

**Characterization and Remediation of Aquifers Contaminated by
Nonaqueous Phase Liquids Using Partitioning Tracers and
Surfactants**

by

Varadarajan Dwarakanath

Dissertation

Presented to the Faculty of the Graduate School of

The University of Texas at Austin

in Partial Fulfillment

of the Requirements

for the Degree of

Doctor of Philosophy


The University of Texas at Austin

May 1997

Copyright
by
Varadarajan Dwarakanath
1997

**Characterization and Remediation of Aquifers Contaminated by
Nonaqueous Phase Liquids Using Partitioning Tracers and
Surfactants**

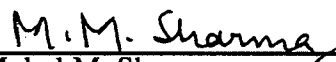
**Approved by
Dissertation Committee:**




Gary A. Pope, Co-supervisor



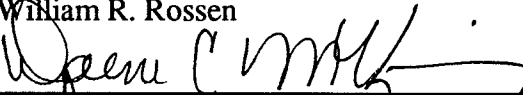
Kamy Sepehrmoori, Co-supervisor




Mukul M. Sharma



William R. Rossen



Daene C. McKinney



William H. Wade

Dedication

This dissertation is dedicated to my guru, Sant Piara Singh Raja whose prayers and inspiration have helped me through all these years.

Acknowledgments

In all my years at the University of Texas, I owe a debt of gratitude to many people. First and foremost, it has been my good fortune to be supervised by Dr. Gary A. Pope. Words are poor substitutes to express my gratitude for his guidance, support and many constructive criticisms which have greatly enriched my learning experience at the University of Texas.

I would also like to thank Dr. Kamy Sepehrnoori for co-supervising this project. A special note of thanks go to Dr. William H. Wade for advice on many aspects of surfactant phase behavior. To the other members of my committee, Dr. Daene C. McKinney, Dr. William R. Rossen and Dr. Mukul M. Sharma, I extend my deepest appreciation for their assistance, comments and suggestions.

I would like reserve a special note of thanks for Dr. Bruce Rouse who helped me get started in my laboratory work and his invaluable help in running all my GC samples and the measurement of alcohol partition coefficients without which this work would have been impossible. I would also like to thank Vinitha Weerasooriya for helping out in difficult surfactant synthesis which was needed in this work.

I have been extremely fortunate to have worked with several individuals who were great friends and helped me learn a lot at school. First of all I would like to thank Dino Kostarelos and Douglas Shotts who were excellent friends and laboratory mates. I would also like to thank Minquan Jin, Allen Whitley, Meng Lim, Adil Abubakar, Kiam Ooi, Taimur Malik, Jeff Edgar and Neil Deeds for their help and support during the course of this work.

The staff at Petroleum and Geosystems Engineering deserves special mention. In this regard I would like to thank Egidio Leitao who worked wonders in procuring equipment and materials which made most of this possible. I would also like to thank Esther Barrientes, Tony Bermudez, Joanna Castillo, Glen Baum and Bob Savicki for their help and support.

Financial support for this work came from EPA/ManTech Environmental Research (Contract No: GL 2000-602-4600), State of Texas ATP-D-404, Air Force Center for Environmental Excellence (Contract No: F41624-95-C-8010), PPG Industries Inc. (Purchase order 654100661) and U.S. EPA (Contract CR-818647-03). I would also like to thank the Department of Energy Research and Environmental Management Science Program.

I would like to thank Lynn Wood (EPA) for his support in the EPA/ManTech Environmental Research project for performing the partitioning tracer test at Hill OU1. Many thanks to Richard Jackson (Intera) who gave me an opportunity to work at both the Phase I and Phase II projects at Hill OU2. A special note of thanks to Hans Meinardous (Intera) for supplying field soil samples and field DNAPL samples for performing several laboratory experiments. Special thanks

also go to Tim Oolman (Radian) for the timely supply and analysis of Hill source water.

I would like to thank my parents, Champa and Krishnasami Varadarajan for their support, my grandparents, my uncle Srini Iyengar for constant encouragement and support. Special note of thanks to my brother Raghu for his friendship during the course of my studies. I would like to thank my friends, Reddy, Srihari, John, Althea and many others for their constant support.

Finally I would like to thank the almighty for making my stay in Austin pleasurable and timely completion of my studies.

Characterization and Remediation of Aquifers Contaminated by Nonaqueous Phase Liquids Using Partitioning Tracers and Surfactants

Publication No. _____

Varadarajan Dwarakanath, Ph.D.

The University of Texas at Austin, 1997

Co-supervisor: Gary A. Pope

Co-supervisor: Kamy Sepehrnoori

The main objectives of this work were the development of the partitioning interwell tracer test for estimation of nonaqueous phase liquid (NAPL) saturation in saturated porous media, performance assessment of surfactant enhanced aquifer remediation using partitioning tracers and screening and selection of environmentally acceptable surfactant solutions for surfactant enhanced aquifer remediation (SEAR) of soils contaminated by NAPLs. The contaminants studied in this work were tetrachloroethylene (PCE), trichloroethylene (TCE), jet fuel (JP4) and contaminant from Hill Air Force Base, site Operational Unit 2 (Hill OU2 DNAPL) and contaminant from Hill Air Force Base, site Operational Unit 1 (Hill OU1 LNAPL)

The first step in screening partitioning tracers involved performing several batch experiments to determine partition coefficients of about 28 alcohols and 10 NAPLs. Partitioning tracer tests were performed to estimate NAPL saturation in soil packs with known amounts of NAPL. A close match between NAPL saturation estimates based on mass balance and partitioning tracers was obtained in column experiments with several NAPLs thus validating the partitioning interwell tracer test as an effective tool for estimating residual NAPL saturation. The next step involved the development of laboratory procedures for designing field partitioning tracer tests. Two field partitioning tracer tests were designed using these procedures. The first field test was a partitioning interwell tracer test (PITT) performed by The University of Florida and EPA at the Operational Unit 1 site at Hill Air Force Base, Utah and the second test was the PITT performed by INTERA Inc. at the Operational Unit 2 site at Hill Air Force Base, Utah.

Surfactants were selected by performing phase behavior experiments with surfactant, NAPL, alcohol, electrolyte and water mixtures. The surfactants used were the anionic surfactants, sodium diamyl sulfosuccinate, sodium dihexyl sulfosuccinate and sodium dioctyl sulfosuccinate. Surfactant solutions with low viscosities and quick equilibration times were selected for use in soil column experiments. Alcohols such as isopropyl alcohol and secondary butyl alcohol were used to minimize gel/liquid crystal formation and emulsions and to lower equilibration times. These favorable characteristics were confirmed by measurement of low pressure losses (hydraulic gradients) across the soil packs during surfactant flooding in several column experiments. The effect of the addition of polymer to the surfactant solution on surfactant remediation was

investigated by performing several surfactant remediation experiments with surfactant, alcohol and polymer solutions. Based on all the column experiments, a laboratory procedure for designing field surfactant enhanced aquifer remediation tests was developed. This was used to design a surfactant flood at Hill AFB, site Operational Unit 2.

Both the laboratory and field results showed that with the proper surfactant selection, laboratory procedures and process design, more than 99% of the DNAPL can be removed from sandy/gravelly soil of the type found in Hill AFB, Utah. This is a much more favorable result than previously reported and a strong indication that surfactant remediation is a viable alternative, perhaps the best alternative for these very difficult DNAPL sites. Partitioning tracers and other site characterization played a key role in this success and were an integral part of all this research.

The main contributions of this work were the validation the PITT for estimation of NAPL saturations and performance assessment of surfactant remediation and development of laboratory procedures for selection of both partitioning tracers and surfactants for application in field PITT and SEAR operations.

Table of Contents

Acknowledgments	v
Abstract	viii
Table of Contents	xi
List of Tables	xxiii
List of Figures	xxx
Chapter 1: Introduction	1
1.1 Motivation	1
1.2 Literature Review	9
1.2.1 Partitioning Tracers	9
1.2.2 Phase Behavior Experiments	13
1.2.3 Soil Column Experiments	17
1.2.4 Field Studies	21
1.3 Review of Chapters	24
Chapter 2: Equipment and Materials	28
2.1 Injection Pumps	28
2.2 Solution Columns	28
2.3 Fluid Reservoirs	29
2.4 Glass Columns	29
2.5 Stainless Steel Screens	29
2.6 Steel Columns	29

2.7 Tubing	30
2.8 Fraction Collectors.....	30
2.9 Pressure Transducers	30
2.10 Carrier Demodulator	31
2.11 Chart Recorder.....	31
2.12 Pressure Gauges, Vacuum Gauges	32
2.13 Balances	32
2.14 Gas Chromatograph (Varian 3400)	32
2.15 Gas Chromatograph (Varian 3400cx SPME)	33
2.16 Gas Chromatograph (Buck Scientific).....	33
2.17 Liquid Scintillation Counter	34
2.18 Couette Viscometer	34
2.19 Filter Press	34
2.20 Spinning Drop Tensiometer.....	35
2.21 Water Deionizer.....	35
2.22 pH Meters	35
2.23 Ottawa Sand.....	36
2.24 Glass Pipettes for Phase Behavior	36
2.25 Glass Vials with Aluminum Lined Caps	36
2.26 Micropipettes	36
2.27 Alcohols and Solvents	37
2.28 Surfactants	37

Chapter 3: Experimental Procedures	40
3.1 Phase Behavior	40
3.2 Static partition coefficient tests	41
3.3 Soil Column Preparation With Clean Ottawa Sand.....	42
3.3.1 soil washing	42
3.3.2 determination of end volume in column	42
3.3.3 soil packing	42
3.4 Saturation of Clean Ottawa Sand.....	43
3.5 Column Preparation With Field Soil	44
3.6 Saturation of Field Soil	45
3.7 NAPL Injection Procedures	45
3.8 Water Injection Procedures.....	46
3.9 Mixing of Alcohol Tracers	47
3.10 Mixing of Radiolabeled Tritium Tracer	47
3.11 Mixing of Surfactant.....	47
3.12 Mixing of Surfactant Alcohol Polymer Solutions	48
3.13 Gas Chromatograph Calibration for Alcohol Tracers	49
3.14 Gas Chromatograph Calibration for Contaminants	49
 Chapter 4: Data Analysis Techniques.....	 56
4.1 Phase Behavior: Measurement of Solubilization Ratios	56
4.1.1 volumetric measurements of solubilization	56
4.1.2 GC measurement of solubilization	59
4.2 Porosity and Pore Volume Determination	60

4.3 Permeability Determination	61
4.4 Estimation of Residual NAPL Saturation in Soil Packs	62
4.5 Performance Assessment of Surfactant Using Mass Balance	63
4.6 Static Partition Coefficient Calculation	63
4.7 Method of Moments To Estimate Pore Volume, NAPL Saturation	64
Chapter 5: Surfactant Phase Behavior Studies	75
5.1 Description of Surfactants	75
5.1.1 Anionic	78
5.1.2 Cationic	78
5.1.3 Nonionic	78
5.1.4 Amphoteric or Zwitterionic	78
5.2 Review of Surfactant Behavior	79
5.2.1 Microemulsions	80
5.2.2 Solubilization parameter and contaminant solubilization	83
5.2.3 Volume fraction diagrams	85
5.2.4 Ternary diagrams	86
5.2.5 Interfacial tensions (IFT)	87
5.3 Surfactant Applicability	89
Chapter 6: Phase Behavior Results	102
6.1 Phase Behavior Results	102
6.1.1 PCE	102
6.1.1.1 Salinity Scans	102

6.1.1.2 Ternary Diagram.....	104
6.1.2 TCE.....	105
6.1.2.1 Salinity Scans.....	105
6.1.2.2 Ternary Diagrams	106
6.1.3 Hill DNAPL.....	106
6.1.3.1 Salinity Scans.....	106
6.1.4 JP4.....	109
6.1.4.1 Salinity Scans.....	109
6.2 Discussion on Phase Behavior	113
6.2.1 Comparison of Phase Behavior Results from Literature	114
6.2.2 Coalescence Times and Liquid Crystal Formation.....	116
6.2.3 Effect of Temperature	118
6.2.4 Effect of Alcohol Concentration.....	119
6.2.5 Effect of Electrolyte Type	121
6.2.6 Effect of Surfactant Tail Length	122
6.2.7 Effect of Polymer.....	123
6.3 Comparison of GC and Volumetric Measurements of Solubilization..	124
Chapter 7: Partition Coefficient Tests	180
7.1 Introduction.....	180
7.1.1 Static Partition Tests	180
7.1.2 Dynamic Partition Tests	181
7.2 Results with Various NAPLs.....	182
7.2.1 Mixture of PCE and DCA.....	182

7.3 Applications of Partition Coefficient Measurement	183
Chapter 8: Column Experiments, Description and Results	192
8.1 Experiments with PCE.....	193
8.1.1 Experiment DW#1	193
Initial Tracer Test	194
Contamination of Soil Column and Relative Permeability	
Experiments	194
Relative Permeability Experiments; Results	195
Tracer Test at Residual Water Saturation	196
Tracer Test at Residual PCE Saturation	196
Surfactant Flood to remediate PCE	197
Tracer Test After Surfactant to Estimate Residual PCE	
Saturation	198
Discussion for Experiment DW#1	199
8.1.2 Experiment DW#2	200
Initial Tracer Test	201
Contamination of Soil Column	202
Tracer Test at Residual PCE Saturation	202
Surfactant Flood to Remediate PCE	203
Tracer test After Surfactant to Estimate Residual PCE	
Saturation	204
Discussion for Experiment DW#2	205
8.1.3 Experiment DW#3	207

Initial Tracer Test	207
Contamination of Soil Column	208
Tracer Test at Residual PCE Saturation	208
Surfactant Flood to Remediate PCE	209
Tracer Test After Surfactant to Estimate Residual PCE Saturation	212
Discussion for Experiment DW#3	213
8.2 Experiments with TCE	214
8.2.1 Experiment DW#4	215
Initial Tracer Test	215
Contamination of Soil Column	216
Tracer Test at Residual TCE Saturation	216
Surfactant Flood to Remediate TCE	217
Tracer Test After Surfactant to Estimate Residual TCE Saturation	219
Discussion for Experiment DW#4	220
8.2.2 Experiment POLYTCE#1	221
Initial Tracer Test	222
Contamination of Soil Column	222
Tracer Test at Residual TCE Saturation	223
Surfactant Flood to Remediate TCE	224
Tracer Test After Surfactant to Estimate Residual TCE Saturation	226
Discussion for Experiment POLYTCE#1	227

8.2.3 Experiment POLYTCE#3.....	229
Initial Tracer Test	230
Contamination of Soil Column	230
Tracer Test at Residual TCE Saturation	231
Surfactant Flood to Remediate TCE.....	231
Tracer Test After surfactant to Estimate Residual TCE	
Saturation	233
Discussion for Experiment POLYTCE#3	234
8.3 Experiments with Hill OU1 LNAPL	235
8.3.1 Experiment OUDNAPL1.....	236
Initial Tracer Test	236
Contamination of Soil Column	237
First Tracer Test at Residual NAPL Saturation	237
Second Tracer Test at Residual NAPL Saturation	238
Discussion for Experiment OUDNAPL1	239
8.3.2 Experiment OUDNAPL2.....	239
First Tracer Test at Residual NAPL Saturation	240
Second Tracer Test at Residual NAPL Saturation	241
Discussion for Experiment OUDNAPL2	242
8.3.3 Experiment OUDNAPL3.....	242
First Tracer Test at Residual NAPL Saturation	243
Second Tracer Test at Residual NAPL Saturation	244
Discussion for Experiment OUDNAPL3	244
Overall Summary of OU1 LNAPL Experiments.....	245

8.4 Experiments with JP4	245
8.4.1 Experiment DW#5	246
Initial Tracer Test	246
Contamination of Soil Column	246
Tracer Test at Residual JP4 Saturation	247
Surfactant Flood to Remediate JP4.....	247
Tracer Test After surfactant to Estimate Residual JP4	
Saturation	248
Discussion for Experiment DW#5	249
8.4.2 Experiment JP4#2	250
Initial Tracer Test	251
Contamination of Soil Column	251
Tracer Test at Residual TCE Saturation	251
Surfactant Flood to Remediate JP4.....	252
Tracer Test After surfactant to Estimate Residual JP4	
Saturation	253
Discussion for Experiment JP4#2	254
8.5 Experiments with HILL OU2 DNAPL	254
8.5.1 Experiment HILLOU2#3	256
Initial Tracer Test	257
Contamination of Soil Column	257
Surfactant Flood to Remediate DNAPL	258
Discussion for Experiment HILLOU2#3.....	258
8.5.2 Experiment HILLOU2#5	259

Initial Tracer Test	260
Surfactant Flood to Remediate DNAPL	260
Tracer Test After Surfactant to Estimate Residual DNAPL	
Saturation	263
Discussion for Experiment HILLOU2#5	264
8.5.3 Experiment HILLOU2#7	265
Initial Tracer Test	265
Contamination of Soil Column	266
Tracer Test at Residual DNAPL Saturation	267
Surfactant Flood to Remediate Contaminant	267
Tracer Test After Surfactant to Estimate Residual DNAPL	
Saturation	270
Discussion for Experiment HILLOU2#7	271
8.5.4 Experiment HILLOU2#8	272
Initial Tracer Test	273
Surfactant Flood to Remediate DNAPL	273
Tracer Test After Surfactant to Estimate Residual DNAPL	
Saturation	276
Discussion for Experiment HILLOU2#8	277
8.6 Summary and Discussion of Experiments	278
8.6.1 Measurement of Hydraulic Gradients	280
8.6.2 Use of Xanthan Gum Polymer	280
8.6.3 Use of Alcohol as a Co-solvent	281
8.6.4 Salinity Gradient	281

Chapter 9: Column Experiments: Discussion	401
9.1 Error Analysis	401
9.1.1 Gas Chromatograph Errors	402
9.1.2 Errors in Pore Volume Measurement	403
9.1.3 Errors in Residual TCE Saturation Measurement	403
9.1.4 Errors in Static Partition Coefficient Measurement.....	404
9.1.5 Error in Saturation Estimation	405
9.1.6 Estimation of Dynamic Partition Coefficients.....	405
9.2 Tracer Adsorption	407
9.3 Surfactant Adsorption	408
9.3 Interfacial Tensions	409
Chapter 10: Laboratory Selection and Design of Partitioning Tracer and Surfactant Injection Tests	420
10.1 Hill AFB: Introduction and Geology	422
10.1.1 Hill OU1	423
10.1.2 Hill OU2	423
10.1.3 Site Description, HILLOU2.....	424
10.2 Partitioning Tracer Design and Selection	425
10.2.1 Partition Coefficient Tests to Measure Partition Coefficients	426
10.2.2 Partitioning Tracer Tests in Clean Field Soil with Field NAPL	427

10.2.3 Partitioning Tracer Tests in Contaminated Field Soil	429
10.3 Recommendations for Field Tests	431
10.3.1 HILLOU1	431
10.3.2 Hill OU2	432
10.4 Surfactant Selection and Design	432
10.4.1 Phase Behavior	432
10.4.2 Column Experiments	434
10.4.2.1 Hydraulic Gradient Measurement.....	436
10.4.2.2 Surfactant Adsorption	437
10.4.2.3 CDC Curves and DNAPL Recovery Mechanism.....	438
10.4.2.4 Performance Assessment	439
10.4.2.5 Selection of a suitable surfactant solution	440
10.5 Recommendations for the HILLOU2 Phase I and the Phase II tests ..	441
 Chapter 11: Summary, Conclusions and Future Work	 450
11.1 Summary	450
11.2 Conclusions.....	452
11.3 Future Work.....	457
Nomenclature.....	458
Appendix A.....	464
Bibliography	468
Vita	484

List of Tables

Table 1.1:	Nonionic surfactants used in remediation literature	25
Table 1.2:	Anionic surfactants used in remediation literature	26
Table 6.1:	Summary of phase behavior experiments with PCE	126
Table 6.2:	Summary of phase behavior experiments with TCE	126
Table 6.3:	Summary of phase behavior experiments with Hill DNAPL	127
Table 6.4:	Summary of phase behavior experiments with Jet fuel	128
Table 6.5:	Comparison of solubilization parameters for several surfactants ...	129
Table 6.6:	Comparison of molar solubilization ratios for several surfactants .	130
Table 6.7:	Summary of abbreviations and surfactant characteristics	131
Table 7.1:	Partition coefficients for several NAPLs	185
Table 7.2:	Partition coefficients for several NAPLs	186
Table 7.3:	Partition coefficients for PCE, DCA mixture	186
Table 8.1:	Brief description of column experiment	282
Table 8.2:	Brief description of column properties	283
Table 8.3:	Initial tracer test summary for experiment DW#1	283
Table 8.4:	Flow rates during drainage relative permeability experiments for DW#1	283
Table 8.5:	Flow rates during imbibition relative permeability experiments for DW#1	284

Table 8.6:	Drainage relative permeability curve for experiment DW#1	284
Table 8.7:	Imbibition relative permeability curve for experiment DW#1	284
Table 8.8:	Tracer test summary at residual water saturation for experiment DW#1	285
Table 8.9:	Tracer test summary at residual PCE saturation for experiment DW#1	285
Table 8.10:	Surfactant flood summary for experiment DW#1	285
Table 8.11:	Tracer test summary for first tracer test after surfactant, experiment DW#1	286
Table 8.12:	Tracer test summary for second tracer test after surfactant, experiment DW#1	286
Table 8.13:	Initial tracer test summary for experiment DW#2	286
Table 8.14:	Contamination summary, experiment DW#2	287
Table 8.15:	Tracer test summary at residual PCE saturation for experiment DW#2	287
Table 8.16:	Residual PCE saturation estimates based on partitioning tracers, experiment DW#2	287
Table 8.17:	Surfactant flood summary for experiment DW#2	288
Table 8.18:	Tracer test summary for tracer test after surfactant, experiment DW#2	288
Table 8.19:	Initial tracer test summary for experiment DW#3	288
Table 8.20:	Contamination summary, experiment DW#3	289
Table 8.21:	Tracer test summary at residual PCE saturation for experiment DW#3	289

Table 8.22: Residual saturation estimates based on partitioning tracers, experiment DW#3	289
Table 8.23: Surfactant flood summary for experiment DW#3	290
Table 8.24: Tracer test summary for tracer test after surfactant, experiment DW#3	290
Table 8.25: Residual saturation estimates after surfactant based on partitioning tracers, experiment DW#3	291
Table 8.26: Initial tracer test summary for experiment DW#4	291
Table 8.27: Contamination summary, experiment DW#4	291
Table 8.28: Tracer test summary at residual TCE saturation for experiment DW#4	292
Table 8.29: Dynamic partition coefficient estimates based on partitioning tracers, experiment DW#4	292
Table 8.30: Surfactant flood summary for experiment DW#4	292
Table 8.31: Tracer test summary for tracer test after surfactant, experiment DW#4	293
Table 8.32: Residual saturation estimates after surfactant based on partitioning tracers, experiment DW#4	293
Table 8.33: Initial tracer test summary for experiment POLYTCE#1	293
Table 8.34: Contamination summary, experiment POLYTCE#1	294
Table 8.35: Tracer test summary at residual TCE saturation for experiment POLYTCE#1	294
Table 8.36: Residual TCE saturation estimates based on partitioning tracers, experiment POLYTCE#1	295

Table 8.37: Surfactant flood summary for experiment POLYTCE#1	295
Table 8.38: Tracer test summary for tracer test after surfactant, experiment POLYTCE#1	296
Table 8.39: Residual saturation estimates after surfactant based on partitioning tracers, experiment POLYTCE#1	296
Table 8.40: Initial tracer test summary for experiment POLYTCE#3	297
Table 8.41: Contamination summary, experiment POLYTCE#3	297
Table 8.42: Tracer test summary at residual TCE saturation for experiment POLYTCE#3	297
Table 8.43: Residual saturation estimates based on tritium tracer, experiment POLYTCE#3	297
Table 8.44: Surfactant flood summary for experiment POLYTCE#3	298
Table 8.45: Tracer test summary for tracer test after surfactant, experiment POLYTCE#3	298
Table 8.46: Residual saturation estimates after surfactant based on partitioning tracers, experiment POLYTCE#3	299
Table 8.47: Initial tracer test summary for experiment OUDNAPL1	299
Table 8.48: Contamination summary, experiment OUDNAPL1	299
Table 8.49: First tracer test summary at residual NAPL saturation for experiment OUDNAPL1	300
Table 8.50: Dynamic partition coefficient estimates based on first set of partitioning tracers, experiment OUDNAPL1	300
Table 8.51: Second tracer test summary at residual NAPL saturation for experiment OUDNAPL1	300

Table 8.52: Dynamic partition coefficient estimates based on second set of partitioning tracers, experiment OUDNAPL1	301
Table 8.53: Comparison of partition coefficients from static partition coefficient tests and column experiments	301
Table 8.54: First tracer test summary at residual NAPL saturation for experiment OUDNAPL2	301
Table 8.55: Residual saturation estimates based on first set of partitioning tracers, experiment OUDNAPL2.....	302
Table 8.56: Second tracer test summary at residual NAPL saturation for experiment OUDNAPL2	302
Table 8.57: Residual saturation estimates based on second set of partitioning tracers, experiment OUDNAPL2.....	303
Table 8.58: First tracer test summary at residual NAPL saturation for experiment OUDNAPL3	303
Table 8.59: Residual saturation estimates based on first set of partitioning tracers, experiment OUDNAPL3.....	304
Table 8.60: Second tracer test summary at residual NAPL saturation for experiment OUDNAPL3	304
Table 8.61: Residual saturation estimates based on first set of partitioning tracers, experiment OUDNAPL3.....	304
Table 8.62: Initial tracer test summary for experiment DW#5	305
Table 8.63: Contamination summary, experiment DW#5	305
Table 8.64: Tracer test summary at residual JP4 saturation for experiment DW#5.....	306

Table 8.65: Residual saturation estimates based on partitioning tracers, experiment DW#5.....	306
Table 8.66: Surfactant flood summary for experiment DW#5	307
Table 8.67: Tracer test summary for tracer test after surfactant, experiment DW#5.....	307
Table 8.68: Initial tracer test summary for experiment JP4#2.....	308
Table 8.69: Contamination summary, experiment JP4#2.....	308
Table 8.70: Tracer test summary at residual JP4 saturation for experiment JP4#2.....	309
Table 8.71: Residual saturation estimates based on partitioning tracers, experiment JP4#2.....	309
Table 8.72: Surfactant flood summary for experiment JP4#2	310
Table 8.73: Tracer test summary for tracer test after surfactant, experiment JP4#2.....	310
Table 8.74: Residual saturation estimates after surfactant based on partitioning tracers, experiment JP4#2	311
Table 8.75: Initial tracer test summary for experiment HILLOU2#3.....	311
Table 8.76: Residual saturation estimates based on partitioning tracers, experiment HILLOU2#3	312
Table 8.77: Surfactant flood summary for experiment HILLOU2#3	312
Table 8.78: Tracer test summary at residual DNAPL saturation for experiment HILLOU2#5	313
Table 8.79: Residual DNAPL saturation estimates based on partitioning tracers, experiment HILLOU2#5.....	313

Table 8.80: Surfactant flood summary for first surfactant flood, experiment HILLOU2#5	313
Table 8.81: Surfactant flood summary for second surfactant flood, experiment HILLOU2#5	314
Table 8.82: Tracer test summary for tracer test after surfactant, experiment HILLOU2#5	314
Table 8.83: Residual saturation estimates after surfactant based on partitioning tracers, experiment HILLOU2#5	314
Table 8.84: Initial tracer test summary for experiment HILLOU2#7	315
Table 8.85: Contamination summary, experiment HILLOU2#7	315
Table 8.86: Tracer test summary at residual DNAPL saturation for experiment HILLOU2#7	316
Table 8.87: Residual DNAPL saturation estimates based on partitioning tracers, experiment HILLOU2#7	316
Table 8.88: Surfactant flood summary, experiment HILLOU2#7	317
Table 8.89: Tracer test summary for tracer test after surfactant, experiment HILLOU2#7	318
Table 8.90: Residual saturation estimates after surfactant based on partitioning tracers, experiment HILLOU2#7	318
Table 8.91: Tracer test summary at residual DNAPL saturation for experiment HILLOU2#8	319
Table 8.92: Residual DNAPL saturation estimates based on partitioning tracers, experiment HILLOU2#8	319
Table 8.93: Surfactant flood summary, experiment HILLOU2#8	320

Table 8.94: Tracer test summary for tracer test after surfactant, experiment HILLOU2#8	320
Table 8.95: Residual saturation estimates after surfactant based on partitioning tracers, experiment HILLOU2#8	321
Table 9.1: Best estimates of partition coefficients	411
Table 9.2: Distribution coefficients for several alcohols in different types of soil.....	412
Table 9.3: Adsorption values for alcohols with different types of soil.....	413
Table 9.4: Surfactant adsorption by Hill field soil.....	413
Table 9.5: Comparison of measured interfacial tensions and interfacial tensions estimated using the Chun Huh relation.....	414
Table 10.1: Summary of phase behavior experiments performed with Hill DNAPL	442
Table 10.2: Cations in Hill groundwater and Hill source water	443
Table 10.3: Anions in Hill groundwater and Hill source water	443
Table 10.4: Summary of column experiments performed for Hill OU2 Phase I and Phase II tests	444
Table 10.5: Performance assessment of surfactant remediation	445

List of Figures

Figure 1.1:	Geological cross section of a DNAPL contaminated site.....	27
Figure 2.1:	Chemical structure of sodium diamyl sulfosuccinate	38
Figure 2.2:	Chemical structure of sodium dihexyl sulfosuccinate	38
Figure 2.3:	Chemical structure of sodium dioctyl sulfosuccinate	39
Figure 3.1:	Set up for packing soil columns.....	51
Figure 3.2:	Teflon tubing used in glass columns to prevent movement of sand	52
Figure 3.3:	Leak testing setup	53
Figure 3.4:	Core saturation setup	54
Figure 3.5:	NAPL saturation setup.....	55
Figure 4.1:	Calculation of Oil Solubilization Ratios in type I systems	70
Figure 4.2:	Calculation of Water Solubilization Ratios in type II systems	71
Figure 4.3:	Comparison of gas chromatograph measurement and volume measurement of contaminant in microemulsion	72
Figure 4.4:	Permeability calculation plot for experiment HILLOU2#8	73
Figure 4.5:	Extrapolation of partitioning tracer data, experiment OUDNAPL3	74
Figure 5.1:	Nature of surfactant molecule.....	91

Figure 5.2:	Examples of anionic and nonionic surfactants	92
Figure 5.3:	Phase behavior of anionic surfactants.....	93
Figure 5.4:	Solubilization parameters plotted against electrolyte concentration.....	94
Figure 5.5:	Contaminant solubilization plotted against electrolyte concentration.....	95
Figure 5.6:	Volume fraction diagram for a surfactant formulation.....	96
Figure 5.7:	Type I ternary with oil, water and surfactant (reproduced from Nelson and Pope, 1978).....	97
Figure 5.8:	Type III ternary with oil, water and surfactant (reproduced from Nelson and Pope, 1978)	98
Figure 5.9:	Type II ternary with oil, water and surfactant (reproduced from Nelson and Pope, 1978).....	99
Figure 5.10:	Ternary diagram of a surfactant formulation.....	100
Figure 5.11:	Illustration showing the relation between phase behavior and interfacial tensions between microemulsions and excess water and oil phases. (illustration based on Figure in Baran <i>et al.</i> , 1994b)	101
Figure 6.1:	Volume fraction diagram for 4% by weight sodium dihexyl sulfosuccinate at 23°C	132
Figure 6.2:	Volume fraction diagram for 4% by weight sodium dihexyl sulfosuccinate at 23°C	133

Figure 6.3:	Solubilization parameters for 4% by weight sodium dihexyl sulfosuccinate	134
Figure 6.4:	Solubilization parameters for 4% by weight sodium dihexyl sulfosuccinate	135
Figure 6.5:	PCE solubilization for 4% by weight sodium dihexyl sulfosuccinate	136
Figure 6.6:	PCE solubilization for 4% by weight sodium dihexyl sulfosuccinate	137
Figure 6.7:	Volume fraction diagram for 2% by weight sodium diamyl sulfosuccinate and 2% by weight sodium dioctyl sulfosuccinate at 23°C	138
Figure 6.8:	Solubilization parameters for 2% by weight sodium diamyl sulfosuccinate and 2% by weight sodium dioctyl sulfosuccinate	139
Figure 6.9:	PCE solubilization for 2% by weight sodium diamyl sulfosuccinate and 2% by weight sodium dioctyl sulfosuccinate	140
Figure 6.10:	Ternary for 1:1 sodium diamyl sulfosuccinate and sodium dioctyl sulfosuccinate, 500 mg/l CaCl ₂ at 23°C	141
Figure 6.11:	Volume fraction diagram for 8% by weight sodium dihexyl sulfosuccinate at 23°C	142
Figure 6.12:	Volume fraction diagram for 8% by weight sodium dihexyl sulfosuccinate at 23°C	143

Figure 6.13: Solubilization parameters for 8% by weight sodium dihexyl sulfosuccinate	144
Figure 6.14: Solubilization parameters for 8% by weight sodium dihexyl sulfosuccinate	145
Figure 6.15: TCE solubilization for 8% by weight sodium dihexyl sulfosuccinate	146
Figure 6.16: TCE solubilization for 8% by weight sodium dihexyl sulfosuccinate	147
Figure 6.17: Ternary for sodium dihexyl sulfosuccinate, 1,000 mg/l NaCl at 23°C	148
Figure 6.18: Volume fraction diagram for 4% by weight sodium dihexyl sulfosuccinate, 4% by weight IPA and 500 mg/l xanthan gum in Hill source water at 23°C.....	149
Figure 6.19: Volume fraction diagram for 4% by weight sodium dihexyl sulfosuccinate, 4% by weight ethanol and 500 mg/l xanthan gum in Hill source water at 23°C	150
Figure 6.20: Solubilization parameters for 4% by weight sodium dihexyl sulfosuccinate, 4% by weight alcohol and 500 mg/l xanthan gum in Hill source water at 23°C	151
Figure 6.21: Hill contaminant solubilization for 4% by weight sodium dihexyl sulfosuccinate, 4% by weight alcohol, 500 mg/l xanthan gum in Hill source water at 23°C.....	152

Figure 6.22:	Volume fraction diagram for 8% by weight sodium dihexyl sulfosuccinate, 8% by weight IPA and 500 mg/l xanthan gum in Hill source water at different temperatures	153
Figure 6.23:	Solubilization parameters for 8% by weight sodium dihexyl sulfosuccinate, 8% by weight IPA and 500 mg/l xanthan gum in Hill source water at different temperatures	154
Figure 6.24:	Hill contaminant solubilization plotted for 8% by weight sodium dihexyl sulfosuccinate, 8% by weight alcohol and 500 mg/l xanthan gum in Hill source water at different temperatures.....	155
Figure 6.25:	Volume fraction diagram for 8% by weight sodium dihexyl sulfosuccinate, 2% by weight IPA in Hill source water at different temperatures	156
Figure 6.26:	Volume fraction diagram for 8% by weight sodium dihexyl sulfosuccinate, 4% by weight IPA in Hill source water at different temperatures	157
Figure 6.27:	Hill contaminant and water solubilization parameters for 8% by weight sodium dihexyl sulfosuccinate and 2% by weight IPA ...	158
Figure 6.28:	Hill contaminant and water solubilization parameters for 8% by weight sodium dihexyl sulfosuccinate, 4% by weight IPA	159
Figure 6.29:	Hill contaminant solubilization for 8% by weight sodium dihexyl sulfosuccinate, 2% by weight IPA in Hill source water .	160
Figure 6.30:	Hill contaminant solubilization for 8% by weight sodium dihexyl sulfosuccinate, 4% by weight IPA in Hill source water .	161

Figure 6.31:	Volume fraction diagram for 2% by weight sodium diheptyl sulfosuccinate, secondary butyl alcohol	162
Figure 6.32:	Jet fuel and water solubilization parameters for 2% by weight sodium diheptyl sulfosuccinate, secondary butyl alcohol	163
Figure 6.33:	Jet fuel solubilization for 2% by weight sodium diheptyl sulfosuccinate, secondary butyl alcohol	164
Figure 6.34:	Volume fraction diagram for 4% by weight sodium diheptyl sulfosuccinate, secondary butyl alcohol	165
Figure 6.35:	Jet fuel and water solubilization parameters for 4% by weight sodium diheptyl sulfosuccinate, secondary butyl alcohol	166
Figure 6.36:	Jet fuel solubilization for 4% by weight sodium diheptyl sulfosuccinate, 2% by weight secondary butyl alcohol	167
Figure 6.37:	Viscosity of 4% by weight sodium diheptyl sulfosuccinate, 8% by weight secondary butyl alcohol plotted against shear rate	168
Figure 6.38:	Volume fraction diagram for 2% by weight sodium dihexyl sulfosuccinate and 2% by weight dioctyl sulfosuccinate, 8% by weight secondary butyl alcohol	169
Figure 6.39:	Solubilization parameters for 2% by weight sodium dihexyl sulfosuccinate and 2% by weight dioctyl sulfosuccinate with 8% by weight secondary butyl alcohol	170
Figure 6.40:	Jet fuel solubilization plotted for 2% by weight sodium dihexyl sulfosuccinate and 2% by weight dioctyl sulfosuccinate, 8% by weight secondary butyl alcohol	171

Figure 6.41:	Effect of temperature on optimal salinity for 4% by weight sodium dihexyl sulfosuccinate solutions with varying amounts of IPA and TCE	172
Figure 6.42:	Effect of temperature on optimal salinity for 8% by weight sodium dihexyl sulfosuccinate solutions with varying amounts of IPA and Hill DNAPL	173
Figure 6.43:	Effect of IPA concentration on optimal salinity and solubilization for 4% by weight sodium dihexyl sulfosuccinate TCE	174
Figure 6.44:	Effect of IPA concentration on optimal salinity and solubilization for 8% by weight sodium dihexyl sulfosuccinate and Hill DNAPL	175
Figure 6.45:	Solubilization parameter and optimal salinity plotted as function of surfactant chain length	176
Figure 6.46:	Volume fraction diagram for 4% by weight sodium dihexyl sulfosuccinate, 8% by weight IPA, xanthan gum at 23°C	177
Figure 6.47:	Comparison of GC and volumetric measurements of contaminant solubilization at different electrolyte concentrations	178
Figure 6.48:	Comparison of GC and volumetric measurements of contaminant solubilization at different surfactant concentrations	179
Figure 7.1:	Partition coefficients for a PCE, DCA mixture	187

Figure 7.2:	Partition coefficients of alcohol tracers with one branched methyl group plotted against solubility for several DNAPLs	188
Figure 7.3:	Partition coefficients of alcohol tracers with one branched methyl group plotted against solubility for several DNAPLs and Jet Fuel	189
Figure 7.4:	Partition coefficients of alcohol tracers with two branched methyl groups plotted against solubility for several DNAPLs	190
Figure 7.5:	Partition coefficients of alcohol tracers with two branched methyl groups plotted against solubility for several DNAPL	191
Figure 8.1:	Initial tracer concentration history, experiment DW#1	322
Figure 8.2:	Drainage relative permeability curve for PCE and water, experiment DW#1	323
Figure 8.3:	Imbibition relative permeability curve for PCE and water, experiment DW#1	324
Figure 8.4:	Tracer concentration history for PCE tracer test at residual water saturation, experiment DW#1	325
Figure 8.5:	Tracer concentration history at residual PCE saturation, experiment DW#1	326
Figure 8.6:	PCE concentration in effluent during surfactant flushing, experiment DW#1	327
Figure 8.7:	Final tracer concentration history for first set of tracers after surfactant, experiment DW#1	328

Figure 8.8	Final tracer concentration history for second set of tracers after surfactant, experiment DW#1	329
Figure 8.9	Initial tracer concentration histories, experiment DW#2.....	330
Figure 8.10	Tracer concentration histories at residual PCE saturation, experiment DW#2.....	331
Figure 8.11:	PCE concentration in effluent during surfactant flushing, experiment DW#2.....	332
Figure 8.12:	Plot showing PCE recovery mechanisms during surfactant flushing, experiment DW#2.....	333
Figure 8.13:	Viscosities of aqueous surfactant solution and middle phase microemulsion, experiment DW#2.....	334
Figure 8.14:	Final tracer concentration history, experiment DW#2	335
Figure 8.15:	Initial tracer concentration history, experiment DW#3	336
Figure 8.16:	Tracer concentration histories at residual PCE saturation, experiment DW#3.....	337
Figure 8.17:	PCE concentration in effluent during surfactant flushing, experiment DW#3.....	338
Figure 8.18:	Plot showing PCE recovery mechanisms during surfactant flushing, experiment DW#3.....	339
Figure 8.19:	Hydraulic gradient across soil column during surfactant flood and post surfactant waterflood, experiment DW#3	340
Figure 8.20:	Viscosity of aqueous surfactant solution, experiment DW#3	341
Figure 8.21:	Final tracer concentration histories, experiment DW#3	342

Figure 8.22: Comparison of initial and final tracer concentration histories, experiment DW#3.....	343
Figure 8.23 Initial tracer concentration history, experiment DW#4.....	344
Figure 8.24: Tracer concentration histories at residual TCE saturation, experiment DW#4.....	345
Figure 8.25: Plot showing PCE concentration history and recovery mechanisms during surfactant flushing, experiment DW#4.....	346
Figure 8.26: Hydraulic gradient across soil column during surfactant flood and post surfactant waterflood, experiment DW#4	347
Figure 8.27: Viscosity of aqueous surfactant solution, experiment DW#4	348
Figure 8.28: Final tracer concentration histories, experiment DW#4	349
Figure 8.29: Initial tracer concentration history, experiment POLYTCE#1	350
Figure 8.30: Tracer concentration histories at residual TCE saturation, experiment POLYTCE#1	351
Figure 8.31: TCE concentration in effluent during surfactant flushing, experiment POLYTCE#1	352
Figure 8.32: TCE concentration during post surfactant waterflood, experiment POLYTCE#1	353
Figure 8.33: Viscosities of aqueous surfactant solution and microemulsions with 500 mg/l xanthan gum polymer, experiment POLYTCE#1	354
Figure 8.34: Hydraulic gradient across soil column during surfactant flood and post surfactant waterflood, experiment POLYTCE#1	355

Figure 8.35:	Comparison of initial and final tracer concentration histories, experiment POLYTCE1	356
Figure 8.36:	Initial tracer concentration history, experiment POLYTCE#3	357
Figure 8.37:	Tracer concentration history at residual TCE saturation, experiment POLYTCE#3	358
Figure 8.38:	TCE concentration history and recovery mechanisms during surfactant flushing, experiment POLYTCE#3	359
Figure 8.39:	Hydraulic gradient across soil column and TCE concentration during surfactant flood and post surfactant waterflood, experiment POLYTCE#3	360
Figure 8.40:	Final tracer concentration histories, experiment POLYTCE#3	361
Figure 8.41:	Initial tracer concentration histories, experiment OUDNAPL1	362
Figure 8.42:	Tracer concentration histories for first set of tracers at residual OU1 NAPL saturation, experiment OUDNAPL1	363
Figure 8.43:	Tracer concentration histories for second set of tracers at residual OU1 NAPL saturation, experiment OUDNAPL1	364
Figure 8.44:	Tracer concentration histories for first set of tracers at residual OU1 NAPL saturation, experiment OUDNAPL2	365
Figure 8.45:	Tracer concentration histories for second set of tracers at residual OU1 NAPL saturation, experiment OUDNAPL2	366
Figure 8.46:	Tracer concentration histories for first set of tracers at residual OU1 NAPL saturation, experiment OUDNAPL3	367
Figure 8.47:	Tracer concentration histories for second set of tracers at residual OU1 NAPL saturation, experiment OUDNAPL3	368

Figure 8.48:	Initial tracer concentration history, experiment DW#5	369
Figure 8.49:	Tracer concentration histories at residual JP4 saturation, experiment DW#5	370
Figure 8.50:	Hydraulic gradient across soil column during surfactant flood and post surfactant waterflood, experiment DW#5	371
Figure 8.51:	Viscosity of aqueous surfactant solution, experiment DW#5	372
Figure 8.52:	Final tracer concentration histories, experiment DW#5	373
Figure 8.53:	Initial tracer concentration history, experiment JP4#2	374
Figure 8.54:	Tracer concentration histories at residual JP4 saturation, experiment JP4#2	375
Figure 8.55:	Viscosity of aqueous surfactant solution, experiment JP4#2	376
Figure 8.56:	Hydraulic gradient across soil column during surfactant flood and post surfactant waterflood, experiment JP4#2	377
Figure 8.57:	Final tracer concentration histories, experiment JP4#2	378
Figure 8.58:	Initial tracer concentration histories, experiment HILLOU2#3 ..	379
Figure 8.59:	Initial tracer concentration histories, experiment HILLOU2#5 ..	380
Figure 8.60:	Comparison of tritium and surfactant concentration histories, experiment HILLOU2#5	381
Figure 8.61:	Comparison of normalized tritium and normalized surfactant concentration histories, experiment HILLOU2#5	382
Figure 8.62:	Hydraulic gradient across soil column during second surfactant flood and post surfactant waterflood, experiment HILLOU2#5 ..	383
Figure 8.63:	Final tracer concentration histories, experiment HILLOU2#5	384
Figure 8.64:	Initial tracer concentration histories, experiment HILLOU2#7 ..	385

Figure 8.65:	Tracer concentration histories at residual DNAPL saturation, experiment HILLOU2#7	386
Figure 8.66:	Plot showing contaminant recovery mechanisms and fraction of DNAPL produced in effluent during surfactant flooding, experiment HILLOU2#7	387
Figure 8.67:	Comparison of tritium and surfactant concentration histories, experiment HILLOU2#7	388
Figure 8.68:	Normalized concentration histories of tritium and surfactant during surfactant and post surfactant polymer flood, experiment HILLOU2#7	389
Figure 8.69:	Tritium and surfactant recoveries during surfactant flood and post surfactant polymer flood, experiment HILLOU2#7	390
Figure 8.70:	Hydraulic gradient across soil column during surfactant flood and post surfactant waterflood, experiment HILLOU2#7	391
Figure 8.71:	Viscosity of aqueous surfactant solution and polymer solution, experiment HILLOU2#7	392
Figure 8.72:	Final tracer concentration histories, experiment HILLOU2#7	393
Figure 8.73:	Initial tracer concentration histories, experiment HILLOU2#8 ..	394
Figure 8.74:	Viscosity of aqueous surfactant solution and polymer solution, experiment HILLOU2#8	395
Figure 8.75:	Hill Contaminant concentration history during surfactant flushing, experiment HILLOU2#8	396
Figure 8.76:	Comparison of normalized tritium and normalized surfactant concentration histories, experiment HILLOU2#8	397

Figure 8.77:	Hydraulic gradient across soil column during surfactant flood and post surfactant waterflood, experiment HILLOU2#8	398
Figure 8.78:	Figure showing the artifact that caused high hydraulic gradients in experiment HILLOU2#8	399
Figure 8.79:	Final tracer concentration histories, experiment HILLOU2#8	400
Figure 9.1:	Comparison of static and dynamic partition coefficients for TCE	415
Figure 9.2:	Comparison of static and dynamic partition coefficients for JP4	416
Figure 9.3:	Comparison of static and dynamic partition coefficients for Hill OU1 NAPL	417
Figure 9.4:	Comparison of static and dynamic partition coefficients for Hill OU2 DNAPL	418
Figure 9.5:	Comparison of measured interfacial tensions and Chun Huh estimates of interfacial tensions	419
Figure 10.1:	Plan View of Hill OU2	446
Figure 10.2:	Solubility of Hill OU2 contaminants as function of surfactant concentration in Hill source water	447
Figure 10.3:	Optimal salinity plotted against temperature for a surfactant solution to be used in Hill OU2	448
Figure 10.4:	Comparison of capillary desaturation data	449

Chapter 1: Introduction

The research presented in this work was part of the ongoing surfactant enhanced aquifer remediation (SEAR) research at the University of Texas at Austin. The main focus of this work was the application of partitioning tracers for estimation of nonaqueous phase liquid (NAPL) saturation in contaminated regions and use of surfactant solutions to remediate contaminated soil. The fundamentals of applying surfactant technology for SEAR applications were adapted from lessons learned from enhanced oil recovery (EOR) research (Pope and Wade, 1995). In the following sections, the motivation for this work, review of previous and ongoing work and a description of all the Chapters is provided

1.1 MOTIVATION

Water is a precious resource. It is used for a variety of applications such as household use, irrigation, hydroelectric power and most industrial processes. About one fifth of the freshwater is supplied from groundwater sources (Solley *et al.*, 1988). Groundwater sources are sometimes contaminated by a variety of pollutants, both organic and inorganic. The inorganic contaminants usually consist of heavy metal ions. Chief among the organic contaminants are chlorinated hydrocarbons and petroleum hydrocarbons.

In this work the terms nonaqueous phase liquid (NAPL) and contaminant are used extensively. The term contaminant refers to a chemical species that is unwanted in a given environment. When this species contaminates air or water, it is termed contaminant. Contaminants can exist in air, water, surfactant solutions

and as an adsorbed component on surfaces. The term NAPL refers to a separate nonaqueous liquid phase. This can be either one contaminant or a mixture of several chemical species. When the term NAPL is used, it means that there is a residual saturation of the nonaqueous liquid. The term concentration is used to characterize contaminant quantity in a given phase and saturation is used to characterize NAPL quantity as a function of pore volume.

When the density of an organic contaminant is greater than 1, it is termed dense nonaqueous phase liquid (DNAPL). Similarly if the density of the contaminant is less than 1, it is termed light nonaqueous phase liquid (LNAPL) (Villaume, 1985; USEPA 1991). Chlorinated hydrocarbons such as tetrachloroethylene (PCE), trichloroethylene (TCE), carbon tetrachloride (CTET) etc. are common DNAPLs and jet fuel, gasoline, diesel etc. are common LNAPLs.

Contamination problems due to LNAPLs are usually limited by the low density of the contaminants which cause them to float on water. LNAPLs are easier to characterize than DNAPLs because of their buoyancy. The presence of LNAPLs in water is usually characterized by odor and taste at typical groundwater levels. On the other hand, contamination of groundwater by chlorinated hydrocarbons are not limited by the water table. They are common contaminants because they exhibit (Pankow and Cherry, 1996):

1. low liquid viscosities (less than 1 cp) and low interfacial tensions which help movement into the subsurface.
2. high volatilities which enables gases to move into the unsaturated zone.
3. low absolute solubilities which limit pump and treat methods.

4. high solubilities (ppm levels) relative to drinking water standards (ppb levels).
5. low degradabilities.

Due to all these properties, chlorinated hydrocarbons can penetrate the soil and contaminate groundwater. Once these NAPLs penetrate the soil, they are held in place in the form of NAPL blobs or ganglia by capillary forces (Hunt *et al.*, 1988a,b; Kueper, 1989). This process of entrapment of NAPL in the subsurface is similar to trapping and release of oil in natural petroleum reservoirs. The factors which affect trapping and mobilization of oil in porous media are described by Stegemeier (1977) and Lake (1989) among many others. The trapped blobs or ganglia remain as sources of contaminant for indefinite time periods in subsurface soils and present a long term threat to groundwater quality as they slowly dissolve into groundwater (Schwille, 1988; Mackay and Cherry 1989; Abriola, 1989; Mercer and Cohen, 1990). In some instances the DNAPL may accumulate in depressions and on top of low permeability formations in the form of pools. In order to eliminate continual contamination of groundwater by slow dissolution of NAPL blobs and pools by flowing water, the source of contamination must be removed.

A figure showing the geological cross section of a DNAPL contaminated aquifer is given in Figure 1.1. This is a cross section of a DNAPL contaminated site Operational Unit 2 at Hill Air Force Base, Utah. A lower confining aquitard can be seen in Figure 1.1. Above the lower confining aquitard there is a permeable sand gravel layer. DNAPL was detected as a pool on top of the aquitard in both the depressions observed in Figure 1.1 (Radian, 1993, Brown,

1997). Laboratory experiments were carried out in this work to design a partitioning tracer test and surfactant flood at Hill Operational Unit 2 to remediate DNAPL from the smaller depression seen in Figure 1.1.

One of the oldest technologies to remediate these NAPL blobs is the pump and treat method. This involves pumping of contaminated water from the contaminated zones followed by treatment of the contaminated water at the surface by air stripping, steam stripping, charcoal filtration and various other means. The recovery of contaminant by pump and treat is dependent on the mass transfer rates between the NAPL and the water flowing across the NAPL-water interface. Remediation of NAPL-contaminated aquifers is limited by parameters such as flow rates, NAPL composition and mass transfer rates (Gellar and Hunt, 1993). These mass transfer rates are in turn dependent on the surface area available for mass transfer (Powers *et al.*, 1991). The dissolution of NAPL under pseudo-steady state and transient conditions has been measured by Powers *et al.*, (1992; 1994). The dissolution kinetics of DNAPL pools was studied by Whelan *et al.*, (1994) who showed that DNAPL mixtures exhibited lower aqueous solubilization than respective aqueous solubility of the contaminants. Pulsed pumping was shown to enhance aqueous contaminant concentrations. Low aqueous solubilization of DNAPL mixtures has also been attributed to dilution effects (Jackson and Mariner, 1995) caused by hydrodynamic dispersion, mixing of contaminated and uncontaminated water, mixing in the extraction system and volatilization of volatile organic carbon compounds during pumping operations. These dilution effects can affect remediation operations adversely. A multiphase flow and transport model for simulating NAPL intrusion, attainment of immobile

state, dissolution and transport in the aqueous phase in both homogeneous and heterogeneous porous media was developed by Mayer and Miller (1996). The model was used to show the importance of porous media heterogeneity on the NAPL dissolution process.

The effectiveness of pump and treat is greatly limited by extremely low solubilities of the contaminants in water and low groundwater velocities (Mackay and Cherry 1989; Fountain *et al.*, 1991). Based on the equilibrium solubilities of the NAPL in water, it takes several years to several decades to remediate typical contaminated zones (Kueper *et al.*, 1993). This is compounded by the fact that the rate of recovery of NAPL decreases as the NAPL blobs get smaller and hence the area available for dissolution is reduced (Powers *et al.*, 1991). For a given porous medium, the only way to increase the NAPL recovery is by either increasing the injection rates which increase the viscous forces on the NAPL and cause mobilization of NAPL or, lowering the interfacial tension between NAPL and water (Hunt *et al.*, 1988a,b). In practice, increasing the injection rate sufficiently high to mobilize NAPL is not feasible (Conrad and Wilson, 1992).

Surfactant remediation is one of the emergent technologies being developed to remediate contaminated soil. Surfactants can be used to vastly increase the solubility of the contaminants in water, hence the potential for increasing the rate of NAPL dissolution (Fountain *et al.*, 1991, 1996). Surfactants also lower the interfacial tension at the water-NAPL interface which if sufficiently low will result in mobilizing the NAPL (Fountain *et al.*, 1991). The goal of surfactant enhanced oil recovery is to achieve ultra-low IFT so that the oil can be economically recovered with a small amount of surfactant that mobilized the

residual oil very efficiently. However, mobilization of DNAPL in aquifers is not always desirable because of concerns of downward migration (Fountain *et al.*, 1991; Pankow and Cherry, 1996).

Before the DNAPL can be removed, it must be located in the subsurface, and this turns out to be very difficult in many cases (Mackay and Cherry, 1989). In the last 15 years of hydrogeological practice, several methods have been developed for characterizing dissolved-phase plumes of contaminants. Conventional coring methods provide point measurements of contaminant concentrations and require interpolation of often sparsely distributed data to estimate total NAPL volumes in the flow domain. The number of sampling locations is usually limited by cost, including the high cost of obtaining the cores and subsequent laboratory analysis for contaminant concentrations. There are several other limitations to coring methods that are site specific and will not be discussed here, but are nevertheless serious problems under some circumstances. Studies of residual DNAPL distribution in heterogeneous, sandy aquifer materials indicate that cores are unlikely to provide reliable estimates of the volume of DNAPL at the field scale because the representative elementary volume of residual DNAPL appears to be much larger than that provided by cores (Mayer and Miller, 1992). It has now become desirable to move away from reliance on core samples alone to estimate DNAPL volumes in the subsurface and to use interwell tests to estimate the residual or pooled DNAPL volumes over meaningful distances (Jin *et al.*, 1995; Wilson and Mackay, 1995). The use of the partitioning interwell tracer test (PITT) to detect and estimate NAPL saturation

was described by Jin *et al.* (1994), Jin (1995), Jin *et al.* (1995) and Whitley *et al.* (1995).

Tracers are chemicals that can be added to fluids in small concentrations and used to follow their movement without affecting their physical properties. Partitioning tracers are tracers which have the ability to partition between two distinct phases. In case of saturated zone partitioning tracer tests, tracers which can partition between NAPL and water are used and in case of vadose zone partitioning tracer tests, tracers which can partition between NAPL and gas phase are used.

The PITT consists of simultaneous injection of several tracers with different partition coefficients an one or more injection wells and measurement of tracer concentrations in one or more extraction or monitoring wells. The non-partitioning or conservative tracers move at the velocity of the carrier phase (water or gas). Due to partitioning of the partitioning tracer molecules between the carrier phase and NAPL, the partitioning tracers are retarded. This retardation is proportional to the volume of NAPL and the partition coefficient. The NAPL saturation can be measured using the difference between the retention times of the partitioning and non-partitioning tracer and the partition coefficient. This can be used for estimation of NAPL saturation before any remedial action is initiated and for performance assessment of remediation.

In all field applications of chemical flooding, performance is limited by the dilution of the injected fluids and bypassing of some zones due to heterogeneities. It is extremely important to minimize these effects in order to minimize costs and maximize performance. In the oil industry, polymers have

been used extensively to improve oil recovery (Lake, 1989 and Sorbie, 1991). The use of mobility control with either polymer or foam also has applicability to aquifer remediation (Pope and Wade, 1995).

From the above discussion it can be seen that partitioning tracers are applicable in locating NAPL contaminated zones and estimation of NAPL saturation and surfactants are applicable in remediation of these contaminated zones. Polymers have potential to maximize partitioning tracer and surfactant performance by providing mobility control. However before this work, laboratory procedures had not been perfected to perform partitioning tracer tests both for estimation of NAPL and performance assessment of remediation. Also, in earlier studies with surfactants, the main focus was on contaminant removal and no attention was paid to factors such as comparison of hydraulic conductivities (permeabilities) before and after remediation. Polymer had not been extensively used in many laboratory experiments with DNAPLs and especially field contaminants. Parameters such as partitioning tracer adsorption and surfactant adsorption by field soil were not quantified.

In this work, a systematic approach for performing soil column experiments is discussed. The goals of this study were;

- (1) development of laboratory procedures for performing partitioning tracer tests.
- (2) development of experimental procedures for selection of suitable partitioning tracers for use in field partitioning interwell tracer tests.
- (3) development of broad guidelines for screening of surfactant solutions using performing phase behavior experiments.

- (4) development of experimental procedures for successful application of surfactants for remediation of soils contaminated with common NAPLs.
- (5) procedures for selection of suitable surfactant/polymer solutions for use in laboratory column experiments and field surfactant applications.

Parameters such as tracer adsorption, surfactant adsorption in field soil from Hill AFB were measured. The soil column hydraulic conductivities before and after surfactant remediation were measured and surfactant solutions that restored the soil to very nearly its original condition i.e. condition before contamination were identified.

1.2 LITERATURE REVIEW

In pursuance of the objectives outlined earlier the literature review was divided into three broad areas. The first area is partitioning tracers, the second area is surfactant phase behavior and the third area is soil column experiments and field tests. All these are reviewed in the following sections.

1.2.1 Partitioning Tracers

Nonaqueous phase liquids (NAPLs) exist in many unsaturated (vadose) and saturated zones. NAPLs are found in a wide variety of hydrogeological environments beneath federal facilities throughout the U.S. Of paramount concern are NAPLs which are denser than water (DNAPLs), in particular chlorinated hydrocarbons such as trichloroethene (trichloroethylene, TCE), tetrachloroethene (tetrachloroethylene, perchloroethylene, PCE), carbon tetrachloride (CTET) and polychlorinated biphenyls (PCBs), which have been identified beneath many DOE facilities. Also of concern are light NAPLs

(LNAPLs) such as fuel hydrocarbons like jet fuel (JP4). Quantifying the amount and spatial distribution of NAPL trapped in porous media at hazardous waste sites is of great importance in determining its environmental impact and in selecting appropriate remediation alternatives. A major portion of this work will focus on the issue of DNAPL characterization, although the methodology is just as applicable to LNAPLs as to DNAPLs.

The concept of the use of partitioning tracers for estimating residual oil saturation was described by Cook (1971) and Deans (1971). This involved the comparison of the mean residence times of partitioning and non-partitioning tracers. The use of a partitioning tracer for reservoir evaluation has been discussed by Casad and Gant (1989). In their work, they recommended iodoethanol radiolabeled with ^{131}I as a partitioning tracer. Extensive work in the area of single well tracer tests was done by Tomich *et al.*, 1973; Sheely, 1978; Sheely and Baldwin, 1982 Descant, 1989 and Ferriera *et al.*, 1992. Interwell partitioning tracer tests have been studied and applied by Allison *et al.*, 1989; Causin and Rochon, 1989; Wood, 1990; Lichtenberger, 1991; Tang and Harker, 1991a,b; and Tang, 1992; and Tang *et al.*, 1995; and Zemel, 1995.

Procedures for measuring the partition coefficients under reservoir conditions are described by Knaepen *et al.* (1990). They used a technique called flow injection analysis (FIA) in which brine with a known initial concentration of a partitioning tracer is continuously circulated through a cell filled with oil until equilibrium is established. Using the partitioning coefficients measured using this technique, the residual oil saturation estimates were accurate to within $\pm 8\%$. The use of perfluorocarbon gas phase partitioning tracers to determine residual oil

saturation was demonstrated by Dugstad *et al.*, 1993. They used perfluoromethylcyclopentane and perfluoromethylcyclohexane. Negligible retention of these tracers was observed in pure Ottawa sand. Slight retention was observed when clay was added to Ottawa sand. Both the above perfluorocarbon tracers were also used by Ljosland *et al.*, 1993 for reservoir characterization.

The main advantage of performing a partitioning interwell tracer test is that the sample volume is large compared to cores or well logs, which provide saturation estimates very near the wellbore only. The selection of partitioning tracers for an interwell test is described by Tang and Harker (1991a). Some field applications of partitioning tracers by the petroleum industry have been described by Tang *et al.* (1991b) and Tang (1992). The application of tracers for characterizing oilfield reservoirs was described by Maroongroge, 1994 and Maroongroge *et al.* (1995).

The applicability of the partitioning tracer interwell test (PITT) to estimate NAPL saturation is described by Jin *et al.* (1994), Jin *et al.* (1995) and Jin (1995). The theory behind the PITT and the use of the method of moments to estimate the residual NAPL saturation has been discussed in detail by Jin (1995). The method of moments is based on using the residence times of the partitioning and non-partitioning tracers and the partition coefficient of the partitioning tracer to measure NAPL saturation.

The application of partitioning tracers to characterize NAPL saturation in vadose zones has been described by Whitley *et al.* (1995), Studer *et al.* (1996) and Whitley (1997). Laboratory experiments were carried out to measure partition coefficients for several perfluorocarbon tracers between TCE and air. These

partition coefficients were used to determine residual TCE saturations in a NAPL PITT (Studer *et al.* 1996).

The design of a partitioning tracer test for field application has been described by Pope *et al.* (1994) in which several laboratory experiments and computer simulations were carried out to design a field PITT at Hill Air Force Base, site Operational Unit 1, Annable *et al.* (1994; 1996). In this study, 1-hexanol and 2,2-dimethyl-3-pentanol were used as partitioning tracers and ethanol and bromide were used as conservative tracers.

Sulfur hexafluoride has been used as a conservative tracer by Wilson and Mackay (1993; 1996) and as a partitioning tracer by Wilson and Mackay (1995) in soil column experiments to determine residual saturations of trichloroethylene, o-dichlorobenzene and dichloromethane. In this work there was no discussion of parameters such as residence times for obtaining good NAPL saturation estimates. Tracer recoveries were not computed. Only one partitioning tracer was recommended as a candidate. For a successful field test several tracers with a range of partition coefficients will be required. In this work results with several partitioning tracers are presented. Several tracers are recommended as candidates for use in field tracer experiments. A field partitioning tracer test using sulfur hexafluoride as a partitioning tracer was conducted by Nelson and Brusseau (1996) to detect NAPL. Very poor tracer recoveries ranging from 4.5% to 73.5% were obtained suggesting poor hydraulic control and possibility of nonequilibrium mass transfer between the tracer and NAPL.

Partitioning tracers were extensively used by Shotts (1996) to determine DNAPL saturation in soils contaminated by TCE and Hill DNAPL and for

performance assessment of surfactant remediation. Based on several experiments conducted in this work NAPL Partitioning Interwell Tracer Tests were designed at Hill AFB, site Operational Unit 1 (Pope *et al.*, 1994a,b) and site Operational Unit 2. These will be discussed Chapters 8,9 and 10. Some results from the field partitioning tracer test at Hill OU2 are given in Brown (1997).

1.2.2 Phase Behavior Experiments

For application of surfactants for NAPL remediation in aquifers, several experiments should be carried out to identify suitable surfactant solutions applicable for specific NAPLs. Depending on the type of remediation required different types of surfactant solutions will be required. In case of enhanced oil recovery (EOR) operations and mobilization dominated SEAR operations it would be advantageous to use a Winsor type III surfactant solution. On the other hand, in instances where a solubilization type SEAR operation is required, a Winsor type I system would be more applicable. In most cases, field NAPL is a mixture of several species. Hence in order to design a suitable surfactant solution, a good understanding of surfactant phase behavior with different organic species is required. In order to develop a good understanding of surfactant phase behavior with organic species several experiments have to be carried out. All the experiments performed to characterize surfactant solutions for use in NAPL recovery can be termed phase behavior experiments. Phase behavior experiments with surfactant, water, alcohol, polymer and electrolyte are extremely important in both surfactant enhanced aquifer remediation (SEAR) and enhanced oil recovery (EOR) applications for selection of optimal surfactant solutions.

Some of the earliest work with surfactant phase behavior was done by Winsor (1954), who defined the various phase environments observed once surfactant, water and oil were mixed (Winsor type I, II and III systems). Winsor type I systems are typically oil in water microemulsions, Winsor type II systems are typically inverted or water in oil microemulsions. The behavior of surfactants and microemulsions is described by Bourrel and Schechter (1988). A good discussion of surfactant behavior is also presented in Rosen (1988).

The applicability of Winsor type III surfactant systems to EOR operations has been investigated by performing phase behavior studies to develop phase diagrams. The objectives were to obtain a good understanding of surfactant phase behavior with regard to various parameters such as salinity, alcohol, electrolyte etc. The applicability of ternary diagrams to design EOR floods and the effect of parameters such as salinity, alcohol concentration and electrolyte on phase behavior was investigated by Healy and Reed (1974). A correlation of the IFT between the microemulsion and excess phases and solubilization parameter was observed by Reed and Healy (1977). The applicability of phase diagrams for better understanding of the mechanisms of chemical flooding and applicability of these in laboratory chemical floods was described by Nelson and Pope (1978). They also defined the three types of phase environments (type II⁻ corresponding to a Winsor type I, type III corresponding to a Winsor type III and type II⁺ corresponding to a Winsor type II system).

A theoretical model that correlates solubilization parameter to IFT was developed by Huh (1979). This is a very useful tool in screening surfactant solutions for EOR operations as the solubilization parameters of various

surfactant solutions can be easily measured and this number can be used to estimate the IFT between oil and surfactant solutions.

The application of surfactant phase behavior for use in enhanced oil recovery (EOR) was described by Pope and Baviere (1991). Since earlier work was aimed towards EOR type operations, extensive work to understand phase behavior of surfactants with oil to identify surfactant solutions with low interfacial tensions was carried out by Salager *et al.* (1979). They also developed concepts relating the optimal salinity of a surfactant formulation to an equivalent alkane carbon number (EACN), surfactant characteristic type and cosolvent/alcohol type. The advantage of the EACN concept is that complex mixtures of hydrocarbons can be assigned one equivalent alkane carbon number and surfactants solutions can be suitably designed. This is very useful in selecting surfactants for sites where the organic phase is composed of several different species of contaminant. Typically surfactant solutions that produced well defined middle phase microemulsions were considered suitable for use in enhanced oil recovery operations since ultra low interfacial tensions were observed in the three-phase region (Reed and Healy, 1977).

In order to use surfactant solutions in field EOR and SEAR applications, surfactant solutions with minimal gel/liquid forming tendencies have to be identified. In order to minimize liquid crystal formation, cosolvents or co-surfactants are added. Middle phase microemulsions could be produced by addition of suitable co-surfactants (Asgharian *et al.*, 1991; 1992) or cosolvents or alcohols (Lalanne-Cassou *et al.*, 1987).

Extensive computer modeling is necessary for design of field scale SEAR and EOR operations. Hence mathematical models are required for modeling surfactant phase behavior. A thermodynamic model for modeling the phase behavior of micellar systems was developed by Prouvost *et al.* (1985). This was used to model phase volume diagrams, salinity requirement diagrams and ternary diagrams. Since most surfactant solutions require the presence of a cosolvent a thermodynamic model was developed by Prouvost *et al.* (1985) for modeling the behavior of alcohol partitioning between various phases. A physical property model was developed by Camilleri *et al.* (1987) for modeling surfactant floods and comparing results with experimental data. This is used in UTCHEM (Delshad *et al.*, 1996), a compositional simulator which can model surfactant flooding.

The basic principles from this surfactant enhanced oil recovery research were adapted to design and perform phase behavior experiments with chlorinated hydrocarbons by Baran *et al.* (1994a,b,c; 1996a,b,c), Jin (1995) and Shotts (1996). One of the important contributions from the Baran *et al.* (1994b, 1996b) work was mixing rules for the hydrocarbons (Salager *et al.*, 1979) were found applicable to chlorinated hydrocarbons. Similar studies with mixed chlorinated hydrocarbons were also carried out by Shiau *et al.* (1996) who proposed a non-ideal mixing model to predict behavior for binary and ternary systems.

In order to quantify the properties of surfactants to remediate the NAPLs, several batch studies have been carried out to quantify parameters such as solubilization ratio, solubilization, temperature dependence, salinity dependence etc. (Edwards *et al.* 1991b; West, 1992; Martel *et al.*, 1993; Baran *et al.*

1994a,b,c, Diallo *et al.*, 1994). Several phase behavior studies were carried out to identify surfactant solutions which produced Winsor type III microemulsions with chlorinated hydrocarbons (Baran *et al.*, 1994a,b,c), jet fuel (Baran *et al.*, 1996a,b,c). Ternary diagrams were used by Martel *et al.* (1993) to study surfactant behavior and select surfactants (Martel and Gelinas, 1996).

Phase behavior experiments were extensively carried out by Jin (1995) with PCE to select suitable solutions to perform column experiments. Similar studies were carried out by Shotts (1996) with TCE and Hill DNAPL for screening surfactant. A summary of some of the surfactants used in earlier remediation research is presented in Tables 1.1 and 1.2.

In this work, phase behavior experiments were carried out with PCE, TCE, jet fuel (JP4) and Hill DNAPL. Surfactant solutions that showed excellent potential in terms of contaminant solubilization, minimal gel forming tendencies, good behavior over a range of temperatures, well defined three phase region, good behavior in the presence of both calcium and sodium ions and quick equilibration/coalescence times were identified as possible candidates for use in SEAR operations. The effect of parameters such as alcohol, polymer, electrolyte and temperature was evaluated. A detailed description of these selection requirements for surfactants is presented in Chapter 10.

1.2.3 Soil Column Experiments

The approach taken in this study was to select surfactant solutions based upon phase behavior experiments. These solutions were then used to remediate

soil columns contaminated by various NAPLs. This approach was highly successful.

The ability of surfactants to remediate organic contaminants from soil has been investigated extensively. One dimensional and two dimensional studies were conducted by The Texas Research Institute (1979, 1985) to remove entrapped gasoline from soil columns and containers using surfactant solutions. The recovery of gasoline was about 80%. Zeigenfuss (1987) conducted similar studies on gasoline entrapped in soil columns. No significant removal of gasoline was observed but plugging of soil columns was observed in many cases.

Ellis *et al.* (1986) performed soil column experiments to evaluate the use of nonionic surfactants for cleaning soil contaminated by PCBs, petroleum hydrocarbons and chlorophenols. Between 60.8% and 68% of the PCBs was remediated in two experiments after ten pore volumes of surfactant and ten pore volumes of water. The efficiency of three alkylphenoethoxylate surfactants and two alkyl ethoxylate surfactants in removing anthracene and biphenyl from a solid surface was evaluated by adsorbing the contaminant from synthetic groundwater on to the solid and desorbing using surfactant solutions in synthetic groundwater (Vigon and Rubin, 1989). They observed that greater than 0.1% by weight surfactant solutions were needed to obtain significant improvement in chemical desorption.

Sodium dodecyl sulfate (SDS) was used by Gannon *et al.* (1989) to remediate soil columns contaminated by dichlorobenzene (DCB), naphthalene and biphenyl. About 65%-90% of the DCB and 90-95% of the naphthalene was recovered in these experiments. In all these experiments, 250 g of soil was

remediated by more than 1,000 ml of SDS. This corresponds to between 15 to 20 pore volumes of surfactant. Abdul *et al.* (1990) evaluated the performance of ethoxylated alcohols, ethoxylated nonylphenols, sulfates and sulfonates to remediate automatic transmission fluid (ATF) from sandy soil. Between 33% and 84% of the ATF was recovered depending on the surfactant used. In these experiments, 100 ml of surfactant solution was used to remediate 5 g of contaminated soil. More studies conducted by Ang and Abdul (1991) demonstrated that 55% and 73% of the ATF could be recovered using alkyl polyoxyethylene glycol after 28 pore volumes of surfactant washing.

Peters *et al.* (1992) screened several surfactant solutions for their effectiveness for remediating diesel fuel from contaminated soil. Total petroleum hydrocarbon (TPH) recoveries ranged from 60%-90%. Similar work was carried out by Fountain *et al.* (1991) who remediated PCE pools from sand boxes using surfactant solutions. The objective of these experiments was solubilization of the PCE pool and surfactant solutions with IFTs of about 2.5-5.0 dynes/cm were used. However emulsion production was observed in these experiments.

Surfactant flushing was successfully employed to enhance the recovery of dodecane (Pennell *et al.*, 1993) and PCE (Pennell *et al.*, 1994; Jin, 1995). Between 90% and 99% of the PCE was recovered as a result of surfactant flooding (Pennell *et al.*, 1994; Jin, 1995). Similar results were reported by Shiau *et al.* (1994) who recovered up to 99% PCE from contaminated soil columns.

In recent work Bourbonais *et al.* (1995) showed that surfactants recovered up to 90% of the total petroleum hydrocarbons (TPHs) from contaminated soil. However they identified problems such as mobilization of fines, difficulty in

removing surfactant residue from soil and surfactant precipitation during surfactant use. A lowering in hydraulic conductivity up to two orders of magnitude was observed by Allred and Brown (1995) when surfactants were flushed through saturated soil columns. Similar results were reported by Renshaw *et al.*, (1997) who proposed that reduction in hydraulic conductivity (permeability) could be attributed to surfactant adsorption by organic clays in the soil.

From the above discussions it is evident that surfactants have potential for remediating sites contaminated by organic compounds. However there are many potential problems (Harwell, 1992, West and Harwell, 1992) that have to be overcome for successful implementation of surfactants in field trials. These problems include surfactant loss by liquid crystal formation, partitioning into a trapped phase, coacervation of surfactant and precipitation of surfactants especially in the presence of calcium ions. In the review of applicability of surfactants in subsurface remediation by West and Harwell (1992), the above mentioned potential problems with surfactants have been described. Some of these problems are surfactant loss by adsorption or by precipitation. The authors are of the opinion that adsorption losses could be significant in case of nonionic surfactants and that anionic surfactants are susceptible to precipitation. Other problems include the possibility of coacervation of surfactant, partitioning of surfactant into the oil phase and chromatographic separation of surfactant mixtures into individual surfactant components. The authors have also concluded that surfactant remediation depends on selecting surfactants for optimum

efficiency by minimizing sorption losses, precipitation, phase changes, environmental acceptability and balanced biodegradation.

Results from this work will show that by careful experimentation and a good understanding of surfactant phase behavior we can identify surfactants that will fulfill most of the above mentioned (demanding) criteria and be used in remediation applications. Problems such as precipitation could be avoided by using a surfactant which shows good behavior in the presence of calcium ions. Surfactant loss by adsorption could be minimized by using anionic surfactants. The addition of alcohols (cosolvents) will also minimize adsorption of surfactant. The surfactants used in this work had very low adsorption, of the order of $0.3 \frac{\text{mg}}{\text{g}}$. The loss of surfactant by partitioning into the oil phase could be minimized by ensuring that Winsor type II behavior is not observed in the subsurface. Problems such as plugging can be avoided by using surfactants that show low coalescence times and minimal gel/liquid crystal forming tendencies. Addition of adequate amounts of cosolvent will also minimize gel/liquid crystal forming tendencies and lower coalescence times. In this work it will be shown that proper surfactants are selected for remediation, up to 99.9% of the NAPL can be recovered by surfactant flooding and the soil can be restored to its original condition.

1.2.4 Field Studies

Surfactants have been employed in field trials to remediate zones contaminated by NAPLs. Some early studies were carried out by Nash *et al.* (1987) who used surfactants to wash soil contaminated by a mixture of jet fuel,

waste oils and a variety of solvents at Volk Field Air National Guard Base, WI. Several surfactants were used to wash seven test cells. Severe plugging and permeability reduction was observed in many test cells and insignificant quantities of NAPL was recovered. Alkaline polymer surfactant mixtures (APS) principles were used by Trost *et al.*, 1989, to remediate viscous oil from an industrial plant site in Florida. A total of 65% of the oil was removed after two alkaline polymer floods. A similar field project was carried out by Pitts *et al.* (1993) who used an alkaline polymer surfactant mixture to remediate wood treating oil from alluvium at a wood treating facility at Laramie, Wyoming. This field test was designed after performing several corefloods in which the performance of ethoxylated nonylphenol with 1,050 mg/l xanthan gum and sodium dodecyl benzene sulfonate with 1,050 mg/l xanthan gum were evaluated. In laboratory experiments, residual oil saturations of 0.01 were achieved after polymer surfactant flooding. In the field tests sheet piling was used to confine the test cells in which polymer surfactant flooding was carried out. The polymer surfactant flood reduced the oil saturation from 0.203 to 0.032 after three pore volumes of alkali-surfactant-polymer flooding. This corresponds to 84% oil recovery.

Based on the experiments conducted in this work a surfactant flood to remediate DNAPL was performed at Hill Air Force Base. This flood was the first surfactant flood performed to remediate a DNAPL pool in an unconfined site. The DNAPL saturation was reduced from 0.036 to 0.0004 by surfactant remediation (Brown *et al.*, 1996b). This corresponds to 99% DNAPL recovery.

No sheet piling was used to confine the aquifer. Such high recovery was obtained in the absence of polymer.

Surfactants have also been used for recovering DNAPLs by Fountain *et al.* (1993, 1994, 1996) at two field sites (CFB Borden and Corpus Christi). At Borden the DNAPL was PCE and at Corpus Christi, the DNAPL was carbon tetrachloride. The PCE pool at the base of the aquifer at Borden was about 50 cm at the beginning of the test and this was reduced to less than 5 cm after surfactant remediation. Subsequent excavation showed that almost all the PCE had been remediated after 14 pore volumes of surfactant flushing. However final PCE saturation estimates were not obtained. The average PCE concentrations in the effluent declined from about 199 mg/l to less than 30 mg/l after surfactant flushing. Similar results were observed by Fountain *et al.* (1993) at Corpus Christi where the carbon tetrachloride concentrations declined from an average of 790 mg/l to less than 10 mg/l based on core data in the center of the treated area. Again an estimate of the percentage of DNAPL recovered was not obtained. In comparison, at the surfactant enhanced aquifer remediation demonstration at Hill Air Force Base (designed as a consequence of this work), about 99% of the DNAPL was recovered after less than three pore volumes of surfactant flooding (Brown *et al.*, 1996b). The total contaminant concentration at the central monitoring well was only 30 mg/l down from about 1,000 mg/l before surfactant remediation.

For successful design of field SEAR projects extensive computer modeling has to be carried out in addition to laboratory experiments. The modeling and design of surfactant enhanced aquifer remediation has been

discussed by Brown (1993; 1997), Brown *et al.*, (1994), Freeze *et al.* (1994) and Brown *et al.*, (1996a). A description of UTCHEM the compositional simulator used for modeling surfactant flooding is given in Delshad *et al.* (1996).

1.3 REVIEW OF CHAPTERS

A brief description of all the equipment and chemicals used is given in Chapter 2. A description of all the experimental procedures is detailed in Chapter 3. In Chapter 4, data analysis techniques are discussed. Various calculations needed for performing experiments are also described. In Chapter 5, a description of phase behavior experiments is provided. The results from phase behavior experiments are discussed in Chapter 6. A description of static partition tests is provided in Chapter 7. Static partition coefficients of several alcohols with various NAPLs is presented. A description of all the soil column experiments, experimental results and discussion of experimental results are presented in Chapter 8. A discussion of error analysis of experimental measurements is presented in Chapter 9. A description of experiments leading towards selection of partitioning tracers and surfactants for field design is presented in Chapter 10. Finally, conclusions and future work are presented in Chapter 11.

Table 1.1: Nonionic surfactants used in remediation literature

Chemical Description	Trade Name	Reference
Nonionic Surfactants		
Alkyl polyglucamides	--	Baran <i>et al.</i> , 1996c
Ethoxylated (20) Sorbitan Mono-oleate	Tween 80	Pennell <i>et al.</i> , 1993
Ethoxylated (20) Sorbitan Mono-oleate	T-Maz	Shiau <i>et al.</i> , 1993, 1995
Ethoxylated nonylphenol	Igepal	West, 1992
Ethoxylated tetramethyl decynediol	Surfynol 485/13	Peters <i>et al.</i> , 1992
Ethylene oxide adducts of fatty alcohols	Witconol SN-70	Abdul <i>et al.</i> , 1990
Ethoxylated alcohol	Adsee 799 Neodol	Ellis <i>et al.</i> , 1985
Ethoxylated nonylphenol	Arkopal N-100	TRI, 1985

Table 1.2: Anionic surfactants used in remediation literature

Chemical Description	Trade Name	Reference
Anionic Surfactants		
Sodium dihexyl sulfosuccinate	Aerosol MA-80I	Shotts, 1996, Baran <i>et al.</i> 1996, Jin, 1995, Pennell, 1994
Sodium diamyl sulfosuccinate	Aerosol AY-100	
Sodium dioctyl sulfosuccinate	Aerosol OT	
Lauryl alcohol ethersulfate	Genepol LRO	Martel <i>et al.</i> 1996
Secondary alkane sulfonate	Hostapur SAS	
Sodium mono and dimethyl naphthalene sulfonate		Shiau <i>et al.</i> 1994
Sodium dodecyl sulfate		
Alkyl diphenyl oxide sulfonates	DOWFAX	Rouse, 1993
Phosphate ester of nonylphenol ethoxylate	Rexophos 25-97	Fountain <i>et al.</i> , 1992
Sodium polyacrylate	Cyanamer P- 35(L)15	Peters <i>et al.</i> , 1992

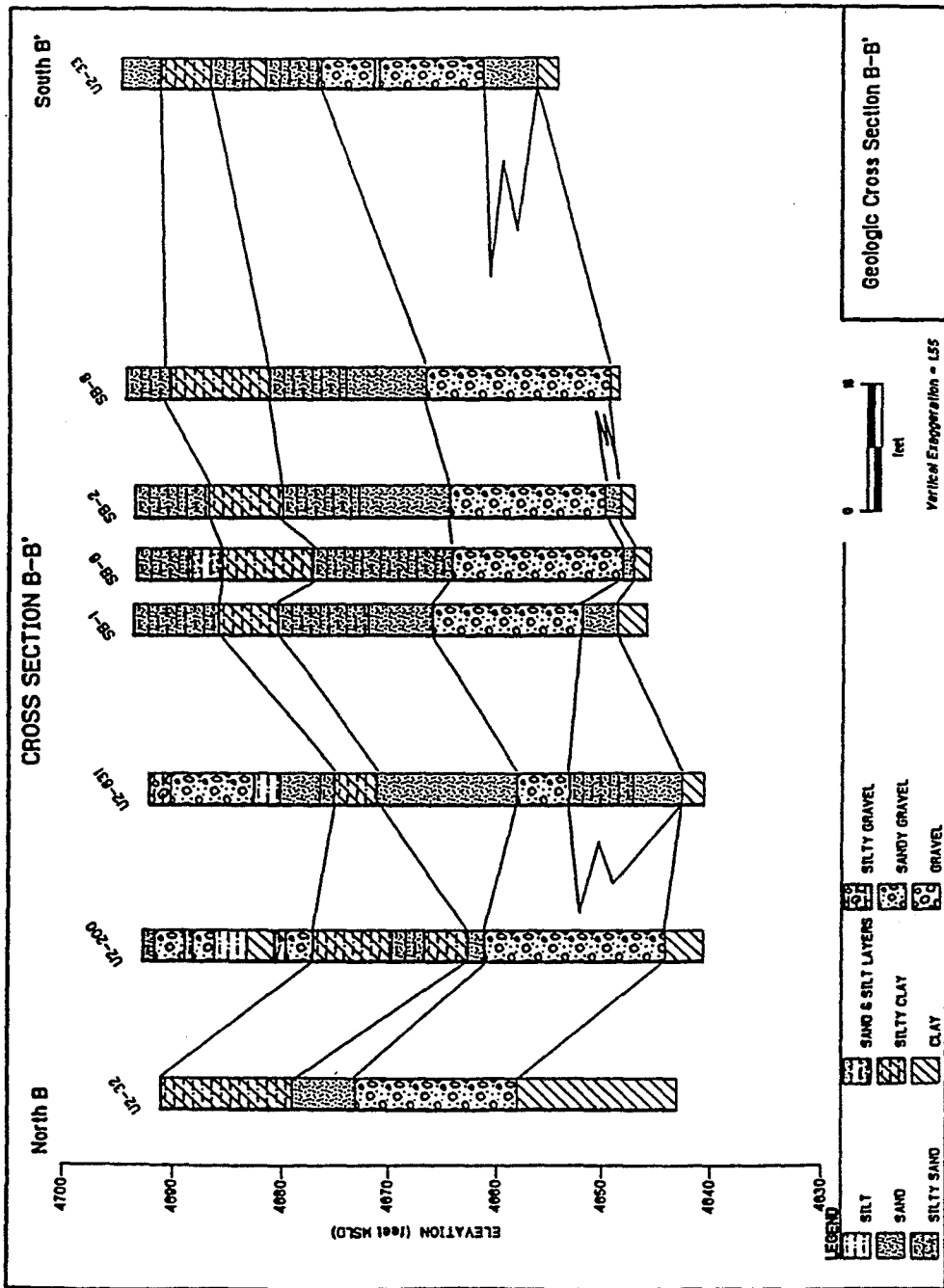


Figure 1.1: Geological cross section of a DNAPL contaminated site

Chapter 2: Equipment and Materials

The equipment and materials used in this research can be divided into several categories. Equipment used for performing experiments such as pumps, pressure transducers, solution reservoirs etc.; equipment used for analytical work such as gas chromatographs, liquid scintillation counter, spinning drop tensiometer etc. and various chemicals used during the experiments such as surfactant, alcohols and solvents are described. A brief description of these is presented in the following sections.

2.1 INJECTION PUMPS

The fluid injection was carried out using Beckman Model 100A solvent metering pumps. This pump is a dual piston pump capable of providing constant flow rates from 0.01 ml/min to 9.99 ml/min and a maximum pressure drop of 10,000 psig. The uniform flow rate was achieved by means of two cam driven reciprocating pistons, each of which displaces 0.1 ml per stroke. Experimental fluids can be pumped directly through the pump unless the fluids are considered corrosive.

2.2 SOLUTION COLUMNS

Glenco glass columns made of borosilicate glass with polypropylene collars and Teflon end pieces were used as solution reservoirs for water, tracer solution and solvents. The columns are 5.0 cm diameter and 60 cm long with a pressure rating of 80 psig. Whenever tracer was stored in the column, a 5 cm diameter, 2.5 cm long Teflon piston with two Viton O rings fitted into grooves cut

around the circumference separated the forcing fluid from the injected fluid in the column. The columns were purchased from VWR Scientific.

2.3 FLUID RESERVOIRS

Temco fluid reservoirs, model CC-20, made of Lexan polycarbonate with Teflon pistons, were employed. These columns were used as storage reservoirs for surfactant solutions during surfactant flushing. These columns had a capacity of 2,000 ml and were rated to 100 psig

2.4 GLASS COLUMNS

The glass columns used for preparing soil packs for all the experiments were purchased from KONTES. The columns were non jacketed, 4.8 cm diameter and either 15 cm or 30 cm long. An adjustable end piece with a Viton O ring was used to confine the soil. These columns were rated up to 15 psig. The columns came with 20 μm polyethylene filters. These were replaced with stainless steel screens.

2.5 STAINLESS STEEL SCREENS

Stainless steel (304 ss) screens were used to contain the sand in the column. The screens used were #60 mesh (250 μm opening) and #150 mesh (99 μm opening).

2.6 STEEL COLUMNS

The steel columns were custom made using a 1 inch outside diameter stainless steel pipe as a column and using 1 inch Swagelok fittings as the end pieces. The 1 inch piece was connected to a 1/2 inch fitting which was finally connected to a Swagelok connector capable of supporting 1/8 inch tubing. A

brass piece was machined into all the Swagelok end pieces to reduce the end volume. Two 30.5 cm long and one 75.0 cm long columns were constructed for experimental work.

2.7 TUBING

Nylon tubing was used for most of the experimental work due to its flexibility and ability to handle relatively high pressures. The tubing was rated to a burst pressure of 1,500 psig. The tubing was 1/8 inch OD and 1/16 inch ID. The commercial name for the tubing is Nylaflo. In some experiments, 1/8 inch OD and 1/16 inch ID 304 stainless steel tubing was used for experimental work.

2.8 FRACTION COLLECTORS

Instrument Specialties Company, (ISCO) fraction collectors were used for collection of effluent samples during tracer tests and surfactant tests. An ISCO model 1850 with a capacity of 140 tubes and model RETRIEVER II with a capacity of 116 tubes were used for all the experiments. The fraction collectors were programmed such that each test tube collected effluent samples for a fixed time and the rack was moved to position a new test tube below the effluent sampling port for the next sample to be collected. Sample volumes and sampling times varied depending on the pore volume of the soil pack and the rate of injection.

2.9 PRESSURE TRANSDUCERS

Differential pressure transducers were used to measure pressure drops across the soil packs during the surfactant flood. In all the initial experiments, Validyne DP15 variable reluctance differential pressure transducers were used.

Deflection of the diaphragm caused by an applied differential pressure is converted to an output voltage which is measured by the carrier demodulator. The transducers have bleed screws on the side of the body to allow them to be filled with mineral oil. A bypass valve is located between the high pressure and low pressure lines to allow the transducers to be zeroed.

In the later experiments, differential transducers with solid state sensors (made by Cole Parmer) were used. In these transducers, differential pressure across the high pressure end and the low pressure end was converted into 4-20 mA current. Using an appropriate resistor, this current was converted into a 0-10 mV output which was calibrated to a pressure reading and printed by the digital chart recorder.

2.10 CARRIER DEMODULATOR

A Validyne model CD-19 carrier demodulator was used with a model MC1 module case. The demodulator was used to convert the AC output from the transducer to a DC voltage which was carried to a chart recorder.

2.11 CHART RECORDER

A Tracor Westronics DDR10 digital chart recorder was used to record pressure data. The output from the carrier demodulator for the Validyne transducers and the direct output from the Cole Parmer transducers was converted into a pressure drop. The pressure drop was logged by printing out the pressure drop at preset time intervals.

2.12 PRESSURE GAUGES, VACUUM GAUGES

Vacuum and pressure gauges used in this work were diaphragm analog gauges (Royal brand) manufactured by Weksler instruments. The vacuum gauge was capable of measuring up to 30 inches of mercury and 15 psid. Pressure gauges capable of measuring up to 100 psid were also used.

2.13 BALANCES

Balances were used for mixing solutions, determining pore volumes of soil packs and weighing columns to estimate NAPL saturation. The various balances used were the Mettler P11N series, (0-10,000 g), the Mettler P1200 series, (0-1,200 g), the Mettler PN323 series, (0-320 g), the Sartorius type 3862, (0-16,000 g), the Sartorius type 1475 (0-4,240 g) and the Sartorius type 1574, (0-420 g). The Mettler balances were analog balances and the Sartorius balances were digital balances.

2.14 GAS CHROMATOGRAPH (VARIAN 3400)

The alcohol tracer analysis and some contaminant analysis was carried out using a Varian model 3400 equipped with a Varian autosampler model 8000. The samples were passed through a 60 m long, 0.53 mm diameter, 5.0 mm thick bonded poly (5% diphenyl, 95% dimethyl siloxane) megabore capillary column (made by SUPELCO). A flame ionization detector was used to detect the alcohols. Detection limits of 10 mg/l for the alcohol tracers, PCE and TCE were obtained. A Varian integrator model 4290 was used to integrate the chromatography curves.

2.15 GAS CHROMATOGRAPH (VARIAN 3400CX SPME)

Head space analysis was used for analyzing TCE concentrations in effluents of column experiments. The gas chromatograph used for the head-space analysis was a Varian Model 3400CX equipped with a Model 8200 Auto-sampler with the Solid Phase Micro Extraction (SPME) adapter and an electrolytic conductivity detector. Control was through the Varian SPME software running on a Digital desktop computer. The SPME fiber used was a nylon fiber with a 100 micrometer coating of polydimethylsiloxane as the absorbent. TCE was adsorbed by the SPME fiber and was later desorbed and separated on a 60 meter long J&W DB-5 poly(5%-diphenyl-95%-dimethylsiloxane) megabore column. Detection limits of up to 1 mg/l TCE were obtained.

2.16 GAS CHROMATOGRAPH (BUCK SCIENTIFIC)

Some tracer analysis was also carried out using the Buck Scientific gas chromatograph manufactured by SRI. This GC was equipped with a flame ionization detector (FID), thermal conductivity detector (TCD) and electron capture detector (ECD). Only the FID was used for the alcohol and contaminant analysis. In this GC, a carbowax 30 m long, 0.5 mm diameter, 1 μ m film thickness capillary megabore column was used. In addition a DYNATECH Precision Sampling Corporation model 311H autosampler modified by SRI was used for continuous analysis of samples. Detection limits of up to 1 mg/l of alcohols was obtained using this GC.

2.17 LIQUID SCINTILLATION COUNTER

A Beckman Liquid Scintillation Counter model LS 9800 was used to measure radioactive ^3H and ^{14}C concentrations. The counter has a capacity of 300 samples and is equipped with a control keyboard, printer, three count channels, 10 user programs, CRT display, H#, quench compensation factor, two phase warning monitor, single, dual and triple label disintegrations per minute (DPM) programs.

Liquid scintillation samples were prepared by adding 0.25 ml of the sample to 5 ml of liquid scintillation cocktail. Liquid scintillation cocktail used was Ready-Solv HP, made by Beckman.

Samples were counted for 2 minutes for two radioactive isotopes, ^3H and ^{14}C and values of disintegrations per minute (DPM) were printed for each sample.

2.18 COUETTE VISCOMETER

A Contraves Low Shear 30 (LS 30) viscometer was used to measure bulk viscosity. The LS 30 is a Couette type viscometer that analyzes the shear stress between a cup and a bob. The stress is converted into a viscosity. The instrument is designed to measure viscosity over shear rates ranging from 0.0174 to 128.5 sec^{-1} . About 1 ml of fluid is required for each measurement.

2.19 FILTER PRESS

Filtration was done using a FANN model 12 BL filter press. This press is of stainless construction with several openings. The fluid was stored in a stainless steel cup with a Viton O ring, which was clamped to the filter press. Polymer

solutions were filtered using a 1.2 μm filter paper at 10 psid. Water was filtered using a 0.45 μm filter paper at 10 psid.

Filters were manufactured by Millipore. These filters were made of a cellulose acetate, cellulose nitrate mixture. The diameter of the filters is 47 mm. Two sizes, 1.2 μm opening and 0.45 μm opening were used.

2.20 SPINNING DROP TENSIOMETER

Low interfacial tensions were measured using a spinning drop tensiometer model 300 manufactured at the University of Texas at Austin. The spinning drop technique was used in obtaining interfacial tension by measuring the shape of a drop of liquid in a more dense liquid contained in a rotating horizontal tube.

2.21 WATER DEIONIZER

A NANOPURE system with a recirculation pump, remote dispenser, resistivity monitor and on/off standby membrane switches was used to supply deionized water for all the experiments. Distilled water was fed into the system and deionized water was obtained at the outlet. The system has three pre-filters and one post filter. The pre filter was made of cellulose acetate fibers with a pore size of 5 μm and the post filter had a pore opening of 0.45 μm to remove particulate matter and microorganisms.

2.22 PH METERS

A ORION Research model 701/digital IONALYZER with a pH combination electrode was used to measure pH of some aqueous samples.

2.23 OTTAWA SAND

The Ottawa sand was obtained from U.S. Silica at Ottawa Illinois. The commercial name for the sand was F-95. The sand was obtained in 50 lb bags from the supplier. More than 99% of the sand particles were between 600 μm (#30 mesh) and 38 μm (400 mesh) with an average size of 170 μm .

2.24 GLASS PIPETTES FOR PHASE BEHAVIOR

Glass pipettes with 5 ml total volume (manufactured by Baxter) and 10 ml total volume (PYREX brand manufactured by Corning) were used for phase behavior studies. The pipettes used were borosilicate glass, serological, sterile pipettes. The pipettes were calibrated down to 0.1 ml. The ends were sealed using a butane burner.

2.25 GLASS VIALS WITH ALUMINUM LINED CAPS

Glass screw vials with solid caps (manufactured by SUPELCO) were used for storing surfactant and tracer samples produced during experiments. The vials were sealed with solid aluminum foil lined caps. Vials with total volumes of 8 ml and 22 ml were used for all the experiments.

2.26 MICROPIPETTES

Two micropipettes, 0-1,000 μl adjustable (PIPETMAN brand) and 250 μl fixed (EPPENDORF brand) were used for making up LSC and GC samples during experiments.

2.27 ALCOHOLS AND SOLVENTS

Several alcohols were used in this work. Isopropanol (2-propanol) was used in large quantities and was purchased from EM Science. The 2,4-dimethyl-3-pentanol was purchased from ACROS Chemicals. All the other heavier alcohols used in the partitioning tracer work were purchased from Aldrich Chemicals.

The solvents, tetrachloroethylene (PCE), trichloroethylene (TCE) and 1,2-dichloroethane (DCA) were purchased from Aldrich Chemicals. The jet fuel was obtained from March AFB and the Hill OU1 LNAPL and Hill OU2 DNAPL were obtained from Hill AFB.

2.28 SURFACTANTS

The surfactants used in this study were sodium diamyl sulfosuccinate, sodium dihexyl sulfosuccinate and sodium dioctyl sulfosuccinate. The surfactants were purchased from CYTEC Chemicals, NJ. The sodium dihexyl sulfosuccinate is commercially available as Aerosol MA-80I and is 80% active. The sodium diamyl sulfosuccinate is sold as 100% active Aerosol AY-100 or 65% active Aerosol AY-65 and the sodium dioctyl sulfosuccinate is sold as the 100% active Aerosol OT-100. The chemical structures for these surfactants are presented in Figures 2.1 through 2.3.

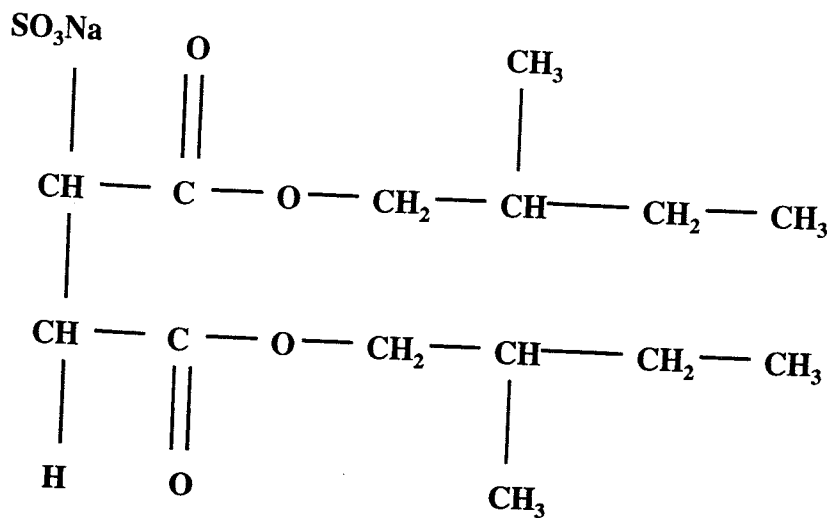


Figure 2.1: Chemical structure of sodium diamyl sulfosuccinate

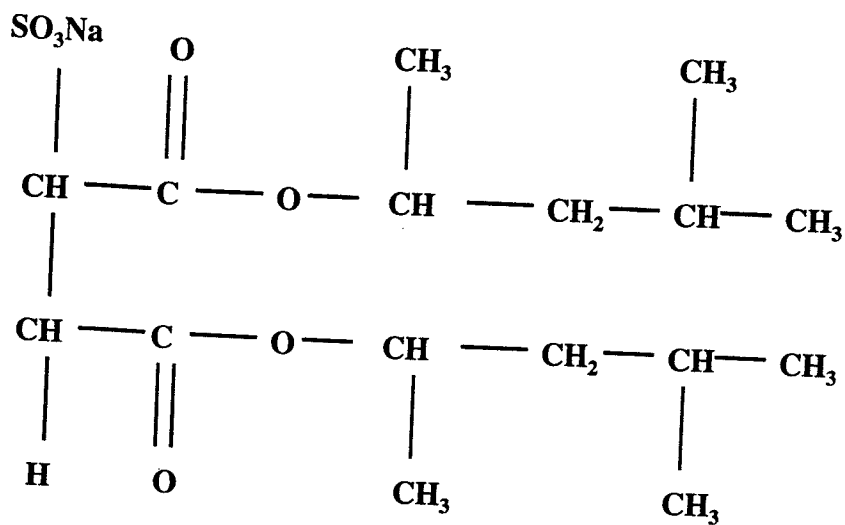


Figure 2.2: Chemical structure of sodium dihexyl sulfosuccinate

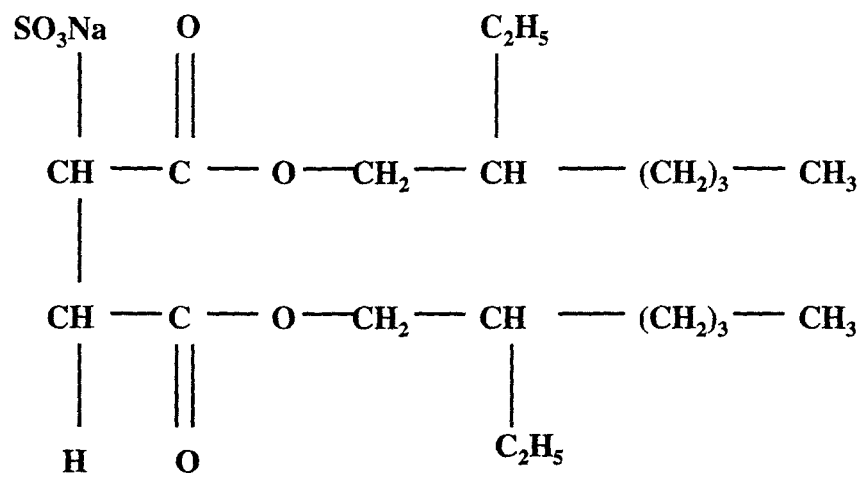


Figure 2.3: Chemical structure of sodium dioctyl sulfosuccinate

Chapter 3: Experimental Procedures

Many experimental procedures were perfected during the completion of this work. All the procedures used during the course of this work are described below.

3.1 PHASE BEHAVIOR

Phase behavior procedures were similar to the procedures used by Baran *et al.* (1994a,b,c and 1996a,b,c) and Jin (1995). All these experiments were carried out at surfactant concentrations greater than the CMC of the surfactant and at different temperatures depending on site specific requirements. For several phase behavior experiments using the contaminant from Hill OU2, the experiments were carried out in a water bath at 12.2°C.

The procedure involved mixing two ml of NAPL with two ml of aqueous surfactant solution (with cosolvent when applicable) in a five cc pipette. The ends were heat sealed to prevent loss due to volatilization. When the NAPL was jet fuel, the ends were sealed with a cork stopper. After pouring the NAPL and surfactant, the relative levels of both the aqueous and oleic phases were measured to obtain an accurate measurement of the actual volume of NAPL and aqueous surfactant solution. The pipette was mixed vigorously by hand and allowed to equilibrate for several hours. For the experiments conducted at 285.2 K, the samples were placed in a test tube rack and placed in a water bath. The samples were allowed to equilibrate for 12 hours, mixed vigorously and placed in the water bath. This was done to ensure that the NAPL and surfactant were given

sufficient time to cool down to the desired temperature. The phase volumes were visually examined every 24 hours until equilibrium was reached. Once equilibrium was reached, the phase volumes were noted down and solubilization parameters and solubilization ratios were calculated.

3.2 STATIC PARTITION COEFFICIENT TESTS

In all the initial experiments with many NAPLs, a 10 ml aliquot of a 1,000 mg/l aqueous standard was placed in a separatory funnel with 10 ml of the NAPL. These samples were prepared in triplicate. The samples were thoroughly shaken for one hour, allowed to separate for 1 hour and re-shaken. This was repeated twice to ensure that the samples were at equilibrium. The samples were then allowed to separate for at least 12 hours, were drained into centrifuge tubes and centrifuged at approximately 1,000 g for 1 hour to allow a complete separation of the phases to occur. Three aqueous aliquots on duplicate aqueous samples were then analyzed with a gas chromatograph for a total of six measurements of the alcohol concentrations in the aqueous phase. One set samples were allowed to equilibrate for 36 hours and the aqueous samples were analyzed to ensure that equilibrium between the aqueous and nonaqueous phases was reached. This procedure was found to be effective to accurately measure partition coefficients less than 15.

For heavier alcohols with higher partition coefficients, all the alcohol tracer would partition into the nonaqueous phase leaving extremely low concentrations of the alcohol in the aqueous phase. Hence, for tracers with higher partition coefficients, 3 ml of NAPL was mixed with 18 ml of aqueous standard in

a 24 ml vial and sealed with aluminum lined caps. The samples were gently shaken and the procedures outlined earlier were repeated.

3.3 SOIL COLUMN PREPARATION WITH CLEAN OTTAWA SAND

Preparation of the soil columns with clean Ottawa sand for column experiments involved many experimental procedures. The soil was washed to remove any organic impurities and packed at a specific rate to ensure uniform packing. The various procedures were are given in the following sections.

3.3.1 soil washing

The sand was mixed with hydrochloric acid (4 N) and settled for 5 hours. The acid was drained and the sand was washed with deionized water until the pH of the sand was 7. The sand was put in an oven for 24 hours at 55°C until the sand was completely dried.

3.3.2 determination of end volume in column

The end pieces of columns were fitted with tubing and valves and weighed dry. The lines were filled with water. The weight of the end pieces saturated with water was measured. The end volume was calculated based on the difference between the weight of the saturated and dry end pieces.

3.3.3 soil packing

The empty column and fittings were weighed before addition of sand. The packing apparatus and column were mounted making sure that the column was set vertically as shown in Figure 3.1. Three 304 stainless steel mesh screens were

used to hold the sand in place. The two screen sizes are 60 mesh (250 μm) and 150 mesh (99 μm). Two 60 mesh screens and one 150 mesh screen were used to confine the sand. The sand was contained in a separatory funnel reservoir and allowed sand to fall out at a slow rate into the column. The column was vibrated using a vibrating jig and packed at a rate of approximately 1 cm (of height in column) per minute for the 2.21 cm diameter steel columns and 0.5 cm (of height in column) per minute for the 4.8 cm diameter glass columns was used while packing. In experiments POLYTCE#1 and POLYTCE#3, a set of layered screens (7 sets of 1.5 mm openings spaced approximately one inch apart) were used to ensure uniform flow of sand into the column. The sand flow was stopped when sand reached the required level. For glass columns, a small piece of Teflon heat shrink tubing was attached to the inlet end piece so that sand would not get inside the gap of the end piece (as shown in Figure 3.2). When steel columns were used, this step was omitted. The sand pack length was measured and the end pieces were adjusted into place. The packed column was weighed with sand for calculation of porosity and pore volume.

3.4 SATURATION OF CLEAN OTTAWA SAND

Once the soil packs were prepared, they had to be pressure tested and vacuum tested for leaks. In order to do this, the columns were hooked up to a testing set up as shown in Figure 3.3. An air pressure of about 10-15 psi was applied and the column was allowed to sit for 2 hours. If a drop in pressure of greater than 0.5 psi was observed after 2 hours, the all the fittings were tightened and process was repeated. This was done to ensure that the column remained leak

free during the course of the experiments. After this a vacuum of about 29 inches mercury was pulled on the column for 30 minutes. The column was allowed to sit for 2 hours and the vacuum gage readings were taken again to ensure that a good vacuum seal was obtained for the column.

A carbon dioxide tank was hooked to the column and carbon dioxide was flushed through the column for 30 minutes with 1 psi differential pressure across the column. The column was sealed and hooked up to the saturation apparatus shown in Figure 3.4. The water used for saturation was deionized and de-aired water. The water was de-aired by pulling a vacuum for 30 minutes. Argon was used as the forcing fluid to drive the water into the sand due to its slight solubility in water. A back pressure regulator was used to provide 10 psi back pressure on the soil pack. The water was flowed into the column at about 3 to 5 cc/min. Every column was flushed with 5 to 6 pore volumes of de-aired water (300 - 800 cc depending on the pore volume). The column was weighed after saturation to calculate the pore volume and porosity.

3.5 COLUMN PREPARATION WITH FIELD SOIL

The procedures with field soil were slightly different. Usually field soil samples are not dry and usually contain gravel and stones, which were sometimes greater than 5 cm in diameter. Field soil is generally obtained in SOLINST cores or loose field soil in bottles or jars collected during drilling operations.

While working with field soil samples, all the work was performed in a fume hood. Proper gloves were always worn. Care was always taken to minimize contact with the soil and fluids. With field cores having high hydraulic

conductivities, 4.8 cm diameter glass columns were used. The contents of the SOLINST core was slowly emptied into the glass column by using a steel piston to force out the contents of the SOLINST into the glass column. The soil in the glass column was compacted by tapping the glass column slowly. Large cobbles and stones, (greater than 2 cm diameter) were removed to ensure that no large spaces remained in the soil pack. Once the desired soil pack length was obtained, the end pieces were adjusted into place and the column was ready for saturation.

3.6 SATURATION OF FIELD SOIL

When field soil was used, a vacuum could not be pulled on the soil pack since this would cause volatilization of any volatile organic compounds present in the soil. The soil pack was hooked up to the saturation apparatus as show in Figure 3.4. In case of field cores from Hill OU1, about 1,000 ml of de-aired 1,000 mg/l NaCl was injected into the pack with 10 psi back pressure using the same procedures as discussed earlier. For field soil packs from Hill OU2, groundwater from Hill OU2 was used to saturate the soil cores.

3.7 NAPL INJECTION PROCEDURES

The procedures employed for saturation of the soil packs with NAPL are the same for packs with Ottawa sand and field soil. The column was hooked up to the saturation setup as shown in Figure 3.5. A setup for DNAPL injection into a soil pack is shown in Figure 3.5. NAPL was stored in 5 cm diameter, 60 cm long chromatography columns. Water was injected into the chromatography column storing the NAPL and used as the forcing fluid to force the NAPL into the soil

pack. The NAPL was injected into the soil pack from the bottom for DNAPLs and from the top for LNAPLs. This was done to ensure gravity stable displacement of the water. An injection rate of 1 ml/min was used for the 2.21 cm diameter steel columns and a rate of 3.0 cc/min was used for 4.8 cm diameter columns. NAPL was injected continuously into the column until no water production was observed. The pressure difference at steady state was measured using a differential pressure transducer to calculate the end point relative permeability of the NAPL.

3.8 WATER INJECTION PROCEDURES

In order to reach residual NAPL saturations, the soil packs were flushed with several pore volumes of water. The setup was similar to the setup shown in Figure 3.5. Water was injected from the top for DNAPLs and from the bottom for LNAPLs. Injection rates of 1.0 ml/min for 2.21 cm diameter columns and 3.0 ml/min for 4.8 cm diameter columns were used during the waterflood. Water was injected into the column until no NAPL observed in the effluent. The pressure difference across the column at residual NAPL saturation was measured to calculate the end point relative permeability to water. The soil pack was weighed and the difference in weights between the uncontaminated and contaminated soil pack and the density of the NAPL was used to calculate the residual NAPL saturation.

3.9 MIXING OF ALCOHOL TRACERS

Tracers were mixed using weight measurements. For example to get a 2,000 mg/l solution of isopropanol in water, 0.5 g of isopropanol was weighed into a 250 ml Erlenmeyer flask. Water was then added to make the total volume to 250 ml.

3.10 MIXING OF RADIOLABELED TRITIUM TRACER

In order to radiolabel tracer solutions, all the alcohols were mixed to the desired concentration. The activity of the tritium was 1 mCurie/ml. Since 2.2×10^9 DPM equals 1 m Curie, to obtain 100 cc of 200,000 DPM/ml tritium, 0.009 ml of 1 mCurie/ml tritium stock was added to 100 ml of alcohol tracer solution. Since this quantity is so small, variations in injected tritium concentration can be observed in all experiments.

3.11 MIXING OF SURFACTANT

Surfactant mixing was always carried out using weight measurements. To obtain a 8% aqueous surfactant solution using the commercially available sodium dihexyl sulfosuccinate (called MA-80I, 80% active surfactant), 100 g of surfactant was added to 900 g of deionized water. To obtain a 8% surfactant, 8% isopropanol and 1,000 mg/l NaCl aqueous solution, 100 g of the commercial sodium dihexyl sulfosuccinate, 80 g of isopropanol, 1 g of NaCl and 819 g of deionized water were mixed up.

3.12 MIXING OF SURFACTANT ALCOHOL POLYMER SOLUTIONS

The procedures for mixing up xanthan gum polymer are described in detail in Garver (1988), Wreath (1989), Wang (1995) and Shotts (1996). The xanthan gum was obtained as a thick broth. The broth (commercial name FLOCON 4800C) was supplied by OFPG (Oil Field Products Group). The broth was 12.3% active. This broth was used for preparing a stock solution of 1% by weight xanthan gum and 2% by weight sodium chloride. The water used for mixing up polymer was filtered using a 0.45 μm filter paper to remove bacteria and undissolved solids and clay dust etc. The stock was further diluted to prepare the surfactant solutions. In order to mix up 250 g of polymer stock, 20.33 g of broth, 5.00 g of sodium chloride and 224.67 g of deionized water were mixed. In all experiments performed with Hill OU2 soil and Hill OU2 DNAPL, filtered Hill source water was used instead of deionized water. Hill source water is the tap water available at Hill Air Force Base with 115 mg/l TDS (see table 10.2). Polymer broth was added first with care being taken not to allow any broth accumulation on the side of the blending jar then mixed in a Waring blender on high for 2 minutes. The solution prepared was labeled, 1% xanthan gum and 2% sodium chloride.

In order to get 500 g of 8% sodium dihexyl sulfosuccinate, 8% isopropanol, 5,850 mg/l NaCl and 500 ppm xanthan gum, 25 g of polymer stock, 50 g of 80% active commercial sodium dihexyl sulfosuccinate (MA-80I), 40 g of isopropanol and 2.43 g of NaCl were added to a conical flask and stirred using a magnetic stir bar for about 2 hours, then filtered in a filter press using a 1.2 μm

Millipore filter at 20 psid. This was the final surfactant/alcohol/polymer solution used for injection into contaminated soil columns.

3.13 GAS CHROMATOGRAPH CALIBRATION FOR ALCOHOL TRACERS

For calibration of the alcohol concentrations in the gas chromatograph, stock solutions of the alcohols were mixed up. For example, for mixing up standards for isopropanol, 2 g of isopropanol was added to a calibrated 1 liter Erlenmeyer flask. Deionized water was added to make up the volume to 1 liter. This solution was labeled 2,000 mg/l isopropanol. Serial dilutions were then performed to obtain 1,000, 500, 250 and 125, 50, 25 mg/L for each set. Standards were always run in duplicate.

3.14 GAS CHROMATOGRAPH CALIBRATION FOR CONTAMINANTS

Gas chromatograph calibrations were obtained for PCE, TCE and Hill DNAPL. No calibration curves could be obtained for jet fuel. The procedures for developing calibration curves for contaminants are similar to the procedures used for alcohols. The procedures varied slightly depending on the type of gas chromatograph used.

For the Varian 3400 gas chromatograph, the microemulsion samples could not be injected into the gas chromatograph due to the possibility of plugging of the chromatography column by the surfactant. Hence calibration curves used were in the range of 100 mg/l to 1,000 mg/l of trichloroethylene or Hill contaminant.

The procedure involved in mixing 2.5 g of contaminant in a 250 ml Erlenmeyer flask and making up the total volume to 250 ml by adding 4% sodium dihexyl sulfosuccinate with 10,000 mg/l NaCl. This was labeled 10,000 mg/l contaminant. By serial dilution with water, 1,000, 500, 250, 125 mg/l standards were prepared.

For the Varian 3400cx gas chromatograph, fluid was not injected into the column. A head space analysis was used for contaminant analysis. Using this gas chromatograph, high contaminant concentrations (15,000 mg/l) could be analyzed directly. Calibrations had to be run at different surfactant concentrations as the concentration of the contaminant in the head space varied with changes in the surfactant concentration in the microemulsion.

The procedure involved mixing 12.5 g of contaminant in a 250 ml Erlenmeyer flask and making up the total volume to 250 ml by adding 8% sodium dihexyl sulfosuccinate with 10,000 mg/l NaCl. This was labeled 50,000 mg/l contaminant. Serial dilutions were performed using an 8% sodium dihexyl sulfosuccinate with 10,000 mg/l sodium chloride solution to obtain 10,000, 7500, 5,000, 2500, 1,250 mg/l contaminant concentrations. The same process was repeated for other surfactant concentrations.

In order to prepare standards at low concentrations, 0.25 g of contaminant was mixed with deionized water in a 250 ml Erlenmeyer flask and the total volume was made up to 250 ml. This was labeled as 1,000 mg/l contaminant. Using serial dilutions with water, 500, 250, 125, 25, 1 mg/l standards were prepared.

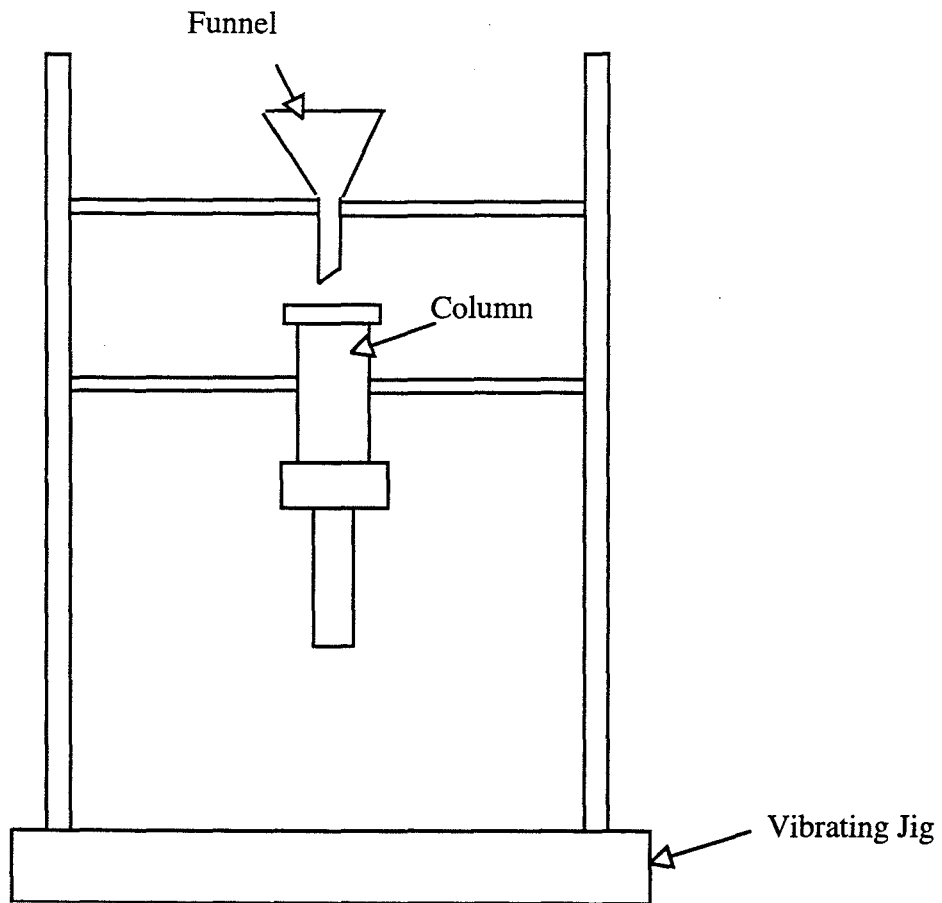


Figure 3.1: Set up for packing soil columns.

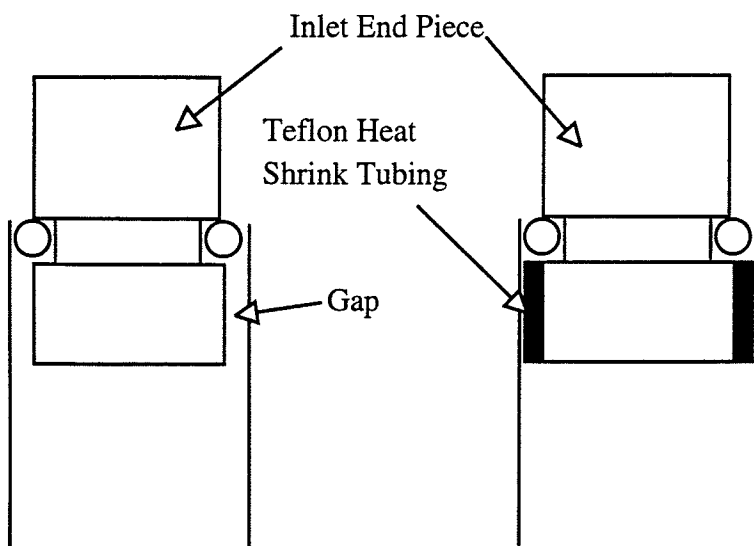


Figure 3.2: Teflon tubing used in glass columns to prevent movement of sand.

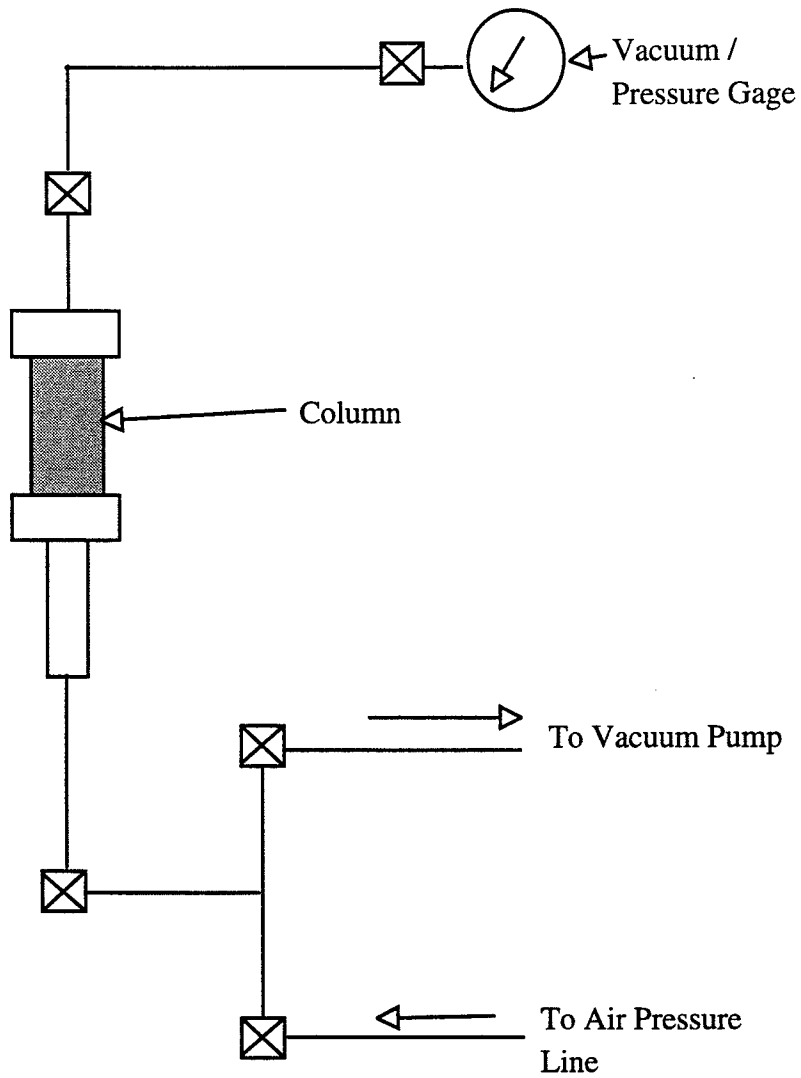


Figure 3.3: Leak testing setup

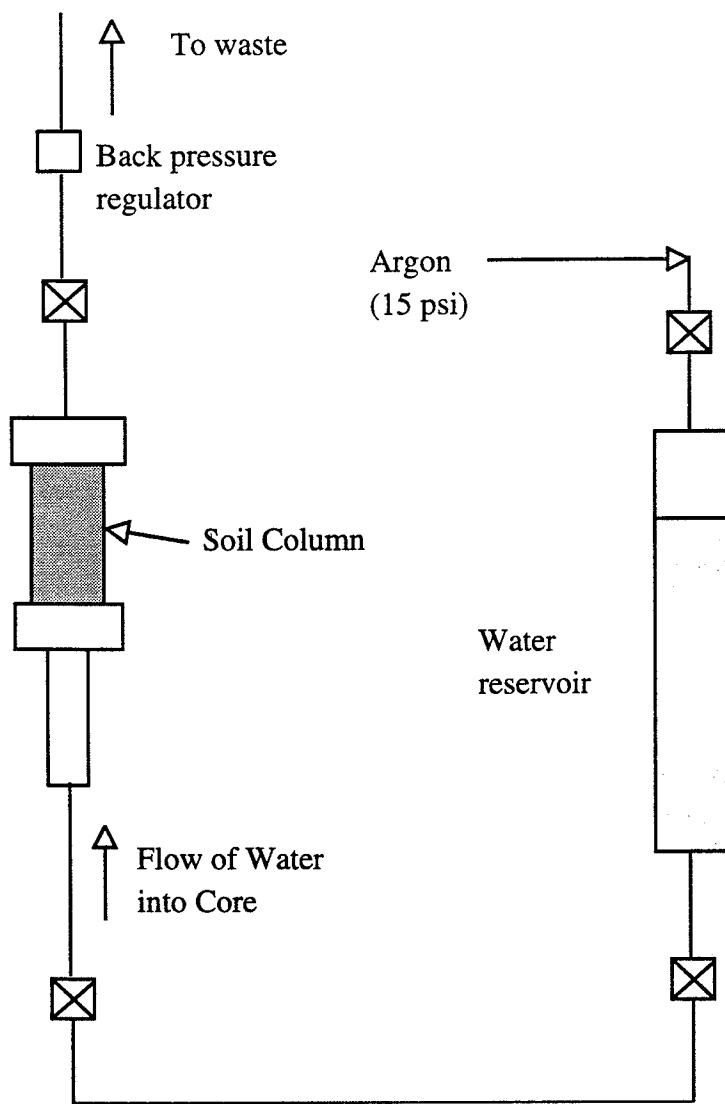


Figure 3.4: Core saturation setup

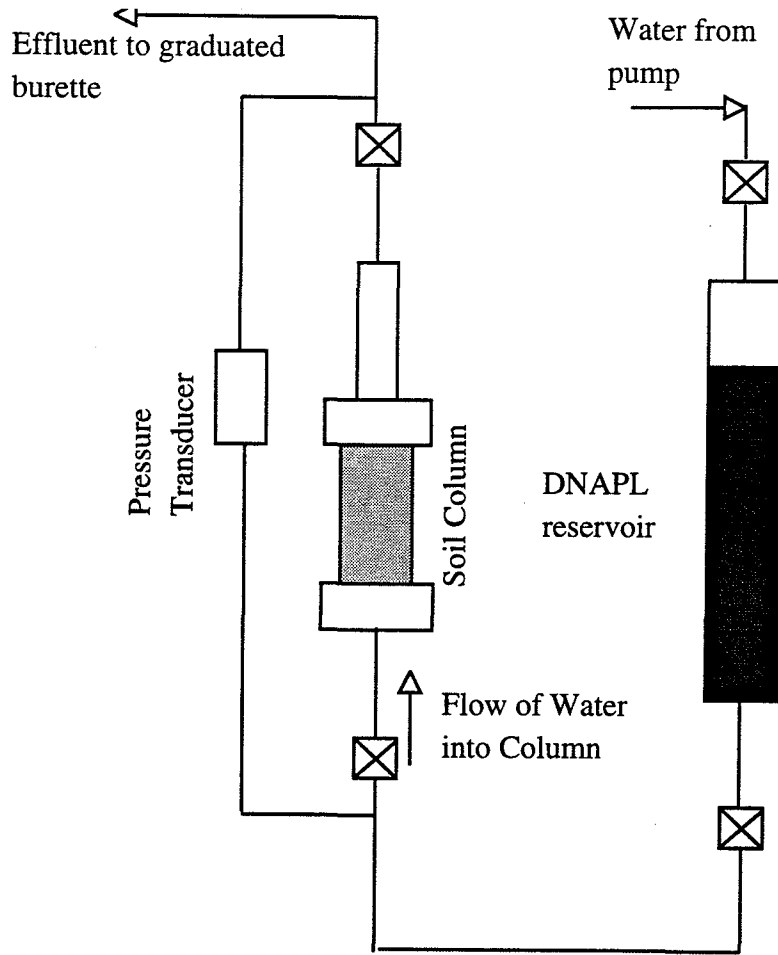


Figure 3.5: NAPL saturation setup

Chapter 4: Data Analysis Techniques

Several techniques were used for data analysis. The theoretical equations that were used to determine permeability, pore volume and saturations for soil column experiments and the solubilization ratios and contaminant solubilization in phase behavior experiments are presented in this Chapter.

4.1 PHASE BEHAVIOR: MEASUREMENT OF SOLUBILIZATION RATIOS

When surfactant is mixed with oil (NAPL) and water above its CMC under certain conditions of temperature etc., a stable phase called microemulsion forms. The volume of oil divided by the volume of surfactant in the microemulsion is defined as the oil solubilization ratio for Winsor type I behavior. The volume of water divided by the volume of surfactant in the microemulsion is defined as the water solubilization ratio for Winsor type II behavior. Both ratios apply for Winsor type III behavior.

4.1.1 volumetric measurements of solubilization

In Figure 4.1, a typical example showing a Winsor type I surfactant system with DNAPL is shown. The volume of DNAPL solubilized can be measured by measuring the change in the interface reading in the graduated pipette. The DNAPL solubilization parameter can be calculated using,

$$\sigma_o = \frac{V_N}{V_S} \quad (4.1)$$

σ_o = NAPL solubilization parameter

V_N = Volume of NAPL solubilized

V_S = Volume of surfactant

In Figure 4.2, a typical example showing a Winsor type II surfactant system with DNAPL is shown. The volume of water solubilized can be measured by measuring the change in the interface reading in the graduated pipette. The water solubilization parameter can be calculated using;

$$\sigma_w = \frac{V_w}{V_S} \quad (4.2)$$

σ_w = water solubilization parameter

V_w = Volume of water solubilized

Both the above equations are used when there is no alcohol in the surfactant solution. When alcohol is present in the surfactant solution, the alcohol partitions between the surfactant micelles, oil and water. Due to partitioning of alcohol into the oil phase the apparent volume of oil solubilized based on volume measurements has to be corrected to calculate the correct oil solubilization parameter.

In order to account for alcohol partitioning into the oil we must consider the alcohol partition coefficient between the oil and water, K_a^O , and the alcohol partition coefficient between the water and surfactant micelles, K_a^S . Both these are defined as follows,

$$K_a^o = \frac{C_a^o}{C_a^w} \quad (4.3)$$

$$K_a^s = \frac{C_a^s}{C_a^w} \quad (4.4)$$

Performing a mass balance on the alcohol,

$$V_A = V_a^o + V_a^s + V_a^w = V_a^o + C_a^w V_w + K_a^s C_a^w V_s \quad (4.5)$$

$$C_a^w = \frac{V_a^o}{V_o \cdot K_a^o \cdot \rho_a} \quad (4.6)$$

Using the above equations the volume of alcohol in oil can be derived as,

$$V_a^o = \frac{V_a}{1 + \frac{1}{K_a^o \cdot \rho_a \cdot V_o} (V_w + K_a^s \cdot V_s)} \quad (4.7)$$

In all our phase behavior experiments, the volume of surfactant is usually small and $V_w \approx V_o$. Hence the above equation can be rewritten as,

$$V_a^o = \frac{V_a}{1 + \frac{1}{K_a^o \cdot \rho_a}} \quad (4.8)$$

Hence the actual volume of oil solubilized after accounting for alcohol partitioning is,

$$V_o = V_o' + V_a^o \quad (4.9)$$

In our experiments isopropanol was used as the cosolvent. The partition coefficient of this alcohol with TCE is less than 0.1 and alcohol partitioning into the oil was not significant at concentrations of alcohol less than 4%. However at higher alcohol concentrations and with heavier alcohols (with higher oil-water partition coefficients), equations 4.7 and 4.9 must be used to calculate oil solubilization.

Generally, the solubilization of the contaminant by the surfactant solution is required for designing a surfactant flood. The contaminant solubilization can be calculated as follows:

$$\sigma_{cme} = \frac{V_N(\text{ml}) \rho_{DNAPL} \left(\frac{\text{g}}{\text{ml}} \right) \frac{1,000\text{mg}}{\text{g}}}{V_{me}(\text{ml}) \cdot \left(\frac{0.001(\text{liter})}{\text{ml}} \right)} \quad (4.10)$$

4.1.2 GC measurement of solubilization

A gas-chromatograph was also used to measure contaminant concentration in microemulsion in some phase behavior experiments. When these measurements were made, experimental techniques to inject surfactant-TCE mixtures in to the GC had not been perfected in our laboratory. Hence dilution by water was used in all samples prior to GC measurement. Samples with expected contaminant concentrations less than 50,000 mg/l were diluted on a 1:50 basis and

samples with contaminant concentrations greater than 50,000 mg/l were diluted on a 1:200 basis. The expected contaminant concentrations were based on volume measurements. A comparison of volume measurements, volume measurements corrected for alcohol concentration and gas chromatograph measurements of Hill contaminant is presented in Figure 4.3. The surfactant mixture used here is 4% by weight sodium dihexyl sulfosuccinate, 4% IPA and 500 mg/l xanthan gum.

From the plot it can be seen that there is a good match between 40,000 mg/l and 60,000 mg/l. At higher contaminant concentrations some scatter can be observed. This can be attributed to dilution errors. Some scatter can also be observed in concentrations less than 40,000 mg/l. Volume measurements are not very accurate at contaminant concentrations less than 40,000 mg/l and GC measurements should be used to measure contaminant concentrations less than 40,000 mg/l.

4.2 POROSITY AND PORE VOLUME DETERMINATION

The porosity and pore volume of the soil columns were determined by mass balance measurements. The weight of the dry unsaturated columns was measured after pulling a vacuum and removing all air from the columns. The weight of the column was measured after complete saturation with water. The porosity and pore volume of the soil pack were calculated using the following formula:

$$\phi = \frac{W_{\text{sat}} - W_{\text{dry}}}{\pi r^2 L} \quad (4.11)$$

$$V_p = \frac{W_{\text{sat}} - W_{\text{dry}}}{\rho_w} \quad (4.12)$$

4.3 PERMEABILITY DETERMINATION

Darcy's law was used to calculate the permeability of soil packs. Water was flowed into the saturated soil pack until steady state was reached. The pressure was measured and the flow rate was changed. This was done for several flow rates and plotted as shown in Figure 4.4. The slope of the $\frac{\Delta\Phi}{\Delta Q}$ curve was determined by regression. At steady state, Darcy's law can be written as,

$$k = \frac{Q\mu L}{A\Delta\Phi_j} \quad (4.13)$$

From Delshad (1990), the potential drop can be defined as;

$$\Delta\Phi_j = \Delta p_T - (\rho_j - \rho_x)gh \text{ for flow upwards into the column} \quad (4.14)$$

$$\Delta\Phi_j = \Delta p_T + (\rho_j - \rho_x)gh \text{ for flow downwards into the column} \quad (4.15)$$

In all permeability measurements, a differential pressure transducer was used to measure Δp_T across the soil column. Since the fluid lines were filled with water and the fluid flowing through the column was water, $\Delta\Phi_j$ was always equal to Δp_T . The permeability of the sand pack was measured by using the calculated value for the slope of $\frac{\Delta\Phi_j}{\Delta Q}$, the length of the soil pack, cross sectional area of the

soil pack and viscosity of water. Using lab units of $\frac{\text{ml}}{\text{min}}$ for flow rate, cp for viscosity, cm for length, cm^2 for cross sectional area and psid for pressure drop, the permeability in Darcies is given by,

$$k(\text{Darcy}) = 0.242 \frac{Q\mu L}{A\Delta\Phi_j} \quad (4.16)$$

4.4 ESTIMATION OF RESIDUAL NAPL SATURATION IN SOIL PACKS

After the NAPL flood and the waterflood, the NAPL saturation can be calculated by performing a volume balance or a mass balance. Volume balance involves in using the volume of water produced during the NAPL flood and the volume of NAPL produced during the waterflood to compute the residual NAPL saturation. Mass balance involves using the difference in weight of the contaminated soil pack at residual NAPL saturation and the clean uncontaminated soil pack saturated with water. The density difference between the NAPL and water is used to estimate the residual NAPL volume.

The following equations were used to estimate the residual NAPL saturation by volume balance.

$$S_N = \frac{V_{wp} - V_{np}}{V_p} \quad (4.17)$$

$$V_{\text{NAPL}} = V_{wp} - V_{np} \quad (4.18)$$

The following equations were used to estimate the residual NAPL saturations by mass balance:

$$S_N = \left(\frac{W_{sn} - W_{sat}}{\rho_N - \rho_w} \right) \frac{1}{V_p} \quad (4.19)$$

$$V_{NAPL} = \left(\frac{W_{sn} - W_{sat}}{\rho_N - \rho_w} \right) \quad (4.20)$$

4.5 PERFORMANCE ASSESSMENT OF SURFACTANT USING MASS BALANCE

Performance assessment of surfactant remediation was done using mass balance measurements. The percentage of NAPL removed by surfactant remediation was calculated using the following equations:

$$N_p = \left(\frac{W_{sn} - W_{sf}}{\rho_N - \rho_w} \right) \quad (4.21)$$

$$f_{N_p} = \frac{V_{NAPL} - N_p}{V_{NAPL}} \quad (4.22)$$

4.6 STATIC PARTITION COEFFICIENT CALCULATION

The static partition coefficient can be defined as,

$$K_i = \frac{C_{i,NAPL}}{C_{i,Water}} \quad (4.23)$$

In all the laboratory work, the concentration of the tracers in the aqueous phase was measured. The concentration of the tracers in the nonaqueous phase was estimated by performing a mass balance between the mass of tracer injected in the aqueous phase and mass measured in the aqueous phase after equilibration. The static partition coefficient was calculated from the following formula:

$$K_i = \frac{V_w}{V_N} \left(\frac{C_{i,I}}{C_{i,Water}} - 1 \right) \quad (4.24)$$

4.7 METHOD OF MOMENTS TO ESTIMATE PORE VOLUME, NAPL SATURATION

The method of moments is a very powerful mathematical technique to calculate various physical quantities. For example, the center of mass in a body can be calculated using the first moment and the center of percussion can be computed using the second moment. Similarly the concepts of moment analysis if applied to flow in porous media can help us compute some physical quantities. It has been shown by Himmelblau and Bischoff (1968) that for a single-phase nonreactive flow in a packed bed, the pore volume is given by the dimensionless mean residence time or first temporal moment calculated from the tracer response resulting from the imposition of an idealized instantaneous tracer pulse (the Dirac delta function) into the vessel entrance stream.

$$\bar{t}_D = \frac{\int_0^{\infty} t_D C_D(t_D) dt_D}{\int_0^{\infty} C_D(t_D) dt_D} \quad (4.25)$$

$$C_D = \text{normalized tracer concentration} = \frac{C - C_o}{C_{i,I} - C_o} \quad (4.26)$$

$$t_D = \text{normalized time or pore volumes injected} = \frac{\int_0^t q dt}{V_p} \quad (4.27)$$

It is convenient to work in terms of volumes and concentrations instead of normalizing all the parameters. The above equation can be expressed as,

$$\bar{V} = \frac{\int_0^{\infty} VC(V) dV}{\int_0^{\infty} C(V) dV} \quad (4.28)$$

If the input tracer has finite slug size V_{ds} , the pore volume is given by,

$$V_p = \bar{V} - \frac{V_{ds}}{2} \quad (4.29)$$

If one conservative tracer is flowing through a porous medium, the pore volume of the porous medium is given by the above equations.

In a soil pack with NAPL at an average residual saturation S_N , and two tracers flowing through it with partition coefficients $K_{N,w}^1$ and $K_{N,w}^2$ (Jin, 1995):

$$S_N = \frac{\bar{t}_2 - \bar{t}_1}{(K_{N,w}^2 - 1)\bar{t}_1 - (K_{N,w}^1 - 1)\bar{t}_2} \quad (4.30)$$

when $K_{N,w}^1 = 0$

$$S_N = Q \frac{\bar{t}_2 - \bar{t}_1}{K_{N,w}^2} \quad (4.31)$$

The detailed description and derivation of the method moments used in this work is given in Jin (1995). The above equation can be rewritten in terms of volumes as,

$$S_N = \frac{\bar{V}_2 - \bar{V}_1}{(K_{N,w}^2 - 1)\bar{V}_1 - (K_{N,w}^1 - 1)\bar{V}_2} \quad (4.32)$$

when $K_{N,w}^1 = 0$

$$S_N = \frac{\bar{V}_2 - \bar{V}_1}{V_p \cdot K_{N,w}^2} \quad (4.33)$$

If one of the tracers is a partitioning tracer and the other one is a nonpartitioning tracer then,

$$S_N = \frac{\bar{V}_p - \bar{V}_n}{(K_{N,w}^p - 1)\bar{V}_n + \bar{V}_p} \quad (4.34)$$

The mass of tracer recovered (M_i) in a tracer test can be calculated from the zeroth moment as follows:

$$M_i = \int_0^{V_f} C_i dV \quad (4.35)$$

In order to estimate the NAPL volume accurately, the tracer response curves should be complete, because much of the information is contained in the tail of the response curves. Unfortunately, the tracer response curves are often incomplete either due to the dilution of the tracer concentration below the detectable limit or to the limitation of the duration of the tracer test, or for some other reason. However, the tracer response curves can be extrapolated with an exponential function provided the duration of the test is sufficient to establish this decline (Pope *et al.*, 1994, Jin, 1995). The first moments of the tracer response curves can be obtained by dividing the data into two parts. The first part represents the data from zero to the time t_b where it becomes exponential, and the second covers the exponential part in which it goes from t_b to infinity. After time t_b , the tracer response is assumed to follow an exponential decline given by:

$$C = C_b e^{-\frac{t-t_b}{a}} \quad (4.36)$$

where $1/a$ is the slope of the straight line when the tracer response curves are plotted on a semi-log scale, and C_b is the tracer concentration at time t_b . A typical example of extrapolation of tracer data is presented in Figure 4.5. By integration of the above the first moment can be rederived as (Jin, 1995):

$$\bar{t} = \frac{\int_0^{t_b} t C dt + a(a + t_b)C_b}{\int_0^{\infty} C dt + aC_b} \quad (4.37)$$

When volumes are used instead of time, the above equation can be rewritten as:

$$\bar{V} = \frac{\int_0^{V_b} V C dV + a(a + V_b)C_b}{\int_0^{\infty} C dV + aC_b} \quad (4.38)$$

The estimation of NAPL saturations is significantly improved by extrapolation. In confined column experiments conducted in this work, extrapolation did not significantly change the NAPL estimates. In field situations

where the system is unconfined and many streamlines do not make it to the production wells, extrapolation of data is an excellent tool to improve the estimates of NAPL saturations.

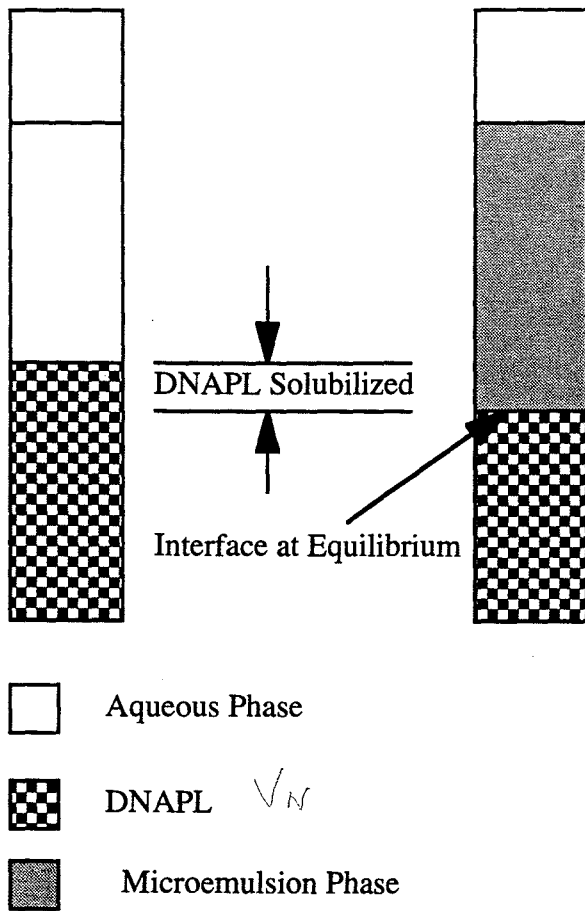


Figure 4.1: Calculation of Oil Solubilization Ratios in type I systems

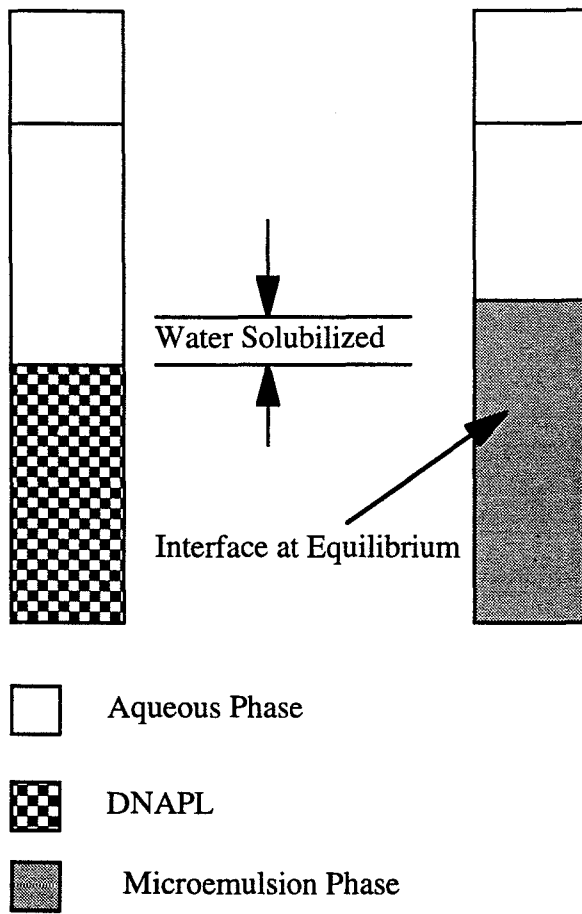


Figure 4.2: Calculation of Water Solubilization Ratios in type II systems

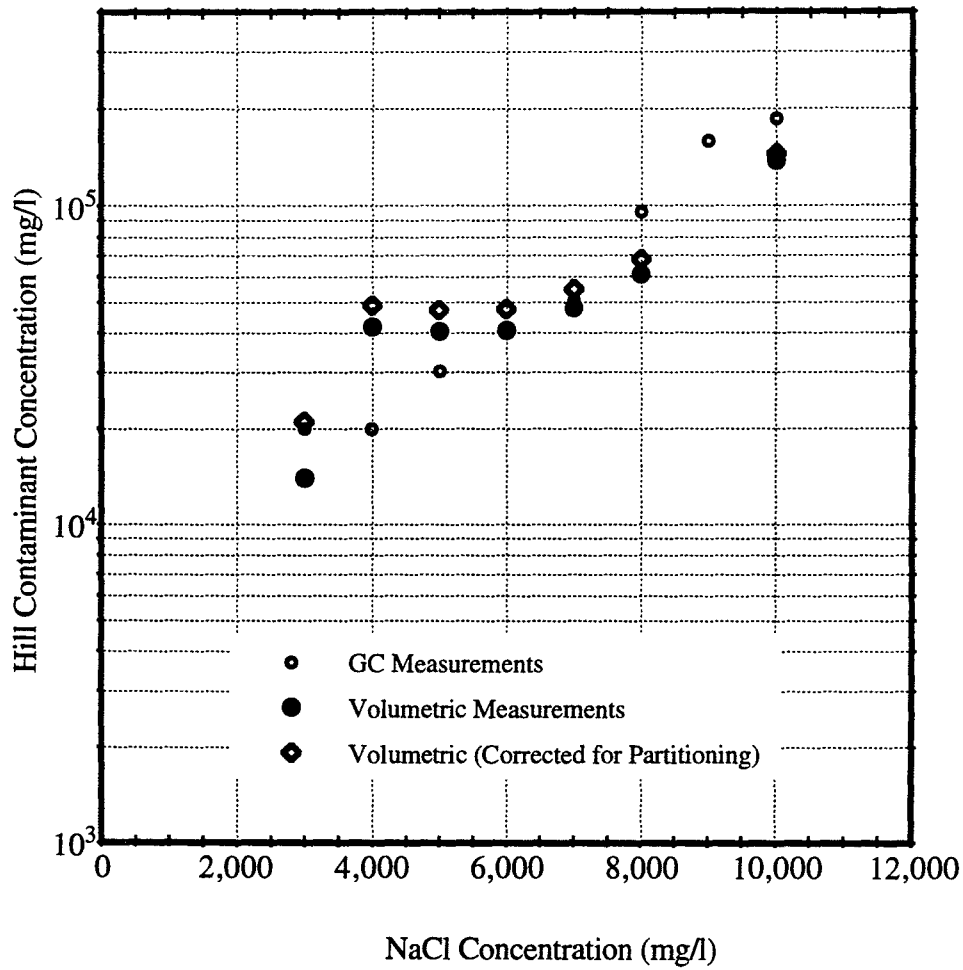


Figure 4.3: Comparison of gas chromatograph measurement and volume measurement of contaminant in microemulsion

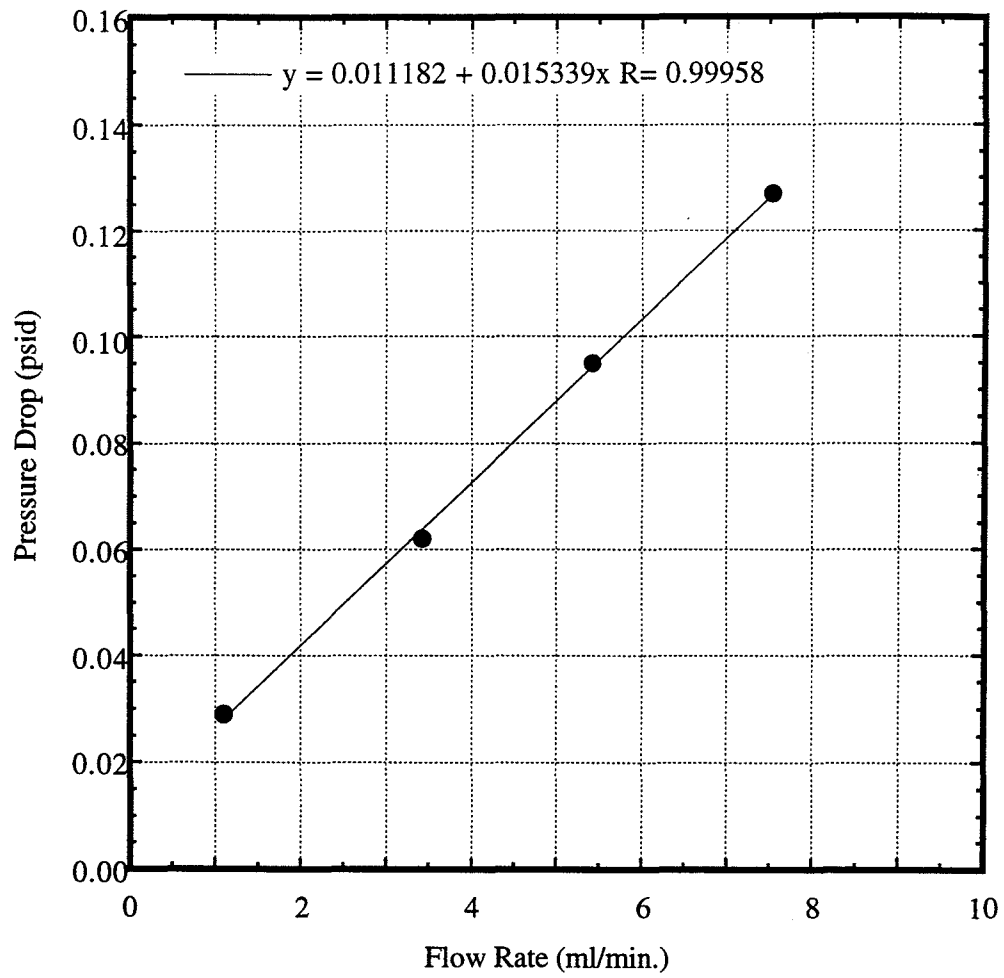


Figure 4.4: Permeability calculation plot for experiment HILLOU2#8

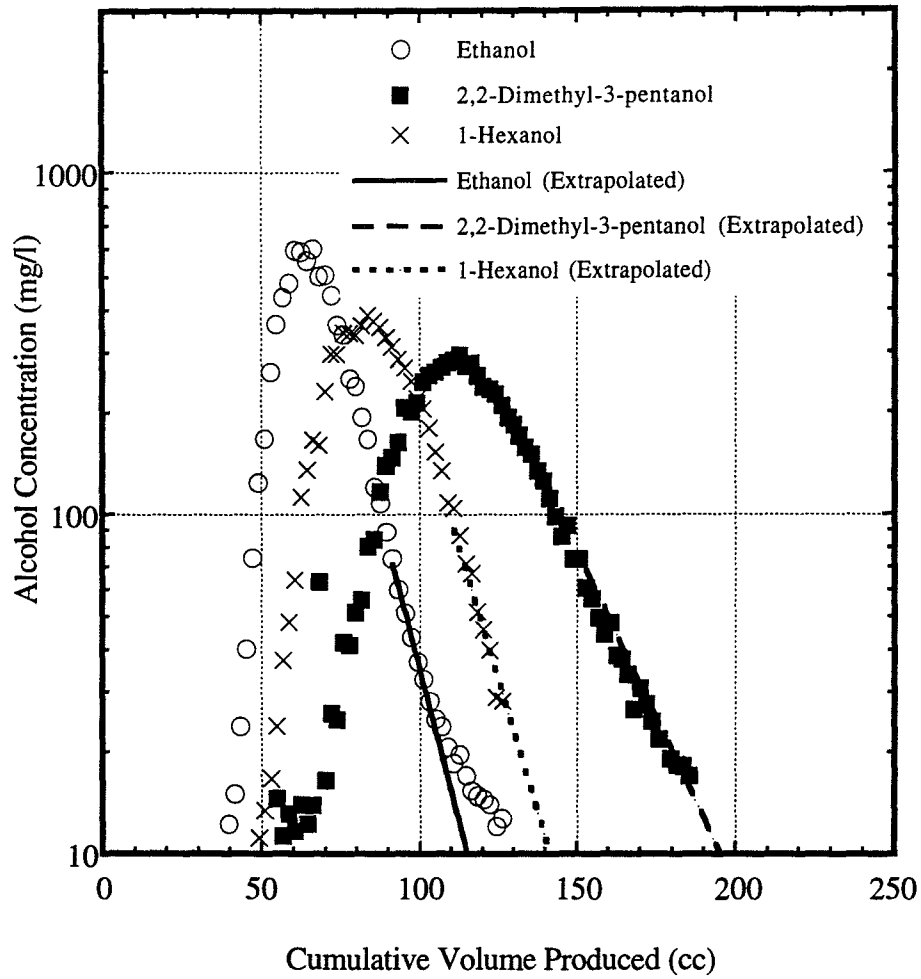


Figure 4.5: Extrapolation of partitioning tracer data, experiment OUDNAPL3

Chapter 5: Surfactant Phase Behavior Studies

Surfactant enhanced aquifer remediation (SEAR) describes the application of surfactants for the recovery of NAPLs from contaminated aquifers. Surfactants have been used for enhanced oil recovery by the oil industry for more than 30 years. However, the application of surfactants for remediation involves a variety of new conditions and criteria, so careful experiments have to be carried out to identify suitable surfactants for specific NAPLs and specific aquifer conditions. The first and very important step in identifying suitable surfactants is to conduct appropriate phase behavior experiments.

Surfactants both increase the solubilization of NAPL constituents and lower the IFT between the NAPL and water. Phase behavior experiments are extremely important to identify surfactant solutions with suitable characteristics such as solubilization ratio and contaminant solubilization, quick equilibration times with absence of liquid crystals. In this Chapter, a brief introduction to surfactants and their behavior is presented.

5.1 DESCRIPTION OF SURFACTANTS

Surfactants or surface active agents are amphiphiles or amphiphilic compounds characterized by possessing in the same molecule, two distinct groups which differ greatly in their solubility relationship (Winsor, 1954). This tendency for surfactant molecules is responsible for their tendency to concentrate at interfaces. Surfactants possess a characteristic structure that consists of molecular components that have little attraction for the organic solvent that are called

lyophobic and components that have a strong attraction for the organic solvent that are called lyophilic group (Myers, 1988). When the solvent is water, the terms lyophobic and lyophilic can be replaced by hydrophilic and hydrophobic.

Due to this unique amphiphilic nature, surfactants are used for a wide range of commercial applications like, enhanced oil recovery, pharmaceutical applications, lubrication etc. (Myers, 1988). A description of surfactant types, properties, behavior, characteristics and applications is given in Rosen (1988). A more detailed description of the thermodynamics of micelle formation and description of various parameters that affect micelle formation, microemulsion formation and surfactant phase behavior is given Bourrel and Schechter (1988).

In order to use surfactants for EOR operations, a good understanding of surfactant properties such as micellization, oil solubilization have to be quantified. In addition, the effect of temperature, pressure, cosolvent, electrolyte, polymer, surfactant adsorption, cation exchange, surfactant-rock interactions etc. also have to be understood and well defined before application of surfactants in field EOR operations. Some of the above are discussed in Bourrel and Schechter (1988). A procedure for designing EOR processes is described by Pope and Baviere (1991). They recommended that the physicochemistry of surfactant solutions (outlined above) should be used as a basis for designing field surfactant floods for EOR.

The lessons learned during surfactant applications to EOR can be used for surfactant enhanced aquifer remediation (Pope and Wade, 1995). The objective of surfactant enhanced aquifer remediation is to recover greater than 95% of the contaminant and restore the soil to its original condition. However, improper application of surfactants in remediation applications can cause several problems

like plugging as observed by Zeigenfuss (1987), reduction in hydraulic conductivity observed by Allred and Brown (1995) and mobilization of fines (Bourbonais *et al.*, 1995). Some of these problems that can be faced during surfactant remediation are surfactant losses by adsorption, precipitation, liquid crystals, coacervation and partitioning into the trapped NAPL (Harwell, 1992).

Many concepts discussed in EOR literature are directly applicable to remediation of aquifers by surfactants. Problems like plugging could be attributed to pore plugging caused by liquid crystal formation and gel formation. Reductions in hydraulic conductivities can be caused by surfactant precipitation due to surfactant rock interaction. Cation exchange in which calcium ions in clays are replaced by sodium ions can cause mobilization of fines as the clays are not held in place by monovalent sodium ions. Most of these mechanisms were well described by EOR literature. One of the objectives of this work was to use the concepts described in the EOR literature to screen surfactants suitable for SEAR applications.

The basic nature of surfactant molecules is given in Figure 5.1. An anionic surfactant (sodium dihexyl sulfosuccinate) and a nonionic surfactant molecule (2,4,5-trimethyl-heptyl-polyglucoside) are presented in Figure 5.2. The most common surfactants are substantially soluble in water. The water solubility is affected by the length of hydrophobic tail, the nature of head group, the valency of counterions and solution environment (Myers, 1988). In general surfactants can be divided into four main classes depending on the type of the hydrophilic groups.

5.1.1 Anionic

Surfactants with a negatively charged hydrophilic group such as carboxyl ($\text{RCOO}^- \text{M}^+$), sulfonate ($\text{RSO}_3^- \text{M}^+$) and sulfate ($\text{ROSO}_3^- \text{M}^+$) are classified as anionic. Examples of commercial anionic surfactants are sodium dihexyl sulfosuccinate (Baran *et al.*, 1996b), sodium dodecyl sulfate (Shiau *et al.*, 1994), alkyl diphenyl oxide sulfonates (Rouse *et al.*, 1993) and phosphate ester of Nonylphenyl ethoxylate (Fountain, 1992).

5.1.2 Cationic

Surfactants with a positively charged hydrophilic group such as quaternary ammonium halides ($\text{R}_4\text{N}^+ \text{Cl}^-$) are classified as cationic.

5.1.3 Nonionic

Surfactants with a hydrophilic group has no charge but derives its water solubility from highly polar groups such as polyoxyethylene or polyol groups are classified as nonionic. Some commercial examples are ethoxylated (20) sorbitan mono-oleate (Pennell *et al.*, 1994), ethoxylated nonylphenol (TRI, 1985), alkyl polyglucamides (Baran *et al.*, 1996c).

5.1.4 Amphoteric or Zwitterionic

Surfactants that have both positive and negative charges such as sulfobetaines $\text{RN}^+(\text{CH}_3)_2\text{CH}_2\text{CH}_2\text{SO}_3^-$ are classified as amphoteric or zwitterionic surfactants.

5.2 REVIEW OF SURFACTANT BEHAVIOR

Due to the unique amphiphilic nature of the surfactant molecules, they tend to aggregate at the interfaces of two fluids. This is responsible for a reduction in the free energy of the system in which they interact. The primary mode of energy reduction is adsorption of the surfactant molecules at all the available surfaces. One physical manifestation of lowering of free energy is the formation of crystals or precipitation of surfactant from solution. Another physical manifestation is the formation of micelles or molecular aggregates. If surfactant is dissolved in water at concentrations greater than the CMC, the surfactant exists almost entirely as micelles (Bourrel and Schechter, 1988; Rosen, 1988; Lake, 1989). The micelle may be looked upon as a crystalline hydrate or a solid crystal so that the energy change in going from the crystal to the micelle is less than the change in going from the crystal to the monomeric species in solution. The formation of micelles greatly increases the solubility of the surfactant in water. The critical micelle concentration and is associated with a sudden decrease in interfacial tension, electrical conductivity, increase in detergency etc. For this and other reasons, all experiments done as part of this research on surfactant remediation were done at concentrations much higher than the CMC.

Most surfactants used in commercial applications are usually water soluble. The solubility of anionic surfactants generally increases with temperature. In case of ionic surfactants, the solubility undergoes a sharp change at a temperature called Krafft point at which the solubility of the surfactant equals

its CMC. Surfactants are usually used above their Krafft points (Rosen, 1988). Nonionic surfactants do not exhibit Krafft point, instead they become less soluble as temperature increases. The sudden onset of turbidity of a nonionic surfactant solution raising the temperature is called the cloud point. At a higher temperature the solution tends to separate into two phases. One of the phases is surfactant-rich whereas in the other phase the surfactant concentration is usually very small (Bourrel and Schechter, 1988). For remediation applications surfactants should be used below the cloud point.

The hydrophobic groups are generally more varied than the hydrophilic groups and include long chain alkyl groups, branched chain alkyl groups, alkylbenzenes, alkylnaphthalenes, polydimethylsiloxanes, polyoxypropylene glycol derivatives, etc. Considering the possible permutations and combinations of all the above groups, a good understanding of surfactant behavior is required for selection of the best surfactants for rapid screening including which phase behavior experiments to perform and how to properly interpret them.

5.2.1 Microemulsions

The term microemulsion is frequently confused with emulsions or macroemulsions. Ordinary emulsions or macroemulsions must be distinguished from microemulsions. Macroemulsions are unstable. Macroemulsions are composed of drops of one liquid phase interspersed within a second immiscible liquid phase. The drops will coalesce into bigger drops and eventually fall out of the emulsion. The larger drops will fall faster and eventually two separate immiscible phases separated by an interface will appear. Microemulsions are

thermodynamically stable and are composed of submicroscopic structures which are so small that Brownian motion keeps them suspended, and coalescence of the drops leads to an increase in free energy. Thus the free energy of a microemulsion is at a minimum and the system is thermodynamically stable compared to macroemulsions which are thermodynamically unstable (Bourrel and Schechter, 1988).

As only anionic surfactants were used in this work, subsequent discussions will emphasize anionic surfactants. When a surfactant, water and NAPL (oil) are mixed and allowed to equilibrate, two or more phases may appear and in many cases most of the surfactant will reside in one of the phases together with various proportions of oil and water. When certain criteria are met, this phase is called a microemulsion. At low electrolyte concentrations, a Winsor type I system with an oil in water microemulsion is formed. As the electrolyte concentration is increased, the system changes from a Winsor type I (type II⁻) to a Winsor type III to a Winsor type II (type II⁺) system with an inverted microemulsion or a water in oil microemulsion. An illustration of surfactant phase behavior and transition between the three types of systems with anionic surfactants is presented in Figure 5.3.

Winsor type I behavior is characterized by swollen micelles surrounded by water. The organic species (hydrocarbon or chlorocarbon) is dissolved in the interior of the micelles. Winsor type II behavior is characterized by swollen inverted micelles with the water dissolved in the center of the micelles. For the type III microemulsions, the structure cannot be easily defined but is thought to be bicontinuous (Bourrel and Schechter, 1988).

When a surfactant solution and an oil are mixed to form a microemulsion, there is coalescence of microemulsion and excess phases. When two drops approach each other, the liquid film of continuous phase separating the two drops will become thinner. If the film becomes thin enough, coalescence will occur (Bourrel and Schechter, 1988). Any mechanism that slows the rate of thinning will slow down the rate of coalescence. When two microemulsion drops approach each other and the liquid film separating them thins, the surfactant molecules in the interface separating the drops will be displaced thus slowing the coalescence rate. This slowing is more likely when the microemulsion is the continuous phase. In many instances, a mixture of microemulsions and excess phases can form macroemulsions. In these macroemulsions, the micellar phase (microemulsion) is the continuous phase and would lead to a slower coalescence rate. Coalescence rates can be increased by increasing the fluidity of interfaces. This can be brought about by addition of alcohol or cosolvent which adsorbs at the water-oil interface and increases the fluidity. This increased fluidity causes breakup of macroemulsions and reduces coalescence times. Other factors which enhance fluidity of interfaces are higher temperature and branching in the surfactant tail.

Depending on a large number of factors, including the structure of the surfactant molecule, the temperature and the presence or absence of certain additives some intermediate liquid-crystalline phases may appear (Bourrel and Schechter, 1988). Stable macroemulsions can be associated with liquid-crystalline structures. In some instances liquid crystals are used to produce stable macroemulsions (Bourrel and Schechter, 1988). Hence an increase in the fluidity

of the water-oil interface would decrease stable macroemulsion formation and also minimize liquid crystal or gel formation. This can be achieved by adding alcohol, increasing temperature and increasing branching in the surfactant tail. As microemulsion transition from a Winsor type I to type III to type II is observed, the viscosity of the micellar phase has been observed to show discontinuities. Higher viscosities and sometimes non Newtonian behavior are observed at the type I to type III transition and type III to type II transition (Bourrel and Schechter, 1988). In order to minimize excessively high viscosities alcohol can be added (Read and Healy, 1977).

From the above discussion on microemulsions it can be seen that a good understanding of microemulsion behavior is paramount for surfactant selection for field EOR and SEAR applications in order to prevent undesirable problems such as pore plugging and loss of hydraulic conductivity which could be caused by low coalescence times and liquid crystal formation.

5.2.2 Solubilization parameter and contaminant solubilization

The solubilization parameter is defined as the ratio of the volume of NAPL or water dissolved to the volume of surfactant present. If V_o , V_w are the volume of NAPL and water dissolved by the surfactant and V_S is the volume of surfactant then the NAPL and water solubilization parameters (solubilization ratio) are defined by the following equations;

$$\sigma_o = \frac{V_o}{V_S} \quad (4.1)$$

$$\sigma_w = \frac{V_w}{V_s} \quad (4.2)$$

Typically, for anionic surfactants with chlorinated solvents like TCE, low values of oil solubilization are observed at low electrolyte concentrations. Higher values of solubilization ratio are observed at optimal salinity. The water solubilization ratio decreases as the electrolyte concentration is increased. The electrolyte concentration at which the volume of oil solubilized equals the volume of water solubilized is termed the optimal salinity. Optimal salinity also refers to a point where the oil solubilization parameter and water solubilization parameter are equal and in case of nonionic surfactant, optimal salinity may refer to a temperature or a surfactant blend which gives rise to optimal conditions. Optimal salinity is a very important and useful reference point for any surfactant and should be measured even if there is no interest in using the surfactant at optimal salinity. Surfactants at optimal salinity are usually associated with ultra-low interfacial tensions and mobilization of residual oil for enhanced oil recovery (EOR). EOR surfactants at optimal salinity typically reduce the IFT to 10^{-3} dyne/cm or less (Pope and Baviere, 1991).

A typical example is shown in Figure 5.4. As seen in Figure 5.4, the oil solubilization ratio increases from 0.2 to about 6.2 and the water solubilization ratio decreases from 7 to 2.8. The optimal salinity is at about 11,250 mg/l NaCl and the solubilization parameter is about 5 at optimal salinity. More results will be presented in the next Chapter. For a given surfactant and oil, the optimal salinity can be reached by changing electrolyte concentration, temperature or

concentration of cosolvent (alcohol). The optimal salinity is also a weak function of pressure, but this is not relevant to low pressure aquifer applications of surfactant. Nonionic surfactants are generally insensitive to electrolyte concentrations, but optimal salinity can be reached by changing the temperature or by blending suitable combinations of surfactants with different molecular structures.

Contaminant solubilization is defined as milligrams of contaminant dissolved in liters of solution. A measure of contaminant solubilization is a preliminary indication of the possible effectiveness of the surfactant. Typically, the solubility of contaminant in the aqueous phase is increased by a factor of 10-1,000 on addition of surfactant. A typical example is presented in Figure 5.5 for a surfactant formulation with contaminant from the Hill Operational Unit 2 site at Utah. The solubility of the contaminant increases from about 20,000 mg/l to 600,000 mg/l by increasing the electrolyte concentration from 3,000 mg/l to 12,000 mg/l. This corresponds to a change from a Winsor type I surfactant system to a Winsor type III surfactant system.

5.2.3 Volume fraction diagrams

Surfactant phase behavior can also be presented in the form of volume fraction diagrams (Shiau, 1994 and Jin, 1995). In case of anionic surfactants the volume fractions of various phases are plotted against the electrolyte concentration. In these experiments, the water oil ratio, surfactant concentration, temperature and cosolvent concentration were fixed. Only the electrolyte concentration was varied. Volume fraction diagrams for nonionic surfactants can

be generated by fixing the total surfactant concentration and varying the fractions of the individual surfactants, or by varying temperature. A good insight on the behavior of the surfactant is obtained by looking at the volume fraction diagrams. The activity of the surfactant can be inferred from the relative fractions of the microemulsion formed. The transition from a Winsor type I system to a Winsor type III to Winsor type II system can be observed. An illustration showing a volume fraction diagram and corresponding phase behavior samples are shown in Figure 5.3. The oleic phase is always shown in the top left hand corner and the aqueous phase is shown in the bottom right hand corner. A good example with Hill DNAPL and sodium dihexyl sulfosuccinate is presented in Figure 5.6. The volume fraction of the microemulsion and oleic phases are observed to be almost equal at low electrolyte concentrations. This is because of low solubilization parameters at low electrolyte concentration. As the transition to the three phase region is approached a significant increase in the volume fraction of the microemulsion phase is observed. The fraction of oil or NAPL is observed to go to zero at the transition point from a Winsor type III system to a Winsor type II system.

5.2.4 Ternary diagrams

Ternary diagrams are an excellent way of characterizing surfactant phase behavior. When oil, water and surfactant are mixed together and allowed to equilibrate, the phase behavior will involve at least three components. When anionic surfactants are used, pressure, temperature and electrolyte concentration are fixed. Ternaries have been used to represent compositions, and functions of

compositions like dilution paths (Read and Healy, 1977; Nelson and Pope, 1978, Lake, 1989). A surfactant -water-oil system can form two or more phases. A ternary representation of phase diagrams is presented in Figures 5.7 through 5.9. In Figure 5.7 a Winsor type I system is presented. Since the overall composition is inside the binodal curve and the tie lines have negative slope, it is a two phase system (type II⁻). Similarly in Figure 5.8 and Figure 5.9, Winsor type III and Winsor type II (type II⁺) systems are presented. The respective oil, water and microemulsion volume fractions are also defined in Figures 5.7 through 5.9. When we perform phase behavior experiments, the overall composition is known and phase volume fractions can be measured at equilibrium. Using these, tie lines and a binodal curve can be drawn. An example of a ternary diagram with tetrachloroethylene and a mixture of sodium diamyl sulfosuccinate and sodium dioctyl sulfosuccinate is presented in Figure 5.10. From Figure 5.10 it can be seen that the surfactant solution forms a Winsor type I system at the given electrolyte concentration, pressure and temperature.

5.2.5 Interfacial tensions (IFT)

Due to the amphiphilic nature of surfactants and their tendency to aggregate at interfaces, the addition of surfactant will bring about a reduction in interfacial tensions between aqueous phases and nonaqueous phases. IFT measurement is required to determine the trapping number make a prediction of the remediation regime (mobilization or solubilization). The effect of trapping number on surfactant remediation has been extensively discussed by Jin (1995). A spinning drop tensiometer (Cayais *et al.*, 1978) was used to measure IFT's. IFT

measurements are time consuming and have a high degree of uncertainty. Hence an easier technique for estimating IFT is useful and is discussed next.

The interfacial tensions can be correlated with the solubilization parameters (Read and Healy, 1977). A qualitative illustration showing the correlation between phase behavior and IFT's is presented in Figure 5.11. In Figure 5.5 it can be seen that there are two interfacial tensions, one between the microemulsion and oil and the other between the microemulsion and water. The interfacial tensions between the aqueous phase and microemulsion phase and nonaqueous phase and microemulsion phase are equal at optimal salinity. A theoretical relationship to predict IFT and solubilization parameter has been developed by Chun Huh (1979) and verified by Glinsmann (1979), Graciaa *et al.* (1981) and Delshad (1981). The IFT can be estimated using the following relation;

$$\gamma = \frac{C}{\sigma^2} \quad (5.1)$$

Based on regression with a large number of measurements with hydrocarbons, the value for C has been estimated to be about 0.3. The main advantage of this correlation is that difficult IFT measurements can be replaced by easier phase behavior experiments. It can also be used to smooth experimental data, spot large errors and as guide to additional measurements.

5.3 SURFACTANT APPLICABILITY

Anionic surfactants are most commonly used for enhanced oil recovery by the petroleum industry (Lake, 1989; Pope and Baviere, 1991). This is because of low adsorption on reservoir rocks, availability and low cost. The low adsorption of anionic surfactants is because of negatively charged hydrophilic groups, which get repelled by the negatively charged surfaces of clays in the subsurface at typical pH's of 6 to 8 for oilfield brines

For applicability in NAPL recovery operations the surfactants must have the following characteristics (Pope and Wade, 1995):

- solubilization potential
- phase behavior
- environmental acceptability
- viscosity of surfactant solutions
- coalescence behavior
- cost and availability
- transport characteristics in porous media
- stability
- sorption characteristics

As in EOR applications, phase behavior is the most important requirement for SEAR applications as solubilization, coalescence behavior, liquid crystal forming tendencies, microemulsion viscosity and IFTs can be related to phase behavior. Historically EOR surfactants were mixed with alcohols or cosolvents to minimize coalescence times, liquid crystal formation and microemulsion

viscosity. At higher temperatures or with surfactants having sufficiently branched tails this was not necessary, but SEAR applications are usually at lower temperatures and addition of alcohol would greatly assist in minimizing many of the above mentioned problems.

Once the phase behavior screening is completed and an acceptable surfactant has been identified, the next step in the screening process is to test the transport characteristics of the surfactant in a porous medium (soil column experiments). This was done with many surfactants identified in this work. Column experiments can help determine the transport characteristics of the surfactant, measure surfactant adsorption and evaluate surfactant performance in terms of the final in oil/NAPL saturation after surfactant flooding. Other parameters such as surfactant rock interaction and effect of surfactant remediation on hydraulic conductivity of the soil can also be studied. Column experiments and discussion of column experiment results are presented in Chapter 8 and Chapter 9.

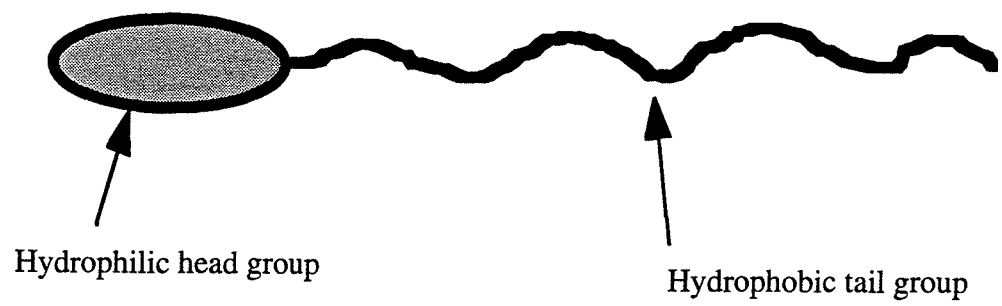


Figure 5.1: Nature of surfactant molecule

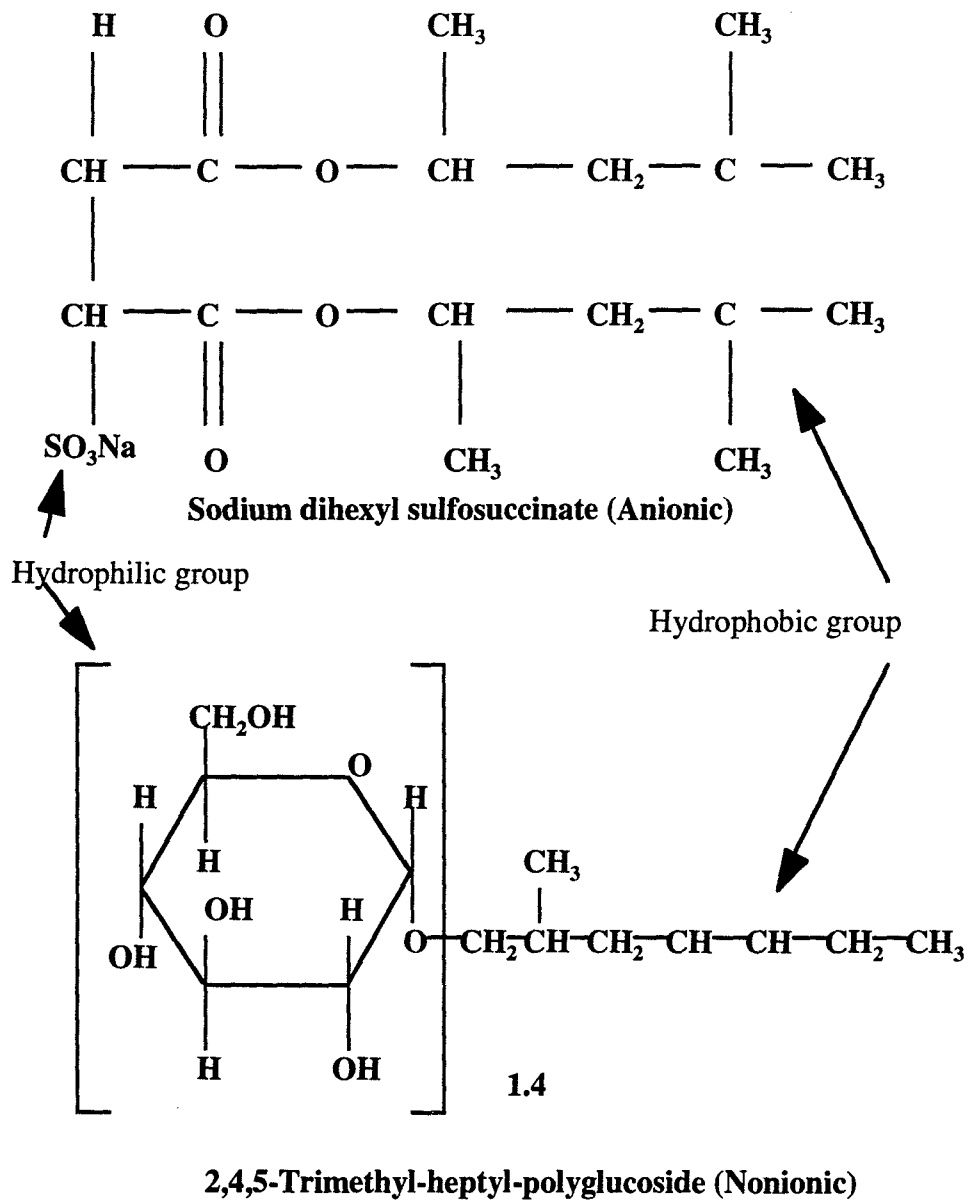


Figure 5.2: Examples of anionic and nonionic surfactants

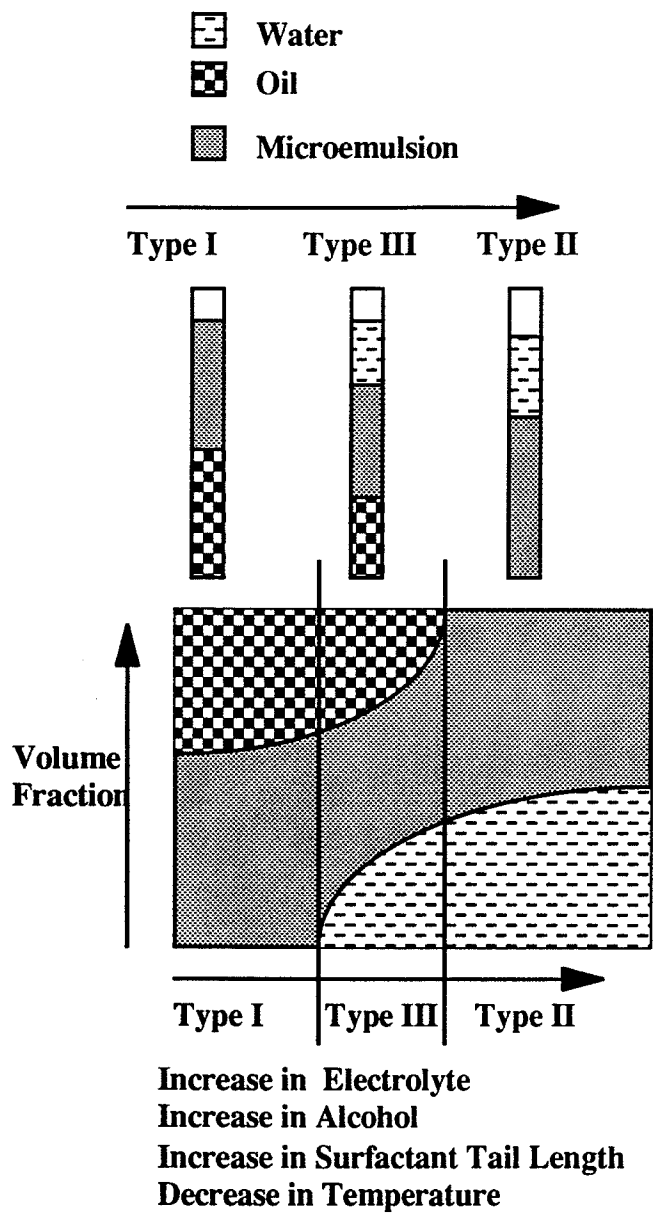


Figure 5.3: Phase behavior of anionic surfactants

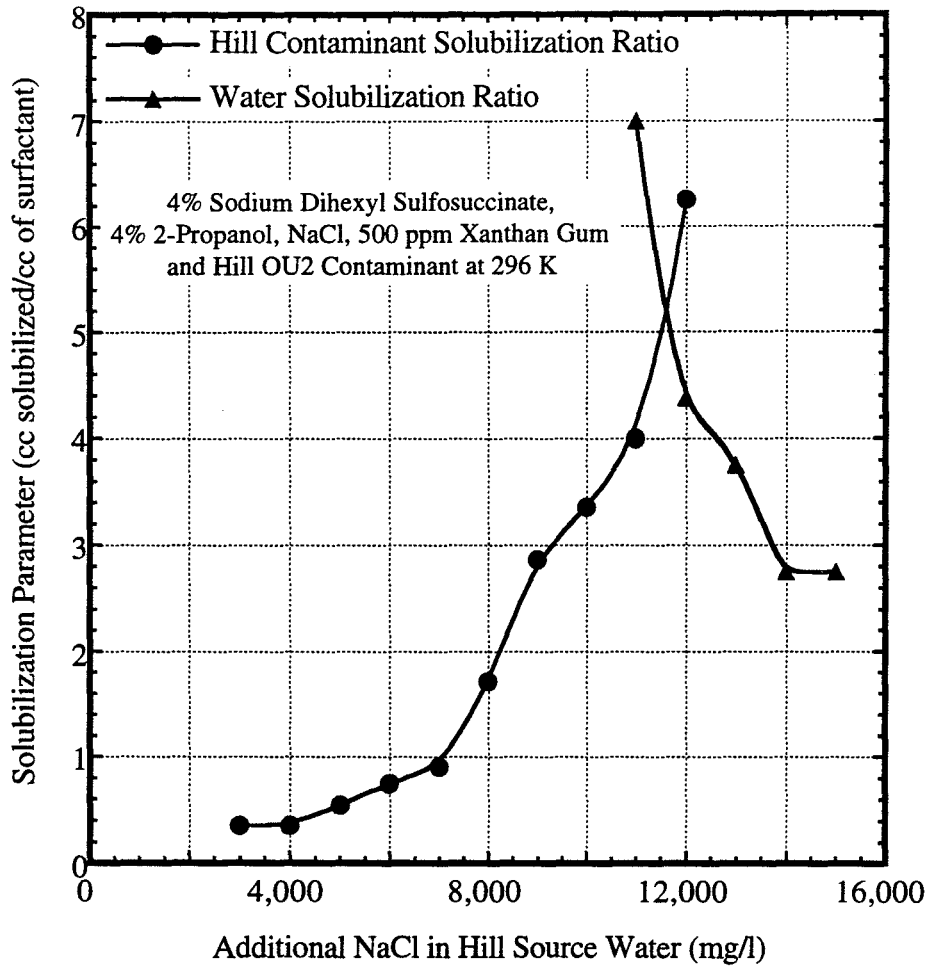


Figure 5.4: Solubilization parameters plotted against electrolyte concentration

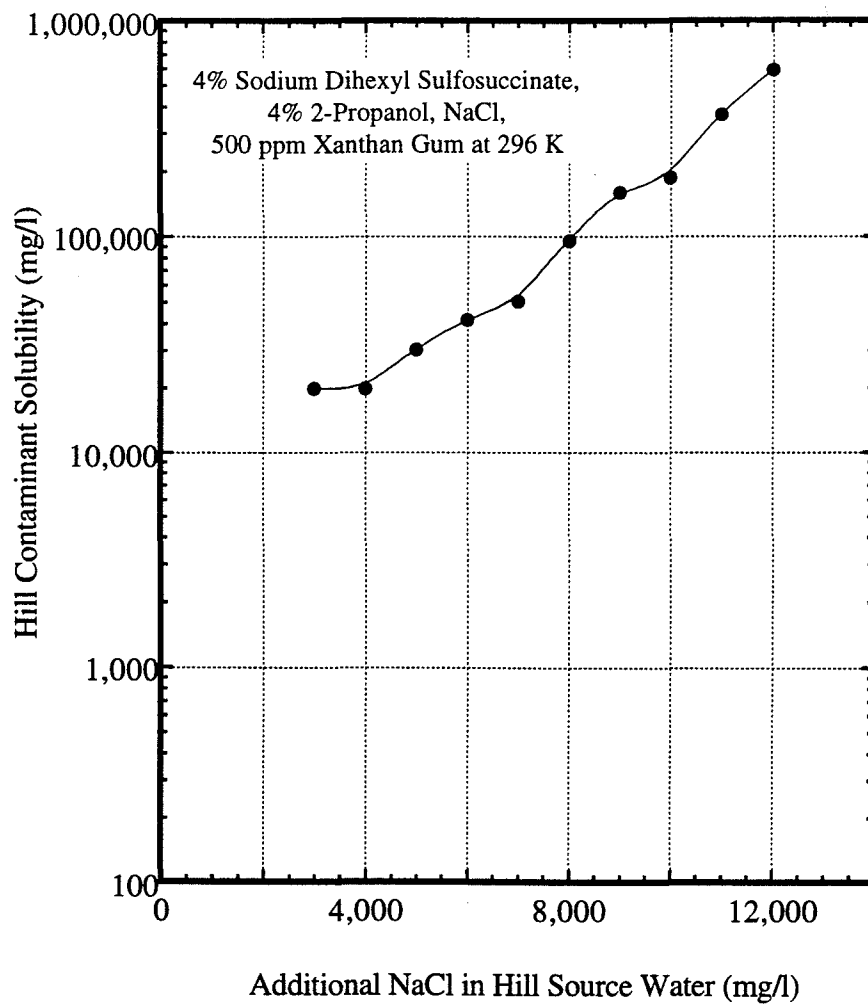


Figure 5.5: Contaminant solubilization plotted against electrolyte concentration

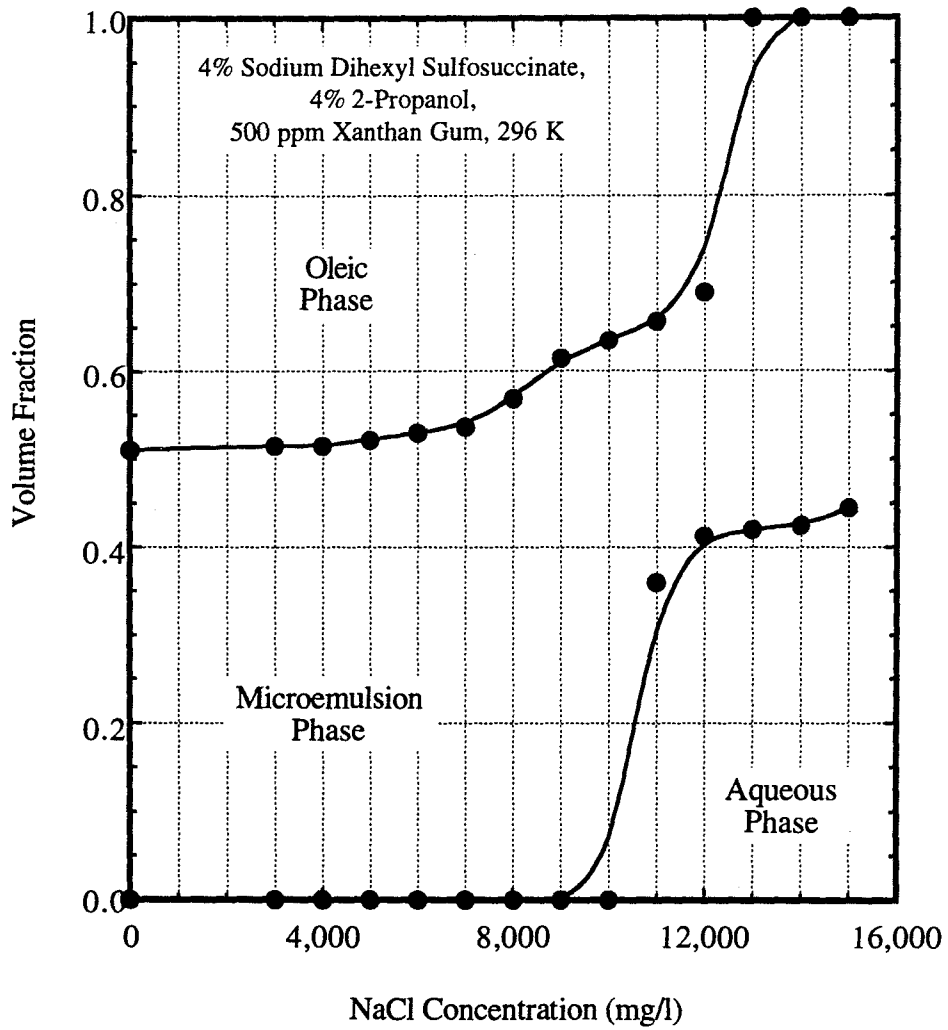


Figure 5.6: Volume fraction diagram for a surfactant formulation

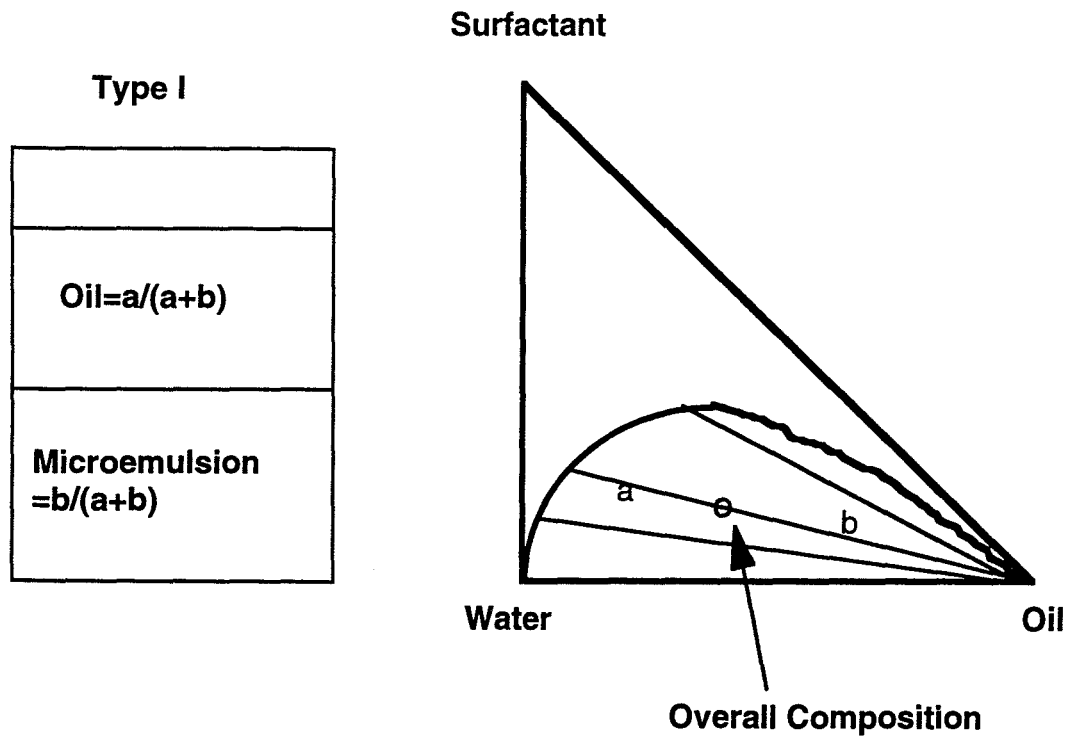


Figure 5.7: Type I ternary with oil, water and surfactant (reproduced from Nelson and Pope, 1978).

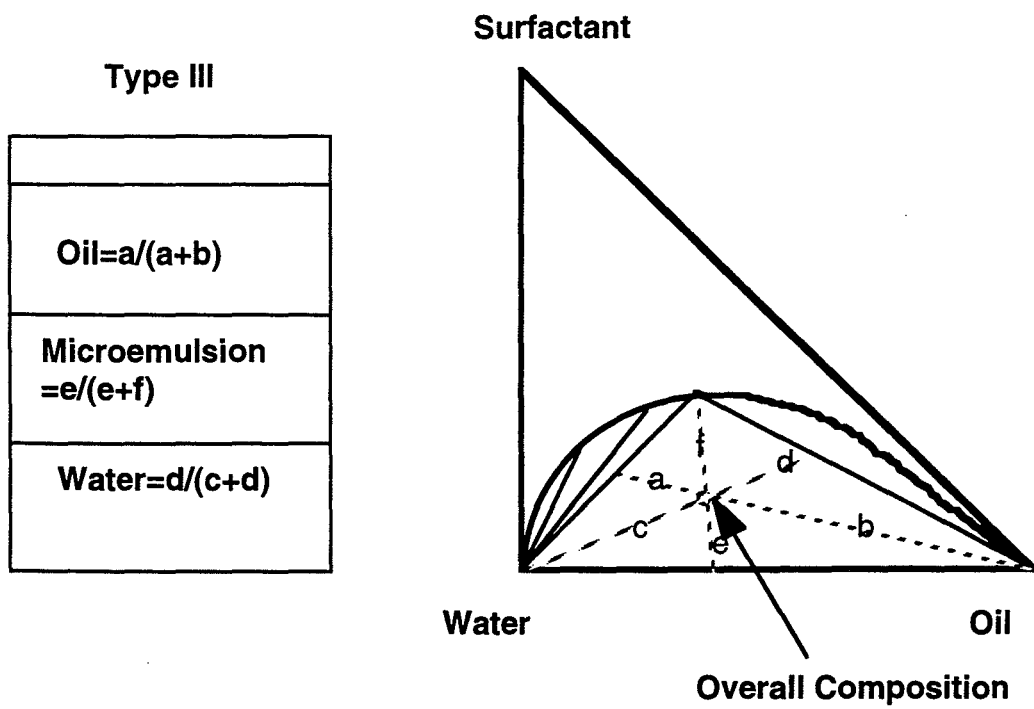


Figure 5.8: Type III ternary with oil, water and surfactant (reproduced from Nelson and Pope, 1978).

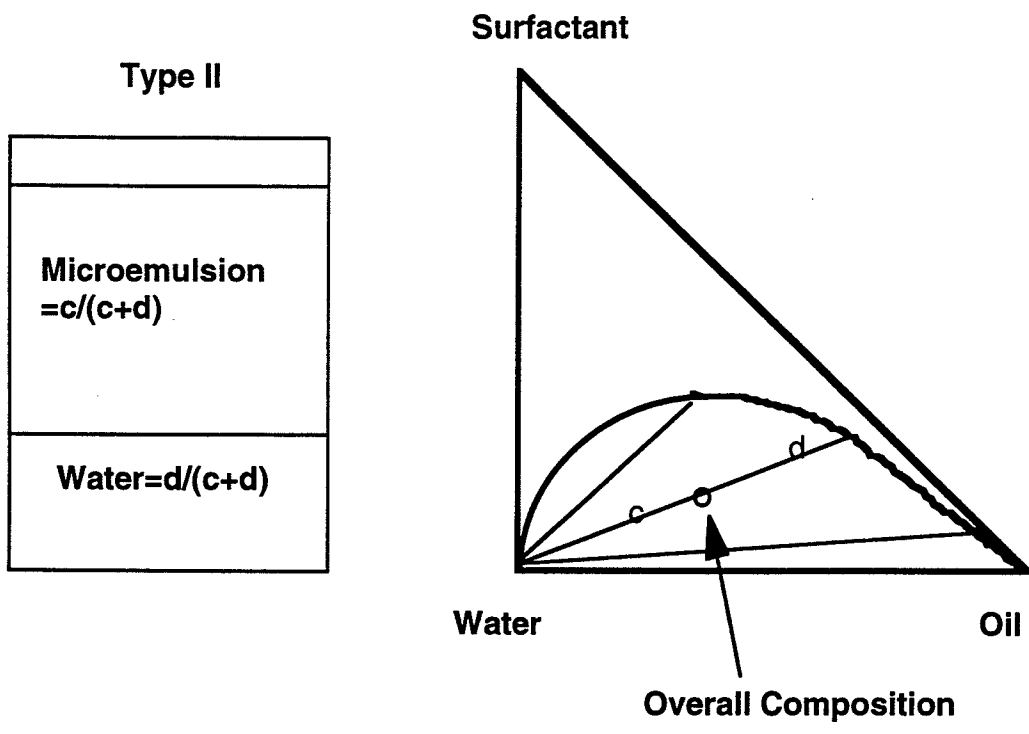


Figure 5.9: Type II ternary with oil, water and surfactant (reproduced from Nelson and Pope, 1978).

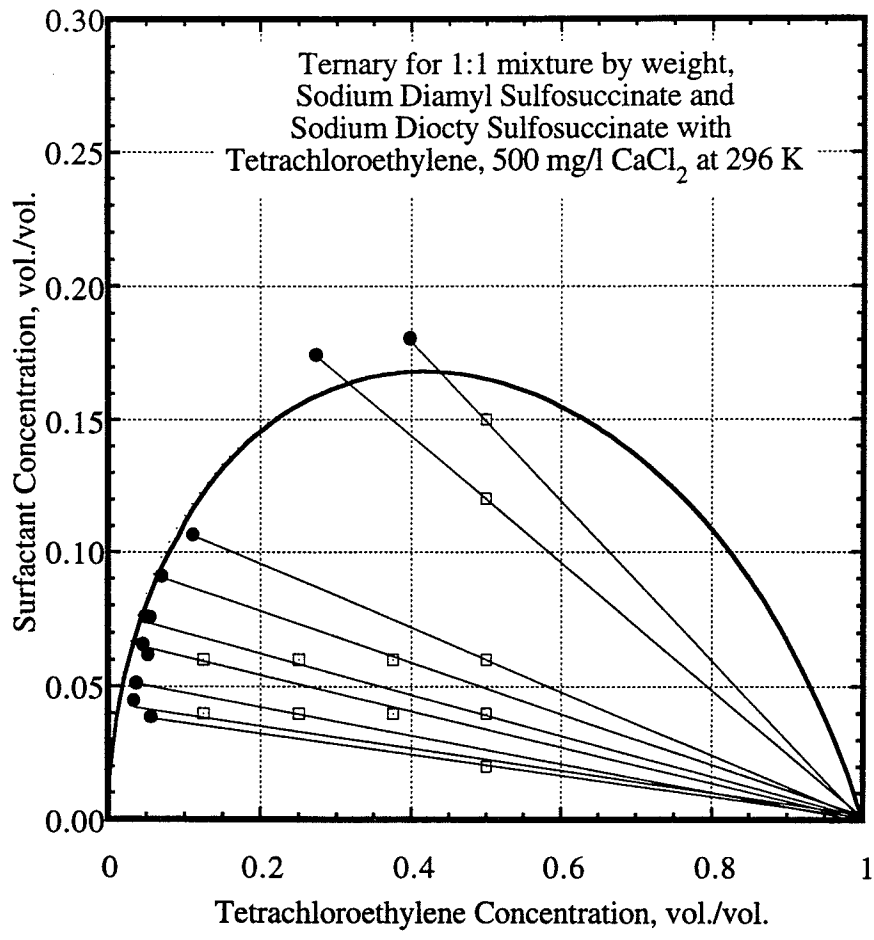


Figure 5.10: Ternary diagram of a surfactant formulation

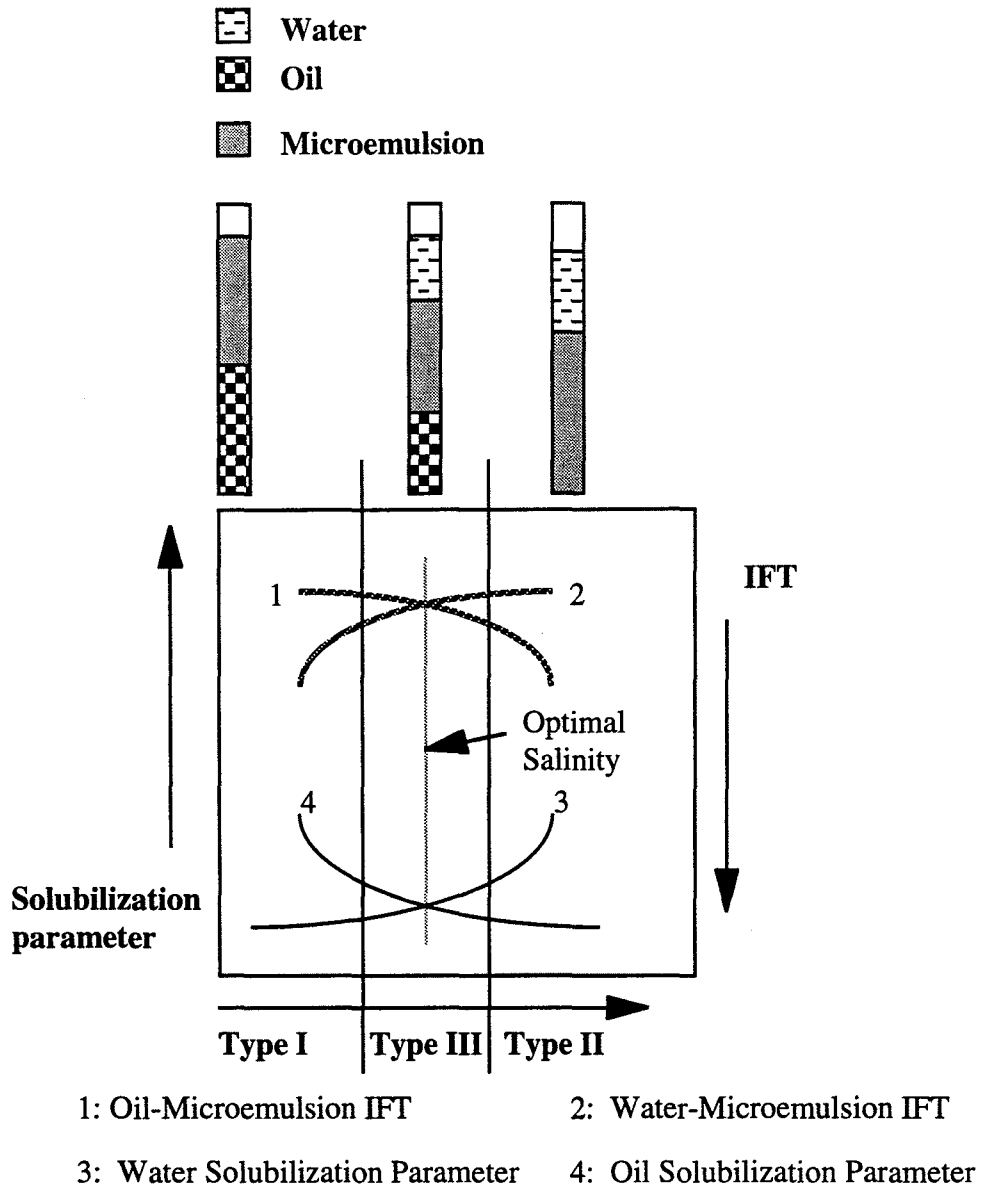


Figure 5.11: Illustration showing the relation between phase behavior and interfacial tensions between microemulsions and excess water and oil phases. (illustration based on Figure in Baran *et al.*, 1994b)

Chapter 6: Phase Behavior Results

In this Chapter, phase behavior results are presented in the form of volume fraction diagrams, solubilization ratio plots and contaminant solubility plots. The effect of contaminant type, electrolyte type, alcohol type and concentration, polymer and temperature on the phase behavior will be discussed.

6.1 PHASE BEHAVIOR RESULTS

The contaminants covered in this study were tetrachloroethylene (PCE), trichloroethylene (TCE), jet fuel (JP4) and Hill OU2 DNAPL from the Hill OU2 site at Hill AFB, Utah. The surfactants used in the study were sodium diamyl sulfosuccinate (C5), sodium dihexyl sulfosuccinate (C6), sodium diheptyl sulfosuccinate (C7) and sodium dioctyl sulfosuccinate (C8). Isopropanol (IPA, IPA), ethanol and secondary butyl alcohol (SBA) were used as the cosolvents to minimize gelling problems and reduce equilibration times. The surfactant structures are presented in Chapter 2.

6.1.1 PCE

The initial phase behavior work with PCE focused on repeating some of the work done by Jin (1995) and confirming and extending his results. A summary of all the phase behavior experiments carried out with PCE is presented in Table 6.1.

6.1.1.1 Salinity Scans

Phase behavior experiments were conducted with 4% by weight sodium dihexyl sulfosuccinate and PCE using both NaCl and CaCl₂ as the electrolyte.

The sodium dihexyl sulfosuccinate used here was commercially available as MA-80I from CYTEC. The volume fraction diagrams are plotted in Figures 6.1 and 6.2. The PCE and water solubilization parameters and PCE solubilization were plotted against electrolyte concentration. The results are plotted in Figures 6.3 through 6.6. The optimal salinities are about 5.5% by weight NaCl and 4.5% by weight CaCl₂, respectively, and the corresponding solubilization parameters are 1.2 and 1.0. Similar experiments were carried out by Baran *et al.*, (1994a) who performed phase behavior experiments with 2% by weight sodium dihexyl sulfosuccinate. This corresponds to a PCE solubilization of about 650,000 mg/l. A comparison of GC measurements and volumetric measurements to calculate contaminant solubilization is given in Chapter 4 and later in this Chapter. Thus, even though a solubilization ratio of 1.2 is not very high for a good surfactant, the enhancement of the solubility of PCE is still very substantial since it is on the order of a 2,000 fold increase. However, 5.5% by weight NaCl (~ 55,000 mg/l) is considered higher than desirable for use in a remedial flood. Furthermore, precipitation of the surfactant was observed in aqueous surfactant solutions at optimal salinity and this increases the chances that pore plugging might occur. The optimal salinity for the 2% by weight sodium dihexyl sulfosuccinate was 4.1% by weight NaCl and 2.4% CaCl₂.

Similar phase behavior experiments were also carried out using a solution of 2% by weight diamyl sulfosuccinate and 2% by weight dioctyl sulfosuccinate using NaCl as the electrolyte. The volume fraction diagram, solubilization parameter and contaminant solubilization data are plotted in Figures 6.7 through 6.9. The optimal salinity is about 8,500 mg/l NaCl. The solubilization parameter

is 7.5 and the PCE concentration is about 700,000 mg/l at optimum salinity. The volume fraction of the middle phase microemulsion at optimum salinity is about 0.3, which is twice that of the volume fraction of the type III microemulsion with sodium dihexyl sulfosuccinate. This is attributed to a the longer hydrophobe of sodium dioctyl sulfosuccinate. The lower optimal salinity and higher solubilization parameter would make sodium dioctyl sulfosuccinate more attractive as a candidate for application in contaminant remediation. However, after performing column experiments (see Chapter 8) in which sodium dioctyl sulfosuccinate was used without any cosolvent, gelling behavior was observed and sodium dioctyl sulfosuccinate was not used in subsequent phase behavior experiments without cosolvents.

6.1.1.2 Ternary Diagram

In order to obtain a better understanding of the surfactant phase behavior with PCE, experiments were conducted to construct a ternary diagram. The surfactant solution used was a 1:1 mixture of sodium diamyl sulfosuccinate and sodium dioctyl sulfosuccinate. The electrolyte used was CaCl_2 and the electrolyte concentration in the water was set at 500 mg/l. Phase behavior experiments were conducted at different surfactant concentrations and different PCE concentrations. The volumes of individual phases were measured and a binodal curve was drawn as shown in Figure 6.10. The tie lines were drawn using the overall composition and assuming that the tie lines all originate from the lower right corner. This is justified because the microemulsion is type I and the solubility of the water and surfactant in PCE is extremely small. The height of the binodal curve was 0.18.

The height of the binodal curve is a very important parameter to be used in modeling surfactant enhanced aquifer remediation (Brown, 1993; Brown *et al.*, 1994).

6.1.2 TCE

Similar phase behavior studies were conducted with TCE. Again, the work was divided into phase behavior experiments aimed toward generating volume fraction diagrams and experiments to obtain ternary diagrams. A summary of all the phase behavior work conducted is presented in Table 6.2.

6.1.2.1 Salinity Scans

Phase behavior experiments were conducted with 8% by weight sodium dihexyl sulfosuccinate and TCE using both NaCl and CaCl₂ as the electrolyte. The volume fraction diagrams are plotted in Figures 6.11 and 6.12. The TCE and water solubilization parameters are shown in Figures 6.13 and 6.14 and TCE solubilization in Figures 6.15 and 6.16. The optimal salinities are about 11,000 mg/l NaCl and 5,000 mg/l CaCl₂ respectively and the solubilization ratios at optimal salinity about 6 and 8. This corresponds to a TCE solubilization of about 700,000 mg/l. This microemulsion showed low equilibration times even with CaCl₂ and did not exhibit any precipitation or gelling problems. Additional phase behavior experiments with TCE were conducted by Shotts (1996) concurrently with this work. A discussion on coalescence, emulsion formation and equilibration times is presented in later sections.

6.1.2.2 Ternary Diagrams

A ternary diagram for 1,000 mg/l NaCl (type I) is shown in Figure 6.17. The maximum height of the binodal curve at this salinity is 0.14.

6.1.3 Hill DNAPL

A lot of phase behavior experiments were performed with Hill DNAPL from the Operational Unit 2 site at Hill AFB Utah. The composition of the Hill DNAPL is described in Chapter 10. TCE was the primary component in the DNAPL. Since the solvents at Hill Air Force Base were primarily used as degreasers, the DNAPL was black in color (due to the presence of dissolved grease). The density of the DNAPL is 1.383 g/cc. The interfacial tension varied between 4 to 7 dyne/cm. These appear to be the first time that DNAPL from a field site has been used in a surfactant study since no other data could be found in the literature. These phase behavior data were used to develop several volume fraction diagrams. A summary of the phase behavior experiments carried out with Hill DNAPL is presented in Table 6.3.

6.1.3.1 Salinity Scans

The main objective of performing several phase behavior studies was to identify surfactant solutions with suitable solubilization parameters and low equilibration times for use in the surfactant flood at Hill OU2 AFB in Utah. Several phase behavior studies were carried out with 500 mg/l xanthan gum polymer. This was done to quantify surfactant-DNAPL behavior in the presence of xanthan gum polymer. The main advantage of using polymer in a field surfactant flood is a better sweep of layers with low permeabilities. Some phase

behavior was carried out by Shotts (1996) in which 4% by weight sodium dihexyl sulfosuccinate and 8% by weight IPA were mixed in Hill source water. One set of experiments was carried out with 500 mg/l xanthan gum and the other set was carried out with 0 mg/l xanthan gum. These results showed no effect of the xanthan gum polymer on the phase behavior within experimental error. In both instances, the optimal salinity was between 9,800 mg/l NaCl and 10,400 mg/l NaCl. The solubilization parameter at optimal salinity was about 4.0. This result is in agreement with observations made with TCE with and without polymer.

The volume fraction diagrams for 4% by weight sodium dihexyl sulfosuccinate, 4% by weight IPA, 500 mg/l xanthan gum and NaCl in Hill source water and 4% by weight sodium dihexyl sulfosuccinate, 4% by weight ethanol, 500 mg/l xanthan gum and NaCl in Hill source water are plotted in Figures 6.18 and 6.19. The solubilization parameters and contaminant solubilization are plotted in Figures 6.20 and 6.21. Satisfactory behavior was observed in all the samples in terms of equilibration times and absence of liquid crystals, emulsions and gels. The equilibration times were less than 15 hours for all samples. The samples at optimal salinity reached equilibrium in less than 12 hours. The optimal salinity was about 11,500 mg/l with both alcohols. The solubilization parameter at optimal salinity was about 5.2 and this corresponded to a contaminant solubilization of about 700,000 mg/l. Since phase behavior results with IPA and ethanol were similar in terms of solubilization and equilibration times, it can be concluded that either IPA or ethanol could be used as a cosolvent.

Phase behavior studies were also conducted using 8% by weight sodium dihexyl sulfosuccinate, 8% by weight IPA and 500 mg/l xanthan gum using both

NaCl and CaCl₂ as the electrolyte mixed in Hill source water. Hill source water was the tap water available at Hill Air Force Base. The composition of Hill source water is given in Table 10.2. The phase behavior for the 8% by weight sodium dihexyl sulfosuccinate, 8% by weight IPA, and 500 mg/l xanthan gum using NaCl was conducted at both 12.2°C and 23°C. Groundwater temperature at Hill Air Force Base was 12.2°C.

The volume fraction diagrams for 8% by weight sodium dihexyl sulfosuccinate, 8% by weight IPA, 500 mg/l xanthan gum and NaCl at 23°C and 12.2°C and 8% by weight sodium dihexyl sulfosuccinate, 8% by weight IPA, 500 mg/l xanthan gum and CaCl₂ at 23°C are plotted in Figure 6.22. The optimal salinity is decreased from 8,300 mg/l at 23°C to 5,850 mg/l at 12.2°C when NaCl was the electrolyte. When CaCl₂ was the electrolyte, the optimal salinity was 4,650 mg/l at 23°C.

The electrolyte concentrations were normalized using the optimal salinity for all the above results and the solubilization parameter data are shown in Figure 6.23. Contaminant solubility data for these experiments (in relation to normalized electrolyte concentration) are plotted in Figure 6.24. A solubilization parameter of between 3.6 to 4.4 was measured at optimal salinity for the three solutions. This corresponds to a solubilization between 425,000 mg/l to 475,000 mg/l contaminant. The data from these phase behavior experiments were used by Brown *et al.* (1996a,b) to design the field tests at Hill AFB OU2.

Additional phase behavior studies were performed with 8% by weight sodium dihexyl sulfosuccinate, 4% by weight IPA, NaCl and Hill source water and 8% by weight sodium dihexyl sulfosuccinate, 2% by weight IPA, NaCl and

Hill source water at different temperatures. This was done for fine tuning the SEAR design at Hill OU2. The electrolyte concentration was normalized by using the optimal salinity at each temperature. The volume fraction diagrams as a function of normalized electrolyte concentration are plotted in Figures 6.25 and 6.26. The solubilization parameters are plotted in Figures 6.27 and 6.28. The contaminant solubilization data are plotted in Figures 6.29 and 6.30, which show that as the temperature decreases, a decrease in optimal salinity is observed. The solubilization parameter at optimal salinity for the solution with 2% by weight IPA was about 6.0 at 23°C and the solubilization parameter at optimal salinity for the solution with 4% by weight IPA was 5.4 at 23°C. The contaminant solubilization was 600,000 mg/l for the surfactant solution with 4% by weight alcohol and 675,000 mg/l with 2% by weight alcohol.

A discussion of all the phase behavior data described in this work and Shotts (1996) will be presented later in this Chapter.

6.1.4 JP4

Many surfactant phase behavior experiments were performed with jet fuel. The jet fuel was obtained from March AFB. Some phase behavior using JP4 has been described by Baran *et al.* (1996b). A summary of all the phase behavior experiments performed in this study is described in Table 6.4.

6.1.4.1 Salinity Scans

The main objective of performing phase behavior experiments with jet fuel was to identify surfactant solutions exhibiting Winsor type III behavior. This

type of behavior gives low interfacial tensions that cause mobilization of the LNAPL in soil column studies.

In many phase behavior experiments conducted without cosolvent, formation of extremely thick gels and macroemulsions were observed. No measurable solubilization was observed (by reading volumes only) in phase behavior samples containing:

1. 4% by weight sodium dihexyl sulfosuccinate
2. 3.6% by weight sodium dihexyl sulfosuccinate and 0.4% by weight sodium dioctyl sulfosuccinate
3. 2.8% by weight sodium dihexyl sulfosuccinate and 1.2% by weight sodium dioctyl sulfosuccinate.

For the surfactant solution containing 2.0% by weight sodium dihexyl sulfosuccinate and 2.0% by weight sodium dioctyl sulfosuccinate, no measurable solubilization was observed for NaCl concentrations from 0 to 2,000 mg/l. The samples however exhibited thick emulsions. Similar results were observed in phase behavior studies with:

1. 2.8% by weight sodium dioctyl sulfosuccinate and 1.2% by weight sodium dihexyl sulfosuccinate
2. 3.6% by weight sodium dioctyl sulfosuccinate and 0.4% by weight sodium dihexyl sulfosuccinate solutions.

The macroemulsion problems were observed to increase as increasing fractions of the sodium dioctyl sulfosuccinate were blended in. No coalescence was observed after 10 days. This is attributed to the increase in the surfactant tail length and lack of branching of sodium dioctyl sulfosuccinate. The length of the

hydrophobic tail of the sodium dioctyl sulfosuccinate molecule is greater than the length of the hydrophobic tail of the sodium dihexyl sulfosuccinate molecule and has less branching.

In order to eliminate the excessive gel/macroemulsion formation, a new surfactant, sodium diheptyl sulfosuccinate was used. This surfactant was synthesized by Weerasooriya (1994). In the initial phase behavior studies with the sodium diheptyl sulfosuccinate, the surfactant solutions containing 2 % by weight sodium diheptyl sulfosuccinate and 2 % by weight secondary butyl alcohol by weight were used. Two sets of experiments were performed. In the first set, NaCl was the electrolyte and in the second set a mixture of NaCl and CaCl₂ at a 9:1 ratio was used. The total electrolyte concentration was varied from 1,000 mg/l to 9,000 mg/l. In both sets of samples, thick macroemulsions were observed after 24 hours of equilibration. In the second set of samples, the sample with 9,000 mg/l total electrolyte (8,100 mg/l NaCl and 900 mg/l CaCl₂) exhibited three phase behavior with an oil solubilization ratio of 6.25 and water solubilization ratio of 7.25. Samples were observed to coalesce after 7 to 10 days. Based on these results, it was decided to increase the alcohol concentration to minimize gel/macroemulsion formation.

In subsequent phase behavior studies, an electrolyte mixture containing a 9:1 mixture of NaCl and CaCl₂ was used with all the surfactant solutions. Phase behavior studies were carried out using 2% and 4% by weight sodium diheptyl sulfosuccinate solutions. The alcohol concentration was varied from 5% by weight to 8% by weight.

The volume fraction diagrams for 2% sodium diheptyl sulfosuccinate with 5% SBA and 8% SBA are plotted in Figure 6.31. The oil and water solubilization parameter data are plotted in Figure 6.32. The optimal salinity increased from 11,500 mg/l to 13,500 mg/l when the alcohol concentration increased from 5% to 8% by weight. The solubilization parameter at optimal salinity decreased from 4.5 to 4.0 when the alcohol concentration was increased from 5% to 8% by weight.

Similarly, the volume fraction diagrams for 4% by weight sodium diheptyl sulfosuccinate with 6% by weight SBA and 8% by weight SBA are plotted in Figure 6.34. The solubilization parameter data and contaminant solubilization data are plotted in Figures 6.35 and 6.36. The optimal salinity increased from 12,000 mg/l to 13,000 mg/l when the alcohol concentration was increased from 6% to 8% by weight. The contaminant solubilization parameter was 4 at optimal salinity in both cases.

In all these experiments, no evidence of gel or liquid crystal formation was observed. The viscosities of the aqueous surfactant solutions were measured as an additional performance measure of the acceptability of these mixtures. The viscosity of a few aqueous solutions of 4% by weight sodium diheptyl sulfosuccinate and 8% by weight secondary butyl alcohol at varying electrolyte concentrations are plotted in Figure 6.37. The viscosities varied between 1.5 to 2.0 cp and Newtonian behavior was observed. Both these are indications that no significant gel or liquid crystal problem existed for these compositions. This was considered an acceptable viscosity for injection into the subsurface. However column studies are still needed as a final check since problems can still occur

despite these favorable screening results e.g. gels can form at lower oil concentrations than tested here.

Since sodium diheptyl sulfosuccinate was not commercially available, it was decided that a 1:1 mixture of sodium dihexyl sulfosuccinate and sodium dioctyl sulfosuccinate be tested in phase behavior experiments. Phase behavior experiments were conducted with a surfactant solution consisting of 2% by weight sodium dioctyl sulfosuccinate, 2% by weight sodium dihexyl sulfosuccinate, 8% by weight secondary butyl alcohol and electrolyte consisting of a mixture of 9:1 NaCl and CaCl₂ by weight. The volume fraction diagram for the solution is plotted in Figure 6.38. The solubilization parameter data are plotted in Figure 6.39 and contaminant solubilization data are plotted in Figure 6.40. A complete volume fraction diagram was not obtained as enough jet fuel was unavailable to complete the phase behavior experiments. The optimal salinity was estimated by extrapolation as 14,000 mg/l of total electrolyte. The solubilization parameter at optimal salinity was estimated as 3.5 and this corresponded to a contaminant solubilization of 300,000 mg/l. The viscosity of the aqueous surfactant solution was measured at 11,000 mg/l total electrolyte concentration. The viscosities ranged between 1.5 and 2.0 cp for shear rates between 0.01 sec⁻¹ to 100 sec⁻¹.

6.2 DISCUSSION ON PHASE BEHAVIOR

Based on all the phase behavior experiments, several conclusions and inferences were drawn. During the course of this work and the work done by Shotts (1996), the effect of various parameters such as temperature, length of

surfactant hydrophobe tail, alcohol concentration and polymer were studied. These are described in the following sections.

6.2.1 Comparison of Phase Behavior Results from Literature

There are many techniques to analyze and discuss phase behavior results. In the petroleum literature, the term solubilization parameter is defined as the ratio of the volume of oil (or water) solubilized and the volume of surfactant (Bourrel and Schechter, 1988; Pope and Baviere, 1991). This is very useful as above the CMC the oil and water solubilization parameters are usually constant for a well behaved surfactant. Another advantage of using this approach is that the interfacial tensions between the microemulsion and excess water or oil phases can be estimated using the Chun Huh equation (Huh, 1979).

Another technique to analyze phase behavior results is to present the solubilization in terms of a molar solubilization ratio (MSR). The molar solubilization ratio can be defined as the average number of molecules solubilized per micelle divided by the aggregation number (Edwards *et al.*, 1991b). From the molar solubilization ratio we can calculate the micelle/aqueous phase partition coefficient can be calculated. Both the MSR and the micelle/aqueous phase partition coefficients can be derived using the following equations (Edwards *et al.*, 1991):

$$\text{MSR} = \frac{S_{N,\text{mic}} - S_{N,\text{cmc}}}{C_{\text{surf}} - \text{CMC}} \quad (6.1)$$

$$X_m = \frac{S_{N,mic} - S_{N,cmc}}{C_{surf} - CMC + S_{N,mic} - S_{N,cmc}} = \frac{MSR}{1 + MSR} \quad (6.2)$$

$$K_m = \frac{X_m}{X_a} = \frac{X_m}{S_{N,cmc} V_{wa}} \quad (6.3)$$

In this work, the phase behavior results are presented in terms of water and oil solubilization parameters. However, some comparisons were made with phase behavior results presented in the literature in order to compare the performance of sodium dihexyl sulfosuccinate with other surfactants used for remediation. The oil solubilization parameter for several surfactant solutions with various contaminants is given in Table 6.5. The molar solubilization ratios for some of the corresponding surfactant solutions are given in Table 6.6. Abbreviations, surfactant chemical names and some surfactant characteristics are given in Table 6.7.

From Table 6.5, it is evident that surfactant solutions with high molar solubilization ratios have high contaminant solubilization. It can also be seen that contaminant solubilization by sodium dihexyl sulfosuccinate is higher than other surfactants used in previous and concurrent work. Since sodium dihexyl sulfosuccinate is an anionic surfactant, an increase in the MSR was observed as more sodium chloride is added to the surfactant solution. This corresponds to a transition from Winsor type I to Winsor type III to Winsor type II behavior. High contaminant solubilization greater than 600,000 mg/l is due to the formation of middle phase microemulsions or presence of Winsor type III behavior.

6.2.2 Coalescence Times and Liquid Crystal Formation

One of the objectives of performing phase behavior experiments was to identify surfactants with low coalescence times since such behavior is one of the most important indicators of good performance in field tests. Complications such as liquid crystal formation and macroemulsion formation have been observed by Reed and Healy (1977) and others testing surfactants for enhanced oil recovery and discussed by Bourrel and Schechter (1988) and Rosen (1988). As early as 1968, alcohols were used and patented by the oil company researchers for the explicit purpose of minimizing problems with gels and emulsions. The worst problems in this study were with jet fuel. Macroemulsion formation was observed and sample coalescence times were in excess of seven days for many samples. This behavior is undesirable as macroemulsions can lead to problems such as pore plugging in the subsurface. The desired behavior is for the emulsions to break and for clean microemulsions to form within a few hours of equilibration in an unshaken pipette.

In phase behavior experiments conducted with TCE and sodium dihexyl sulfosuccinate, when surfactant and TCE were mixed a milky white emulsion was formed. These emulsions coalesced in less than 24 hours when no alcohol was added forming clear (with a bluish tinge) microemulsion phases. In experiments with Hill DNAPL, a chocolate brown emulsion was formed on mixing surfactant and DNAPL. After coalescence, a transparent golden brown microemulsion was observed. When Hill DNAPL was used, the emulsions were much thicker and in the presence of 2% by weight isopropanol they were observed to coalesce in less

than 24 hours at 23°C. When the alcohol concentration was increased to 4% isopropanol by weight, the coalescence time was reduced to less than 15 hours. Samples at optimal salinity were observed to coalesce in less than 4 hours. When polymer was added to the surfactant, coalescence times were slower but after 20 hours no evidence of macroemulsions or liquid crystals were observed.

Some surfactant solutions are prone to precipitation and liquid crystal formation in the presence of CaCl_2 . Hence, it was important to use CaCl_2 as the electrolyte to study the sensitivity of the surfactant solution to Ca^{++} . When a sodium-rich anionic surfactant solution is injected into the subsurface, the sodium ions replace the calcium ions on the clay by cation exchange. Hence, there is an overall movement of calcium ions from the clays to the micelles and replacement of the calcium ions by sodium ions on the clay. This causes an increase in the calcium ion concentration in the surfactant solution as the surfactant solution flows through the subsurface. The presence of calcium ions decreases the optimal salinity as observed earlier in phase behavior results with CaCl_2 . Hence, if enough calcium is released during surfactant flooding, the remediation regime may be shifted to Winsor type II (type II⁺). Type II behavior is undesirable since it promotes high surfactant retention in the form of microemulsion trapping. Phase behavior experiments with CaCl_2 were performed in order to characterize the effect of CaCl_2 on surfactant phase behavior and determine at what point type II behavior would occur.

6.2.3 Effect of Temperature

Anionic surfactants are affected by changes in temperature. A higher probability of gel and liquid crystal formation and longer equilibration times are expected at lower temperatures. The optimal salinity of anionic surfactants such as alkyl sulfates or sulfonates increases as the temperature increases. This was observed in several phase behavior experiments with both TCE and Hill DNAPL using sulfosuccinates which are sulfonates. This type of behavior is caused by an increase in the relative solubility of the anionic surfactant in the aqueous phase compared to the solubility of the anionic surfactant in the nonaqueous phase as temperature is increased. Hence, more electrolyte is required to cause a phase change of the microemulsion from Winsor type I to Winsor type III.

In Figures 6.41 and 6.42, the effect of temperature on optimal salinity for surfactant solutions with TCE and Hill DNAPL is presented. As reported by Salager *et al.* (1979), a linear trend between the optimal salinity and temperature on a semi log plot is observed for both TCE and Hill DNAPL in both figures.

In order to compare the phase behavior for a given anionic surfactant at different temperatures, the electrolyte concentration in the surfactant is normalized by the optimal salinity at a given temperature. The solubilization data are plotted against the normalized electrolyte concentration. Even though the optimal salinity changes as temperature varies, the phase behavior essentially remains unchanged. The relative width of the three phase region with respect to the optimal salinity remains constant. This is confirmed by results in Figures 6.27 and 6.28 where the solubilization parameter data of Hill DNAPL with two

surfactants at different temperatures are plotted. Within experimental error, the data overlay each other. Similar overlap within experimental error is observed when the contaminant solubilization is plotted against normalized electrolyte concentration in Figures 6.29 and 6.30.

This is very useful in designing field surfactant floods. The exact optimal salinity for a given surfactant at a required temperature can be determined using the correlation between optimal salinity and temperature. Using the normalized phase behavior diagrams, solubilization parameter data and contaminant solubilization can be determined at the required temperature.

6.2.4 Effect of Alcohol Concentration

Alcohol was used as a cosolvent in many surfactant solutions. The main purpose of the addition of alcohol was lowering the equilibration times of the microemulsions. This was attributed to alcohol partitioning between the oil, water and surfactant micelles. Heavier alcohols partition strongly to the oil and micelles and shift the phase behavior from type I to III or even II. In this work, heavier alcohols like pentanol and hexanol were not used as cosolvents. Instead, isopropanol, ethanol and secondary butyl alcohol were used. This was done mainly for elimination of gels/liquid crystals and not for lowering optimal salinity, although a slow decrease does occur.

Also, a lower solubilization parameter and a corresponding reduction in contaminant solubilization was observed, which is consistent with the well known behavior in the EOR literature e.g. Salager *et al.* (1979). A good example is presented in Figure 6.43 (data from Shotts, 1996). The surfactant concentration

was fixed at 4 % by weight sodium dihexyl sulfosuccinate and the isopropanol concentration was varied between 0% and 8% by weight. Both the solubilization parameter and optimal salinity are observed to decrease linearly. The optimal salinity is lowered from 12,500 mg/l NaCl for the solution with no IPA to 5,000 mg/l NaCl for the solution with 20% by weight IPA at 23°C. The solubilization parameter correspondingly decreased from 6.5 to 4.5. Similar results were observed for a solution of 8% by weight sodium dihexyl sulfosuccinate mixed in Hill source water and Hill DNAPL at different alcohol concentrations and temperatures as shown in Figure 6.44. It is seen that the behavior of the Hill DNAPL is similar to that of pure TCE. The optimal salinity for the 8% by weight sodium dihexyl sulfosuccinate decreased from 11,600 mg/l at 2% by weight IPA to 8,300 mg/l at 8% by weight IPA at 23°C. The solubilization parameter correspondingly decreased from 6.2 to 4.4 when the alcohol concentration was increased from 2% by weight to 8% by weight.

The molecular weight of the alcohol significantly affects the type of phase behavior observed. Alcohols like methanol, ethanol and IPA that partition very slightly into contaminants like TCE, PCE and jet fuel do not cause significant reduction in the optimal salinity whereas heavier alcohols like secondary butyl alcohol, pentanol and hexanol will cause lower optimal salinity. This is attributed to the partitioning of the heavier alcohols between the aqueous and the oleic phase which causes a change in phase behavior. For a solution containing 3.6% by weight sodium dihexyl sulfosuccinate, 0.4% by weight sodium dioctyl sulfosuccinate, 8% by weight IPA and 500 mg/l xanthan gum, the optimal salinity

was 5,800 mg/l NaCl (data from Shotts, 1996). When the IPA was replaced with secondary butyl alcohol, the optimal salinity decreased to 5,200 mg/l.

One exception in surfactant phase behavior on addition of alcohol was observed when experiments were carried out with jet fuel and the sulfosuccinate surfactants using secondary butyl alcohol as the cosolvent. The optimal salinity was observed to increase on addition of increasing amounts of SBA. For a surfactant solution with 2% by weight sodium diheptyl sulfosuccinate with 5% by weight SBA, the optimal salinity was at 11,500 mg/l electrolyte (90% NaCl and 10% CaCl₂). When the alcohol concentration was increased to 8% by weight the optimal salinity increased to 13,500 mg/l. The solubilization parameter was observed to decrease as expected. Thus, alcohols always decrease the optimal solubilization, but this is a favorable tradeoff provided problems with emulsions, gels and liquid crystals are eliminated.

6.2.5 Effect of Electrolyte Type

The effect of the type of electrolyte used for mixing the surfactant solution is extremely important. For a surfactant solution consisting of 2% by weight sodium diamyl sulfosuccinate and 2% by weight dioctyl sulfosuccinate with CaCl₂ and PCE at 21°C, the optimal salinity was 1,200 mg/l (Jin, 1995). When the CaCl₂ was replaced with NaCl, the optimal salinity was 9,000 mg/l. Similarly, the optimal salinity for a solution containing 4% by weight sodium dihexyl sulfosuccinate using PCE was observed to decrease from 5.5% to 4.5% when NaCl was replaced by CaCl₂. Similar results were obtained with TCE where the optimal salinity for a surfactant solution containing 8% by weight

sodium dihexyl sulfosuccinate decreased from 11,000 mg/l with NaCl to 5,000 mg/l with CaCl₂. During phase behavior studies with 8% by weight sodium dihexyl sulfosuccinate, 8% by weight IPA and Hill DNAPL the optimal salinity decreased from 8,300 mg/l NaCl to 4,650 mg/l CaCl₂. This lowering of optimal salinity in the presence of CaCl₂ is attributed to the divalent nature of the calcium ions as compared to the monovalent nature of sodium ions.

6.2.6 Effect of Surfactant Tail Length

The effect of surfactant tail length and branching on phase behavior is extremely important. Higher oil solubilities are caused by longer surfactant tails. This translates into higher oil solubilization parameters and lower optimal salinities. A longer surfactant tail also makes the surfactant solution more susceptible to liquid crystal formation. This is because longer surfactant tails tend to stack up to form liquid crystals. The sodium dihexyl sulfosuccinate used in this work was a twin tailed surfactant and hence minimal liquid crystal formation was observed in most experiments.

The effect of the tail length on solubilization parameter and optimal salinity is shown in Figure 6.45. A surfactant solution containing 8% by weight surfactant, 8% by weight IPA and NaCl was used for phase behavior. The fraction of sodium dihexyl sulfosuccinate was increased from 0.5 to 1 in the surfactant mixture and correspondingly the fraction of sodium diamyl sulfosuccinate was decreased from 0.5 to 0. Sodium dihexyl sulfosuccinate has a longer tail than the sodium diamyl sulfosuccinate. A decrease in optimal salinity and increase in solubilization parameter is observed when the fraction of sodium

dihexyl sulfosuccinate in the surfactant solution is increased. The optimal salinity for a solution with 4% by weight sodium diamyl sulfosuccinate and 4% by weight sodium dihexyl sulfosuccinate was 10,400 mg/l NaCl with a solubilization parameter of 4.5. In comparison, for 8% by weight sodium dihexyl sulfosuccinate, the optimal salinity dropped to 7,400 mg/l NaCl and the solubilization parameter increased to 5.2. This is directly due to the increased surfactant tail length of the sodium dihexyl sulfosuccinate over the sodium diamyl sulfosuccinate.

6.2.7 Effect of Polymer

The addition of polymer has many advantages for remediation. Due to the increased viscosity of the surfactant solution when polymer is added to it increased sweep efficiency is obtained. Increased sweep efficiency corresponds to a mitigation of aquifer heterogeneities. Almost all of the undesirable effects of heterogeneity can be eliminated if the viscosity of the displacing solution is sufficiently high (Lake, 1989; Sorbie, 1991; Pope and Wade, 1995). However, in order to use polymer successfully, several phase behavior experiments have to be carried out to quantify the effect of polymer on phase behavior, coalescence times, etc. The polymer used here was xanthan gum. Xanthan gum is a highly biodegradable commercial food additive. Many studies were carried out by Shotts (1996) in which phase behavior studies were conducted with surfactant solutions containing polymer and surfactant solutions without polymer. An example is presented in Figure 6.46 for a solution containing 4% by weight sodium dihexyl sulfosuccinate, 8% by weight IPA and NaCl with TCE with and

without 500 mg/l xanthan gum. A very close overlap is observed between both volume fraction diagrams indicating that addition of polymer did not cause any change in phase behavior.

An important exception was observed when polymer was used in phase behavior experiments at the lower critical salinity, (transition between type I and III) where gel formation in the aqueous phase was observed. Similar behavior was observed by Tsaur (1978) and Shotts (1996). This is due to the very high concentration of polymer in the aqueous phase at the lower critical salinity as microemulsion phase is just being formed. This behavior was minimized by addition of sufficient quantities of isopropanol. It can be avoided by changing the salinity and other variables as well.

6.3 COMPARISON OF GC AND VOLUMETRIC MEASUREMENTS OF SOLUBILIZATION

The contaminant solubilization data presented in this work were calculated by volumetric measurements (discussed in Chapter 4). A comparison of volumetric measurements of Hill OU2 contaminant solubilization and gas chromatograph measurements of contaminant solubilization is made in Figures 6.47 and 6.48. The surfactant mixture used in Figure 6.47 is 4% by weight sodium dihexyl sulfosuccinate, 4% IPA and 500 mg/l xanthan gum at different sodium chloride concentrations in Hill source water. A similar comparison is made in Figure 6.48 for the solubilization data at different surfactant concentrations and temperatures. In general the GC measurements are more accurate at low contaminant concentrations (<20,000 mg/l) and the volumetric data are more accurate at high contaminant concentrations (>20,000 mg/l). Since

the volumetric measurements are both much faster and more accurate at the high contaminant concentrations of most interest in this study, this was the method used the most.

Table 6.1: Summary of phase behavior experiments with PCE.

Surfactant solution	Type of Experiment
4% by weight Sodium dihexyl sulfosuccinate, NaCl,	Volume fraction diagrams, salinity scan
4% by weight Sodium dihexyl sulfosuccinate, CaCl ₂	Volume fraction diagrams, salinity scan
2% by weight Sodium diamyl sulfosuccinate, 2% by weight sodium dioctyl sulfosuccinate, NaCl	Volume fraction diagrams, salinity scan
1:1 sodium diamyl sulfosuccinate and sodium dioctyl sulfosuccinate, CaCl ₂	Ternary diagram

Table 6.2: Summary of phase behavior experiments with TCE.

Surfactant solution	Type of Experiment
8% by weight Sodium dihexyl sulfosuccinate, NaCl,	Volume fraction diagrams, salinity scan
8% by weight Sodium dihexyl sulfosuccinate, CaCl ₂	Volume fraction diagrams, salinity scan
Sodium dihexyl sulfosuccinate, NaCl	Ternary diagram
Sodium dihexyl sulfosuccinate, NaCl, IPA	Ternary diagram

Table 6.3: Summary of phase behavior experiments with Hill DNAPL.

Surfactant solution	Type of Experiment
4% by weight Sodium dihexyl sulfosuccinate, 4% by weight IPA, NaCl, xanthan gum, Hill source water	Volume fraction diagrams, salinity scan
4% by weight Sodium dihexyl sulfosuccinate, 4% by weight ethanol, NaCl, xanthan gum, Hill source water	Volume fraction diagrams, salinity scan
8% by weight Sodium dihexyl sulfosuccinate, 8% by weight IPA, NaCl, xanthan gum, Hill source water	Volume fraction diagrams, salinity scan
8% by weight Sodium dihexyl sulfosuccinate, 2% by weight IPA, NaCl, Hill source water at different temperatures	Volume fraction diagrams, salinity scan
8% by weight Sodium dihexyl sulfosuccinate, 4% by weight IPA, NaCl, Hill source water at different temperatures	Volume fraction diagrams, salinity scan

Table 6.4: Summary of phase behavior experiments with Jet fuel.

Surfactant solution	Type of Experiment
4% by weight sodium dihexyl sulfosuccinate	Salinity scan, volume fraction diagrams using NaCl.
3.6% by weight sodium dihexyl sulfosuccinate, 0.4% by weight sodium dioctyl sulfosuccinate	Salinity scan, volume fraction diagrams using NaCl.
2.8% by weight sodium dihexyl sulfosuccinate, 1.2% by weight sodium dioctyl sulfosuccinate	Salinity scan, volume fraction diagrams using NaCl.
2.0% by weight sodium dihexyl sulfosuccinate, 2.0% by weight sodium dioctyl sulfosuccinate	Salinity scan, volume fraction diagrams using NaCl.
2.0% by weight sodium dihexyl sulfosuccinate, 2.0% by weight sodium dioctyl sulfosuccinate	Salinity scan, volume fraction diagrams using NaCl.
1.2% by weight sodium dihexyl sulfosuccinate, 2.8% by weight sodium dioctyl sulfosuccinate	Salinity scan, volume fraction diagrams using NaCl.
0.4% by weight sodium dihexyl sulfosuccinate, 3.6% by weight sodium dioctyl sulfosuccinate	Salinity scan, volume fraction diagrams using NaCl.
2% by weight sodium diheptyl sulfosuccinate, 5% by weight secondary butyl alcohol	Salinity scan, volume fraction diagrams using NaCl.
2% by weight sodium diheptyl sulfosuccinate, 8% by weight secondary butyl alcohol	Salinity scan, volume fraction diagrams using 9:1, NaCl and CaCl ₂ .
4% by weight sodium diheptyl sulfosuccinate, 6% by weight secondary butyl alcohol	Salinity scan, volume fraction diagrams.
4% by weight sodium diheptyl sulfosuccinate, 8% by weight secondary butyl alcohol	Salinity scan, volume fraction diagrams.
2.0% by weight sodium dihexyl sulfosuccinate, 2.0% by weight sodium dioctyl sulfosuccinate, 8% by weight secondary butyl alcohol	Salinity scan, volume fraction diagrams.

Table 6.5: Comparison of solubilization parameters for several surfactants

Surfactant	Electrolyte Concentration (mg/l)	NAPL	Solubilization Parameter (cc/cc)	Solubilization mg/l
8% MA-80I	1,000 mg/l NaCl	TCE	0.31	35,000
8% MA-80I	4,000 mg/l NaCl	TCE	0.47	52,000
8% MA-80I	10,000 mg/l NaCl	TCE	3.44	314,000
8% MA-80I	11,750 mg/l NaCl	TCE	9.84	965,000
8% MA-80I	7,500 mg/l NaCl	PCE	0.26	27,000
8% MA-80I	30,000 mg/l NaCl	PCE	0.44	47,000
8% MA-80I	52,500 mg/l NaCl	PCE	1.09	618,000
8% MA-80I	67,500 mg/l NaCl	PCE	1.21	772,000
0.03% Tergitol	no electrolyte	Phenanthrene		43
1.44% SDS	121 mg/l TDS	TCE	0.17	3,613
19.33% TMAZ28	121 mg/l TDS	TCE	0.01	4,000
6.33% TMAZ20	121 mg/l TDS	TCE	0.17	15,727
6.55% TMAZ60	121 mg/l TDS	TCE	0.23	21,803
5% AOT and SMDNS	121 mg/l TDS	TCE		594,000
5% AOT and SMDNS	121 mg/l TDS	PCE		619,000
Rexophos 25/97		PCE		9,000
Alkasurf NP10		PCE		22,000

Table 6.6: Comparison of molar solubilization ratios for several surfactants

Surfactant	Electrolyte Concentration (mg/l)	NAPL	MSR	Reference
8% MA-80I	1,000 mg/l NaCl	TCE	1.30	Dwarakanath, 1997
8% MA-80I	4,000 mg/l NaCl	TCE	2.58	Dwarakanath, 1997
8% MA-80I	10,000 mg/l NaCl	TCE	11.84	Dwarakanath, 1997
8% MA-80I	11,750 mg/l NaCl	TCE	36.48	Dwarakanath, 1997
8% MA-80I	7,500 mg/l NaCl	PCE	0.80	Dwarakanath, 1997
8% MA-80I	30,000 mg/l NaCl	PCE	1.38	Dwarakanath, 1997
8% MA-80I	52,500 mg/l NaCl	PCE	18.51	Dwarakanath, 1997
8% MA-80I	67,500 mg/l NaCl	PCE	23.13	Dwarakanath, 1997
0.03% Tergitol	no electrolyte	Phenanthrene	0.16	Edwards <i>et al.</i> , 1991
1.44% SDS	121 mg/l TDS	TCE	0.39	Shiau <i>et al.</i> , 1994
19.33% TMAZ28	121 mg/l TDS	TCE	0.45	Shiau <i>et al.</i> , 1994
6.33% TMAZ20	121 mg/l TDS	TCE	2.27	Shiau <i>et al.</i> , 1994
6.55% TMAZ60	121 mg/l TDS	TCE	3.15	Shiau <i>et al.</i> , 1994

Table 6.7: Summary of abbreviations and surfactant characteristics

Abbreviation	Chemical Name	Molecular Weight	CMC (weight %)
MA-80I	Sodium dihexyl sulfosuccinate	388	0.2
SDS	Sodium dodecyl sulfate	288	0.03
TMAZ28	POE(80) sorbitan monolaurate	3866	0.39
TMAZ20	POE(20) sorbitan monolaurate	1266	0.13
TMAZ60	POE (20) sorbitan monostearate	1310	
AOT	Sodium dioctyl sulfosuccinate		
SMDNS	sodium mono and dimethyl naphthalene sulfonate		
Rexophos 25/97	nonylphenol ethoxylate phosphate		
Alkasurf NP10	nonylphenol ethoxylate		

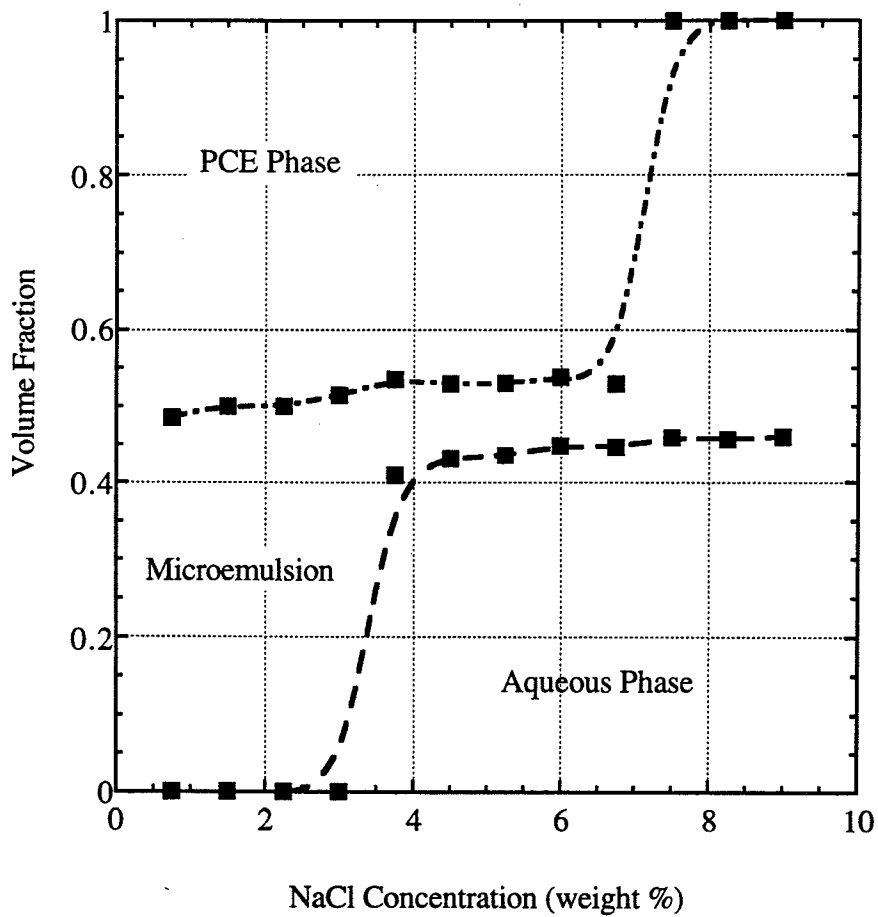


Figure 6.1: Volume fraction diagram for 4% by weight sodium dihexyl sulfosuccinate at 23°C.

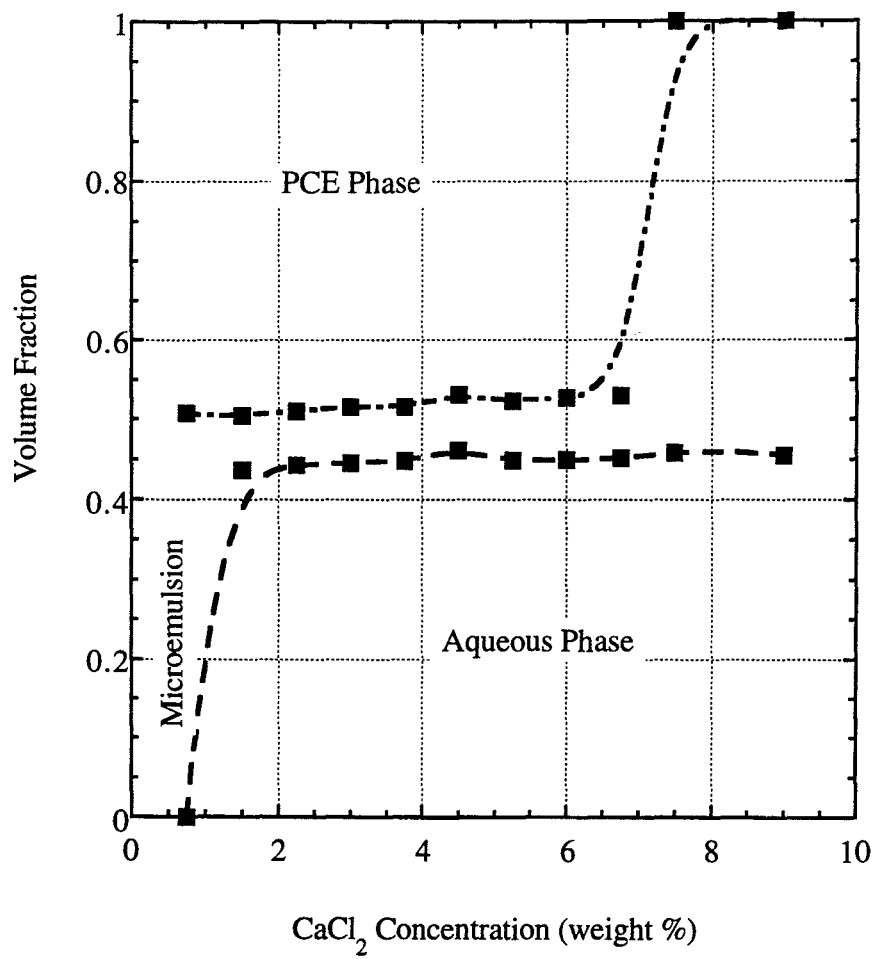


Figure 6.2: Volume fraction diagram for 4% by weight sodium dihexyl sulfosuccinate at 23°C.

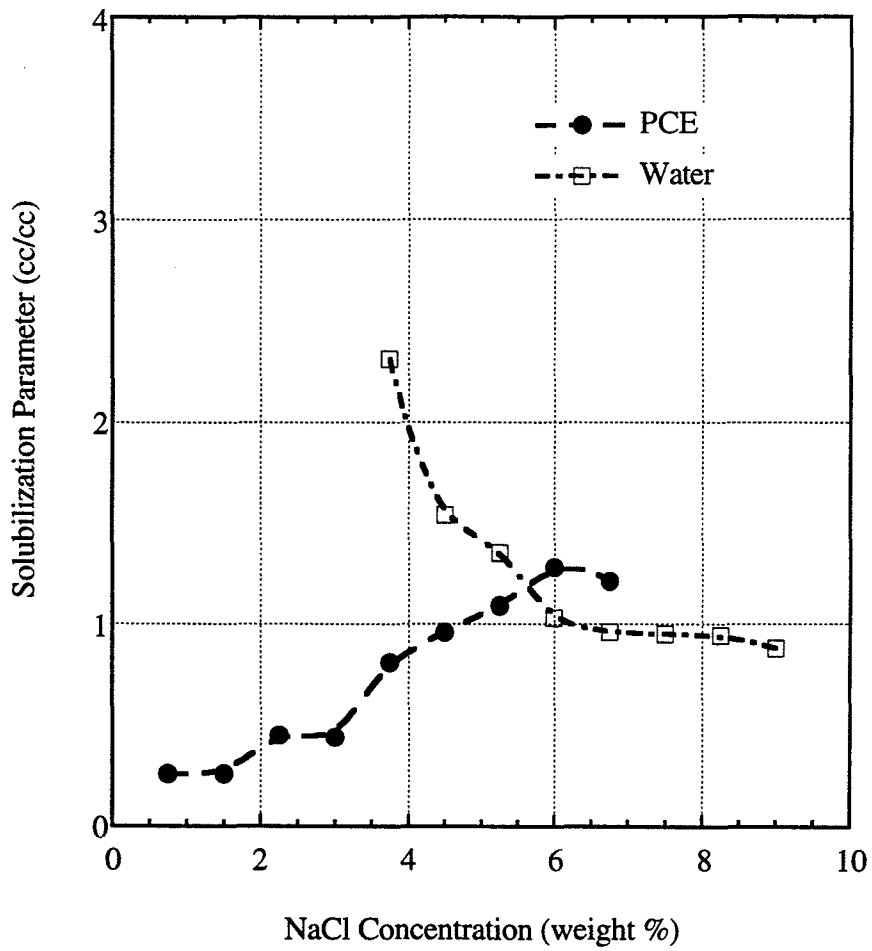


Figure 6.3: Solubilization parameters for 4% by weight sodium dihexyl sulfosuccinate.

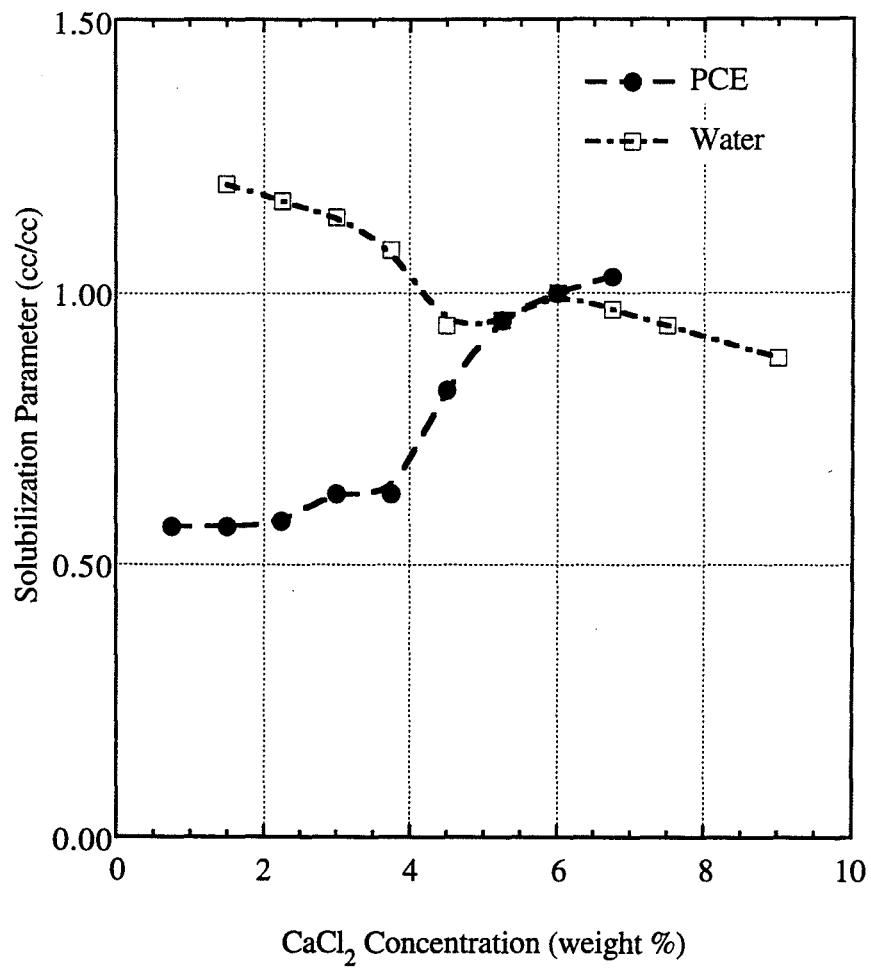


Figure 6.4: Solubilization parameters for 4% by weight sodium dihexyl sulfosuccinate.

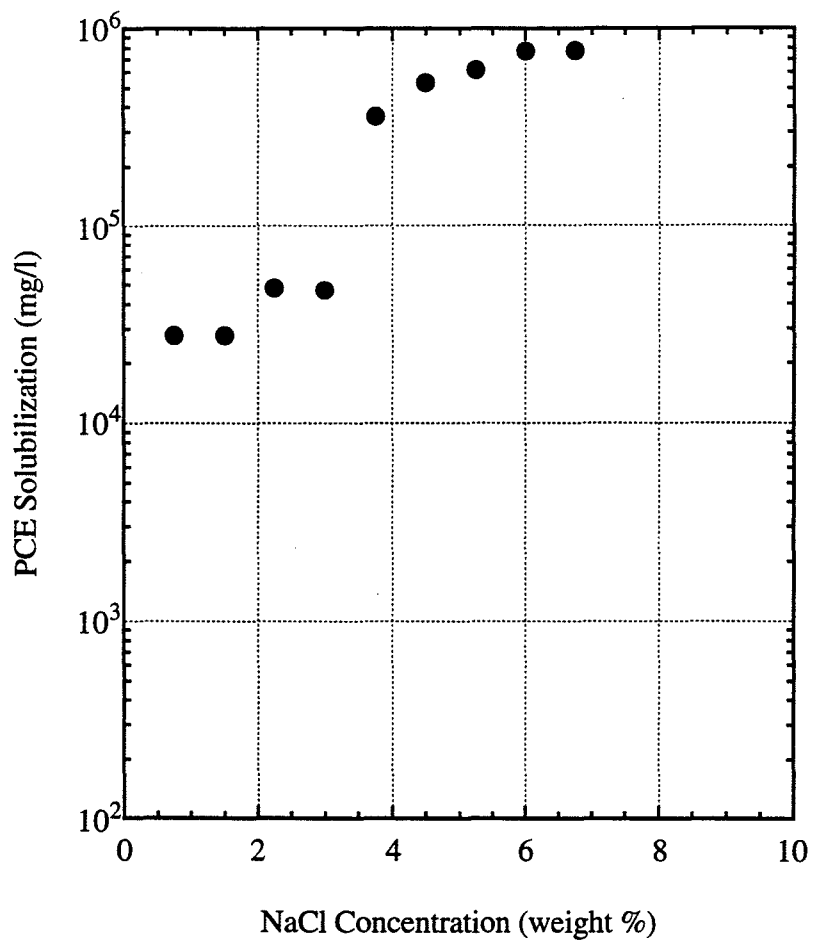


Figure 6.5: PCE solubilization for 4% by weight sodium dihexyl sulfosuccinate.

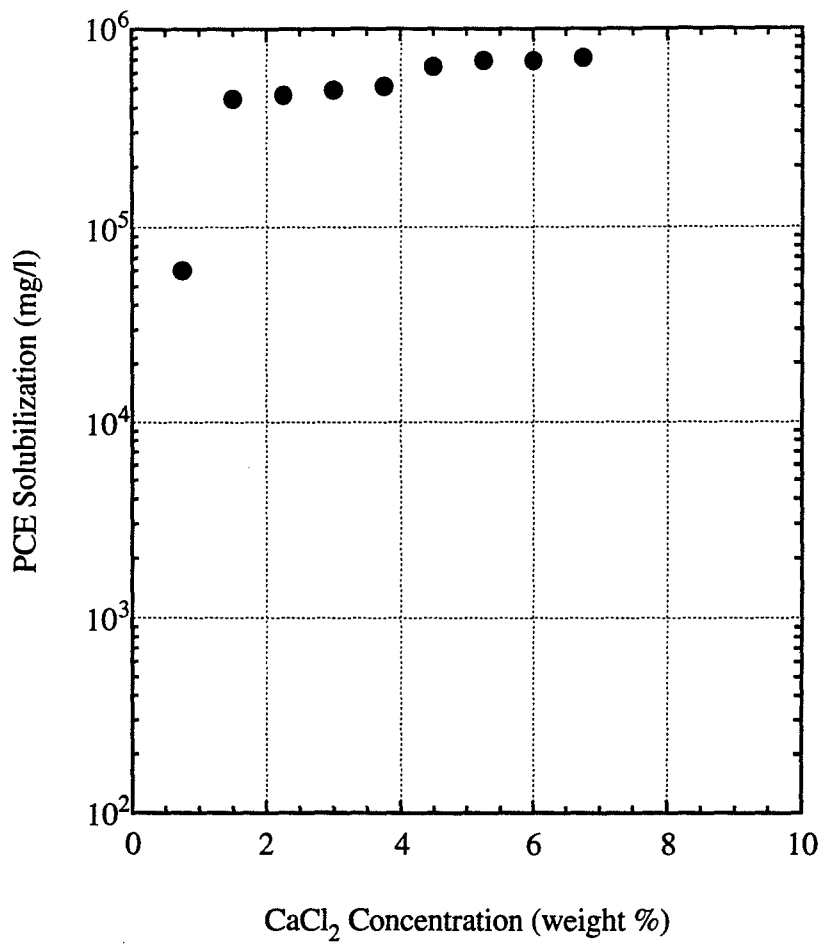


Figure 6.6: PCE solubilization for 4% by weight sodium dihexyl sulfosuccinate.

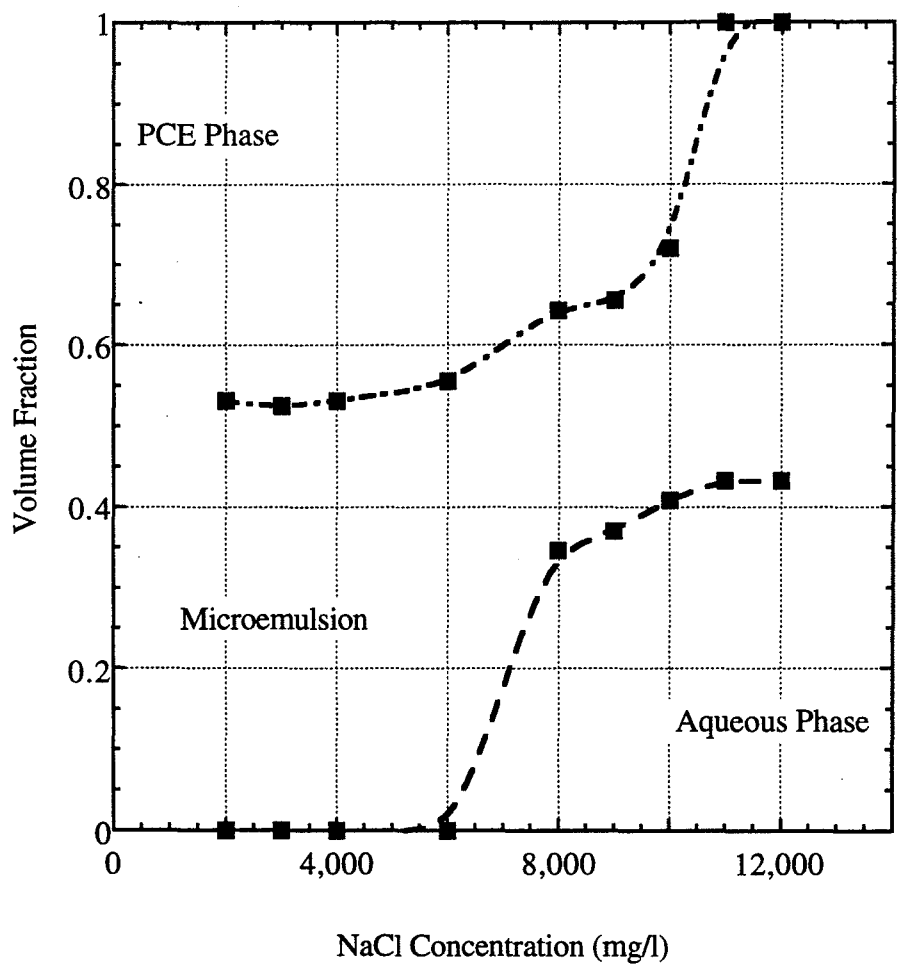


Figure 6.7: Volume fraction diagram for 2% by weight sodium diamyl sulfosuccinate and 2% by weight sodium dioctyl sulfosuccinate at 23°C.

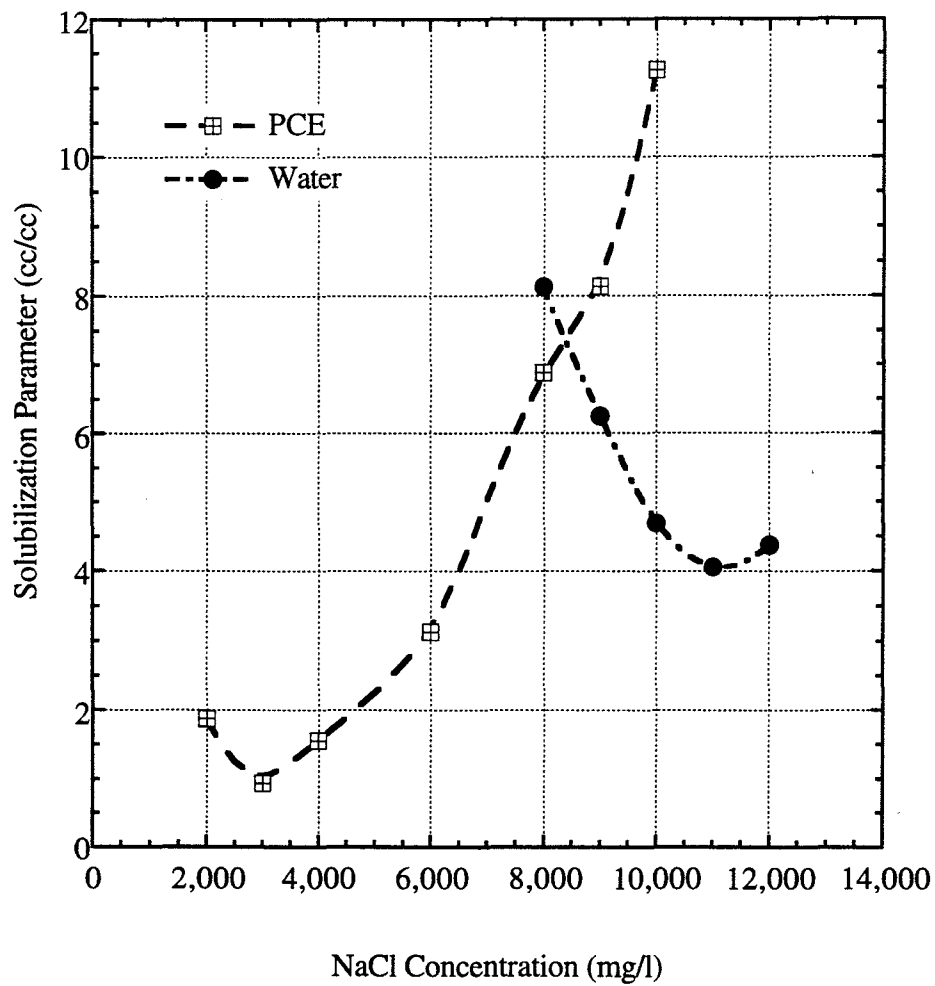


Figure 6.8: Solubilization parameters for 2% by weight sodium diamyl sulfosuccinate and 2% by weight sodium dioctyl sulfosuccinate.

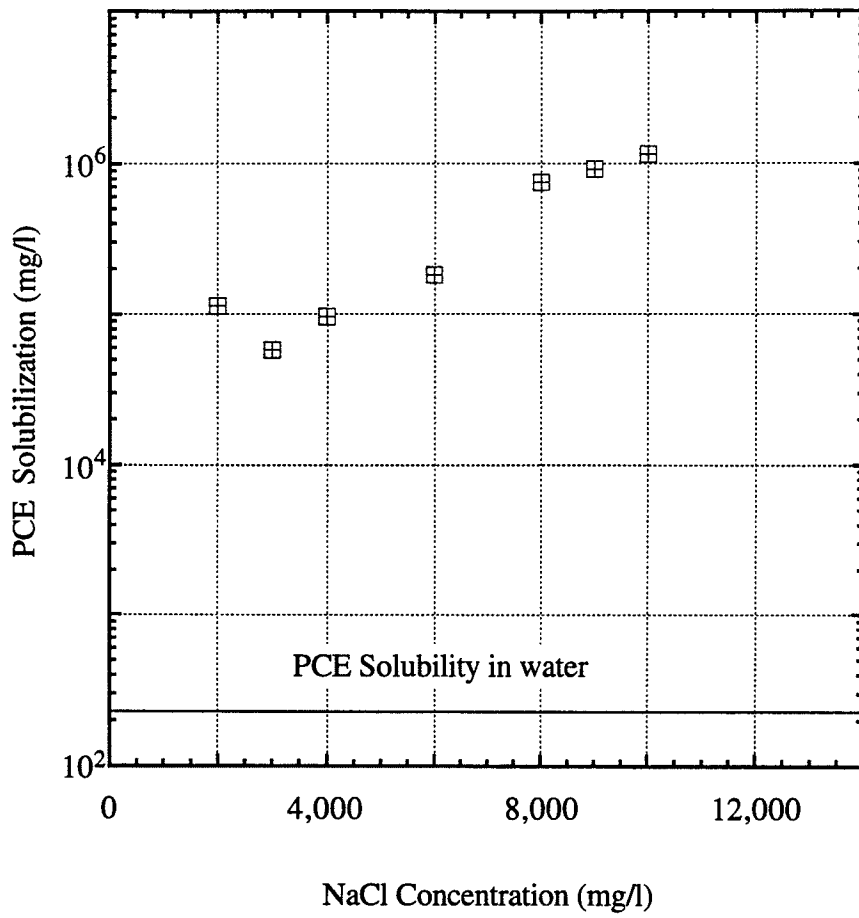


Figure 6.9: PCE solubilization for 2% by weight sodium diamyl sulfosuccinate and 2% by weight sodium dioctyl sulfosuccinate.

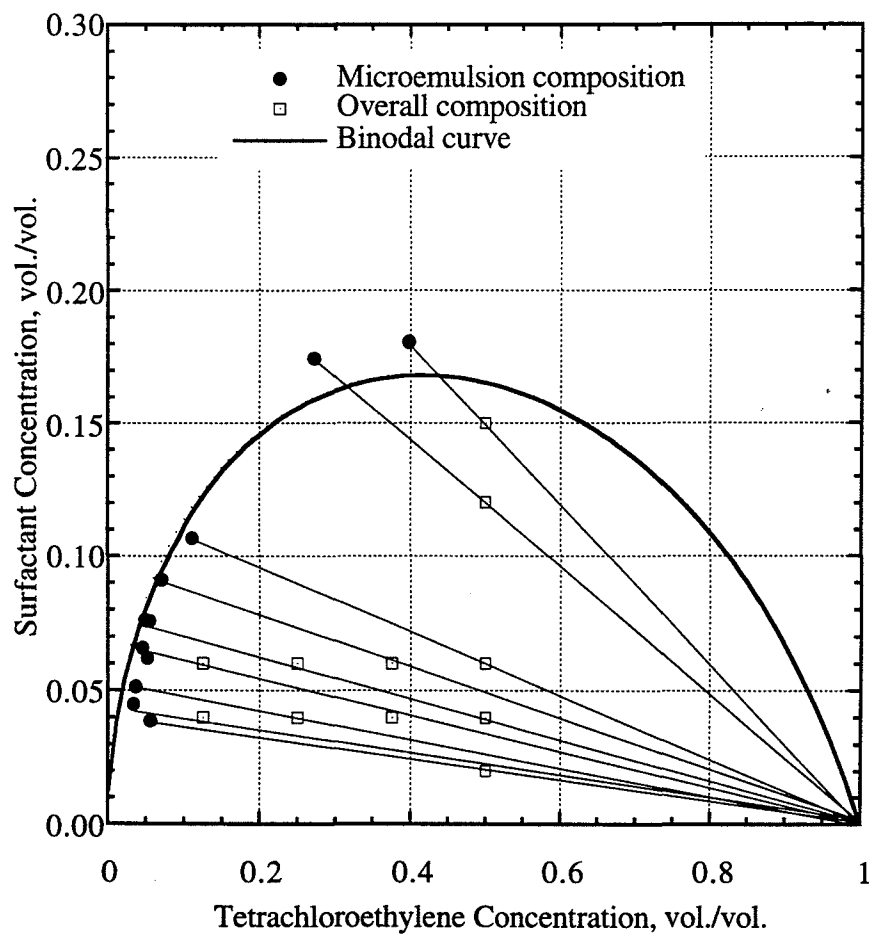


Figure 6.10: Ternary for 1:1 sodium diamyl sulfosuccinate and sodium dioctyl sulfosuccinate, 500 mg/l CaCl_2 at 23°C.

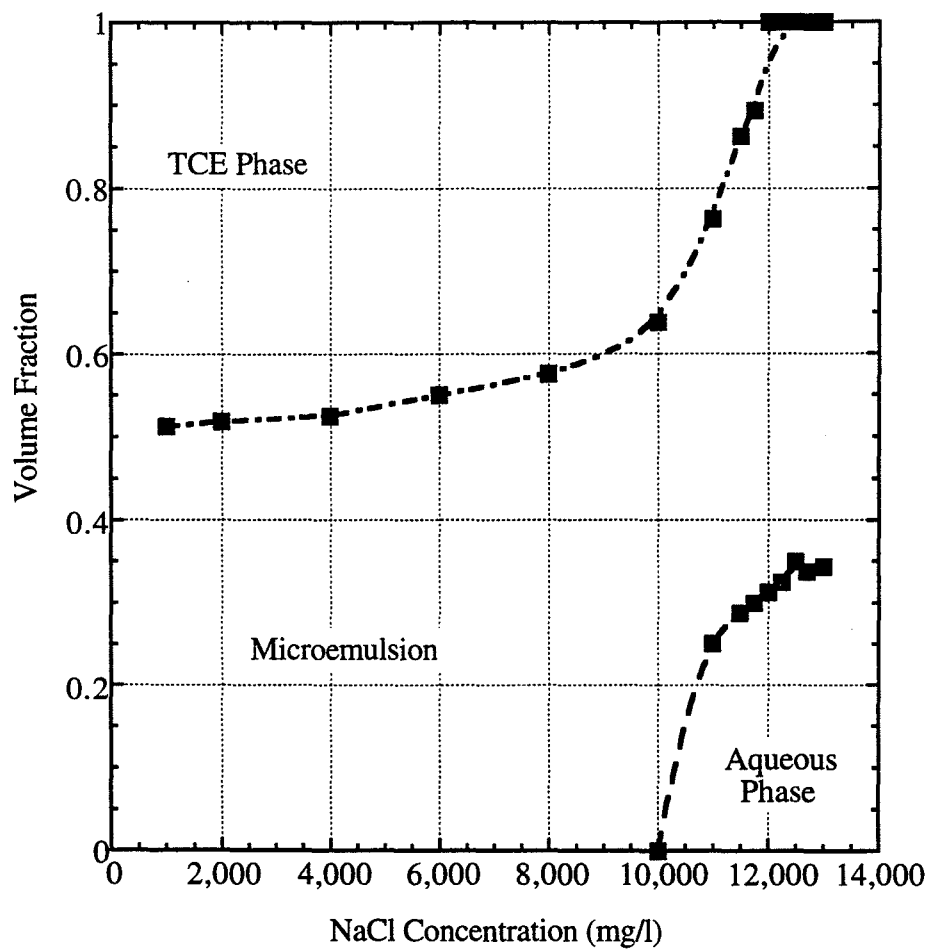


Figure 6.11: Volume fraction diagram for 8% by weight sodium dihexyl sulfosuccinate at 23°C.

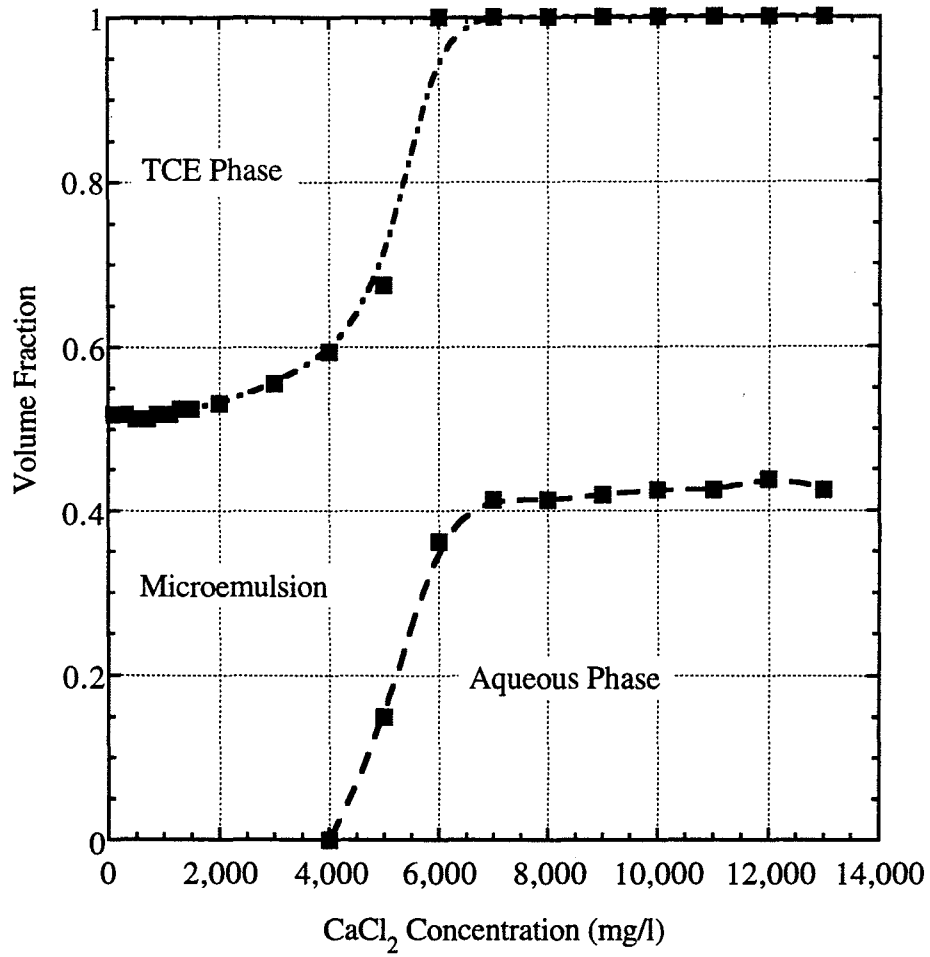


Figure 6.12: Volume fraction diagram for 8% by weight sodium dihexyl sulfosuccinate at 23°C.

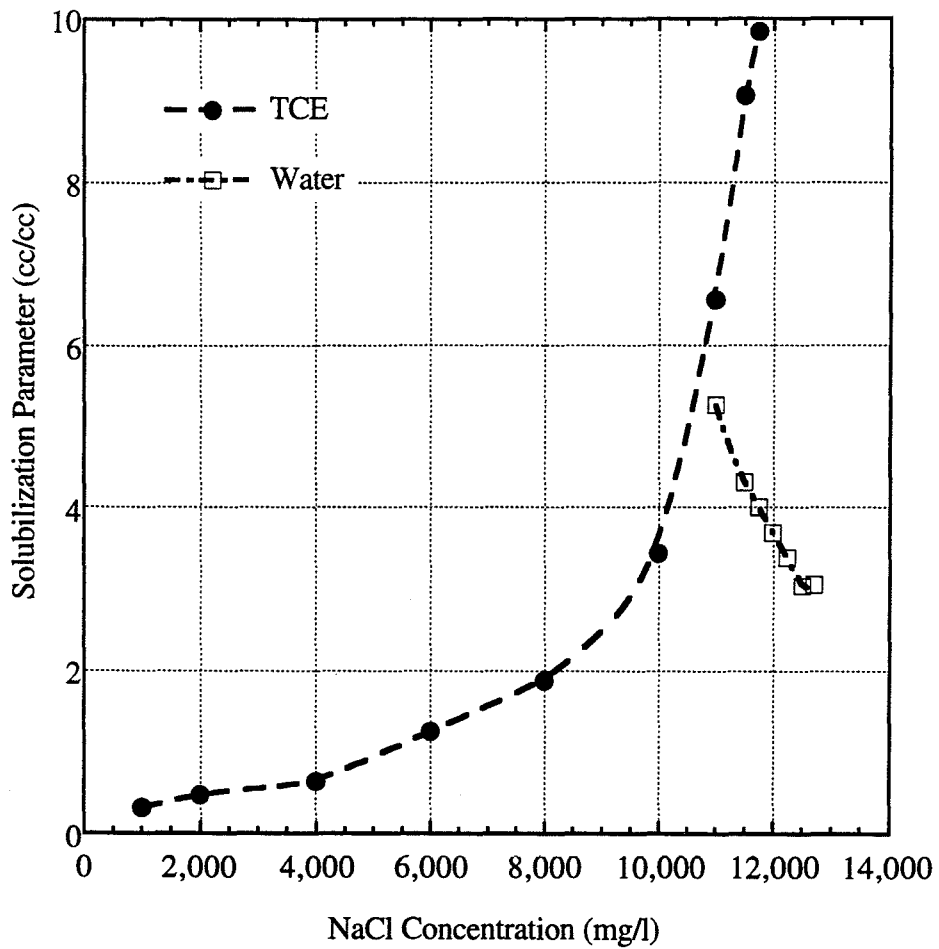


Figure 6.13: Solubilization parameters for 8% by weight sodium dihexyl sulfosuccinate.

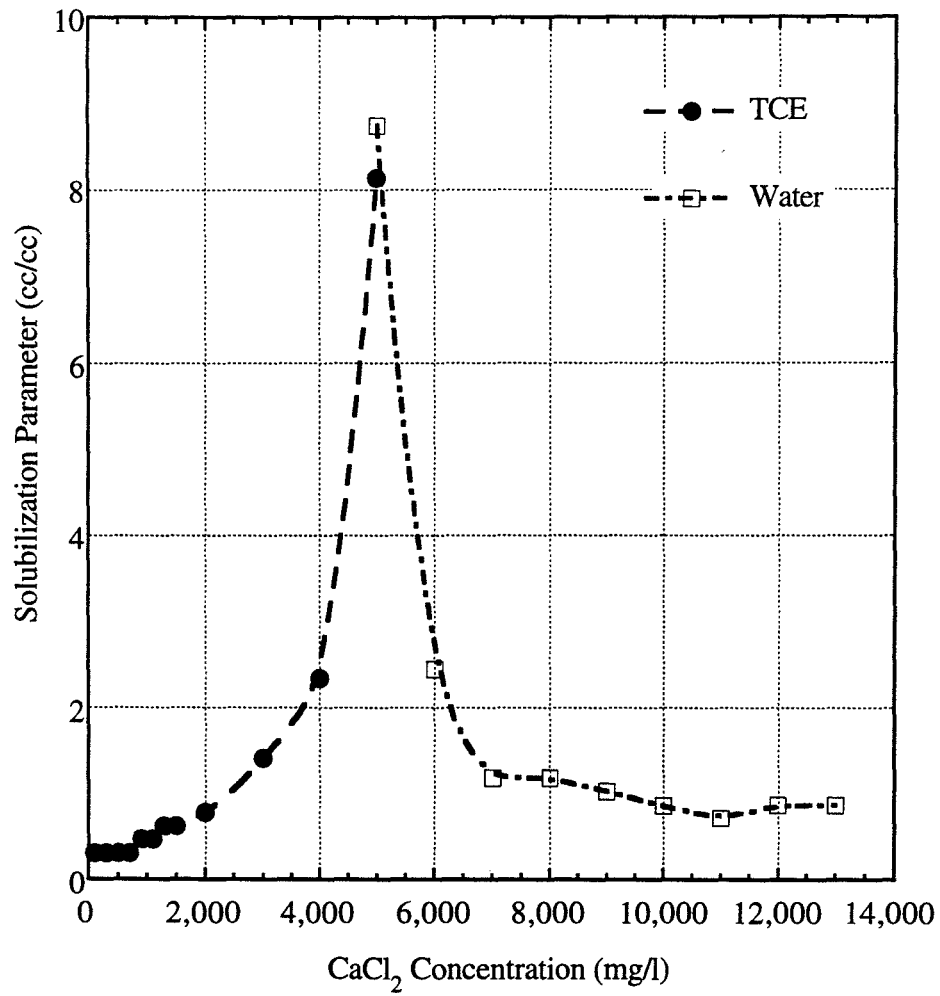


Figure 6.14: Solubilization parameters for 8% by weight sodium dihexyl sulfosuccinate.

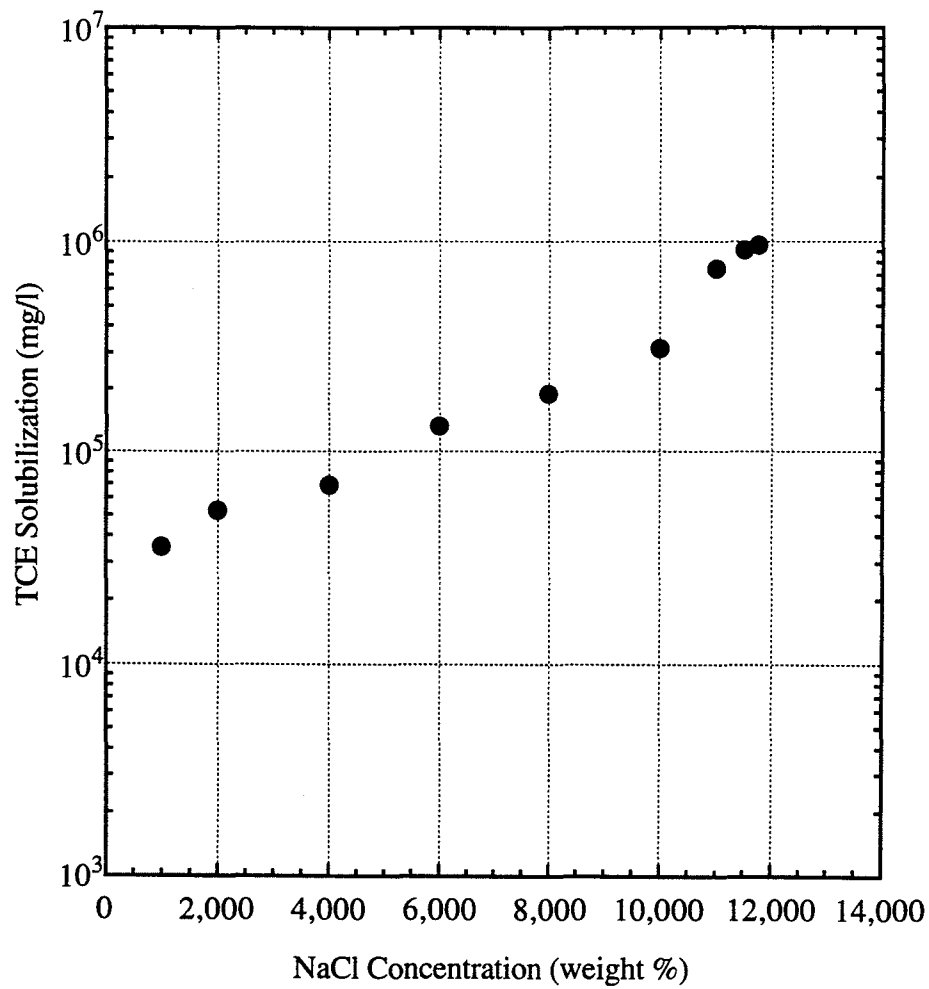


Figure 6.15: TCE solubilization for 8% by weight sodium dihexyl sulfosuccinate.

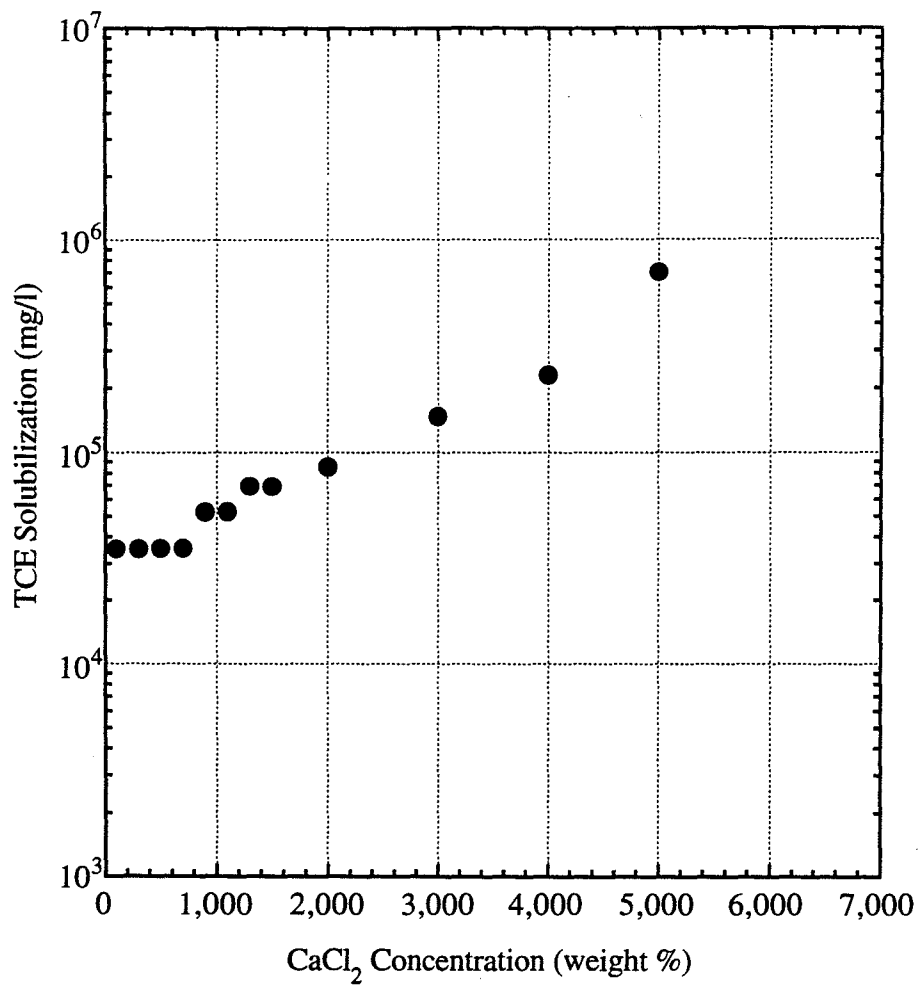


Figure 6.16: TCE solubilization for 8% by weight sodium dihexyl sulfosuccinate.

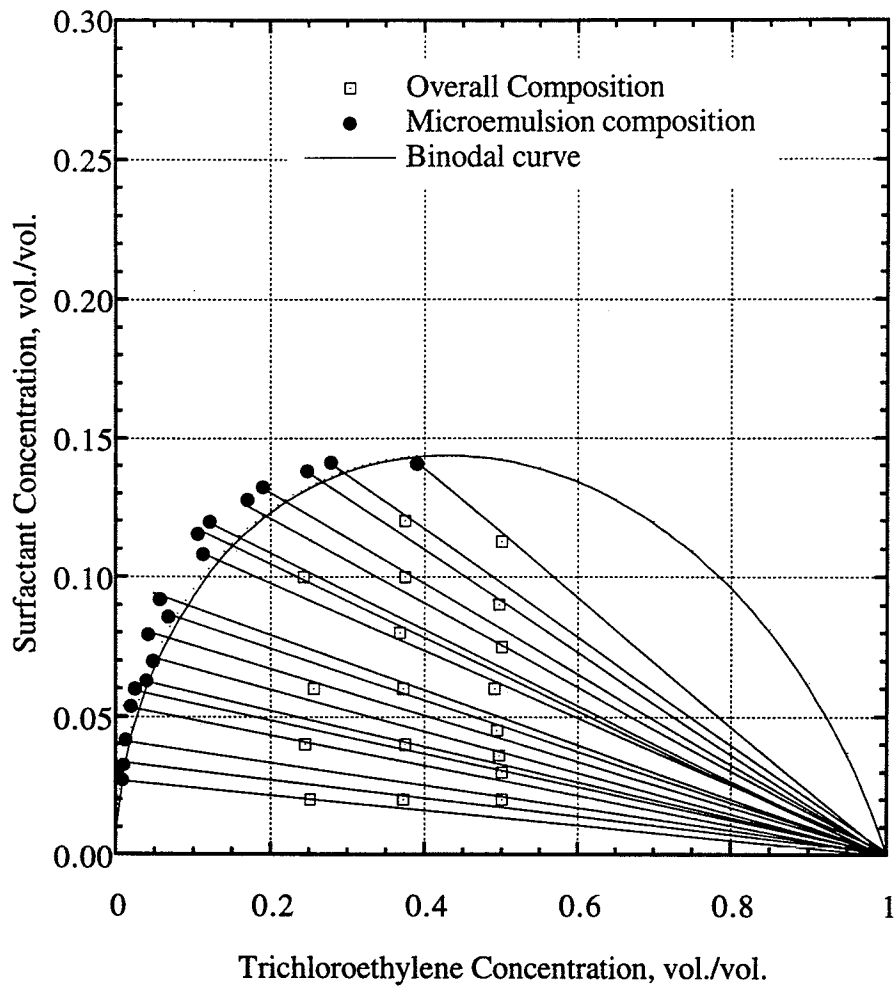


Figure 6.17: Ternary for sodium dihexyl sulfosuccinate, 1,000 mg/l NaCl at 23°C.

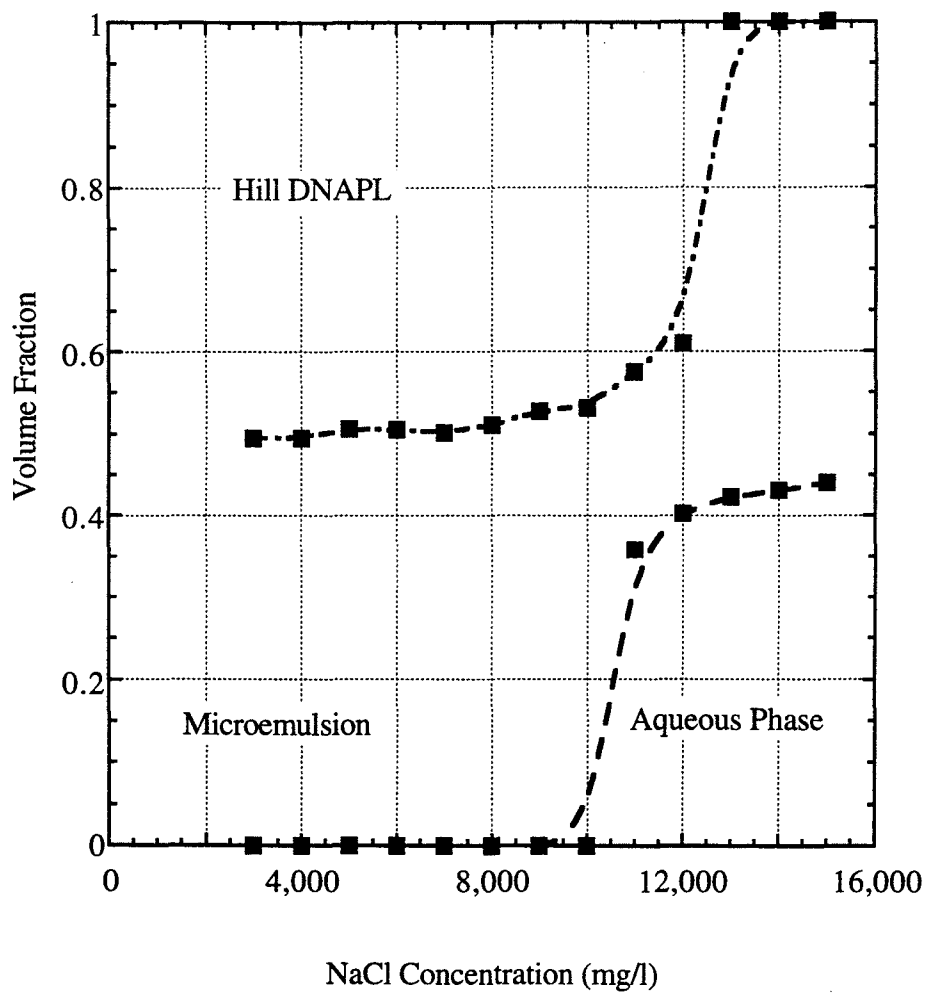


Figure 6.18: Volume fraction diagram for 4% by weight sodium dihexyl sulfosuccinate, 4% by weight IPA and 500 mg/l xanthan gum in Hill source water at 23°C.

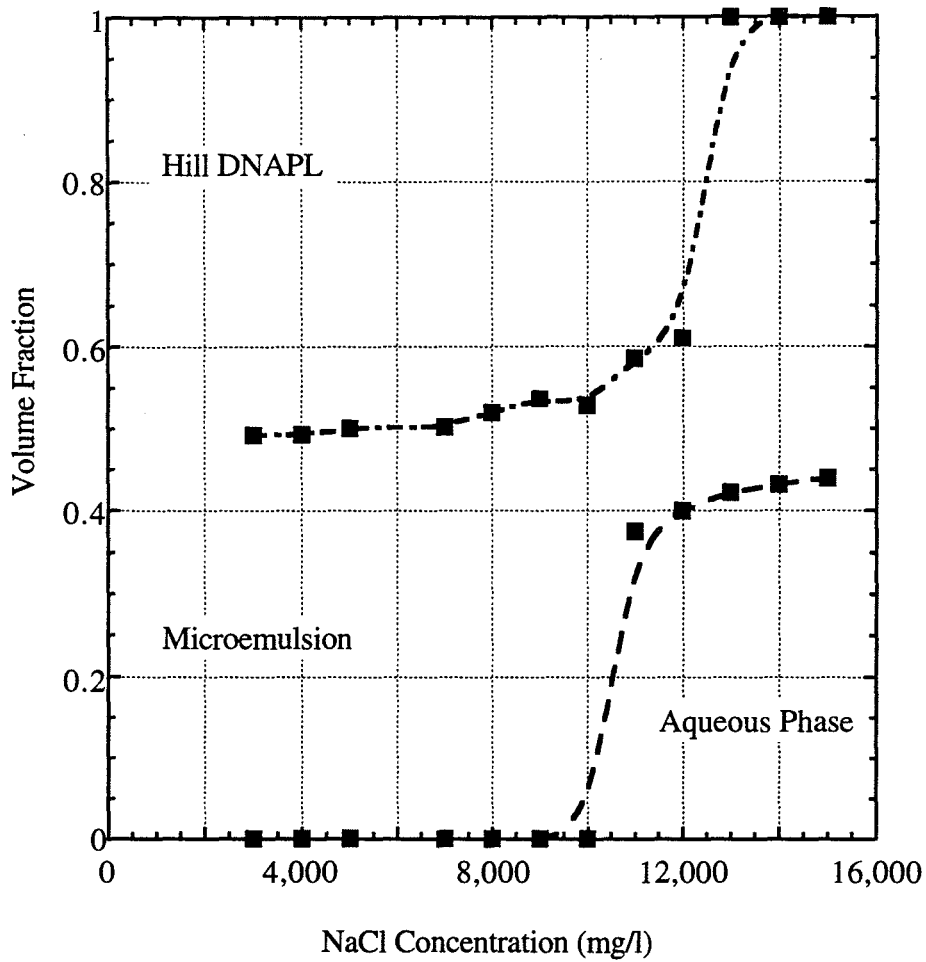


Figure 6.19: Volume fraction diagram for 4% by weight sodium dihexyl sulfosuccinate, 4% by weight ethanol and 500 mg/l xanthan gum in Hill source water at 23°C.

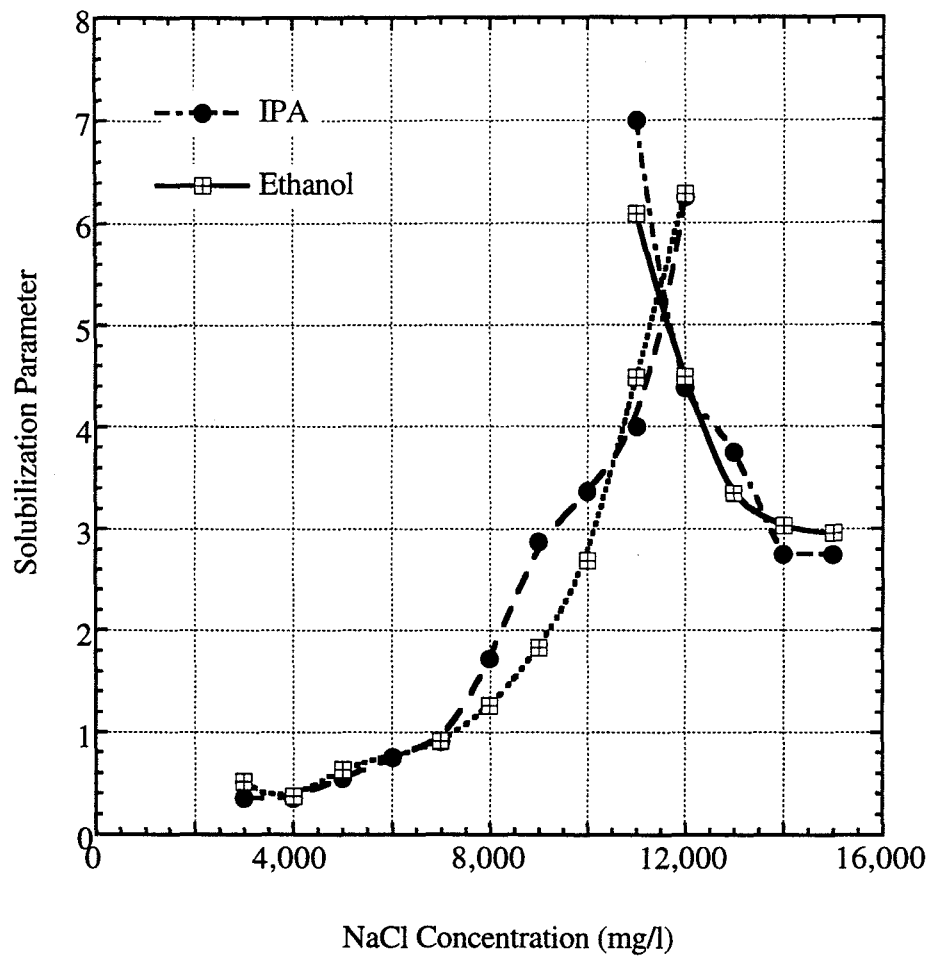


Figure 6.20: Solubilization parameters for 4% by weight sodium dihexyl sulfosuccinate, 4% by weight alcohol and 500 mg/l xanthan gum in Hill source water at 23°C.

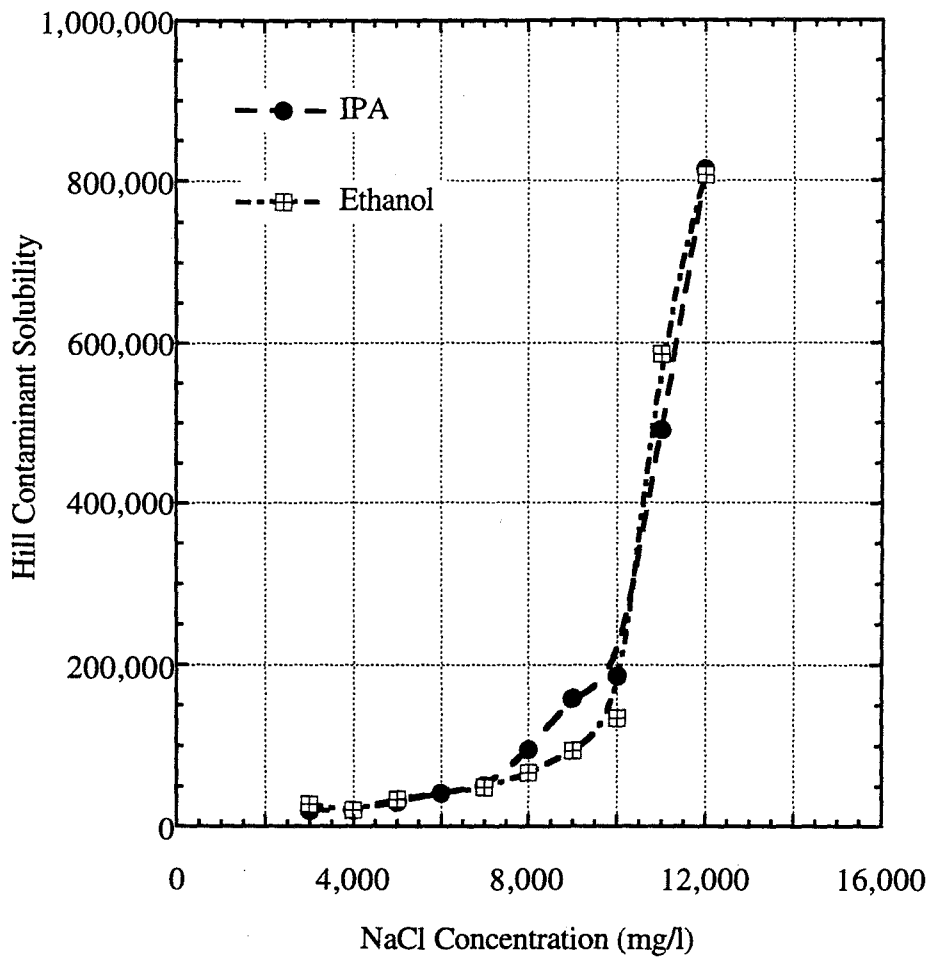


Figure 6.21: Hill contaminant solubilization for 4% by weight sodium dihexyl sulfosuccinate, 4% by weight alcohol, 500 mg/l xanthan gum in Hill source water at 23°C.

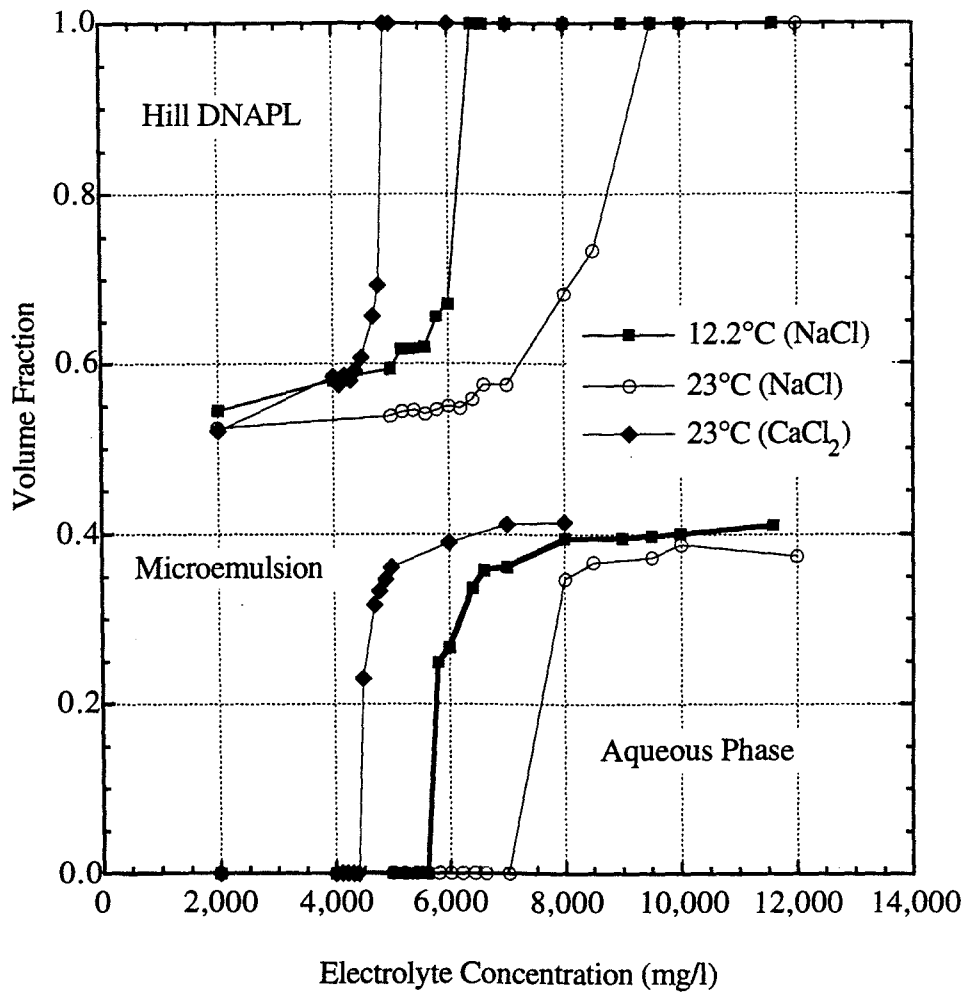


Figure 6.22: Volume fraction diagram for 8% by weight sodium dihexyl sulfosuccinate, 8% by weight IPA and 500 mg/l xanthan gum in Hill source water at different temperatures.

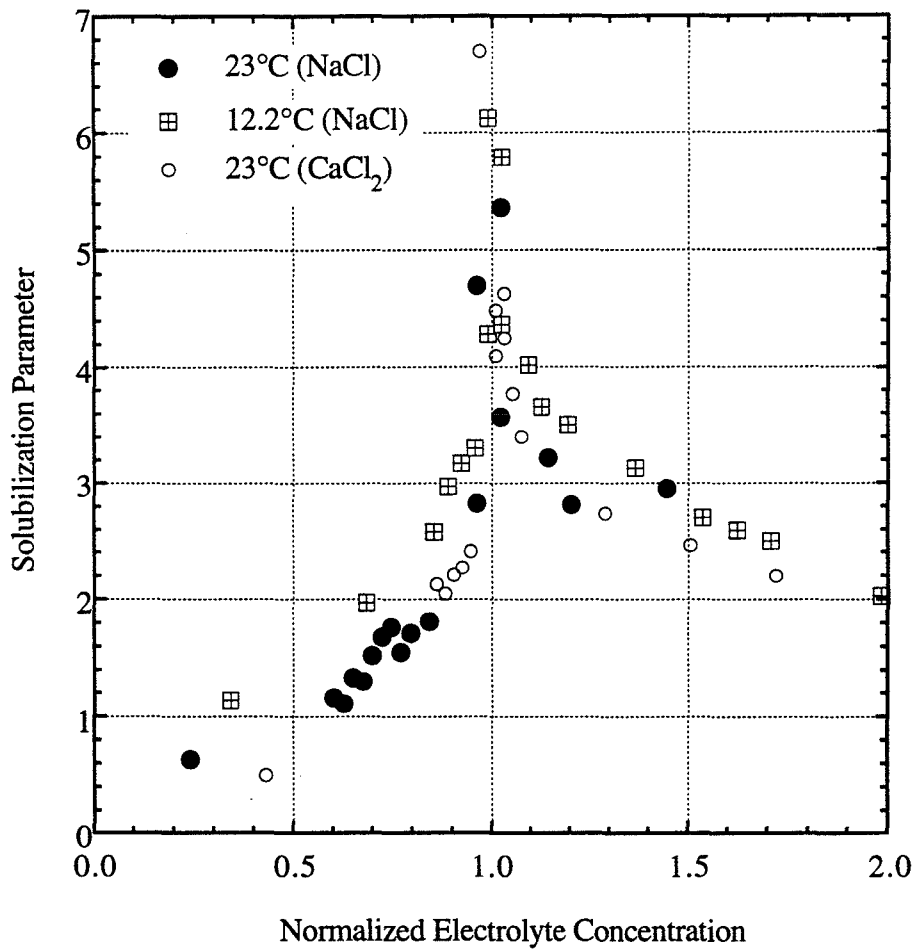


Figure 6.23: Solubilization parameters for 8% by weight sodium dihexyl sulfosuccinate, 8% by weight IPA and 500 mg/l xanthan gum in Hill source water at different temperatures.

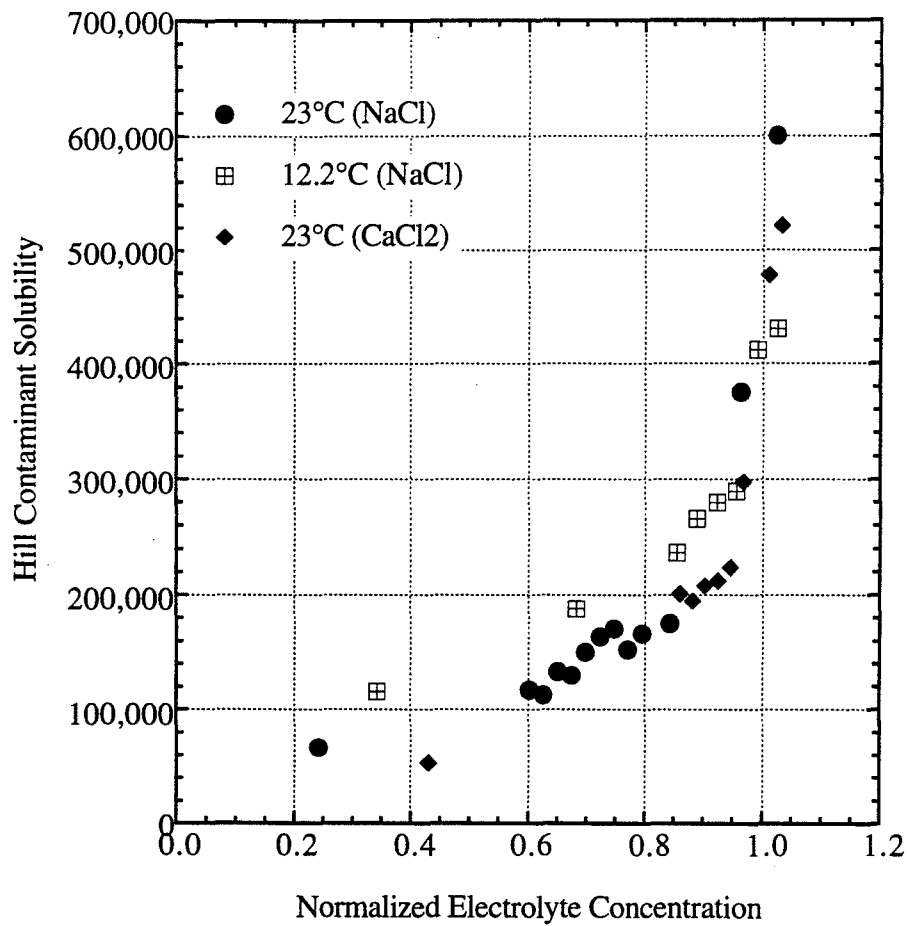


Figure 6.24: Hill contaminant solubilization plotted for 8% by weight sodium dihexyl sulfosuccinate, 8% by weight alcohol and 500 mg/l xanthan gum in Hill source water at different temperatures.

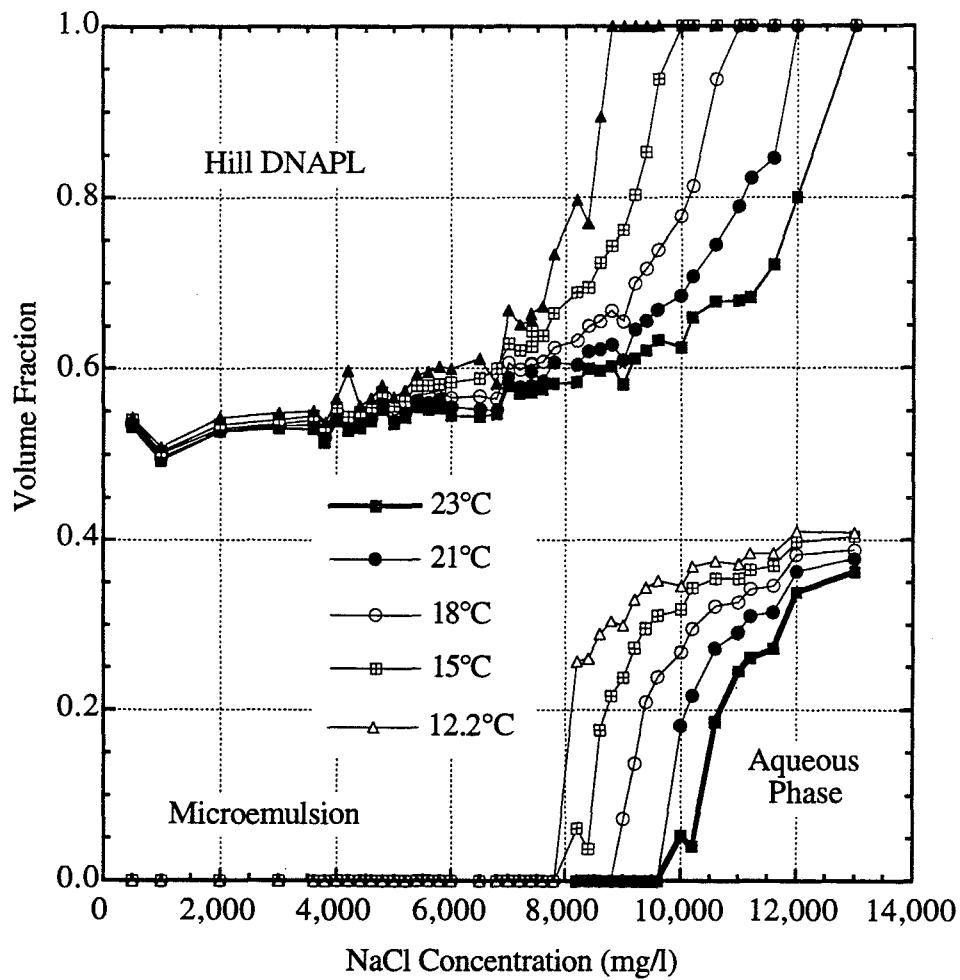


Figure 6.25: Volume fraction diagram for 8% by weight sodium dihexyl sulfosuccinate, 2% by weight IPA in Hill source water at different temperatures.

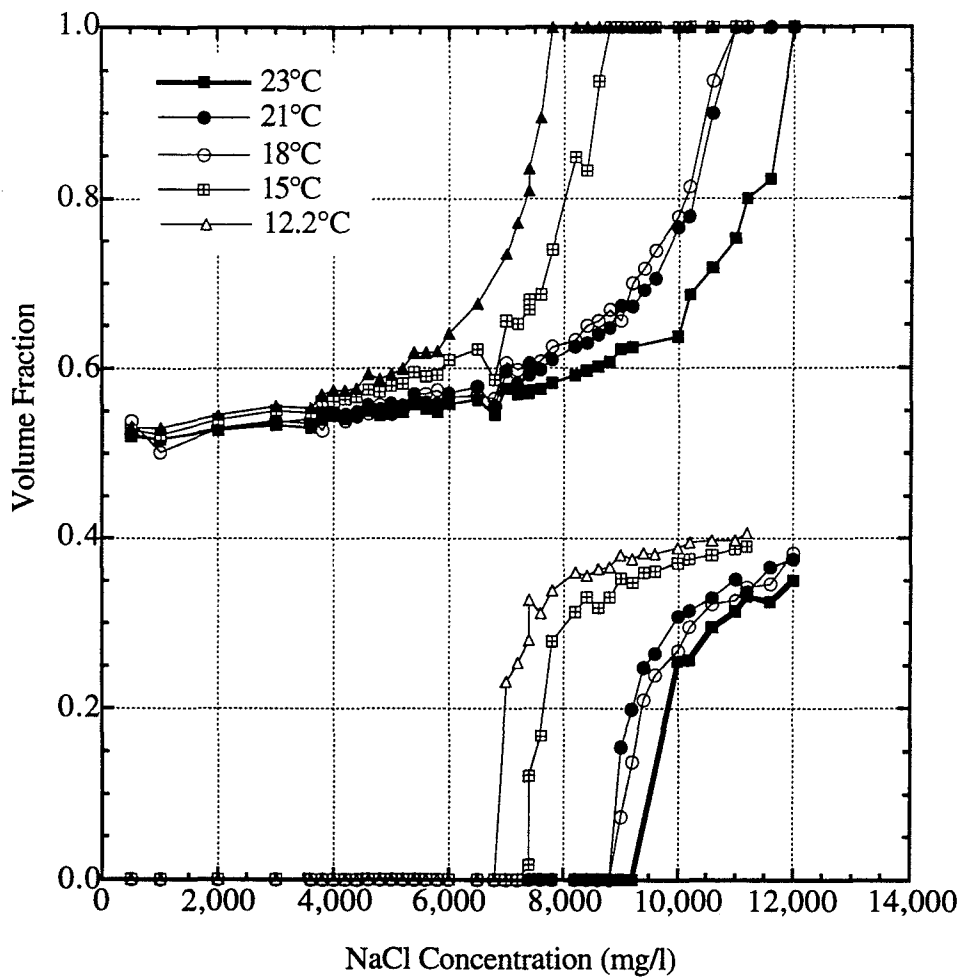


Figure 6.26: Volume fraction diagram for 8% by weight sodium dihexyl sulfosuccinate, 4% by weight IPA in Hill source water at different temperatures.

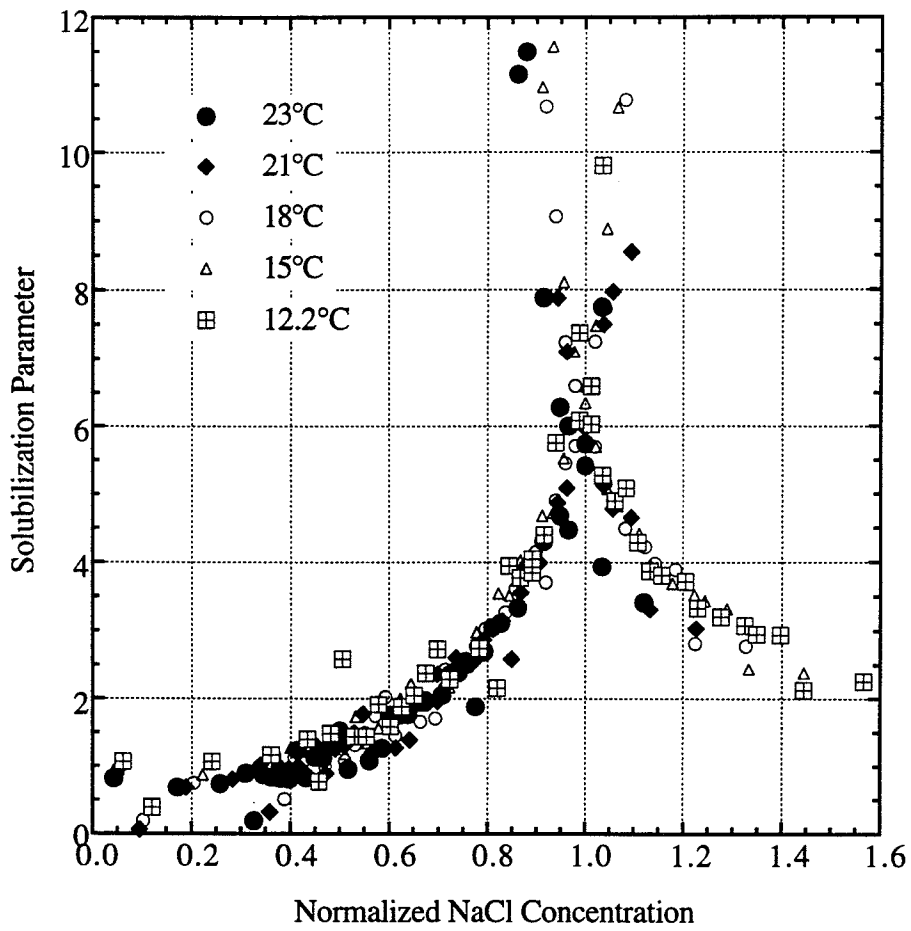


Figure 6.27: Hill contaminant and water solubilization parameters for 8% by weight sodium dihexyl sulfosuccinate and 2% by weight IPA.

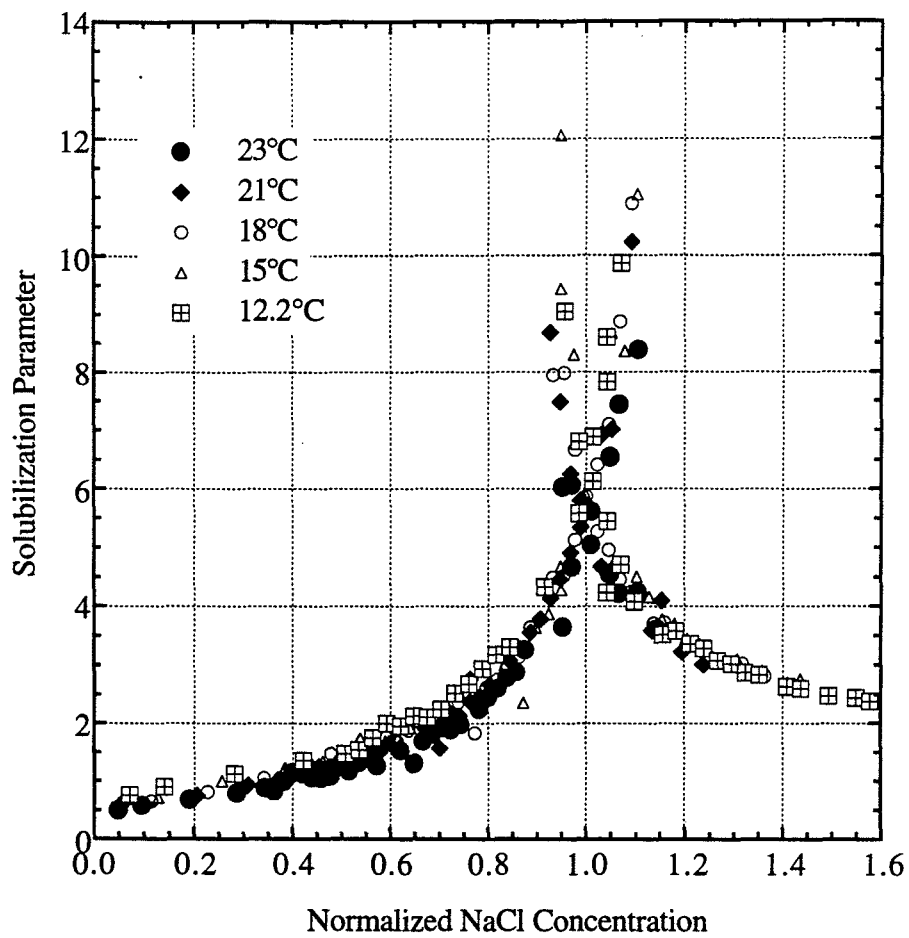


Figure 6.28: Hill contaminant and water solubilization parameters for 8% by weight sodium dihexyl sulfosuccinate, 4% by weight IPA.

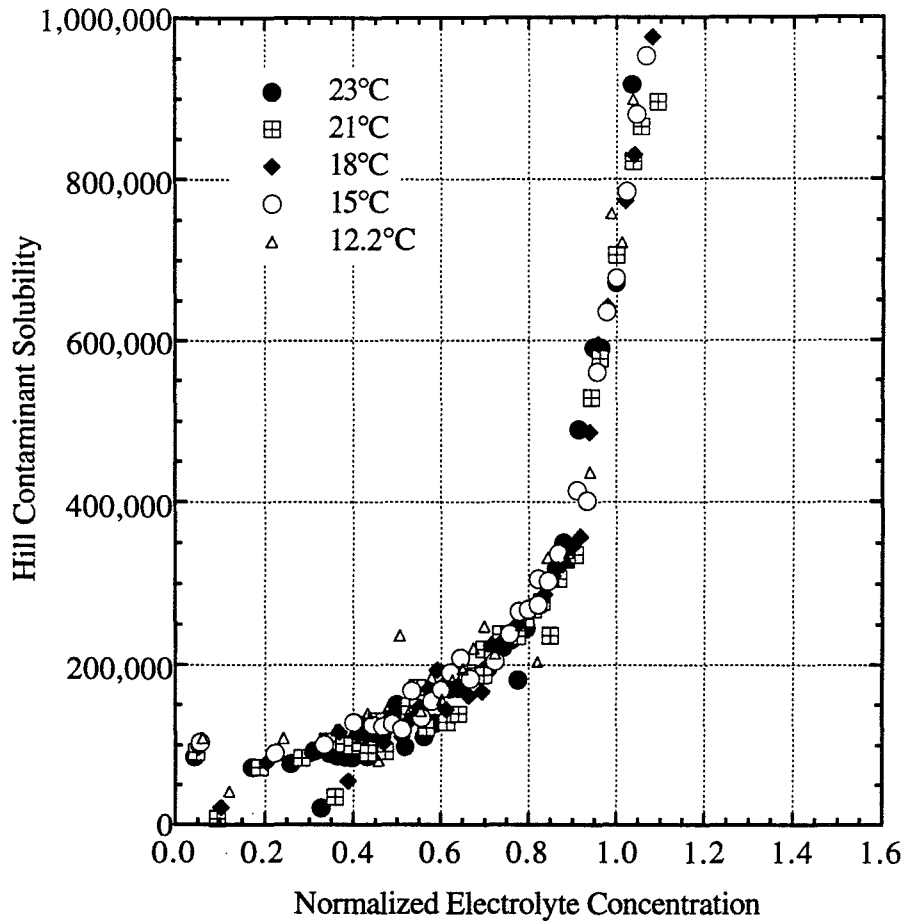


Figure 6.29: Hill contaminant solubilization for 8% by weight sodium dihexyl sulfosuccinate, 2% by weight IPA in Hill source water.

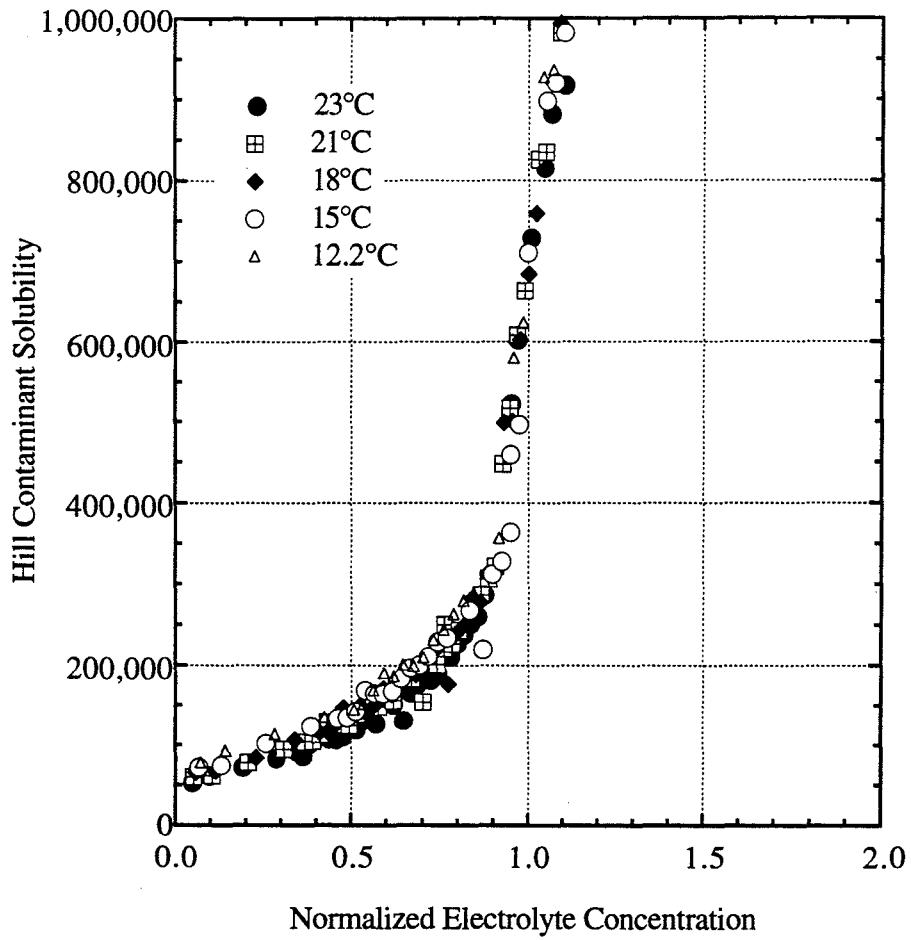


Figure 6.30: Hill contaminant solubilization for 8% by weight sodium dihexyl sulfosuccinate, 4% by weight IPA in Hill source water.

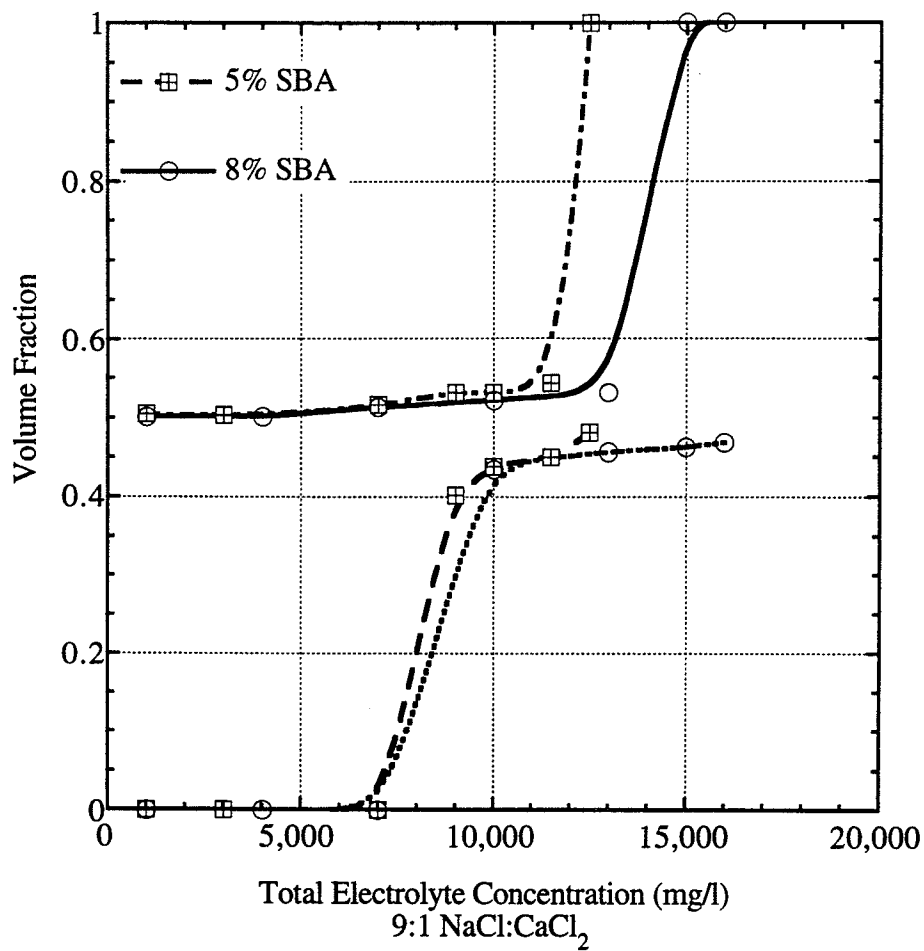


Figure 6.31: Volume fraction diagram for 2% by weight sodium diheptyl sulfosuccinate, secondary butyl alcohol.

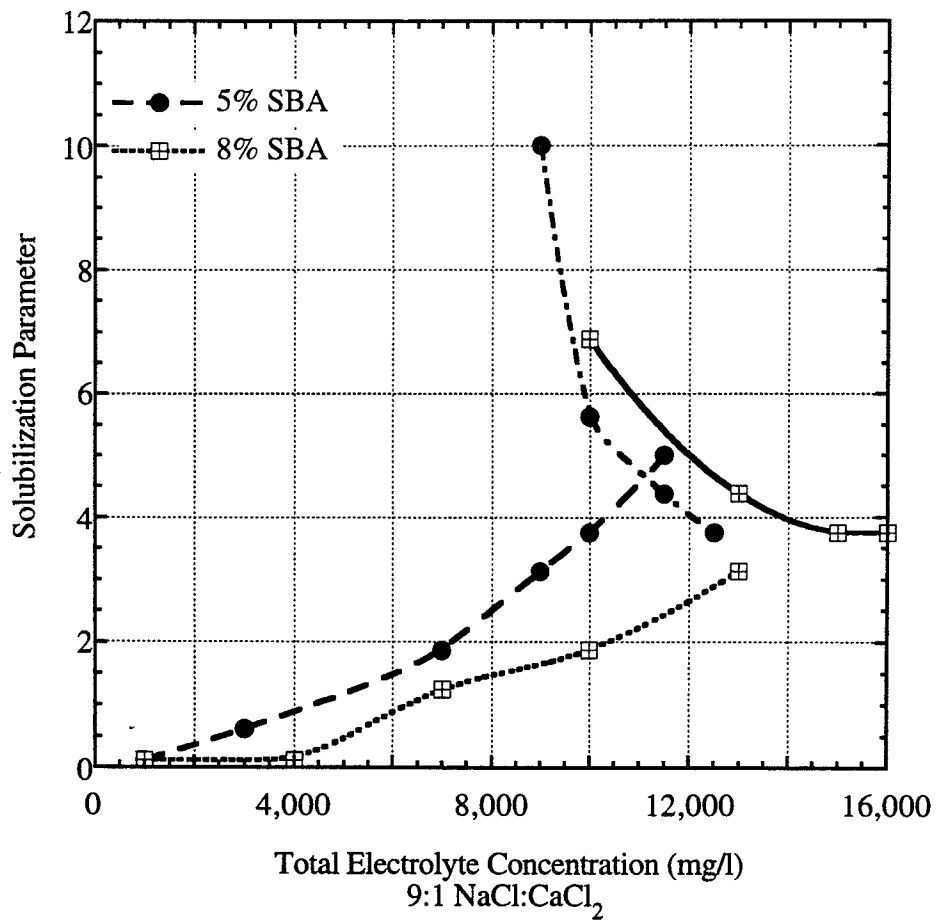


Figure 6.32: Jet fuel and water solubilization parameters for 2% by weight sodium diheptyl sulfosuccinate, secondary butyl alcohol.

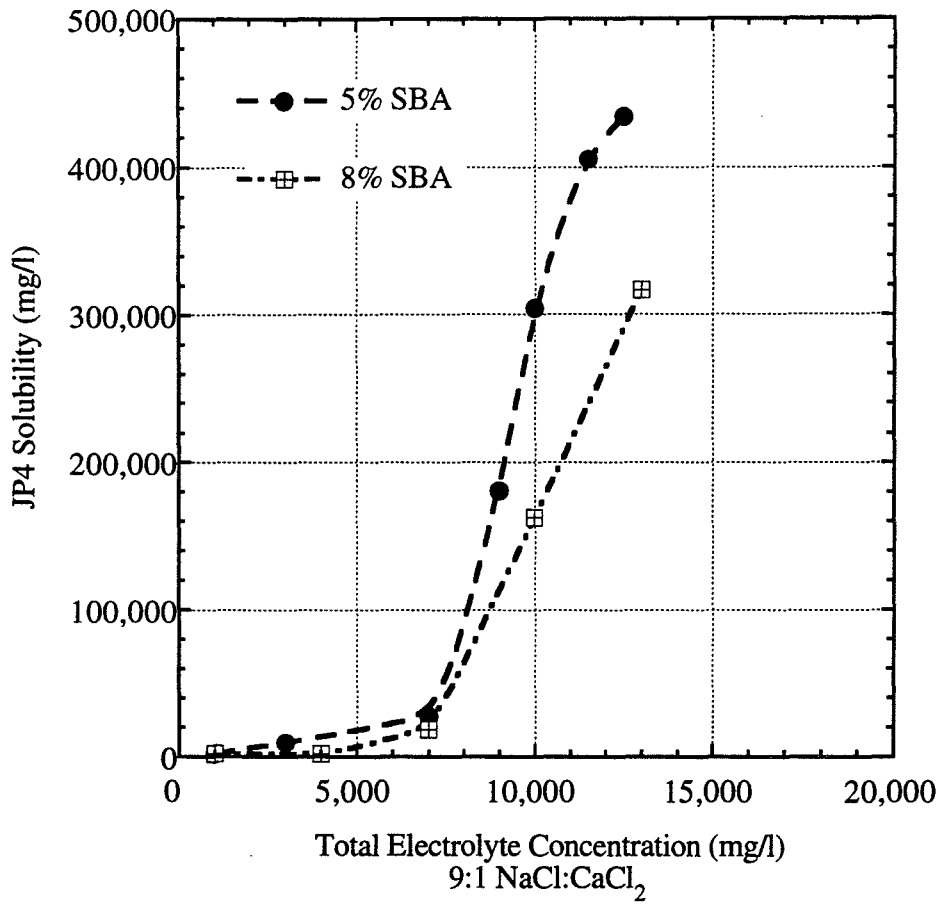


Figure 6.33: Jet fuel solubilization for 2% by weight sodium diheptyl sulfosuccinate, secondary butyl alcohol.

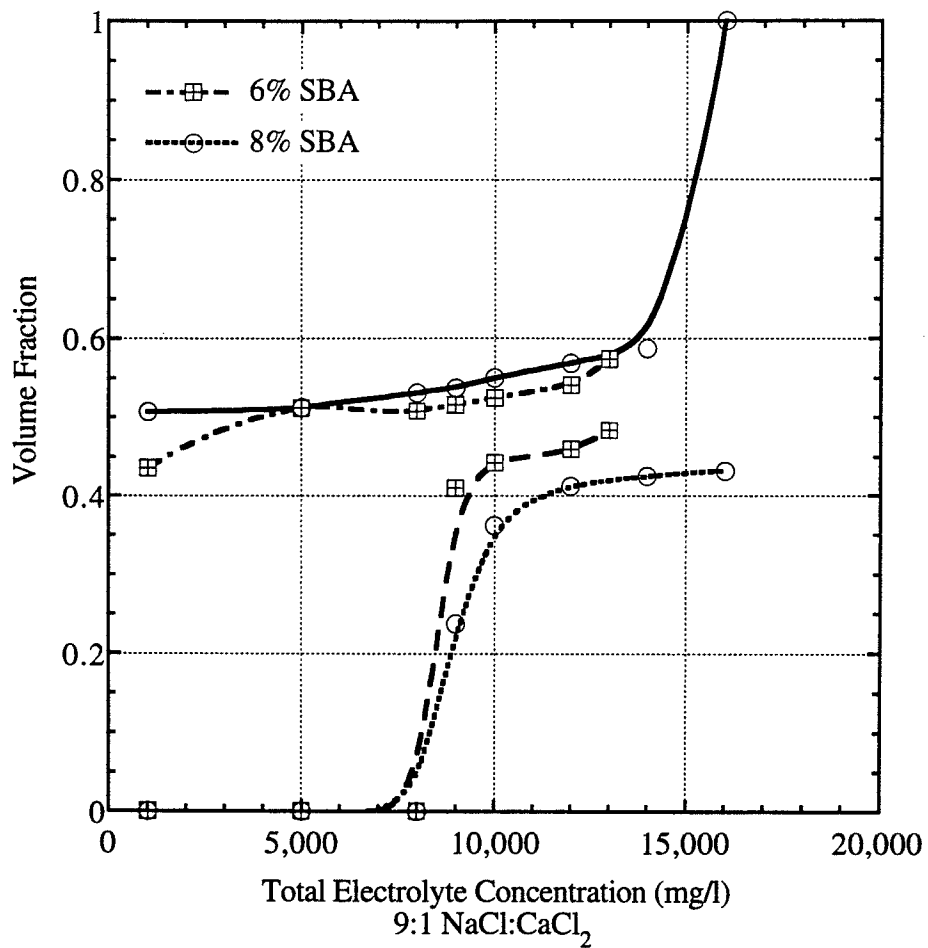


Figure 6.34: Volume fraction diagram for 4% by weight sodium diheptyl sulfosuccinate, secondary butyl alcohol.

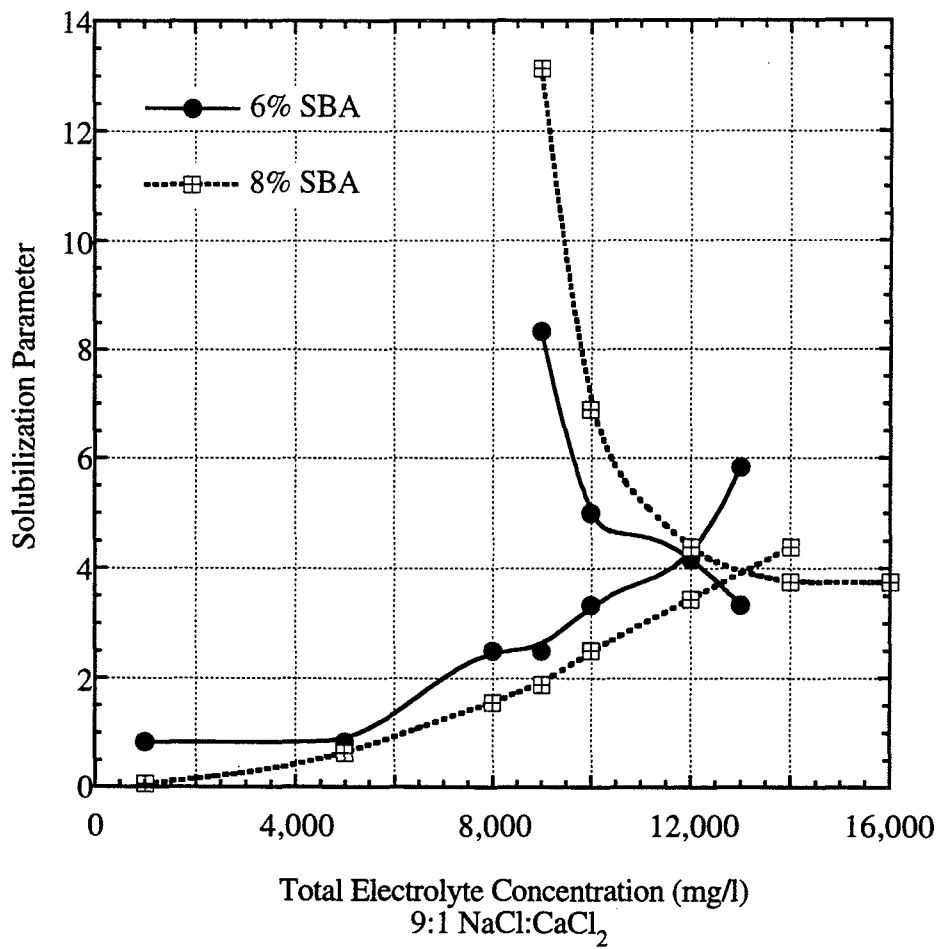


Figure 6.35: Jet fuel and water solubilization parameters for 4% by weight sodium diheptyl sulfosuccinate, secondary butyl alcohol.

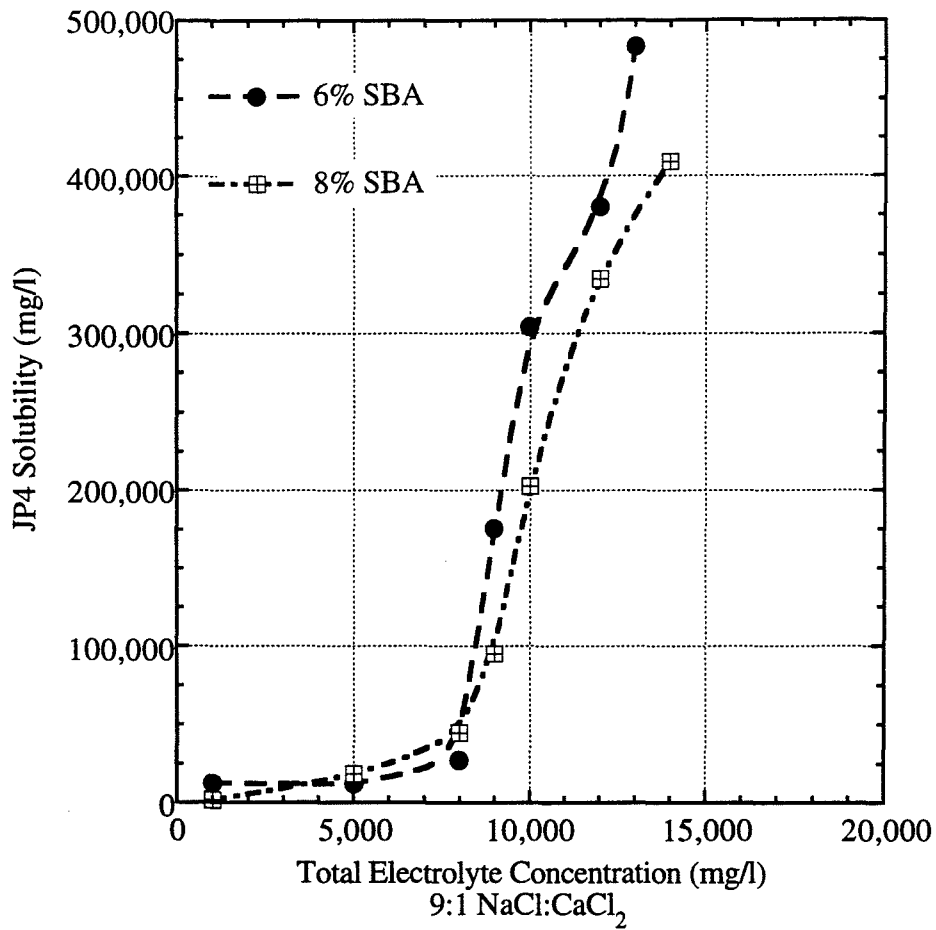


Figure 6.36: Jet fuel solubilization for 4% by weight sodium diheptyl sulfosuccinate, 2% by weight secondary butyl alcohol.

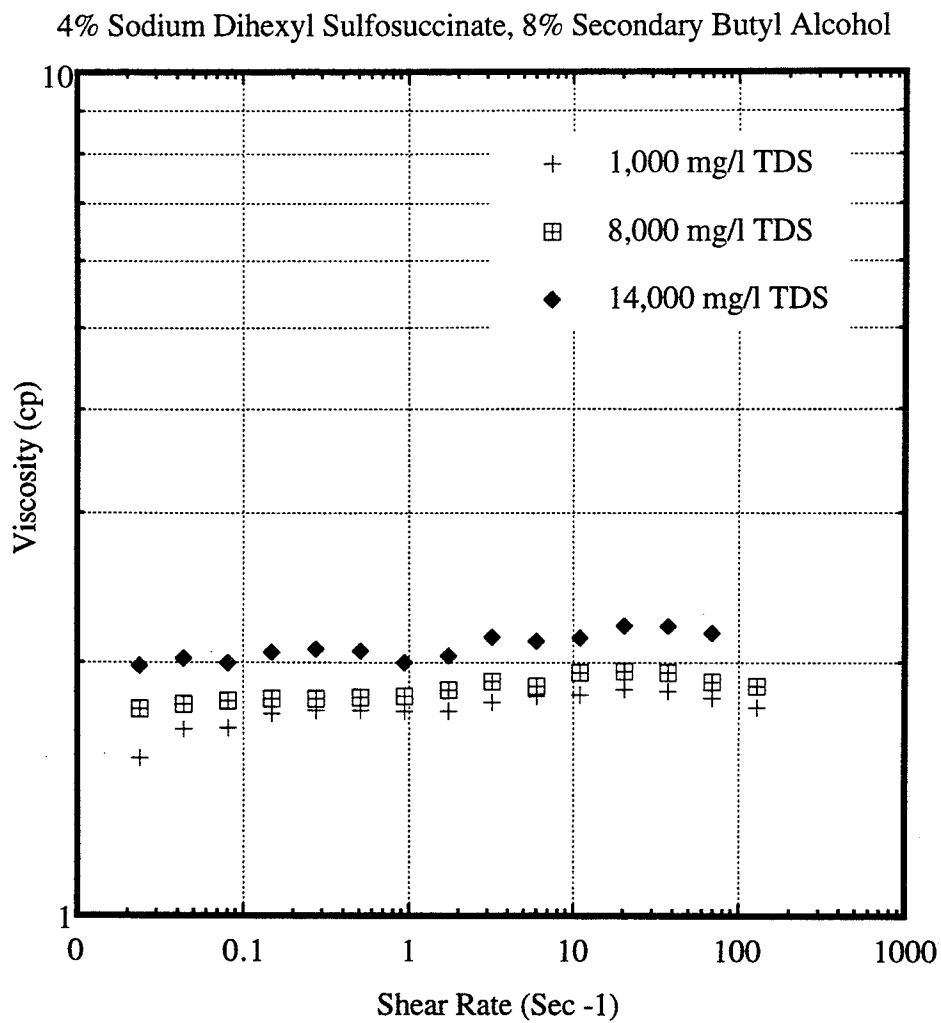


Figure 6.37: Viscosity of 4% by weight sodium diheptyl sulfosuccinate, 8% by weight secondary butyl alcohol plotted against shear rate.

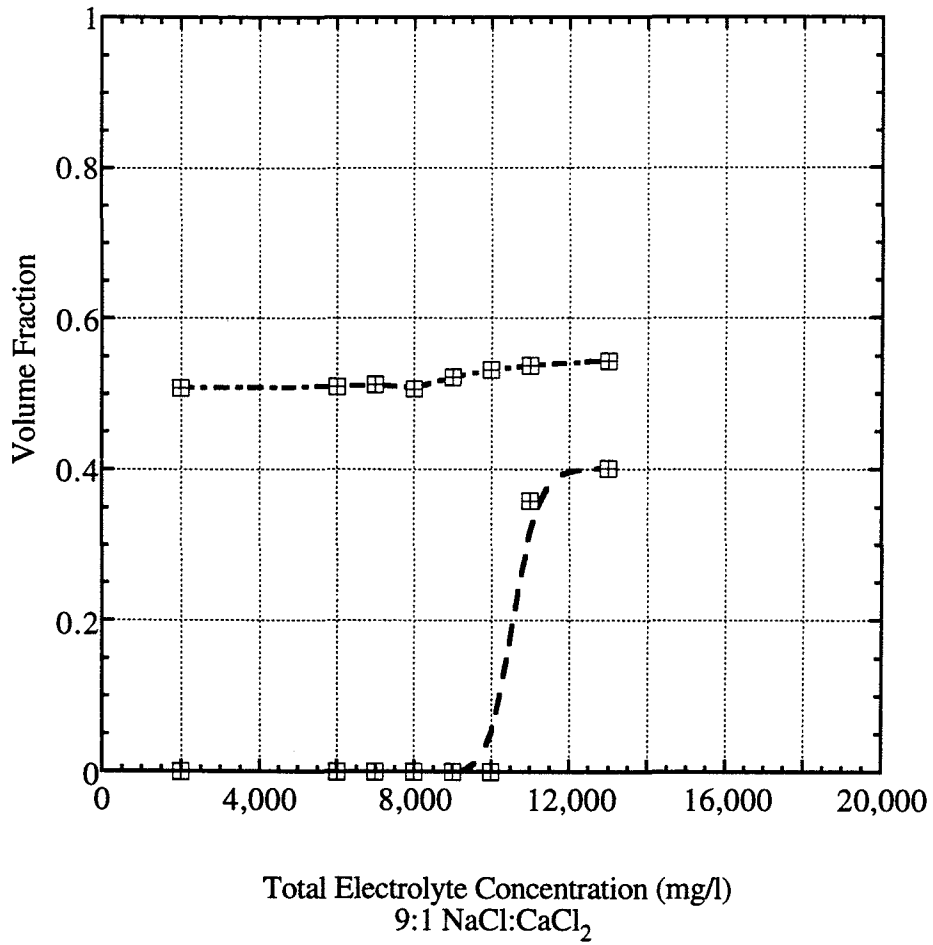


Figure 6.38: Volume fraction diagram for 2% by weight sodium dihexyl sulfosuccinate and 2% by weight dioctyl sulfosuccinate, 8% by weight secondary butyl alcohol.

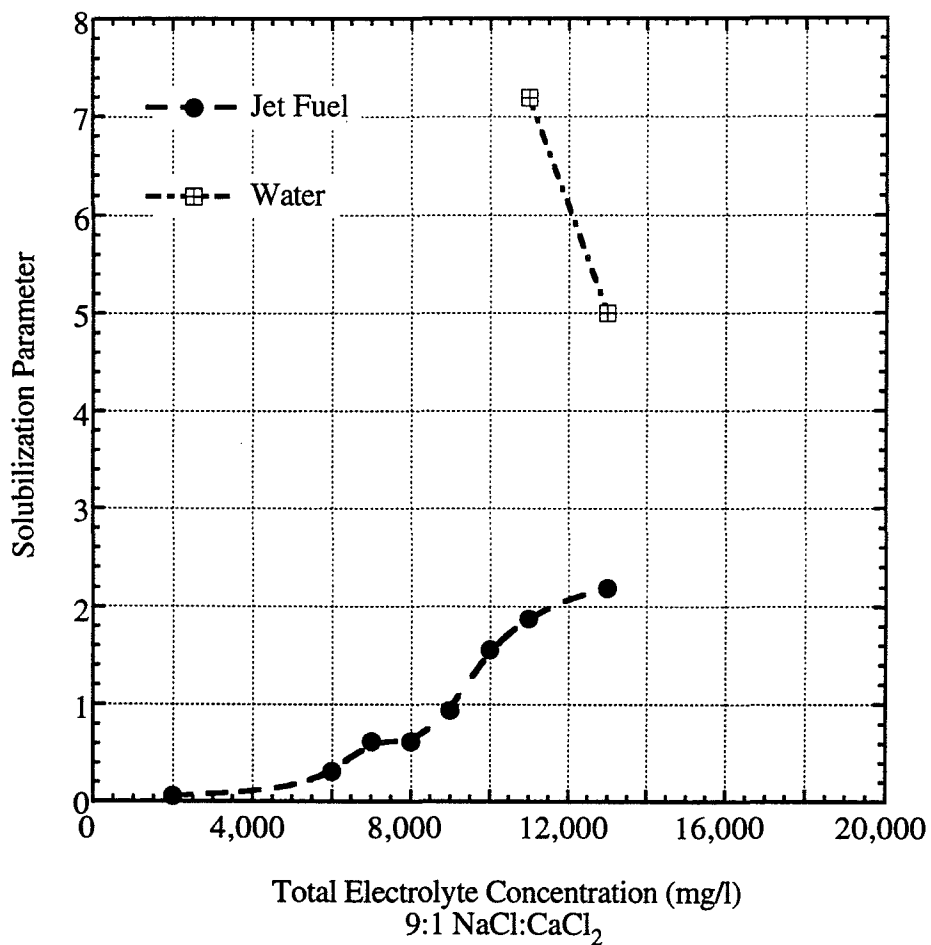


Figure 6.39: Solubilization parameters for 2% by weight sodium dihexyl sulfosuccinate and 2% by weight dioctyl sulfosuccinate with 8% by weight secondary butyl alcohol.

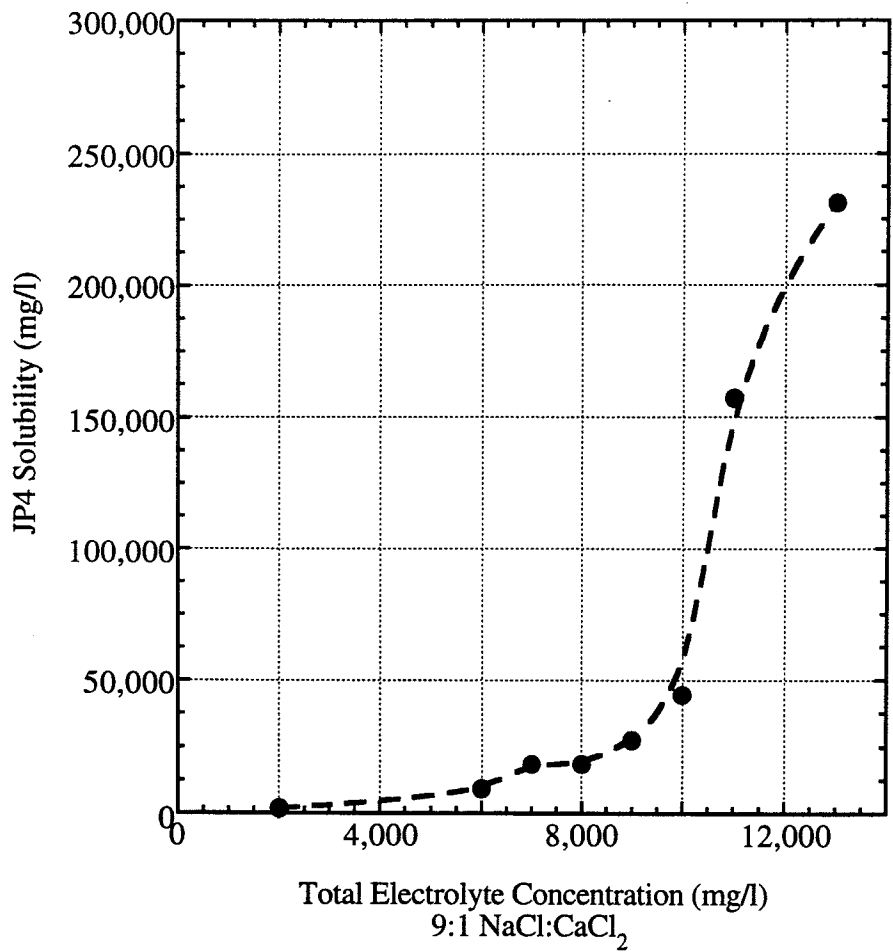


Figure 6.40: Jet fuel solubilization plotted for 2% by weight sodium dihexyl sulfosuccinate and 2% by weight dioctyl sulfosuccinate, 8% by weight secondary butyl alcohol.

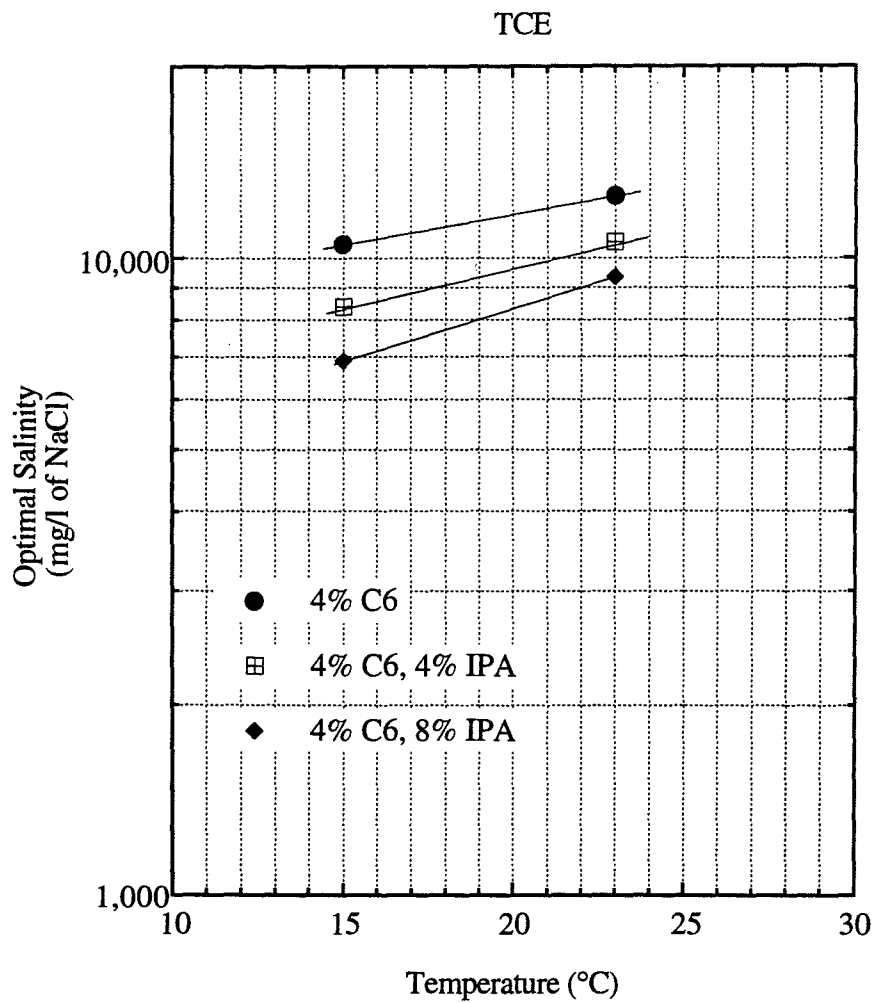


Figure 6.41: Effect of temperature on optimal salinity for 4% by weight sodium dihexyl sulfosuccinate solutions with varying amounts of IPA and TCE.

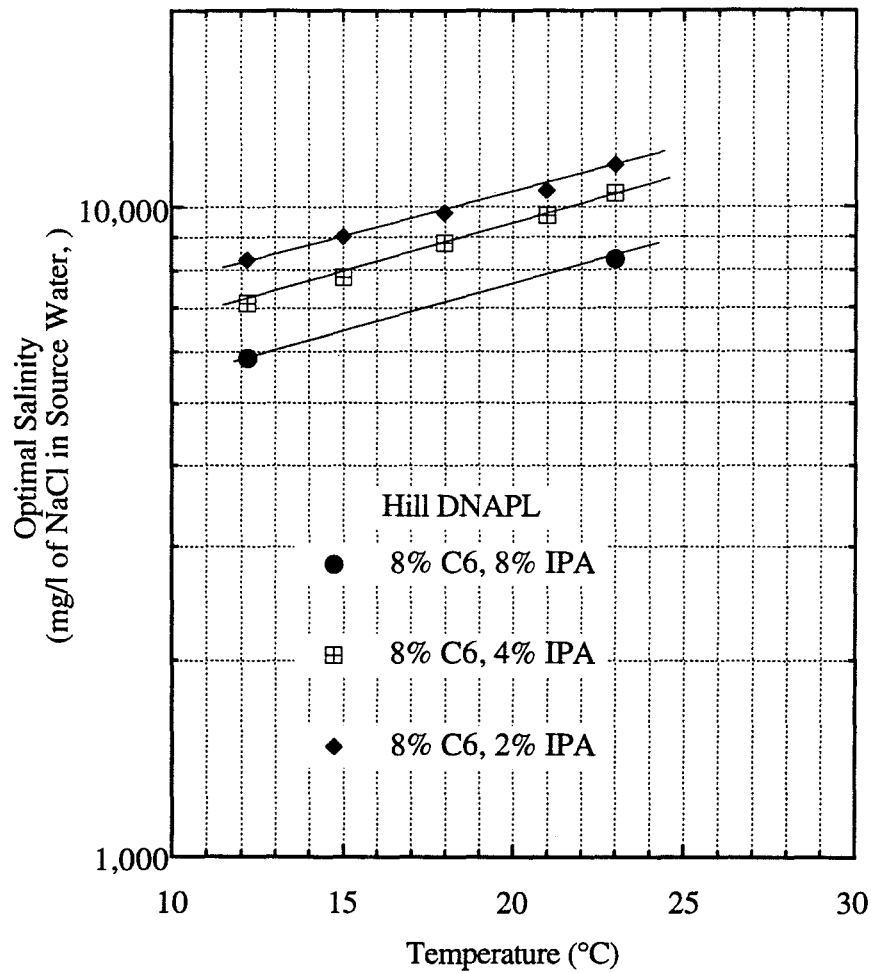


Figure 6.42: Effect of temperature on optimal salinity for 8% by weight sodium dihexyl sulfosuccinate solutions with varying amounts of IPA and Hill DNAPL.



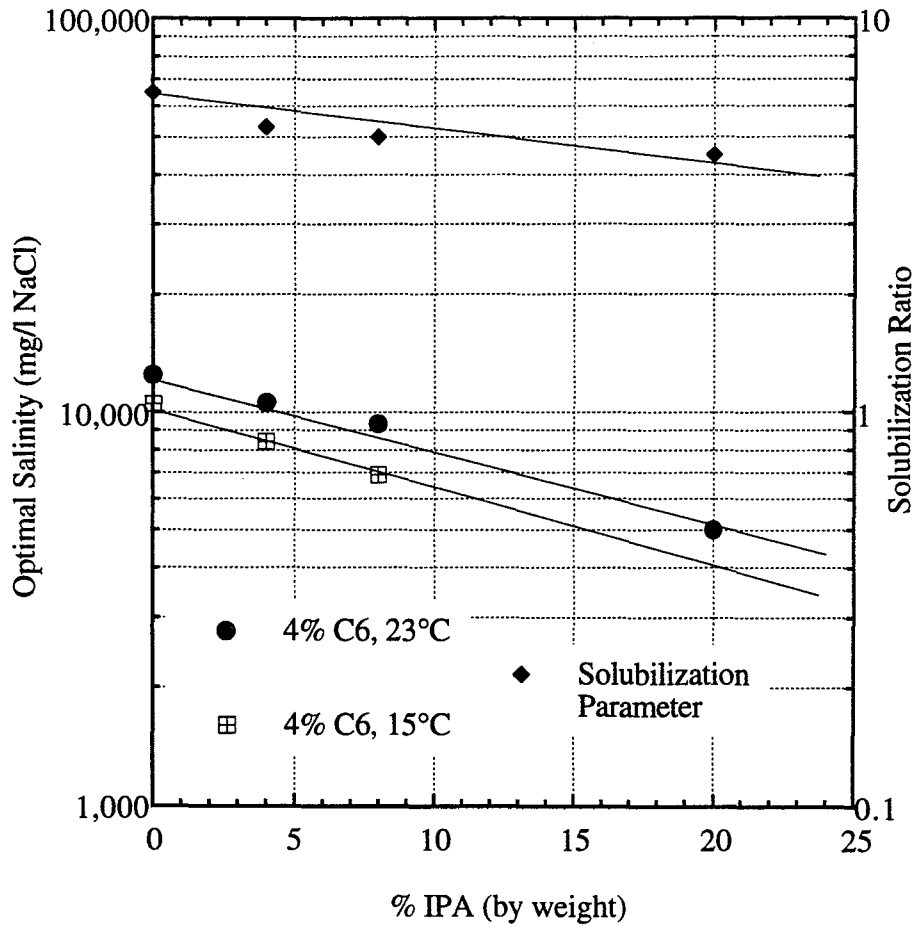


Figure 6.43: Effect of IPA concentration on optimal salinity and solubilization for 4% by weight sodium dihexyl sulfosuccinate TCE.

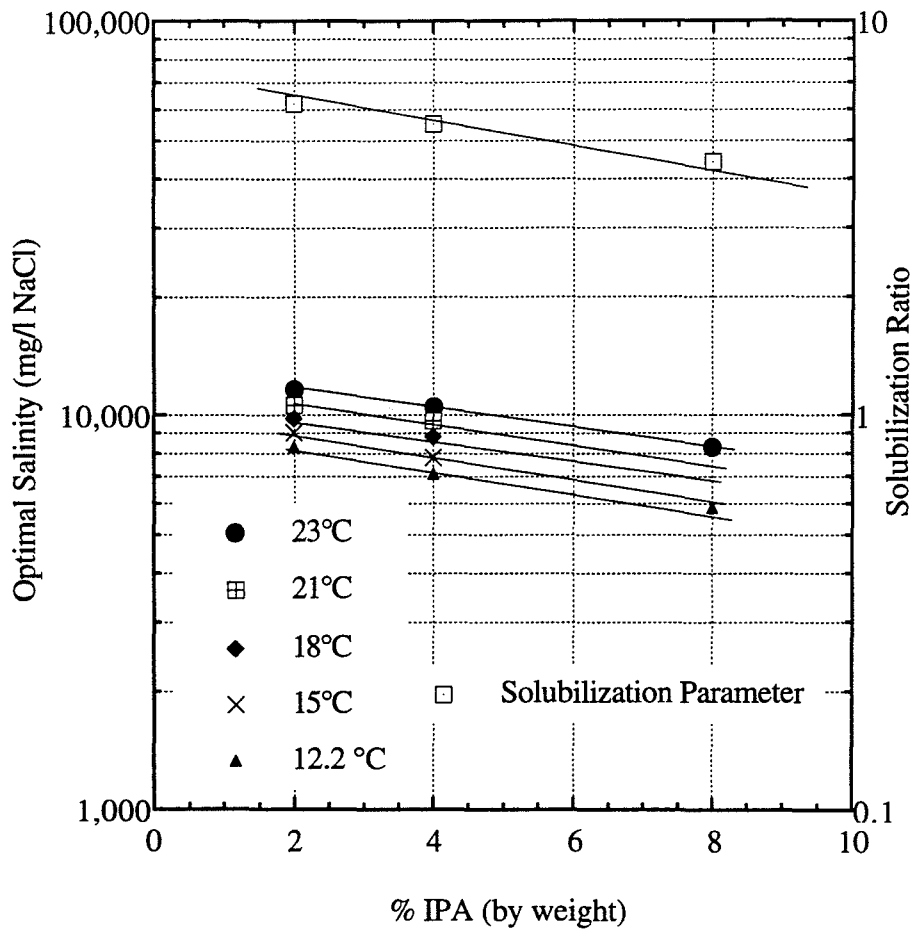


Figure 6.44: Effect of IPA concentration on optimal salinity and solubilization for 8% by weight sodium dihexyl sulfosuccinate and Hill DNAPL.

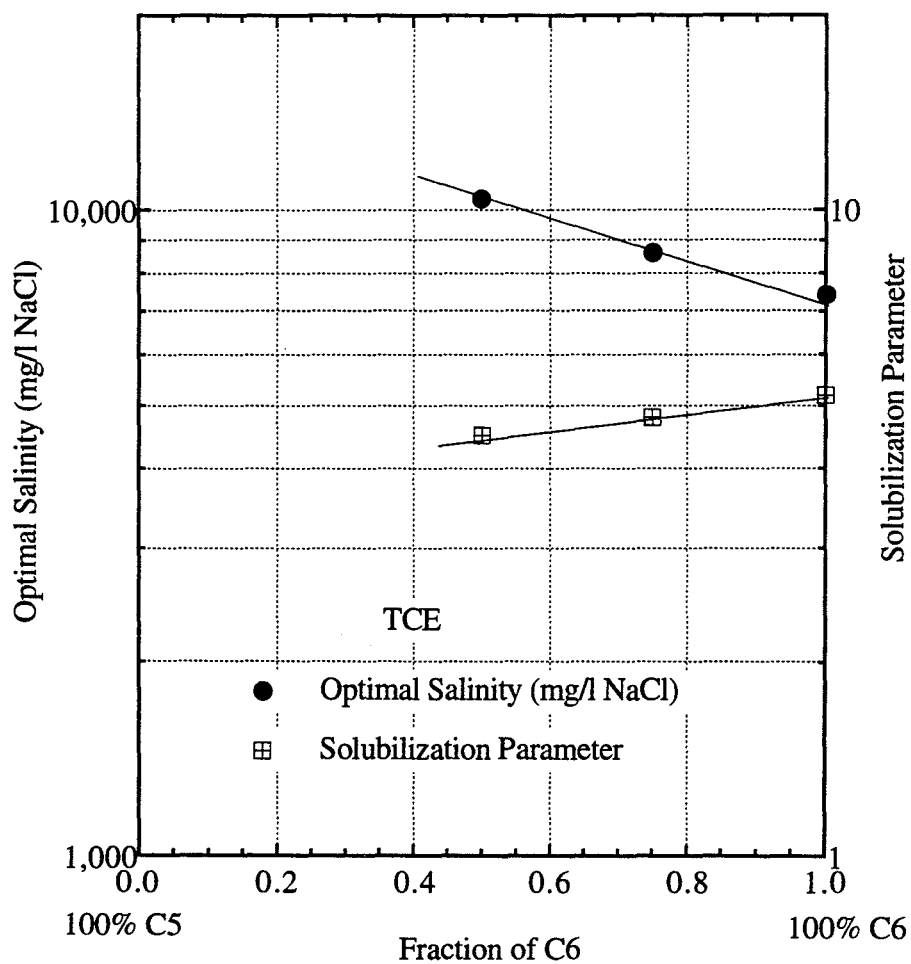


Figure 6.45: Solubilization parameter and optimal salinity plotted as function of surfactant chain length.

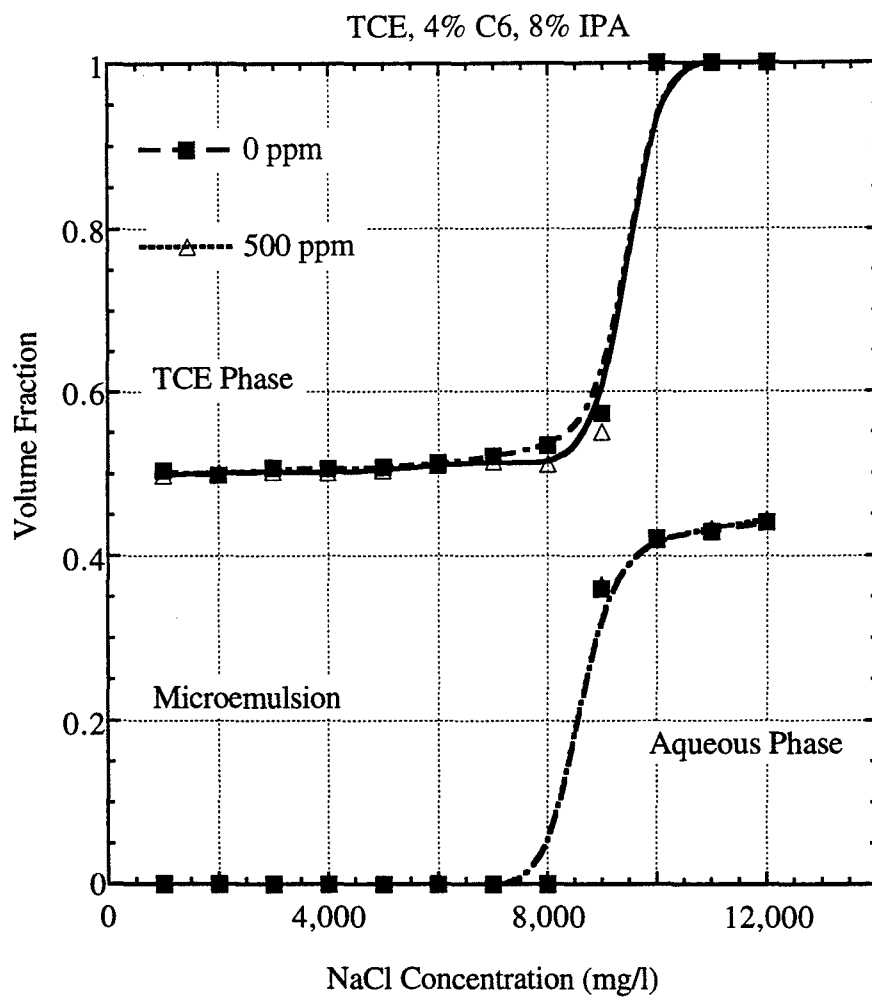


Figure 6.46: Volume fraction diagram for 4% by weight sodium dihexyl sulfosuccinate, 8% by weight IPA, xanthan gum at 23°C.

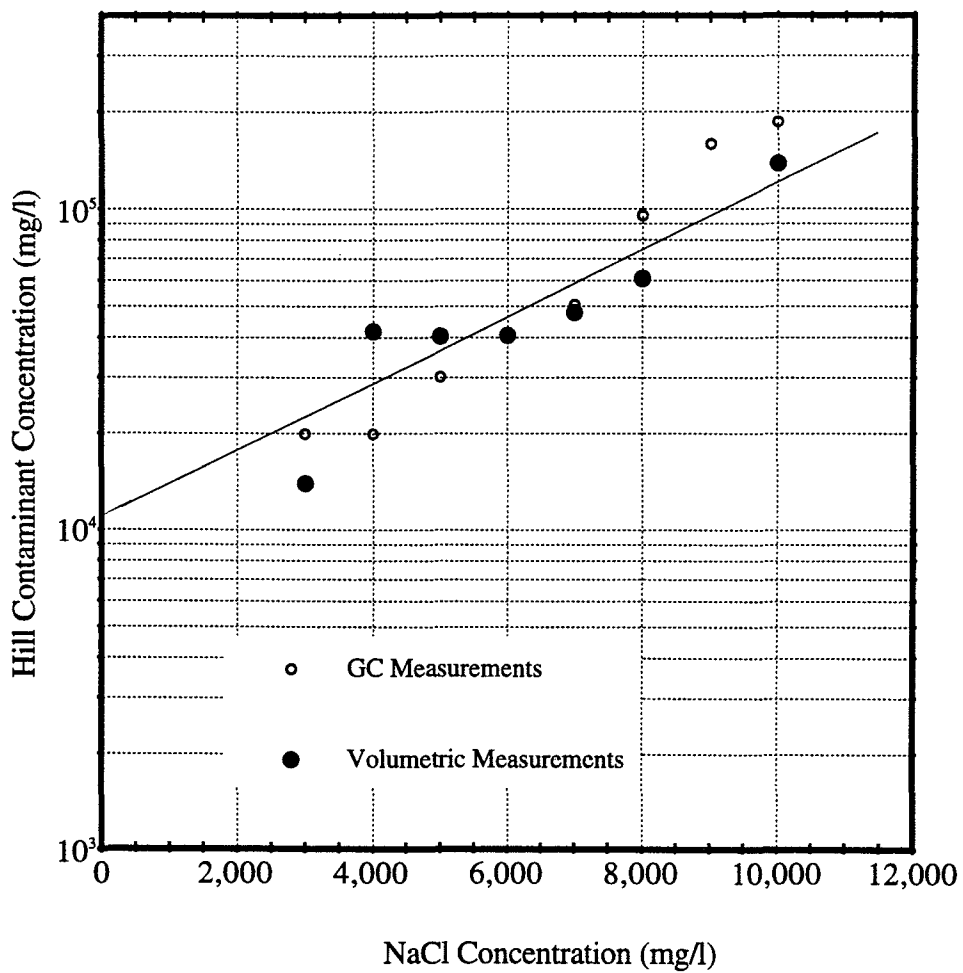


Figure 6.47: Comparison of GC and volumetric measurements of contaminant solubilization at different electrolyte concentrations.

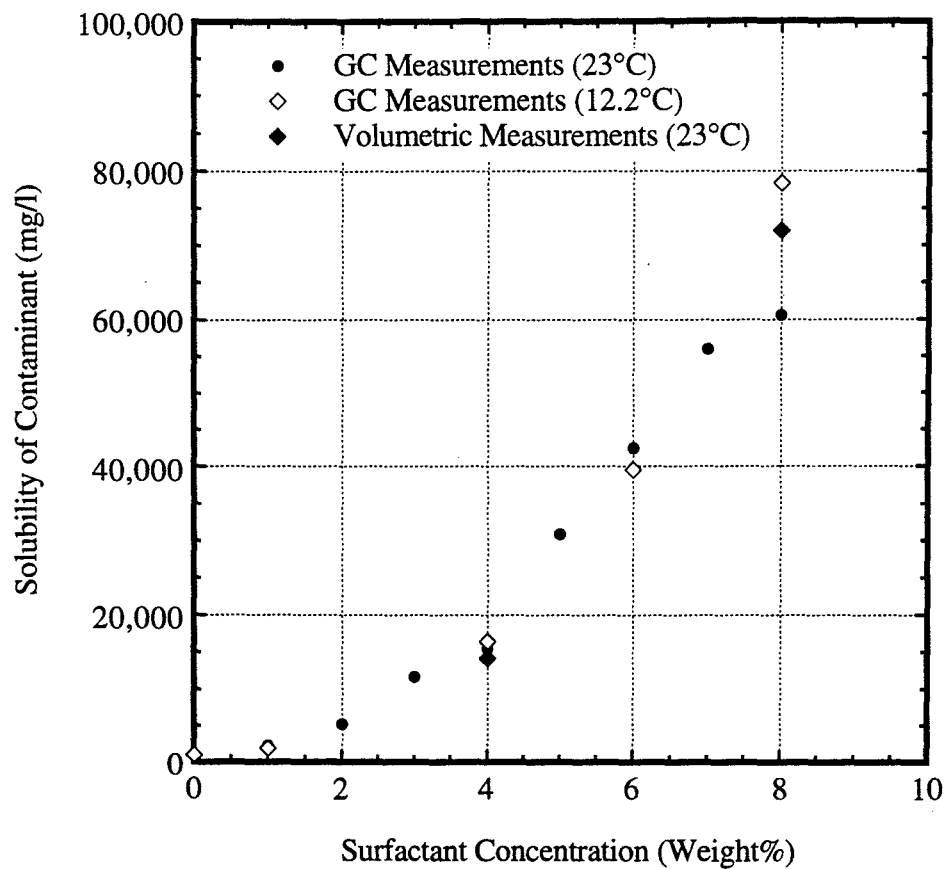


Figure 6.48: Comparison of GC and volumetric measurements of contaminant solubilization at different surfactant concentrations.

Chapter 7: Partition Coefficient Tests

7.1 INTRODUCTION

Partitioning of a species 'i' can be described as mass transfer of the species between two distinct phases. When the partitioning species is a solute at a sufficiently low concentration that it does not significantly affect the properties of the solvents (density, viscosity etc.), then it is called a tracer. The subject of this research is the partitioning of chemical tracers between liquid phases.

The partition coefficient of a tracer species 'i' between NAPL and water has been defined as,

$$K_i = \frac{C_{i,NAPL}}{C_{i,Water}} \quad (4.23)$$

Once tracer candidates are identified, partition coefficients should be measured to determine if they are in the given range for a given application. Static partition coefficient tests and dynamic partition coefficient tests can be performed to measure partition coefficients. Both these tests are described in the following sections. In this work, partition coefficients were measured by both static and dynamic methods.

7.1.1 Static Partition Tests

As the name suggests, static partition coefficient tests are performed under static conditions. The tracer is usually mixed in the aqueous phase. Fixed volumes of aqueous phases (with tracer) and NAPL are mixed and allowed to

equilibrate. Ideally the concentration of the tracer is measured in both the phases after equilibration and the partition coefficient is computed. Static tests are easy to perform and many tracers can be screened at one time. The concentration of the tracers is often more difficult to measure in the NAPL than the water. Hence, the concentration of the tracers in the nonaqueous phase is often computed using mass balance. This can be difficult for tracers with extremely high partition coefficients. For tracers with high partition coefficients (>50), larger volumes of the tracer solution may be mixed with a smaller volume of NAPL to allow for more precise measurement of aqueous phase tracer concentrations.

7.1.2 Dynamic Partition Tests

In this case a soil pack with a NAPL at a known saturation is flushed with a suite of tracers. Ideally one of the tracers is a conservative tracer with a partition coefficient of zero (for example tritiated water). The first moments of all the tracers and the known residual saturation are then used to compute the partition coefficient using the following equation;

$$K_i = \frac{\bar{V}_p - \bar{V}_n}{V_p \cdot S_N} \quad (7.1)$$

The main advantage of a dynamic partition coefficient experiment is that the tracer concentrations do not need to be measured as accurately since the estimated partition coefficients depend on the separation of tracer pulses rather than absolute concentrations. The disadvantages are that dynamic tests are much harder to perform, take a much longer time to complete, need extremely accurate

measurement of residual NAPL saturation and in instances where the DNAPL is highly soluble in water (for example 1,2-Dichloroethane) the residual saturation will change significantly during a tracer test due to water flushing. However, it is very important to perform such tests to ensure that the tracers perform as expected in field soil and to check consistency and precision of the data. Furthermore, dynamic tests are needed to determine the minimum residence time required for equilibrium partitioning, which is a complex function of many variables such as temperature, wettability etc.

7.2 RESULTS WITH VARIOUS NAPLS

Partition coefficients for 28 alcohol tracer candidates were measured with 10 NAPLs using both static partition coefficient tests and dynamic partition coefficient tests (column experiments). The measured K values were almost always within experimental error and hence the combined results are presented. The NAPLs were, tetrachloroethylene (PCE), trichloroethylene (TCE), 1,2-dichloroethane (DCA), carbon tetrachloride (CTET), dichlorobenzene (DCB), 1,1,1-trichloroethane (TCA), trichloromethane (TCM or chloroform), jet fuel (JP4), Hill OU1 NAPL, Hill OU2 NAPL and a mixture of PCE and DCA. The partition coefficients for various NAPLs with various alcohols are presented in Table 7.1 and Table 7.2.

7.2.1 Mixture of PCE and DCA

Field NAPLs are usually mixtures of various organic contaminants. In one contaminated field site at PPG Lake Charles Louisiana, it was known that PCE and DCA were the primary contaminants of concern. Hence partition

coefficients were measured at various fractions of PCE and DCA. The results are presented in Table 7.3 and Figure 7.1. The curve drawn is a smooth curve through all the points.

7.3 APPLICATIONS OF PARTITION COEFFICIENT MEASUREMENT

Based on the experimental measurement of these partition coefficients, the activity coefficients of the tracers in the nonaqueous phase can be computed. Using all this information, a suitable code for estimation of the activity coefficients of the tracers in the nonaqueous phase can be computed for various contaminant mixtures. The aqueous phase activity coefficient can be computed using (Wang *et al.*, 1996);

$$\gamma_i^\infty = \frac{1}{x_i} \quad (7.2)$$

Using the aqueous phase and nonaqueous phase activity coefficients, partition coefficients for various NAPLs and NAPL mixtures can be computed (Wang *et al.*, 1996).

When the partition coefficients for the alcohol tracers are plotted against the solubility of the tracer in water, a linear trend can be observed. In Figures 7.2 and 7.3, the partition coefficients are plotted against the solubility of the alcohols in water for alcohols with one branched methyl group. A similar plot in which partition coefficients are plotted against the solubility of the alcohols in water for alcohols with two branched methyl groups. In all these plots a linear trend can be observed for similar types of alcohols. This can be used as a quick and easy

method to make a preliminary selection of partitioning tracers with appropriate partition coefficients. For example, from Figure 7.2, if a partition coefficient of 100 is needed with trichloroethylene, then an alcohol with one branched methyl group and a solubility of 0.4% can be used. As there are a large number of alcohol isomers with various solubilities, a suitable alcohol can be identified and the partition coefficients predicted.

Table 7.1: Partition coefficients for several NAPLs

Alcohol	PCE	TCE	TCA	CTET	TCM	JP4	DCB
Ethanol	0.0	0.0	0.1	0.0	0.3	0.0	0.0
Iso-Propanol	0.0	0.1	0.1	0.0	1.1	0.0	0.1
1-Pentanol	1.4	3.8	3.1	1.9	10.8	0.9	2.2
2-Methyl-2-Butanol	0.4	1.3	0.7	0.9	3.1	0.5	0.7
1-Hexanol	6.8	18.6	15.2	11.0	57.5	4.0	13.2
1-Heptanol		163.1					
2-Methyl-1-Pentanol	5.4	14.5	11.6	7.8	36.7	3.9	9.0
3-Methyl-1-Pentanol	4.7	12.8	9.7	6.5	41.2	2.8	8.4
2-Methyl-2-Pentanol	2.6	6.3	5.1	3.4	19.7	1.7	3.4
3-Methyl-2-Pentanol	6.2	11.3	8.2	5.9	32.5	2.8	6.0
4-Methyl-1-Pentanol	5.7	16.0	12.8	8.5	58.9	3.7	9.2
2-Methyl-3-Pentanol	5.2	13.2	9.7	7.7	32.6	4.3	7.1
4-Methyl-2-Pentanol	3.8	10.2	7.4	5.1	30.2	2.3	4.9
3-Methyl-3-Pentanol	2.2	4.5	4.4	3.3	18.3	1.5	3.2
2-Ethyl-1-Butanol	9.6	13.0	10.8	7.5	37.3	3.4	7.7
2,3-Dimethyl-2-Butanol	2.8	6.3	4.4	3.3	16.4	1.7	3.0
3,3-Dimethyl-2-Butanol	4.5	9.6	8.9	6.5	31.5	3.2	5.8
3,3-Dimethyl-1-Butanol	3.8	9.5	6.7	4.1	25.9	2.1	4.4
3-Methyl-3-Hexanol	11.8	27.9	20.6	15.9	68.3	7.9	14.4
2-Methyl-3-Hexanol	20.0	43.2	35.4	29.8	81.2	9.9	23.8
3-Methyl-2-Hexanol	19.2	56.9	42.2	30.0		12.4	29.3
2-Methyl-2-Hexanol	10.9	28.1	21.8	16.1	70.1	7.8	14.9
5-Methyl-2-Hexanol	17.1	55.3	39.8	30.4	554.1	10.3	33.7
3-Ethyl-3-Pentanol	13.9	31.9	23.9	17.1	99.2	8.3	16.4
4,4-Dimethyl-2-Pentanol	22.6	51.3	37.6	24.7		12.0	22.1
2,3-Dimethyl-3-Pentanol	12.3	29.0	23.8	17.6	81.6	8.2	15.8
2,4-Dimethyl-3-pentanol		38.2					
2,2-Dimethyl-3-Pentanol	26.4	80.2	45.1	39.1	292.5	19.2	32.4

Table 7.2: Partition coefficients for several NAPLs

Alcohol	DCA	OU1	OU2
Ethanol		0.0	0.0
Iso-Propanol		0.0	0.1
1-Propanol			0.2
1-Pentanol	3.4		
1-Hexanol	28.4	4.4	30.2
1-Heptanol	80.2		140.5
2-Methyl-2-butanol			0.2
2-Methyl-2-Pentanol		1.3	
3-Methyl-3-Pentanol	7.7		6.2
2-Ethyl-1-Butanol			12.5
2,3-Dimethyl-2-Butanol		1.5	
3-Methyl-3-Hexanol		5.5	
3-Methyl-2-Hexanol		12.8	
2-Methyl-2-Hexanol		6.0	
2,4-Dimethyl-3-Pentanol			49.9
2,2-Dimethyl-3-Pentanol		12.9	68.3

Table 7.3: Partition coefficients for PCE, DCA mixture

PCE mole fraction	DCA mole fraction	Partition Coefficient
0.000	1.000	6.4
0.421	0.579	13.2
0.685	0.315	19.0
0.867	0.133	24.1
1.000	0.000	28.4

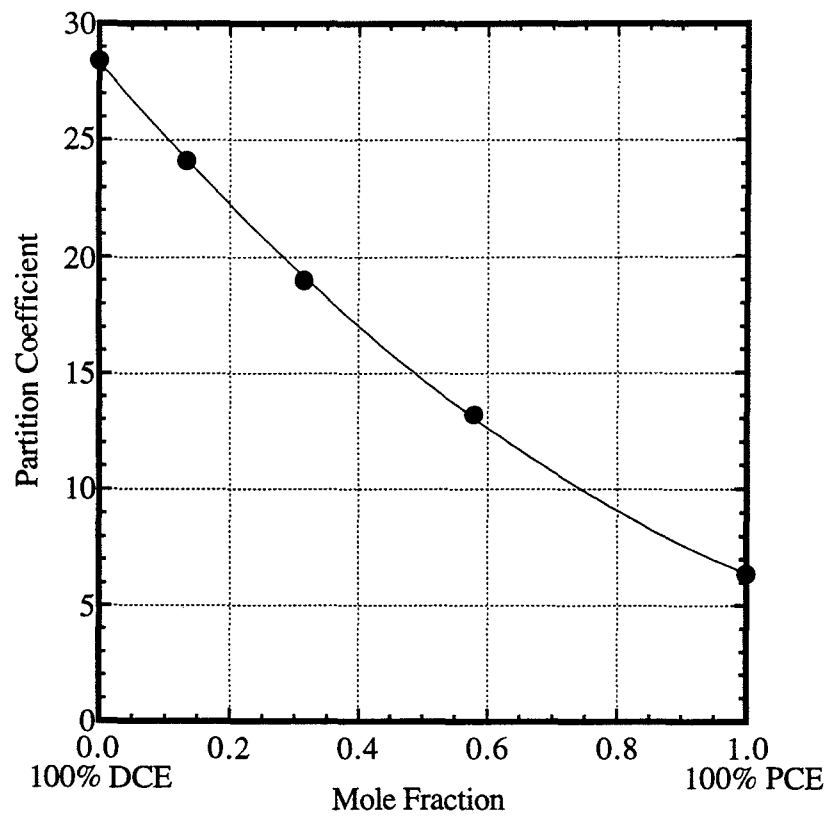


Figure 7.1: Partition coefficients for a PCE, DCA mixture

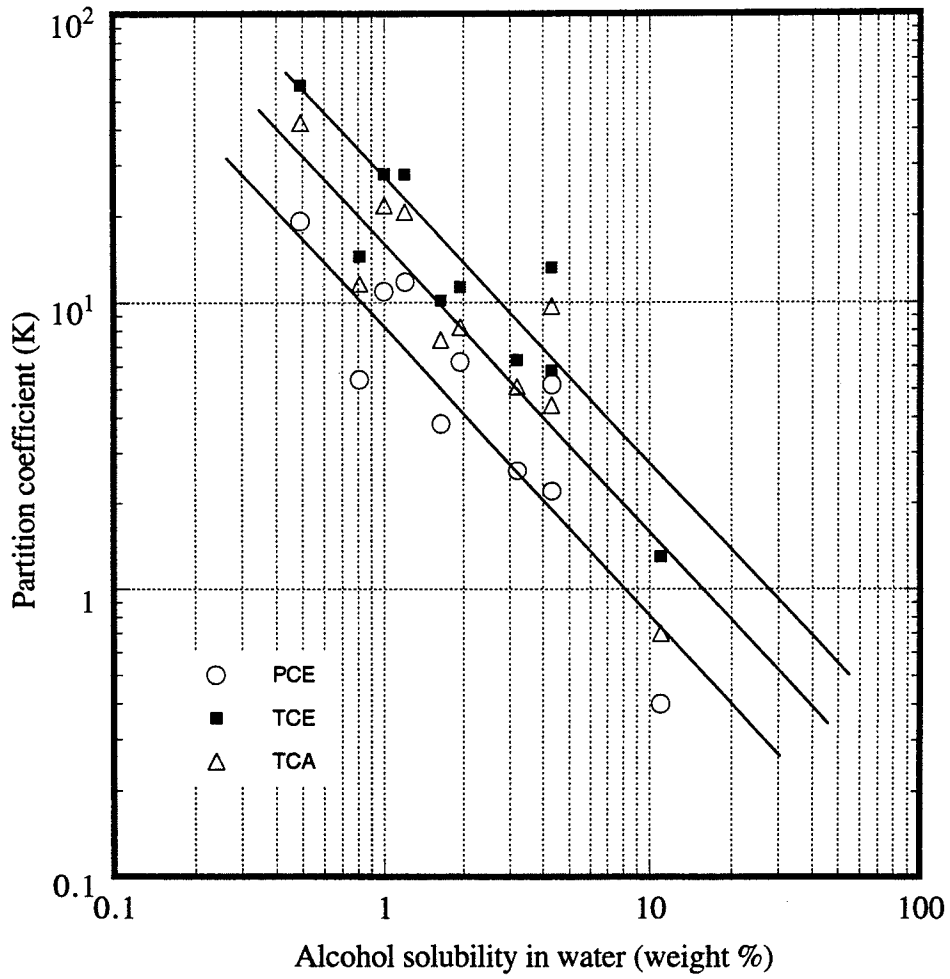


Figure 7.2: Partition coefficients of alcohol tracers with one branched methyl group plotted against solubility for several DNAPLs.

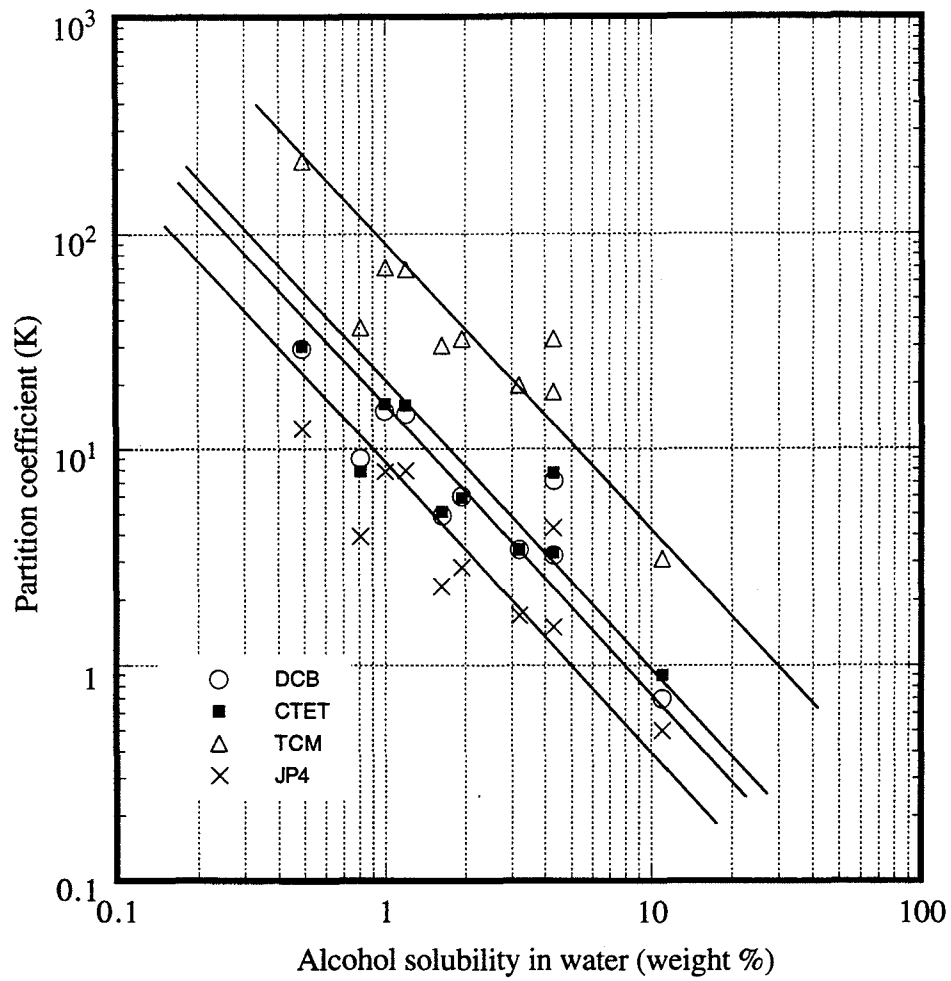


Figure 7.3: Partition coefficients of alcohol tracers with one branched methyl group plotted against solubility for several DNAPLs and Jet Fuel

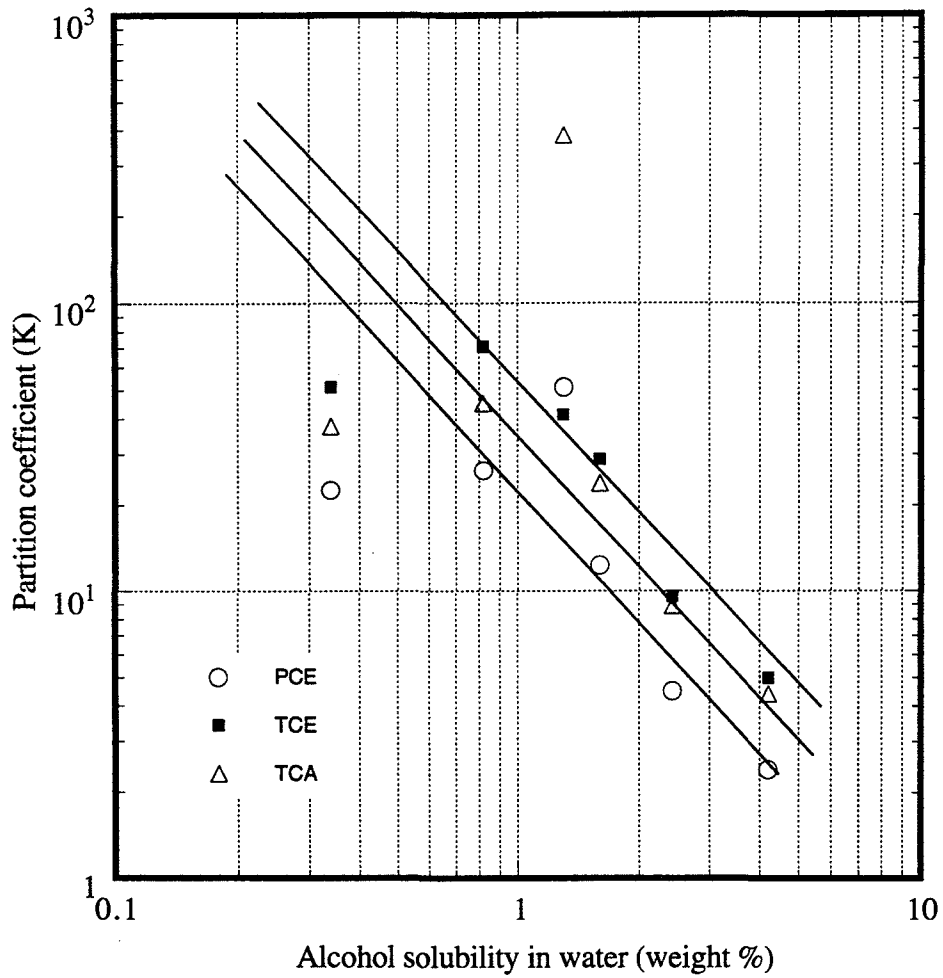


Figure 7.4: Partition coefficients of alcohol tracers with two branched methyl groups plotted against solubility for several DNAPLs.

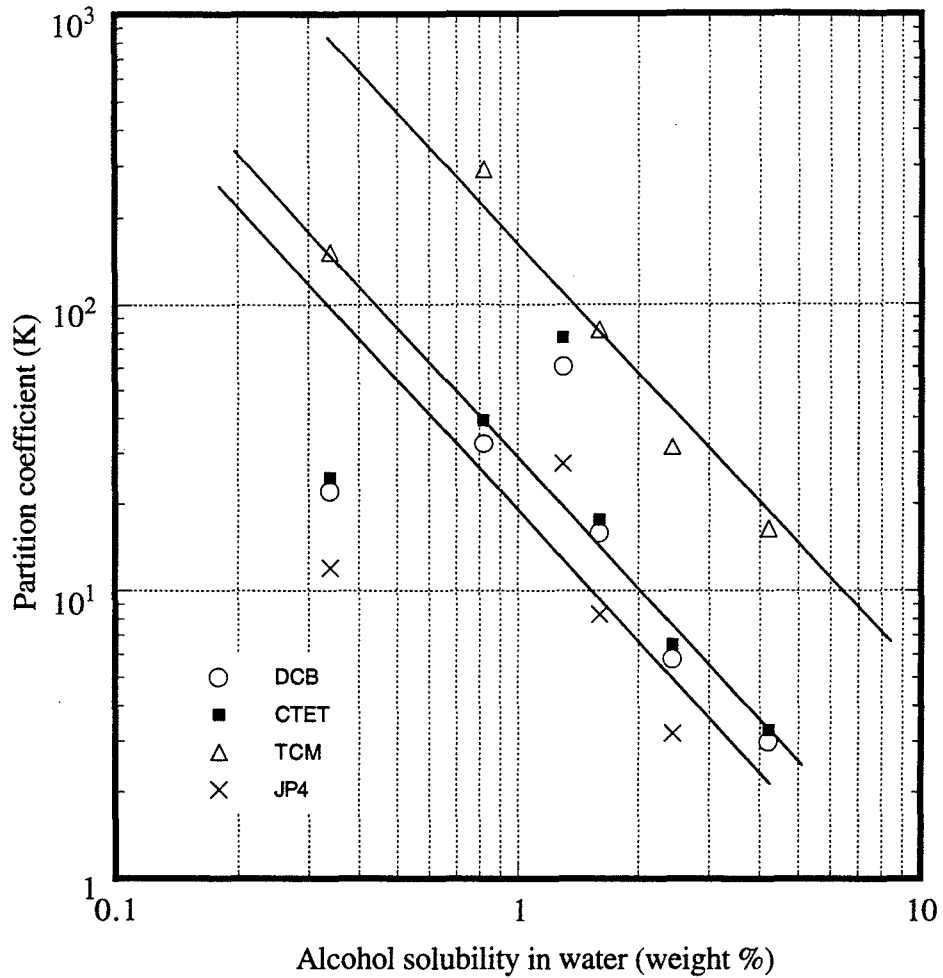


Figure 7.5: Partition coefficients of alcohol tracers with two branched methyl groups plotted against solubility for several DNAPLs.

Chapter 8: Column Experiments, Description and Results

Phase behavior experiments can be used to identify surfactants for use in remediation operations. But in order to use a surfactant solution in field SEAR operations, it is necessary to quantify the behavior of surfactants under dynamic conditions. This can be done in soil column experiments. Essential data that must be collected include recovery of the contaminant, hydraulic gradient (pressure drop) across the soil column during surfactant flooding and surfactant retention due to adsorption or other mechanisms. Surfactant solutions that exhibit high head losses during use in column experiments are usually associated with gels/liquid crystals or emulsions. These cause plugging of pore throats, loss of hydraulic conductivity and consequently high head losses. The main objective of this work was to identify surfactant solutions which exhibited good behavior under dynamic conditions and could be recommended for use in field applications.

Column experiments were also needed to establish the validity of the partitioning tracer test to estimate residual NAPL saturations before and after surfactant flooding to assess the performance of surfactant remediation.

One of the main contributions of this work was the perfection of experimental techniques for performing partitioning tracer tests and surfactant remediation tests in columns packed with Ottawa sand and field soil. A total of fifteen experiments were performed. The contaminants used in these experiments were tetrachloroethylene (PCE), trichloroethylene (TCE), jet fuel (JP4), Hill Operational Unit 1 LNAPL (Hill OU1 NAPL) from Hill AFB and Hill Operational

Unit 2 DNAPL (Hill OU2 DNAPL) from Hill AFB. PCE, TCE and Hill OU2 DNAPL are DNAPLs and JP4 and Hill OU1 NAPL are LNAPLs.

A brief summary of column experiments showing the number of experiments performed and different NAPLs is given in Table 8.1. Soil column properties are given in Table 8.2. The preliminary work in all the experiments in terms of soil washing, soil packing and saturation with water is described in detail in Chapter 3. The description, results and discussion for all the column experiments are presented in the following sections. A discussion on error analysis of all experimental measurements and interfacial tensions is presented in Chapter 9.

8.1 EXPERIMENTS WITH PCE

A total of three experiments were performed with PCE. These experiments were experiments DW#1, DW#2 and DW#3. Experiments DW#1 and DW#2 were low IFT mobilization experiments and experiment DW#3 was a higher IFT solubilization experiment.

8.1.1 Experiment DW#1

Experiment DW#1 was the first experiment performed in this work. The objectives of this experiment were to gain experience in performing soil column experiments and to compare with the results obtained by Jin (1995). The experiment was divided into several parts: the initial tracer test, relative permeability measurement with PCE and water, tracer test at residual water saturation to estimate residual water saturation, tracer test at residual PCE saturation to estimate residual water saturation, surfactant flood for remediation of soil column and post surfactant tracer tests after surfactant flood for performance assessment. In all the other

experiments, the same sequence was followed. However relative permeability measurements were not carried out in the other soil column experiments. The soil column length, diameter, porosity and permeability are presented in Table 8.2.

Initial Tracer Test

The first part of the experiment was the initial tracer test. Tritium was used as the tracer. Tracer was injected until the measured tracer concentration in the effluent equaled the injected tracer concentration. In this experiment, the method of moments was not used to estimate pore volume. Material balance was performed by measuring the volume of fluid injected and volume of fluid produced. A summary of the initial tracer test showing the fluids used, the tracer concentration and pore volume estimates based on volume balance and the initial tracer test is given in Table 8.3. The tracer concentration history is plotted in Figure 8.1. Based on the initial tracer test, a pore volume of 93.0 cc was estimated compared to the pore volume of 87.4 cc based on volume balance. These do not agree very well. In subsequent experiments, the difference between the weight of the soil column before saturation with water and weight of the soil column after saturation was water was used for estimation of pore volume. This technique is termed mass balance in this work.

Contamination of Soil Column and Relative Permeability Experiments

The column was oriented vertically. Contamination of the soil column was carried out by injecting PCE into the column from the bottom. While injecting PCE, water was also injected and a steady state relative permeability experiment with PCE and water was performed. PCE and water were injected using two

different pumps at fixed flow rates. The samples were collected in graduated test tubes and the pressure drop at steady state was measured. The flow rates for both PCE and water were changed and the above procedure was repeated. The drainage and imbibition relative permeability curves were estimated based on steady state flow rates and pressure measurements. The rates used for both the drainage and imbibition relative permeability experiments are given in Table 8.4 and Table 8.5.

Relative Permeability Experiments; Results

Using Darcy's law at steady state, the relative permeability can be calculated by the following equation;

$$\frac{Q_j \mu L}{A \Delta \Phi_j k} = k_{ri} \tag{8.1}$$

From Delshad (1990), the potential drop can be defined as;

$$\Delta \Phi_j = \Delta p_T - (\rho_j - \rho_x)gh \text{ for flow upwards into the column} \tag{8.2}$$

$$\Delta \Phi_j = \Delta p_T + (\rho_j - \rho_x)gh \text{ for flow downwards into the column} \tag{8.3}$$

Also from the above,

$$H = \frac{\Delta \Phi_j}{\rho_j g} \tag{8.4}$$

$$H_D = \frac{H}{L} \tag{8.5}$$

Using the above equations, the relative permeability was calculated at different saturations of PCE. The results for the drainage relative permeability experiment are given in Table 8.6. The saturations of the PCE phase and water phase were estimated using the difference between the amounts of PCE and water injected and produced. The drainage relative permeability is plotted in Figure 8.2.

Imbibition relative permeability data are presented in Table 8.7. The imbibition relative permeability data are plotted in Figure 8.3. Since some errors were made in the volume measurements during the imbibition portion of the experiment, the errors in the saturations are unfortunately quite large and time did not permit a repeat of this experiment. Nevertheless some rough indication of the relative permeability was obtained and is useful.

Tracer Test at Residual Water Saturation

At the end of the drainage relative permeability test, a tracer test using ^{14}C radiolabeled PCE was performed. A slug of PCE was injected followed by flooding with non-radioactive PCE. The details of this test are given in Table 8.8. The tracer concentration history is plotted in Figure 8.4. Enough non-radioactive PCE was not injected to characterize the complete tracer concentration history. Hence moment analysis could not be used for estimating residual water saturation.

Tracer Test at Residual PCE Saturation

At the end of the imbibition relative permeability test, the column was flooded with water to reach residual PCE saturation. At residual PCE saturation, a tracer test using tritium as tracer was performed. A slug of tritium was injected

followed by flooding with water. The details of this test are given in Table 8.9. The tracer concentration history at residual PCE saturation is plotted in Figure 8.5. Based on tritium data, an aqueous pore volume of 72 cc was calculated. Using an initial pore volume of 93.0 cc, a waterflood residual PCE saturation of 0.226 was calculated.

Surfactant Flood to remediate PCE

A solution of 2% sodium diamyl sulfosuccinate, 2% dioctyl sulfosuccinate with 500 mg/l CaCl_2 was injected at an interstitial velocity of 0.15 m/day (0.3 cc/min). This surfactant solution was a Winsor type I solution with a PCE solubilization parameter of 1.2 and PCE solubilization of 80,000 mg/l. The IFT between the microemulsion and excess PCE was 0.02 dynes/cm. A total of 1072.5 cc (11.5 pore volumes) of surfactant solution was injected. The total PCE recovery was calculated by adding the volume of free PCE produced and PCE in microemulsion produced during surfactant flooding. A total of 16.4 cc of free PCE was produced during the surfactant flood. The volume of PCE in the soil column was estimated as 21 cc. Hence only 77.9% of the PCE was recovered.

Out the total volume of PCE produced, 16.0 cc was mobilized as free PCE and 0.4 cc was solubilized. The term free PCE describes the PCE produced as a separate nonaqueous phase. The concentration of the PCE in the effluent was observed to fall below 200 mg/l (solubility of PCE in water) after four pore volumes of surfactant flooding. The PCE concentration history during the surfactant flood is plotted in Figure 8.6.

In this experiment, the pressure drop across the soil column during the surfactant flood was not measured. At 2.7 pore volumes of total production, the sampling interval was changed from 10 minutes to 16 minutes. An increase in PCE concentration in the effluent from 200 mg/l to 1,000 mg/l was observed. After 6.1 pore volumes of total production, the pump was stopped for 66 hours. The PCE concentration in effluent was observed to increase from about 100 mg/l to 500 mg/l. The pump was stopped again for 11 hours at 8.2 pore volumes when the PCE concentration was observed to increase from 100 mg/l to 300 mg/l.

After surfactant injection, about 1,300 cc (14 pore volumes) of water was injected at 0.15 m/day interstitial velocity (0.3 cc/min) to remove the surfactant. After 14 pore volumes of waterflooding, about 50 cc of water was injected at 3 cc/min to determine the permeability of the soil column after remediation. The permeability at the end of the post surfactant waterflood was measured as 0.6 Darcies compared to the initial permeability of 5.9 Darcies. This is probably due to plugging of the soil column by gel/liquid crystal formation. A summary of the surfactant flood for experiment DW#1 is given in Table 8.10.

Tracer Test After Surfactant to Estimate Residual PCE Saturation

After 11.5 pore volumes of surfactant and more than 14.0 pore volumes of post surfactant waterflooding, tritium tracer was injected into the soil column to estimate the final residual PCE saturation. About 171.5 cc (1.8 pore volumes) of tracer was injected followed by 230 cc of water at an interstitial velocity of 1.5 m/day (3.1 cc/min). This test was repeated by injecting 102.4 cc (1.1 pore volumes) of tracer followed by injecting 180 cc of water at 1.5 m/day (3.0 cc/min).

Both these tests are summarized in Tables 8.11 and 8.12. The tracer concentration histories from both these experiments are plotted in Figures 8.7 and 8.8 respectively. The aqueous pore volume of the soil column was 20.5 cc for the first test and 10.5 cc for the second test. Both these values are much lower than the initial aqueous pore volume of 93.0 cc for the uncontaminated column. This shows that there was plugging of the soil column by surfactant.

Discussion for Experiment DW#1

Even though experiment DW#1 was full of many errors and mistakes, useful observations, conclusions and inferences were drawn. The weight of the soil column was not used for estimating PCE saturation. Volume balance was the only means to estimate initial pore volume and residual PCE saturation. Hence an accurate determination of initial pore volume and residual PCE saturation was not obtained. In general, volume balance of DNAPL was prone to errors. A poor match of the initial pore volume estimate between volume measurement and the tracer measurements also led to errors in estimation of residual PCE saturation. The tracer estimate of pore volume was used for all calculations.

In the initial tracer test, sampling and analysis was not carried out during the post tracer waterflood (carried out to recover tracer). Hence, the down sweep side of the tracer concentration history was not obtained. Sampling and analysis of tracer during this period would have enabled performing a moment analysis for a more accurate determination of the pore volume. Similarly during the tracer test at the end of the PCE flood, enough samples were not analyzed to characterize the complete tracer concentration history. A poor estimation of residual PCE volume

gave rise to poor estimation of PCE recovery i.e. 77.9% recovery based on material balance estimates.

During analysis of effluent samples during the surfactant flood, many observations were made. PCE concentration was observed to increase when sample size was increased from 3 to 7.8 cc. This increase in PCE concentration in the effluent when sample size was increased could not be explained. But the sudden increase observed when the pump was stopped two times was attributed to desorption of adsorbed PCE by the Teflon end pieces during the shut in period. This may also account for a persistent PCE tail of the order of 60 to 90 mg/l after 10 pore volumes of flooding.

A look at the final tracer breakthrough curves show early breakthrough times and small aqueous pore volumes. In the first post surfactant tracer the aqueous pore volume was 20.5 cc and in the second post surfactant tracer the swept volume was 10.5 cc. Both these numbers were substantially below the initial pore volume of 93 cc based on tracers. Based on these results and a final permeability measurement of 0.6 Darcies, it can be inferred that there was pore plugging by surfactant. This caused a reduction in aqueous pore volume of the soil pack. Pore plugging could have been caused by formation of gels and liquid crystals in the surfactant during the surfactant flood.

8.1.2 Experiment DW#2

In experiment DW#2, a stainless steel column was used to eliminate the plastic end pieces which have potential for adsorbing and desorbing chlorinated solvents such as PCE. In addition to volume balance (used in DW#1), the

difference in weight of the uncontaminated soil column and the contaminated soil column was used to estimate the residual PCE saturation (mass balance). In this experiment, a small slug of tracer was injected into the column followed by injection of water instead of injecting more than one pore volume of tracer. The method of moments was used to determine the pore volume. Alcohol partitioning tracers were used for the first time for estimation of residual PCE saturation. A surfactant capable of producing a Winsor type III microemulsion was used to remediate the contaminated soil column. The soil column length, diameter, porosity and permeability are presented in Table 8.2.

Initial Tracer Test

In this experiment, tritium, isopropyl alcohol (IPA) and 2,3-dimethyl-2-butanol were used to estimate pore volume. About 3.8 cc of tracer solution was injected followed by a waterflood at an interstitial velocity of 11 m/day (1 cc/min). The residence time of the tracers was 0.7 hours. The samples were analyzed using a gas chromatograph (GC) for the alcohols and liquid scintillation counter (LSC) for tritium samples. The method of moments was used to calculate pore volume of the soil column. The tracer concentration history is plotted in Figure 8.9. A summary of the initial tracer test is given in Table 8.13.

An excellent match between pore volume estimates based on volume balance and tracers was obtained. The average pore volume based on tracers was 42.5 cc and the pore volume based on volume balance was 41.2 cc. The tracer recoveries were around 100% within experimental error.

Contamination of Soil Column

The column was oriented vertically. Contamination of the soil column was carried out by injecting PCE into the column from the bottom until residual water saturation was reached followed by injection of water from the top of the column until residual PCE saturation was reached. The pressure gradient across the soil column at steady state during the PCE flood was 1.0 psi/ft (at 1 cc/min). The pressure gradient across the soil column at steady state during the waterflood was 0.52 psi/ft (at 1 cc/min). The end point PCE relative permeability was measured at residual water saturation and the end point water relative permeability was measured at residual PCE saturation. A summary of contamination of the soil column is given in Table 8.14. A residual water saturation of 0.323 was reached at the end of the PCE flood and a residual PCE saturation of 0.202 (mass balance) was reached at the end of the waterflood.

Tracer Test at Residual PCE Saturation

A suite of conservative and partitioning tracers was injected into the soil column at an interstitial velocity of 0.6 m/day (0.05 cc/min) to measure residual PCE saturation. The injected tracers were tritium, IPA and 2,3-dimethyl-2-butanol. The mean residence time for tritium and IPA was 11.2 hours and for 2,3-dimethyl-2-butanol it was 19 hours. The samples were analyzed using a gas chromatograph for the alcohol tracer concentrations and a liquid scintillation counter for tritium concentration. The tracer concentration history is plotted in Figure 8.10. The retardation of 2,3-dimethyl-2-butanol is observed in Figure 8.10. A summary of the partitioning tracer test is given in Table 8.15.

The residual PCE saturation based on partitioning tracers was calculated based on the retention time and the measured partition coefficient of the partitioning tracers. When tritium was used as the conservative tracer and 2,3-dimethyl-2-butanol was used as the partitioning tracer, a PCE saturation of 0.195 was calculated. When IPA was used instead of tritium, a saturation of 0.175 was calculated. A summary of residual PCE saturation estimates based on mass balance, volume balance and partitioning tracers is given in Table 8.16.

Surfactant Flood to Remediate PCE

A solution of 2% sodium diamyl sulfosuccinate, 2% dioctyl sulfosuccinate with 1,300 mg/l CaCl_2 was injected at 0.6 m/day (0.05 cc/min). This surfactant solution was a Winsor type III solution with a PCE solubilization parameter of 12.5 and PCE solubilization of about 1,000,000 mg/l. The IFT between the excess PCE and microemulsion was 0.01 dynes/cm. A total of 614.4 cc (14.7 pore volumes) of surfactant solution was injected. A total of 7.7 cc of PCE was mobilized and produced as free PCE and 0.35 cc was solubilized in the microemulsion. Based on this, a total of 98% PCE was recovered. About 94% of the PCE was mobilized and 4% was solubilized. This experiment is summarized in Table 8.17.

The PCE concentration history is plotted in Figure 8.11. The relative amount of PCE solubilized and mobilized and the total amount of PCE recovered as a function of pore volumes produced are plotted in Figure 8.12. Concentrations of PCE greater than 50,000 mg/l correspond to two-phase samples containing both microemulsion and free PCE. The maximum PCE concentration measured in the effluent was 850,000 mg/l compared to the equilibrium phase behavior value of

about 1,000,000 mg/l. The pump was stopped for 22 hours at 12 pore volumes. An increase in PCE concentration from about 130 mg/l to 330 mg/l was observed followed by a decline to about 130 mg/l. A persistent PCE tail on the order of 150 mg/l was observed. This was greater than the PCE tail of about 60-90 mg/l in experiment DW#1.

An attempt was made to measure pressure drops using a 5 psid and a 20 psid Validyne transducer. The pressure drop went off range for both transducers. A 100 psid Validyne transducer was then used to measure the pressure drop. A pressure drop of 32 psi. was measured across the soil column during the surfactant flood. The column was then flushed with 500 cc (11.9 pore volumes) of 500 mg/l CaCl₂.

Since extremely high pressure drops were measured during the surfactant flood, the viscosities of the flooding surfactant solutions and the microemulsions were measured as an aid to understanding why the hydraulic gradient was so high. The viscosities of the aqueous surfactant solution and the middle phase microemulsion are plotted as a function of shear rate in Figure 8.13. The viscosity of the aqueous surfactant solution is non-Newtonian and high. Even at high shear rates, the viscosity is about 7-10 cp. The permeability of the soil after surfactant remediation was 1.5 Darcies compared to the initial permeability of 15.4 Darcies.

Tracer test After Surfactant to Estimate Residual PCE Saturation

After 14.7 pore volumes of surfactant and 11.9 pore volumes of post surfactant waterflooding, tritium tracer was injected into the soil column to estimate the final residual PCE saturation. About 4.3 cc (0.1 pore volumes) of tracer was

injected followed by a waterflood at an interstitial velocity of 0.6 m/d (0.05 cc/min). The breakthrough of tracer in the post surfactant tracer occurred much earlier than tracer breakthrough in the initial tracer test. The results from this test are summarized in Table 8.18. The tracer concentration history is plotted in Figure 8.14. The apparent aqueous pore volume of the soil column was 15.4 cc in this tracer test compared to an initial pore volume of 42.5 cc. This is clearly an indication of bypassing due to the plugging problem rather than the true pore volume.

Discussion for Experiment DW#2

The main improvement in experiment DW#2 was a good match between initial pore volume estimates using tracers and material balance measurements. The pore volume estimate based on mass balance and tracers agreed to within $\pm 3.5\%$. Since no retardation of alcohol tracers was observed during the initial tracer test in clean Ottawa sand, it can be inferred that there was no measurable alcohol tracer adsorption. This was further validated by tracer recoveries which were $100\pm 10\%$. This variation in tracer recovery was due to analysis error in the tracer injectate sample and some error associated with GC analysis.

An excellent match was obtained between the volume balance estimate and mass balance estimate of residual PCE saturation. The residual PCE saturation based on mass balance was 0.181 compared to 0.208 using tritium and 2,3-dimethyl-2-butanol. Only 57.3% 2,3-dimethyl-2-butanol was recovered during the tracer test but the estimate of residual PCE saturation was not affected by the low tracer recovery.

The PCE concentration history showed two separate peaks in experiment DW#2. This was attributed to poor design at the effluent end of the soil pack. The tubing from the column to the fraction collector had a loop which trapped the heavier PCE. When the loop was removed, the PCE trapped in the loop was produced giving rise to the second PCE peak.

Based on contaminant recovery curves, more than 97.7% PCE was recovered by surfactant remediation. By comparing the PCE concentration history in experiment DW#1 and DW#2 it is observed that the persistent PCE tail in experiment DW#2 has a higher concentration (130 to 160 mg/l) compared to experiment DW#1 (60 to 90 mg/l). This result was observed despite the use of a steel column without any Teflon end pieces in experiment DW#2. This can be explained by the occurrence of a greater number of surfactant hemi-micelles due to an increased concentration of CaCl_2 in experiment DW#2 (1,300 mg/L as opposed to 500 mg/L). Since a salinity gradient was not used to break up the hemi-micelles, PCE was retained in large hemi-micelles and slowly partitioned into the flowing surfactant thereby causing persistent PCE concentration in the effluent. A smaller increase in PCE concentration on stoppage of the pump was observed in experiment DW#2 compared to experiment DW#1. This is because the steel column had no Teflon end pieces to desorb any PCE. The small increase in PCE concentration was due to desorption of PCE by the nylon tubing between the column and the fraction collector.

A look at the final tracer curve showed extremely small break through times and a smaller aqueous pore volumes. Based on an aqueous pore volume of 20.8 cc (lower than a pore volume of 42.5 cc) and a final permeability measurement of 1.5

Darcies, it can be inferred that there was pore plugging which caused reduction in aqueous pore volume through the soil pack. This was further substantiated by the non Newtonian behavior observed in Figure 8.13 between viscosity of the aqueous surfactant solution and shear rate. In general, surfactant solutions exhibiting non Newtonian behavior without addition of polymer are indicative of gel and liquid crystal formation. These gels and liquid crystals can cause pore plugging and excessive pressure drops and a reduction in aqueous volume as observed in experiments DW#1 and DW#2.

8.1.3 Experiment DW#3

In experiment DW#3, both mass balance and partitioning tracers were used for performance assessment of surfactant remediation. The mass balance estimate of performance assessment was calculated by comparing the weight of the soil column before contamination (at 100% water saturation) and the weight of the soil column after surfactant remediation. Pressure drops were measured across the column during the surfactant flood. This number was converted into a hydraulic gradient and plotted against cumulative volume produced. The initial soil permeability before contamination of the soil column was compared to the permeability after surfactant remediation to assess efficacy of surfactant remediation. The soil column length, diameter, porosity and permeability are presented in Table 8.2.

Initial Tracer Test

In this experiment, tritium was used to estimate pore volume. About 4.4 cc of tritium was injected followed by a waterflood at an interstitial velocity of 11

m/day (1 cc/min). The samples were analyzed using a LSC. The tracer concentration history is plotted in Figure 8.15. A summary of the initial tracer test is given in Table 8.19. The pore volume based on tritium was 44.4 cc and the pore volume based on mass balance was 42.8 cc.

Contamination of Soil Column

The column was oriented vertically. Contamination of the soil column was carried out by injecting PCE into the column from the bottom until residual water saturation was reached, followed by injection of water from the top of the column until residual PCE saturation was reached. The end point PCE relative permeability was measured at residual water saturation and the end point water relative permeability was measured at residual PCE saturation. A summary of contamination of the soil column is given in Table 8.20. A residual water saturation of 0.392 was reached at the end of the PCE flood and a residual PCE saturation of 0.181 (mass balance) was reached at the end of the waterflood.

Tracer Test at Residual PCE Saturation

A suite of conservative and partitioning tracers was injected into the soil column at an interstitial velocity of 1.5 m/day (0.15 cc/min) to measure residual PCE saturation. The injected tracers were tritium, IPA and 2,3-dimethyl-2-butanol. Sampling and analysis procedures were similar to procedures followed in experiment DW#2. The mean residence time for tritium and IPA was 3.6 hours and for 2,3-dimethyl-2-butanol it was 6.2 hours. The samples were analyzed using a GC for the alcohol tracer concentrations and a LSC for tritium concentration. The

tracer concentration histories are plotted in Figure 8.16. A summary of the partitioning tracer test is given in Table 8.21.

The residual PCE saturation based on partitioning tracers was calculated based on the retention time of the partitioning tracers. When tritium was used as the conservative tracer and 2,3-dimethyl-2-butanol was used as the partitioning tracer, a PCE saturation of 0.208 was estimated. When IPA was used instead of tritium a saturation of 0.205 was estimated. A summary of residual PCE saturation estimates based on mass balance, volume balance and partitioning tracers are given in Table 8.22.

Surfactant Flood to Remediate PCE

A solution of 4% sodium dihexyl sulfosuccinate with 25,000 mg/l of NaCl was injected at 0.6 m/day (0.06 cc/min). The flow rate was increased to 1.2 m/day (0.12 cc/min) after 2.2 pore volumes of injection and increased to 2.4 m/day (0.24 cc/min) after a total of 5.5 pore volumes of injection. This surfactant solution was a Winsor type I solution with a PCE solubilization parameter of 0.9 and PCE solubilization of 58,000 mg/l. The IFT between the microemulsion and excess PCE was 0.14 dynes/cm. A total of 557.5 cc (12.8 pore volumes) of surfactant solution was injected. A total of 1.3 cc of PCE was mobilized and produced as free PCE and 3.9 cc was solubilized in the microemulsion. Based on this, 17% of the PCE was mobilized and the rest was solubilized. The surfactant flood is summarized in Table 8.23.

The PCE concentration history during the surfactant flood is plotted in Figure 8.17. In Figure 8.18, the relative amounts of PCE solubilized and

mobilized and the total amount of PCE recovered as a function of pore volumes produced are plotted in Figure 8.17. Concentrations of PCE greater than 50,000 mg/l correspond to two-phase samples containing both microemulsion and PCE. The maximum PCE concentration measured in the effluent was 45,000 mg/l compared to the equilibrium phase behavior value of 58,000 mg/l. From Figure 8.17 it can be seen that about 70% of the PCE is recovered as a result of surfactant flooding. This number is incorrect as both partitioning tracers and mass balance measurements indicated better performance by surfactant flooding. In addition to material balance, partitioning tracers and mass balance were used for performance assessment of surfactant remediation. Based on mass balance (comparison of weights of the soil column before contamination by PCE and after surfactant remediation), 100.5% of the PCE was recovered. The final saturation of PCE after surfactant remediation was 0.004.

From the PCE concentration history in Figures 8.17 and 8.18, a steady plateau in the PCE concentration of about 30,000 mg/l to 45,000 mg/l is observed. This is due to slow solubilization of the PCE ganglia in the Ottawa sand. After 5 pore volumes, the PCE concentration was observed to rapidly decline to less than 1,000 mg/l. Several effluent samples at the end of the surfactant flood could not be analyzed. The soil column was flushed with 227 cc (5.2 pore volumes) of 1,000 mg/l NaCl after surfactant flooding.

Since the pressure drops across the column for experiment DW#2 were extremely high and could not be measured during the surfactant flood, one of the main objectives of experiment DW#3 was to measure pressure drops across the soil column. Pressure drop was converted into a dimensionless hydraulic gradient and

plotted against the pore volumes. The hydraulic gradient during the surfactant flood is plotted in Figure 8.19. A quick look at the plot shows a lot of experimental noise as the transducers were not sensitive enough to measure such low hydraulic gradients during the surfactant flood. The average hydraulic gradient across the column was low, on the order of 0.05-0.10 in the beginning of the surfactant flood (A hydraulic gradient of 1 psi/ft = 2.3 m/m). The average hydraulic gradient was observed to increase from about 0.07 to 0.15 when the injection rate was increased from 0.06 cc/min to 0.12 cc/min. A hydraulic gradient of about 0.32 was measured at an injection rate of 0.24 cc/min. Once the waterflood was started, the hydraulic gradient declined to less than 0.15. Such low head losses can be attributed to low viscosity and minimal gel forming tendencies of the surfactant solution.

The viscosity for the injected surfactant solution for experiment DW#3 is plotted in Figure 8.20. The viscosity of the injected surfactant is extremely low (about 1.3-1.4 cp) and independent of shear rate with the noise in the data at the very low shear stresses of these measurements. Even though the pressure measurements indicated low hydraulic gradients during the surfactant flood, more accurate pressure measurements are needed for proper understanding of the process of surfactant remediation. The permeability of the soil after surfactant remediation was 6.9 Darcies compared to the initial permeability of 7.3 Darcies. This shows that the soil column can be restored to very nearly its original condition after surfactant remediation since these values are the same within experimental error.

Tracer Test After Surfactant to Estimate Residual PCE Saturation

After 12.8 pore volumes of surfactant and 5.2 pore volumes of post surfactant waterflooding, a suite of conservative and partitioning tracers was injected into the soil column to estimate final residual PCE saturation. The tracers used were tritium, IPA and 2,3-dimethyl-2-butanol. About 6.4 cc of tracer solution was injected at an interstitial velocity of 1.5 m/day (0.15 cc/min) followed by flooding with 1,000 mg/l NaCl. The effluent was analyzed for alcohols and tritium and the residual PCE saturation was calculated. The tracer concentration history for this tracer test is plotted in Figure 8.21. Negligible retardation of 2,3-dimethyl-2-butanol is observed. This implies a low PCE saturation as a result of surfactant remediation.

Tracer concentration histories for tracer tests before contamination of the soil column and after surfactant remediation are plotted in Figure 8.22. A very close overlap between initial tracer and post surfactant tracer is observed in Figure 8.22. This means that the soil has been restored to very nearly its original condition after surfactant remediation.

The final partitioning tracer test is summarized in Table 8.24. Based on the partitioning tracers, the PCE saturation after surfactant flooding was 0.005 compared to a waterflood residual PCE saturation of 0.181. This corresponded to a recovery of 97.2% of PCE. A summary of the residual saturations after surfactant is given in Table 8.25.

Discussion for Experiment DW#3

The pore volume estimates based on mass balance, volume balance and tracers in experiment DW#3 were in excellent agreement (within $\pm 3.5\%$). The tracer recovery was consistent with recoveries observed in experiment DW#2.

As in experiment DW#2, an excellent match was obtained between the volume balance estimate and mass balance estimate of residual PCE saturation. The partitioning tracer estimates of the residual PCE saturation agreed to within $\pm 3\%$ saturation of PCE. The recovery of all the tracers was low during the partitioning tracer test. Despite low tracer recovery the saturation estimation was in excellent agreement with mass balance estimates.

From the PCE concentration history it can be seen that high PCE concentrations corresponding to free phase PCE were observed in the first pore volume. This was followed by a PCE concentration plateau of about 20,000 mg/l to 35,000 mg/l in the next four pore volumes. There was some delay in analyzing the samples in the first 2 pore volumes and this accounted for scatter observed in the experimental measurements.

An increase in the flow rate did not change the effluent PCE concentration. The flow rate was changed two times during the surfactant and both times there was no change in the effluent PCE concentration. From this it can be inferred that there was equilibrium solubilization of the contaminant. The recovery of PCE based on the PCE concentration history curve was about 70%, but the recovery based on mass balance was 100.5%. PCE is a fairly volatile contaminant. The microemulsion samples produced during the surfactant were not analyzed

immediately. Typically the samples were allowed to sit in the tube rack in the fraction collector until a new rack moved into the sampling port. This caused additional delay in analysis of effluent samples. This delay in sample analysis caused PCE loss by volatilization. In addition, GC errors in PCE measurement could also account for under prediction of PCE recovery based on material balance. The recovery based on the weight of the soil column was used as primary means for performance assessment of surfactant remediation. This number was confirmed by partitioning tracers which estimated low PCE saturations after surfactant remediation.

Based on the average residual PCE saturation of 0.005 calculated after surfactant flooding, the close match between the initial tracer concentration history and final tracer concentration histories and a close match between the initial permeability and final permeability after surfactant flooding it can be concluded that the soil pack had been restored to very nearly its original condition after surfactant flooding.

Based on the plot showing the head losses across the soil column during surfactant flooding, it can be inferred that the surfactant solution used in this experiment did not cause any pore plugging and gelling problems. Gradients observed during the experiment (less than 0.3) are acceptable field hydraulic gradients.

8.2 EXPERIMENTS WITH TCE

A total of three column experiments were conducted with TCE as the contaminant. The first experiment was a solubilization-type experiment (DW#4).

The second experiment was a solubilization-type experiment with xanthan gum polymer and IPA used as a co-solvent (POLYTCE#1). The final experiment (POLYTCE#3) was a mobilization type experiment aimed at quick remediation of contaminated soil.

8.2.1 Experiment DW#4

In experiment DW#4, a dynamic partition coefficient test was performed in which the partition coefficients of two alcohols, 2,3-dimethyl-2-butanol and 2-methyl-2-hexanol were determined. The residence times of the tracers and known TCE saturation in the soil column were used to calculate the partition coefficients. These tracers were used in the subsequent column experiment to estimate residual TCE saturation. The ability of sodium dihexyl sulfosuccinate to remediate Ottawa sand contaminated by TCE was evaluated. Performance assessment of surfactant remediation was done by using partitioning tracers and mass balance measurements. The soil column length, diameter, porosity and permeability are presented in Table 8.2.

Initial Tracer Test

In this experiment, tritium was used to estimate pore volume. About 4.3 cc of tracer was injected followed by a waterflood at an interstitial velocity of 11 m/day (1 cc/min). The samples were analyzed using a LSC. The tracer concentration history is plotted in Figure 8.23. A summary of the initial tracer test is given in Table 8.26. The average pore volume based on the initial tritium tracer was 43.0 cc. The pore volume based on mass balance was 40.4 cc and the pore volume estimate based on volume balance was 41.4 cc.

Contamination of Soil Column

The column was oriented vertically. Contamination of the soil column was carried out by injecting TCE into the column from the bottom until residual water saturation was reached followed by injection of water from the top of the column until residual TCE saturation was reached. Both the TCE flood and waterflood were carried out at an interstitial velocity of 11 m/day (1 cc/min). The pressure gradient across the soil column at steady state during the TCE flood was 0.99 psi/ft (at 1 cc/min). The pressure gradient across the soil column at steady state during the waterflood was 0.78 psi/ft (at 1 cc/min). The end point TCE relative permeability was measured at residual water saturation and the end point water relative permeability was measured at residual TCE saturation. A summary of contamination of the soil column is given in Table 8.27. A residual water saturation of 0.263 was reached at the end of the TCE flood and a residual TCE saturation of 0.176 (mass balance) was reached at the end of the waterflood.

Tracer Test at Residual TCE Saturation

A suite of conservative and partitioning tracers was injected into the soil column to measure the partition coefficients of two alcohol tracers. The injected tracers were IPA, 2,3-dimethyl-2-butanol and 2-methyl-2-hexanol. Sampling and analysis procedures were similar to procedures followed in experiments DW#2 and DW#3. A total of 4.5 cc of tracer solution was injected followed by a waterflood at an interstitial velocity of 1.5 m/day (0.15 cc/min). The tracer concentration histories were plotted Figure 8.24. A summary of the partitioning tracer test is given in Table 8.28.

The residual TCE saturation and the mean residence times of the partitioning tracers were used to compute the partition coefficients. A retardation factor of 2.39 was measured for 2,3-dimethyl-2-butanol and a retardation factor of 7.17 was measured for 2-methyl-2-hexanol. This corresponded to a residence time of 11 hours for 2,3-dimethyl-2-butanol and for 2-methyl-2-hexanol it was 33 hours. Based on these retardation factors, the partition coefficient for 2,3-dimethyl-2-butanol was calculated as 6.3 and the partition coefficient for 2-methyl-2-hexanol was 28.1. The partition coefficients for both these alcohols determined by the partitioning tracer test are summarized in Table 8.29.

Surfactant Flood to Remediate TCE

A solution of 8% sodium dihexyl sulfosuccinate with 2,000 mg/NaCl was injected at an interstitial velocity of 1.3 m/day (0.13 cc/min). This surfactant solution was a Winsor type I solution with a TCE solubilization parameter of 0.5 and TCE solubilization of 52,000 mg/l. The IFT between the excess TCE and microemulsion was 0.20 dynes/cm. A total of 361.3 cc (8.7 pore volumes) of surfactant solution was injected. A total of 0.3 cc of TCE was mobilized and produced as free TCE and the rest was solubilized in microemulsion. This experiment was a solubilization dominated experiment as less than 5% of the TCE was mobilized. After 2.4 pore volumes of total production there were some GC problems. Hence many samples could not be analyzed for TCE immediately after collection. TCE was lost by volatilization from these samples and this is reflected in the scatter observed in the TCE concentration in the effluent after 2.4 pore volumes. The surfactant flood is summarized in Table 8.30.

The TCE concentration history during the surfactant flood and the amount of TCE recovered are plotted in Figure 8.25. The maximum TCE concentration measured in the effluent was 32,000 mg/l compared to an equilibrium phase behavior value of 52,000 mg/l. From this Figure it can be seen that about 35 % of the TCE was recovered as a result of surfactant remediation. In addition to material balance of TCE using GC measurements, mass balance and partitioning tracers were used for performance assessment of surfactant remediation. Based on weighing the soil column before and after surfactant remediation, 100.0% of the TCE was recovered. Similar results were obtained from partitioning tracer results which showed that 96.9% of the TCE was recovered.

Pressures were measured across the soil column during the surfactant flood and post surfactant waterflood in experiment DW#4. The hydraulic gradient across the soil column during the surfactant flood and post surfactant waterflood is plotted in Figure 8.26. In this experiment, the hydraulic gradient at the beginning of the surfactant flood was about 0.17. This increased to about 0.38 when breakthrough of TCE was observed. This was followed by a slow decline to 0.17. The hydraulic gradients were observed to increase when the pump was stopped two times during the surfactant flood. Once the pump was started again, the hydraulic gradient was observed to decline to lower values. Such increases in hydraulic gradient can be attributed to thixotropic behavior of the injected surfactant solution. This behavior must be avoided for successful application of surfactants in field applications as this behavior is usually associated with gels and liquid crystal formation. This behavior can be minimized by the addition of alcohol. This was done in subsequent experiments. The soil column was flushed with 200 cc (4.6

pore volumes) of 2,000 mg/l NaCl. Once the waterflood was started, the hydraulic gradient declined to less than 0.25 after 4 pore volumes of waterflooding. Such low head losses can be attributed to the low viscosity of the injected surfactant solution. The variation of viscosity of the injected surfactant solution with shear rate for experiment DW#4 is plotted in Figure 8.27. The viscosity of the injected surfactant is low (about 1.5 cp) and constant with shear rate exhibited Newtonian behavior. This type of behavior is suitable for surfactant remediation. After surfactant remediation and post surfactant waterflooding, the permeability of the soil column was measured as 6.9 Darcies compared to the initial permeability of 7.3 Darcies which is essential the same.

Tracer Test After Surfactant to Estimate Residual TCE Saturation

After 8.7 pore volumes of surfactant and 4.2 pore volumes of post surfactant waterflooding, a suite of conservative and partitioning tracers was injected into the soil column to estimate final residual TCE saturation. The tracers used were IPA, 2,3-dimethyl-2-butanol and 2-methyl-2-hexanol. About 6.4 cc of tracer solution was injected at an interstitial velocity of 1.5 m/day (0.15 cc/min) followed by flooding with 2,000 mg/l NaCl. The effluent was analyzed for the alcohols and the residual TCE saturation was calculated. The tracer concentration history for this tracer test is plotted in Figure 8.28. Negligible delay of both the partitioning tracers is observed. This implies a low TCE saturation as a result of surfactant flooding.

The final partitioning tracer test is summarized in Table 8.31. Based on partitioning tracers, the TCE saturation after surfactant flooding was 0.0054

compared to a waterflood residual TCE saturation of 0.176. This corresponded to a recovery of 96.9% of TCE. A summary of the residual TCE saturations after surfactant flooding is given in Table 8.32.

Discussion for Experiment DW#4

In experiment DW#4, the known saturation of TCE was used to estimate partition coefficients for two alcohol tracers, 2,3-dimethyl-2-butanol and 2-methyl-2-hexanol. The partition coefficients measured in this experiment were used to estimate TCE saturations in the next experiment. A dynamic partition coefficient of 6.3 was measured for 2,3-dimethyl-2-butanol compared to a static partition coefficient of 5.2. The static and dynamic coefficients for 2-methyl-2-hexanol were 26.8 and 28.1 respectively. These discrepancies will be discussed in the section on error analysis in Chapter 9.

During the surfactant flood, TCE concentrations of the order of 1,000 to 1,400 mg/l were measured in the effluent before surfactant breakthrough. This corresponded to the equilibrium solubility of TCE in water. This also confirmed local equilibrium conditions. After surfactant breakthrough, TCE concentrations of about 20,000 mg/l were measured in the effluent. As in experiment DW#3, a decline was observed after about 4 pore volumes of flooding. The concentration history curve could not be accurately measured due to loss of TCE by volatilization. The samples were stored for more than 72 hours before analysis. This caused loss of TCE by volatilization and measurement of lower TCE concentrations in the effluent from the soil pack. This accounted for a recovery of only 35% of the TCE. However based on mass balance measurements, about 100% of the TCE was

removed from the column. In subsequent experiments, samples were stored in vials with aluminum lined caps to minimize losses by volatilization.

A look at the hydraulic gradient graph showed an increase in hydraulic gradient until there was some TCE mobilization and surfactant breakthrough. This was followed by a decline to a lower hydraulic gradient. This decline would be expected as the relative permeability to the surfactant solution increased as the TCE was slowly being solubilized. The sudden increase in hydraulic gradient when the pump was stopped may be attributed to thixotropic behavior of the microemulsion. This kind of behavior can be eliminated by addition of sufficient quantities of alcohol (like IPA or ethanol) which break up gels and liquid crystals.

An average residual saturation of 0.0054 was computed based on the post surfactant tracer results. This meant that almost all the TCE was removed from the soil column. This number compared well with mass balance estimates which indicated that 100.0% of the TCE was recovered. From the close match between the initial tracer and final curves and a close match between the initial permeability and final permeability, it can be concluded that the soil pack had been restored to very nearly its original condition after surfactant remediation.

8.2.2 Experiment POLYTCE#1

In experiment POLYTCE#1, a series of screens was used while packing the sand. This was done to ensure better packing. The main objective was the evaluation of a surfactant, alcohol, NaCl, xanthan gum polymer aqueous solution for remediation of a soil column contaminated with TCE. The performance of 2,3-dimethyl-2-butanol and 2-methyl-2-hexanol as partitioning tracers for estimation of

TCE saturation was evaluated. Pressure drops were measured across the soil column during the surfactant flood and the post surfactant waterflood. Partitioning tracers were used for performance assessment and this number was compared to TCE recovery estimates obtained from mass balance of the column. The initial soil permeability before contamination of the soil column was compared to the final permeability after surfactant remediation to evaluate the efficacy of the surfactant/polymer solution. The soil column length, diameter, porosity and permeability are presented in Table 8.2.

Initial Tracer Test

In this experiment, tritium was used to estimate pore volume. About 16.4 cc of tracer was injected followed by a waterflood at an interstitial velocity of 6.9 m/day (3 cc/min). The samples were analyzed using a LSC. The tracer concentration history is plotted in Figure 8.29. A summary of the initial tracer test is given in Table 8.33. The pore volume based on tritium was 168.4 cc and the pore volume based on mass balance was 168.6 cc.

Contamination of Soil Column

Contamination procedures were the same as in experiment DW#4. The column was oriented vertically. Contamination of the soil column was carried out by injection of water from the bottom until residual water saturation was reached, followed by injection of water from the top of the column until residual TCE saturation was reached. In this experiment, the TCE flood for contaminating the soil column and waterflood to reach residual TCE saturation were carried out at an interstitial velocity of 6.9 m/day (3 cc/min). The pressure gradient across the soil

column at steady state during the DNAPL flood was 1.39 psi/ft (at 3 cc/min). The pressure gradient across the soil column at steady state during the waterflood was 0.72 psi/ft (at 3 cc/min). The end point TCE relative permeability was measured at residual water saturation and the end point water relative permeability was measured at residual TCE saturation. A summary of contamination of the soil column is given in Table 8.34. A residual water saturation of 0.325 was reached at the end of the TCE flood and a residual TCE saturation of 0.198 (mass balance) was reached at the end of the waterflood.

Tracer Test at Residual TCE Saturation

A suite of conservative and partitioning tracers was injected into the soil column to evaluate the performance of partitioning tracers to estimate residual TCE saturation. About 16.7 cc of tracer solution was injected followed by a waterflood at an interstitial velocity of 1.8 m/day (0.8 cc/min). The tracers used were tritium, IPA, 2,3-dimethyl-2-butanol and 2-methyl-2-hexanol. Sampling and analysis procedures were similar to procedures followed in earlier experiments. The tracer concentration history is plotted in Figure 8.30. The mean residence time for tritium and IPA was 2.9 hours. For 2,3-dimethyl-2-butanol, it was 7.2 hours and for 2-methyl-2-hexanol it was 14.4 hours. The samples were analyzed using a gas chromatograph for the alcohol tracer concentrations and a liquid scintillation counter for tritium concentration. This tracer test is summarized in Table 8.35.

The partition coefficients calculated from the previous experiment (experiment DW#4) were used to compute residual TCE saturation. The average TCE saturation based on partitioning tracers was 0.199 and the residual TCE

saturation based on mass balance was 0.198. A summary of residual TCE saturation estimates based on mass balance, volume balance and partitioning tracers is given in Table 8.36.

Surfactant Flood to Remediate TCE

An aqueous solution consisting of 4% sodium dihexyl sulfosuccinate, 8% IPA, 500 mg/l xanthan gum polymer with 4,000 mg/l NaCl was injected at an interstitial velocity of 1.8 m/day (0.8 cc/min). This surfactant solution was a Winsor type I solution with a TCE solubilization parameter of 0.6 and TCE solubilization of 39,000 mg/l. The IFT between the microemulsion and excess TCE was 0.19 dynes/cm. A total of 2003.9 cc (11.9 pore volumes) of surfactant/polymer/alcohol solution was injected. A 5 psid Validyne differential pressure transducer was used to measure pressure drops across the soil column during the surfactant flood and post surfactant waterflood. A polymer flood with 500 mg/l by weight xanthan gum, 8% IPA and 500 mg/l NaCl was started after surfactant injection. Polymer was used to aid in the efficiency of displacing the surfactant solution from the soil column. The polymer solution was injected for approximately 330 cc (2.0 pore volumes). The column was weighed after the polymer flood. A waterflood using 500 mg/l NaCl was used to remove the polymer after 13.9 total pore volumes. The injection continued for approximately 5,900 cc at which point the total amount of injected fluid through the soil column was approximately 50 pore volumes. The surfactant flood is summarized in Table 8.37.

The TCE concentration history during the surfactant flood is plotted in Figure 8.31. This experiment was a solubilization-type experiment and less than 3% of the TCE was mobilized. The maximum TCE concentration measured in the effluent was 38,000 mg/l. This number was in excellent agreement with the equilibrium phase behavior value of 39,000 mg/l. A plateau of TCE concentration of about 25,000 mg/l to 35,000 mg/l is observed for about 8 pore volumes. This is due to slow solubilization of the TCE ganglia in the Ottawa sand. A steady decline in TCE concentration from about 25,000 mg/l to about 30 mg/l is observed between 8 and 12 pore volumes. The TCE concentration was observed to increase to about 100 mg/l when the polymer flood was started. This is probably due to break up of hemi-micelles due to the salinity gradient caused by flooding with fresh water.

An attempt was made to characterize the persistent TCE tail. Hence a water flood with 500 mg/l NaCl was continued after the alcohol/polymer flood and the TCE concentrations were measured and plotted against cumulative pore volumes (Figure 8.32). The TCE concentration was observed to drop to about 3 to 5 mg/l. The pump was stopped for 10 days and injection was restarted. The TCE concentration was observed to increase to greater than 1,000 mg/l. A decline in the TCE concentration was observed on continued flooding with water. This can be attributed to adsorption of TCE by Teflon end pieces in the soil column and nylon tubing during saturation of the column and desorption during the waterflood.

In order to characterize the gel forming tendencies of the surfactant/alcohol polymer/solution at various TCE concentrations, viscosities of the surfactant solution with varying amounts of TCE were measured as a function of shear rate. These viscosities are plotted in Figure 8.33. The viscosities are the same in the

whole range of TCE concentrations studied. Based on Figure 8.33, it can be seen that the viscosity of the all the solutions is the same within experimental error. Hence it can be inferred that there was minimal liquid crystal/gel formation with the surfactant solution used in this experiment.

The pressure drops were measured across the soil column during surfactant flooding. The hydraulic gradient during the surfactant flood is plotted in Figure 8.34. A steady increase in hydraulic gradient until surfactant/polymer breakthrough is observed. This was followed by a steady hydraulic gradient until polymer/alcohol injection which increased the hydraulic gradient. The hydraulic gradient declined rapidly after the start of freshwater injection to less than 0.2. Gradients observed in this experiment were low despite the use of the more viscous surfactant/alcohol/polymer solution. Gradients observed in this experiment were acceptable hydraulic gradients considering the increased viscosity of the surfactant polymer solution being injected into the soil column. The permeability of the soil after surfactant remediation was 4.9 Darcies compared to the initial permeability of 5.8 Darcies.

Tracer Test After Surfactant to Estimate Residual TCE Saturation

After 11.9 pore volumes of surfactant/polymer/alcohol, 2.0 pore volumes of polymer/alcohol and 35 pore volumes of post surfactant waterflooding a suite of conservative and partitioning tracers was injected into the soil column to estimate the final residual TCE saturation. The tracers used were tritium, IPA, 2,3-dimethyl-2-butanol and 2-methyl-2-hexanol. About 17.5 cc of tracer solution was injected at an interstitial velocity of 1.8 m/day (0.8 cc/min) followed by flooding

with 500 mg/l NaCl. The effluent was analyzed for the alcohols and tritium and the residual TCE saturation was calculated. The tracer concentration history for this tracer test is plotted in Figure 8.35. Negligible delay of the partitioning tracers is observed in Figure 8.35. This implies a low TCE saturation as a result of surfactant remediation.

The final partitioning tracer test is summarized in Table 8.38. The residual TCE saturation estimates based on partitioning tracers is given in Table 8.39. Based on the partitioning tracers the average TCE saturation after surfactant was 0.00016. This corresponded to a recovery of 99.9% TCE. Based on mass balance measurements, 101.2% TCE was recovered. These measurements are in excellent agreement.

Discussion for Experiment POLYTCE#1

Based on partitioning tracers using dynamic partition coefficients measured in experiment DW#4, an average residual TCE saturation of 0.199 was calculated compared to a waterflood residual TCE saturation of 0.198 based on mass balance measurements. From this it can be concluded that partition coefficients can be accurately measured by performing a dynamic partition coefficient test as in experiment DW#4 provided that the rates are low enough that equilibrium partitioning occurs.

During the surfactant flood, very uniform TCE concentrations on the order of 25,000 mg/l to 38,000 mg/l were measured in the effluent. This number is much closer to the equilibrium solubilization of 39,000 mg/l compared to earlier experiments. This could be attributed to the use of polymer. The increased

viscosity of the polymer causes better sweep of the contaminated regions and promotes more uniform conditions. The increase in TCE concentration when the surfactant flood was switched to an alcohol/polymer flood (in 500 mg/l NaCl) could be attributed to the breakup of hemi-micelles by the fresh water. This suggests that a fresh water flood following anionic surfactant flood may be good strategy in many cases.

The sudden increase in TCE concentration to $> 1,000$ mg/l after 10 days of stopping can be attributed to desorption of TCE by the Teflon end pieces in the glass column. This also confirmed results observed in experiment DW#1. The persistent TCE tail even after 50 pore volumes could be attributed to desorption by the Teflon end pieces and nylon tubing.

The increase in hydraulic gradient after injection of surfactant was due to the increased viscosity of the injected surfactant/polymer solution. Even though a hydraulic gradient of about 2 to 2.5 may be high for some shallow groundwater applications, it must be noted that injected solutions are subjected to high shear near the wellbore. Since xanthan gum polymer is shear thinning, this would translate into lower apparent viscosity of the injected solution and hence lower hydraulic gradients by a factor on the order of 2. The xanthan gum concentration could also be decreased if necessary to control viscosity of the injected polymer solution or the injection rate into the well could be reduced. The hydraulic gradient is observed to decline very rapidly on water injection. This is due to fingering and early break through of the water through the viscous polymer in the soil column. Displacement of polymer by water is an inefficient process and many pore volumes of water are required to flush the polymer out completely.

A close overlap of partitioning and nonpartitioning tracers was observed in tracer results after surfactant flooding. Based on the method of moments, an average residual saturation of 0.00016 was computed. This meant that almost all the TCE was removed from the soil column. This value is in excellent agreement with mass balance measurements which indicate that 101.2% of the TCE was recovered. From the close match between the initial and final tracer curves and a close match between the initial permeability and final permeability, it can be concluded that the soil pack had been restored to very nearly its original condition after surfactant polymer remediation.

8.2.3 Experiment POLYTCE#3

In experiment POLYTCE#3, the main objective was the evaluation of a surfactant, alcohol, sodium chloride solution for quick remediation of a soil column contaminated with TCE. The effect of Teflon end pieces and nylon tubing on the persistent release of TCE after surfactant remediation was studied by eliminating all the Teflon pieces and nylon tubing from the column. Pressure drops were measured across the column during the surfactant flood and the post surfactant waterflood. This was extremely important as this experiment was an ultra-low IFT experiment and mobilization of TCE was expected. Partitioning tracers were used only for performance assessment and this number was compared to the TCE recovery estimate obtained from mass balance on the column. The soil column permeability was measured after surfactant remediation and this number was compared to the initial permeability. The soil column length, diameter, porosity and permeability are presented in Table 8.2.

Initial Tracer Test

In this experiment, tritium was used to estimate pore volume. The effluent was analyzed for tritium concentration using a LSC. About 11.7 cc of tracer was injected followed by a waterflood at 17.6 m/day (1.6 cc/min). The tracer concentration history is plotted in Figure 8.36. A summary of the initial tracer test is given in Table 8.40. The pore volume based on tritium was 103.4 cc and the pore volume based on mass balance was 101.1 cc.

Contamination of Soil Column

The column was oriented vertically. Contamination of the soil column was carried out by injecting TCE into the column from the bottom until residual water saturation was reached followed by injection of water from the top of the column until residual TCE saturation was reached. In this experiment, both the TCE flood for contaminating the soil column and waterflood to reach residual TCE saturation were carried out at 11 m/day (1.0 cc/min). The pressure gradient across the soil column at steady state during the DNAPL flood was 0.79 psi/ft (at 1 cc/min). The pressure gradient across the soil column at steady state during the waterflood was 0.56 psi/ft (at 1 cc/min). The end point TCE relative permeability was measured at residual water saturation the end point water relative permeability was measured at residual TCE saturation. A summary of contamination of the soil column is given in Table 8.41. A residual water saturation of 0.314 was reached at the end of the TCE flood and a residual TCE saturation of 0.163 (mass balance) was reached at the end of the waterflood.

Tracer Test at Residual TCE Saturation

Tritium was used as a tracer to estimate the residual TCE saturation. The difference between the aqueous pore volume calculated from the initial tritium tracer test and the tritium tracer test at residual TCE saturation was used to estimate the residual TCE saturation. About 12.1 cc of tracer was injected followed by a water flood at an interstitial velocity of 16.5 m/day (1.5 cc/min). The samples were analyzed using a liquid scintillation counter for tritium concentration. This tracer test is summarized in Table 8.42. The tracer concentration history is plotted in Figure 8.42. The summary of residual TCE saturation estimates based on mass balance and tritium tracer is given in Table 8.43. Based on mass balance, the residual TCE saturation was 0.163. Based on tritium tracer it was 0.165.

Surfactant Flood to Remediate TCE

An aqueous solution of 4% sodium dihexyl sulfosuccinate, 8% IPA and 9,350 mg/l NaCl was injected at an interstitial velocity of 1.4 m/day (0.13 cc/min). This surfactant solution was a Winsor type III solution with a TCE solubilization ratio of 3.8 and a TCE solubilization of 516,000 mg/l. The IFT between the excess TCE and microemulsion was 0.02 dynes/cm. A total of 102 cc (1 pore volume) of this surfactant solution was injected followed by injection of 100 cc (1 pore volume) of 4% sodium dihexyl sulfosuccinate, 8% IPA and 500 mg/l NaCl. This was followed by the injection of 200 cc (2 pore volumes) of 500 mg/l NaCl to remove surfactant. The column was weighed after the post surfactant waterflood and TCE recovery was estimated based on comparing the weight of the column

before contamination and the final weight after surfactant remediation. The surfactant flood is summarized in Table 8.44.

The TCE concentration during the surfactant flood and the relative amount of TCE mobilized and solubilized during the surfactant flood is plotted in Figure 8.38. About 16.1 cc of TCE was mobilized. This corresponded to 96% of the TCE initially present in the column. The high TCE concentrations on the order of 10^6 mg/l correspond to free TCE produced during the surfactant flood. A sharp decline in TCE concentrations from 10^6 mg/l to about 10^4 mg/l at one pore volume of total injection is observed. This is due to mobilization of 96% of the TCE present in the column. Based on material balance estimates obtained from adding the volume of TCE mobilized and GC measurements, about 101.5% of the TCE was recovered. This is in agreement with mass balance estimates of TCE recovery which estimated that 100.0% TCE was recovered by surfactant flooding.

In experiment POLYTCE#3 a persistent TCE concentration on the order of 25-50 mg/l was measured at the end of the surfactant flood and post surfactant waterflood. Nylon tubing was used to connect the soil column to the fraction collector. The nylon tubing was replaced by stainless steel tubing and TCE concentration in the effluent was measured. The TCE concentration was observed to fall below 1 mg/l (detection limit for TCE in our GC). The pump was stopped for 2 days and water injection was resumed. No TCE could be measured in the effluent. Hence, it could be seen that surfactant remediation could reduce TCE concentration to less than 1 mg/l. Hence it can be concluded that the persistent TCE tail observed in earlier experiments was due to adsorption of contaminant by Teflon end pieces and nylon tubing.

The pressure drop was measured across the soil column during the surfactant flood and post surfactant waterflood. The pressure drops were converted into hydraulic gradients during surfactant flood and post surfactant waterflood. The variation of hydraulic gradient and TCE concentration during the surfactant flood is plotted in Figure 8.39. A low hydraulic gradient of the order of 0.1 was measured at the beginning of the surfactant flood. A steady increase in the hydraulic gradient to 0.6 was observed until TCE breakthrough. This was followed by a steady decline to a hydraulic gradient of 0.09. No evidence of gelling was observed as evidenced by low hydraulic gradients measured during surfactant flooding. This increase in hydraulic gradient was because of mobilization of TCE and multi-phase flow during the surfactant flood. Once all the mobilized TCE was produced, a decline in the hydraulic gradient was observed. After surfactant flooding and post surfactant waterflooding, the permeability of the soil column was 6.2 Darcies compared to the initial permeability of 6.8 Darcies which is essentially the same.

Tracer Test After surfactant to Estimate Residual TCE Saturation

After 2 pore volumes of surfactant and 5 more volumes of water, a suite of conservative and partitioning tracers was injected into the soil column to estimate the final TCE saturation. The tracers used were ethanol, 2,3-dimethyl-2-butanol and 3-methyl-3-hexanol. About 10.7 cc of tracer solution was injected at an interstitial velocity of 2.8 m/day (0.22 cc/min) followed by flooding with 500 mg/l NaCl. The effluent was analyzed for alcohols and the residual TCE saturation was calculated. The tracer concentration history for this tracer test is plotted in Figure

8.40. Negligible delay of the partitioning tracers is observed. This implies a low TCE saturation as a result of surfactant flooding.

The final partitioning tracer test is summarized in Table 8.45. A summary of the residual TCE saturations after surfactant flooding is given in Table 8.46. Based on the partitioning tracers, the TCE saturation after surfactant flooding was 0.00025. This corresponded to a recovery of 99.8% TCE.

Discussion for Experiment POLYTCE#3

Compared to experiment POLYTCE#1, a very small amount, (only one pore volume) of surfactant was required to clean up the contaminated soil column. Hence it can be concluded that under proper design conditions, mobilization can be used as an excellent remediation alternative for cleanup of sites contaminated by NAPLs. The persistent TCE tails observed in previous experiments were attributed to adsorption by Teflon end pieces in glass columns and nylon tubing. Since the TCE concentration was measured to less than 1 mg/l after 2.5 pore volumes of flooding, it can be concluded that surfactant flooding can reduce contaminant concentrations to extremely low levels by eliminating the source of contaminant.

As in previous experiments, low hydraulic gradients were measured during surfactant flooding. Low hydraulic gradients also signified the absence of significant emulsions, gels and liquid crystals. The hydraulic gradients were observed to track the remediation of TCE closely. A decrease in hydraulic gradient when all the TCE was mobilized signified the removal of TCE and hence corresponded to an increase in permeability and decrease in pressure drops (hydraulic gradient).

An excellent match between the initial permeability and final permeability and a close match between TCE removal estimates based on mass balance and partitioning tracers suggested that the soil had been almost completely remediated and very nearly restored to its original condition.

8.3 EXPERIMENTS WITH HILL OU1 LNAPL

A total of three experiments were conducted with Hill OU1 LNAPL. All these experiments were partitioning tracer tests. In the first experiment, Ottawa sand was contaminated with Hill OU1 LNAPL and performance of partitioning tracers to estimate a known residual LNAPL saturation was evaluated. The other two experiments used contaminated soil from Hill OU1. The main objective of these experiments was to select a suitable tracer combination for use in the field partitioning tracer test conducted by the University of Florida and EPA RSKERL during October, 1994. This was the first such test ever conducted. The complete design including computer modeling (Jin, 1995) was done by the University of Texas at Austin can be found in Pope *et al.* (1994).

The site OU1 at Hill Air Force Base has a number of contaminant sources located across the site. Several chemical disposal pits were used to dispose of aviation fuels (JP4) and chlorinated solvents (Annable *et al.*, 1996). Up gradient of the cell is a fire training area which may also have contributed unextinguished fuels and combustion by products at the site. The resulting NAPL was lighter than water with a density of 0.89 g/cc, viscosity of 0.8 cp and was black in color. The porosity of the aquifer was between 0.3 and 0.4. The LNAPL was composed of five main constituents, 1,1,1-trichloroethane, toluene, 1,2-dichlorobenzene, n-

decane, and naphthalene in addition to some dissolved grease, unextinguished fuels and combustion products at the site.

8.3.1 Experiment OUDNAPL1

In experiment OUDNAPL1, the main objective was the evaluation of the performance of several partitioning tracers for estimation of residual Hill OU1 LNAPL saturation. The dynamic partition coefficients of eight alcohol tracers were measured in two partitioning tracer tests conducted at residual Hill OU1 LNAPL saturation in Ottawa sand. The dynamic partition coefficients for the alcohol tracers were calculated using the known LNAPL saturation and the mean residence times of the partitioning tracers in the soil column. This number was then compared with the static partition coefficients. In subsequent experiments the dynamic partition coefficient measured in experiment OUDNAPL1 was used to estimate the residual LNAPL saturation in soil column. The soil column length, diameter, porosity and permeability are presented in Table 8.2.

Initial Tracer Test

A suite of alcohol tracers was injected into the soil column for estimation of pore volume in the uncontaminated soil column. The alcohol tracers used were IPA, 2,3-dimethyl-2-butanol and 2-methyl-2-hexanol. About 4.7 cc of tracer solution was injected followed by a waterflood at an interstitial velocity of 11 m/day (1 cc/min). The effluent was analyzed using a GC. A summary of the initial tracer test is given in Table 8.47. The tracer concentration history is plotted in Figure 8.41. The pore volume based on mass balance was 43.0 cc and the average pore volume based on tracers was 45.2 cc.

Contamination of Soil Column

The column was oriented vertically. Contamination of the soil column was carried out by injecting Hill OU1 LNAPL into the column from the top until residual water saturation was reached followed by injection of water from the bottom of the column until residual LNAPL saturation was reached. In this experiment, both the LNAPL flood for contaminating the soil column and waterflood to reach residual LNAPL saturation were carried out at an interstitial velocity of 11 m/day (1 cc/min). A summary of contamination of the soil column is given in Table 8.48. A residual water saturation of 0.126 was reached at the end of the NAPL flood. Based on volume balance estimates a residual LNAPL saturation of 0.179 was reached at the end of the waterflood.

First Tracer Test at Residual NAPL Saturation

A suite of partitioning and conservative tracers was injected into the soil column to measure the dynamic partition coefficients of two alcohol tracers. IPA was used as the conservative tracer and 2,3-dimethyl-2-butanol and 2-methyl-2-hexanol were used as the partitioning tracers. A total of 6.1 cc of tracer solution was injected followed by a waterflood at 2.3 m/day (0.24 cc/min). The tracer concentration history for this tracer test is plotted in Figure 8.42. A summary of the partitioning tracer test is given in Table 8.49.

A retardation factor of 1.29 was measured for the 2,3-dimethyl-2-butanol. This corresponded to a residence time of 4 hours. For 2-methyl-2-hexanol, a retardation of 2.26 was measured. This corresponded to a residence time of 7 hours. Based on these retardation numbers and a waterflood residual LNAPL

saturation of 0.179, the partition coefficient for 2,3-dimethyl-2-butanol was calculated as 1.3 and the partition coefficient for 2-methyl-2-hexanol was 5.8. The dynamic partition coefficients for both these alcohols are summarized in Table 8.50. A more detailed discussion on both static and dynamic partition coefficient tests is given in Chapter 9.

Second Tracer Test at Residual NAPL Saturation

In the second tracer test, a suite of partitioning and conservative tracers was injected into the soil column to measure the partition coefficients of three other alcohol tracers. Ethanol was used as the conservative tracer and 2-methyl-2-pentanol, 2,2-dimethyl-3-pentanol and 3-methyl-2-hexanol were used as the partitioning tracers. A total of 8.4 cc of tracer solution was injected followed by a waterflood at an interstitial velocity of 2.3 m/day (0.24 c/min). The tracer concentration history for this tracer test is plotted in Figure 8.43. A summary of the partitioning tracer test is given in Table 8.51.

A retardation factor of 1.28 was measured for the 2-methyl-2-pentanol. This corresponded to a residence time of 4 hours. For the 2,2-dimethyl-3-pentanol, a retardation of 3.81 was measured. This corresponded to a residence time of 12 hours. For the 3-methyl-2-hexanol, a retardation factor of 3.18 was measured. This corresponded to a residence time of 10 hours. Based on these retardation factors and a waterflood residual saturation of 0.179, the partition coefficients for 2-methyl-2-pentanol, 2,2-dimethyl-3-pentanol and 3-methyl-2-hexanol were calculated as 1.3, 12.9 and 10.0 respectively. The partition coefficients for both these alcohols are summarized in Table 8.52.

A comparison of the dynamic partition coefficients and static partition coefficients is given in Table 8.53.

Discussion for Experiment OUDNAPL1

The error analysis of both static and dynamic measurements of partition coefficients will be in Chapter 9. A comparison of static and dynamic partition coefficients showed a close match between both values within experimental error. A higher deviation was observed for 3-methyl-2-hexanol. This alcohol was not recommended for the field test at Hill OU1. Tracer recoveries were close to 100% for all tracers except the 2,2-dimethyl-3-pentanol in the second set of tracers. This could be attributed to a sudden decline in concentration observed in Figure 9.43 after 130 cc of flooding. No reason was found to describe the observed behavior. Despite low recovery, an excellent match between the static partition coefficient and dynamic partition coefficient for 2,2-dimethyl-3-pentanol was observed.

8.3.2 Experiment OUDNAPL2

Contaminated field soil from Hill Air Force Base site Operational Unit 1 was used in experiment OUDNAPL2. The soil was obtained from zones 16.25 ft to 16.50 ft and 16.50 ft to 16.75 ft from well U1-145 (samples EPA007-1,2). A Kontes borosilicate column 4.8 cm diameter and 15 cm long was used with an adjustable plunger to apply some confining stress. A 99 μm stainless steel mesh was used to hold the sand in place. The column was saturated with 1,000 mg/l NaCl water. Soil packing and saturation procedures are described in Chapter 3.

The tracers screened in experiment OUDNAPL1 were used in experiment OUDNAPL2. The dynamic partition coefficients calculated in experiment

OUNAPL1 were used to compute the residual LNAPL saturation. Based on soil core data, the expected LNAPL saturations in contaminated field soil were between 0.03 and 0.05. In order to obtain accurate results from partitioning tracer tests, retardation factors between 1.2 and 4.0 are required. Based on the expected residual LNAPL saturations, partition coefficients between 4.0 and 13.0 were used in soil column experiments. Since the initial LNAPL saturation of the soil cores was not known, 2,3-dimethyl-2-butanol, with a partition coefficient of 1.3 was used in experiment OUNAPL2. The soil column length, diameter, porosity and permeability are presented in Table 8.2.

First Tracer Test at Residual NAPL Saturation

A suite of five tracers was injected into the soil column to estimate the initial aqueous pore volume and initial LNAPL saturation.. The tracers used were tritium, ethanol, 2,3-dimethyl-2-butanol, 2-methyl-2-hexanol and 3-methyl-2-hexanol. About 6.1 cc of tracer solution was injected followed by a waterflood at an interstitial velocity of 0.6 m/day (0.2 cc/min). A summary of the tracer test is given in Table 8.54. The tracer concentration history is plotted in Figure 8.44. The retention time was 3.9 hours for ethanol, for 2,3-dimethyl-2-butanol it was 4.1 hours, for 2-methyl-2-hexanol it was 4.8 hours and for 3-methyl-2-hexanol it was 5.6 hours.

Based on the dynamic partition coefficients measured in experiment OUNAPL1 and the mean residence times for the tracers, an average residual LNAPL saturation of 0.035 was estimated. The residual saturation estimates based on the first set of partitioning tracers in experiment OUNAPL2 are summarized in

Table 8.55. A negative saturation was obtained using tritium and 2,3-dimethyl-2-butanol. This is because of low retardation caused by the low LNAPL saturation and low partition coefficient of the 2,3-dimethyl-2-butanol.

Second Tracer Test at Residual NAPL Saturation

After the initial tracer test, 1.7 cc of LNAPL was injected into the soil column at 0.2 cc/min followed by 85 cc of water at 0.4 cc/min. No LNAPL was produced in the effluent. The addition of 1.7 cc of LNAPL corresponded to an increase in the LNAPL saturation by 3.2%. Hence based on the average LNAPL saturation estimated by the initial tracer test and the volume of additional LNAPL added, the expected average LNAPL saturation before the second tracer test was 0.067.

A second suite of tracers was injected into the soil column. The tracers were tritium, ethanol, 2,3-dimethyl-2-butanol, 2-methyl-2-hexanol and 3-methyl-2-hexanol. About 6.0 cc of tracer solution was injected followed by a waterflood at an interstitial velocity of 0.6 m/day (0.2 cc/min). A summary of the tracer test is given in Table 8.56. The tracer concentration history for this tracer test is plotted in Figure 8.45. The retention time was 3.9 hours for ethanol and tritium, for 2,3-dimethyl-2-butanol it was 4.2 hours, for 2-methyl-2-hexanol it was 4.9 hours and for 3-methyl-2-hexanol it was 6.0 hours.

An average residual LNAPL saturation of 0.060 was estimated from the moment analysis of the partitioning tracers in experiment OUDNAPL2. The residual saturation estimates based on the second set of partitioning tracers in

experiment OUDNAPL2 are summarized in Table 8.57. This number is in excellent agreement with the expected saturation of 0.067.

Discussion for Experiment OUDNAPL2

Dynamic partition coefficients used in experiment OUDNAPL1 were used in estimating LNAPL saturation in experiment OUDNAPL2. A negative saturation difference was obtained in using the tritium and 2,3-dimethyl-2-butanol. This was due to the low partition coefficient of 2,3-dimethyl butanol and low saturation of LNAPL in the soil pack. This caused similar retention times for both tritium and 2,3-dimethyl-2-butanol. As a rule, a retardation factor of greater than 1.2 is needed for obtaining a good estimate of residual saturation (Jin, 1995). Ethanol seemed to give better results as a conservative tracer. No reasonable explanation was found to explain this discrepancy.

A look at the residual saturation estimates in the first and second tracer tests showed a standard deviation of $\pm 2\%$ LNAPL saturation. This is within the experimental error of the partitioning tracer test. The average expected LNAPL saturation before the second partitioning tracer test was 0.067. Based on the second set of partitioning tracers a value of 0.060 was calculated. This is an excellent estimate within experimental error. Since the standard deviation in the saturation estimate was $\pm 2\%$ LNAPL saturation, it can be concluded that the second partitioning tracer test accurately determined the residual LNAPL saturation.

8.3.3 Experiment OUDNAPL3

Contaminated field soil from Hill AFB site Operational Unit 1 was used in experiment OUDNAPL3. The soil was obtained from zones 17.00 ft to 17.25 ft

and 18.50 ft to 19.00 ft from well U1-147 (samples EPA007-6,7). A Kontes borosilicate column 4.8 cm diameter and 15 cm long was used with an adjustable plunger to apply some confining stress. A 99 μm stainless steel mesh was used to hold the sand in place. As in experiment OUDNAPL2, the column was saturated with 1,000 mg/l NaCl water. The performance of 1-hexanol and 2,2-dimethyl-3-pentanol for estimating LNAPL saturation was evaluated as both tracers were candidates to be used in the field partitioning tracer test at Hill AFB sit OU1. The soil column length, diameter, porosity and permeability are presented in Table 8.2.

First Tracer Test at Residual NAPL Saturation

A suite of four tracers was injected into the soil column to estimate the initial aqueous pore volume and initial LNAPL saturation. The tracers used were tritium, ethanol, 1-hexanol and 2,2-dimethyl-3-pentanol. Tritium and ethanol are conservative tracers. Hexanol and 2,2-dimethyl-3-pentanol are partitioning tracers under these conditions. About 7.0 cc of tracer solution was injected followed by a waterflood at an interstitial velocity of 0.6 m/day (0.2 cc/min). A summary of the tracer test is given in Table 8.58. The tracer concentration history is plotted in Figure 8.46. The retention time was 5.4 hours for ethanol and tritium, for 1-hexanol it was 7.1 hours, and for 2,2-dimethyl-3-pentanol it was 9.5 hours.

Based on the dynamic partition coefficients measured in experiment OUDNAPL1 and the mean residence times for the tracers, an average residual LNAPL saturation of 0.063 was estimated. The residual saturation estimates based on the first set of partitioning tracers in experiment OUDNAPL3 are summarized in Table 8.59. In Figure 8.46, a sudden decrease in the 2,2-dimethyl-3-pentanol

concentration was observed at 140 cc of total flooding. This was due to volatilization of the alcohol due to delay in analysis of samples. The partitioning tracer experiment was repeated.

Second Tracer Test at Residual NAPL Saturation

After the initial tracer test, another suite of tracers was injected into the soil column. The tracers were tritium, ethanol, 1-hexanol and 2,2-dimethyl-3-pentanol. About 6.3 cc of tracer solution was injected followed by a waterflood at an interstitial velocity of 0.6 m/day (0.2 cc/min). A summary of the tracer test is given in Table 8.60. The tracer concentration history is plotted in Figure 8.47. The retention time was 5.2 hours for ethanol and tritium, for 1-hexanol it was 6.9 hours, and for 2,2-dimethyl-3-pentanol it was 9.5 hours.

Based on the dynamic partition coefficients measured in experiment OUDNAPL1 and the mean residence times for the tracers, an average residual LNAPL saturation of 0.061 was estimated. The residual saturation estimates based on the second set of partitioning tracers in experiment OUDNAPL1 are summarized in Table 8.61.

Discussion for Experiment OUDNAPL3

In both sets of tracer tests in experiment OUDNAPL3, retardation factors of 1.3 to 1.4 for the 1-hexanol and 1.8 to 1.9 for the 2,2-dimethyl-3-pentanol were observed. This corresponded to an average LNAPL saturation of 0.062. Tracer recoveries were excellent in the second set of partitioning tracers. Based on these retardation factors and excellent tracer recoveries, 1-hexanol and 2,2-dimethyl-3-

pentanol were recommended as the partitioning tracers and ethanol was recommended as the conservative tracer for the field test at Hill OU1.

Overall Summary of OU1 LNAPL Experiments

Based on the results obtained from the partitioning tracer experiments performed with Hill OU1 LNAPL and Hill field soil, the first field partitioning tracer test was designed and performed to estimate residual LNAPL saturations. This was a brilliant and innovative program in which column experiment results were used as modeling inputs for UTCHEM. Sensitivity analysis of various parameters on the field test was performed and the field test was designed based on the results obtained from soil column studies and extensive computer modeling. The design the field partitioning tracer test is described in Pope *et al.*, (1994) and Jin (1995). The results of this field partitioning tracer test are described by Annable *et al.* (1994).

8.4 EXPERIMENTS WITH JP4

A total of two column experiments were conducted using jet fuel as the contaminant. Both these experiments were aimed towards mobilization of LNAPL (experiment DW#5 and JP4#2). Pressure drops were accurately measured during the surfactant flood to look for possible emulsion/gel/liquid crystal problems. In both these experiments, secondary butyl alcohol (SBA) was used as the co-solvent to avoid liquid crystal/gel formation. The jet fuel was obtained from March Air Force Base. It was golden yellow in color with a density of 0.76 g/cc. The viscosity of jet fuel was 0.8 cp.

8.4.1 Experiment DW#5

In experiment DW#5, the performance of partitioning tracers for estimation of residual JP4 saturation was evaluated. A surfactant/alcohol solution was used to remediate the contaminated soil column. A Winsor type I surfactant solution was used in experiment DW#5. Pressure drops were measured during the surfactant flood and post surfactant waterflood and partitioning tracers were used for performance assessment of surfactant remediation. The soil column length, diameter, porosity and permeability are presented in Table 8.2.

Initial Tracer Test

A suite of alcohol tracers was used for estimation of pore volume in the uncontaminated soil column. The alcohols used were IPA, 2,3-dimethyl-2-butanol and 2-methyl-2-hexanol. The samples were analyzed using a GC. A total of 18.3 cc tracer solution was injected followed by a waterflood at an interstitial velocity of 3.5 m/day (1.6 cc/min). A summary of the initial tracer test is given in Table 8.62. The pore volume based on mass balance measurements was 101.1 cc and the pore volume based on tracers was 100.0 cc. The tracer concentration history is plotted in Figure 8.48. From Figure 8.48 a close overlap of both partitioning and nonpartitioning tracers is observed. This indicates negligible adsorption of alcohols by Ottawa sand. A more detailed analysis of alcohol adsorption is given in Chapter 9.

Contamination of Soil Column

The column was oriented vertically. Contamination of the soil column was carried out by injecting JP4 into the top of the column until residual water saturation

was reached. This was followed by injection of water from the top of the column until residual JP4 saturation was reached. Both the JP4 flood and waterflood were carried out at an interstitial velocity of 6.9 m/day (3.0 cc/min). The end point jet fuel relative permeability was measured at residual water saturation and the end point water relative permeability was measured at residual JP4 saturation. A summary of contamination of the soil column is given in Table 8.63. A residual water saturation of 0.506 was reached at the end of the JP4 flood and a residual JP4 saturation of 0.163 (mass balance) was reached at the end of the waterflood.

Tracer Test at Residual JP4 Saturation

A suite of conservative and partitioning tracers was injected into the soil column to evaluate the performance of partitioning tracers to estimate residual JP4 saturation. The tracers used were IPA, 2,3-dimethyl-2-butanol and 2-methyl-2-hexanol. About 17.5 cc of tracer solution was injected followed by a waterflood at an interstitial velocity of 1.3 m/day (0.58 cc/min). The effluent was analyzed using a GC. This tracer test is summarized in Table 8.64. The tracer concentration history is plotted in Figure 8.49. Based on partitioning tracers, an average residual saturation of 0.178 was calculated compared to a waterflood residual saturation of 0.163 based on mass balance. A summary of residual saturation estimates based on partitioning tracers is given in Table 8.65.

Surfactant Flood to Remediate JP4

A surfactant solution consisting of 0.6% by weight sodium dihexyl sulfosuccinate, 1.4% by weight sodium dioctyl sulfosuccinate and 2% by weight secondary butyl alcohol was injected at 1.3 m/day (0.56 cc/min). This surfactant

solution was a Winsor type I surfactant solution with a JP4 solubilization parameter of 2.8 and JP4 solubilization of 45,000 mg/l. A total of 296.2 cc (3.0 pore volumes) of surfactant was injected followed by injection of 500 cc (5 pore volumes) of 250 mg/l NaCl at 1.3 m/day (0.56 cc/min). The effluent could not be analyzed for JP4 concentration as analytical techniques for measuring JP4 concentration in microemulsion had not been perfected.

The surfactant flood is summarized in Table 8.66. A total of 9.3 cc of free phase jet fuel was mobilized. The pressure differential was observed to rise linearly throughout the surfactant flood. A hydraulic gradient of 30 was measured at 300 cc of total production when the surfactant flood was stopped. The waterflood was started and the hydraulic gradient was observed to drop to less than 1 after 15 cc of injection. This can be attributed to premature breakthrough due to a viscous fingering effect i.e. the fresh water flowing through the path of least resistance. The hydraulic gradient is plotted against cumulative volumes produced in Figure 8.50. The viscosity of the injected surfactant solution is plotted in Figure 8.51. Non-Newtonian behavior is observed for the aqueous surfactant solution.

Movement of sand grains was observed at the end of the surfactant flood and the beginning of the waterflood. Based on mass balance, 117% JP4 was recovered.

Tracer Test After surfactant to Estimate Residual JP4 Saturation

After 3 pore volumes of surfactant flooding and 5 pore volumes of waterflooding, a suite of conservative and partitioning tracers was injected into the soil column to estimate the final residual JP4 saturation. The tracers used were

ethanol, 2,2-dimethyl-3-pentanol and 1-hexanol. About 13.1 cc of tracer solution was injected followed by a waterflood at 1.3 m/day (0.56 cc/min). Early breakthrough of the tracer was observed. This can be attributed to possible plugging of the soil column caused by gelling and/or liquid crystal formation of the surfactant solution. The tracer concentration history is plotted in Figure 8.52. The aqueous pore volume of the soil column was about 8 cc compared to the initial pore volume of 101 cc, which clearly indicates plugging. This tracer test is summarized in Table 8.67.

Discussion for Experiment DW#5

In experiment DW#5, the performance of two alcohol tracers for estimation of JP4 saturation was evaluated. The tracers used were, 2,3-dimethyl-2-butanol and 2-methyl-2-hexanol. The average residual saturation estimated using partitioning tracers and mass balance agreed to within a saturation of ± 0.015 . From this it can be inferred that partitioning tracers are effective in determining residual JP4 saturations.

A total of 13.1 cc of free JP4 was mobilized during the surfactant flood. Two samples showed three phase behavior. During the surfactant flood, an increase in the hydraulic gradient was observed during the surfactant flood. High hydraulic gradients were attributed to the formation of liquid crystals and gels in the surfactant solution. A surfactant solution consisting of a mixture of sodium dioctyl sulfosuccinate and sodium dihexyl sulfosuccinate was used in this experiment. Sodium dioctyl sulfosuccinate has a longer tail and less branching compared to sodium dihexyl sulfosuccinate. Surfactants with longer tails are more susceptible to

liquid crystal/gel formation. The formation of gels and liquid crystals caused pore plugging thereby leading to excessive hydraulic gradients during the surfactant flood. This was further confirmed by the aqueous pore volume of 8 cc measured by the final tracer test. In order to avoid plugging due to liquid crystal/gel formation, additional amounts of alcohol must be added. The addition of alcohol increases the fluidity of interfaces, increases the entropy and melts liquid crystals and gels. The hydraulic gradient was observed to decline rapidly once the post-surfactant waterflood was started. This can be attributed to viscous fingering of water through plugged soil.

8.4.2 Experiment JP4#2

In experiment DW#5 excessive hydraulic gradients across the soil column were observed during surfactant flooding. An attempt was made to rectify this problem by using a surfactant solution with a higher concentration of co-solvent. The additional alcohol was aimed at minimizing liquid crystal/gel formation and prevention of plugging of the soil column by surfactant flooding. Partitioning tracers were used for estimation of jet fuel saturation and for performance assessment of surfactant remediation. Pressure drops were measured during the surfactant flood and post surfactant waterflood to look for possible gel/liquid crystal formation and measure the permeability of the soil column after surfactant flooding. The soil column length, diameter, porosity and permeability are presented in Table 8.2.

Initial Tracer Test

In this experiment, tritium was used to estimate pore volume. About 4.7 cc of tritium was injected followed by a waterflood at an interstitial velocity of 11 m/day (1 cc/min). The effluent was analyzed for tritium concentration using a LSC. The tracer concentration history is plotted in Figure 8.53. A summary of the initial tracer test is given in Table 8.68. The pore volume based on tritium was 41.8 cc, the pore volume based on mass balance was 41.4 cc.

Contamination of Soil Column

The column was oriented vertically. Contamination of the soil column was carried out by injecting JP4 into the top of the column until residual water saturation was reached. This was followed by injection of water from the bottom of the column until residual JP4 saturation was reached. Both the JP4 flood and waterflood were carried out at an interstitial velocity of 11 m/day (1.0 cc/min). The end point jet fuel relative permeability was measured at residual water saturation and the end point water permeability was measured at residual jet fuel saturation. A summary of contamination of the soil column is given in Table 8.69. A residual water saturation of 0.338 was reached at the end of the JP4 flood and a residual JP4 saturation of 0.151 (mass balance) was reached at the end of the waterflood.

Tracer Test at Residual TCE Saturation

A suite of conservative and partitioning tracers was injected into the soil column at to evaluate the performance of partitioning tracers for estimation of residual JP4 saturation. The tracers used were ethanol, 2,3-dimethyl-3-pentanol and 2-methyl-3-pentanol. About 4.9 cc of tracer solution was injected followed by

a waterflood at an interstitial velocity of 2.1 m/day (0.20 cc/min). The effluent was analyzed using a GC. The mean retention time was 3.0 hours for ethanol, for 2-methyl-3-pentanol it was 5.1 hours and for 2,3-dimethyl-3-pentanol it was 8.3 hours. This tracer test is summarized in Table 8.70. The tracer concentration history is plotted in Figure 8.54. Based on partitioning tracers, the average waterflood residual jet fuel saturation was 0.159 compared to a waterflood residual jet fuel saturation of 0.151 based on mass balance measurements. A summary of residual saturation estimates based on partitioning tracers is given in Table 8.71.

Surfactant Flood to Remediate JP4

A solution consisting of 2.0% by weight sodium dihexyl sulfosuccinate, 2.0% by weight sodium dioctyl sulfosuccinate, 8% by weight secondary butyl alcohol, 11,700 mg/l NaCl and 1,300 mg/l CaCl₂ was injected into the column at an interstitial velocity of 1.7 m/day (0.16 cc/min). This solution exhibited Winsor type III behavior with a solubilization parameter of 2.2. The interfacial tension between the excess JP4 and microemulsion was not measured. A total of 242 cc (5.8 pore volumes) of surfactant was injected. This was followed by injection of 65 cc (1.6 pore volumes) of 2.0 % sodium dihexyl sulfosuccinate 8% secondary butyl alcohol and 500 mg/l NaCl to remove sodium dioctyl sulfosuccinate from the soil column. Finally the column was flushed with 500 mg/l NaCl to remove surfactant. This was done because, sodium dioctyl sulfosuccinate was prone to forming gels at co-solvent concentrations of less than 2 weight %. Hence 1.6 pore volumes of a surfactant solution containing 2.0 % sodium dihexyl sulfosuccinate 8% secondary butyl alcohol and 500 mg/l NaCl was flushed through the soil column to remove the

sodium dioctyl sulfosuccinate. The surfactant was used to ensure complete dissolution of secondary butyl alcohol. The surfactant flood is summarized in Table 8.72.

The viscosity of the aqueous surfactant solution was measured before injection to ensure that the solution exhibited a low viscosity Newtonian behavior. The variation of viscosity of the aqueous surfactant solution with shear rate is plotted in Figure 8.55. From the Figure it can be seen that the viscosity was observed to vary between 1.7 cp and 1.9 cp and exhibited Newtonian behavior.

Low hydraulic gradients were measured across the soil column during the surfactant flood and post surfactant waterflood. The hydraulic gradients across the soil column during the surfactant flood and post surfactant waterflood are plotted in Figure 8.56. The hydraulic gradient was observed to increase steadily for the first 1.2 pore volumes of production. This corresponded to the production of free JP4. This was followed by a decline to a hydraulic gradient of 0.2 at the end of the surfactant flood. A further decline of the hydraulic gradient was observed when the waterflood was started. The permeability of the soil after surfactant remediation was 6.9 Darcies compared to the initial permeability of 7.3 Darcies.

Tracer Test After surfactant to Estimate Residual JP4 Saturation

A suite of conservative and partitioning tracers was injected into the soil column after the surfactant flood and post surfactant waterflood estimate the final residual jet fuel saturation. The tracers used were ethanol, 2-methyl-3-pentanol and 2,3-dimethyl-3-pentanol. A total of 4.6 cc of tracer solution was injected followed by a waterflood at an interstitial velocity of 2.1 m/day (0.2 cc/min). Low

retardation of partitioning tracers was observed. The tracer concentration history is plotted in Figure 8.57. This tracer test is summarized in Table 8.73. Based on the partitioning tracers, a residual jet fuel saturation of 0.035 was measured after surfactant flooding compared to an average residual saturation of 0.027 based on mass balance. The residual saturation based on partitioning tracers is summarized in Table 8.74.

Discussion for Experiment JP4#2

In this experiment, the alcohol concentration was increased to 8% in the surfactant solution to minimize the gel/liquid crystal formation and high hydraulic gradients observed in experiment DW#5. The hydraulic gradients during the surfactant flood were low and no evidence of gel/liquid formation was observed. From this it can be concluded that addition of alcohol minimized gel/liquid formation and promoted quick coalescence and equilibration during surfactant flooding. However, all the JP4 was not recovered in this experiment. A residual saturation of 0.027 based on mass balance and a residual saturation of 0.035 based on partitioning tracers was estimated after the surfactant flood. Compared to NAPL recoveries in earlier and later experiments, this is a low recovery. No satisfactory reason could be found for this low recovery. Since the main object of this work was to focus on DNAPL removal, no further surfactant flooding experiments were conducted with jet fuel.

8.5 EXPERIMENTS WITH HILL OU2 DNAPL

Several column experiments were performed for the design of the Phase I pilot tracer/surfactant injection test and Phase II surfactant enhanced aquifer

remediation (SEAR) tests at the Operational Unit 2 site at Hill Air Force Base, Utah. Four experiments were performed by the author of this work and are described in the following sections and additional experiments were performed concurrently by Shotts (1996) due to the limited time of only a few months available to design these field tests during May and August of 1996.

The soil samples as received in SOLINST cores contained numerous large cobbles and stones which were removed prior to packing the glass column (4.8 cm internal diameter). Sometimes it was necessary to use more than one sample for the soil column in order to obtain columns of sufficient length to do partitioning tracer and surfactant flooding experiments. In one experiment, HILLOU2#7, loose field soil stored in jars was used. The procedure for packing and saturating field soil is described in Chapter 3.

All the soil column experiments conducted by the author used Hill field soil. Tracer tests were conducted to quantify tracer adsorption and determine minimum residence times required for obtaining meaningful results from partitioning tracer tests. Radio-labeled surfactant was used in three column experiments to quantify surfactant adsorption by Hill field soil. Finally both tracer tests and surfactant injection tests were conducted in a soil column at 12.2°C to study the performance of partitioning tracers and surfactants at groundwater temperature. Results from these experiments will be used in Chapter 10 for lab design of the field tests at the Operational Unit 2 site at Hill Air Force Base.

The DNAPL at Hill Air Force Base, site OU2 was mainly comprised of chlorinated hydrocarbons such as trichloroethylene (TCE), tetrachloroethylene (PCE) and 1,1,1-trichloroethane (TCA). These solvents were used as degreasers

and disposed in shallow trenches. The average TCE concentration in the DNAPL was 73%, the average PCE concentration was 8%, the average TCA concentration was 14%, and the average Freon 113 concentration was 3%. The rest was made up of carbon tetrachloride, toluene and dissolved grease. The density of the DNAPL was 1.383 g/cc, the DNAPL was black in color and showed a strong tendency to form foam and emulsions when mixed strongly with water. The interfacial tension between the Hill DNAPL and water was between 4 and 7 dynes/cm.

8.5.1 Experiment HILLOU2#3

Experiment HILLOU2#3 was the first experiment conducted with contaminated Hill field soil. The main objectives were evaluation of performance of partitioning tracers for estimation of DNAPL in place and prevention of mobilization of free DNAPL during surfactant flood by using a surfactant solution with an appropriate interfacial tension between the microemulsion and excess DNAPL.

Contaminated field soil from Hill AFB site Operational Unit 2 was used in experiment HILLOU2#3. The soil was obtained from zones 40 ft to 41.5 ft from well SB-205. The soil was a silty gravelly soil. Large cobbles and stones were removed prior to packing. The porosity of the soil column was 0.453 and the permeability was 7.1 Darcies. A Kontes borosilicate column 4.8 cm diameter and 15 cm long was used with an adjustable plunger to apply some confining stress. A 99 μm steel mesh was used to hold the sand in place. The soil column was saturated with ground water from Hill Operational Unit 2. Based on all the earlier soil column experiments it was determined that sodium dihexyl sulfosuccinate was

an excellent candidate surfactant to remediate soils contaminated by PCE and TCE. Since the Hill DNAPL was composed largely of PCE, TCE and other contaminants, it was decided to test the performance of sodium dihexyl sulfosuccinate with Hill DNAPL in phase behavior experiments and soil column experiments.

In all the experiments, the terms Hill source water and Hill groundwater will be used. The term Hill groundwater refers to the groundwater from the Hill OU2 and Hill source water refers to the tap water available at Hill Air Force Base. The composition of Hill groundwater and Hill source water is given in Tables 10.2 and 10.3 in Chapter 10. The soil column length, diameter, porosity and permeability are presented in Table 8.2.

Initial Tracer Test

A suite of five tracers was injected into the soil column for estimation of DNAPL initially present in the soil. The tracers used were tritium, IPA, 3-methyl-3-pentanol, 1-hexanol and 2,2-dimethyl-3-pentanol. About of 6.3 cc of tracer solution was injected followed by a waterflood at an interstitial velocity of 0.8 m/day (0.35 cc/min). A summary of the tracer test is given in Table 8.75. The tracer saturation estimates based on partitioning tracers are summarized in Table 8.76. An average DNAPL saturation of 0.011 was estimated based on partitioning tracers. The tracer concentration history is plotted in Figure 8.58.

Contamination of Soil Column

The column was oriented vertically. Hill DNAPL was injected into the soil column from the bottom at an interstitial velocity of 9.1 m/day (4.0 cc/min). A total

of 9.6 cc of Hill DNAPL was injected. This was followed by injection of water from the top of the soil column at an interstitial velocity of 9.1 m/day (4.0 cc/min). A total of 1.2 cc of free phase DNAPL was produced. A residual DNAPL saturation of 0.089 was calculated based on the volume of DNAPL added during contamination of the soil column and the initial DNAPL saturation based on partitioning tracers.

Surfactant Flood to Remediate DNAPL

A solution consisting of 5% by weight sodium diamyl sulfosuccinate in Hill source water was injected into the soil column at an interstitial velocity of 2.2 m/day (0.24 cc/min) with the soil column oriented horizontally. A total of 148.8 cc (1.3 pore volumes) of surfactant was injected followed by flooding with 120 cc (1.1 pore volumes) of Hill source water. A small bank of DNAPL was observed but no free DNAPL was produced as the column was oriented horizontally. The IFT between the microemulsion and excess DNAPL was measured as 0.4 dyne/cm. Since the objective of this experiment was solubilization and since a bank of DNAPL was observed, no more work was carried out with this soil column.

Discussion for Experiment HILLOU2#3

The main objective of experiment HILLOU2#3 was to avoid mobilization of movement of free phase DNAPL. Since a bank of free phase DNAPL was observed, no more work was carried out in column HILLOU2#3. The formation of the free phase DNAPL bank was attributed to low IFT measured between Hill DNAPL and the surfactant solution. A more detailed discussion will be presented in Chapter 10 in the discussion of Capillary Desaturation Curves (CDC).

8.5.2 Experiment HILLOU2#5

Column experiment HILLOU2#5 was performed in order to evaluate the adsorption of sodium dihexyl sulfosuccinate by Hill field soil using ^{14}C labeled surfactant. This surfactant was prepared by Weerasooriya (University of Texas, 1995). Surfactant concentrations were measured using a Beckman liquid scintillation counter.

The performance of 2-ethyl-1-butanol and 1-pentanol to estimate residual DNAPL saturation was evaluated. These tracers were candidate tracers for use in the field test at Hill AFB. The ability of a surfactant/alcohol/polymer solution to completely remediate the contaminated soil column was also investigated by flooding the contaminated column using a solution consisting of 4% sodium dihexyl sulfosuccinate, 8% IPA, 500 mg/l xanthan gum, 10,600 mg/l NaCl in Hill source water. This surfactant solution exhibited Winsor type III behavior and was at optimal salinity. This was done to evaluate the performance of a surfactant/alcohol/polymer solution for remediating contaminated Hill field soil. Hence partitioning tracers were used to determine residual DNAPL saturations after surfactant remediation. This was done to assess performance of surfactant flooding.

A 4.8 cm diameter, 15 cm long Kontes glass column was used with an adjustable plunger to confine the sand. SOLINST core from well SB-6, sample SB-609 from a depth of 43.8 ft to 44.3 ft and sample SB-606 from a depth of 42 ft were used in experiment HILLOU2#5. The soil used in this experiment was also silty gravely soil with some fine sand present. The soil packing procedures and soil

saturation procedures are described in Chapter 3. Hill groundwater (150 mg/l TDS) was used for initial saturation of the soil column. The soil column length, diameter, porosity and permeability are presented in Table 8.2.

Initial Tracer Test

A suite of tracers were used for estimation of DNAPL already present in the soil column. The tracers used were tritium, 1-pentanol, and 2-ethyl-1-butanol. About of 9.5 cc of tracer solution was injected followed by a waterflood at an interstitial velocity of 0.8 m/day (0.35 cc/min). The residence time was 3.8 hours for 1-pentanol and for 2-ethyl-1-butanol it was 5.9 hours. The tracer concentration history is plotted in Figure 8.59. The initial tracer test is summarized in Table 8.78. The residual DNAPL saturations based on partitioning tracers are given in Table 8.79. A discussion on measurement of partition coefficients for alcohols between NAPLs and water is given in Chapter 7. The partition coefficients of several alcohols with Hill DNAPL are given in Table 7.2. An average residual DNAPL saturation of 0.129 was estimated based on partitioning tracers.

Surfactant Flood to Remediate DNAPL

Two surfactant injections were performed in experiment HILLOU2#5. The first surfactant flood was aimed at quantifying surfactant adsorption by Hill field soil. A 4% by weight sodium dihexyl sulfosuccinate mixed in Hill source water was injected into the soil column at an interstitial velocity of 1.2 m/day (0.5 cc/min). The soil column orientation was horizontal. A total of 25.9 cc (0.47 pore volumes) of surfactant was injected. This was followed by flooding with 150 cc

(2.7 pore volumes) of Hill source water (110 mg/l TDS). The surfactant was radiolabeled with ^{14}C and tritium was used as a conservative tracer.

The oil solubilization parameter of this surfactant solution was 0.29 and this corresponds to a contaminant solubilization of 16,000 mg/l. The interfacial tension between the microemulsion and excess DNAPL was measured as 0.2 dyne/cm. The surfactant flood is summarized in Table 8.80.

Both the tritium and surfactant (^{14}C) concentrations were measured using a liquid scintillation counter and a comparison of the tritium and surfactant concentration histories is plotted in Figure 8.60. A close overlap of normalized tritium and surfactant concentrations is observed in Figure 8.61. The surfactant concentration was observed to decline to less than 0.1% after 180 cc of total production, which is less than the CMC of the surfactant of 0.2 weight %. About 92.5% of the surfactant was recovered. The surfactant adsorption was calculated as 0.313 mg/g from the mass balance. Based upon the simultaneous breakthrough of tritium and ^{14}C as well as subsequent adsorption tests, the adsorption was probably even less than this low value (see Chapter 9).

The soil column was kept horizontal during the surfactant flood and post surfactant waterflood to remove surfactant. No DNAPL was produced during these floods. The soil column orientation was switched to vertical and the soil column was flushed with 200 cc of 10,600 mg/l NaCl (3.6 pore volumes) to equilibrate the soil at the desired electrolyte concentration before injecting the second surfactant slug. This electrolyte concentration corresponded to the optimal salinity for 4% by weight sodium dihexyl sulfosuccinate, 8% isopropanol and 500 mg/l xanthan gum mixed in Hill source water. During this stage 5.4 cc of DNAPL was produced.

The second surfactant flood was performed using a surfactant/alcohol/polymer mixture to remediate the remaining DNAPL in the soil column. The performance of a surfactant/alcohol/polymer mixture for remediating the DNAPL contaminated soil column was evaluated. A total of 125.9 cc (2.3 pore volumes) of 4% by weight sodium dihexyl sulfosuccinate, 8% IPA, 10,600 mg/l NaCl, 500 mg/l xanthan gum was injected at an interstitial velocity of 1.2 m/day (0.5 cc/min). After the surfactant injection, the soil column was flushed with 100 cc (1.8 pore volumes) of 150 mg/l NaCl and 150 cc (2.7 pore volumes) of 150 mg/l CaCl₂ to remove the surfactant from the soil column. The second surfactant flood is summarized in Table 8.81.

The solubilization parameter of this surfactant was 4.0 and this corresponds to a contaminant solubilization of about 500,000 mg/l. A total of 6.0 cc of DNAPL was produced during the second surfactant flood. Hence a total of 11.4 cc of DNAPL was produced as a result of surfactant flooding. Based on the initial tracer test, the DNAPL volume was estimated as 7.2 cc, but after two surfactant floods a total of 11.4 cc of DNAPL was produced. This means that the initial partitioning tracer test under predicted the DNAPL saturation in the soil column. This is due to insufficient residence time for the partitioning tracers in the soil column and will be discussed later.

The hydraulic gradient across the soil column was measured during the second surfactant flood. The hydraulic gradient is plotted against the cumulative volume produced in Figure 8.62. A hydraulic gradient between 0.5 and 0.9 was measured during this surfactant flood. When surfactant injection was stopped and injection of 150 mg/l NaCl was started, the hydraulic gradient was observed to

increase sharply. This is due to possible migration of fines due to the absence of calcium ions in the waterflood. The hydraulic gradient was observed to decrease when 150 cc of 150 mg/l CaCl_2 was injected into the soil column. This will be discussed later.

Tracer Test After Surfactant to Estimate Residual DNAPL Saturation

After both the surfactant floods and the post-surfactant waterflood to remove surfactant, a suite of conservative and partitioning tracers was injected into the soil column to estimate the final residual DNAPL saturation. This was done because there was no other means to estimate DNAPL removal. Since the soil column was contaminated initially, mass balance measurements could not be used to estimate % DNAPL recovered. Recoveries based on GC measurements were generally prone to errors as observed in experiments DW#3 and DW#4. Hence partitioning tracers were employed as a means for performance assessment of surfactant flooding. The tracers used were tritium, 3-methyl-3-pentanol, 2,2-dimethyl-3-pentanol and 1-hexanol. A total of 9.1 cc of tracer solution was injected followed by a waterflood at an interstitial velocity of 0.8 m/day (0.34 cc/min). The effluent was analyzed using a LSC and GC and the residual DNAPL saturation after surfactant flooding was calculated. The tracer concentration history is plotted in Figure 8.63. The tracer test is summarized in Table 8.82. The residual DNAPL saturation estimates based on partitioning tracers are summarized in Table 8.83. Negligible delay of the partitioning tracers can be observed in Figure 8.63. Based on partitioning tracers a final DNAPL saturation of 0.0054 was calculated. This is a very low DNAPL saturation and indicated that the dihexyl sulfosuccinate was likely

to be a very good choice for use in the field tests at Hill OU2 and justified continued testing of it in the laboratory.

Discussion for Experiment HILLOU2#5

The average residual DNAPL saturation estimated by partitioning tracers was 0.129. This corresponded to 7.2 cc of DNAPL but 11.4 cc of free DNAPL was recovered. This discrepancy can be explained by possibility of DNAPL existing as a pool in the soil column. Here a pool is defined by the occurrence of a locally high DNAPL saturation. Hence, the process of detection by the partitioning tracers might have been limited by the diffusion time of partitioning tracers into the pool of DNAPL due to limited surface area of contact. The partitioning tracers had only 3.9 to 6 hours of residence time in the column. These results suggested that a longer residence time might be needed for the partitioning tracers. In experiments HILLOU2#7 and HILLOU2#8, this was evaluated by using a residence time between 19 and 42 hours for the partitioning tracers.

The pressure drops suddenly increased when the waterflood (150 mg/l NaCl) was started. This could be attributed to the replacement of calcium ions by sodium ions in the clays. This replacement caused swelling and movement of clays. These clays probably migrated and blocked pore throats leading to decreased permeability and higher pressure drops (hydraulic gradients). The addition of 150 mg/l CaCl_2 probably reversed the swelling of clays and moved them away from the pore throats. Hence it can be concluded that for field application of surfactant flooding, the surfactant solution and the post surfactant waterflood must have a sufficient quantity of calcium ions to prevent ion exchange i.e. replacement of

calcium ions by sodium ions in clays. This ion exchange can cause fines production, pore plugging and high hydraulic gradients.

8.5.3 Experiment HILLOU2#7

In this experiment partitioning tracers were injected into uncontaminated Hill field soil in order to quantify tracer adsorption by field soil. In experiment HILLOU2#5, a close match between DNAPL saturation based on tracers and the volume of DNAPL recovered during surfactant remediation could not be obtained as partitioning tracers estimated the DNAPL volume as 7.2 cc, but a total of 11.4 cc of DNAPL was mobilized. Since this was probably due inadequate residence times of the tracers in the contaminated soil column, the performance of 1-pentanol for estimation of residual DNAPL saturation was evaluated by increasing the residence time for the tracer. Heavier alcohols like 2,2-dimethyl-3-pentanol and 1-heptanol were used for performance assessment of surfactant remediation. Surfactant adsorption of a Winsor type III surfactant solution was quantified by using radiolabeled surfactant.

A 4.8 cm diameter, 30 cm long Kontes glass column was used with an adjustable plunger to confine the sand. Loose soil samples from well SB-5, sample SB-505 from depths 35 ft to 41.8 ft were used in experiment HILLOU2#7. These samples were uncontaminated soil samples and were stored in glass jars. The soil column length, diameter, porosity and permeability are presented in Table 8.2.

Initial Tracer Test

In this experiment, a suite of partitioning tracers was injected into uncontaminated Hill field soil to quantify alcohol adsorption. The tracers used were

tritium, IPA, 3-methyl-3-pentanol, 2,2-dimethyl-3-pentanol and 1-hexanol. A total of 18.2 cc of tracer solution was injected followed by a waterflood at an interstitial velocity of 0.36 m/day (0.12 cc/min). The retention time for all the alcohols was 19.4 hours. The tracer concentration history is plotted in Figure 8.64. Negligible retardation is observed for all tracers. Tracer adsorption by Hill field soil is further discussed in Chapter 9. The initial tracer test is summarized in Table 8.84.

Contamination of Soil Column

The column was oriented vertically. Contamination of the soil column was carried out by injecting Hill DNAPL into the column from the bottom until residual water saturation was reached followed by injection of water from the top of the column until residual DNAPL saturation was reached. The DNAPL flood was carried out at 9 m/day (3.0 cc/min). The waterflood was carried out at 27 m/day (9 cc/min). A higher rate was used for the waterflood as the DNAPL was slowly being stripped and did not reach equilibrium at a waterflood flow rate of 3.0 cc/min. The pressure gradient across the soil column at steady state during the DNAPL flood was 0.83 psi/ft (at 3 cc/min). The pressure gradient across the soil column at steady state during the waterflood was 4.02 psi/ft (at 9 cc/min). The end point DNAPL relative permeability was measured at residual water saturation and the end point water relative permeability was measured at residual DNAPL saturation. A summary of contamination of the soil column is given in Table 8.85. A residual water saturation of 0.506 was reached at the end of the contaminant flood and a residual DNAPL saturation of 0.261 (mass balance) was reached at the end of the waterflood.

Tracer Test at Residual DNAPL Saturation

Tritium and 1-pentanol were used for estimation of residual DNAPL saturation. A total of 29.2 cc of tracer solution was injected followed by a waterflood at an interstitial velocity of 0.24 m/day (0.08 cc/min). Samples were analyzed using a LSC and GC. The tracer concentration history for this tracer test is plotted in Figure 8.65. The mean residence time for the 1-pentanol was 42 hours. A retardation factor of 2.34 was measured for 1-pentanol. Based on the residence times of tritium and 1-pentanol, a DNAPL saturation of 0.255 was calculated compared to a DNAPL saturation of 0.261 based on mass balance. The tracer test at residual DNAPL saturation is summarized in Table 8.86. The residual saturation estimate based on tracers is given in Table 8.87.

Surfactant Flood to Remediate Contaminant

A surfactant solution consisting of 4% by weight sodium dihexyl sulfosuccinate (commercial name Aerosol MA-80I), 4% IPA, 500 mg/l xanthan gum and 11,250 mg/l NaCl mixed in Hill source water was injected at an interstitial velocity of 1.2 m/day (0.5 cc/min). Xanthan gum polymer acts as a viscosifier. The increased viscosity of the polymer would help in mitigating aquifer heterogeneities. The performance of surfactant/polymer/alcohol solutions to remediate DNAPL contaminated field soil was evaluated in this experiment. The viscosity of the injected surfactant solution and post-surfactant polymer solution is plotted in Figure 8.71. The surfactant solution used in this experiment was a Winsor type III solution close to optimal salinity. For the first 150 cc of injection, the injection rate was only 0.6 m/day (0.25 cc/min). The surfactant was tagged

with ^{14}C labeled sodium dihexyl sulfosuccinate at a ^{14}C concentration of 13,027 DPM/ml.. Tritium was used as a conservative tracer to measure retardation of surfactant by Hill field soil (concentration of 8,604 DPM/ml).

A total of 300.7 cc (2.1 pore volumes) of surfactant was injected. This was followed by 377.3 cc (2.6 pore volumes) of 500 mg/l xanthan gum polymer in Hill source water to remove surfactant. The post-surfactant polymer flood with 500 mg/l xanthan gum polymer mixed in Hill source water was used to provide a salinity gradient (Pope and Baviere, 1991). This is discussed later in this Chapter. The surfactant flood is summarized in Table 8.88.

The solubilization parameter of this surfactant solution was 4.3. This corresponded to a contaminant solubilization of 600,000 mg/l in the middle phase microemulsion. The IFT measured between the microemulsion and excess DNAPL was 0.01 dyne/cm. A total of 26.8 cc of free DNAPL was produced during the surfactant flood. This corresponded to 73.6 % of DNAPL present in the soil column. The rest of the DNAPL was solubilized as microemulsion and produced. The relative percentages of contaminant produced as DNAPL and solubilized are plotted in Figure 8.66.

For the first 105 cc (0.73 pore volumes) of production, DNAPL was produced. This was followed by production of three phase samples for the next 160 cc (1.1 pore volumes) of production and then single phase samples. The tritium concentration was measured in the aqueous phase. The surfactant concentration was measured in aqueous and microemulsion phases. The comparison of the tritium concentration in the aqueous phase and the surfactant concentration in both the middle phase microemulsion and the aqueous phase is

plotted in Figure 8.67. Even though 4% surfactant was injected, surfactant concentrations of up to 16% were measured in the effluent microemulsion samples. When tritium and surfactant concentrations normalized by their injected values are plotted against cumulative volume produced, a close overlap is observed after 265 cc (1.85 pore volumes) of production (Figure 8.68).

In order to make more sense of this information, the recoveries of tritium and surfactant were plotted as a function of cumulative volume produced. This is plotted in Figure 8.69. A slight delay in surfactant recovery compared to tritium recovery is observed. This can be attributed to the concentration of surfactant in the middle phase microemulsion. However, after cessation in the production of middle phase microemulsion, both tritium and surfactant recoveries overlap within experimental error.

Based on mass balance measurement, 100.4% of the waterflood residual DNAPL was recovered. Based on adding the volume of DNAPL mobilized and solubilized in the effluent samples, 98.4% DNAPL was recovered as a result of surfactant remediation. Based upon LSC measurement of the effluent samples, 103.1% tritium and 101.6% surfactant was recovered. From this it can be inferred that there is negligible adsorption of surfactant by Hill field soil.

Pressure drops were measured across the soil column during the surfactant flood and converted into a hydraulic gradient. The hydraulic gradient during surfactant flood and post surfactant polymer flood for experiment HILLOU2#7 is plotted in Figure 8.70. The hydraulic gradient at the beginning of surfactant injection was 0.23. When surfactant was injected into the soil column, the hydraulic gradient increased to a peak of 1.2 at about 170 cc (1.2 pore volumes) of

total production. DNAPL breakthrough was observed at 30 cc (0.21 pore volumes) of total production. At about 150 cc of total production, the injection rate was increased to an interstitial velocity of 1.2 m/day. A slow decline in the hydraulic gradient to 0.85 at 300 cc of total injection.

A polymer flood with 500 mg/l xanthan gum in Hill source water was started at an interstitial velocity of 1.2 m/day after 2.1 pore volumes of surfactant/alcohol/polymer injection. The hydraulic gradient was further observed to decline to about 0.27 after a total of 500 cc of polymer flooding. This hydraulic gradient is about four times the expected hydraulic gradient with water flowing through the soil column at the same flow rate. Based on this it can be inferred that 500 mg/l xanthan gum polymer is about 4 times as viscous as water. The viscosities of the aqueous surfactant solution and injected post surfactant polymer solution are plotted in Figure 8.71. Viscosities of about 4 cp are observed at shear rates of 100 sec^{-1} for both solutions. From this it can be inferred that for the Hill field soil used in experiment HILLOU2#7, the injected solutions would be subjected to a shear rates of about 100 sec^{-1} . A permeability of 4.5 Darcies was measured at the end of the surfactant flood compared to the initial permeability of 5.9 Darcies.

Tracer Test After Surfactant to Estimate Residual DNAPL Saturation

After 2.1 pore volumes of surfactant/polymer flooding and 2.6 pore volumes of polymer flooding, a suite of conservative and partitioning tracers was injected into the soil to estimate the final residual DNAPL saturation. The tracers used were tritium, 2,2-dimethyl-3-pentanol, 1-hexanol and 1-heptanol. The tracers

were mixed in 500 mg/l xanthan gum in Hill source water. About 14.6 cc of tracer solution was injected followed by flooding with 500 mg/l xanthan gum in Hill source water at an interstitial velocity of 0.4 m/day (0.14 cc/min). The effluent was analyzed for the alcohols and tritium using a GC and LSC and the residual DNAPL saturation was calculated. The final tracer concentration histories are plotted in Figure 8.72. Retardation factors between 1.01 and 1.02 were measured for the various partitioning tracers. Based on these retardation factors, an average residual DNAPL saturation of 0.00016 was estimated using partitioning tracers. This corresponded to a recovery of 99.9% DNAPL and is considered the most accurate of the three performance measures used. The final partitioning tracer test is summarized in Table 8.89. The residual DNAPL saturation estimates based on partitioning tracers are given in Table 8.90.

Discussion for Experiment HILLOU2#7

Based on the initial tracer concentration history curve in uncontaminated Hill field soil, negligible retardation of the tracers was observed. Based on it can be concluded that there is negligible adsorption of the alcohol tracers by Hill field soil. This is further explained in later sections.

Based on the excellent match between the tracer estimate of residual DNAPL saturation and the mass balance estimate of residual DNAPL saturation it can be concluded that a residence time of 42 hours was sufficient for an accurate determination of residual DNAPL saturation.

The surfactant concentration was reduced to less than 0.1 % after 2.1 pore volumes of polymer injection after the surfactant flood. In addition, about 101% of

the surfactant and 103% of the tritium were recovered and based on this it can be concluded that there was negligible adsorption of the surfactant by the Hill field soil.

The hydraulic gradients were low during the course of the surfactant/polymer flood and allowing for the enhanced viscosities due to the 500 mg/l xanthan gum polymer. Low hydraulic gradients and absence of liquid crystals/gels/emulsions were due to the presence of 4% isopropanol. Also, the permeability of the soil pack after remediation (4.5 Darcy) was extremely close to the initial permeability (5.9 Darcy). Based on this information it can be inferred that the surfactant solution did not cause any problems such as pore plugging and that the soil was restored to very nearly its original condition after surfactant remediation.

A close overlap of partitioning and nonpartitioning tracers was observed in the final tracer test. Based on the final partitioning tracer test and the method of moments, an average residual saturation of 0.00016 was computed. This remarkably low value indicated that this surfactant is extremely effective in removing essentially all the Hill DNAPL from Hill field soil. This highly favorable result was confirmed by still other lab tests and finally the field test.

8.5.4 Experiment HILLOU2#8

The objectives in experiment HILLOU2#8 were the same as in experiment HILLOU2#7. However, the whole experiment was carried out at 12.2°C rather than 23°C to evaluate the surfactant at groundwater temperature.

A 4.8 cm diameter, 15 cm long Kontes glass column was used with an adjustable plunger to confine the sand. Contaminated soil stored in SOLINST core from well SB-6, sample SB-610 from depths 44.3 ft to 44.8 ft was used. The surfactant concentration was increased to 8% by weight and the alcohol concentration was correspondingly increased to 8% by weight. The surfactant was radiolabeled with ^{14}C to measure adsorption by field soil. The soil column length, diameter, porosity and permeability are presented in Table 8.2.

Initial Tracer Test

A suite of tracers was used for estimation of DNAPL already present in the soil column. The tracers used were tritium, 1-pentanol, and 2-ethyl-1-butanol. About 9.6 cc of tracer solution was injected followed by a waterflood at an interstitial velocity of 0.16 m/day (0.08 cc/min). The residence time was 18.2 hours for 1-pentanol and for 2-ethyl-1-butanol it was 28.3 hours. The tracer concentration history is plotted Figure 8.73. The initial tracer test is summarized in Table 8.91. The residual DNAPL saturations based on partitioning tracers are given in Table 8.92. Based on partitioning tracers an average initial DNAPL saturation of 0.082 was estimated.

Surfactant Flood to Remediate DNAPL

The ability of a surfactant/polymer/alcohol solution to remediate contaminated Hill field soil was evaluated in this experiment. The optimal salinity for a surfactant solution containing 8% sodium dihexyl sulfosuccinate, 8% isopropyl alcohol, 500 mg/l xanthan gum mixed in Hill source water at 12.2°C is 5,850 mg/l NaCl. Hence a pre-flush with 110 cc (1.6 pore volumes) of 5,850 mg/l

NaCl was carried out to equilibrate the soil at the desired electrolyte concentration before injecting surfactant. In this phase, 0.5 cc of DNAPL was mobilized. A surfactant solution consisting of 8% by weight sodium dihexyl sulfosuccinate, 8% IPA, 500 mg/l xanthan gum and 5,850 mg/l NaCl in Hill source water was used to remediate the contaminated soil column. A total of 122.3 cc (1.8 pore volumes) of surfactant was injected at an interstitial velocity of 0.3 m/day (0.15 cc/min) followed by flooding with 180 cc (2.6 pore volumes) of 500 mg/l xanthan gum in Hill source water to remove surfactant. Both the partitioning tracer test and the surfactant flood were carried out at 12.2°C by placing the soil column in a water bath. A 0.3 m long coiled stainless steel tubing was used as a heat exchanger for cooling the injected surfactant solution. The surfactant flood is summarized in Table 8.93.

The solubilization parameter of the surfactant solution was 3.8 and this corresponded to a solubilization of 425,000 mg/l in the middle phase microemulsion. The IFT measured for between the microemulsion and excess DNAPL was 0.01 dyne/cm.

A total of 2.25 cc of free phase DNAPL was produced during the surfactant flood. This corresponded to 40.4% of the DNAPL in the soil column. Another 1.6 cc of the DNAPL was solubilized in the microemulsion and produced as dissolved contaminant for a total of 3.85 cc. The contaminant concentration history during the surfactant flood and polymer flood are plotted in Figure 8.75. Since 0.5 cc of DNAPL was produced in the pre-flush, a total of 4.35 cc of DNAPL was recovered from the column. The concentration of the contaminant decreased to less than 10 mg/l after 280 cc (4 pore volumes) of total flooding. The field DNAPL is a

complex mixture with three main components, PCE, TCE and TCA. A surfactant solution containing 8% sodium dihexyl sulfosuccinate and 10,000 mg/l NaCl was used to make stock solutions containing 50,000 mg/l, 40,000 mg/l, 30,000 mg/l, 10,000 mg/l contaminant. By further serial dilution, standards containing 1,000 mg/l, 500 mg/l, 250 mg/l, 125 mg/l and 10 mg/l of Hill contaminant were prepared. These samples were run through a GC and calibration curves corresponding to the TCE peaks were prepared. These standards were used to estimate contaminant concentrations in the effluent samples from the soil column.

Radiolabeled surfactant was used for quantifying surfactant adsorption and surfactant recovery. A comparison of normalized tritium and surfactant concentrations is shown in Figure 8.76. A close overlap between tritium and surfactant concentrations is observed in Figure 8.76. The surfactant concentration was observed to fall below 0.1% concentration after 275 cc (4 pore volumes) of total flooding. This is below the CMC of the surfactant of 0.2 weight %. About 96.0% of the surfactant was recovered compared to 99.0% tritium recovery.

Two differential pressure transducers were used to measure the pressure drop across the soil column during surfactant flooding. Transducer 1 was designed to measure pressure in the range of 0 to 1 psi and transducer 2 was designed to measure pressures in the range of 0 to 5 psi. The pressures were converted into hydraulic gradients and the hydraulic gradient is plotted against the cumulative volume produced in Figure 8.77. The hydraulic gradient at residual DNAPL saturation at the beginning of the test was 0.13. When injection of surfactant was started, the hydraulic gradient increased to 0.25. DNAPL breakthrough was observed at 30 cc (0.4 pore volumes) of total production and the hydraulic gradient

increased to about 0.9 followed by a decline to 0.45 at 50 cc (0.7 pore volumes) of total volume produced. Based on the increased viscosity of polymer, a maximum gradient of about 0.8 was expected. The maximum gradient achieved during DNAPL mobilization during the surfactant flood was about 0.9.

A sudden increase in hydraulic gradient to about 1.6 was observed. Since the column was placed in a water bath and the line connecting the water bath to the fraction collector was at room temperature, the change in the temperature caused phase separation of the microemulsion into excess DNAPL and microemulsion in the line connecting the soil column to the fraction collector. Since the DNAPL is much heavier than the surfactant solution, it was accumulated in the effluent line connecting the soil column to the fraction collector. This is shown in Figure 8.78. Such artifacts which can cause high gradients must be avoided. This accumulation of DNAPL in the line caused a higher hydraulic gradient. At 120 cc (1.7 pore volumes) of total volume produced, the column was briefly removed from the water bath and all the fluid (including the excess DNAPL) in the effluent line was drained. The soil column was placed in the water bath and injection was restarted. At this point the hydraulic gradient was observed to fall below 0.3.

Tracer Test After Surfactant to Estimate Residual DNAPL Saturation

After 1.8 pore volumes of surfactant flooding and 2.6 pore volumes of polymer flooding, a suite of conservative and partitioning tracers was injected into the soil column to estimate the final residual DNAPL saturation. The process of flushing out polymer from a soil column is a very inefficient process. This is because we are trying to flush a more viscous solution using a less viscous fluid. If

water is injected into a medium saturated with polymer, it would finger through and take many pore volumes to completely flush out the polymer. A partitioning tracer experiment conducted under such conditions would give erroneous results as the tracers will not flow through all parts of the porous medium due to viscous fingering. In order to prevent this, tracers were mixed in 500 mg/l xanthan gum in Hill source water. The tracers used were IPA, 2,2-dimethyl-3-pentanol, 1-hexanol and 1-heptanol. A total of 9.0 cc of tracer solution was injected followed by followed by flooding with 500 mg/l xanthan gum in Hill source water at an interstitial velocity of 0.22 m/day (0.11 cc/min). The effluent was analyzed for the alcohols and tritium using a GC and LSC and the residual DNAPL saturation was calculated. The tracer concentration is plotted in Figure 8.79. Negligible delay of the partitioning tracers is observed. An average residual DNAPL saturation of 0.0015 was calculated based on partitioning tracers. This corresponded to a recovery of 98.1% of the DNAPL initially present in the soil column. The final partitioning tracer test is summarized in Table 8.94. The residual DNAPL saturation estimates based on partitioning tracers is given in Table 8.95.

Discussion for Experiment HILLOU2#8

A residence time of 18 hours gave good results from partitioning tracer tests based on results obtained in experiment HILLOU2#8. A residence time of about 6 hours did not give us good results in experiment HILLOU2#5. From these results it can be inferred that a residence time of 18 hours or greater for the partitioning tracers in the field would be likely to give us good results.

The lower temperature in experiment HILLOU2#8 did not pose any problems such as high hydraulic gradients. Hence, it can be concluded that a solution of 8% sodium dihexyl sulfosuccinate, 8% isopropanol, 500 mg/l xanthan gum, 5,850 mg/l NaCl in Hill source water at 12.2°C would be an excellent candidate for use in the SEAR demonstration at Hill AFB. In the first 50 cc of total injection, there was mobilization of DNAPL. The rest of the DNAPL was solubilized as microemulsion and produced. The contaminant concentration in the effluent was observed to fall below 100 mg/l after about 150 cc of total injection (2.2 pore volumes) and to less than 10 mg/l after 280 cc (4.1 pore volumes).

For column HILLOU2#8, 96% of the surfactant was recovered compared to 99% of the tritium. These are the same within experimental error. Based on this and all the previous experiments, it can be concluded that there is negligible adsorption of the surfactant by the field soil. A more detailed discussion of adsorption is given in Chapter 9.

The 1-heptanol is slightly retarded in Figure 8.79. The retardation factors for the partitioning tracers varied between 1.06 and 1.14. Based on the method of moments, an average residual saturation of 0.0015 was computed. Although this is not as quite as good as experiment HILLOU2#7, this is still a good result.

8.6 SUMMARY AND DISCUSSION OF EXPERIMENTS

In this Chapter, partitioning tracer and surfactant flood results from many soil column experiments are presented. These columns are contaminated by PCE, TCE, JP4 and Hill field DNAPL. A comparison of results obtained from this work and results from earlier literature is presented in this section.

Many laboratory soil column studies have been conducted for evaluating the performance of surfactants to remediate NAPL contaminated soils. Ellis *et al.* (1986) recovered between 60.8% and 68% of polychlorinated biphenyls (PCBs), petroleum hydrocarbons and chlorophenols in two soil column experiments using nonionic surfactants. Gannon *et al.* (1989) recovered between 65% and 90% of dichlorobenzene (DCB) and 90% to 95% naphthalene by flushing soil with sodium dodecyl sulfate (SDS). Abdul *et al.* (1990) recovered between 33% and 84% of the automotive transmission fluid (ATF) using surfactants. More studies conducted by Ang and Abdul (1991) demonstrated that 55% and 73% of the ATF could be recovered using alkyl polyoxyethylene glycol after 28 pore volumes of surfactant washing.

Peters *et al.* (1992) screened several surfactant solutions for their effectiveness for remediating diesel fuel from contaminated soil. Total petroleum hydrocarbon (TPH) recoveries ranged from 60%-90%. Similar results were reported by Bourbonais *et al.* (1995).

Surfactant flushing was successfully employed to enhance the recovery of dodecane (Pennell *et al.*, 1993) and PCE (Pennell *et al.*, 1994; Jin, 1995). Between 90% and 99% of the PCE was recovered as a result of surfactant flooding (Pennell *et al.*, 1994; Jin, 1995). Similar results were reported by Shiau *et al.* (1994) and Shiau (1995c) who recovered between 90% and 99% PCE and TCE from contaminated soil columns using both solubilization and mobilization experiments.

In comparison to earlier literature, up to 99.9% of the NAPL has been recovered in several experiments conducted in this work. This is significantly

better than earlier results. This recovery was based on both partitioning tracer results and mass balance measurements. These remarkably high recoveries have been reported for both TCE and Hill DNAPL. In earlier literature, column experiment results with field DNAPL showing recoveries up to 99.9% have not been reported. In addition to high recoveries, many new features about surfactant flooding have been highlighted. Some of these are discussed in the following sections.

8.6.1 Measurement of Hydraulic Gradients

The measurement of pressure drops across the soil column during the surfactant flood is used to quantify surfactant behavior in the porous medium. Surfactant solutions which cause excessive hydraulic gradients are shown to cause problems such as plugging and lowering of permeability and hence are undesirable for use in remediation applications. In this work, surfactants which show low hydraulic gradients during surfactant flooding have been identified. When used in soil column experiments, these surfactants have shown very small permeability reduction and have restored the soil to very nearly its original condition.

8.6.2 Use of Xanthan Gum Polymer

Several column experiments with xanthan gum polymer in this work have shown that surfactant/polymer/alcohol solutions can be used to remediate DNAPL contaminated soil columns. The higher hydraulic gradients during the surfactant flood were consistent with the higher viscosity of the surfactant/polymer/alcohol solutions and no evidence of gels/liquid crystals/emulsions were observed.

8.6.3 Use of Alcohol as a Co-solvent

In this work, alcohols have been used as co-solvents in many soil column experiments. The addition of alcohol as a co-solvent lowered the viscosity of the aqueous surfactant solutions, minimized gels/liquid crystals/emulsions and increased coalescence rates. In the experiments with jet fuel, the addition of alcohol eliminated high hydraulic gradients and plugging of the soil column.

8.6.4 Salinity Gradient

The main premise of using a salinity gradient is that it takes advantage of the favorable properties of the surfactant first at high salinity and then at low salinity. This is done by reducing the polymer flood salinity to below the lower critical salinity at which the phase behavior changes from type III to type I. This causes miscibility between the surfactant and polymer and a more effective flushing of the microemulsion and surfactant from the aquifer. A salinity gradient will also cause lower adsorption of surfactant if it is reversible with salinity. This was used in several soil column experiments in which a surfactant solution at a higher electrolyte concentration was flushed out with a surfactant solution at a lower electrolyte concentration. In experiments POLYTCE#3 and HILLOU2#7, up to 99.9% of the DNAPL was recovered as a result of surfactant flooding using the salinity gradient concept.

Table 8.1: Brief description of column experiment

Experiment	NAPL	Column type	Comments
DW#1	PCE	Glass	Surfactant
DW#2	PCE	Steel	Partitioning tracers and surfactant
DW#3	PCE	Steel	Partitioning tracers and surfactant
OUNAPL1	Hill OU1	Steel	Partitioning tracers
OUNAPL2	Hill OU1	Glass	Partitioning tracers
OUNAPL3	Hill OU1	Glass	Partitioning tracers
DW#5	JP4	Glass	Partitioning tracers and surfactant
JP4#2	JP4	Steel	Partitioning tracers and surfactant
DW#4	TCE	Steel	Partitioning tracers and surfactant
POLYTCE#1	TCE	Glass	Partitioning tracers and surfactant with polymer
POLYTCE#3	TCE	Steel	Partitioning tracers and surfactant
HILLOU2#3	Hill OU2	Glass	Partitioning tracers and surfactant flood
HILLOU2#5	Hill OU2	Glass	Partitioning tracers and radiolabeled surfactant to measure adsorption
HILLOU2#7	Hill OU2	Glass	Partitioning tracers, radiolabeled surfactant with polymer
HILLOU2#8	Hill OU2	Glass	Partitioning tracers, radiolabeled surfactant with polymer at 12.2°C

Table 8.2: Brief description of column properties

Experiment	Length (cm)	Diameter (cm)	Porosity	Permeability (Darcy)
DW#1	13.18	4.80	0.390	5.9
DW#2	30.50	2.21	0.352	15.4
DW#3	30.50	2.21	0.381	7.3
ODNAPL1	30.50	2.21	0.380	7.2
ODNAPL2	9.20	4.80	0.291	7.3
ODNAPL3	10.2	4.80	0.366	8.7
DW#5	15.00	4.80	0.372	7.1
JP4#2	30.50	2.21	0.357	8.8
DW#4	30.50	2.21	0.355	8.3
POLYTCE#1	26.8	4.80	0.347	5.8
POLYTCE#3	75.00	2.21	0.351	6.8
HILLOU2#3	13.70	4.80	0.453	7.1
HILLOU2#5	8.90	4.80	0.420	3.84
HILLOU2#7	21.60	4.80	0.365	5.9
HILLOU2#8	9.8	4.80	0.384	7.7

Table 8.3: Initial tracer test summary for experiment DW#1

Electrolyte Concentration	500 mg/l CaCl ₂
Tracers Used	Tritium
Volume of Tracer Injected	154.4 cc
Injection Rate	4.0 cc/min
Injected Tracer Concentrations	
Tritium	29, 504 DPM/ml
% Tracer Recovered	--
Pore Volume (tracers)	93.0 cc
Pore Volume (volume balance)	87.4 cc

Table 8.4: Flow rates during drainage relative permeability experiments for DW#1.

PCE Flow Rate (cc/min)	Water Flow Rate (cc/min)
0.00	3.30
0.50	2.65
0.85	2.10
1.20	1.60
1.65	1.10
2.10	0.50
2.40	0.00

Table 8.5: Flow rates during imbibition relative permeability experiments for DW#1.

PCE Flow Rate (cc/min)	Water Flow Rate (cc/min)
2.4	0.00
2.20	0.45
1.75	1.00
1.35	1.50
0.90	2.10
0.55	2.65
0.0	3.30

Table 8.6: Drainage relative permeability curve for experiment DW#1.

PCE flow rate (cc/min)	Water flow rate (cc/min)	K _{rw}	K _{ro}	S _w
2.40	0.00	0.0000	0.0637	0.372
2.10	0.50	0.0123	0.0511	0.439
1.65	1.10	0.0264	0.0391	0.499
1.20	1.60	0.0388	0.0288	0.540
0.85	2.10	0.0549	0.0220	0.580
0.50	2.65	0.0784	0.0146	0.630

Table 8.7: Imbibition relative permeability curve for experiment DW#1.

PCE flow rate (cc/min)	Water flow rate (cc/min)	K _{rw}	K _{ro}	S _w
0.00	3.28	0.1782	0.0000	0.774
0.55	2.65	0.0977	0.0201	0.632
0.90	2.20	0.0697	0.0282	0.580
1.50	1.35	0.0361	0.0396	0.531
1.75	1.00	0.0304	0.0526	0.500
2.20	0.45	0.0137	0.0662	0.429
2.40	0.00	0.0000	0.0637	0.372

Table 8.8: Tracer test summary at residual water saturation for experiment DW#1.

Tracers Used	¹⁴ C labeled PCE
Volume of Tracer Injected	26.0 cc
Injection Rate	2.6 cc/min
Injected Tracer Concentrations	
¹⁴ C	8,650 DPM/ml
Residual Water Saturation (tracer)	--
Residual Water Saturation (volume)	0.372

Table 8.9: Tracer test summary at residual PCE saturation for experiment DW#1.

Tracers Used	Tritium
Volume of Tracer Injected	98.0 cc
Injection Rate	3.0 cc/min
Injected Tracer Concentrations	
Tritium	18,916 DPM/ml
Residual PCE Saturation (tracer)	0.226

Table 8.10: Surfactant flood summary for experiment DW#1

Surfactant Used	2% sodium diamyl sulfosuccinate, 2% sodium dioctyl sulfosuccinate, 500 mg/l CaCl ₂ .
Volume of Surfactant Injected	1072.5 cc
Injection Rate	0.3 cc/min
Phase Behavior	Winsor type I
PCE Solubilization	80,000 mg/l
Interfacial tension	0.02 dyn/cm
Volume of PCE Mobilized	16.0 cc
Volume of PCE solubilized	0.4 cc
% PCE recovered	77.9 %
Permeability After Surfactant Flooding	0.9 Darcy
Initial Permeability	5.9 Darcy

Table 8.11: Tracer test summary for first tracer test after surfactant, experiment DW#1.

Tracers Used	Tritium
Volume of Tracer Injected	171.5 cc
Injection Rate	3.1 cc/min
Injected Tracer Concentrations	
Tritium	20,840 DPM/ml
Aqueous pore volume	20.5 cc

Table 8.12: Tracer test summary for second tracer test after surfactant, experiment DW#1.

Tracers Used	Tritium
Volume of Tracer Injected	102.4 cc
Injection Rate	3.1 cc/min
Injected Tracer Concentrations	
Tritium	20,840 DPM/ml
Aqueous pore volume	10.5 cc

Table 8.13: Initial tracer test summary for experiment DW#2.

Electrolyte Concentration	500 mg/l CaCl ₂
Tracers Used	Tritium, IPA, 2,3-Dimethyl-2-butanol.
Volume of Tracer Injected	3.8 cc
Injection Rate	1.0 cc/min
Injected Tracer Concentrations	
Tritium	154,880 DPM/ml
IPA	6,836 mg/l
2,3-Dimethyl-2-butanol	4,342 mg/l
% Tracer Recovered	
Tritium	110.6 %
IPA	107.9 %
2,3-Dimethyl-2-butanol	112.7 %
Pore Volume (tracers)	42.5 cc
Pore Volume (volume balance)	41.2 cc

Table 8.14: Contamination summary, experiment DW#2

Electrolyte Concentration	500 mg/l CaCl ₂
PCE Injection Rate	1.0 cc/min
Volume of PCE Injected	60 cc
Residual Water Saturation	0.323
PCE Relative Permeability at Residual Water Saturation	0.216
Water Injection Rate	1.0 cc/min
Water Relative Permeability at Residual PCE Saturation	0.179

Table 8.15: Tracer test summary at residual PCE saturation for experiment DW#2.

Electrolyte Concentration	1,300 mg/l CaCl ₂
Tracers Used	Tritium, IPA, 2,3-Dimethyl-2-butanol.
Volume of Tracer Injected	3.7 cc
Injection Rate	0.05 cc/min
Injected Tracer Concentrations	
Tritium (K=0.0)	156,868 DPM/ml
IPA (K=0.1)	7,629 mg/l
2,3-Dimethyl-2-butanol (K=2.8)	5,283 mg/l
% Tracer Recovered	
Tritium	103.8 %
IPA	90.7 %
2,3-Dimethyl-2-butanol (23DM2B)	63.5 %

Table 8.16: Residual PCE saturation estimates based on partitioning tracers, experiment DW#2.

Residual PCE saturation (Tritium, 23DM2B)	0.195
Residual PCE saturation (IPA, 23DM2B)	0.175
Residual PCE saturation (volume)	0.197
Residual PCE saturation (mass)	0.202

Table 8.17: Surfactant flood summary for experiment DW#2.

Surfactant Used	2% sodium diamyl sulfosuccinate, 2% sodium dioctyl sulfosuccinate, 1,300 mg/l CaCl ₂
Volume of Surfactant Injected	614.4 cc
Injection Rate	0.05 cc/min
Phase Behavior	Winsor type III
PCE Solubilization	1,000,000 mg/l
Interfacial tension	0.01 dyn/cm
Volume of PCE Mobilized	7.7 cc
Volume of PCE solubilized	0.35 cc
% PCE recovered (material balance)	97.8%
Permeability after Surfactant Flood	1.5 Darcy
Initial Permeability	15.4 Darcy

Table 8.18: Tracer test summary for tracer test after surfactant, experiment DW#2.

Tracers Used	Tritium
Volume of Tracer Injected	4.3 cc
Injection Rate	0.05 cc
Injected Tracer Concentrations	
Tritium	38,337 DPM/ml
Aqueous pore volume	15.4 cc

Table 8.19: Initial tracer test summary for experiment DW#3.

Electrolyte Concentration	500 mg/l NaCl
Tracers Used	Tritium
Volume of Tracer Injected	4.4 cc
Injection Rate	1.0 cc
Injected Tracer Concentrations	
Tritium	171,344 DPM/ml
% Tracer Recovered	
Tritium	113.7%
Pore Volume (tracers)	44.4 cc
Pore Volume (volume balance)	42.8 cc

Table 8.20: Contamination summary, experiment DW#3.

Electrolyte Concentration	500 mg/l NaCl
PCE Injection Rate	1.0 cc/min
Volume of PCE Injected	60 cc
Residual Water Saturation	0.392
PCE Relative Permeability at Residual Water Saturation	0.354
Water Injection Rate	1.0
Water Relative Permeability at Residual PCE Saturation	0.436

Table 8.21: Tracer test summary at residual PCE saturation for experiment DW#3.

Electrolyte Concentration	25,000 mg/l NaCl
Tracers Used	Tritium, IPA and 2,3-Dimethyl-2-butanol
Volume of Tracer Injected	7.4 cc
Injection Rate	0.15 cc/min
Injected Tracer Concentrations	
Tritium (K=0.0)	170,800 DPM/ml
IPA (K=0.1)	4,260 mg/l
2,3-Dimethyl-2-butanol (K=2.8)	2,170 mg/l
% Tracer Recovered	
Tritium	77.5 %
IPA	61.9%
2,3-Dimethyl-2-butanol (23DM2B)	57.1 %

Table 8.22: Residual saturation estimates based on partitioning tracers, experiment DW#3.

Residual PCE saturation (Tritium, 23DM2B)	0.208
Residual PCE saturation (IPA, 23DM2B)	0.205
Residual PCE saturation (volume)	0.174
Residual PCE saturation (mass)	0.181

Table 8.23: Surfactant flood summary for experiment DW#3.

Surfactant Used	4% sodium dihexyl sulfosuccinate, 25,000 mg/l NaCl.
Volume of Surfactant Injected	557.5 cc
Injection Rate	0.06 cc/min for first 2.2 PV, 0.12 cc/min for next 3.3 PV and 0.24 cc/min for the rest.
Phase Behavior	Winsor type I
PCE Solubilization	58,000 mg/l
Interfacial tension	0.14 dyne/cm.
Volume of PCE Mobilized	1.3 cc
Volume of PCE solubilized	3.9
% PCE recovered (material balance)	70.0 %
% PCE recovered (mass balance)	100.5 %
% PCE recovered (tracers)	97.2 %
Permeability after Surfactant Flood	6.9 Darcy
Initial Permeability	7.3 Darcy

Table 8.24: Tracer test summary for tracer test after surfactant, experiment DW#3.

Electrolyte Concentration	1,000 mg/l NaCl
Tracers Used	Tritium, IPA and 2,3-Dimethyl-2-butanol
Volume of Tracer Injected	6.4 cc
Injection Rate	0.15 cc/min
Injected Tracer Concentrations	
Tritium	177,161 DPM/ml
IPA	4,174 mg/l
2,3-Dimethyl-2-butanol	2,174 mg/l
% Tracer Recovered	
Tritium	96.6 %
IPA	84.9 %
2,3-Dimethyl-2-butanol (23DM2B)	59.6 %

Table 8.25: Residual saturation estimates after surfactant based on partitioning tracers, experiment DW#3.

Residual PCE saturation (Tritium, 23DM2B)	0.007
Residual PCE saturation (IPA, 23DM2B)	0.003

Table 8.26: Initial tracer test summary for experiment DW#4.

Electrolyte Concentration	500 mg/l NaCl
Tracers Used	Tritium
Volume of Tracer Injected	4.3 cc
Injection Rate	1.0 cc/min
Injected Tracer Concentrations	
Tritium	213,378 DPM/ml
% Tracer Recovered	103.6 %
Pore Volume (tracer)	43.0 cc
Pore Volume (mass balance)	40.4 cc
Pore Volume (volume balance)	41.4 cc

Table 8.27: Contamination summary, experiment DW#4.

Electrolyte Concentration	500 mg/l NaCl
TCE Injection Rate	1.0
Volume of TCE Injected	80 cc
Residual Water Saturation	0.263
TCE Relative Permeability at Residual Water Saturation	0.286
Water Injection Rate	1.0 cc/min
TCE Saturation (mass balance)	0.175
TCE Saturation (volume balance)	0.179
Water Relative Permeability at Residual TCE Saturation	0.306

Table 8.28: Tracer test summary at residual TCE saturation for experiment DW#4.

Electrolyte Concentration	2,000 mg/l NaCl
Tracers Used	IPA, 2,3-Dimethyl-2-butanol and 2-Methyl-2-hexanol
Volume of Tracer Injected	4.5 cc
Injection Rate	0.15 cc/min
Injected Tracer Concentrations	
IPA	4,784 mg/l
2,3-Dimethyl-2-butanol	4,736 mg/l
2-Methyl-2-hexanol	3,597 mg/l
% Tracer Recovered	
IPA	92.1 %
2,3-Dimethyl-2-butanol	82.2 %
2-Methyl-2-hexanol	70.6 %

Table 8.29: Dynamic partition coefficient estimates based on partitioning tracers, experiment DW#4.

Tracer	Partition Coefficient
2,3-Dimethyl-2-butanol	6.3
2-Methyl-2-hexanol	28.1

Table 8.30: Surfactant flood summary for experiment DW#4.

Surfactant Used	8% sodium dihexyl sulfosuccinate, 2,000 mg/l NaCl
Volume of Surfactant Injected	361.3 cc
Injection Rate	0.13 cc/min
Phase Behavior	Winsor type I
TCE Solubilization	52,000 mg/l
Interfacial tension	0.20 dyne/cm.
Volume of TCE Mobilized	0.3 cc
Volume of TCE solubilized	--
% TCE Recovered (mass balance)	100.0 %
% TCE Recovered (tracers)	96.9 %
Permeability after Surfactant Flood	7.1 Darcy
Initial Permeability	8.3 Darcy

Table 8.31: Tracer test summary for tracer test after surfactant, experiment DW#4.

Electrolyte Concentration	2,000 mg/l NaCl
Tracers Used	IPA, 2,3-Dimethyl-2-butanol and 2-Methyl-2-hexanol
Volume of Tracer Injected	6.4 cc
Injection Rate	0.15 cc/min
Injected Tracer Concentrations	
IPA	5,720 mg/l
2,3-Dimethyl-2-butanol (23DM2B)	4,711 mg/l
2-Methyl-2-hexanol (2M2HX)	5,742 mg/l
% Tracer Recovered	
IPA	94.9 %
2,3-Dimethyl-2-butanol	72.9 %
2-Methyl-2-hexanol	68.5 %

Table 8.32: Residual saturation estimates after surfactant based on partitioning tracers, experiment DW#4.

Residual PCE saturation (IPA, 23DM2B)	0.0029
Residual PCE saturation (2M2HX, 23DM2B)	0.008

Table 8.33: Initial tracer test summary for experiment POLYTCE#1.

Electrolyte Concentration	500 mg/l NaCl
Tracers Used	Tritium
Volume of Tracer Injected	16.4 cc
Injection Rate	3.0 cc/min
Injected Tracer Concentrations	
Tritium	212,470 DPM/ml
% Tracer Recovered	105.1 %
Pore Volume (tracer)	168.4 cc
Pore Volume (mass balance)	168.6 cc

Table 8.34: Contamination summary, experiment POLYTCE#1.

Electrolyte Concentration	500 mg/l NaCl
TCE Injection Rate	3.0 cc/min
Volume of TCE Injected	200 cc
Residual Water Saturation	0.325
TCE Relative Permeability at Residual Water Saturation	0.178
Water Injection Rate	3.0 cc/min
Water Relative Permeability at Residual TCE Saturation	0.295

Table 8.35: Tracer test summary at residual TCE saturation for experiment POLYTCE#1.

Electrolyte Concentration	4,000 mg/l NaCl
Tracers Used	Tritium (K=0.0), IPA (K=0.1), 2,3-Dimethyl-2-butanol (K=6.3) and 2-Methyl-2-hexanol (K=28.1)
Volume of Tracer Injected	16.7 cc
Injection Rate	0.80 cc/min
Injected Tracer Concentrations	
Tritium (0.0)	213,692 DPM/ml
IPA (0.1)	3,206 mg/l
2,3-Dimethyl-2-butanol (6.3)	2,980 mg/l
2-Methyl-2-hexanol (28.1)	3,071 mg/l
% Tracer Recovered	
Tritium	100.8 %
IPA	120.3 %
2,3-Dimethyl-2-butanol (23DM2B)	134.8 %
2-Methyl-2-hexanol (2M2HX)	107.1 %

Table 8.36: Residual TCE saturation estimates based on partitioning tracers, experiment POLYTCE#1.

Residual TCE Saturation (tritium, 23DM2B)	0.196
Residual TCE Saturation (IPA, 23DM2B)	0.197
Residual TCE Saturation (tritium, 2M2HX)	0.202
Residual TCE Saturation (IPA, 2M2HX)	0.202
Residual TCE Saturation (mass balance)	0.198
Residual TCE Saturation (volume balance)	0.193

Table 8.37: Surfactant flood summary for experiment POLYTCE#1.

Surfactant Used	4% sodium dihexyl sulfosuccinate, 8% IPA, 4,000 mg/l NaCl
Volume of Surfactant Injected	2003.9 cc
Post Surfactant Polymer Flood	330 cc of 500 ppm xanthan gum, 500 mg/l NaCl
Post Surfactant Water Flood	5,900 cc of 500 mg/l NaCl
Injection Rate	0.80 cc/min
Phase Behavior	Winsor type I
TCE Solubilization	32,000 mg/l
Interfacial tension	0.19 dyne/cm.
Volume of TCE Mobilized	< 0.1 cc
Volume of TCE solubilized	--
% TCE Recovered (mass balance)	101.2 %
% TCE Recovered (tracers)	99.9 %
Permeability after Surfactant Flood	4.9 Darcy
Initial Permeability	5.8 Darcy

Table 8.38: Tracer test summary for tracer test after surfactant, experiment POLYTCE#1.

Electrolyte Concentration	4,000 mg/l NaCl
Tracers Used	Tritium (K=0.0), IPA (K=0.1), 2,3-Dimethyl-2-butanol (K=6.3) and 2-Methyl-2-hexanol (K=28.1)
Volume of Tracer Injected	17.5 cc
Injection Rate	0.80 cc/min
Injected Tracer Concentrations	
Tritium (0.0)	213,692 DPM/ml
IPA (0.1)	2,795 mg/l
2,3-Dimethyl-2-butanol (K=6.3)	2,407 mg/l
2-Methyl-2-hexanol (K=28.1)	2,475 mg/l
% Tracer Recovered	
Tritium	99.1 %
IPA	107.4 %
2,3-Dimethyl-2-butanol (23DM2B)	115.3 %
2-Methyl-2-hexanol (2M2HX)	115.3 %

Table 8.39: Residual saturation estimates after surfactant based on partitioning tracers, experiment POLYTCE#1.

Residual TCE Saturation (tritium, 23DM2B)	0.00036
Residual TCE Saturation (IPA, 23DM2B)	0.00010
Residual TCE Saturation (tritium, 2M2HX)	0.00013
Residual TCE Saturation (IPA, 2M2HX)	0.00005

Table 8.40: Initial tracer test summary for experiment POLYTCE#3.

Electrolyte Concentration	500 mg/l NaCl
Tracers Used	Tritium
Volume of Tracer Injected	11.7 cc
Injection Rate	1.6 cc/min
Injected Tracer Concentrations	
Tritium	66,779 DPM/ml
% Tracer Recovered	106.1 %
Pore Volume (tracer)	103.4 cc
Pore Volume (mass balance)	101.1 cc

Table 8.41: Contamination summary, experiment POLYTCE#3.

Electrolyte Concentration	500 mg/l NaCl
TCE Injection Rate	1.0
Volume of TCE Injected	120 cc
Residual Water Saturation	0.314
TCE Relative Permeability at Residual Water Saturation	0.351
Water Injection Rate	1.0 cc/min
Water Relative Permeability at Residual TCE Saturation	0.491

Table 8.42: Tracer test summary at residual TCE saturation for experiment POLYTCE#3.

Electrolyte Concentration	9,350 mg/l NaCl
Tracers Used	Tritium
Volume of Tracer Injected	12.1 cc
Injection Rate	1.5 cc/min
Injected Tracer Concentrations	
Tritium	66,779 DPM/ml
% Tracer Recovered	
Tritium	106.3 %

Table 8.43: Residual saturation estimates based on tritium tracer, experiment POLYTCE#3.

Residual TCE Saturation (tritium)	0.165
Residual TCE Saturation (mass balance)	0.163

Table 8.44: Surfactant flood summary for experiment POLYTCE#3.

Surfactant Used	4% sodium dihexyl sulfosuccinate, 8% IPA, 9,350 mg/l NaCl
Volume of Surfactant Injected	102 cc
Post Surfactant Flood	4% sodium dihexyl sulfosuccinate, 8% IPA, 500 mg/l NaCl
Post Surfactant Water Flood	200 cc of 500 mg/l NaCl
Injection Rate	0.13 cc/min
Phase Behavior	Winsor type III
TCE Solubilization	516,000 mg/l
Interfacial tension	0.02 dyne/cm.
Volume of TCE Mobilized	16.1 cc
Volume of TCE solubilized	0.6 cc
% TCE Recovered (mass balance)	100.0 %
% TCE Recovered (tracers)	99.8 %
Permeability after Surfactant Flood	6.2 Darcy
Initial Permeability	6.8 Darcy

Table 8.45: Tracer test summary for tracer test after surfactant, experiment POLYTCE#3.

Electrolyte Concentration	500 mg/l NaCl
Tracers Used	Ethanol, 2,3-Dimethyl-2-butanol and 3-Methyl-3-hexanol
Volume of Tracer Injected	10.7 cc
Injection Rate	0.22 cc/min
Injected Tracer Concentrations	
Ethanol (K=0.1)	1,212 mg/l
2,3-Dimethyl-2-butanol (K=6.3)	1,129 mg/l
3-Methyl-3-hexanol (K=27.9)	1,134 mg/l
% Tracer Recovered	
Ethanol (Eth)	82.6 %
2,3-Dimethyl-2-butanol (23DM2B)	94.7 %
3-Methyl-3-hexanol (3M3HX)	98.5 %

Table 8.46: Residual saturation estimates after surfactant based on partitioning tracers, experiment POLYTCE#3.

Residual TCE Saturation (Eth, 23DM2B)	0.00036
Residual TCE Saturation (Eth, 3M3HX)	0.00013

Table 8.47: Initial tracer test summary for experiment OUDNAPL1.

Electrolyte Concentration	500 mg/l NaCl
Tracers Used	IPA, 2,3-Dimethyl-2-butanol and 2-Methyl-2-hexanol
Volume of Tracer Injected	4.7 cc
Injection Rate	1.0 cc/min
Injected Tracer Concentrations	
IPA (K=0.0)	4,992 mg/l
2,3-Dimethyl-2-butanol	4,906 mg/l
2-Methyl-2-hexanol	4,899 mg/l
% Tracer Recovered	
IPA	94.2 %
2,3-Dimethyl-2-butanol	88.3 %
2-Methyl-2-hexanol	94.6 %
Average Pore Volume (tracers)	45.2 cc
Pore Volume (volume balance)	42.7 cc
Pore Volume (mass balance)	43.0 cc

Table 8.48: Contamination summary, experiment OUDNAPL1.

Electrolyte Concentration	500 mg/l NaCl
NAPL Injection Rate	1.0 cc/min
Volume of NAPL Injected	65 cc
Residual Water Saturation	0.126
Water Injection Rate	1.0 cc/min

Table 8.49: First tracer test summary at residual NAPL saturation for experiment OUDNAPL1.

Electrolyte Concentration	1,000 mg/l NaCl
Tracers Used	IPA, 2,3-Dimethyl-2-butanol and 2-Methyl-2-hexanol
Volume of Tracer Injected	6.1 cc
Injection Rate	0.24 cc/min
Injected Tracer Concentrations	
IPA (K=0.0)	5,625 mg/l
2,3-Dimethyl-2-butanol	6,055 mg/l
2-Methyl-2-hexanol	5,955 mg/l
% Tracer Recovered	
IPA	87.5 %
2,3-Dimethyl-2-butanol	93.9 %
2-Methyl-2-hexanol	78.3 %

Table 8.50: Dynamic partition coefficient estimates based on first set of partitioning tracers, experiment OUDNAPL1.

Tracer	Partition Coefficient
2,3-Dimethyl-2-butanol	1.3
2-Methyl-2-hexanol	5.8

Table 8.51: Second tracer test summary at residual NAPL saturation for experiment OUDNAPL1.

Electrolyte Concentration	1,000 mg/l NaCl
Tracers Used	IPA, 2,3-Dimethyl-2-butanol and 2-Methyl-2-hexanol
Volume of Tracer Injected	8.4 cc
Injection Rate	0.24 cc/min
Injected Tracer Concentrations	
Ethanol	2,394 mg/l
2-Methyl-2-pentanol (2,115 mg/l
2,2-Dimethyl-3-pentanol	2,080 mg/l
3-Methyl-2-hexanol	1,530 mg/l
% Tracer Recovered	
Ethanol	86.5 %
2-Methyl-2-pentanol	97.0 %
2,2-Dimethyl-3-pentanol	108.2 %
3-Methyl-2-hexanol	53.0 %

Table 8.52: Dynamic partition coefficient estimates based on second set of partitioning tracers, experiment OUDNAPL1.

Tracer	Partition Coefficient
2-Methyl-2-pentanol	1.3
2,2-Dimethyl-3-pentanol	10.0
3-Methyl-2-hexanol	12.9

Table 8.53: Comparison of partition coefficients from static partition coefficient tests and column experiments.

Alcohol	Static K	Dynamic K
2,3-Dimethyl-2-butanol	1.5	1.3
2-Methyl-2-pentanol	1.3	1.3
2-Methyl-2-hexanol	6.0	5.8
3-Methyl-2-hexanol	12.8	10.0
2,2-Dimethyl-3-pentanol	12.9	12.9

Table 8.54: First tracer test summary at residual NAPL saturation for experiment OUDNAPL2.

Electrolyte Concentration	1,000 mg/l NaCl
Tracers Used	Tritium, Ethanol, 2,3-Dimethyl-2-butanol, 2-Methyl-2-hexanol and 3-Methyl-2-hexanol
Volume of Tracer Injected	6.1 cc
Injection Rate	0.2 cc/min
Injected Tracer Concentrations	
Tritium (K=0.0)	167,786 DPM/ml
Ethanol (K=0.0)	3,127 mg/l
2,3-Dimethyl-2-butanol (K=1.3)	3,431 mg/l
2-Methyl-2-hexanol (K=5.8)	3,051 mg/l
3-Methyl-2-hexanol (K=10.0)	2,626 mg/l
% Tracer Recovered	
Tritium (Tr)	107.7 %
Ethanol (Eth)	79.9 %
2,3-Dimethyl-2-butanol (23DM2B)	73.2 %
2-Methyl-2-hexanol (2M2HX)	78.0 %
3-Methyl-2-hexanol (3M2HX)	62.7 %
Average Pore Volume (tracers)	50.4 cc

Table 8.55: Residual saturation estimates based on first set of partitioning tracers, experiment OUDNAPL2.

Residual NAPL Saturation (Eth, 23DM2B)	0.042
Residual NAPL Saturation (Eth, 2M2HX)	0.041
Residual NAPL Saturation (Eth, 3M2HX)	0.042
Residual NAPL Saturation (Tr, 23DM2B)	-0.025
Residual NAPL Saturation (Tr, 2M2HX)	0.023
Residual NAPL Saturation (Tr, 3M2HX)	0.031
Average NAPL Saturation	0.035

Table 8.56: Second tracer test summary at residual NAPL saturation for experiment OUDNAPL2.

Electrolyte Concentration	1,000 mg/l NaCl
Tracers Used	Tritium, Ethanol, 2,3-Dimethyl-2-butanol, 2-Methyl-2-hexanol and 3-Methyl-2-hexanol
Volume of Tracer Injected	6.1 cc
Injection Rate	0.2 cc/min
Injected Tracer Concentrations	
Tritium (K=0.0)	167,786 DPM/ml
Ethanol (K=0.0)	3,292 mg/l
2,3-Dimethyl-2-butanol (K=1.3)	3,417 mg/l
2-Methyl-2-hexanol (K=5.8)	3,056 mg/l
3-Methyl-2-hexanol (K=10.0)	2,276 mg/l
% Tracer Recovered	
Tritium (Tr)	87.8 %
Ethanol (Eth)	73.2 %
2,3-Dimethyl-2-butanol (23DM2B)	89.2 %
2-Methyl-2-hexanol (2M2HX)	73.1 %
3-Methyl-2-hexanol (3M2HX)	57.4 %

Table 8.57: Residual saturation estimates based on second set of partitioning tracers, experiment OUDNAPL2.

Residual NAPL Saturation (Eth, 23DM2B)	0.085
Residual NAPL Saturation (Eth, 2M2HX)	0.061
Residual NAPL Saturation (Eth, 3M2HX)	0.066
Residual NAPL Saturation (Tr, 23DM2B)	0.006
Residual NAPL Saturation (Tr, 2M2HX)	0.039
Residual NAPL Saturation (Tr, 3M2HX)	0.051
Average NAPL Saturation	0.060
Expected NAPL Saturation	0.067

Table 8.58: First tracer test summary at residual NAPL saturation for experiment OUDNAPL3.

Electrolyte Concentration	1,000 mg/l NaCl
Tracers Used	Tritium, Ethanol, 1-Hexanol and 2,2-Dimethyl-3-pentanol
Volume of Tracer Injected	7.0 cc
Injection Rate	0.2 cc/min
Injected Tracer Concentrations	
Tritium (K=0.0)	137,085 DPM/ml
Ethanol (K=0.0)	2,636 mg/l
1-Hexanol (K=4.4)	2,335 mg/l
2,2-Dimethyl-3-pentanol (K=12.9)	2,421 mg/l
% Tracer Recovered	
Tritium (Tr)	88.0 %
Ethanol (Eth)	84.8 %
1-Hexanol (1Hex)	80.0 %
2,2-Dimethyl-3-pentanol (22DM3P)	66.6 %

Table 8.59: Residual saturation estimates based on first set of partitioning tracers, experiment OUDNAPL3.

Residual NAPL Saturation (Eth, 1Hex)	0.073
Residual NAPL Saturation (Eth, 22DM3P)	0.058
Residual NAPL Saturation (Tr, 1Hex)	0.065
Residual NAPL Saturation (Tr, 22DM3P)	0.055
Average NAPL Saturation	0.063
Average Pore Volume (tracers)	68.3 cc

Table 8.60: Second tracer test summary at residual NAPL saturation for experiment OUDNAPL3.

Electrolyte Concentration	1,000 mg/l NaCl
Tracers Used	Tritium, Ethanol, 1-Hexanol and 2,2-Dimethyl-3-pentanol
Volume of Tracer Injected	6.3 cc
Injection Rate	0.2 cc/min
Injected Tracer Concentrations	
Tritium (K=0.0)	137,085 DPM/ml
Ethanol (K=0.0)	2,636 mg/l
1-Hexanol (K=4.4)	2,335 mg/l
2,2-Dimethyl-3-pentanol (K=12.9)	2,421 mg/l
% Tracer Recovered	
Tritium (Tr)	100.2 %
Ethanol (Eth)	92.4 %
1-Hexanol (1Hex)	95.6 %
2,2-Dimethyl-3-pentanol (22DM3P)	104.4 %

Table 8.61: Residual saturation estimates based on first set of partitioning tracers, experiment OUDNAPL3.

Residual NAPL Saturation (Eth, 1Hex)	0.067
Residual NAPL Saturation (Eth, 22DM3P)	0.059
Residual NAPL Saturation (Tr, 1Hex)	0.062
Residual NAPL Saturation (Tr, 22DM3P)	0.057
Average NAPL Saturation	0.061
Average Pore Volume (tracers)	67.6 cc

Table 8.62: Initial tracer test summary for experiment DW#5.

Electrolyte Concentration	500 mg/l NaCl
Tracers Used	IPA, 2,3-Dimethyl-2-butanol and 2-Methyl-2-hexanol
Volume of Tracer Injected	18.3 cc
Injection Rate	1.6 cc/min
Injected Tracer Concentrations	
IPA	5,004 mg/l
2,3-Dimethyl-2-butanol	4,977 mg/l
2-Methyl-2-hexanol	5,626 mg/l
% Tracer Recovered	
IPA	91.9 %
2,3-Dimethyl-2-butanol	92.2 %
2-Methyl-2-hexanol	91.4 %
Pore Volume (tracers)	100.0 cc
Pore Volume (mass balance)	101.1 cc
Pore Volume (volume balance)	101.0 cc

Table 8.63: Contamination summary, experiment DW#5

Electrolyte Concentration	500 mg/l NaCl
JP4 Injection Rate	3.0 cc/min
Volume of JP4 Injected	120 cc
Residual Water Saturation	0.506
JP4 Relative Permeability at Residual Water Saturation	0.181
Water Injection Rate	3.0 cc/min
Water Relative Permeability at Residual JP4 Saturation	0.231

Table 8.64: Tracer test summary at residual JP4 saturation for experiment DW#5.

Electrolyte Concentration	6,000 mg/l NaCl
Tracers Used	IPA, 2,3-Dimethyl-2-butanol and 2-Methyl-2-hexanol
Volume of Tracer Injected	17.5 cc
Injection Rate	0.58 cc/min
Injected Tracer Concentrations	
IPA (K=0.0)	4,857 mg/l
2,3-Dimethyl-2-butanol (K=1.7)	4,671 mg/l
2-Methyl-2-hexanol (K=7.8)	4,922 mg/l
% Tracer Recovered	
IPA	103.1 %
2,3-Dimethyl-2-butanol (23DM2B)	95.3 %
2-Methyl-2-hexanol (2M2HX)	101.9 %

Table 8.65: Residual saturation estimates based on partitioning tracers, experiment DW#5

Residual NAPL Saturation (IPA, 23DM2B)	0.175
Residual NAPL Saturation (IPA, 2M2HX)	0.182
Residual NAPL Saturation (mass balance)	0.163
Residual NAPL Saturation (volume balance)	0.166

Table 8.66: Surfactant flood summary for experiment DW#5.

Surfactant Used	0.6% sodium dioctyl sulfosuccinate, 1.4% sodium dihexyl sulfosuccinate, 2% secondary butyl alcohol and 6,000 mg/l NaCl
Volume of Surfactant Injected	296.2 cc
Post Surfactant Water Flood	500 cc of 250 mg/l NaCl
Injection Rate	0.56 cc/min
Phase Behavior	Winsor type I
JP4 Solubilization	45,000 mg/l
Volume of JP4 Mobilized	9.3 cc
Volume of JP4 solubilized	--
% JP4 Recovered (mass balance)	117.0 %
% TCE Recovered (tracers)	--
Permeability after Surfactant Flood	--
Initial Permeability	6.8 Darcy

Table 8.67: Tracer test summary for tracer test after surfactant, experiment DW#5.

Electrolyte Concentration	250 mg/l NaCl
Tracers Used	Ethanol, 2,2-Dimethyl-3-pentanol and 1-Hexanol
Volume of Tracer Injected	13.1 cc
Injection Rate	0.56 cc/min
Injected Tracer Concentrations	
Ethanol (K=0.0)	2,973 mg/l
2,2-Dimethyl-3-pentanol (19.2)	2,556 mg/l
1-Hexanol (K=4.0)	2,540 mg/l
Aqueous Pore Volume	8 cc

Table 8.68: Initial tracer test summary for experiment JP4#2.

Electrolyte Concentration	500 mg/l NaCl
Tracers Used	Tritium
Volume of Tracer Injected	4.7 cc
Injection Rate	1.0 cc/min
Injected Tracer Concentrations	
Tritium	141,970 DPM/mg/l
% Tracer Recovered	
Tritium	100.1 %
Average Pore Volume (tracers)	41.8 cc
Pore Volume (mass balance)	41.4 cc

Table 8.69: Contamination summary, experiment JP4#2.

Electrolyte Concentration	500 mg/l NaCl
NAPL Injection Rate	1.0 cc/min
Volume of JP4 Injected	70 cc
Residual Water Saturation	0.338
JP4 Relative Permeability at Residual Water Saturation	0.178
Water Injection Rate	1.0 cc/min
Water Relative Permeability at Residual JP4 Saturation	0.281
Residual JP4 Saturation (mass balance)	0.151

Table 8.70: Tracer test summary at residual JP4 saturation for experiment JP4#2.

Electrolyte Concentration	11,700 mg/l NaCl, 1,300 mg/l CaCl ₂
Tracers Used	Ethanol, 2,3-Dimethyl-3-pentanol and 2-Methyl-3-pentanol
Volume of Tracer Injected	4.9 cc
Injection Rate	0.20 cc/min
Injected Tracer Concentrations	
Ethanol (K=0.0)	12,557 mg/l
2,3-Dimethyl-3-pentanol (K=8.2)	3,237 mg/l
2-Methyl-3-pentanol (K=4.3)	3,193 mg/l
% Tracer Recovered	
Ethanol (Eth)	129.9 %
2,3-Dimethyl-3-pentanol (23DM3P)	106.1 %
2-Methyl-3-pentanol (2M3P)	106.7 %

Table 8.71: Residual saturation estimates based on partitioning tracers, experiment JP4#2.

Residual JP4 saturation (Eth, 23DM3P)	0.142
Residual JP4 saturation (Eth, 2M3P)	0.177
Residual JP4 saturation (volume)	0.155
Residual JP4 saturation (mass)	0.151

Table 8.72: Surfactant flood summary for experiment JP4#2.

Surfactant Used	2% sodium dihexyl sulfosuccinate, 2% sodium dioctyl sulfosuccinate, 8% secondary butyl alcohol and 11,700 mg/l NaCl and 1,300 mg/l CaCl ₂
Volume of Surfactant Injected	242.0 cc
Second Surfactant Injection	2% sodium dihexyl sulfosuccinate, 8% secondary butyl alcohol and 500 mg/l NaCl
Injection Rate	0.16 cc/min
Phase Behavior	Winsor type III
JP4 Solubilization	230,000 mg/l
Volume of JP4 Mobilized	4.9 cc
Volume of JP4 produced as middle phase microemulsion	0.8 cc
Residual JP4 Saturation after Surfactant (mass balance)	0.023
Residual JP4 Saturation after Surfactant (tracers)	0.035
Permeability after Surfactant Flood	6.9 Darcy
Initial Permeability	7.3 Darcy

Table 8.73: Tracer test summary for tracer test after surfactant, experiment JP4#2.

Electrolyte Concentration	500 mg/l NaCl
Tracers Used	Ethanol, 2,3-Dimethyl-3-pentanol and 2-Methyl-3-pentanol
Volume of Tracer Injected	4.6 cc
Injection Rate	0.20 cc/min
Injected Tracer Concentrations	
Ethanol (K=0.0)	12,767 mg/l
2,3-Dimethyl-3-pentanol (K=8.2)	3,219 mg/l
2-Methyl-3-pentanol (K=4.3)	3,196 mg/l
% Tracer Recovered	
Ethanol (Eth)	116.4 %
2,3-Dimethyl-3-pentanol (23DM3P)	119.7 %
2-Methyl-3-pentanol (2M3P)	108.1 %

Table 8.74: Residual saturation estimates after surfactant based on partitioning tracers, experiment JP4#2.

Residual JP4 saturation (Eth, 23DM3P)	0.041
Residual JP4 saturation (Eth, 2M3P)	0.029
Residual JP4 saturation (mass)	0.027

Table 8.75: Initial tracer test summary for experiment HILLOU2#3.

Electrolyte Concentration	Hill Ground Water
Tracers Used	Tritium, IPA, 3-Methyl-3-pentanol, 1-Hexanol and 2,2-Dimethyl-3-pentanol
Volume of Tracer Injected	6.3 cc
Injection Rate	0.35 cc/min
Injected Tracer Concentrations	
Tritium	72,084 DPM/mg/l
IPA (K=0.1)	2,446 mg/l
3-Methyl-3-pentanol (K=6.2)	2,253 mg/l
1-Hexanol (K=30.2)	1,670 mg/l
2,2-Dimethyl-3-pentanol (K=68.3)	1,679 mg/l
% Tracer Recovered	
Tritium (Tr)	94.2 %
IPA	91.2 %
3-Methyl-3-pentanol (3M3P)	87.3 %
1-Hexanol (1Hex)	90.1 %
2,2-Dimethyl-3-pentanol (22DM3P)	94.2 %
Average Pore Volume (tracers)	113.7 cc

Table 8.76: Residual saturation estimates based on partitioning tracers, experiment HILLOU2#3.

Residual Hill DNAPL saturation (Tr, 3M3P)	0.022
Residual Hill DNAPL saturation (Tr, 22DM3P)	0.006
Residual Hill DNAPL saturation (Tr, 1Hex)	0.001
Residual Hill DNAPL saturation (IPA, 3M3P)	0.026
Residual Hill DNAPL saturation (IPA, 22DM3P)	0.007
Residual Hill DNAPL saturation (IPA, 1Hex)	0.001
Average Saturation (tracers)	0.011

Table 8.77: Surfactant flood summary for experiment HILLOU2#3.

Surfactant Used	5% sodium diamyl sulfosuccinate in Hill source water.
Volume of Surfactant Injected	148.8 cc
Post Surfactant Injection	120.0 cc of Hill source water
Injection Rate	0.24 cc/min
Phase Behavior	Winsor type I
Contaminant Solubilization	5,000 mg/l
Interfacial tension	0.40 dyne/cm.

Table 8.78: Tracer test summary at residual DNAPL saturation for experiment HILLOU2#5.

Electrolyte Concentration	Hill source water
Tracers Used	Tritium, 1-Pentanol and 2-Ethyl-1-butanol
Volume of Tracer Injected	9.5 cc
Injection Rate	0.35 cc/min
Injected Tracer Concentrations	
Tritium (K=0.0)	78,713 DPM/ml
1-Pentanol (K=3.9)	1,835 mg/l
2-Ethyl-1-butanol (K=12.5)	1,734 mg/l
% Tracer Recovered	
Tritium (Tr)	93.9 %
1-Pentanol (1Pent)	95.5 %
2-Ethyl-1-butanol (2E1B)	76.3 %
Average Pore Volume (tracers)	55.3 cc

Table 8.79: Residual DNAPL saturation estimates based on partitioning tracers, experiment HILLOU2#5.

Residual DNAPL Saturation (Tr, 1Pent)	0.147
Residual DNAPL Saturation (Tr, 2E1B)	0.111

Table 8.80: Surfactant flood summary for first surfactant flood, experiment HILLOU2#5.

Surfactant Used	4% sodium dihexyl sulfosuccinate in Hill source water
Volume of Surfactant Injected	25.9 cc
Tritium Concentration in Surfactant	133,587 DPM/ml
¹⁴ C Concentration in Surfactant	18,830 DPM/ml
% Surfactant Recovered	92.5 %
% Tritium Recovered	105.7
Post Surfactant Waterflood	150 cc of Hill source water
Injection Rate	0.50 cc/min
Phase Behavior	Winsor type I
Contaminant Solubilization	16,000 mg/l
Interfacial tension	0.20 dyne/cm.
Volume of DNAPL Mobilized	5.4 cc

Table 8.81: Surfactant flood summary for second surfactant flood, experiment HILLOU2#5.

Surfactant Used	4% sodium dihexyl sulfosuccinate, 10,600 mg/l NaCl, 500 ppm xanthan gum in Hill source water
Volume of Surfactant Injected	125.9 cc
Post Surfactant Flood	100 cc of 150 mg/l NaCl and 150 cc of 150 mg/l CaCl ₂
Injection Rate	0.50 cc/min
Phase Behavior	Winsor type III
Contaminant Solubilization	500,000 mg/l
Volume of DNAPL Mobilized	6.8 cc
% DNAPL Recovered (tracers)	98.2%

Table 8.82: Tracer test summary for tracer test after surfactant, experiment HILLOU2#5.

Electrolyte Concentration	Hill source water
Tracers Used	Tritium, 3-Methyl-3-pentanol, 2,2-Dimethyl-3-pentanol and 1-Hexanol
Volume of Tracer Injected	9.1 cc
Injection Rate	0.34 cc/min
Injected Tracer Concentrations	
Tritium	89,991 DPM/ml
3-Methyl-3-pentanol (K=6.2)	1,835 mg/l
2,2-Dimethyl-3-pentanol (K=68.3)	1,985 mg/l
1-Hexanol (30.2)	2,084 mg/l
% Tracer Recovered	
Tritium (Tr)	82.6 %
3-Methyl-3-pentanol (3M3P)	111.6 %
2,2-Dimethyl-3-pentanol (22DM3P)	97.8 %
1-Hexanol (1Hex)	97.8 %

Table 8.83: Residual saturation estimates after surfactant based on partitioning tracers, experiment HILLOU2#5.

Residual DNAPL Saturation (Tr, 3M3P)	0.0029
Residual DNAPL Saturation (Tr, 22DM3P)	0.0069
Residual DNAPL Saturation (Tr, 1Hex)	0.0066

Table 8.84: Initial tracer test summary for experiment HILLOU2#7.

Electrolyte Concentration	Hill Groundwater
Tracers Used	Tritium, IPA, 3-Methyl-3-pentanol, 2,2-Dimethyl-3-pentanol and 1-Hexanol
Volume of Tracer Injected	18.2 cc
Injection Rate	0.12 cc/min
Injected Tracer Concentrations	
Tritium	71,340 DPM/ml
IPA	2,442 mg/l
3-Methyl-3-pentanol	2,179 mg/l
2,2-Dimethyl-3-pentanol	1,404 mg/l
1-Hexanol	1,625 mg/l
% Tracer Recovered	
Tritium	106.2 %
IPA	106.9 %
3-Methyl-3-pentanol (K=6.2)	104.7 %
2,2-Dimethyl-3-pentanol (68.3)	100.1 %
1-Hexanol (K=30.2)	109.3 %
Pore Volume Tracers	142.7 cc

Table 8.85: Contamination summary, experiment HILLOU2#7.

Electrolyte Concentration	Hill Groundwater
DNAPL Injection Rate	3.0 cc/min
Volume of DNAPL Injected	180 cc
Residual Water Saturation	0.506
DNAPL Relative Permeability at Residual Water Saturation	0.118
Water Injection Rate	9.0 cc/min
Water Relative Permeability at Residual DNAPL Saturation	0.109

Table 8.86: Tracer test summary at residual DNAPL saturation for experiment HILLOU2#7.

Electrolyte Concentration	Hill Groundwater
Tracers Used	Tritium and 1-Pentanol
Volume of Tracer Injected	29.2 cc
Injection Rate	0.08 cc/min
Injected Tracer Concentrations	
Tritium (K=0.0)	84,688 DPM/ml
1-Pentanol (K=3.9)	3,325 mg/l
% Tracer Recovered	
Tritium (Tr)	95.7 %
1-Pentanol (1Pent)	71.7 %

Table 8.87: Residual DNAPL saturation estimates based on partitioning tracers, experiment HILLOU2#7.

Residual DNAPL saturation (Tr, 1Pent)	0.255
Residual DNAPL saturation (Tr)	0.262
Residual DNAPL saturation (volume)	0.254
Residual DNAPL saturation (mass)	0.261

Table 8.88: Surfactant flood summary, experiment HILLOU2#7.

Surfactant Used	4% sodium dihexyl sulfosuccinate, 4% IPA, 11,250 mg/l NaCl and 500 ppm xanthan gum in Hill source water
Volume of Surfactant Injected	300.7 cc
Tritium Concentration in Surfactant	8,604 DPM/ml
¹⁴ C Concentration in Surfactant	13,027 DPM/ml
% Surfactant Recovered	101.6 %
% Tritium Recovered	103.1 %
Post Surfactant Flood	377.3 cc of 500 ppm santhan gum in Hill source water
Injection Rate	0.25 cc/min for first 150 cc and 0.5 cc/min for rest of the test.
Phase Behavior	Winsor type III
Contaminant Solubilization	600,000 mg/l
Interfacial tension	0.01 dyne/cm.
Volume of DNAPL Mobilized	26.8 cc
% DNAPL Recovered (material balance)	98.4%
% DNAPL Recovered (mass balance)	100.4%
% DNAPL Recovered (tracers)	99.9%
Permeability after Surfactant Flood	4.5 Darcy
Initial Permeability	5.9 Darcy

Table 8.89: Tracer test summary for tracer test after surfactant, experiment HILLOU2#7.

Electrolyte Concentration	Hill source water
Tracers Used	Tritium, 2,2-Dimethyl-3-pentanol, 1-Hexanol and 1-Heptanol
Volume of Tracer Injected	14.6 cc
Injection Rate	0.14 cc/min
Injected Tracer Concentrations	
Tritium (K=0.0)	164,536 DPM/ml
2,2-Dimethyl-3-pentanol (K=68.3)	2,002 mg/l
1-Hexanol (K=30.2)	2,000 mg/l
1-Heptanol (K=140.5)	1,000 mg/l
% Tracer Recovered	
Tritium (Tr)	105.0 %
2,2-Dimethyl-3-pentanol (22DM3P)	71.7 %
1-Hexanol (1Hex)	84.8 %
1-Heptanol (1Hept)	87.4 %

Table 8.90: Residual saturation estimates after surfactant based on partitioning tracers, experiment HILLOU2#7.

Residual DNAPL Saturation (Tr, 22DM3P)	0.00016
Residual DNAPL Saturation (Tr, 1Hex)	0.00013
Residual DNAPL Saturation (Tr, 1Hept)	0.00020

Table 8.91: Tracer test summary at residual DNAPL saturation for experiment HILLOU2#8.

Electrolyte Concentration	Hill source water
Tracers Used	Tritium, 1-Pentanol and 2-Ethyl-1-butanol
Volume of Tracer Injected	9.6 cc
Injection Rate	0.08 cc/min
Injected Tracer Concentrations	
Tritium	75,132 DPM/ml
1-Pentanol (K=3.9)	4,144 mg/l
2-Ethyl-1-butanol (K=12.5)	3,964 mg/l
% Tracer Recovered	
Tritium (Tr)	109.9 %
1-Pentanol (1Pent)	117.7 %
2-Ethyl-1-butanol (2E1B)	97.1 %
Average Pore Volume (tracers)	68.2 cc

Table 8.92: Residual DNAPL saturation estimates based on partitioning tracers, experiment HILLOU2#8.

Residual TCE Saturation (Tr, 1Pent)	0.078
Residual TCE Saturation (Tr, 2E1B)	0.085

Table 8.93: Surfactant flood summary, experiment HILLOU2#8.

Surfactant Used	8% sodium dihexyl sulfosuccinate, 8% IPA, 5,850 mg/l NaCl and 500 ppm xanthan gum in Hill source water and 285.2 K.
Volume of Surfactant Injected	122.3 cc
Tritium Concentration in Surfactant	59,705 DPM/ml
¹⁴ C Concentration in Surfactant	38,346 DPM/ml
% Surfactant Recovered	96.0 %
% Tritium Recovered	99.0 %
Post Surfactant Flood	180 cc of 500 ppm santhan gum in Hill source water
Injection Rate	0.15 cc/min
Phase Behavior	Winsor type III
Contaminant Solubilization	425,000 mg/l
Interfacial tension	0.01 dyne/cm.
Volume of DNAPL Mobilized	2.25 cc
% DNAPL Recovered (tracers)	98.1%
Permeability after Surfactant Flood	7.7 Darcy
Permeability at Residual DNAPL saturation	0.7 Darcy

Table 8.94: Tracer test summary for tracer test after surfactant, experiment HILLOU2#8.

Electrolyte Concentration	Hill source water
Tracers Used	IPA, 2,2-Dimethyl-3-pentanol, 1-Hexanol and 1-Heptanol
Volume of Tracer Injected	8.0 cc
Injection Rate	0.11 cc/min
Injected Tracer Concentrations	
IPA	2,718 mg/l
2,2-Dimethyl-3-pentanol	2,350 mg/l
1-Hexanol	2,055 mg/l
1-Heptanol	1,375 mg/l
% Tracer Recovered	
IPA	110.7 %
2,2-Dimethyl-3-pentanol (22DM3P)	92.4 %
1-Hexanol (1Hex)	101.7 %
1-Heptanol (1Hept)	121.4%

Table 8.95: Residual saturation estimates after surfactant based on partitioning tracers, experiment HILLOU2#8.

Residual DNAPL Saturation (IPA, 22DM3P)	0.0012
Residual DNAPL Saturation (IPA, 1Hex)	0.0023
Residual DNAPL Saturation (IPA, 1Hept)	0.0010

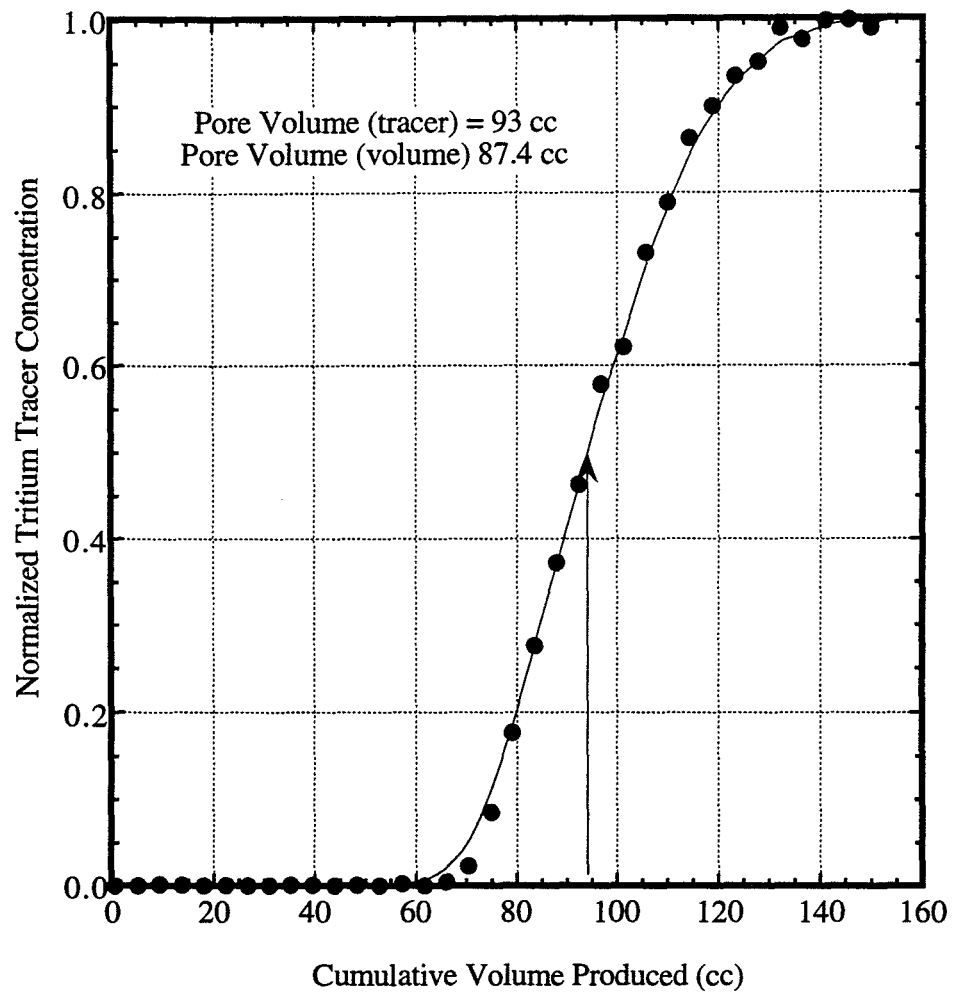


Figure 8.1: Initial tracer concentration history, experiment DW#1.

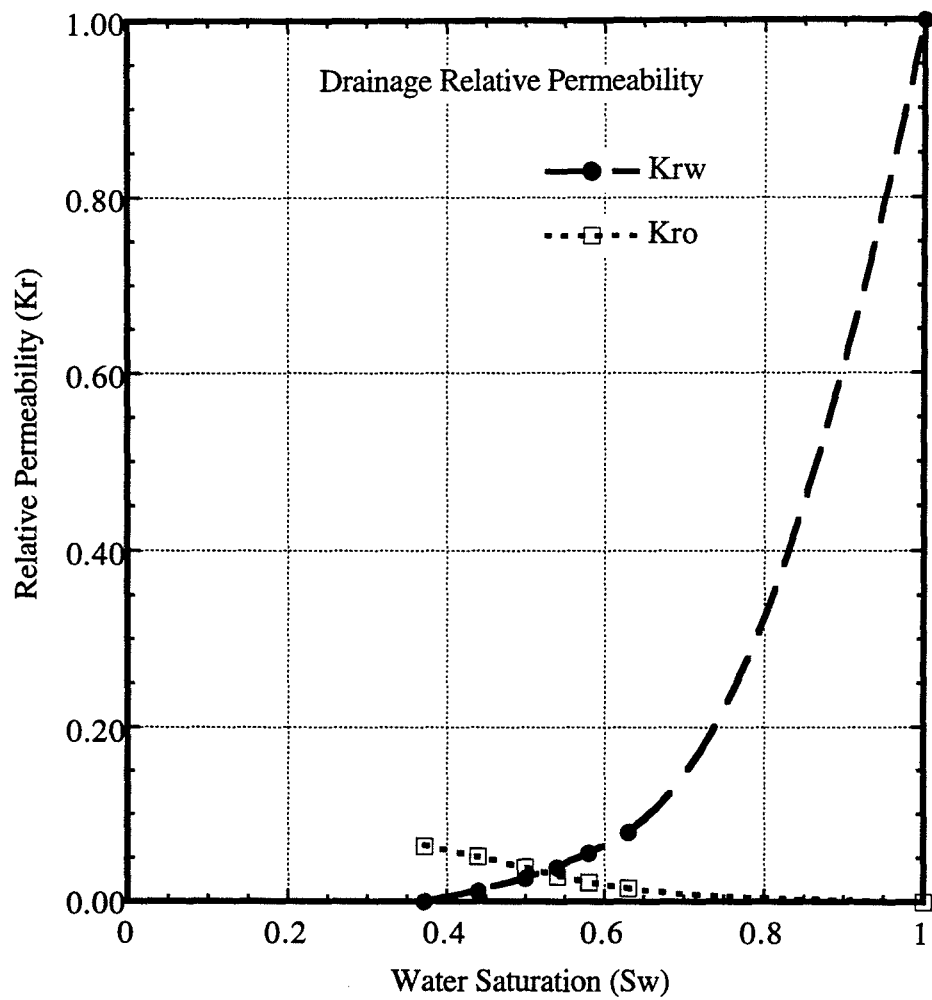


Figure 8.2: Drainage relative permeability curve for PCE and water, experiment DW#1.

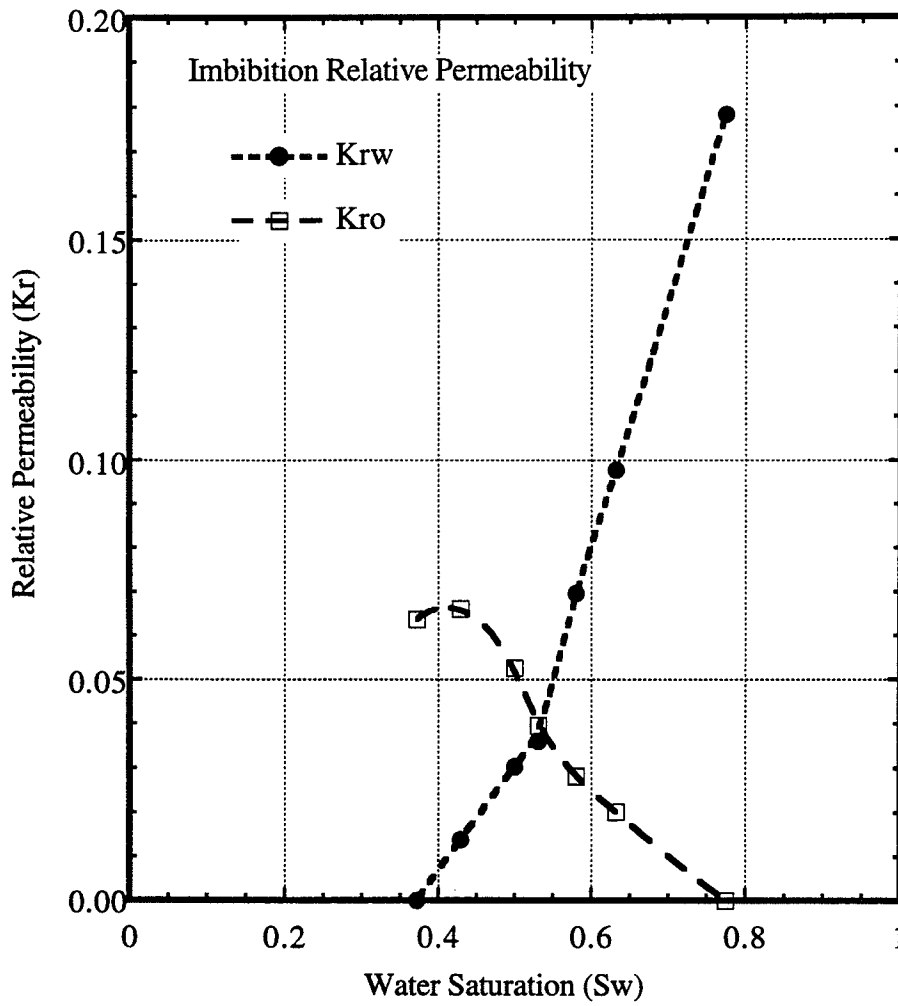


Figure 8.3: Imbibition relative permeability curve for PCE and water, experiment DW#1.

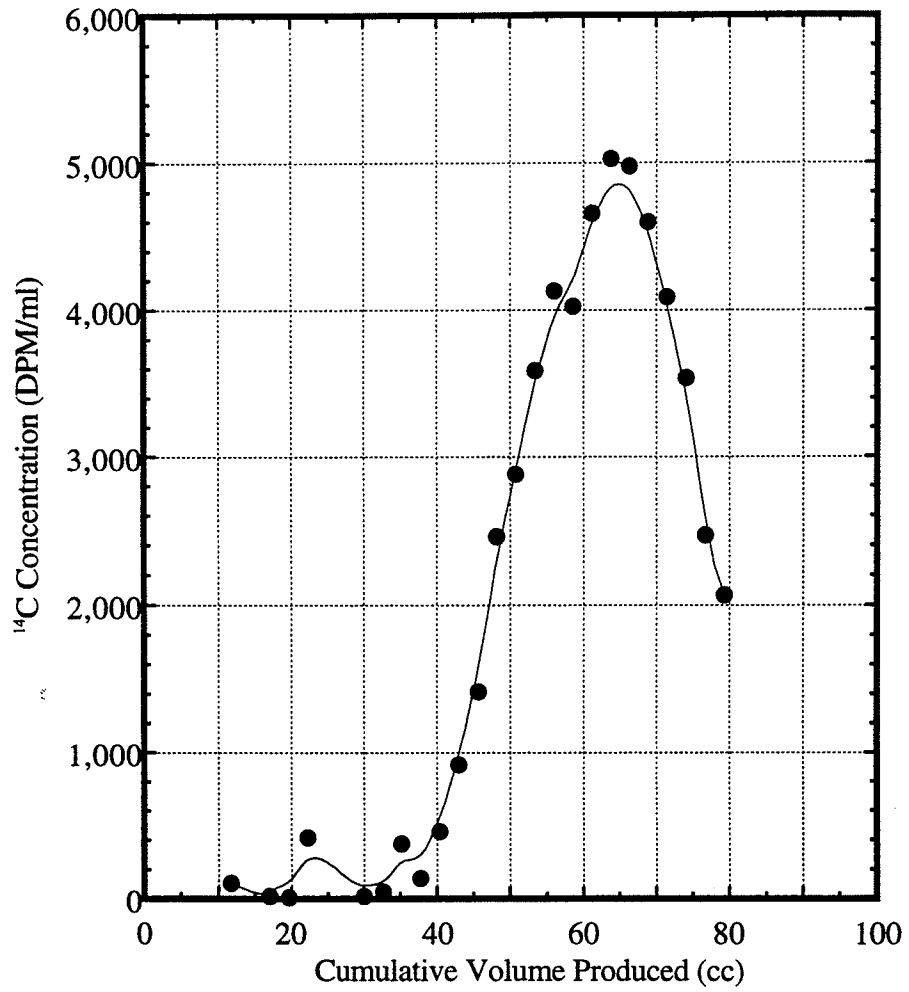


Figure 8.4: Tracer concentration history for PCE tracer test at residual water saturation, experiment DW#1.

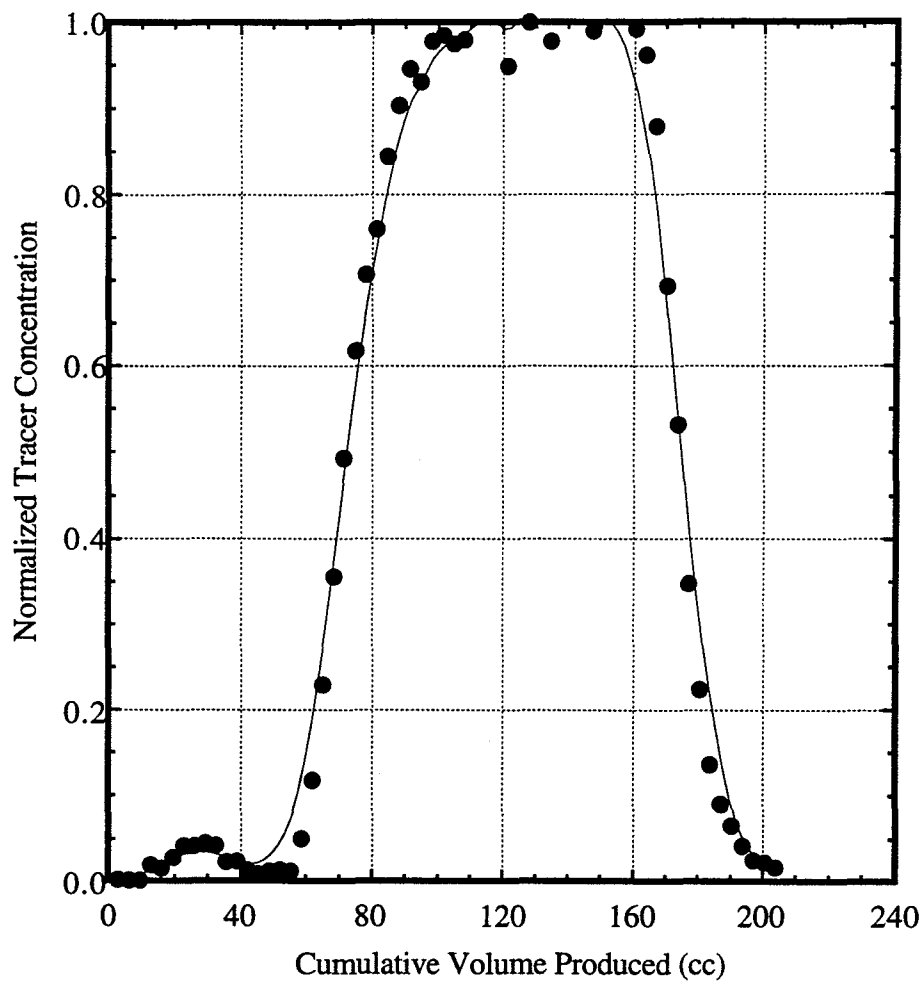


Figure 8.5: Tracer concentration history at residual PCE saturation, experiment DW#1.

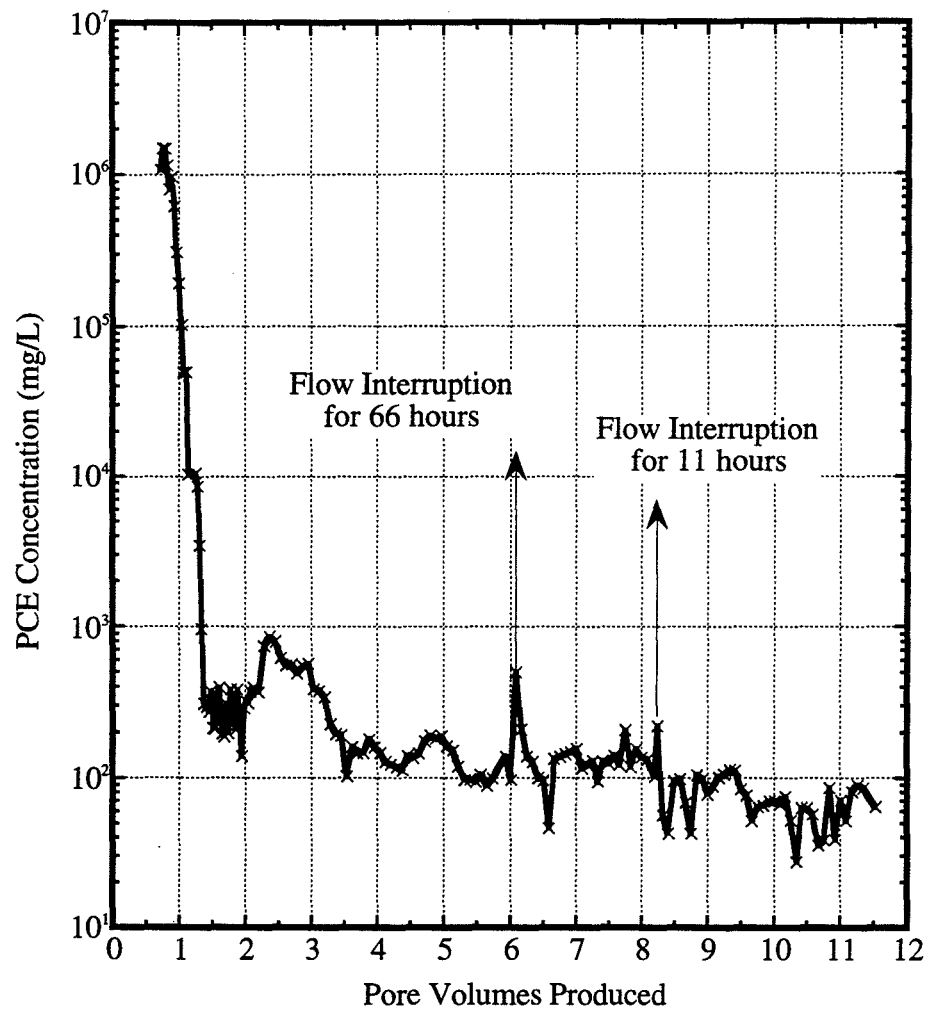


Figure 8.6: PCE concentration in effluent during surfactant flushing, experiment DW#1.

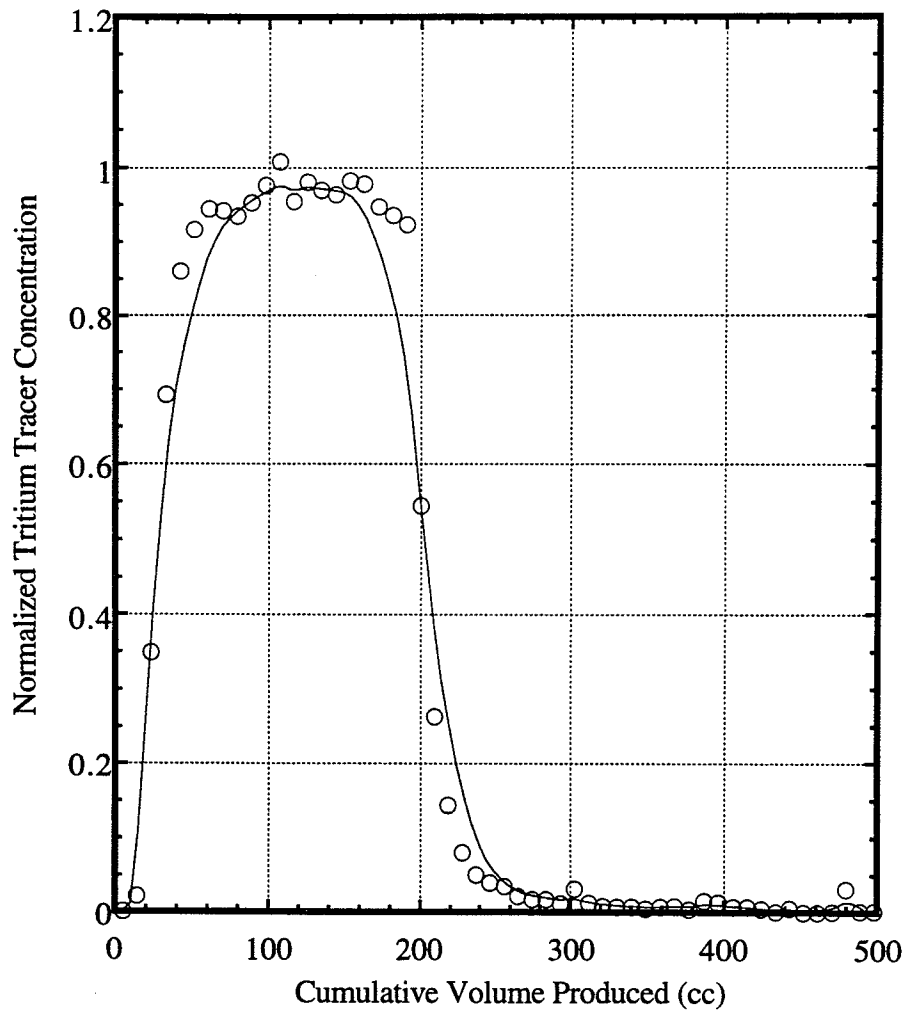


Figure 8.7: Final tracer concentration history for first set of tracers after surfactant, experiment DW#1.

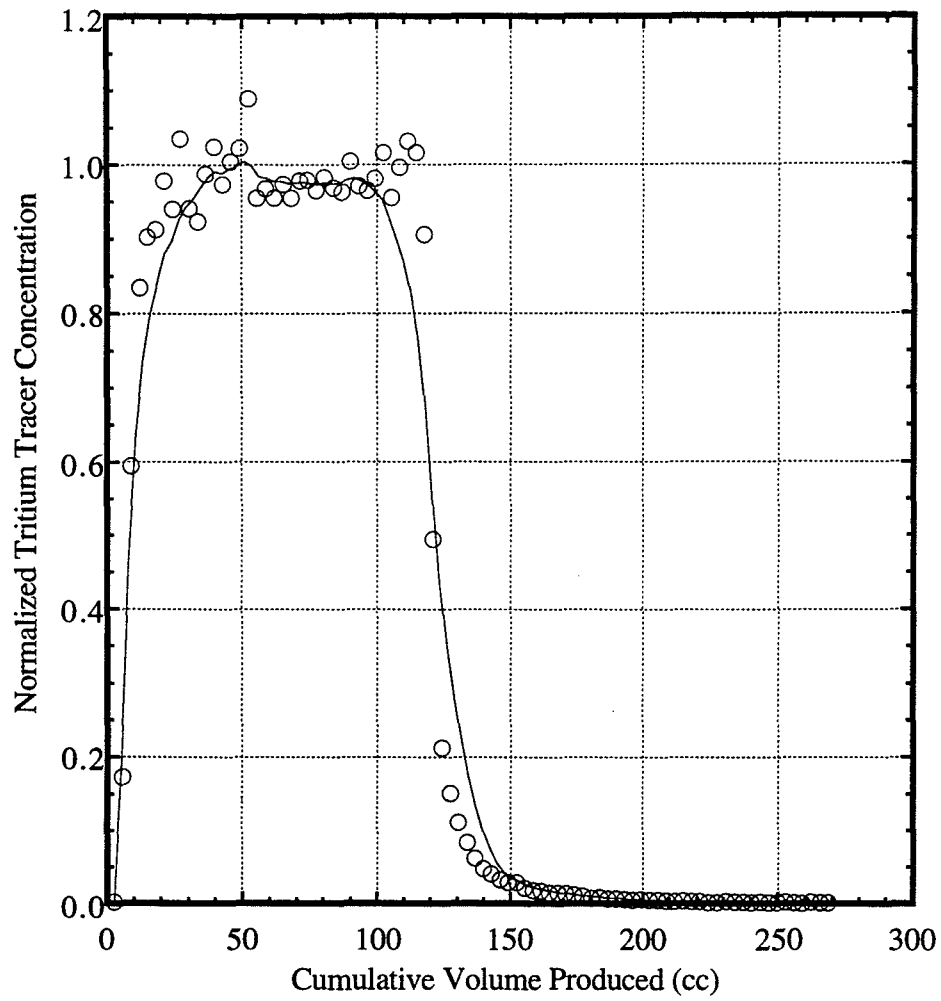


Figure 8.8 Final tracer concentration history for second set of tracers after surfactant, experiment DW#1.

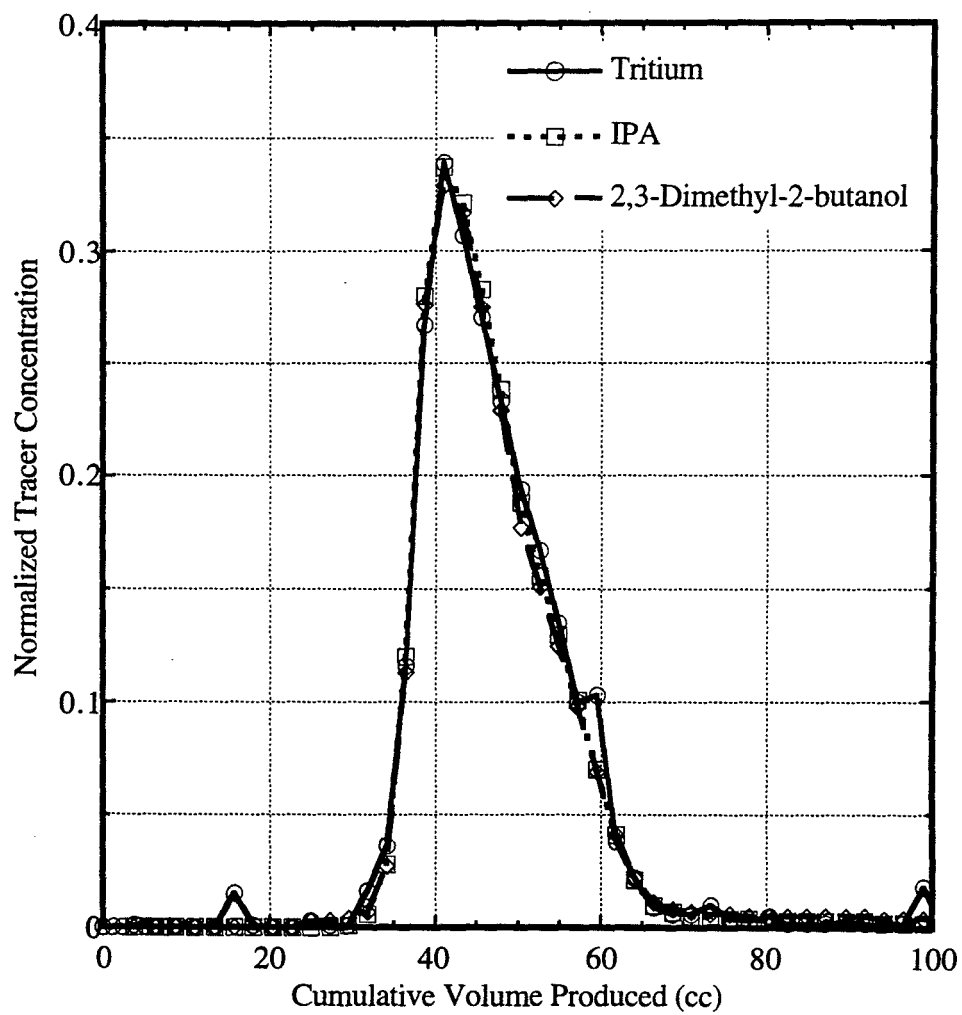


Figure 8.9 Initial tracer concentration histories, experiment DW#2.

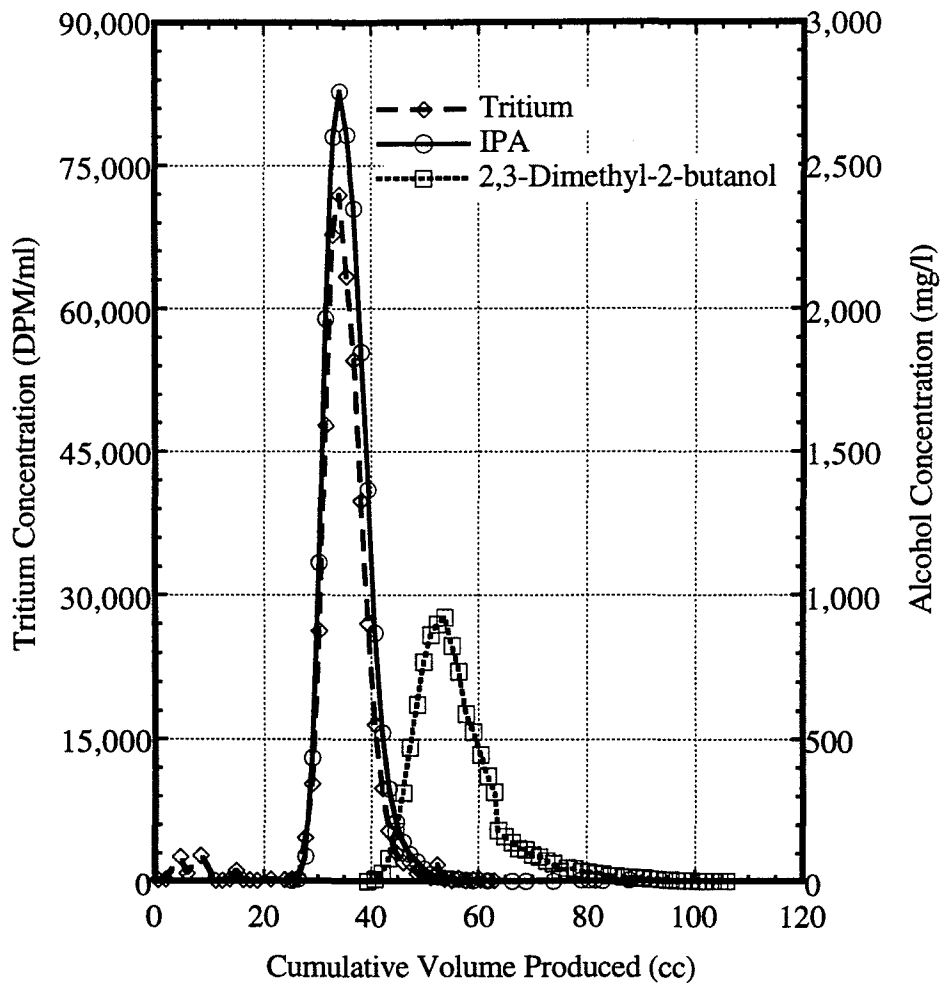


Figure 8.10 Tracer concentration histories at residual PCE saturation, experiment DW#2.

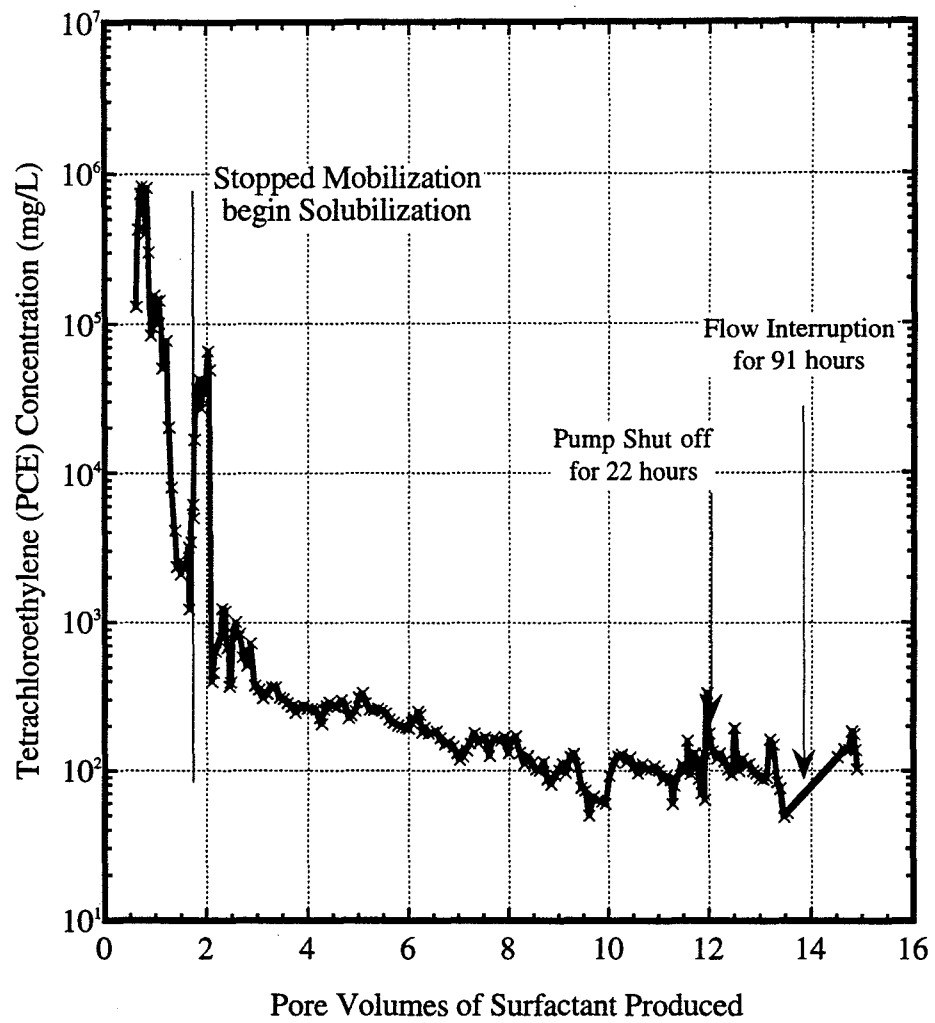


Figure 8.11: PCE concentration in effluent during surfactant flushing, experiment DW#2.

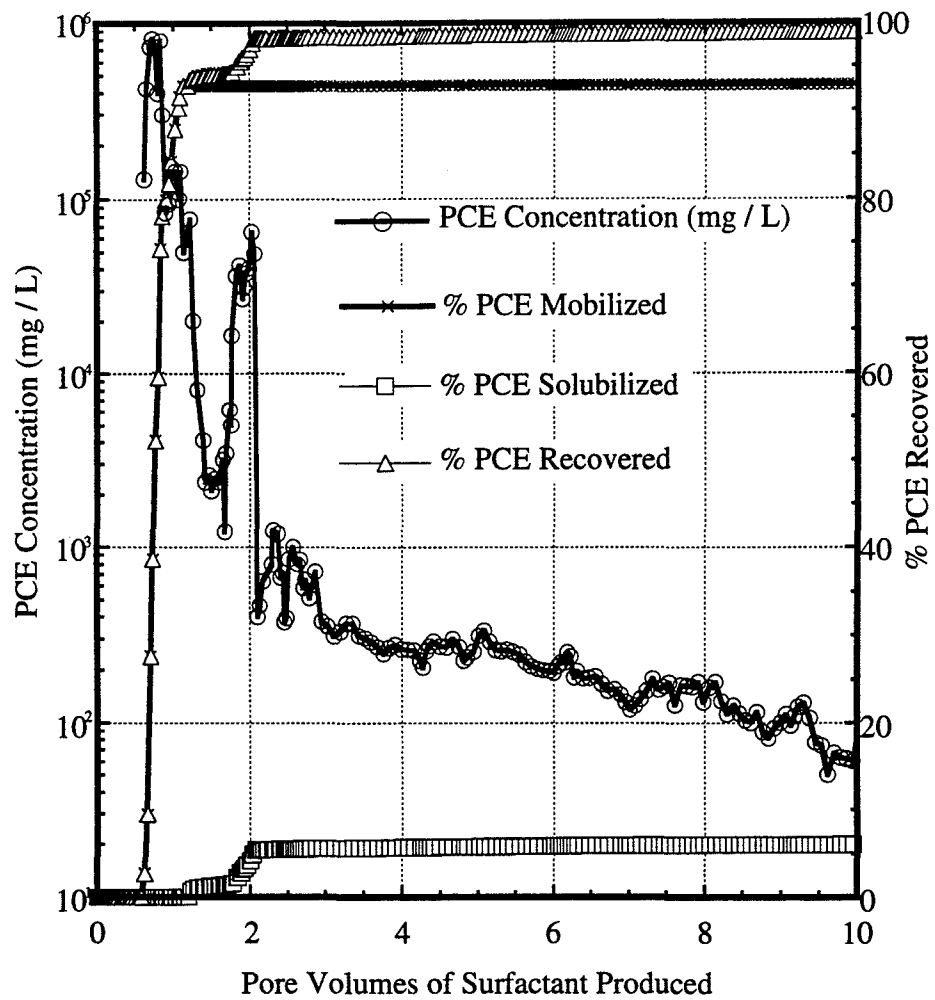


Figure 8.12: Plot showing PCE recovery mechanisms during surfactant flushing, experiment DW#2.

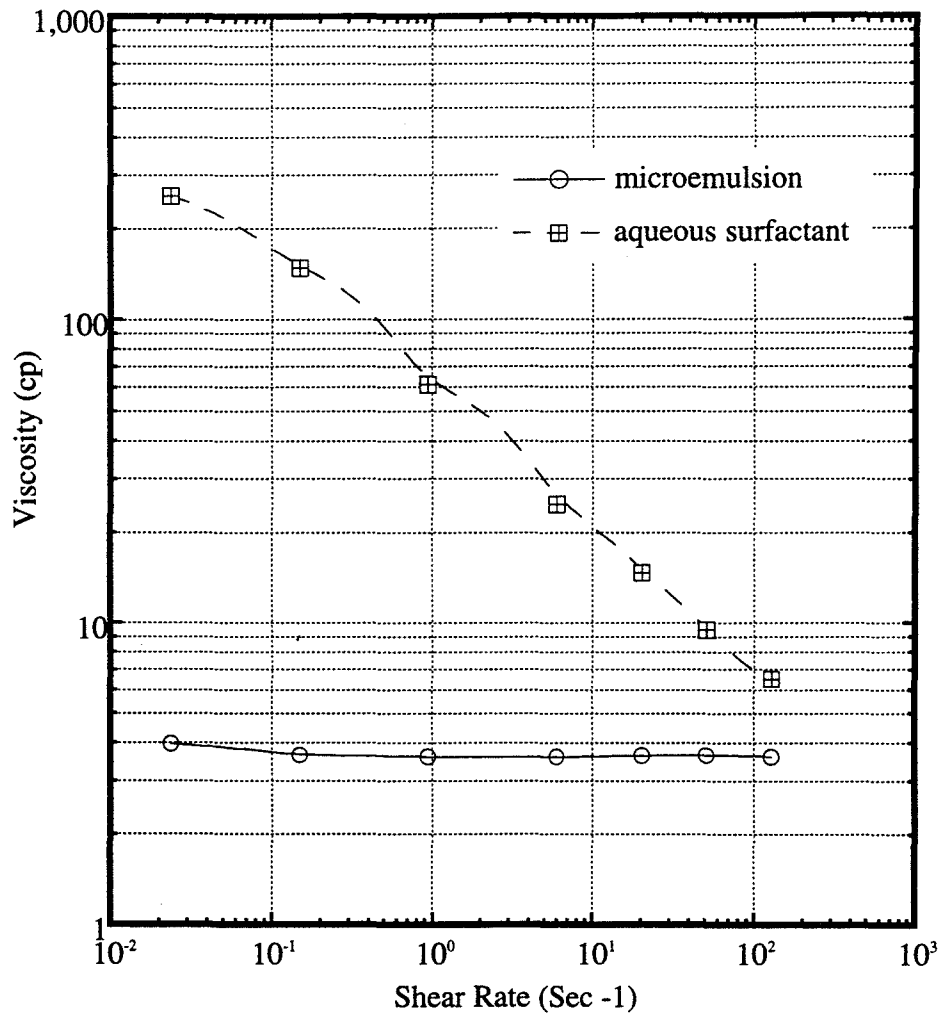


Figure 8.13: Viscosities of aqueous surfactant solution and middle phase microemulsion, experiment DW#2.

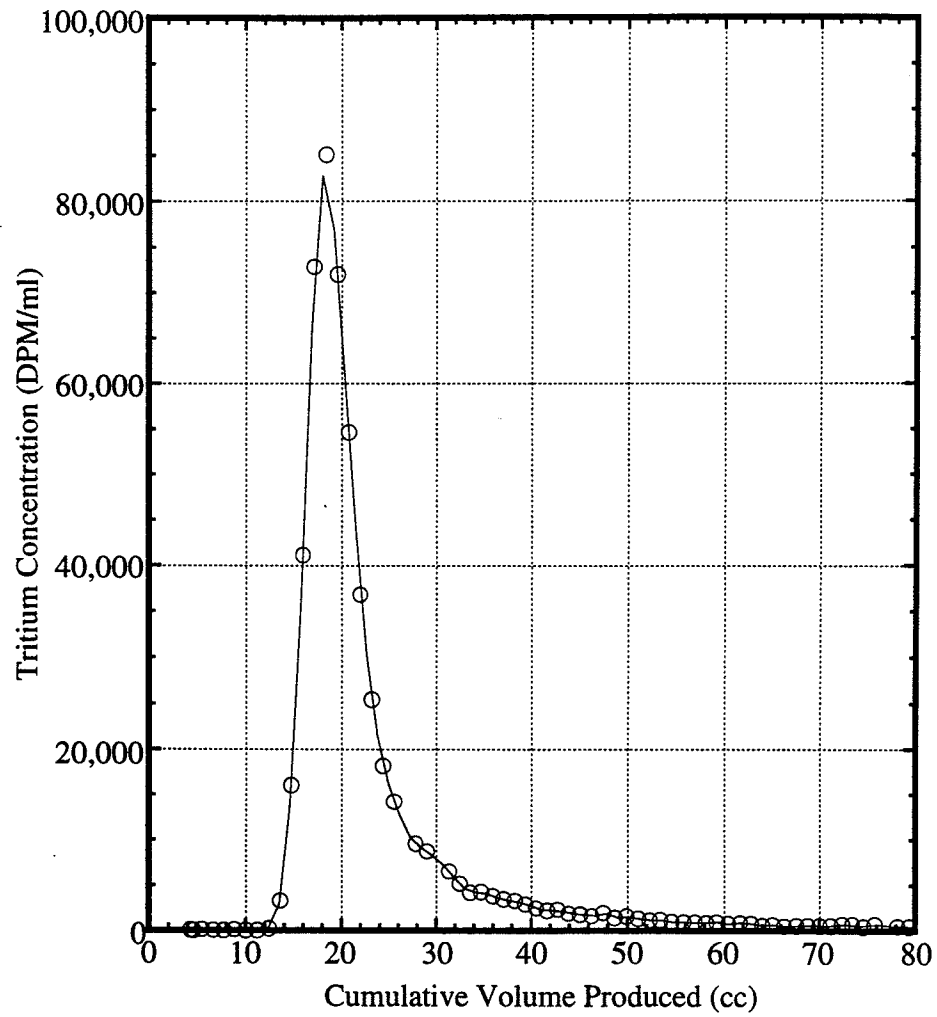


Figure 8.14: Final tracer concentration history, experiment DW#2.

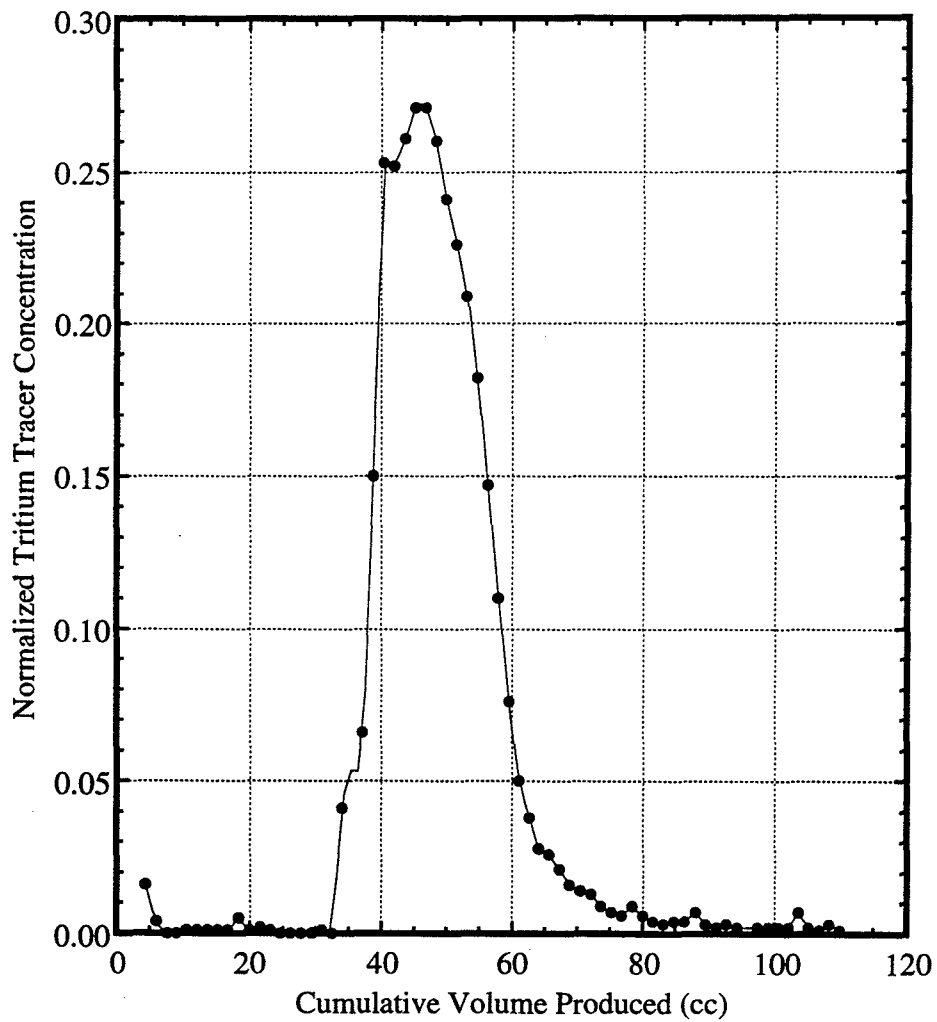


Figure 8.15: Initial tracer concentration history, experiment DW#3.

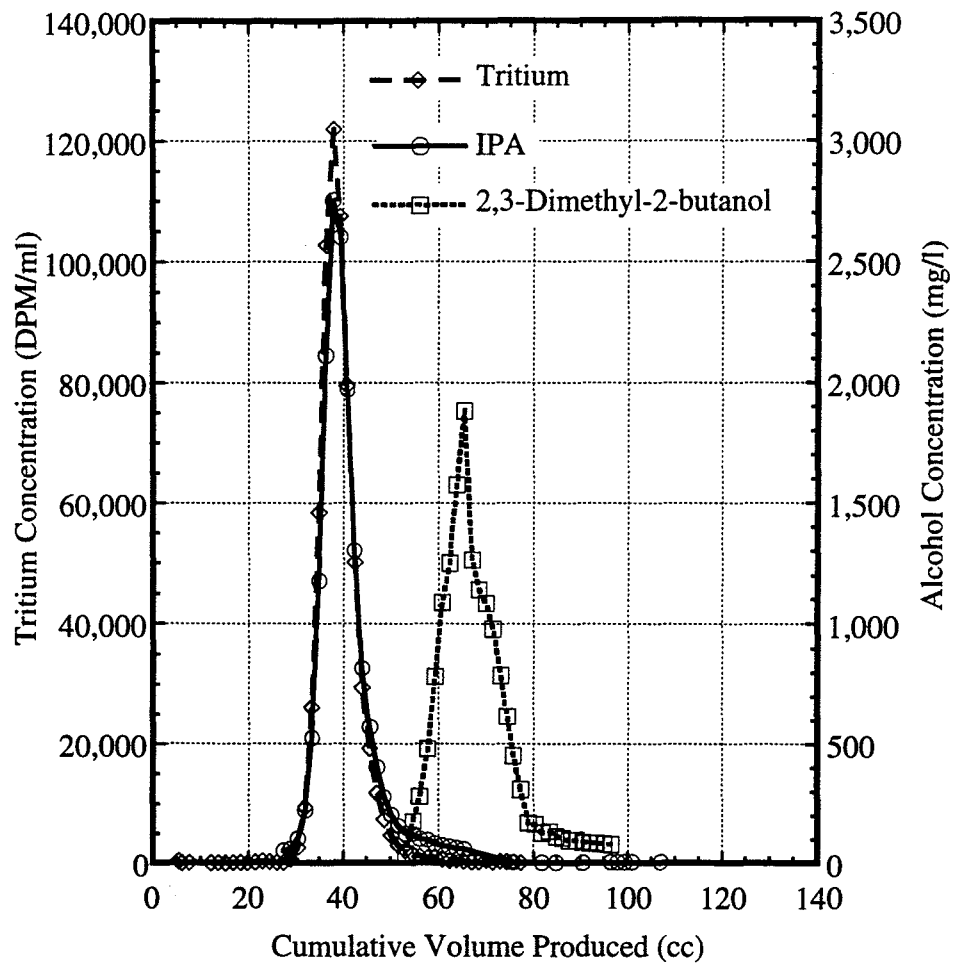


Figure 8.16: Tracer concentration histories at residual PCE saturation, experiment DW#3.

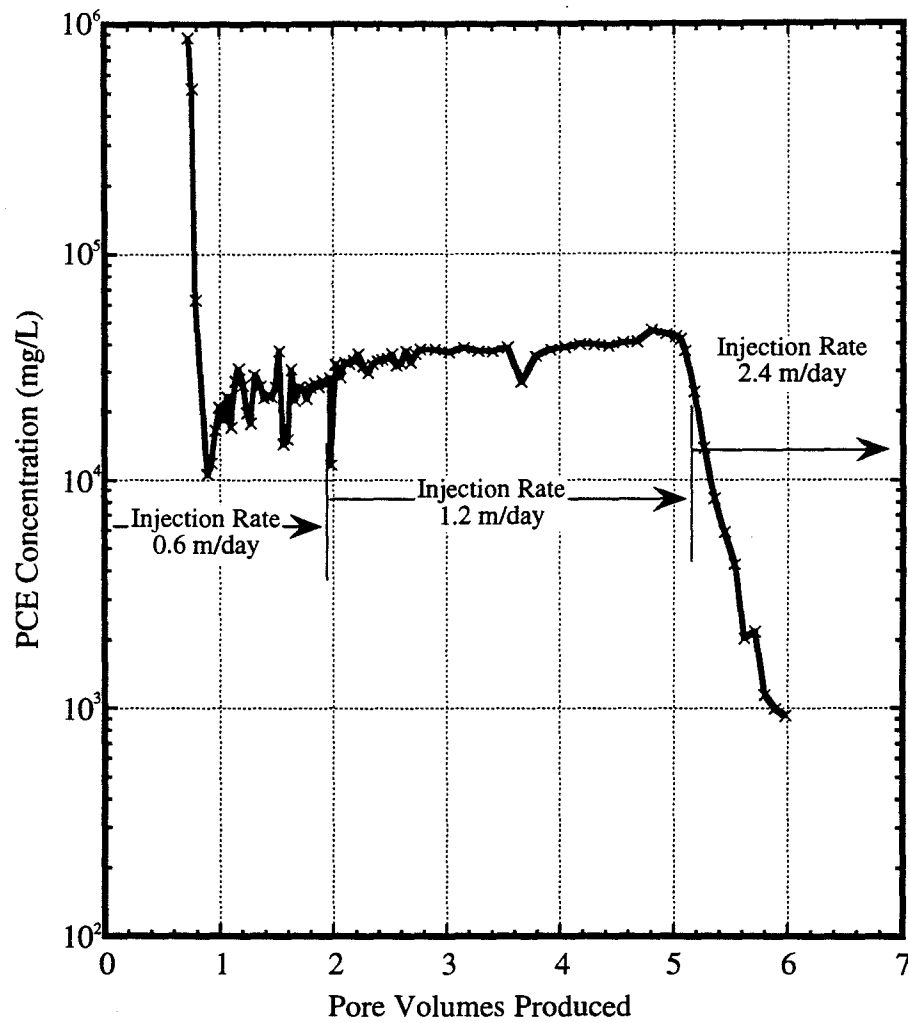


Figure 8.17: PCE concentration in effluent during surfactant flushing, experiment DW#3.

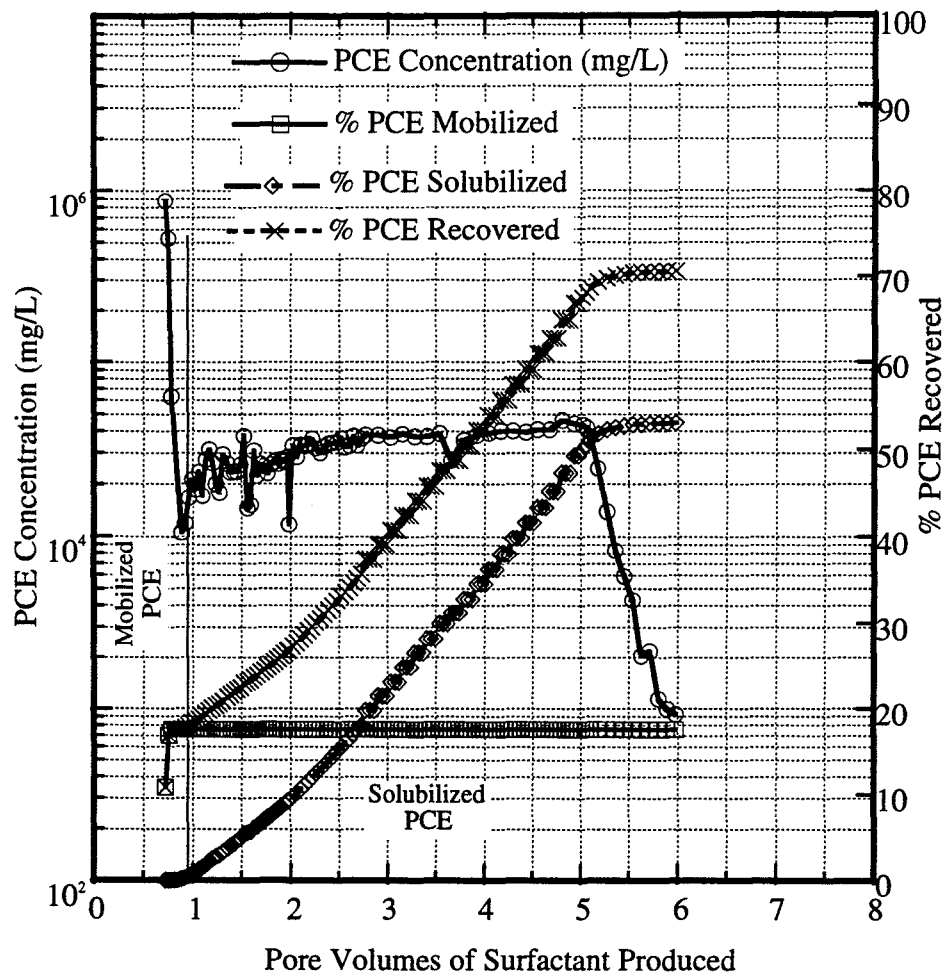


Figure 8.18: Plot showing PCE recovery mechanisms during surfactant flushing, experiment DW#3.

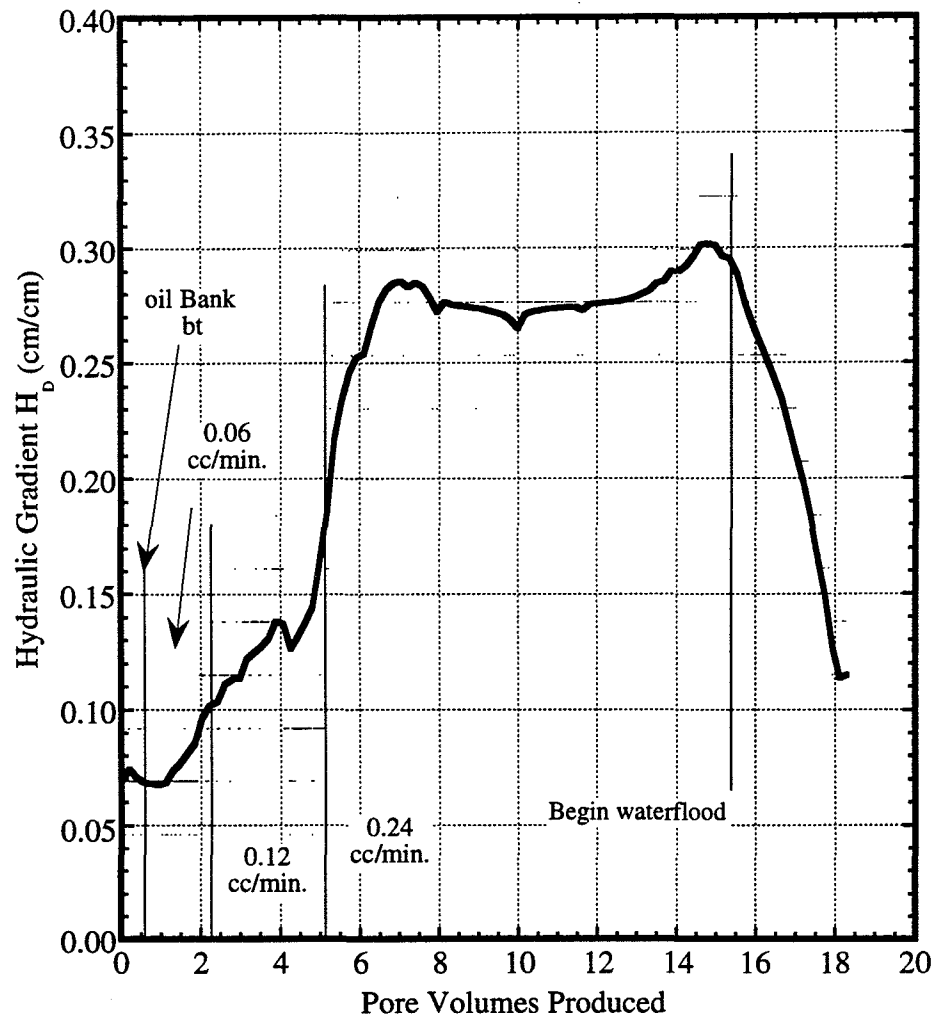


Figure 8.19: Hydraulic gradient across soil column during surfactant flood and post surfactant waterflood, experiment DW#3.

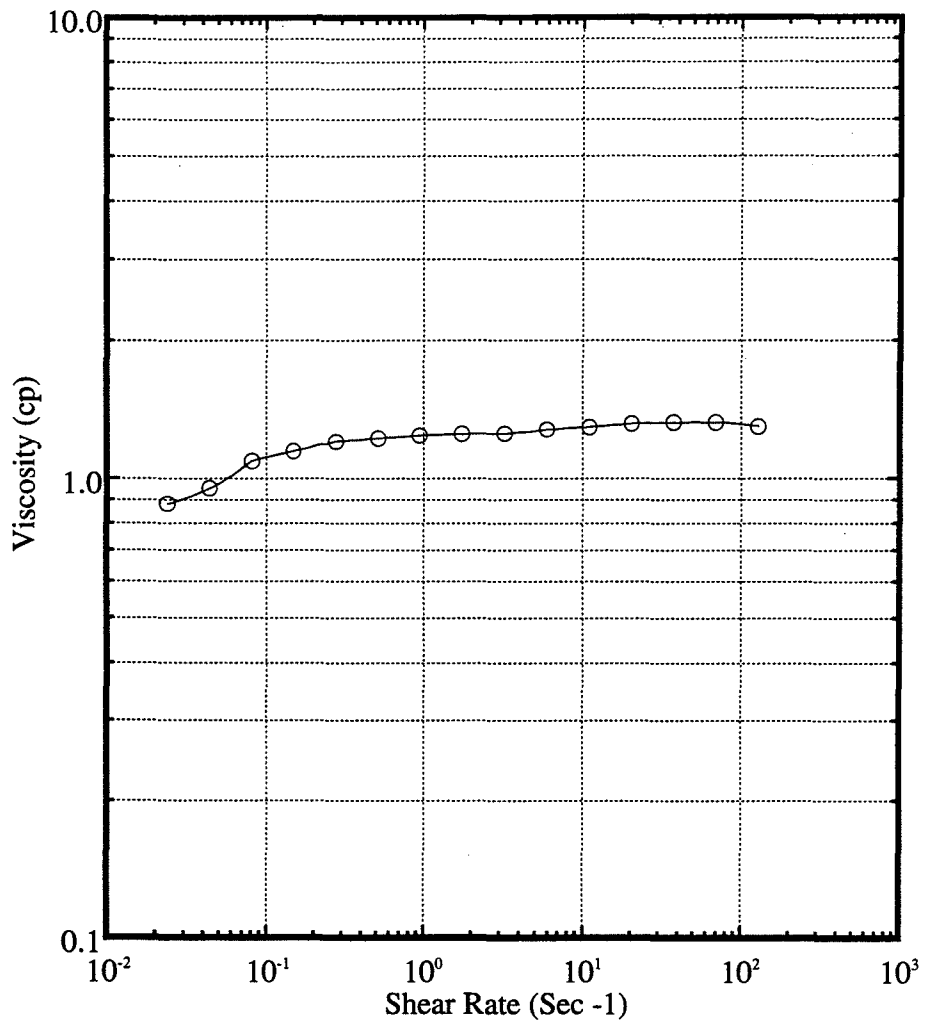


Figure 8.20: Viscosity of aqueous surfactant solution, experiment DW#3.

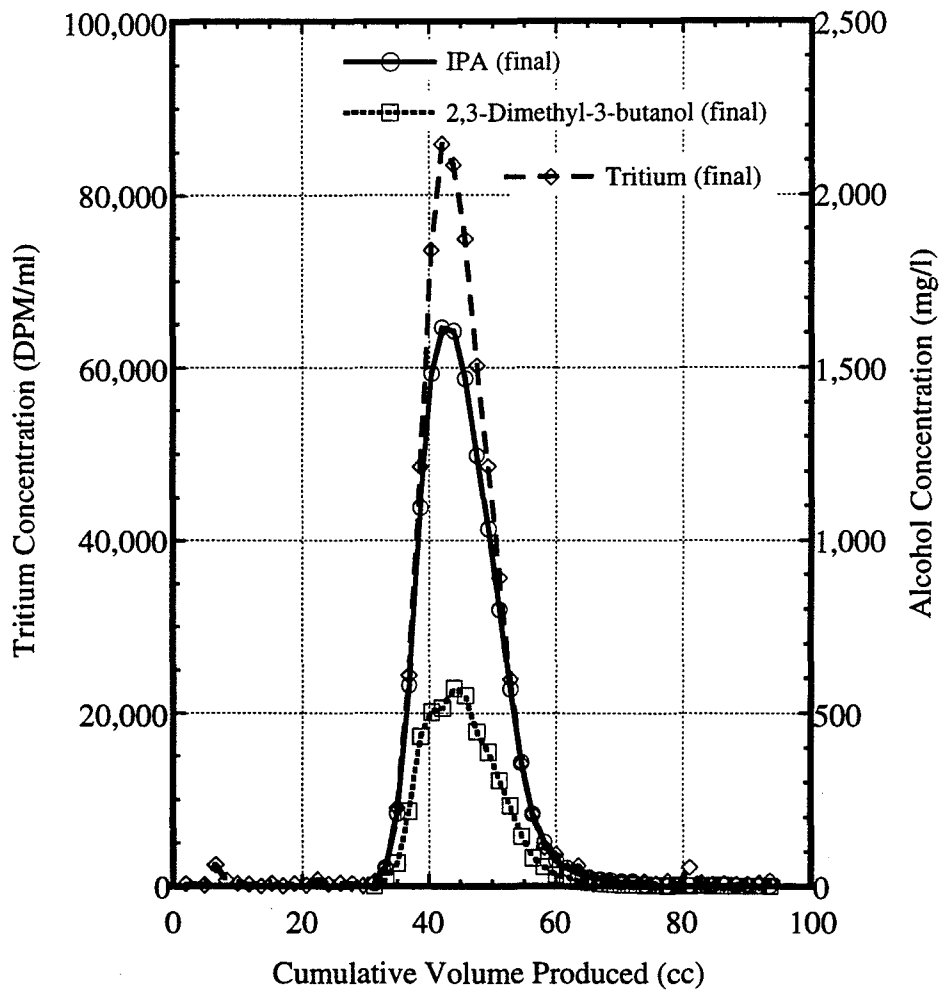


Figure 8.21: Final tracer concentration histories, experiment DW#3.

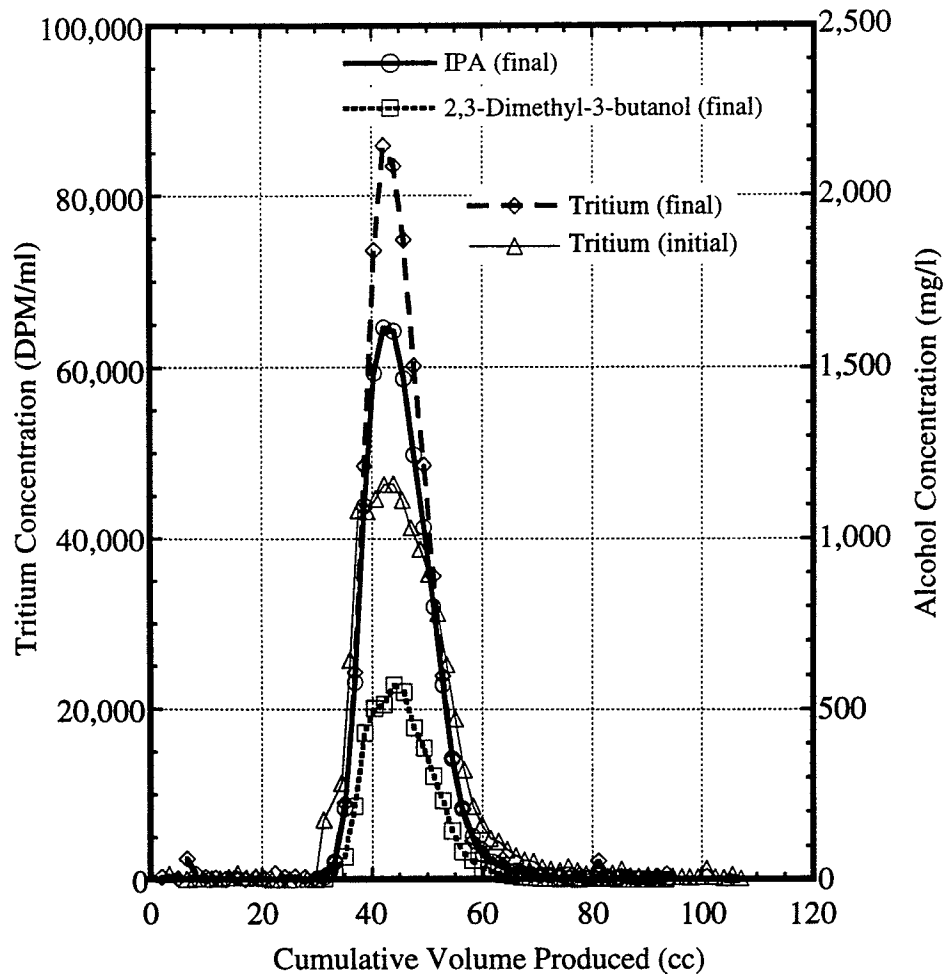


Figure 8.22: Comparison of initial and final tracer concentration histories, experiment DW#3.

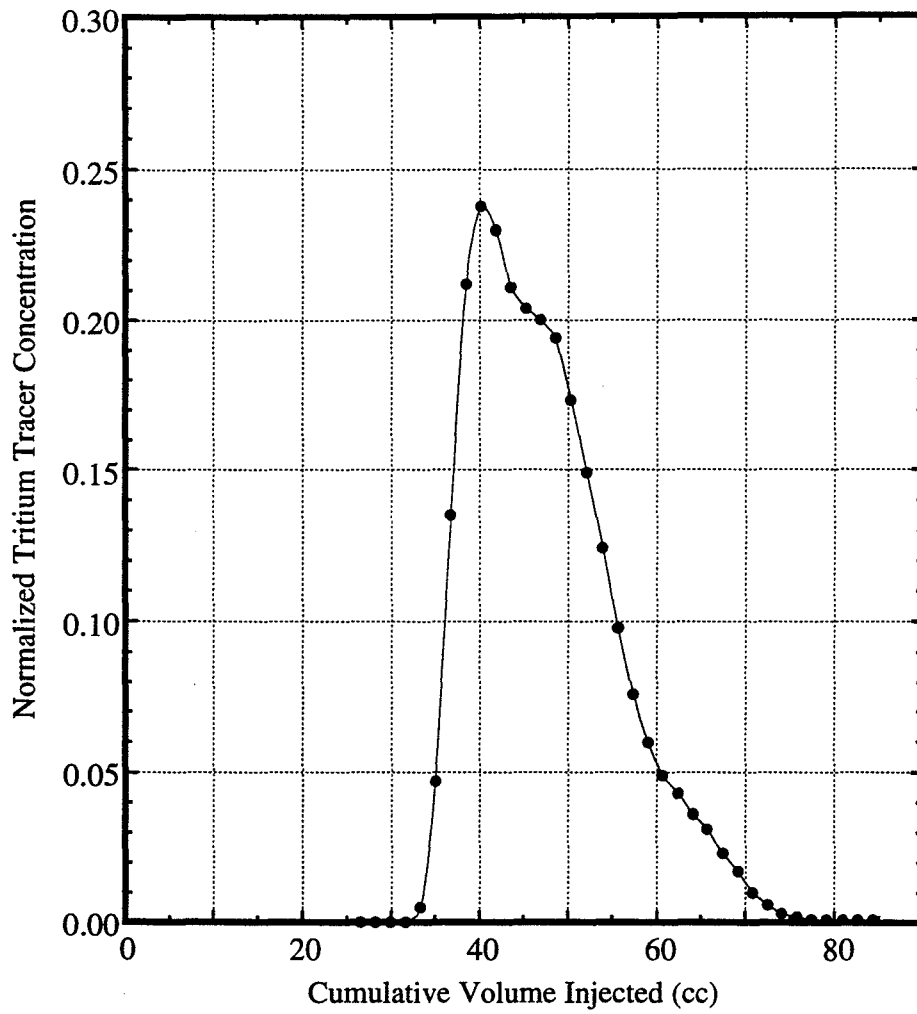


Figure 8.23 Initial tracer concentration history, experiment DW#4.

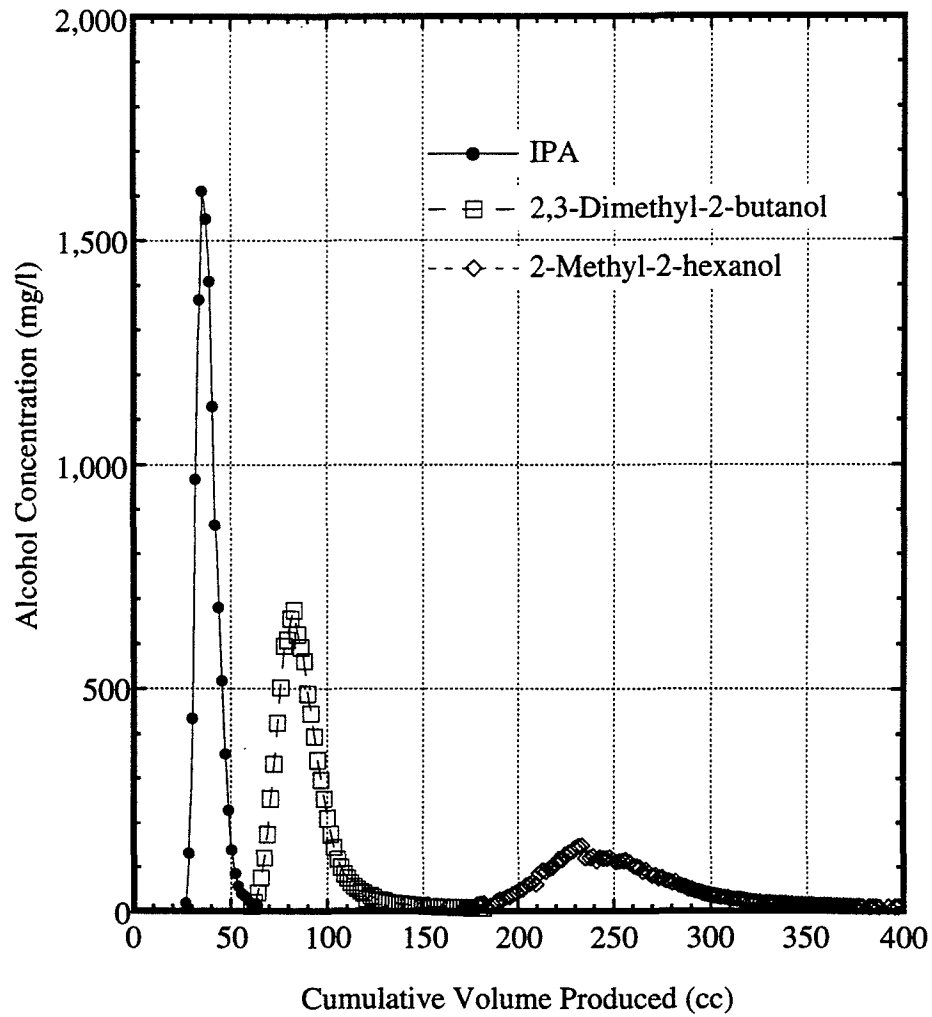


Figure 8.24: Tracer concentration histories at residual TCE saturation, experiment DW#4.

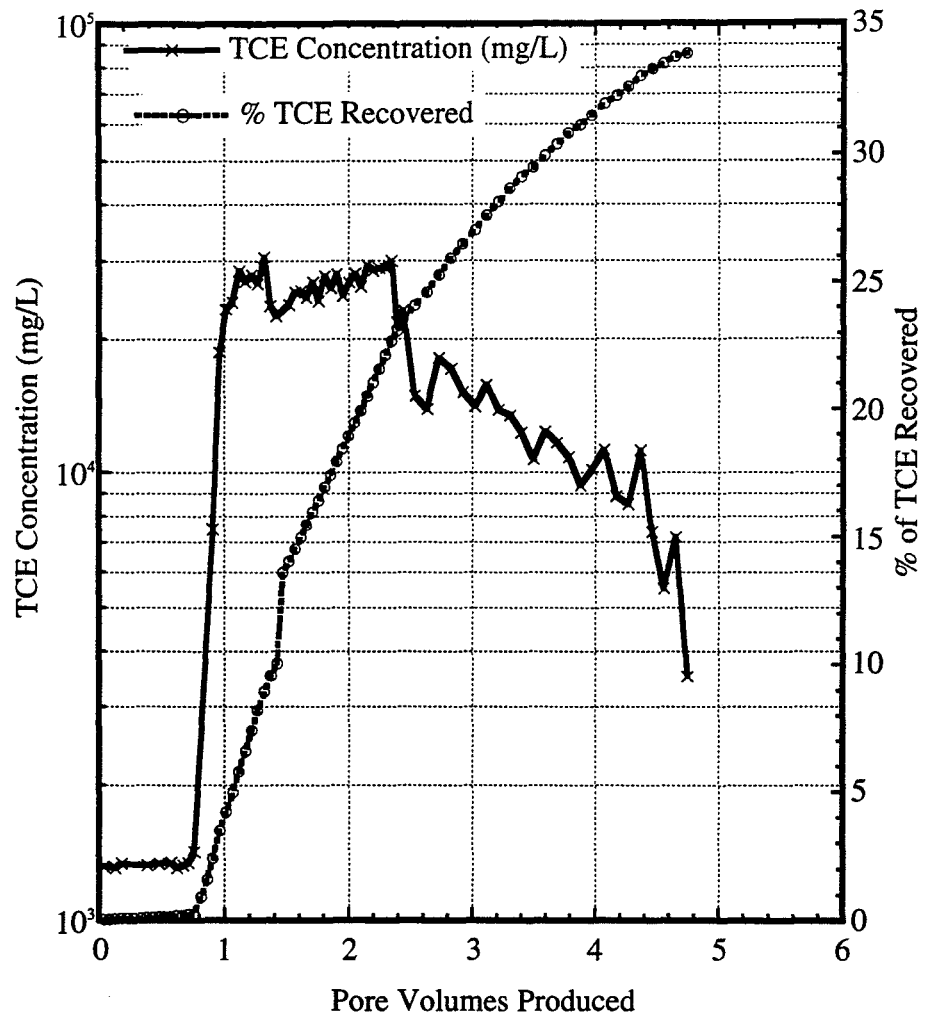


Figure 8.25: Plot showing PCE concentration history and recovery mechanisms during surfactant flushing, experiment DW#4.

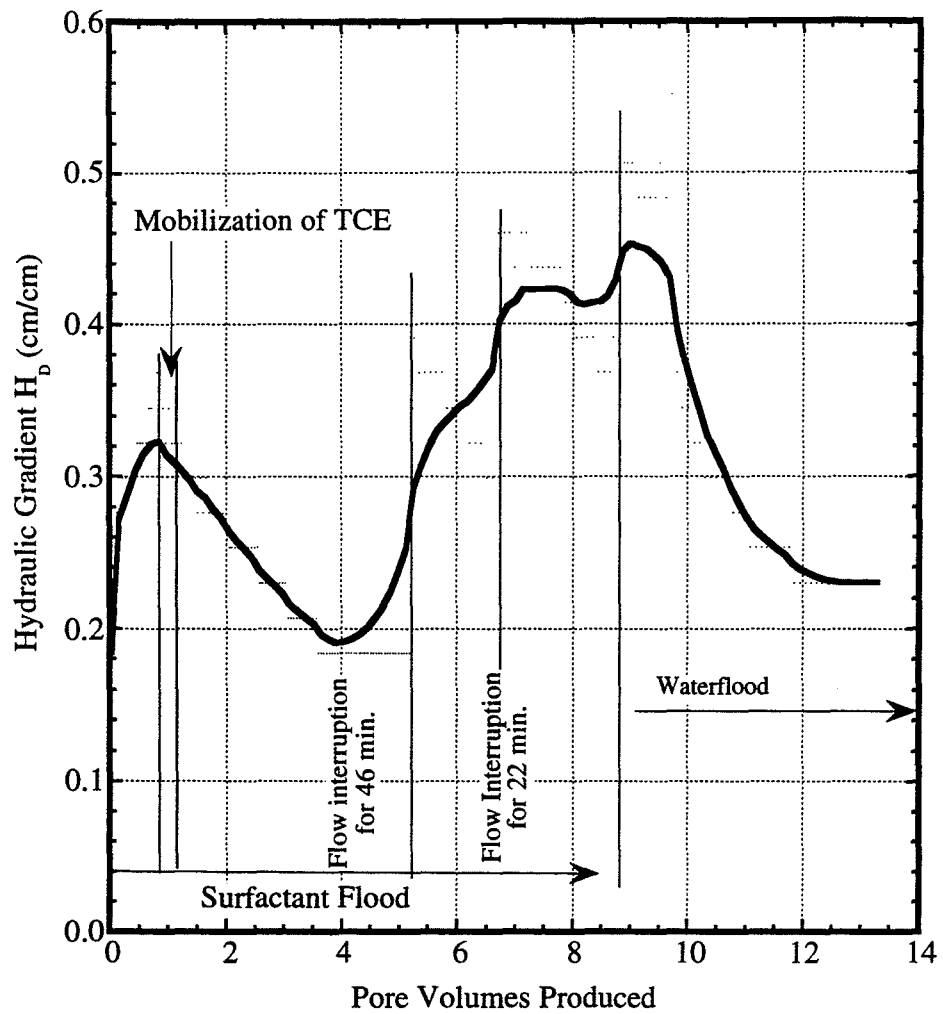


Figure 8.26: Hydraulic gradient across soil column during surfactant flood and post surfactant waterflood, experiment DW#4.

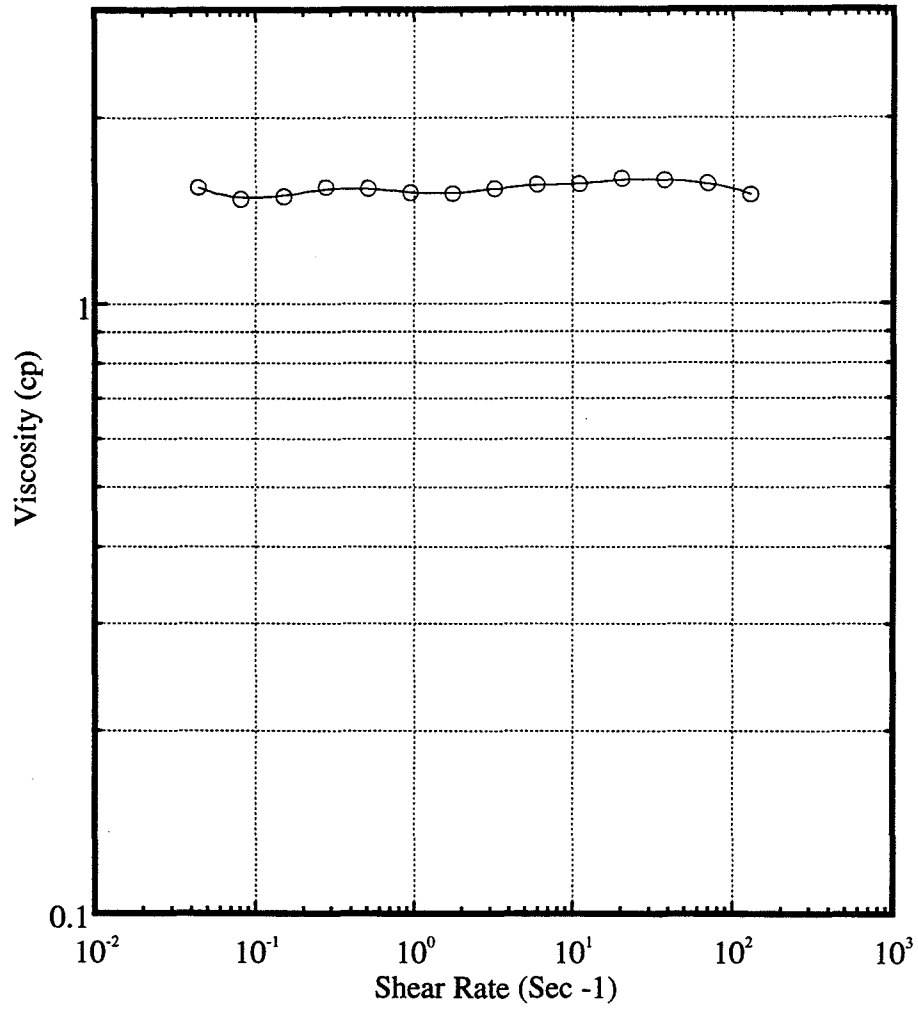


Figure 8.27: Viscosity of aqueous surfactant solution, experiment DW#4.

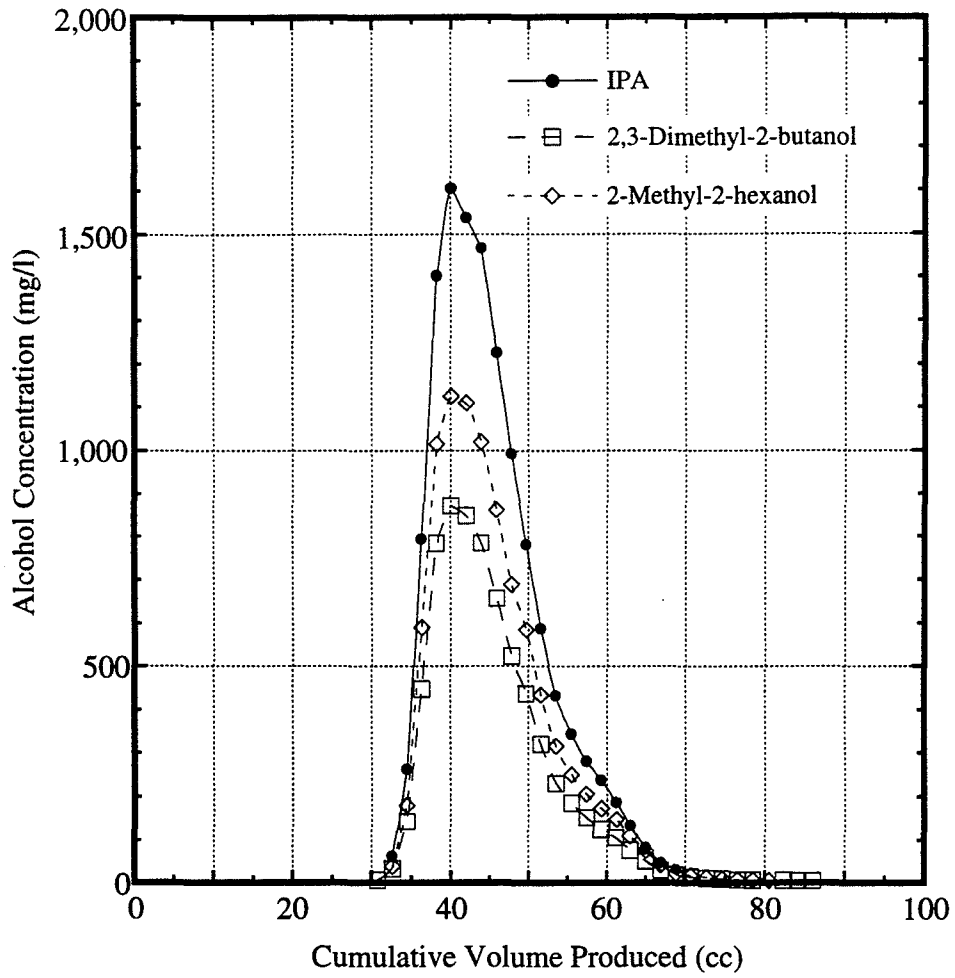


Figure 8.28: Final tracer concentration histories, experiment DW#4.

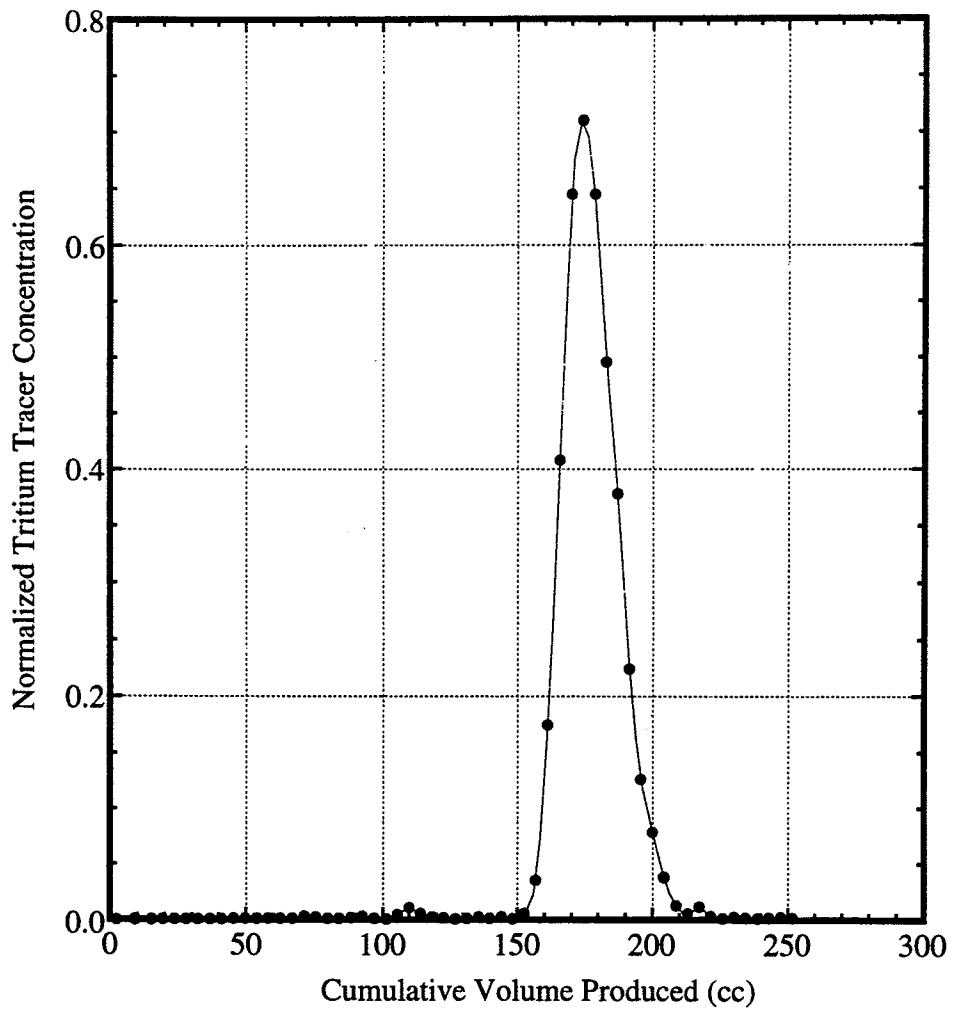


Figure 8.29: Initial tracer concentration history, experiment POLYTCE#1.

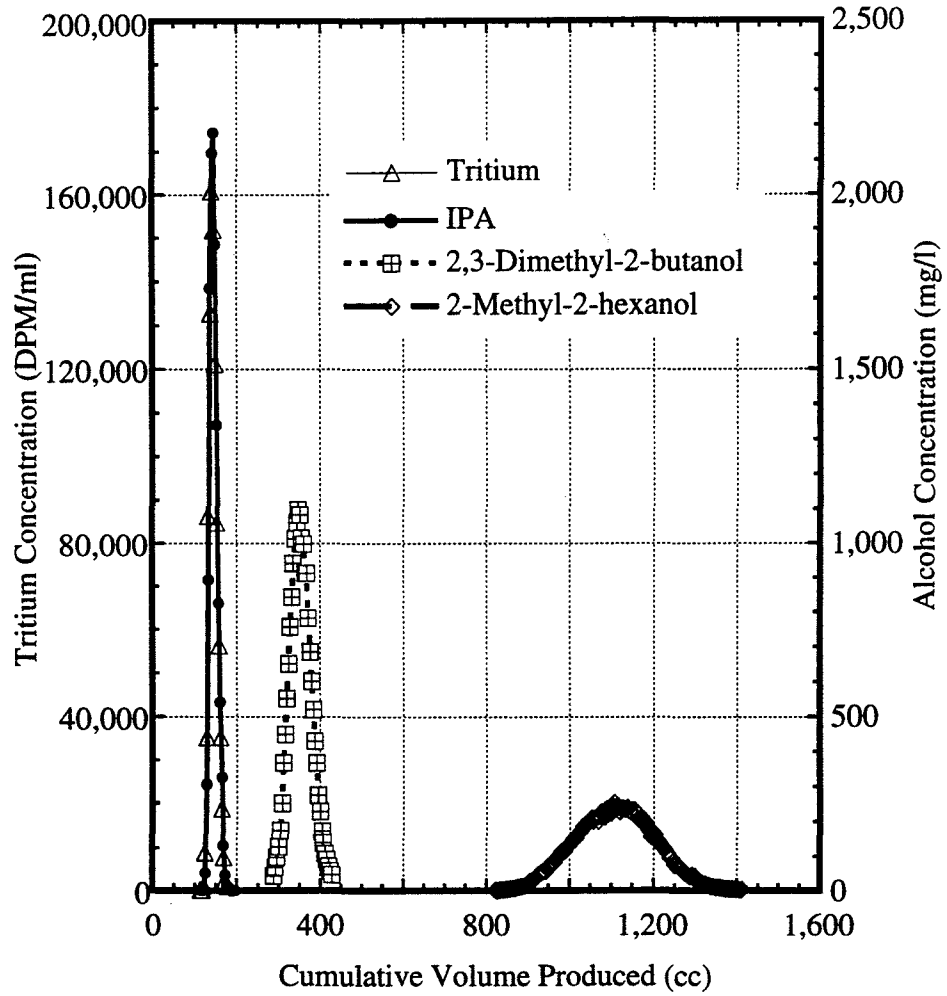


Figure 8.30: Tracer concentration histories at residual TCE saturation, experiment POLYTCE#1.

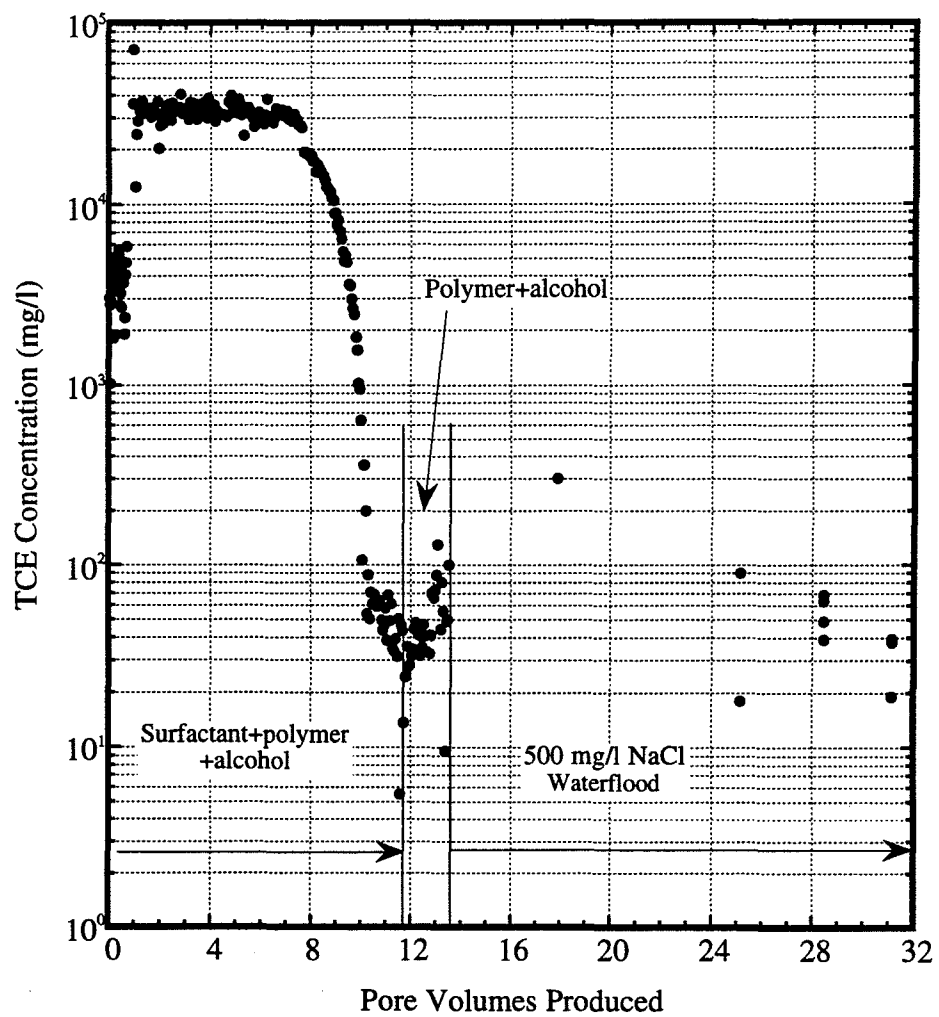


Figure 8.31: TCE concentration in effluent during surfactant flushing, experiment POLYTCE#1.

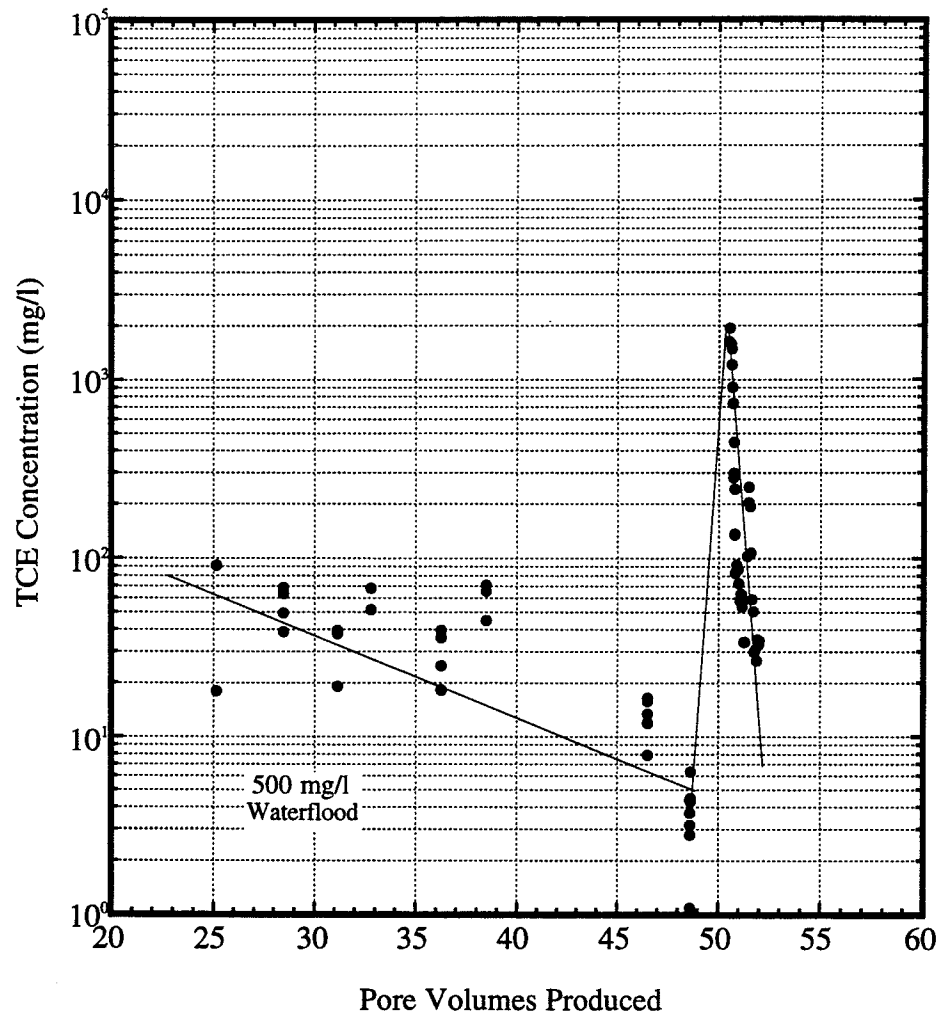


Figure 8.32: TCE concentration during post surfactant waterflood, experiment POLYTCE#1.

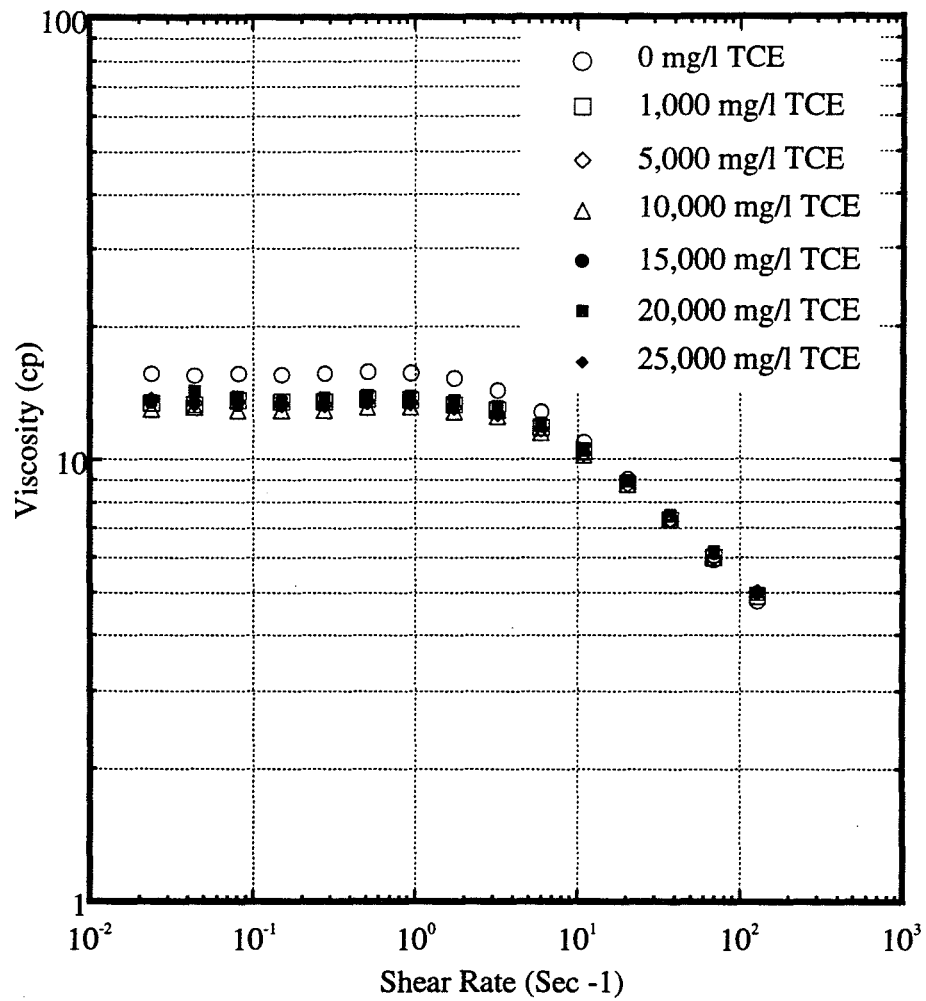


Figure 8.33: Viscosities of aqueous surfactant solution and microemulsions with 500 mg/l xanthan gum polymer, experiment POLYTCE#1.

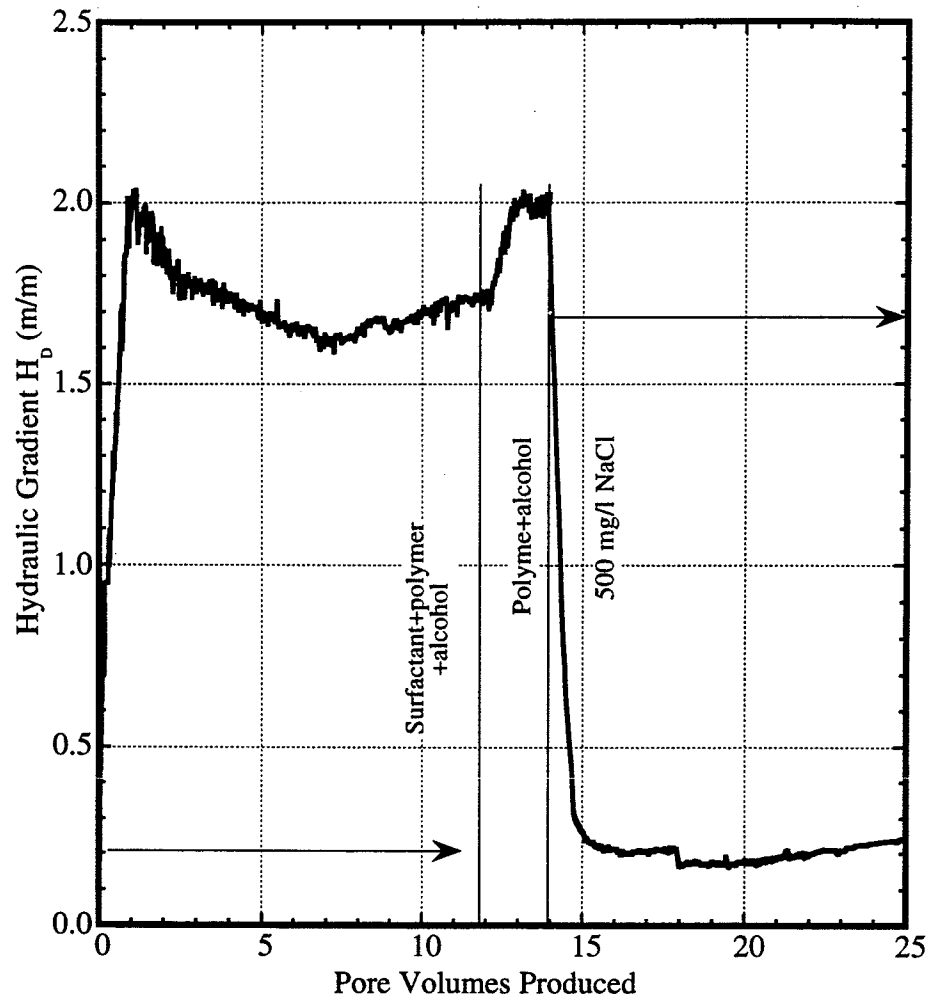


Figure 8.34: Hydraulic gradient across soil column during surfactant flood and post surfactant waterflood, experiment POLYTCE#1.

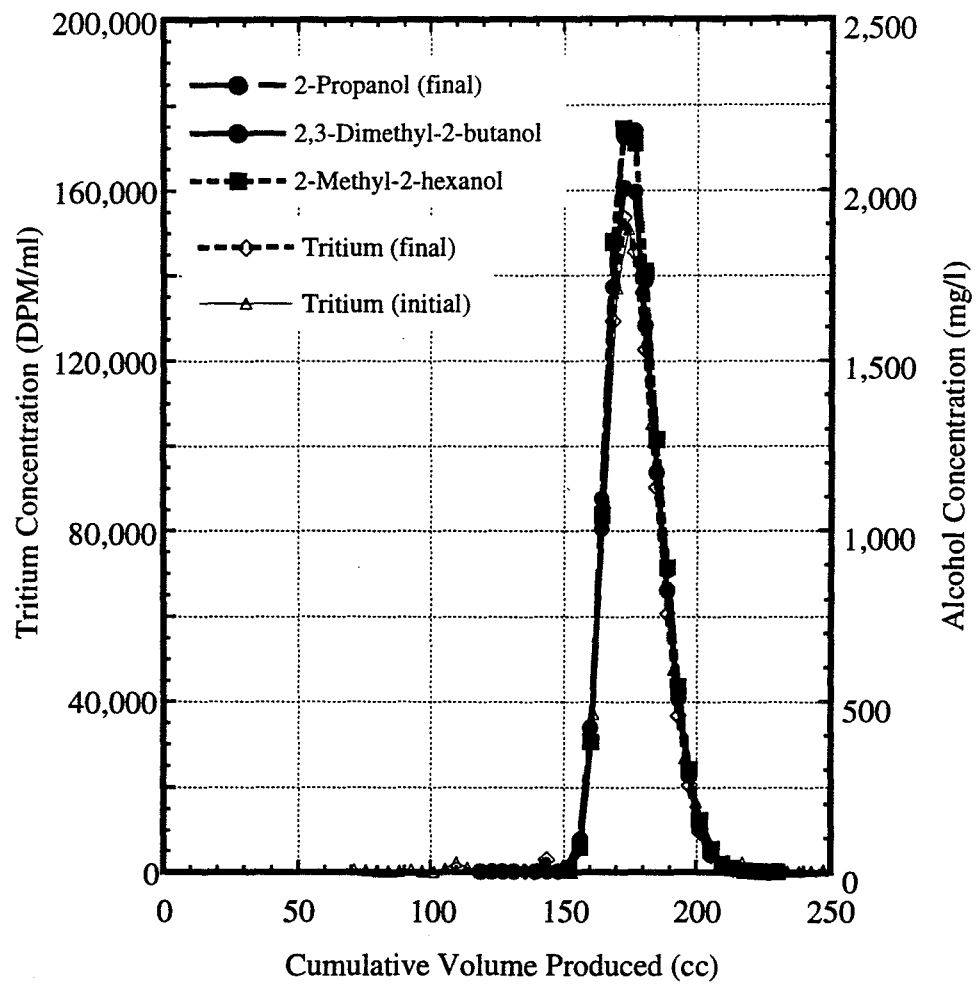


Figure 8.35: Comparison of initial and final tracer concentration histories, experiment POLYTCE1.

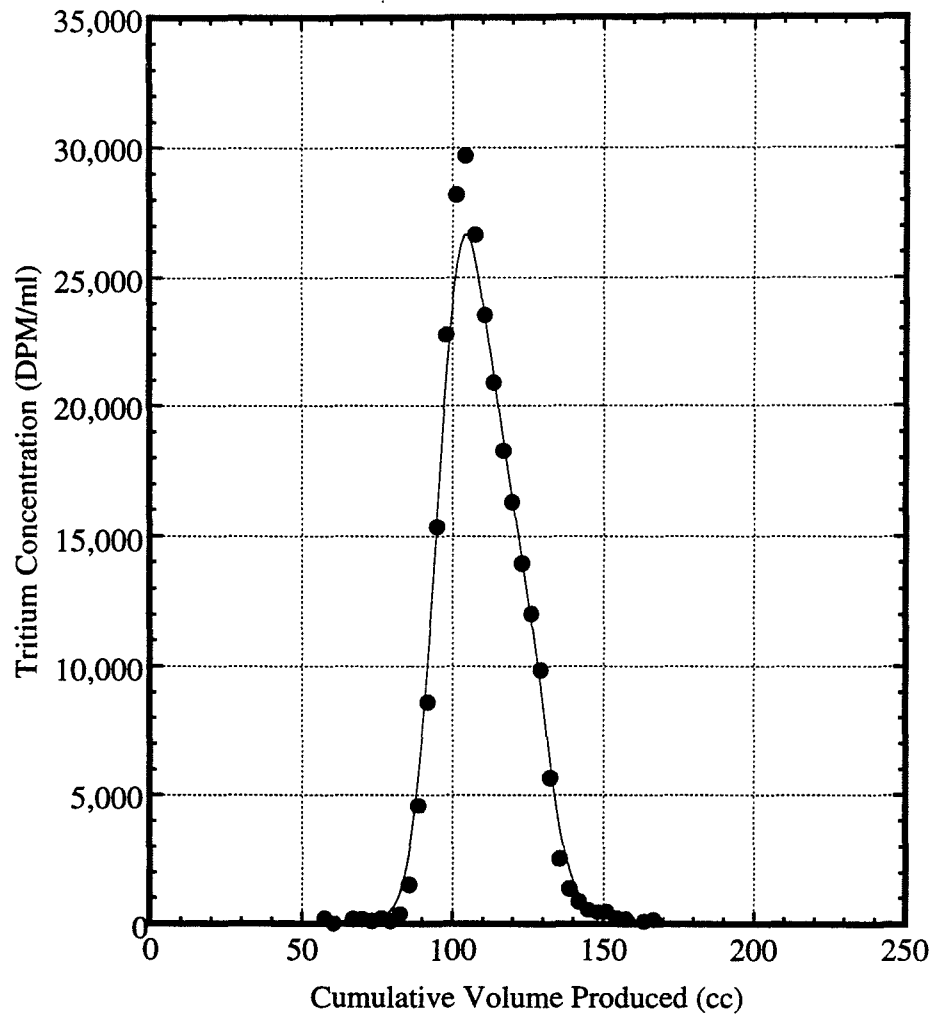


Figure 8.36: Initial tracer concentration history, experiment POLYTCE#3.

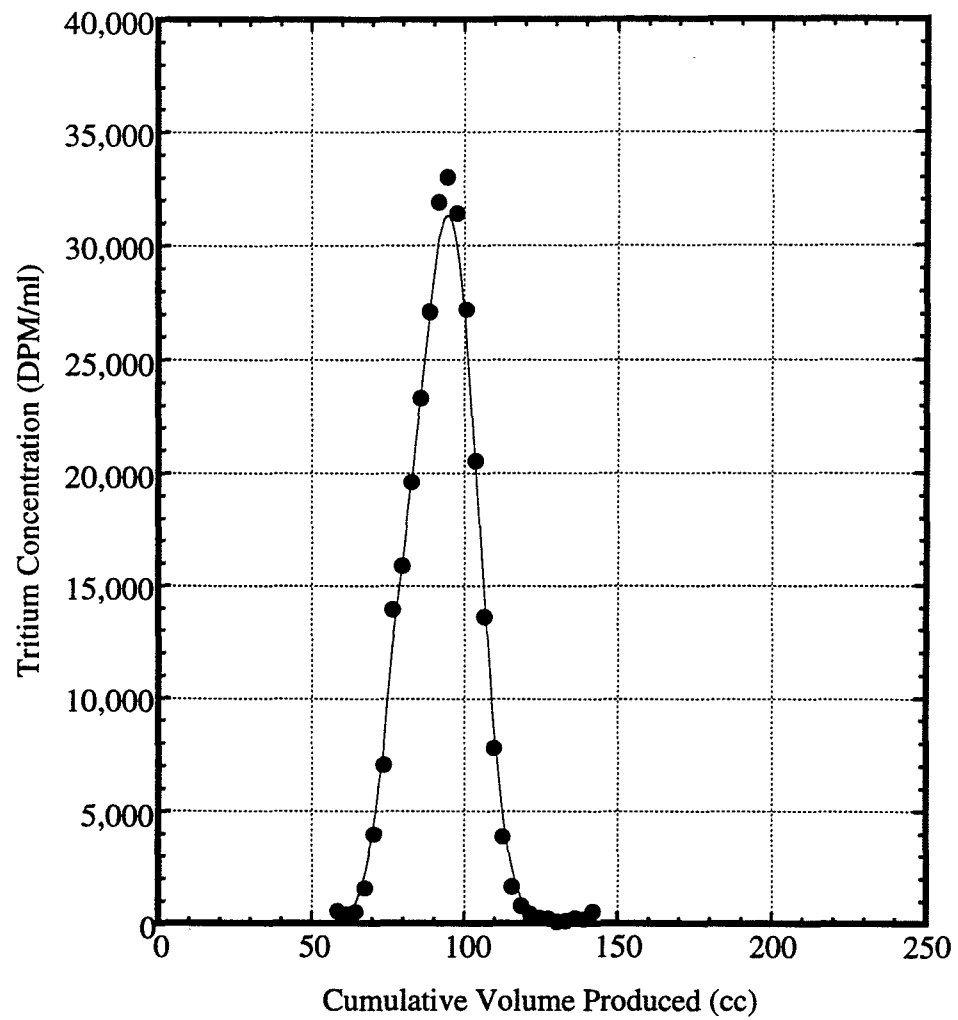


Figure 8.37: Tracer concentration history at residual TCE saturation, experiment POLYTCE#3.

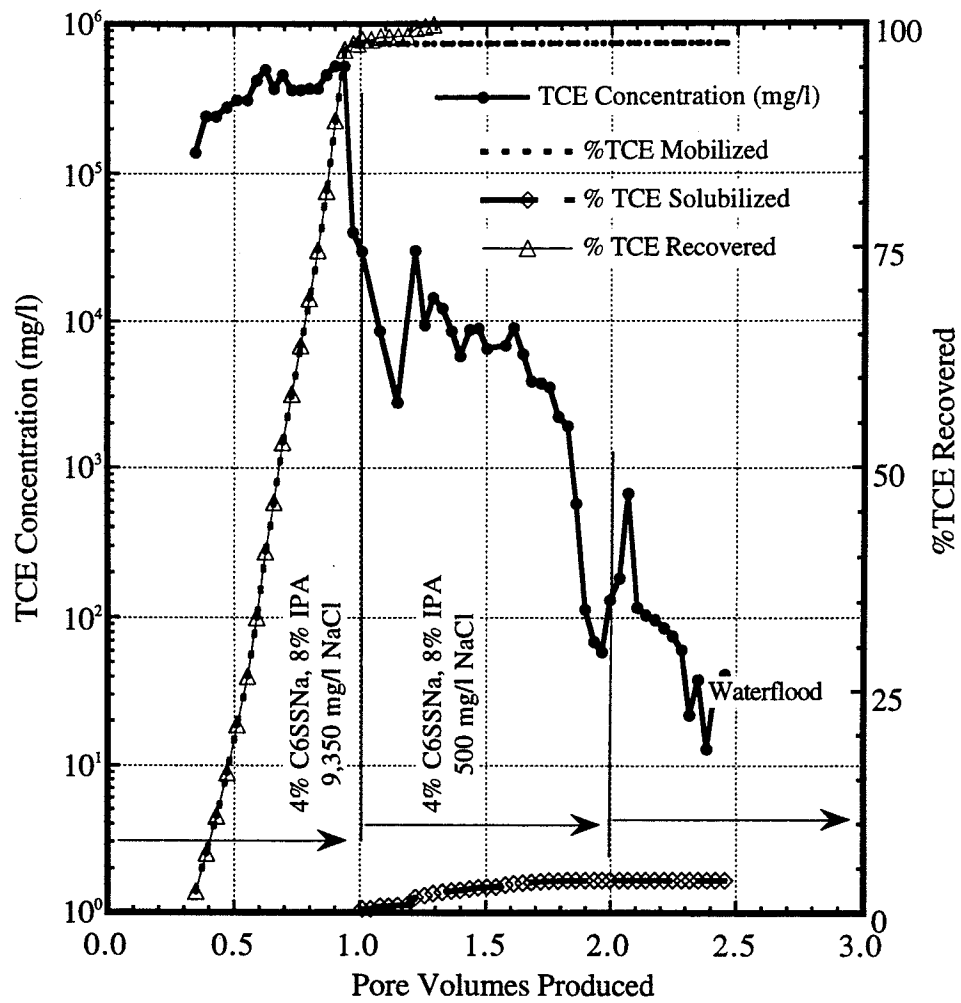


Figure 8.38: TCE concentration history and recovery mechanisms during surfactant flushing, experiment POLYTCE#3.

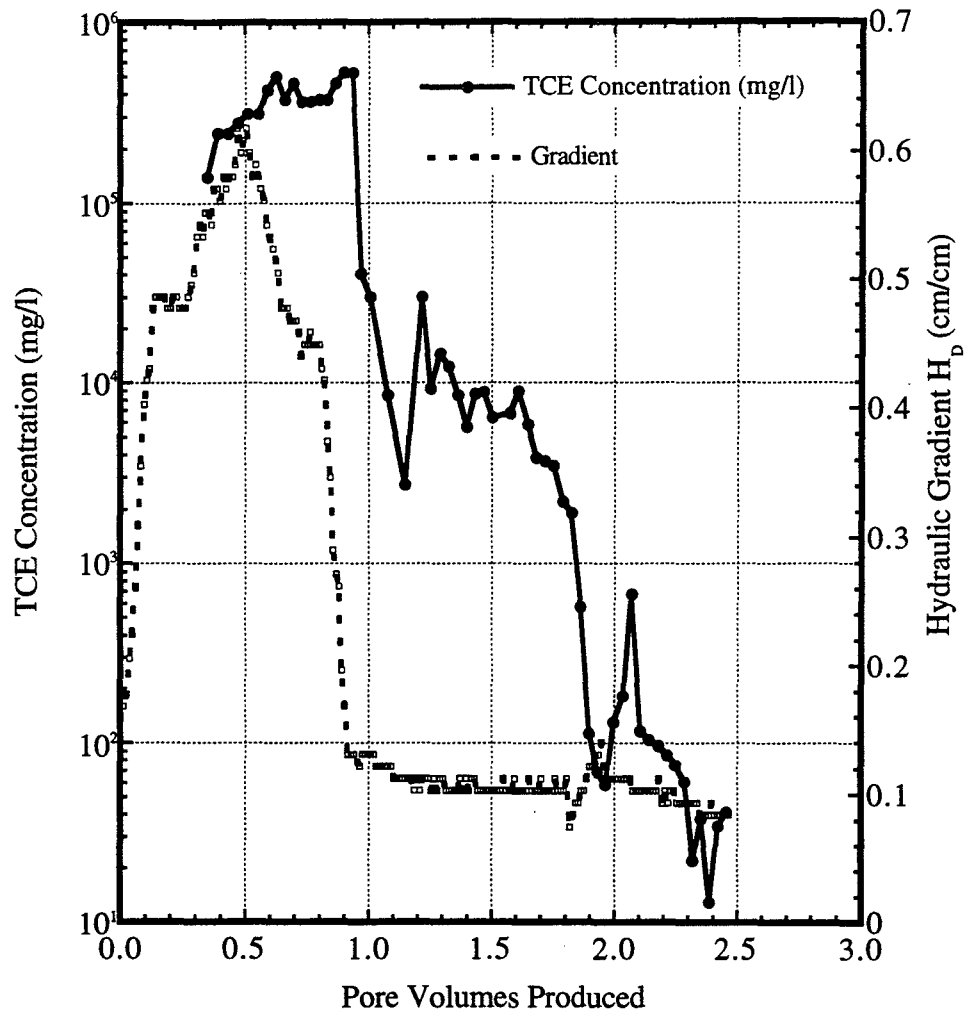


Figure 8.39: Hydraulic gradient across soil column and TCE concentration during surfactant flood and post surfactant waterflood, experiment POLYTCE#3.

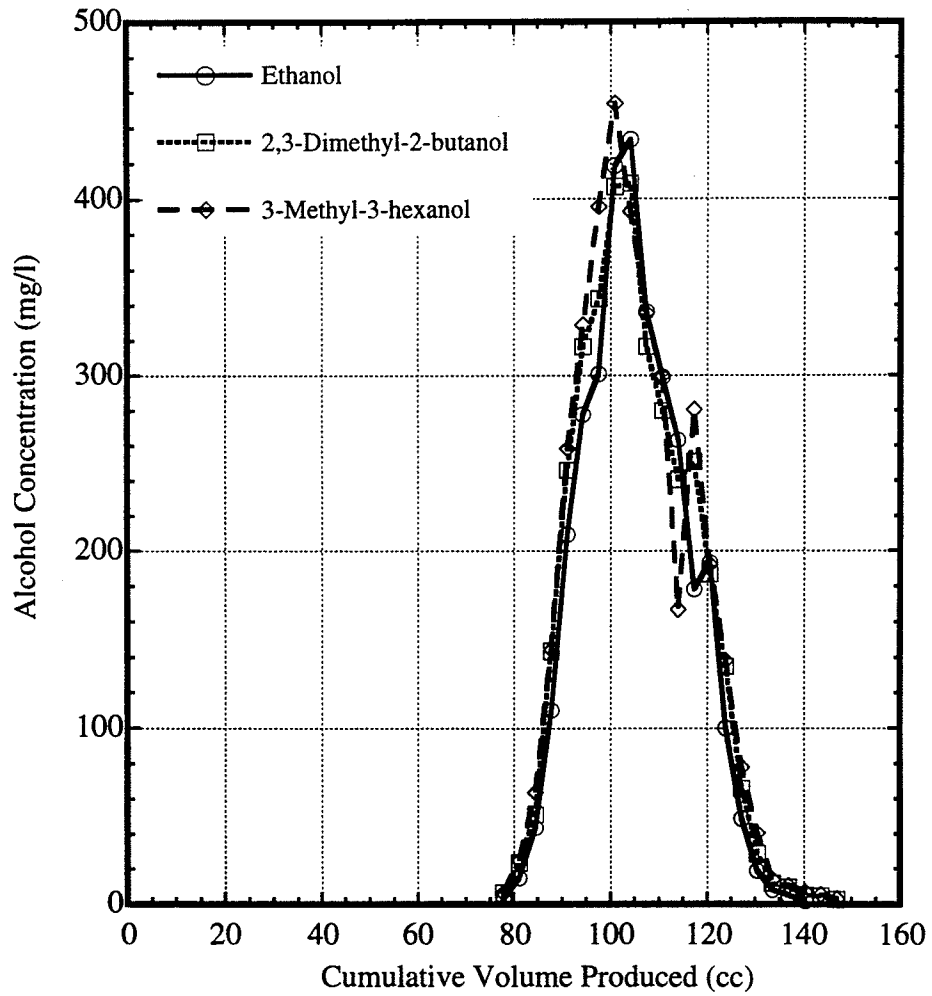


Figure 8.40: Final tracer concentration histories, experiment POLYTCE#3.

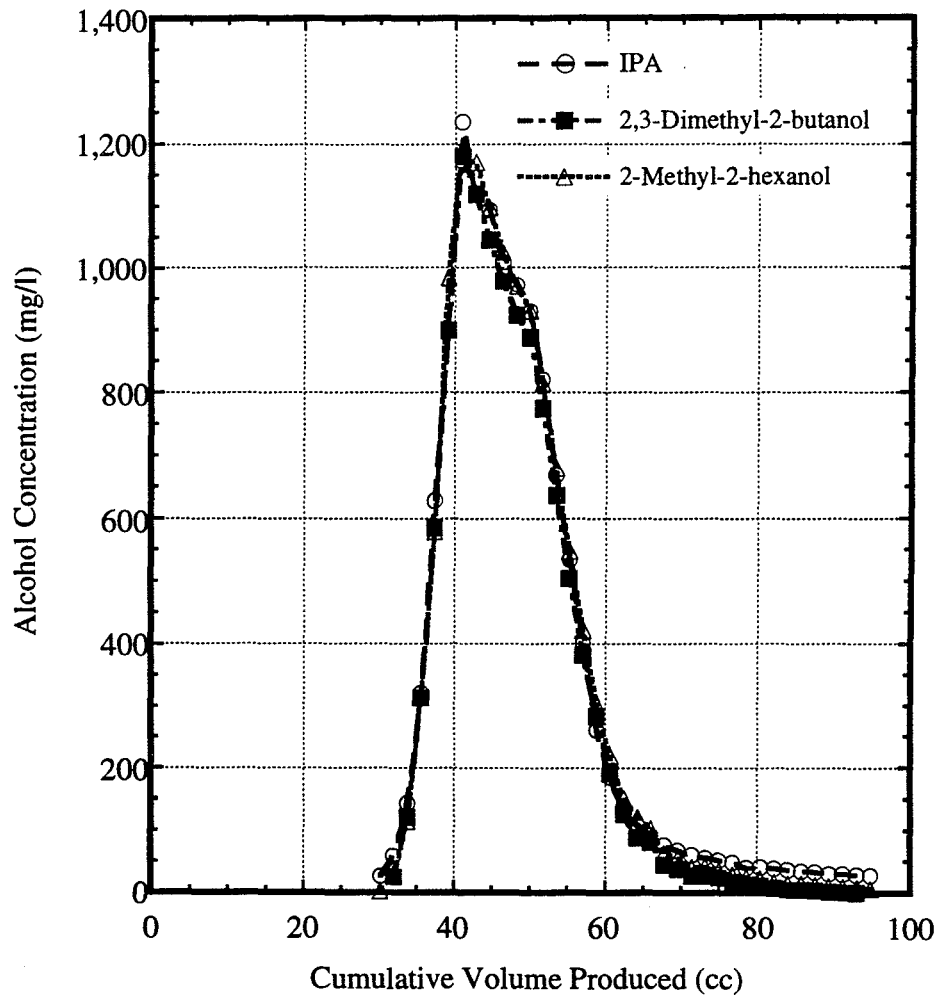


Figure 8.41: Initial tracer concentration histories, experiment OUDNAPL1.

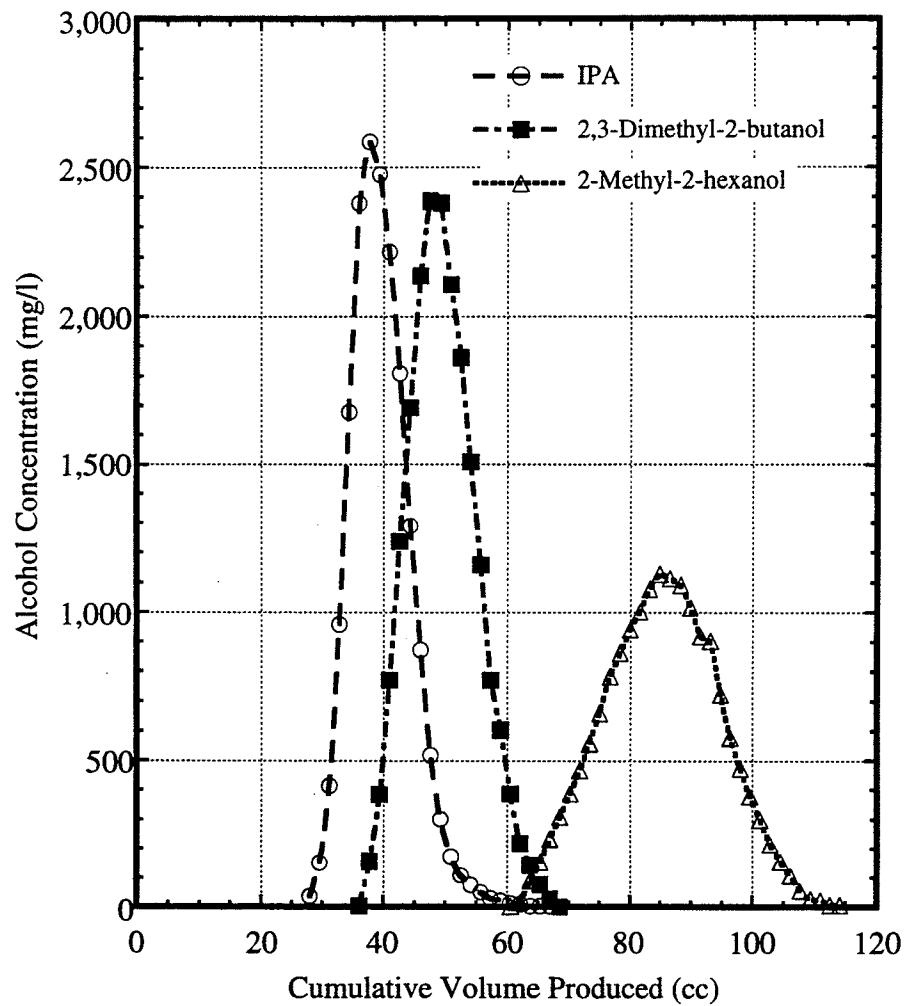


Figure 8.42: Tracer concentration histories for first set of tracers at residual OU1 NAPL saturation, experiment OUDNAPL1.

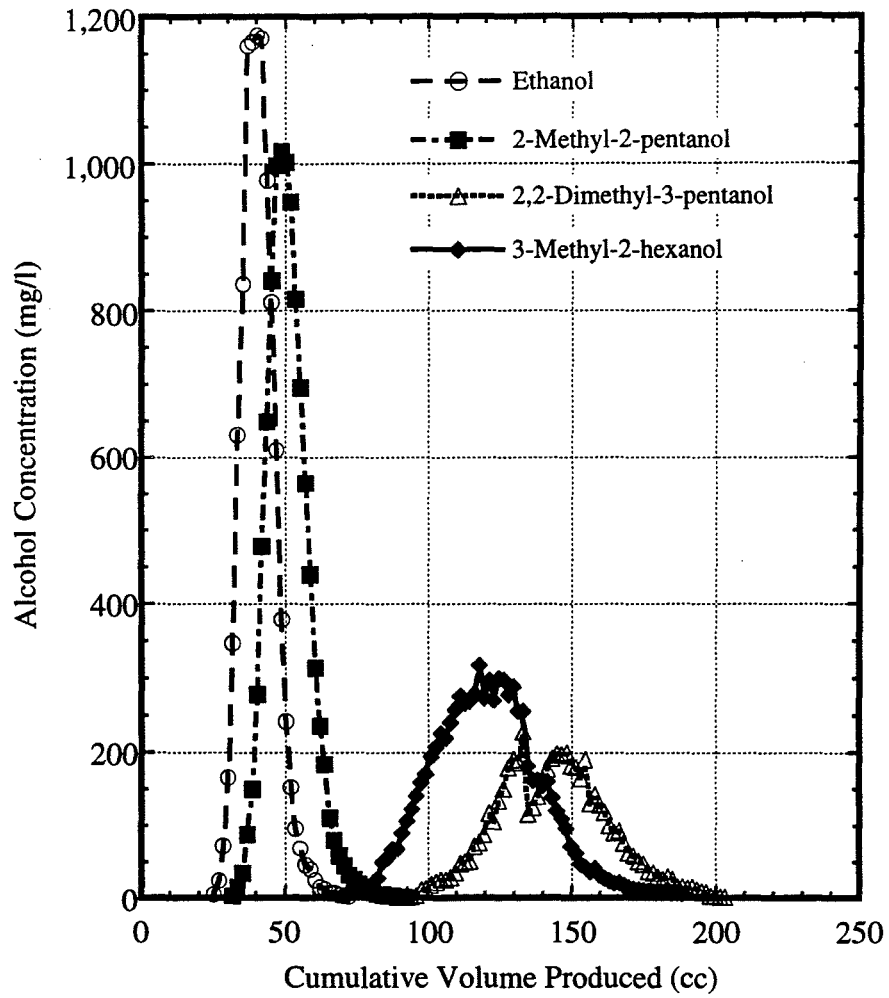


Figure 8.43: Tracer concentration histories for second set of tracers at residual OUI NAPL saturation, experiment OUDNAPL1.

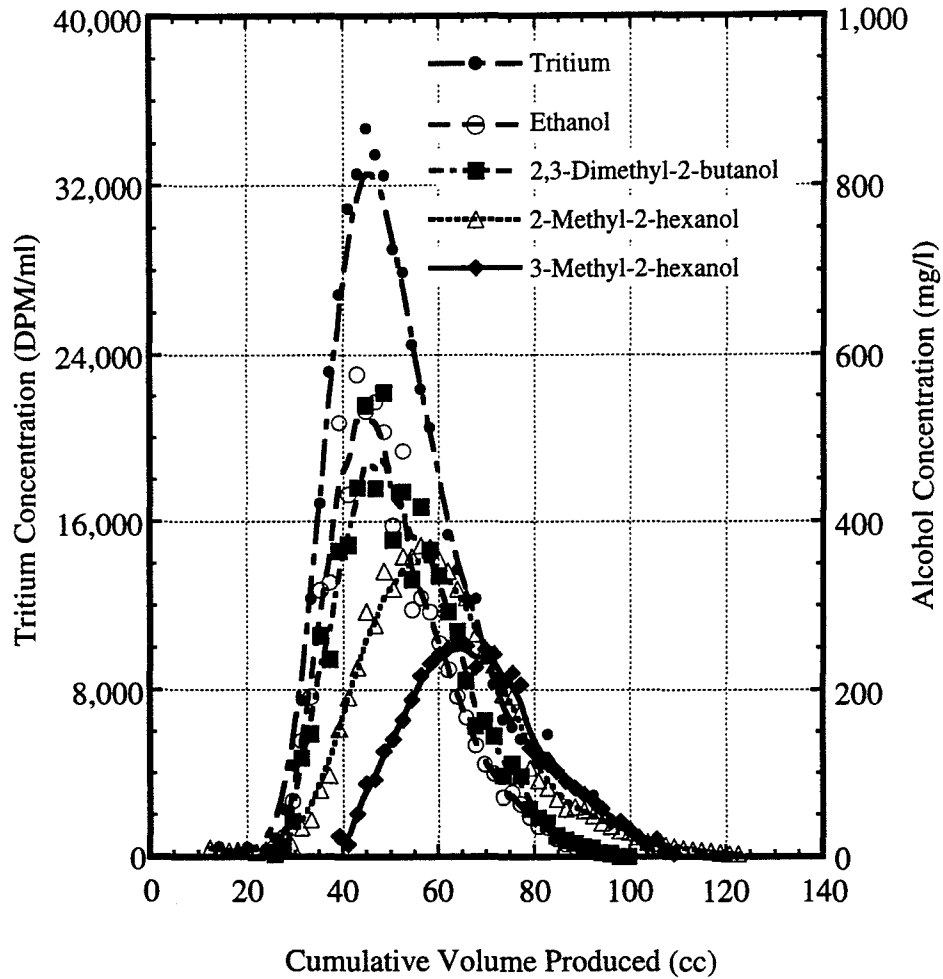


Figure 8.44: Tracer concentration histories for first set of tracers at residual OU1 NAPL saturation, experiment OUDNAPL2.

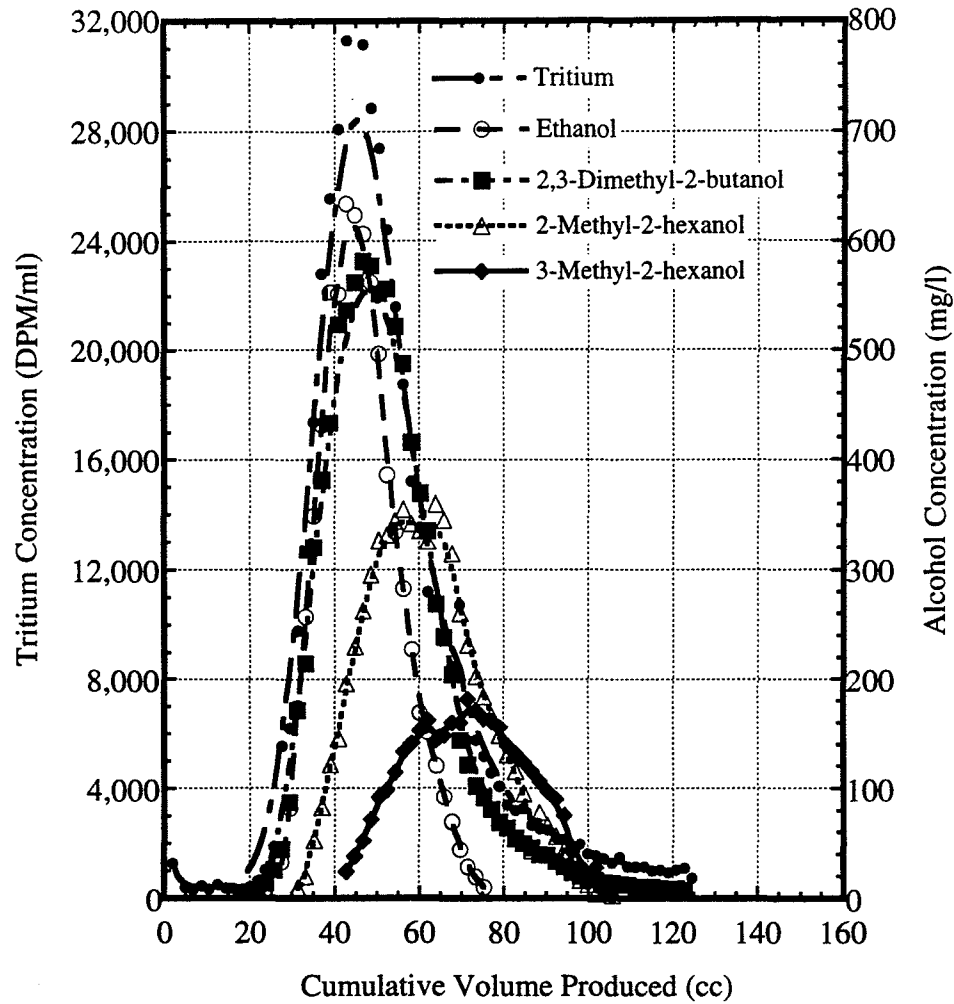


Figure 8.45: Tracer concentration histories for second set of tracers at residual OU1 NAPL saturation, experiment OUDNAPL2.

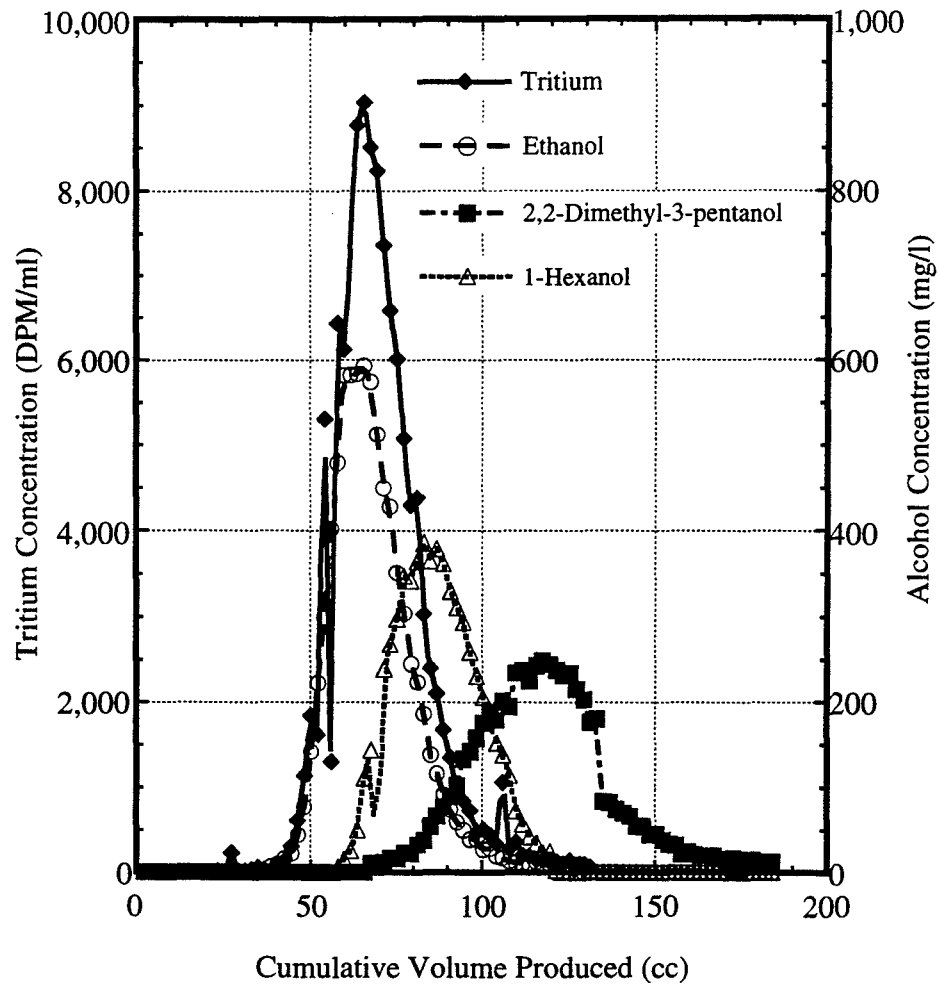


Figure 8.46: Tracer concentration histories for first set of tracers at residual OU1 NAPL saturation, experiment OUDNAPL3.

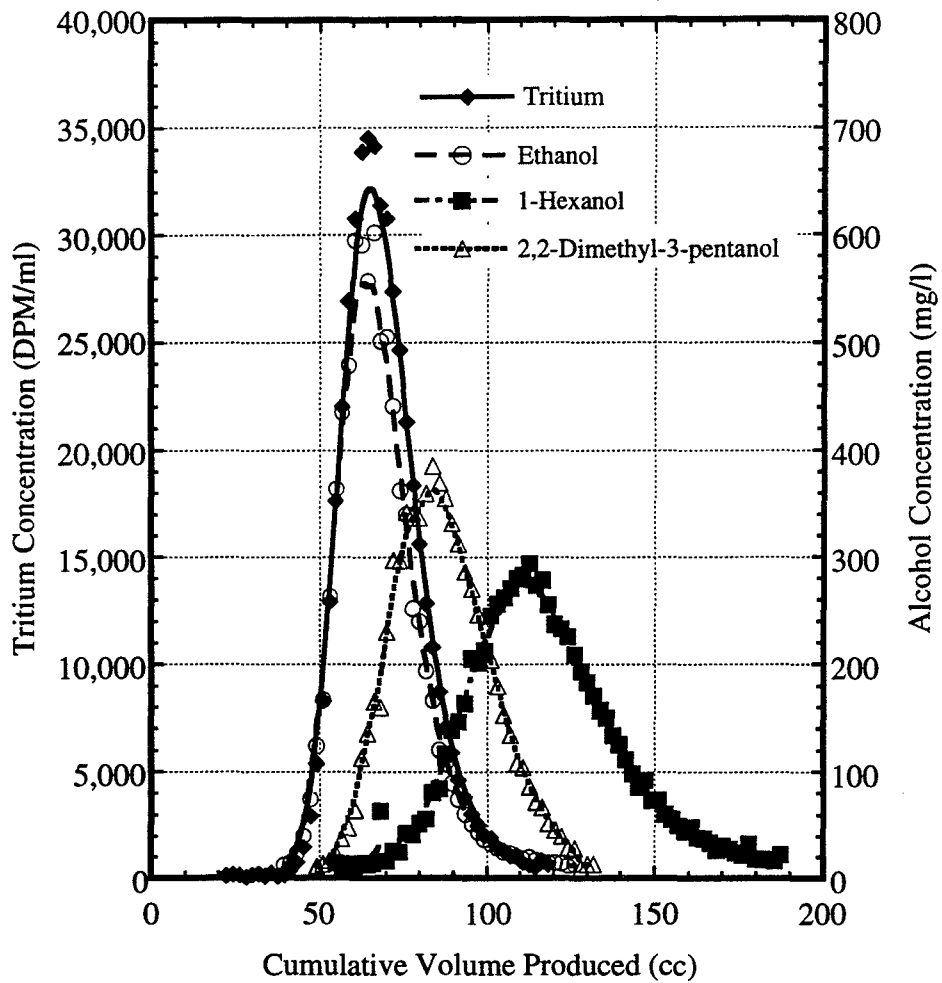


Figure 8.47: Tracer concentration histories for second set of tracers at residual OUI NAPL saturation, experiment OUDNAPL3.

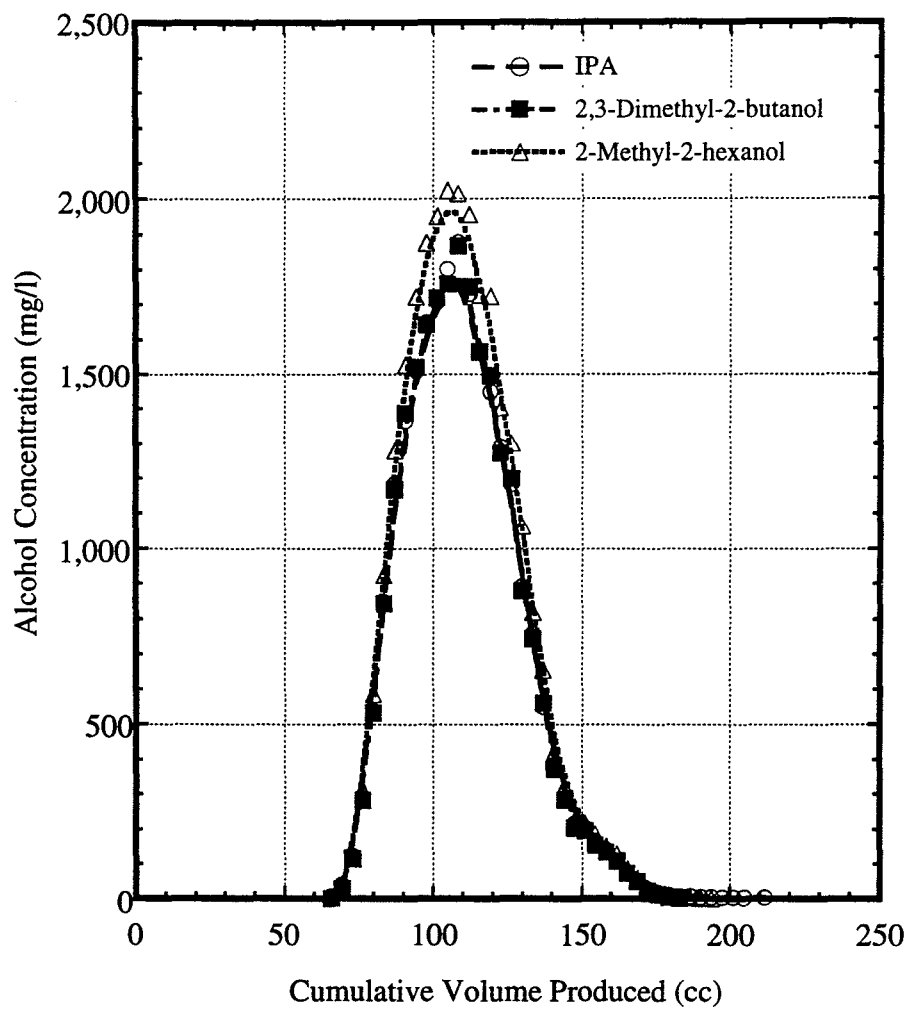


Figure 8.48: Initial tracer concentration history, experiment DW#5.

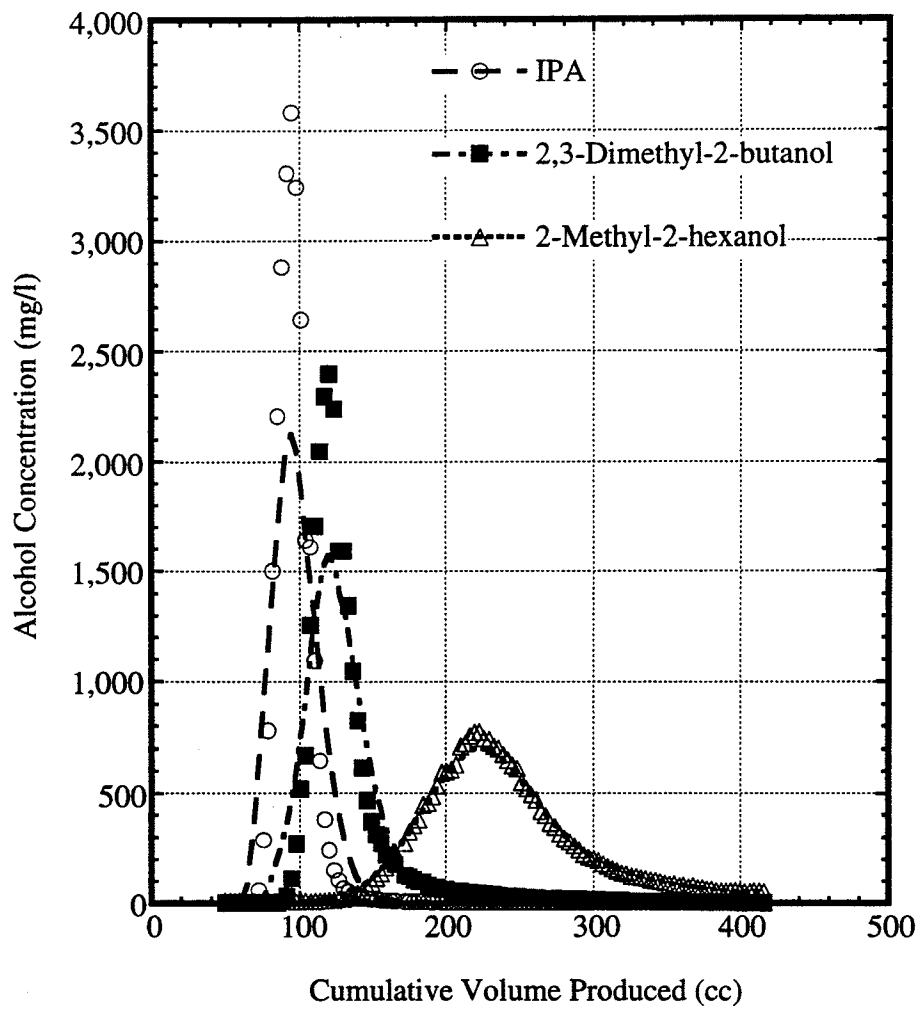


Figure 8.49: Tracer concentration histories at residual JP4 saturation, experiment DW#5.

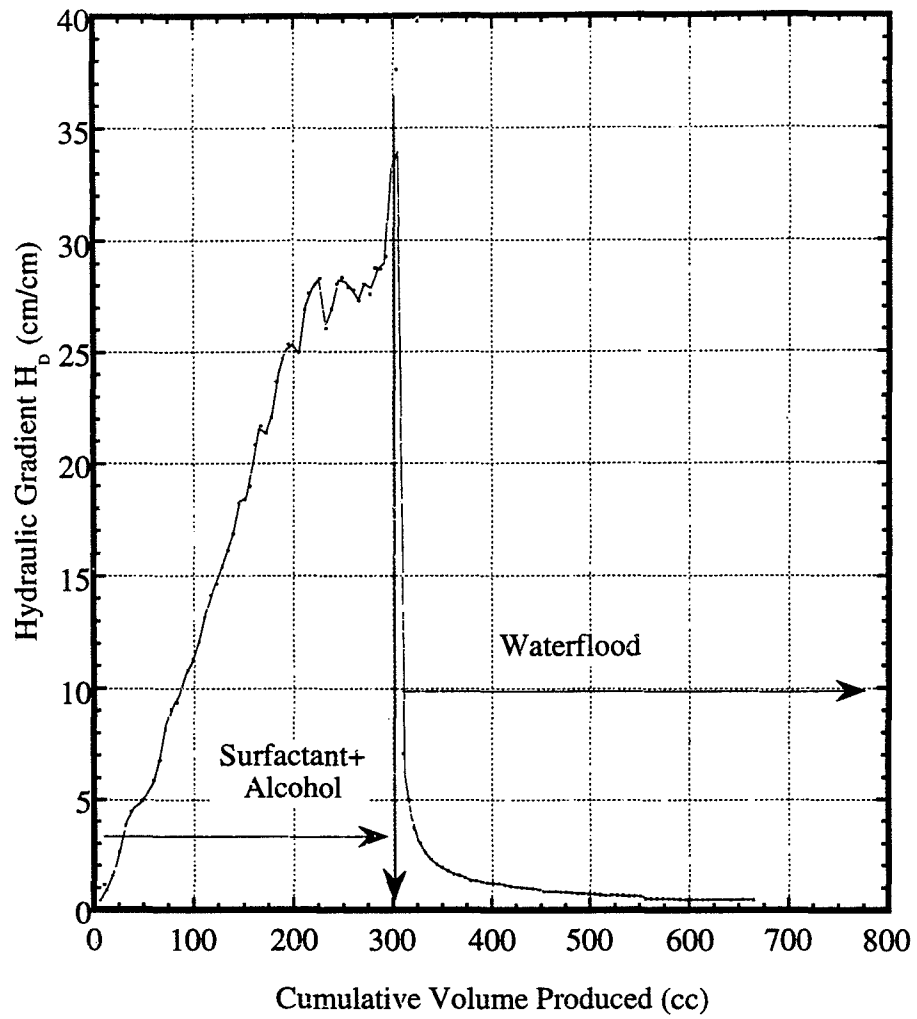


Figure 8.50: Hydraulic gradient across soil column during surfactant flood and post surfactant waterflood, experiment DW#5.

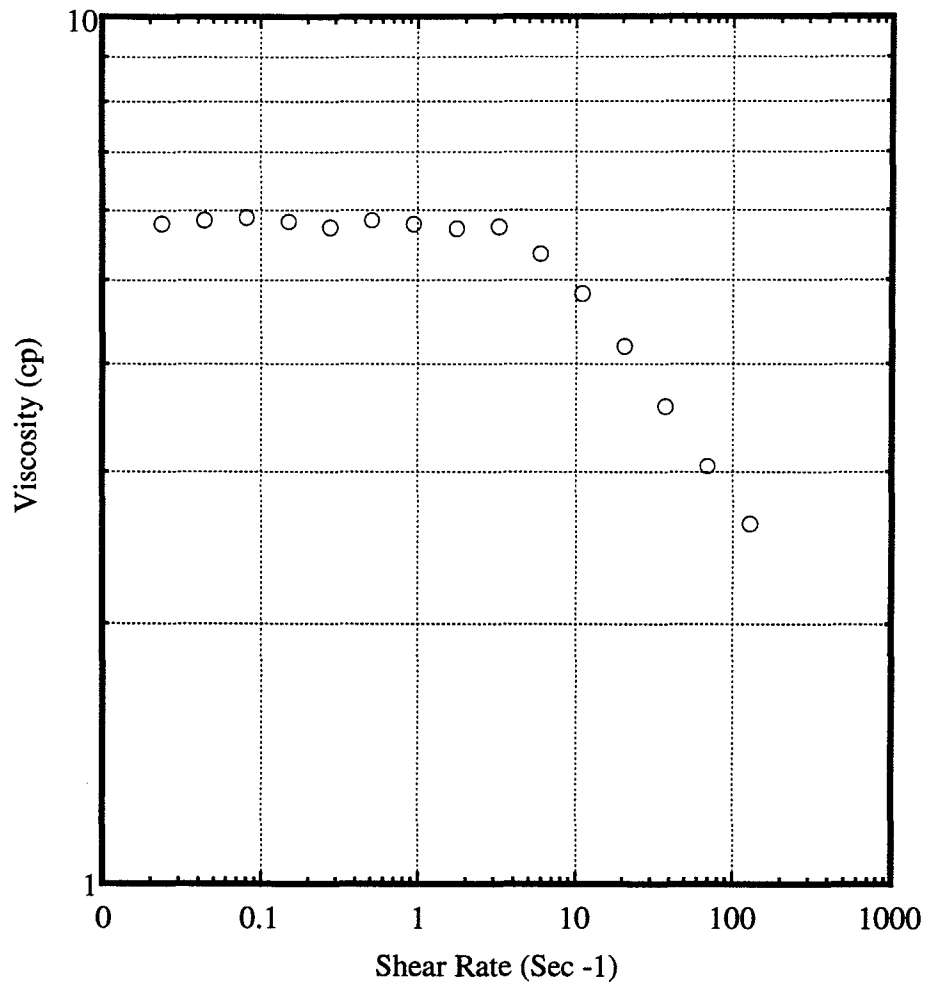


Figure 8.51: Viscosity of aqueous surfactant solution, experiment DW#5.

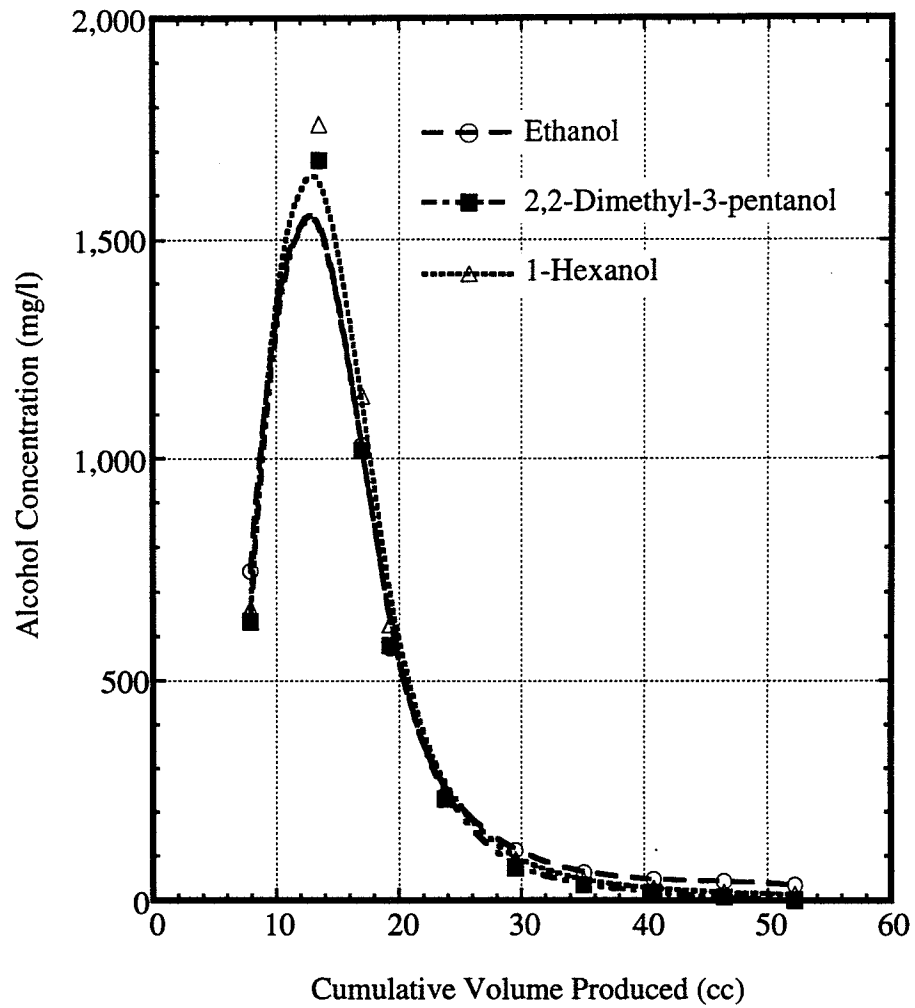


Figure 8.52: Final tracer concentration histories, experiment DW#5.

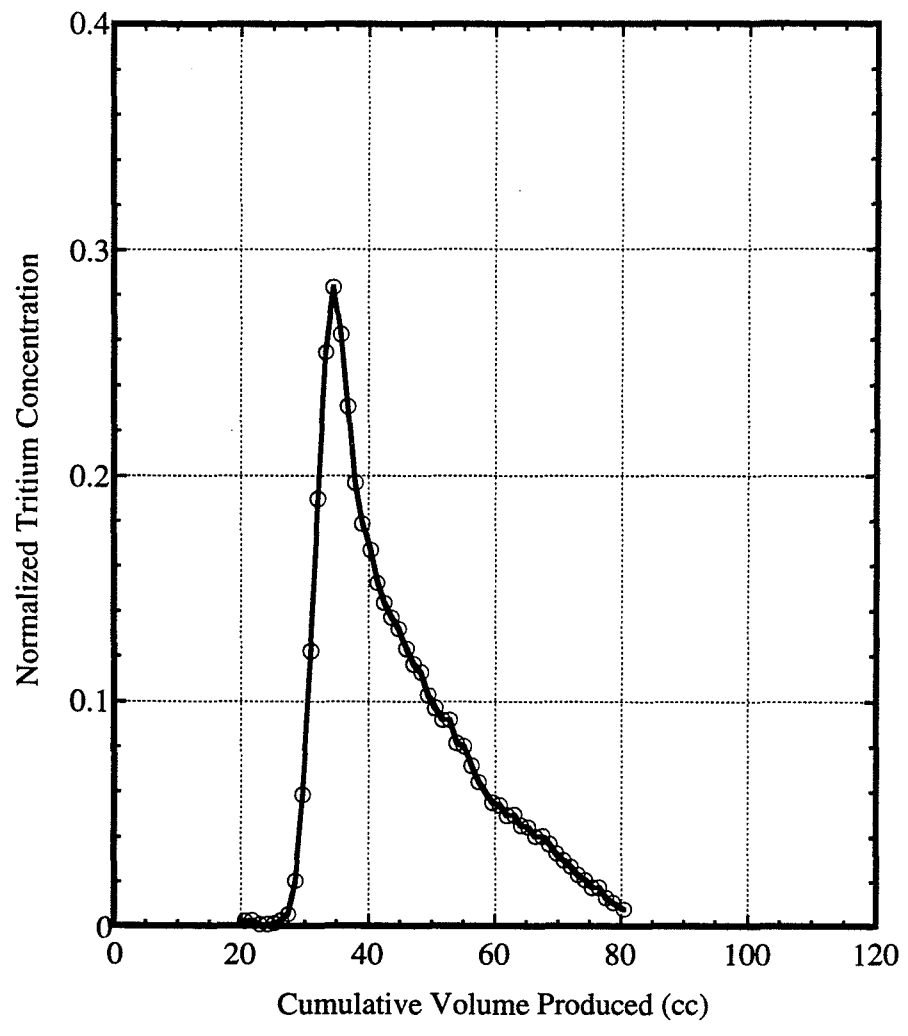


Figure 8.53: Initial tracer concentration history, experiment JP4#2.

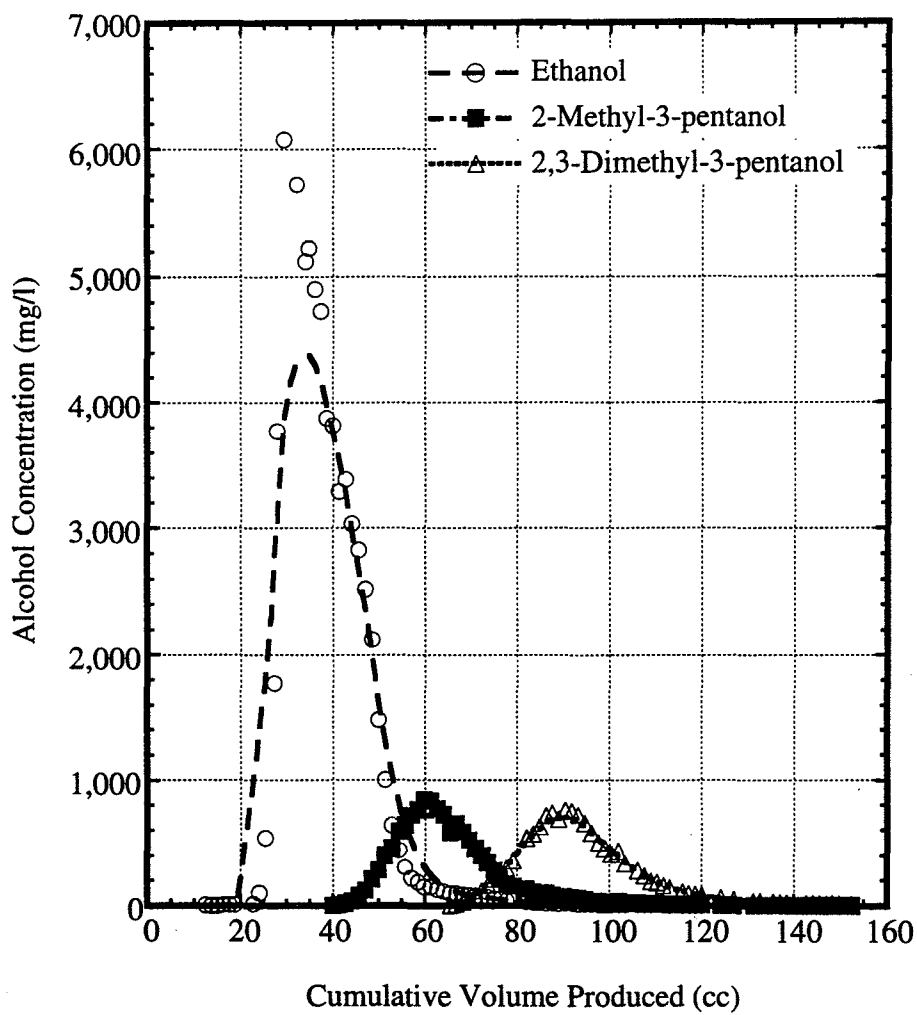


Figure 8.54: Tracer concentration histories at residual JP4 saturation, experiment JP4#2.

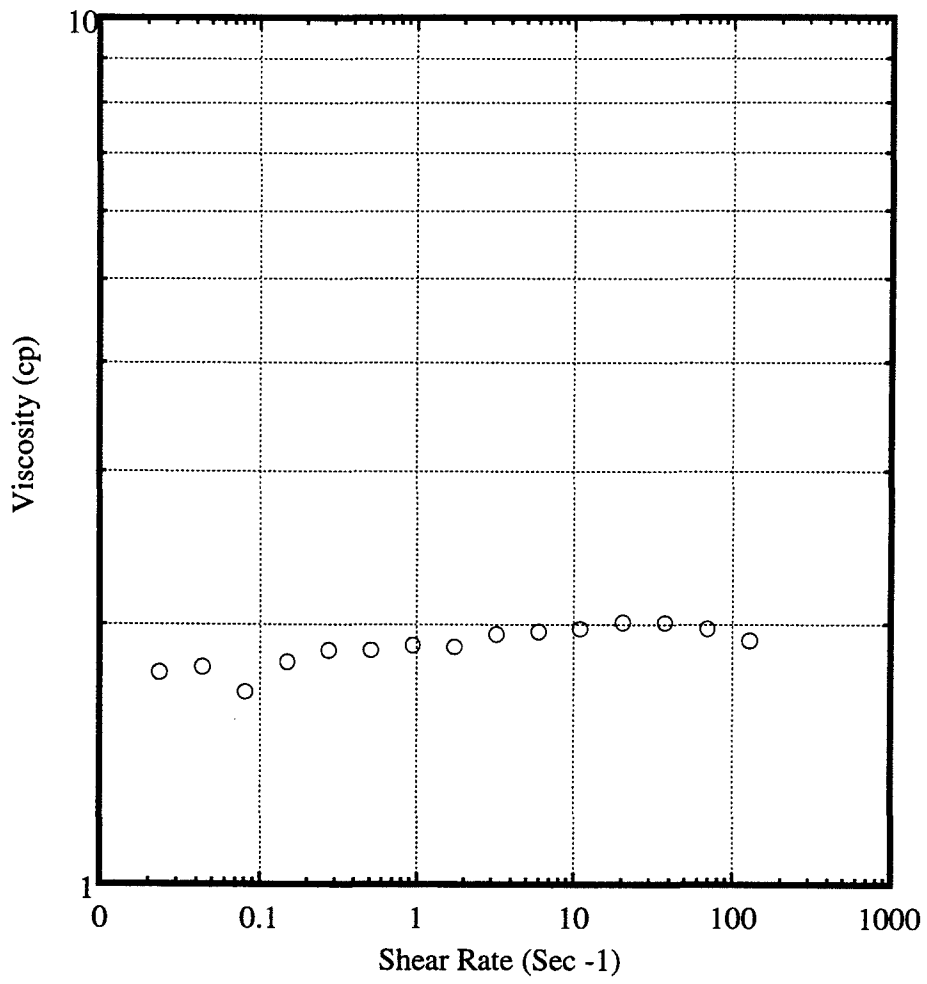


Figure 8.55: Viscosity of aqueous surfactant solution, experiment JP4#2.

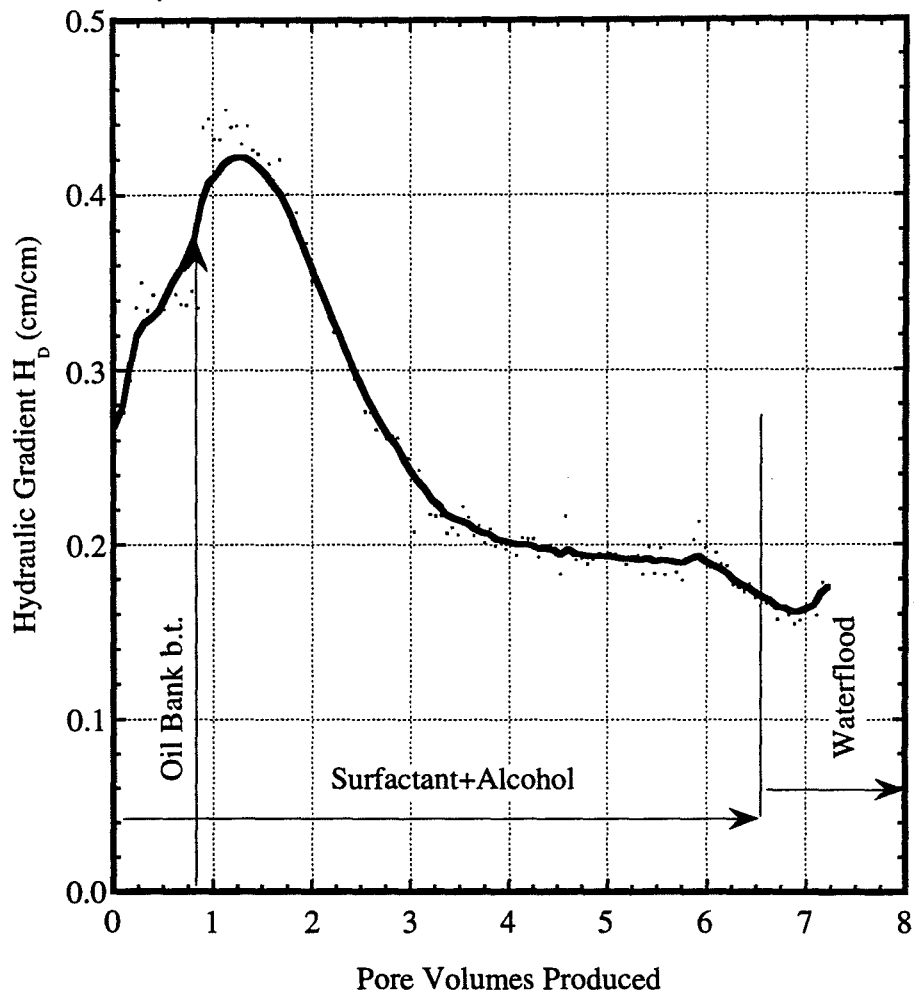


Figure 8.56: Hydraulic gradient across soil column during surfactant flood and post surfactant waterflood, experiment JP4#2.

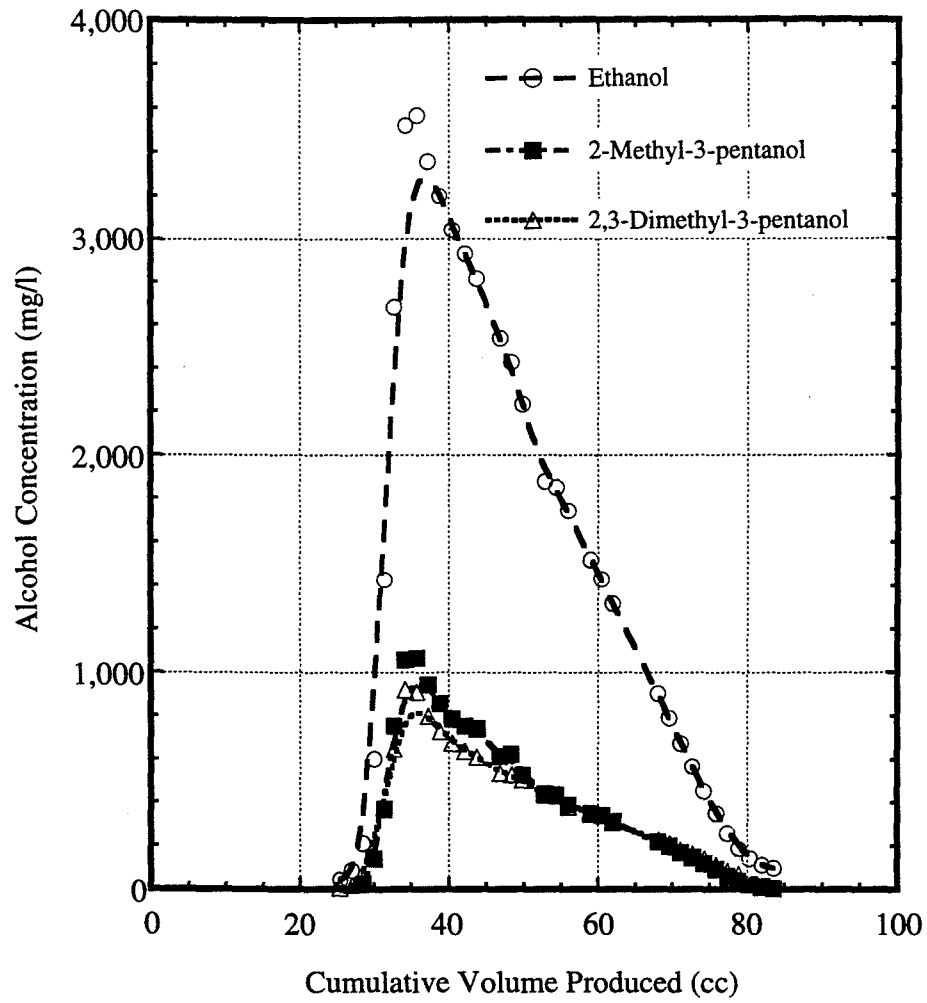


Figure 8.57: Final tracer concentration histories, experiment JP4#2.

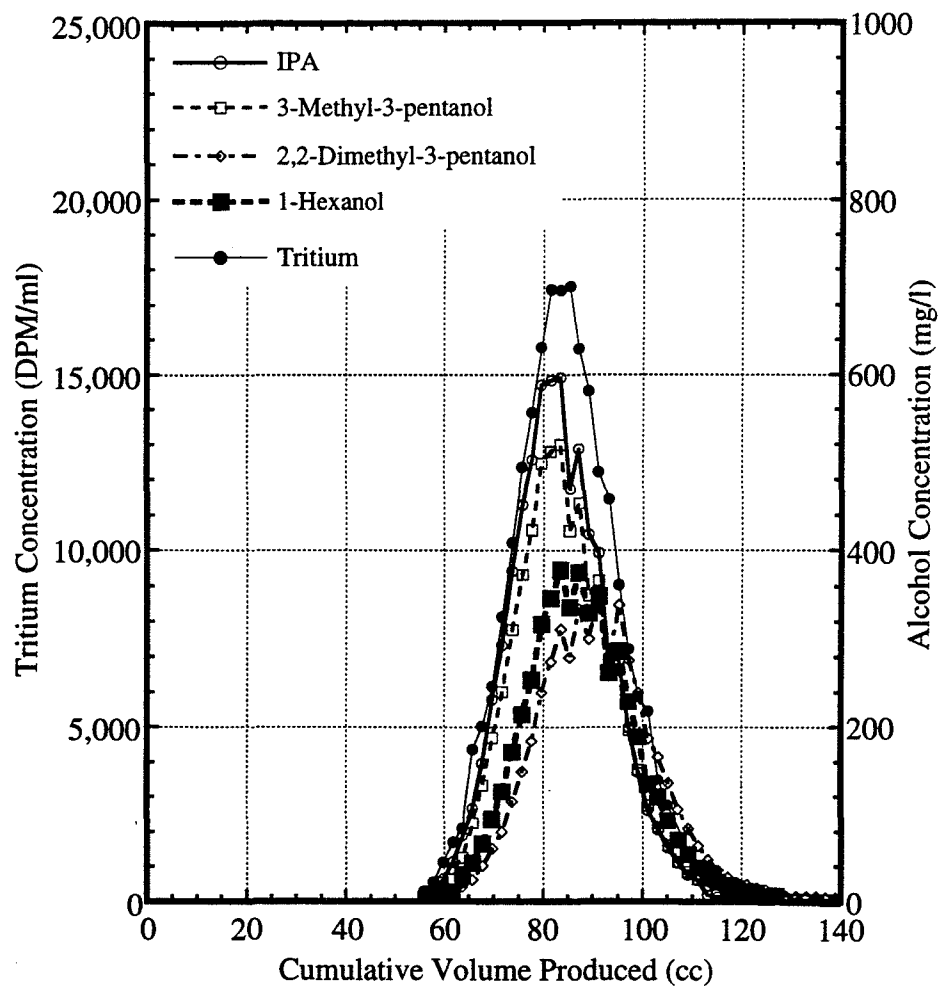


Figure 8.58: Initial tracer concentration histories, experiment HILLOU2#3.

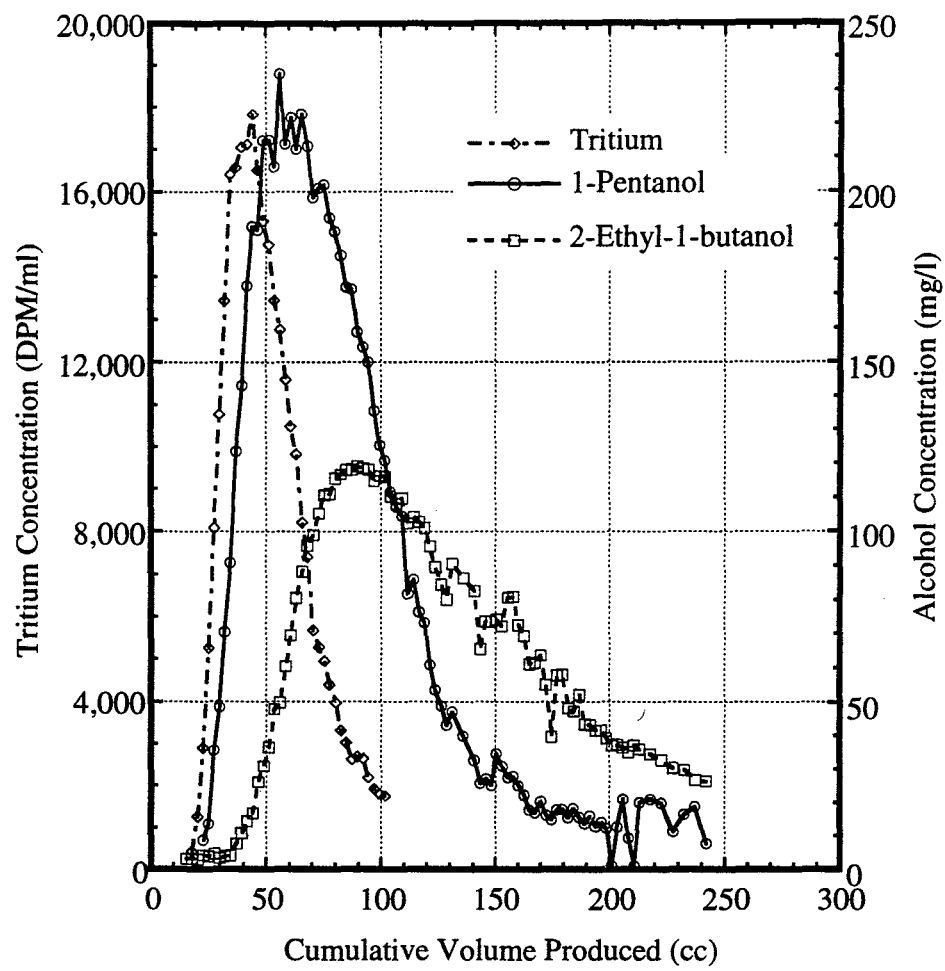


Figure 8.59: Initial tracer concentration histories, experiment HILLOU2#5.

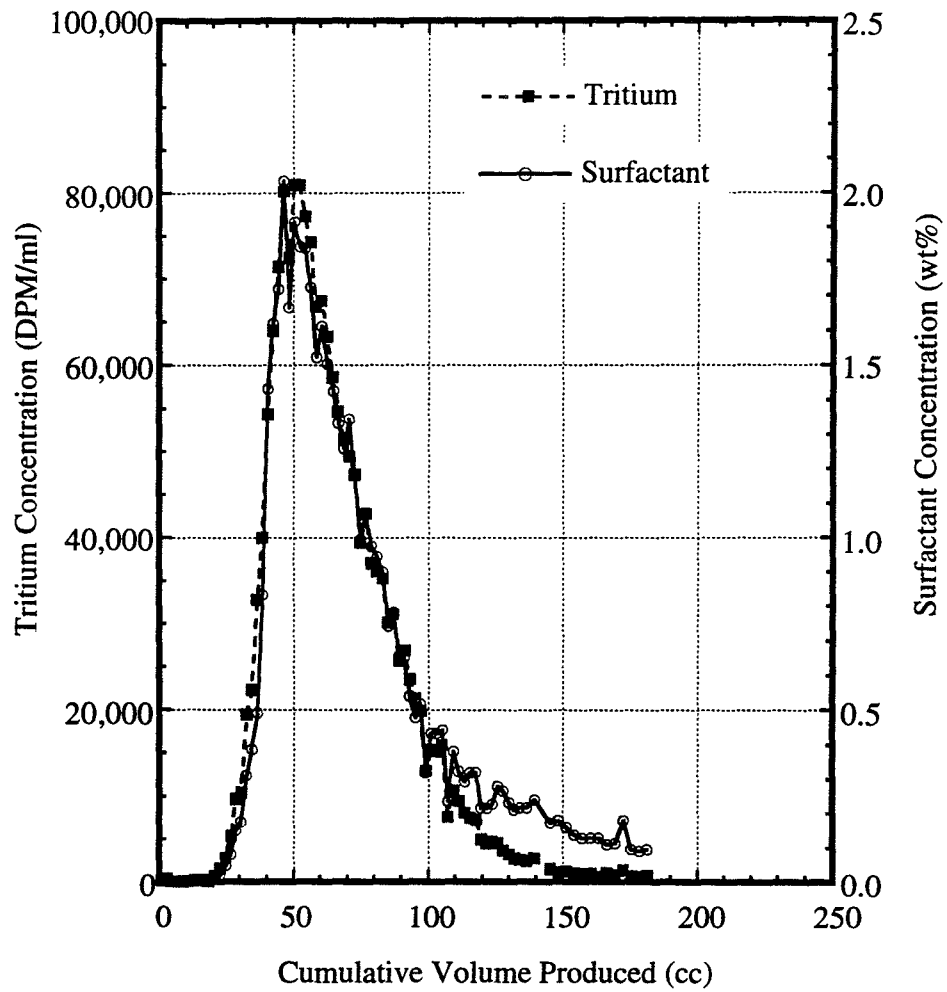


Figure 8.60: Comparison of tritium and surfactant concentration histories, experiment HILLOU2#5.

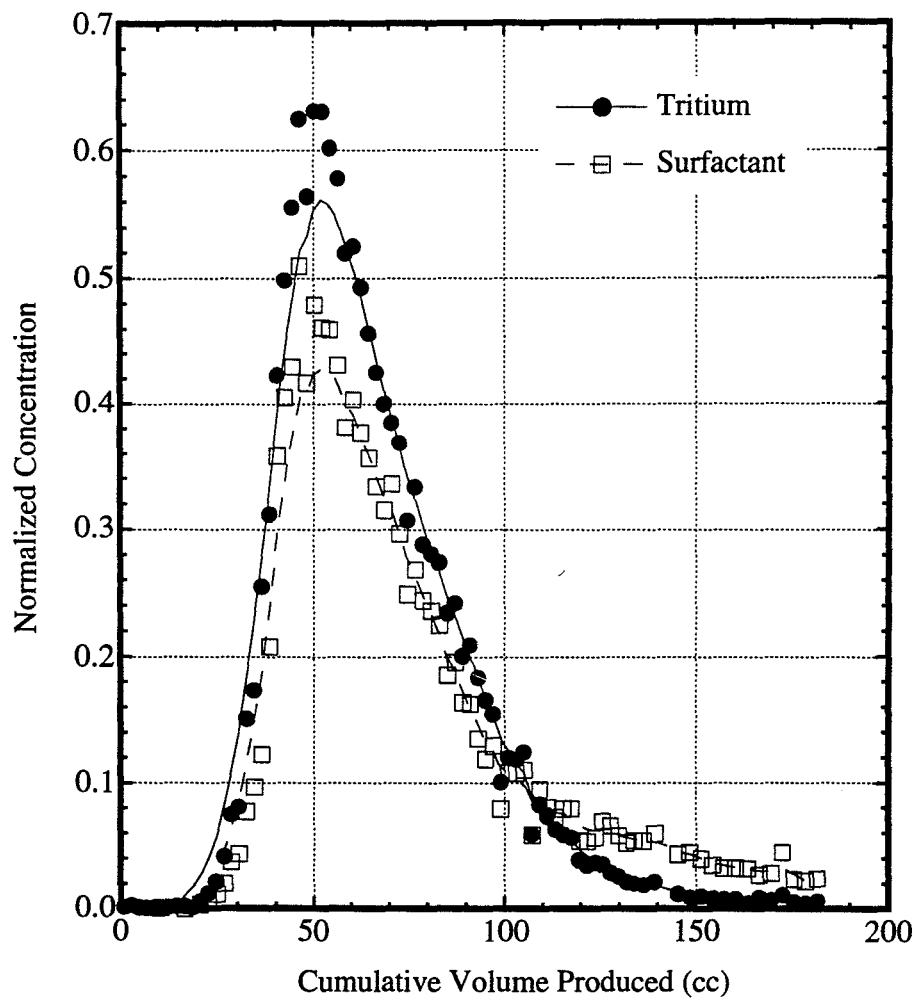


Figure 8.61: Comparison of normalized tritium and normalized surfactant concentration histories, experiment HILLOU2#5.

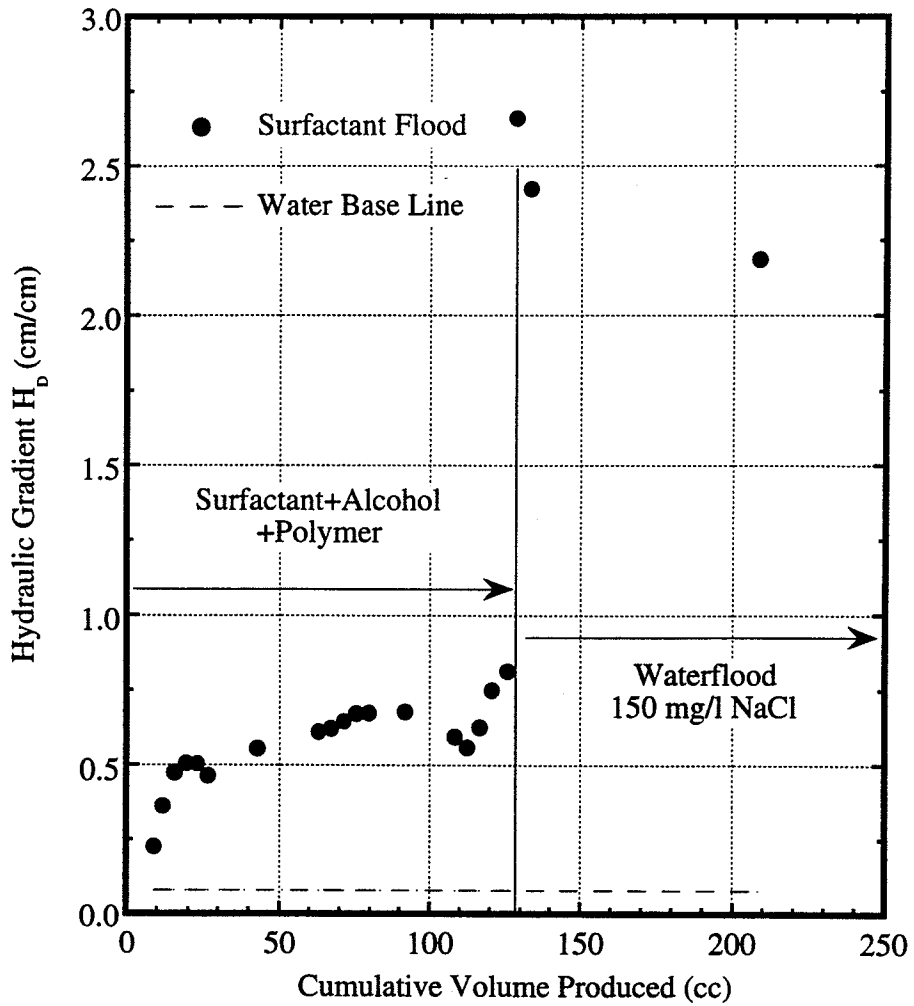


Figure 8.62: Hydraulic gradient across soil column during second surfactant flood and post surfactant waterflood, experiment HILLOU2#5.

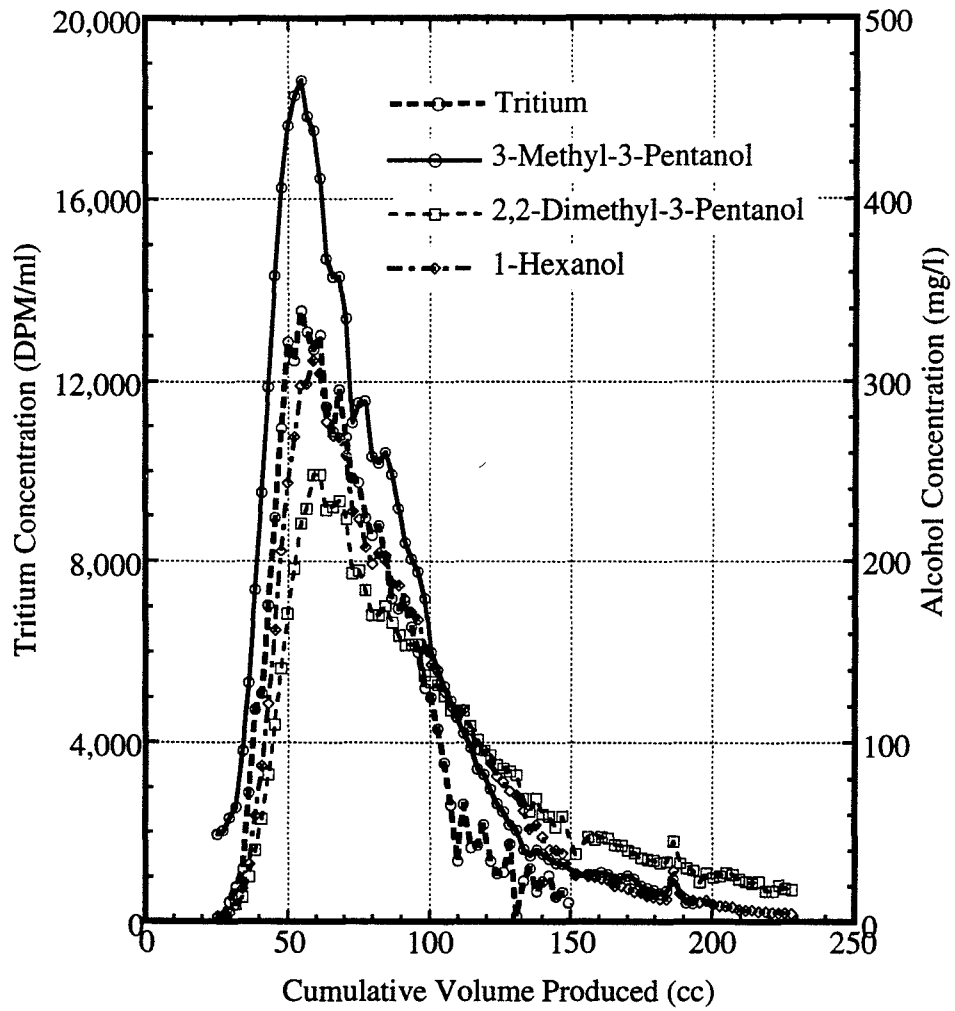


Figure 8.63: Final tracer concentration histories, experiment HILLOU2#5.

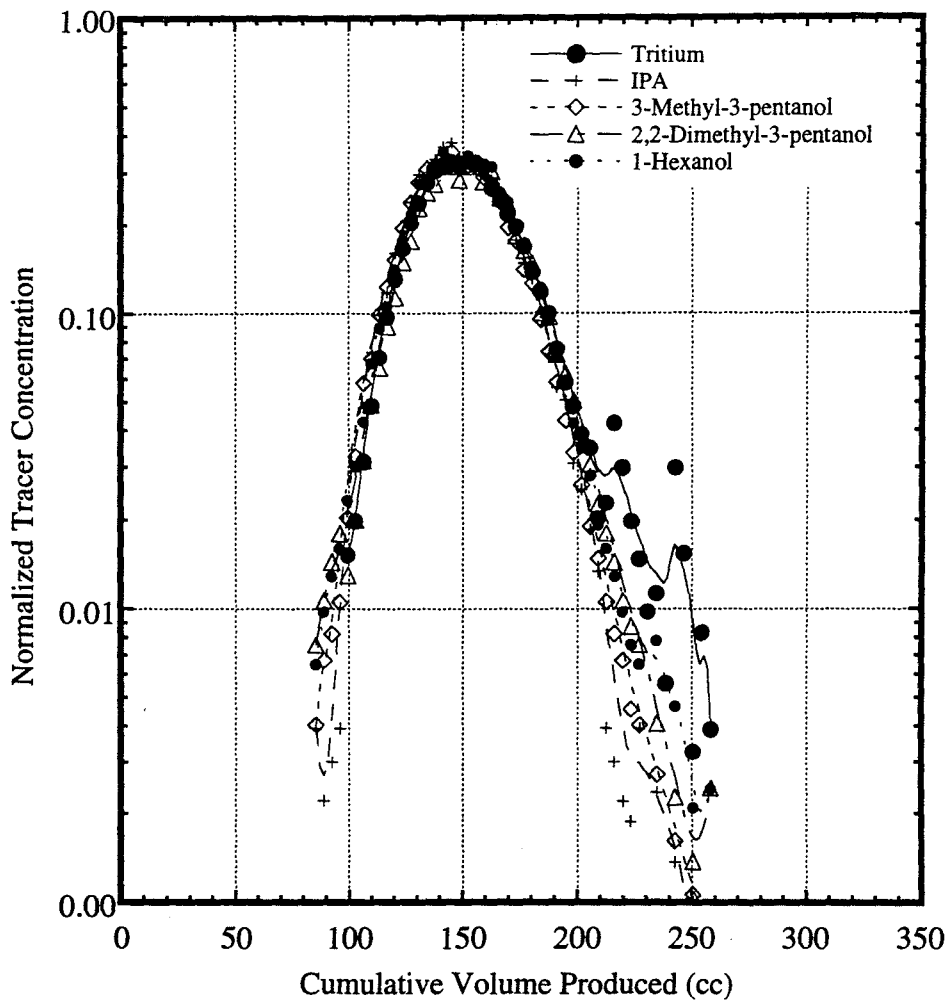


Figure 8.64: Initial tracer concentration histories, experiment HILLOU2#7.

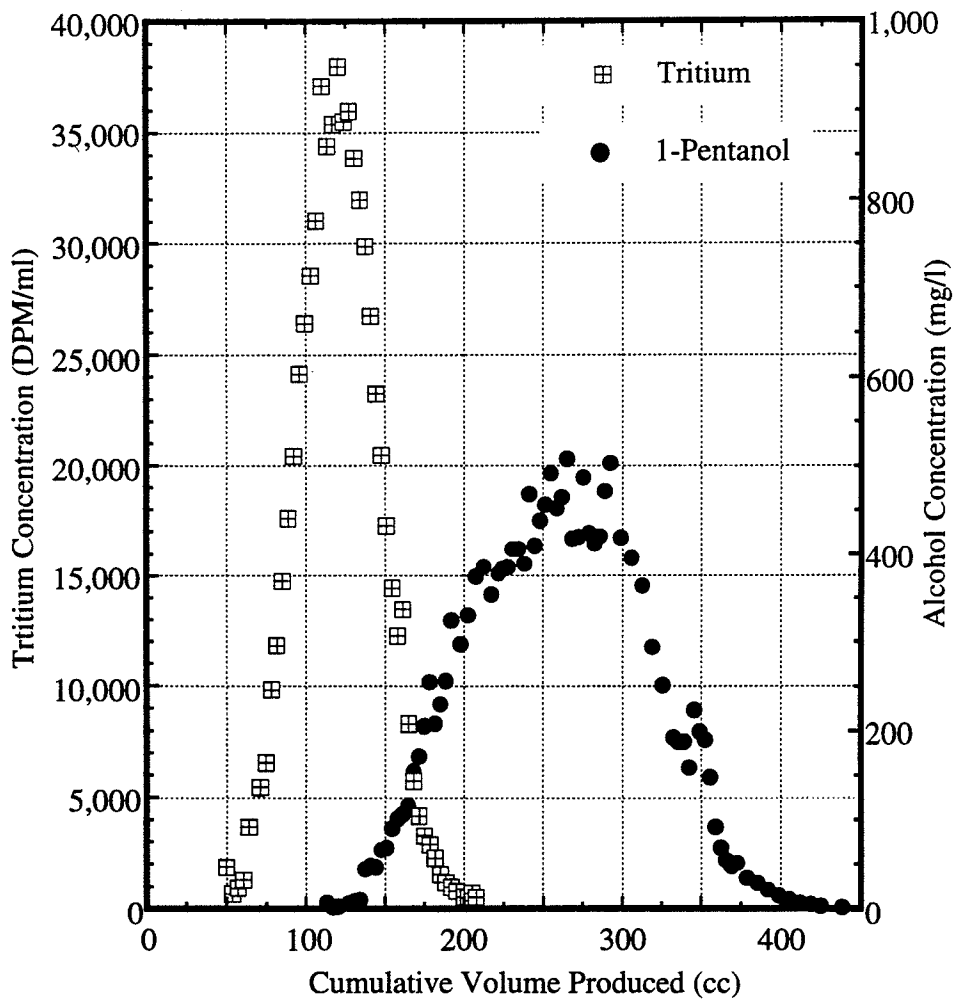


Figure 8.65: Tracer concentration histories at residual DNAPL saturation, experiment HILLOU2#7.

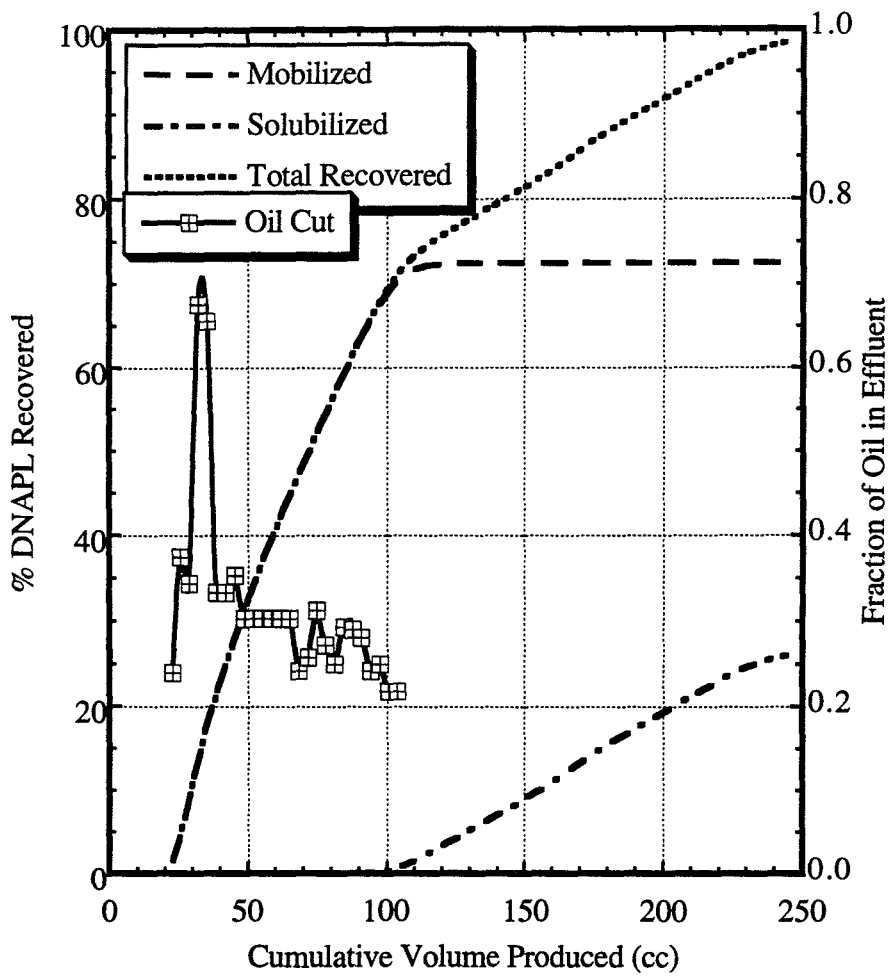


Figure 8.66: Plot showing contaminant recovery mechanisms and fraction of DNAPL produced in effluent during surfactant flooding, experiment HILLOU2#7.

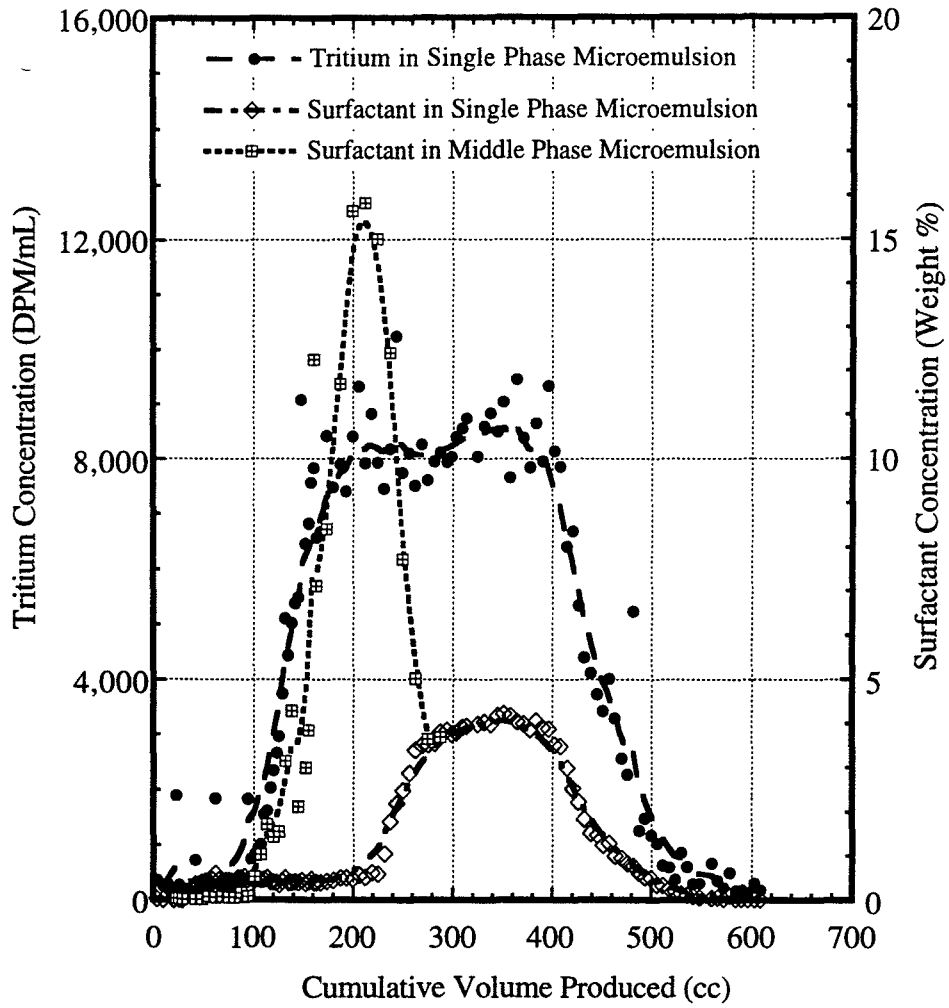


Figure 8.67: Comparison of tritium and surfactant concentration histories, experiment HILLOU2#7.

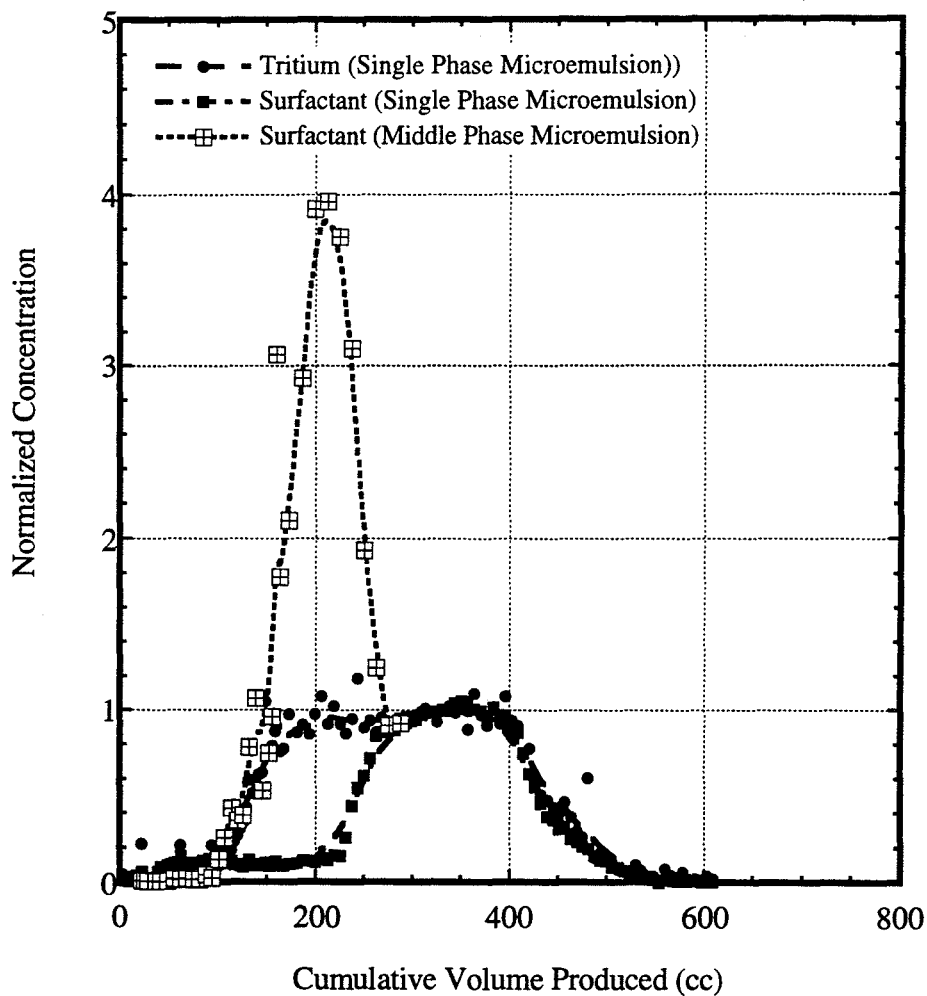


Figure 8.68: Normalized concentration histories of tritium and surfactant during surfactant and post surfactant polymer flood, experiment HILLOU2#7.

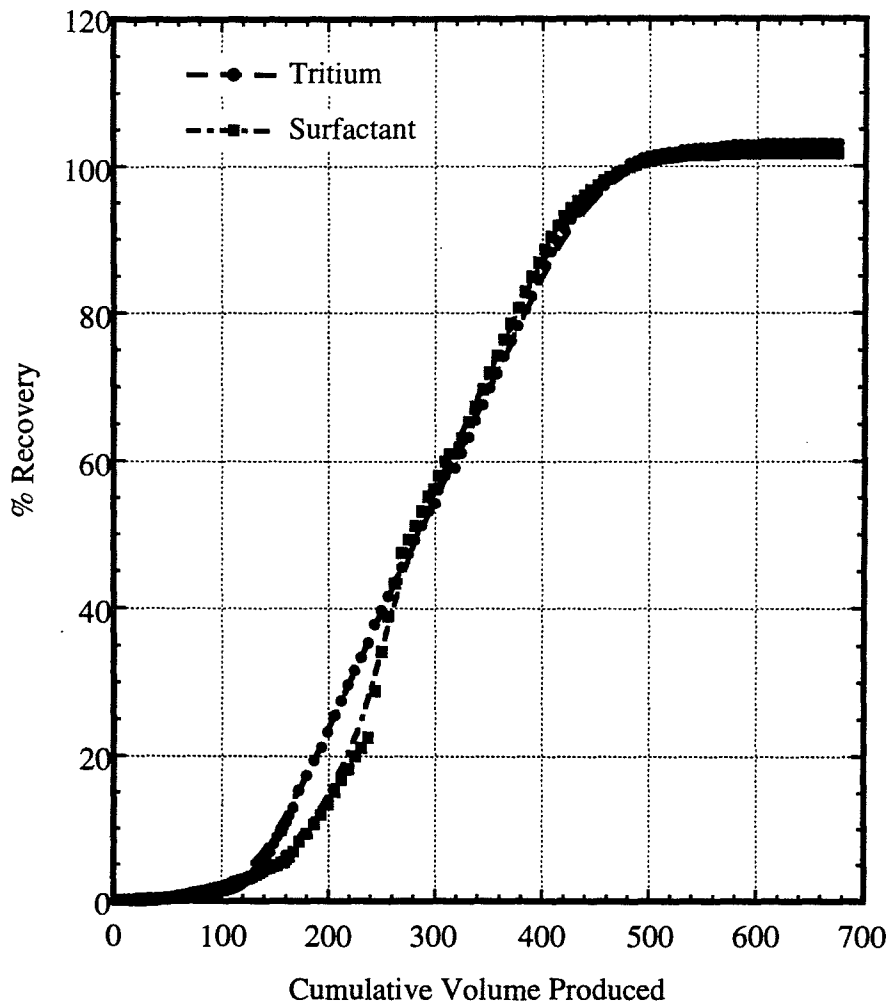


Figure 8.69: Tritium and surfactant recoveries during surfactant flood and post surfactant polymer flood, experiment HILLOU2#7.

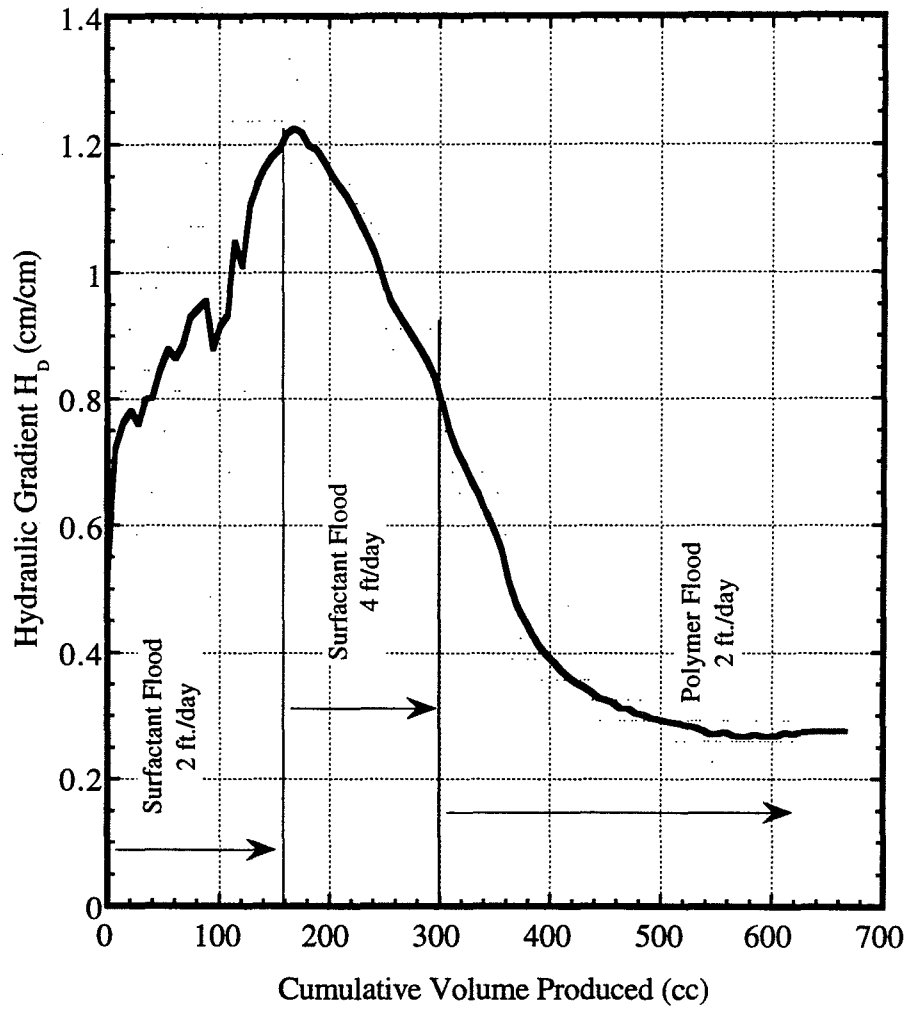


Figure 8.70: Hydraulic gradient across soil column during surfactant flood and post surfactant waterflood, experiment HILLOU2#7.

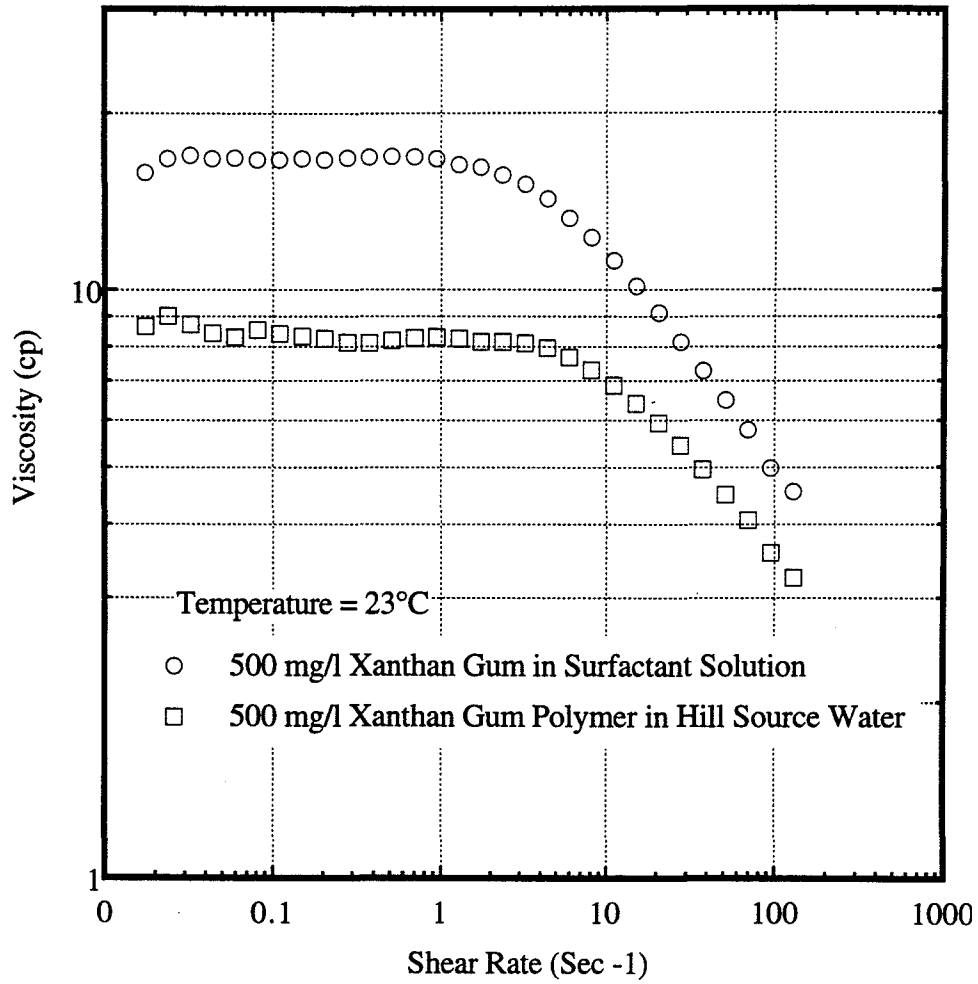


Figure 8.71: Viscosity of aqueous surfactant solution and polymer solution, experiment HILLOU2#7.

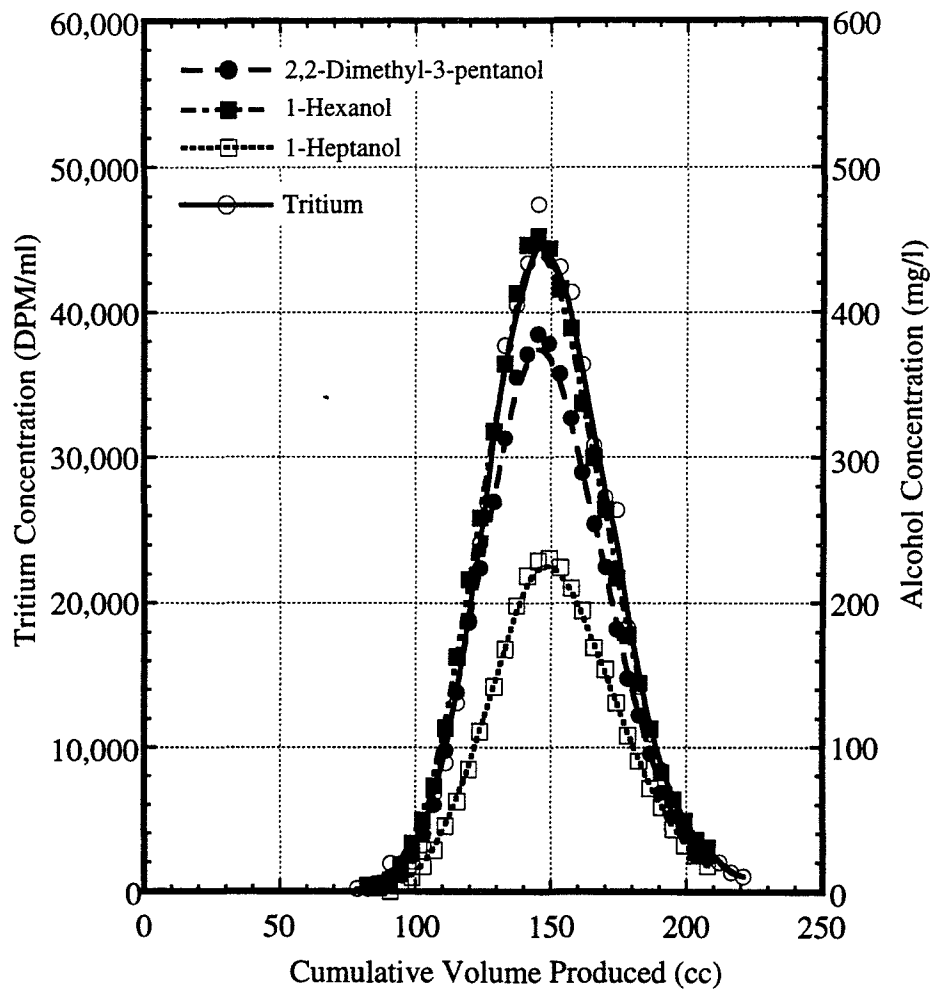


Figure 8.72: Final tracer concentration histories, experiment HILLOU2#7.

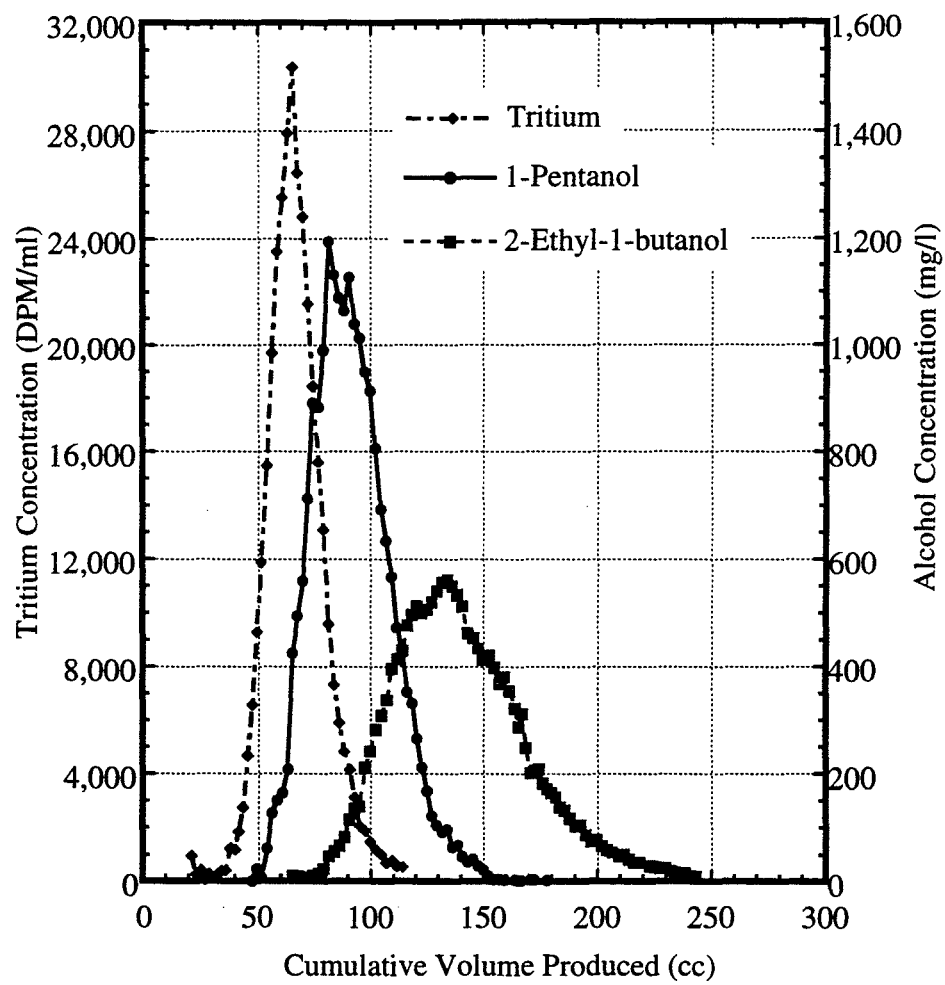


Figure 8.73: Initial tracer concentration histories, experiment HILLOU2#8.

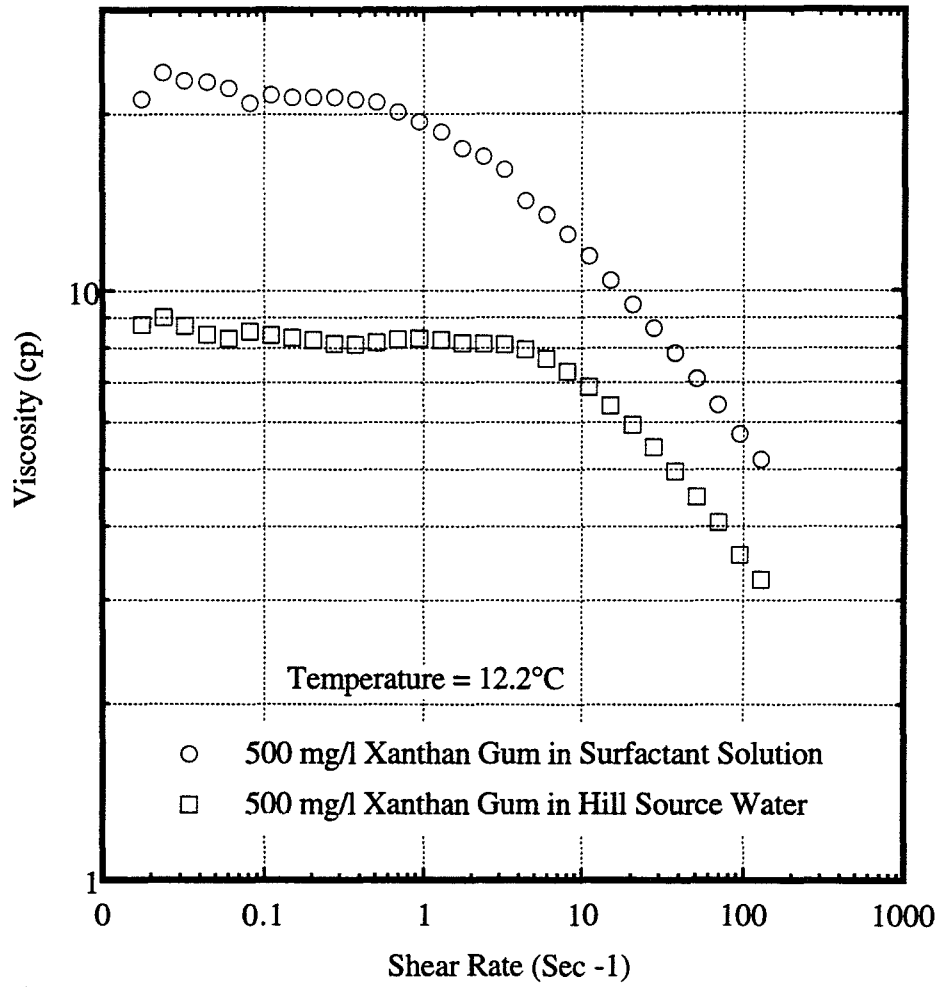


Figure 8.74: Viscosity of aqueous surfactant solution and polymer solution, experiment HILLOU2#8.

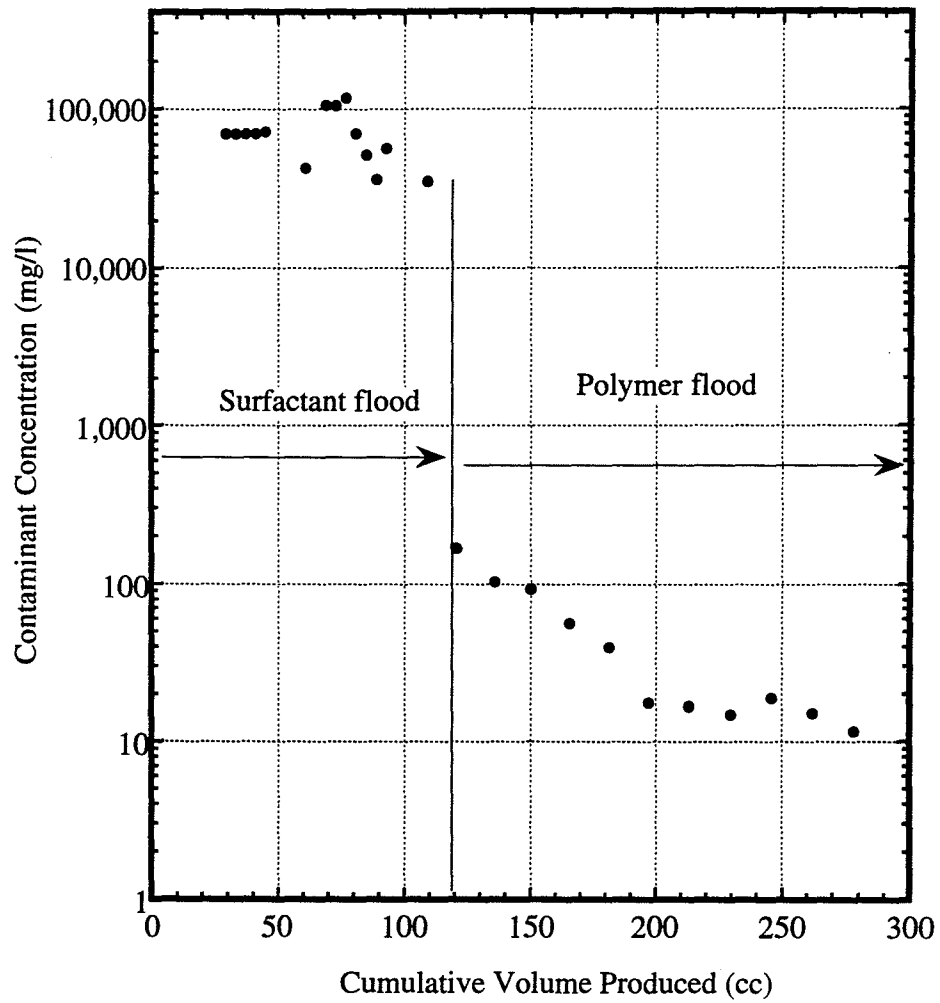


Figure 8.75: Hill Contaminant concentration history during surfactant flushing, experiment HILLOU2#8.

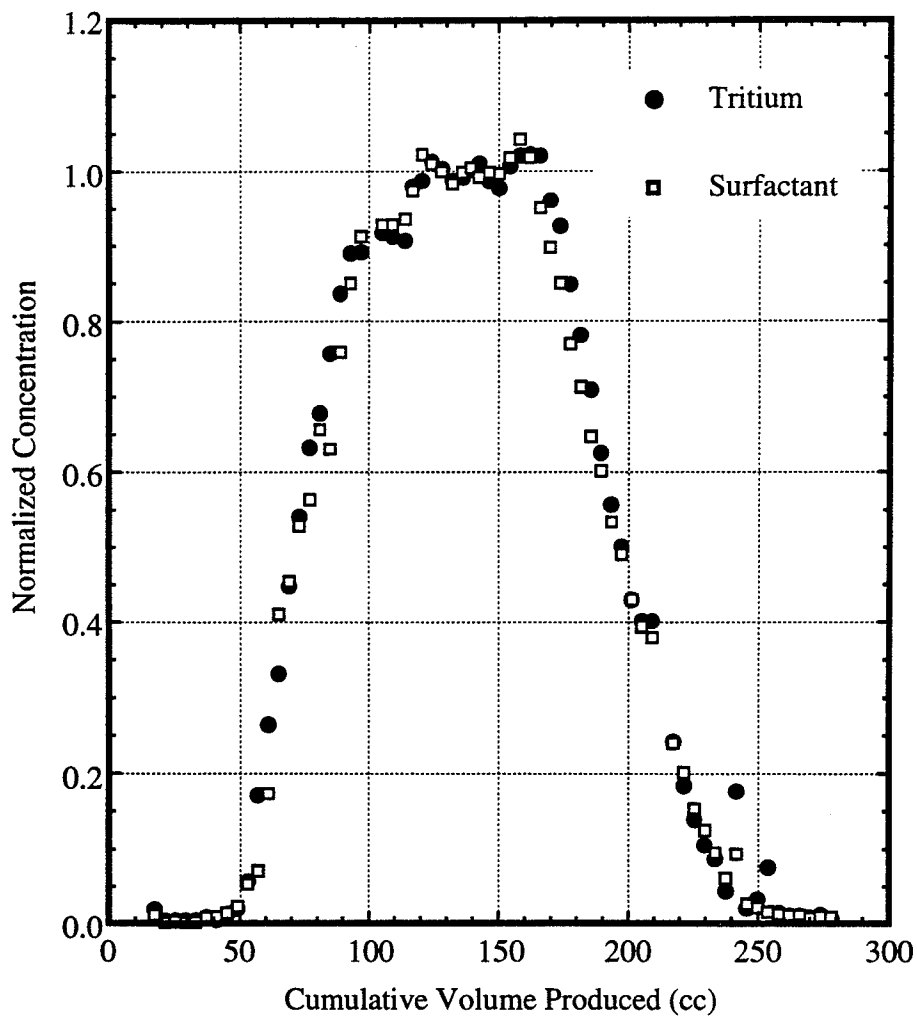


Figure 8.76: Comparison of normalized tritium and normalized surfactant concentration histories, experiment HILLOU2#8.

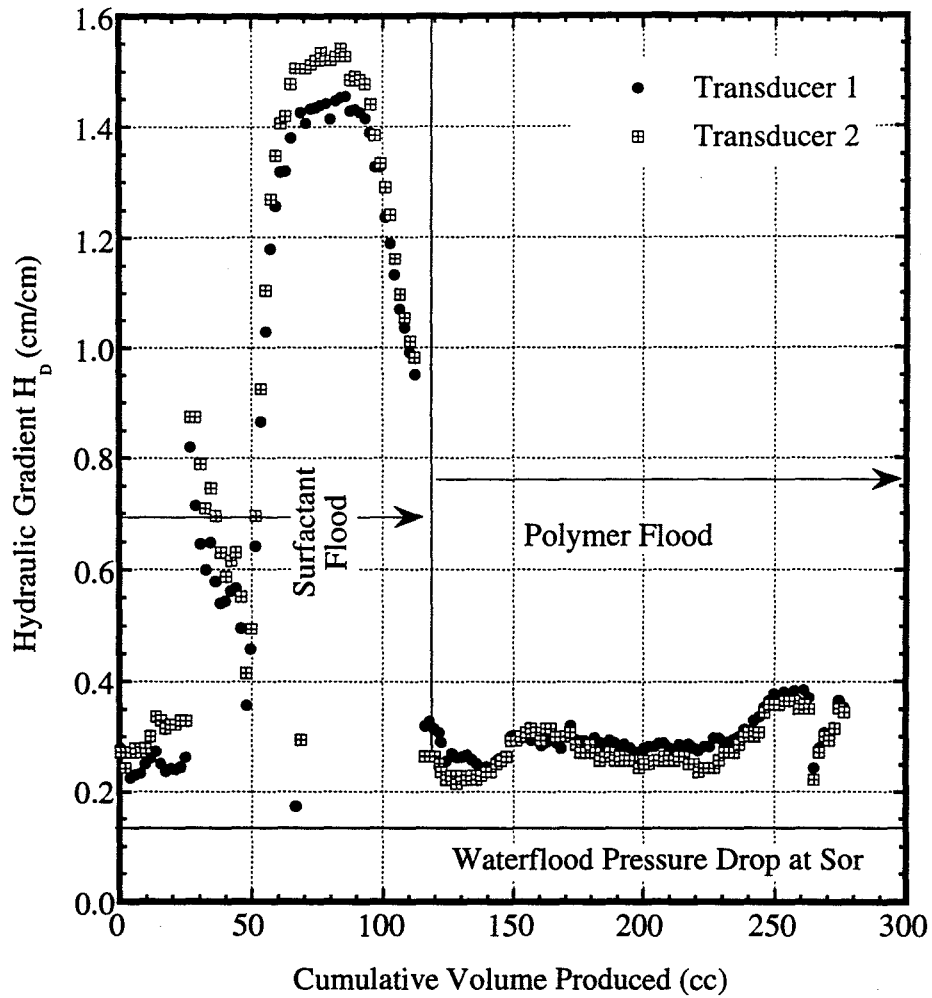


Figure 8.77: Hydraulic gradient across soil column during surfactant flood and post surfactant waterflood, experiment HILLOU2#8.

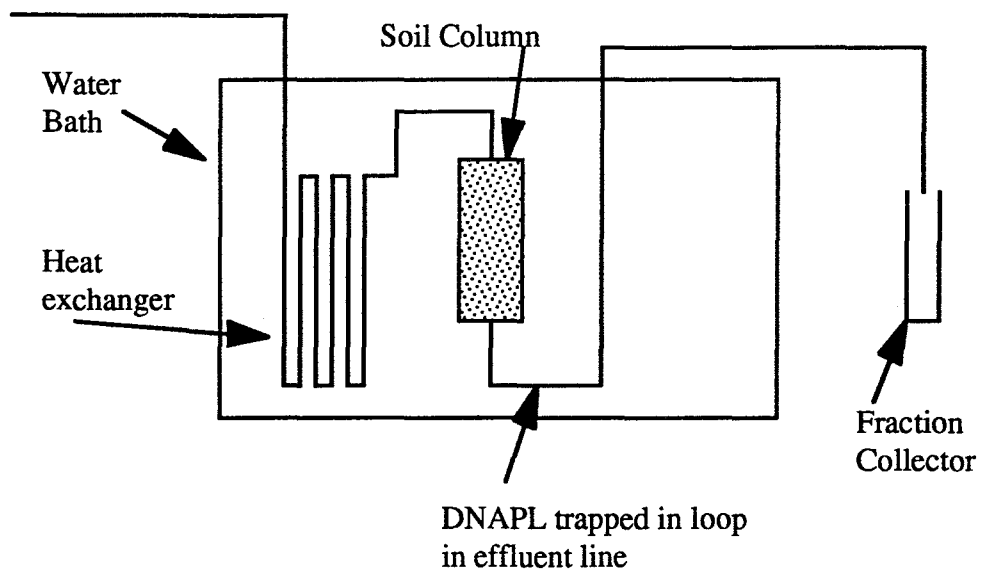


Figure 8.78: Figure showing the artifact that caused high hydraulic gradients in experiment HILLOU2#8.

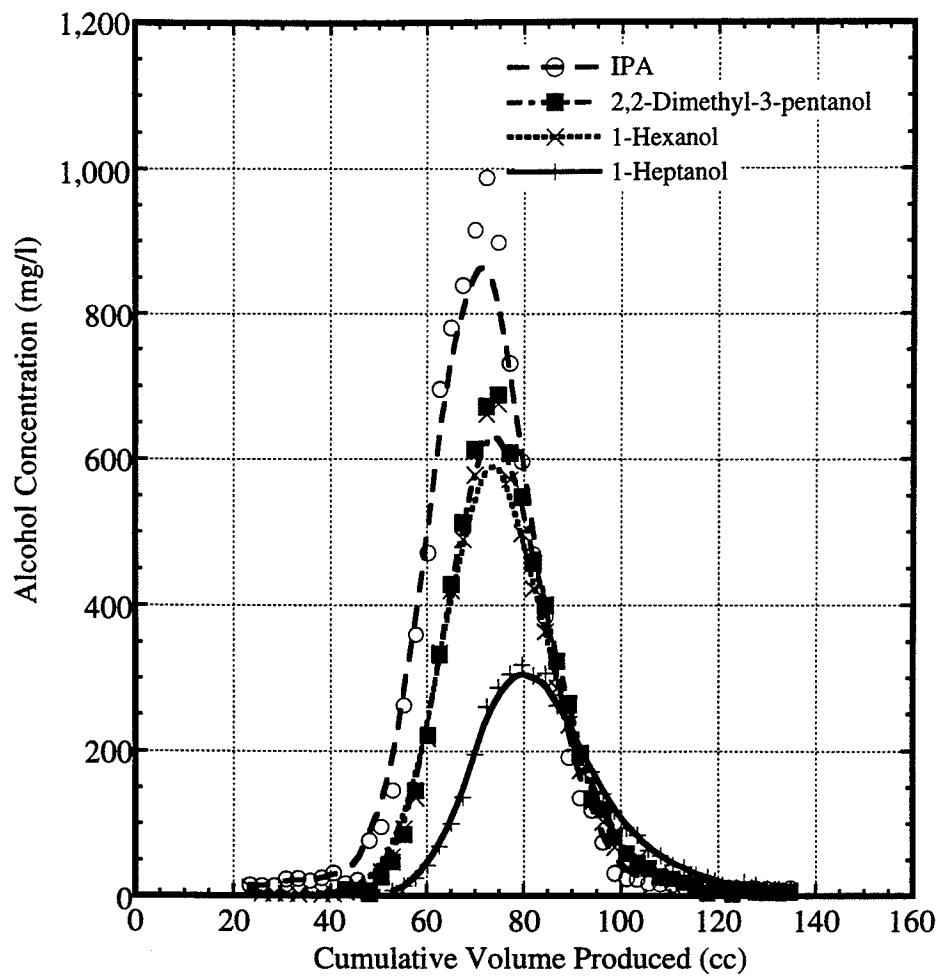


Figure 8.79: Final tracer concentration histories, experiment HILLOU2#8.

Chapter 9: Column Experiments: Discussion

A description of all the column experiments, column experiment results and discussion of experimental results from column experiments were presented in the previous Chapter. In this Chapter, a section on error analysis has been added to estimate the accuracy of experimental measurements. A discussion of interfacial tensions between the excess NAPL and surfactant is also made in this Chapter.

9.1 ERROR ANALYSIS

One of the important contributions of this work was the development of laboratory techniques and expertise for development of the partitioning tracer technology for estimation of NAPL and performance assessment of surfactant remediation. In order to validate this new technology as a viable option for estimation of NAPL saturation, a thorough error analysis of all experimental measurements was made. This was carried out to improve estimation of parameters required for analysis of partitioning tracer test data (for e.g. partition coefficients).

Two terms are widely used in discussions of reliability of data, precision and accuracy. Precision describes the reproducibility of results i.e. agreement between numerical values for two or more measurements. Accuracy describes the correctness of the experimental result. In trying to estimate residual NAPL saturations using partitioning tracers an error analysis had to be performed on various experimentally measured parameters.

In order to estimate residual NAPL saturation using partitioning tracers, partition coefficients of alcohols have to be measured. This can be done by using

static partition coefficient tests and dynamic partition coefficient tests (Chapter 7). Both these measurements are affected by GC errors, volume measurement errors etc. Similarly for estimation of pore volume, errors in weight measurement and density measurement etc. would cause erroneous results.

In the following sections the main sources of error in making residual saturation measurements will be discussed.

9.1.1 Gas Chromatograph Errors

GC errors can be broadly divided into two main areas:

1. GC errors in reproducibility
2. GC errors in making standards

The errors in reproducibility include errors in injection of samples into GC columns and errors in integration of GC chromatograms. This can be done by repeating GC analysis on one sample. For the Varian 3400 GC, the reproducibility was $\pm 3.5\%$ of the sample concentration. The detection limit was 10 mg/l. For the SRI GC, the reproducibility was $\pm 3.0\%$.

GC errors in making standards were attributable to the errors in mixing up weights of respective alcohols, weight of water and density of the tracer solution. The calculations are presented in Appendix A. The errors in making up standards were about $\pm 2.6\%$. The total error in the GC measurements is the sum of the reproducibility errors and errors in making standards. Hence, the total error in GC measurements was 6.1%.

9.1.2 Errors in Pore Volume Measurement

Pore volume estimation based on mass balance has been discussed in Chapter 4. The formula for determining pore volume is,

$$V_p = \frac{W_{\text{sat}} - W_{\text{dry}}}{\rho_w} \quad (4.5)$$

The errors are in measuring the weights of the dry and saturated column and density of the saturating water. The calculations are presented in Appendix A. The average error in pore volume estimation was 0.5%.

Pore volume can also be estimated using tracers. An error analysis was carried out by comparing the standard deviation between initial pore volume estimates based on tracers and estimates based on mass balance. The pore volume estimates based on tracers were within $\pm 3.5\%$ of pore volume estimates based on mass balance.

9.1.3 Errors in Residual TCE Saturation Measurement

The residual TCE saturation in a contaminated soil column can be computed using;

$$S_N = \left(\frac{W_{\text{sn}} - W_{\text{sat}}}{\rho_N - \rho_w} \right) \frac{1}{V_p} \quad (4.10)$$

The errors are in measuring the weights of the dry and saturated column and density of the saturating water, density of NAPL and error in pore volume

estimation. The calculations are presented in Appendix A. The average error in pore volume estimation was 2.5%.

9.1.4 Errors in Static Partition Coefficient Measurement

The static partition coefficient has been defined in Chapter 4 as;

$$K_i = \frac{C_{i,NAPL}}{C_{i,Water}} \quad (4.23)$$

K_i = partition coefficient of tracer species 'i'

$C_{i,NAPL}$ = concentration of tracer species 'i' in the nonaqueous phase at equilibrium.

$C_{i,Water}$ = concentration of tracer species 'i' in the initial water before equilibration with the NAPL

In all the laboratory work, the static partition coefficient was calculated from the following formula;

$$K_i = \frac{V_W}{V_N} \left(\frac{C_{i,I}}{C_{i,Water}} - 1 \right) \quad (4.15)$$

V_W = the volume of the aqueous phase

$C_{i,I}$ = the concentration of tracer component 'i' in the injected tracer.

The errors are in measuring the volumes of water and NAPL and GC errors in measurement of concentration. The calculations are presented in Appendix A. The average error in the static partition coefficients is estimated to be about 12%.

9.1.5 Error in Saturation Estimation

In order to estimate errors in saturation using partitioning tracers, a total of eleven experiments were evaluated. In these experiments, the residual NAPL saturations estimated using partitioning tracer results were compared with residual NAPL saturations using mass balance measurements. Results from three experiments were taken from Shotts (1996), results from one from Edgar (1997) and one from Ooi (1998) in addition to the six experiments from this study for a total of eleven experiments. The residual NAPL saturation was calculated using the following formula.

$$S_N = \frac{\bar{V}_2 - \bar{V}_1}{V_p \cdot K_{N,w}^2} \quad (4.33)$$

A standard deviation of 7.0% was observed between the residual NAPL saturations based on mass balance and residual NAPL saturation based on partitioning tracers.

9.1.6 Estimation of Dynamic Partition Coefficients

If a known saturation is used to estimate the dynamic partition coefficient of the tracer as discussed in Chapter 7 using the following formula;

$$K_i = \frac{\bar{V}_p - \bar{V}_n}{V_p \cdot S_N} \quad (7.1)$$

The source of errors will include the errors in the experimental first temporal moments of the concentration and the errors in $V_N = V_p \cdot S_N$ but is still likely to be less than the average error in static partition coefficients of about 12%. This will be true if column experiments have been done with long enough residence times, good mass balance, no sampling mistakes and so forth.

A refined estimate of the partition coefficients can be made by plotting the static and dynamic values as in Figure 9.1. In an ideal situation with zero errors, both static and dynamic partition coefficients should plot on the same 45° straight line.

In Figure 9.1, a plot showing the comparison of static partition coefficients and dynamic partition coefficients for TCE is presented. In general an excellent match between the static partition coefficients and dynamic partition coefficients was observed. The measured value for the static partition coefficient of 2,3-dimethyl-2-butanol was 5.2. The dynamic partition coefficients were observed to vary between 6.2 and 6.9. Similarly a dynamic partition coefficient of 100 was estimated for 1-heptanol. This was based on 2-D sand tank experiments conducted by Kostarelos (1997). In this experiment an estimate of TCE saturation based on mass balance could not be obtained since the tank is too big to weigh on a mass balance. This could account for error in estimation of dynamic partition coefficients. However in a later experiment conducted by Edgar (1997), a dynamic

partition coefficient of 153.7 was calculated. The standard deviation between the static partition coefficients and dynamic partition coefficients was 6.5%.

Similar plots showing the comparison between static partition coefficients and dynamic partition coefficients for several alcohols with JP4, Hill OU1 NAPL and Hill OU2 DNAPL are presented in Figures 9.2, 9.3 and 9.4. In general, an excellent match between static partition coefficients and dynamic partition coefficients was observed within experimental error. If a good match between static partition coefficients and dynamic partition coefficients is not observed, more experimental measurements have to be carried out to check the validity of previous results. For example, the column tests could be repeated at rates to check for adequate residence time to reach local partitioning equilibrium.

Based on this analysis, the best estimate of partition coefficients were estimated for several alcohols with TCE. These results are given in Table 9.1.

9.2 TRACER ADSORPTION

An attempt was made to quantify tracer adsorption in several soil column experiments. These experiments are experiment DW#5 in uncontaminated Ottawa sand and experiment HILLOU2#7 in uncontaminated Hill field soil, experiment PPG#5 (Shotts, 1996) in field soil from PPG site at Lake Charles Louisiana, experiment Plant 4#1 in field soil from AFB Plant 4 at Fort Worth (Shotts, 1996). The retardation due to sorption by field soil can be defined by (Fetter, 1993),

$$R_f = 1 + \frac{\rho_b}{\phi} K_d \quad (9.1)$$

Using IPA as the conservative tracer and the other tracers as partitioning tracers, the distribution coefficient can be measured. The distribution coefficient for several alcohols are summarized in Table 9.2. The measured values of K_d for all the soils are between 0.0001 and 0.002. For comparison the K_d of ethanol in Na-montmorillonite is on the order of 0.00015 cc/g (for a surface area of $0.6 \frac{m^2}{g}$, Schwarzenbach, *et al.*, 1993) and the K_d for tetrachloroethylene of 0.003 cc/g in porous silica (surface area of $0.6 \frac{m^2}{g}$, Schwarzenbach, *et al.*, 1993). Significantly different values for K_d in PPG soil were not observed for alcohols such as 1-heptanol and 2,2-dimethyl-3-pentanol.

The values of tracer adsorption computed from the R_f values vary between -100 $\mu\text{g/g}$ and 5,000 $\mu\text{g/g}$ (Table 9.3). This corresponds to a retardation factor of 1.028. The error in the first moment of the tracer measurements is of the order of $\pm 3.5\%$ and this corresponds to an adsorption of $\pm 8,500 \mu\text{g/g}$. The values of adsorption measured by all the experiments is less than 8,500 $\mu\text{g/g}$. Hence it can be concluded that there is negligible adsorption of alcohol tracers by the different types of soils studied in this work compared to the retardation caused by very small saturations of NAPL in the same soils.

9.3 SURFACTANT ADSORPTION

In order to quantify surfactant adsorption in Hill field soil, radiolabeled surfactant was used in experiments HILLOU2#5, HILLOU2#6 and HILLOU2#8. Analysis was limited to experiments HILLOU2#5 and HILLOU2#8.

The retardation factors were calculated based on the difference in first moments between tritium and surfactant. The retardation factors and distribution coefficients (K_d) of surfactant for both experiments HILLOU2#5 and HILLOU2#8 are presented in Table 9.4.

A high adsorption was measured in experiment HILLOU2#5. This experiment was the first experiment carried out with radiolabeled surfactant. Since a small amount of surfactant (<0.5 PV) was injected, LSC errors dominated leading to a high tailing off of surfactant concentrations at the end of the surfactant flood. In experiment HILLOU2#8, a large amount of surfactant was injected (>2 PV) and this effect was not observed. Based on mass balance, 96% of surfactant was produced. Based on the retardation factor compared to tritium, a small adsorption (< 165 $\mu\text{g/g}$) corresponding to a distribution coefficient (K_d) of 0.00017 was measured in experiment HILLOU2#8. In previous work carried out by Rouse *et al.* (1993), the value of adsorption was measured as 11,400 $\mu\text{g/g}$. For alkyl diphenyl oxide disulfonates, the value of adsorption was measured as 1,600 $\mu\text{g/g}$. The values of adsorption measured in both experiment HILLOU2#5 and HILLOU2#7 were well below 0.1 cc/g. Based on these results, it can be concluded that there is negligible adsorption of surfactant by Hill field soil.

9.3 INTERFACIAL TENSIONS

Interfacial tensions between the microemulsion and excess NAPL were measured. The Chun-Huh theoretical equation was also used to estimate the interfacial tension between the excess NAPL and microemulsion. The Chun-Huh equation can be written as follows:

$$\gamma = \frac{C}{\sigma^2} \quad (5.1)$$

A comparison of interfacial tensions between excess NAPL and microemulsion for many surfactant solutions is given in Table 9.5. The interfacial tensions have been plotted as a function of solubilization parameter in Figure 9.6. A better match between the Chun Huh estimate of interfacial tension and measured values is observed at higher solubilization parameters (about 3 to 4). At lower solubilization parameters, a good match is not obtained. Interfacial tension measurements are very hard to perform and are associated with large experimental error. This may partly account for the results observed in Figure 9.6.

Table 9.1: Best estimates of partition coefficients.

Alcohol	TCE best estimate	TCE static
2,3-Dimethyl-2-butanol	5.8	5.2
3-Methyl-3-pentanol	4.4	4.5
1-Pentanol	3.8	3.8
1-Hexanol	17.9	18.7
2-Ethyl-1-butanol	12.8	13.0
2-Methyl-2-hexanol	27.6	26.8
1-Heptanol	158.4	163.1

Table 9.2: Distribution coefficients for several alcohols in different types of soil.

Alcohol	K_d (l/Kg)	K_d (l/Kg)	K_d (l/Kg)	K_d (l/Kg)
	Ottawa	Hill	PPG	Plant 4
2,3-Dimethyl-2-butanol	0.00003			
3-Methyl-3-pentanol		-0.00011		0.00371
1-Hexanol		0.00295	-0.00018	0.00439
2-Methyl-2-hexanol	0.00016			
2,2-Dimethyl-3-pentanol		0.00485		0.00292
1-Heptanol			-0.00203	

Table 9.3: Adsorption values for alcohols with different types of soil.

Alcohol	Adsorption Ottawa $\mu\text{g/g}$	Adsorption Hill $\mu\text{g/g}$	Adsorption PPG $\mu\text{g/g}$	Adsorption Plant 4 $\mu\text{g/g}$
2,3-Dimethyl-2-butanol	28			
3-Methyl-3-pentanol		-112		3,705
1-Hexanol		2,947	-180	4,385
2-Methyl-2-hexanol	160			
2,2-Dimethyl-3-pentanol		4,852		2,918
1-Heptanol			-2,032	

Table 9.4: Surfactant adsorption by Hill field soil.

Experiment	Retardation Factor R_f	Distribution Coefficient K_d l/kg	Surfactant Adsorption $\mu\text{g/g}$
HILLOU2#5	1.13230	0.02315	23,150
HILLOU2#8	1.00094	0.00017	165

Table 9.5: Comparison of measured interfacial tensions and interfacial tensions estimated using the Chun Huh relation.

Surfactant Solution	NAPL	Measured IFT dyne/cm	Estimated IFT dyne/cm
2% sodium diamyl sulfosuccinate, 2% sodium dioctyl sulfosuccinate, 500 mg/l CaCl ₂	PCE	0.02	0.20
2% sodium diamyl sulfosuccinate, 2% sodium dioctyl sulfosuccinate, 1,300 mg/l CaCl ₂	PCE	0.01	0.0002
4% sodium dihexyl sulfosuccinate, 25,000 mg/l NaCl	PCE	0.14	0.37
8% sodium dihexyl sulfosuccinate, 2,000 mg/l NaCl	TCE	0.20	1.2
4% sodium dihexyl sulfosuccinate, 8% IPA, 4,000 mg/l NaCl, 500 mg/l Xanthan gum	TCE	0.19	0.83
4% sodium dihexyl sulfosuccinate, 8% IPA, 9,350 mg/l NaCl, 500 mg/l Xanthan gum	TCE	0.02	0.02
5% Sodium diamyl sulfosuccinate in Hill source water	Hill DNAPL	0.4	57.39
4% sodium dihexyl sulfosuccinate in Hill source water	Hill DNAPL	0.2	5.67
4% sodium dihexyl sulfosuccinate, 4% IPA, 11,250 mg/l NaCl and 500 mg/l Xanthan gum	Hill DNAPL	0.01	0.02
8% sodium dihexyl sulfosuccinate, 8% IPA, 5,850 mg/l NaCl and 500 mg/l Xanthan gum	Hill DNAPL	0.01	0.02

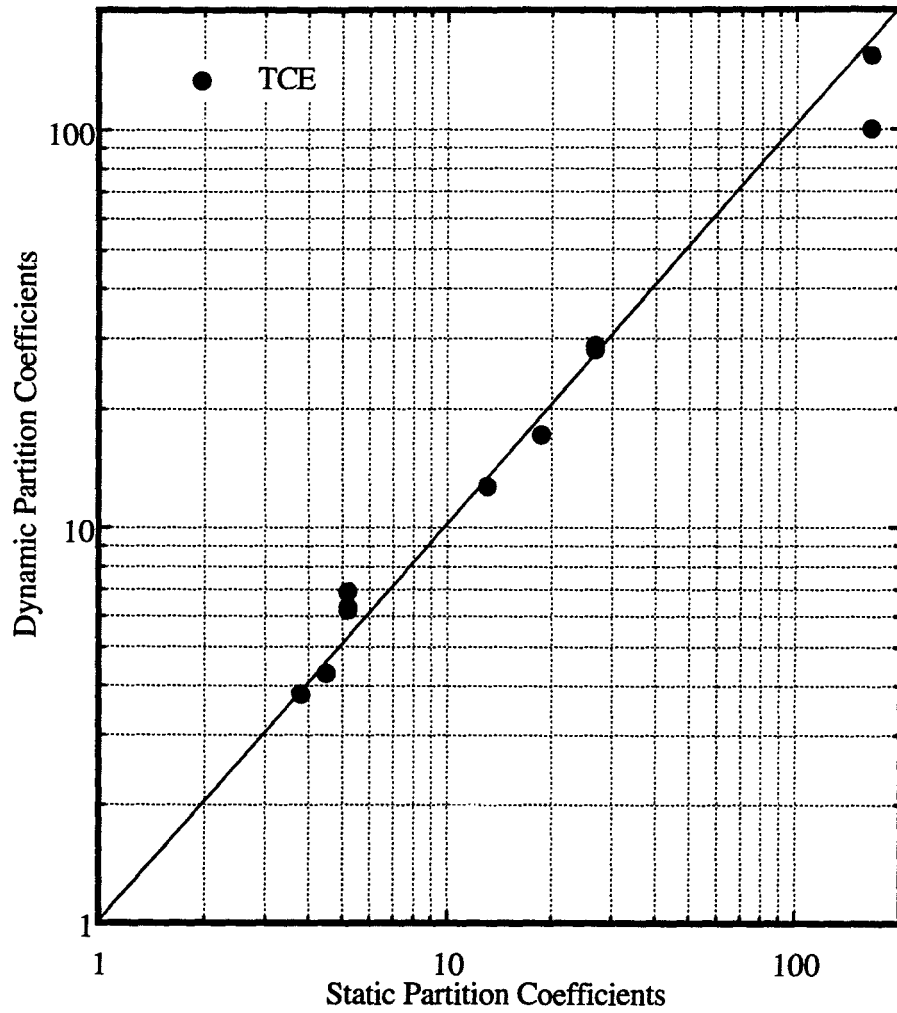


Figure 9.1: Comparison of static and dynamic partition coefficients for TCE.

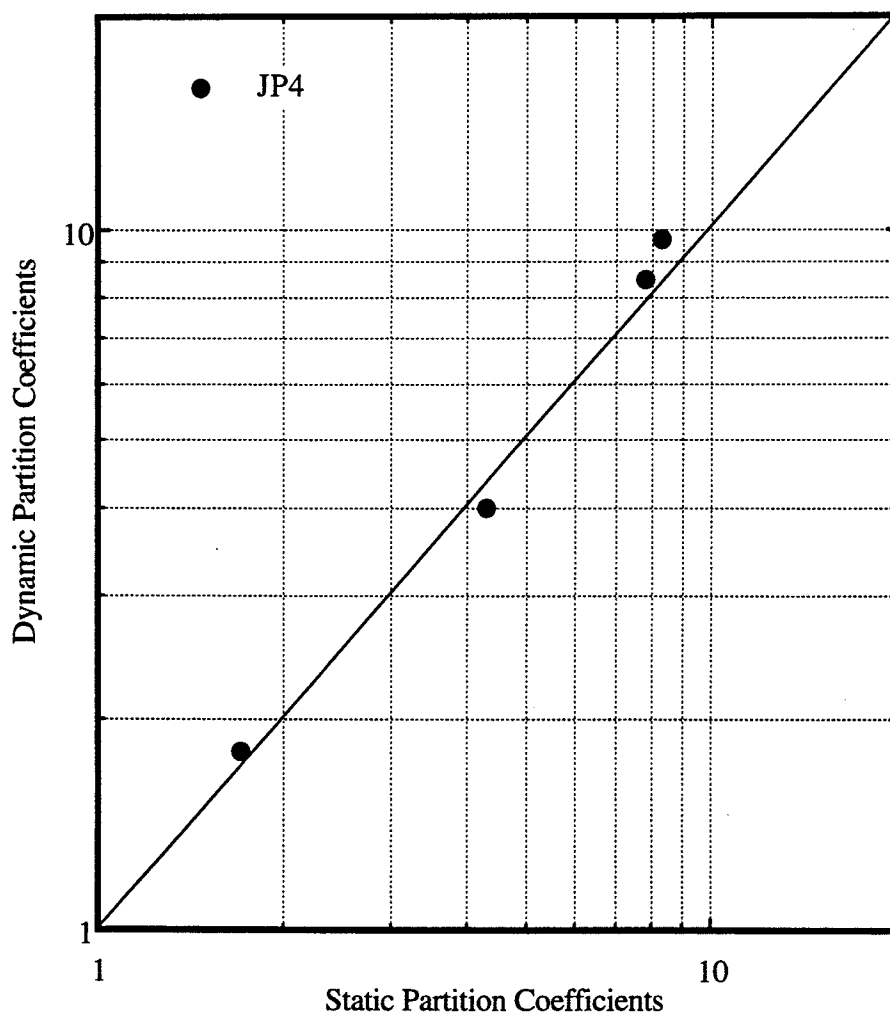


Figure 9.2: Comparison of static and dynamic partition coefficients for JP4.

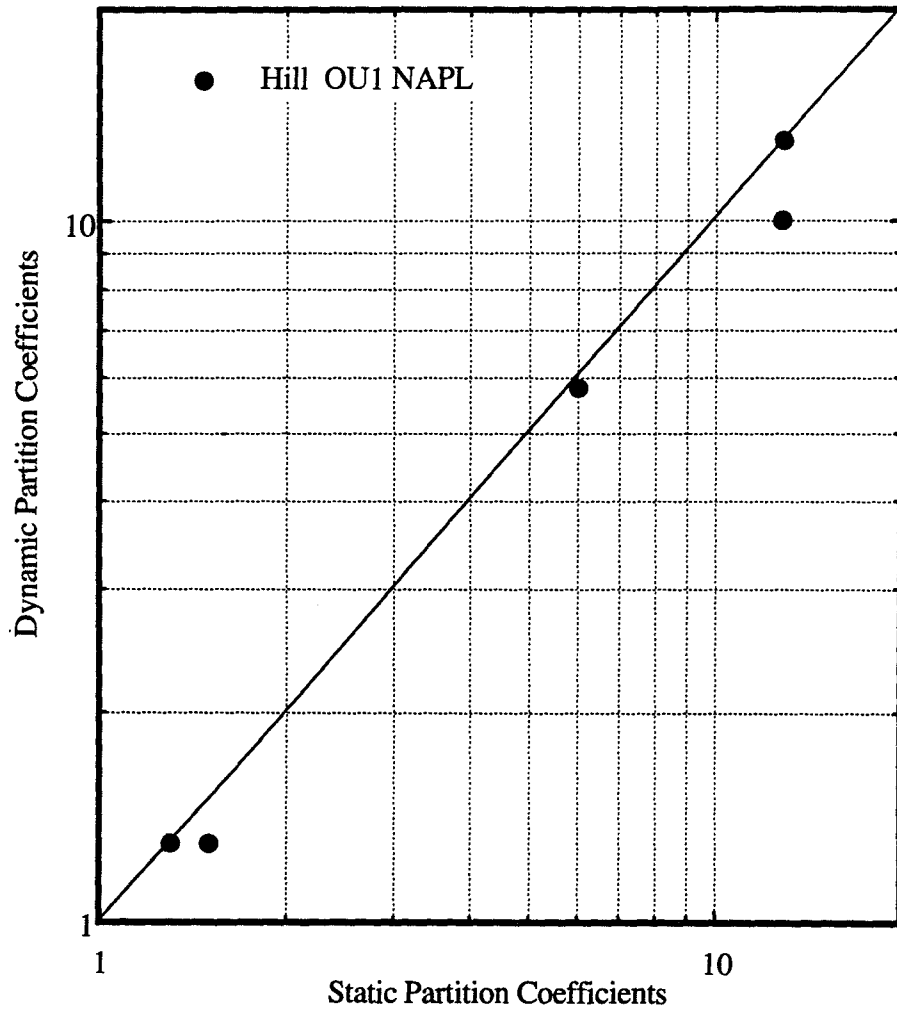


Figure 9.3: Comparison of static and dynamic partition coefficients for Hill OU1 NAPL

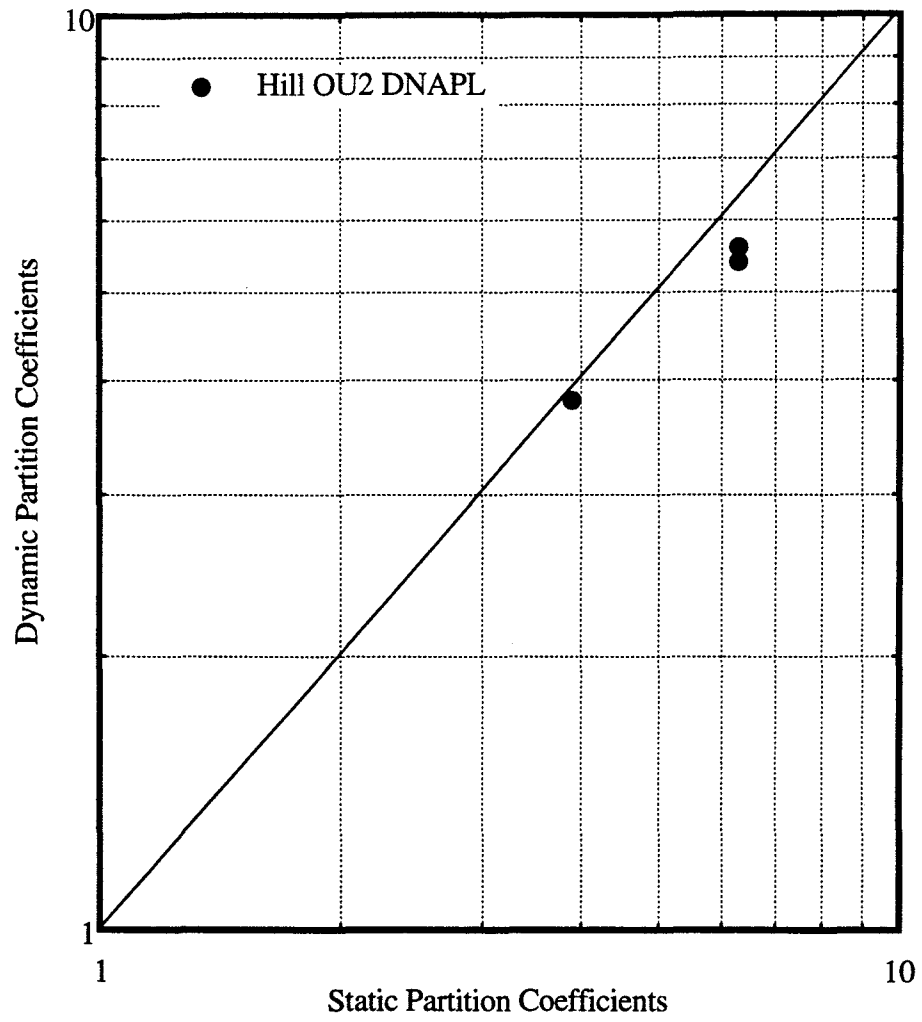


Figure 9.4: Comparison of static and dynamic partition coefficients for Hill OU2 DNAPL

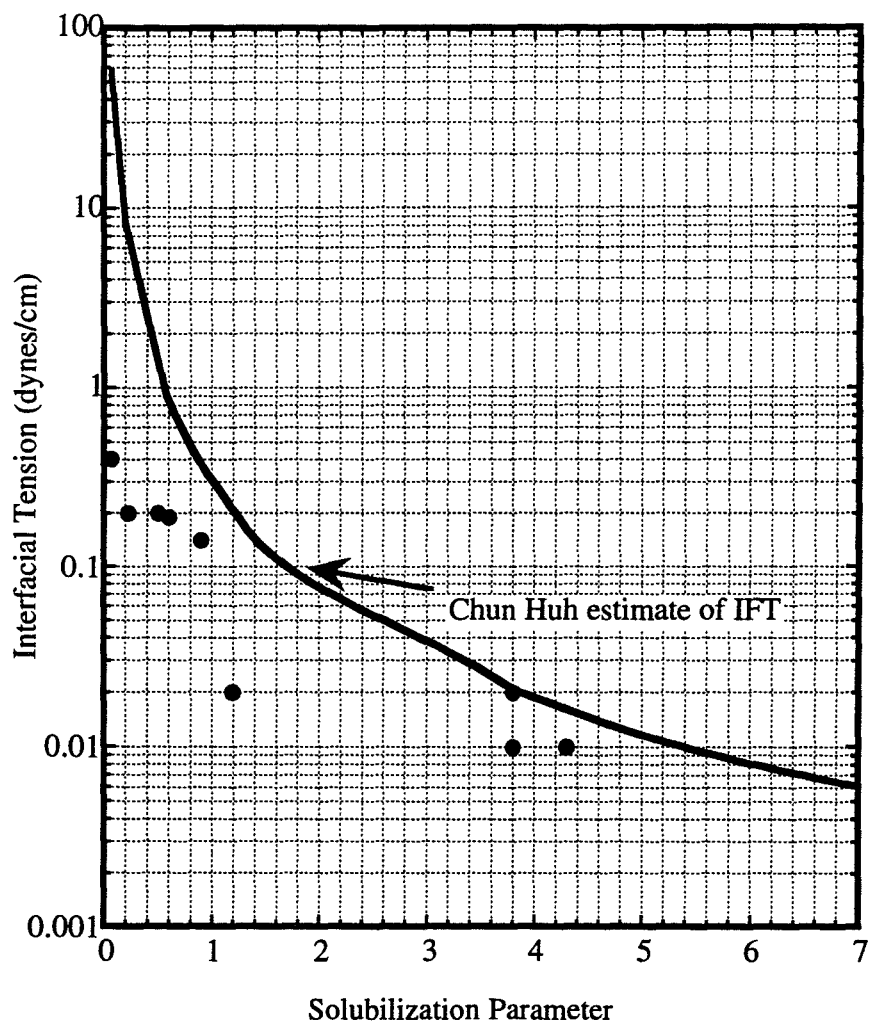


Figure 9.5: Comparison of measured interfacial tensions and Chun Huh estimates of interfacial tensions.

Chapter 10: Laboratory Selection and Design of Partitioning Tracer and Surfactant Injection Tests

For successful field tests to be implemented, several tasks have to be completed. Laboratory studies have to be carried out in order to select partitioning tracers and suitable surfactant solutions. Numerical simulations have to be carried out using the measured lab parameters to design field tests. This work was part of a much larger research effort. A lot of the experimental work was aimed at determining various input parameters for UTCHEM (Delshad *et al.*, 1996) to design for both partitioning tracer tests and surfactant injection tests. The applicability of UTCHEM to model field scale surfactant injection and partitioning tracer tests has been confirmed by (Brown, 1993, Brown *et al.*, 1994; Freeze *et al.*, 1995; Brown *et al.*, 1996a,b and Jin, 1995). A more detailed description of modeling of surfactant remediation using UTCHEM is presented in Brown (1997).

One of the main objectives of this work was application of the partitioning tracer technology and surfactant technology for application in field partitioning tracer tests and field surfactant injection tests. In pursuance of these objectives, partitioning tracers were selected for two interwell partitioning tracer tests. The first test was conducted by EPA and the University of Florida at Hill Air Force Base, site Operational Unit 1. The second test was conducted by INTERA Inc. at Hill Air Force Base, site Operational Unit 2. Laboratory procedures were developed for selection and solution of surfactant solutions for use in surfactant enhanced aquifer remediation at Hill OU2.

Soil samples from the field were usually in form of SOLINST cores and loose field soil stored in glass jars. The experimental approach for partitioning tracer selection was to perform partitioning tracer tests with field NAPL and Ottawa sand. This was followed by performing partitioning tracer tests in uncontaminated field soil to quantify tracer adsorption. After this partitioning tracer tests were performed in contaminated field soil with unknown NAPL saturation and the performance of partitioning tracers in estimating residual NAPL saturation was evaluated.

During the surfactant selection phase, phase behavior experiments were performed with surfactant, alcohol, polymer and electrolyte. Surfactant solutions exhibiting low viscosities, quick equilibration times and well defined three phase regions were selected for use in soil column experiments. Several column experiments were performed both with Ottawa sand and Hill field soil. In the first stage, surfactant solutions were used to flood Ottawa sand contaminated with field DNAPL. The next step involved surfactant flooding field soil at residual DNAPL saturation. The final stage involved performing the surfactant flood at aquifer temperature. Surfactant adsorption was quantified by using radiolabeled surfactant. Pressure drop across soil packs was measured during surfactant remediation to ensure that the surfactant solution was not susceptible to gel/liquid crystal formation. Concurrently a biodegradation study was underway by Dr. Larry Britton of VISTA Chemicals to test the Aerosol MA-80I surfactant's rate of biodegradation at low concentrations of surfactant and contaminant expected after the field test.

A description of both the Hill OU1 and the Hill OU2 sites are described in the following sections.

10.1 HILL AFB: INTRODUCTION AND GEOLOGY

Hill Air Force Base is located about twenty five miles north of Salt Lake City and five miles south of Ogden in a town called Layton. The base covers approximately 6,700 acres in Davis and Weber counties with the majority of the base in Davis county. The base is situated just west of the Wasatch mountains, on a plateau formed by the relict Weber delta approximately 300 feet above the valley floor. Surface elevations at Hill AFB range from 4,600 ft above mean sea level along the western boundary to about 5,000 ft above mean sea level near the eastern boundary.

The climate at Hill AFB is semiarid with a mean annual precipitation of 20.1 inches and an average temperature of 51°F. Average wind speed is about 4.7 knots with reported gusts up to 90 knots.

Hill AFB is located in a basin and range geologic setting, situated on the seismically active Wasatch Fault Zone, which has experienced more than 13,000 feet of vertical displacement during its active lifetime. The dominant regional geologic structures in the area are horsts (uplifted crystal blocks) and grabens (downdropped crustal blocks) created by normal faulting associated with regional extensional forces. The Wasatch Range immediately east of the base and Antelope and Fremont islands in the Great Salt Lake are horsts. The area between is a graben basin that has been filled with a thick sequence of sediments eroded from the surrounding highlands. The depth to the bedrock in the basin ranges from

approximately 1,500 feet on the east side of the base to about 7,500 feet on the west side of the base. The plateau on which the base is situated is composed of deltaic sediments deposited by the Weber river as it entered the Lake Bonneville and older lakes.

10.1.1 Hill OU1

The contaminant in Hill OU1 is an LNAPL. Operable Unit 1 (OU1) at Hill AFB has a number of contaminant sources located across the site. The remediation test cell is located hydraulically down gradient of two Chemical Disposal Pits (CDPs) which were used to dispose of predominantly aviation fuels (JP4) and chlorinated solvents in the 40's and the 50's. Also, up gradient of the cell is former Fire Training Area (FTA) which may have contributed unextinguished fuels and combustion byproducts to the site. The resulting NAPL is lighter than water and exists as a plume covering several acres, as evidenced by up to 0.4 feet of free product measured in wells.

10.1.2 Hill OU2

The contaminant in Hill OU2 is a DNAPL. Base records indicate that from 1967 to 1975 the OU2 site known as Chemical Disposal Pit #3 was used to dispose of unknown quantities of TCE bottoms from a solvent recovery unit and sludge from vapor degreasers. There are also reports of the site receiving an unknown volume of plating tank bottoms in the early 1940's. The disposal area consisted of at least two disposal trenches at the site trending north-northwest which are estimated to have been approximately 6 feet deep. Size estimates based on geophysical surveys, aerial photo interpretations and soil boring data indicate that

two trenches were about 10 feet wide and had lengths of approximately 50 and 100 feet, respectively.

10.1.3 Site Description, HILLOU2

A detailed site description of only Hill OU2 was obtained as both the surfactant and partitioning tracers were selected by The University of Texas at Austin. The OU2 Site at Hill AFB and the locations of recovery Well U2-1 and the recently drilled SB series of borings are shown in Figure 10.1. Chemical disposal trenches, used for disposal of spent degreasing solvents, were located to the south of U2-1; the exact location is unknown.

Depth to the water table (approx. 4670 ft MSL) is 20 ft to 25 ft below ground surface in the U2-1 area, and varies seasonally by several feet. The dotted line to the east and west of the pattern indicates an estimated contour line for the 4670 ft MSL depth of the aquitard, the Alpine Formation, underlying the aquifer. The aerial extent of the saturated zone and the north-south alignment of the saturated zone trough or "channel" is indicated by the dotted line. The deepest part of this trough (presumably near the center) also determines the probable path of the DNAPL contaminant. Once the DNAPL migrated downwards to the aquitard (or any zone of sufficiently low permeability above the aquitard), the DNAPL migrated downslope along the trough, to the north and south of the trenches.

DNAPL has been detected in pools both to the north (Well U2-1, U2-31, U2-32, SB-1, SB-6) and to the south (Well U2-34) of the disposal trenches. From October 1993 to June 1994, 23,000 gallons of DNAPL and over 1,000,000 gallons of contaminated groundwater were produced from these wells (Radian, 1994a) and

by the start of the AFCEE field tests in late 1995, the total volume of DNAPL treated at the Radian steam stripper was more than 32,000 gallons.

During September and October 1995, the eight SB series wells were drilled by INTERA. DNAPL was detected in borings SB-1, SB-2, SB-5, and SB-6. The highest DNAPL saturations were measured in two wells (SB-1 and SB-6) in the center of the aquitard contour (presumably located in the deepest part of the channel). The other two wells drilled through the center of the channel, SB-2 and SB-8, had no samples measured in the aquifer just above the aquitard. Two of the SB wells encountered possible evidence of these trenches. In SB-6, the drilling log noted "a dark reddish concretion" that may have been the remains of a rusted metal barrel, at 7.8 ft BGS (below ground surface). In SB-8, the drilling log noted a "white material in shoe - plastic drum" at 17.5 ft BGS. If the disposal trenches are within the pattern area, DNAPL may be located throughout the unsaturated zone in some areas, rather than only in the aquifer immediately overlying the aquitard.

The measured TCE concentration in the DNAPL varies from 63% to 80%, averaging 73%. The 1,1,1 TCA concentration varies from 12% to 15%, averaging 14%. The PCE concentration varies from 5% to 13%, averaging 8%. The Freon 113 concentration varies from 0% to 7%, averaging 3%. Carbon tetrachloride, toluene, and dichloromethane are present in concentrations less than 1%

10.2 PARTITIONING TRACER DESIGN AND SELECTION

In order to use partitioning tracers for estimation of NAPL in place, several selection criteria have to be met (Tang and Harker, 1991a, Jin *et al.*, 1995). The main requirements are:

1. low detection limits on a gas chromatograph (or any other suitable method)
2. Acceptable partition coefficients to obtain retardation factors between 1.2 and 4.0
3. long term chemical stability
4. family of compounds with similar properties
5. negligible adsorption to the porous matrix
6. low toxicity
7. environmental acceptance and biodegradability
8. adequate water solubility
9. cost effectiveness

The tracers chosen consist of long chained aliphatic alcohols. The approach for selection of partitioning tracers for use in field tracer tests is described in the following sections.

10.2.1 Partition Coefficient Tests to Measure Partition Coefficients

In order to perform a partitioning tracer test, accurate measurement of partition coefficients is required. A definition of the partition coefficient is given in Chapter 7. Depending on the type of application and residual saturation of NAPL present in the contaminated area, a range of partition coefficients will be required. In general higher partition coefficients will be required for post surfactant PITTs to be used for performance assessment of surfactant flooding or co-solvent flooding etc. A retardation factor between 1.2 and 4.0 is a good rule of thumb for the appropriate range for most partitioning tracer tests, but the precise values should be optimized for each specific field test using a suitable model such as UTCHEM and

will vary somewhat depending on the accuracy of the analytical method etc. For a saturated zone, the retardation factor is related to the NAPL saturation S_N by,

$$R_f = 1 + \frac{K_i S_N}{1 - S_N} \quad (10.1)$$

Both static and dynamic partition coefficient tests can be performed to determine the partition coefficients. For the Hill OU1 PITT tracer selection, static partition coefficient tests were used for quick measurement of the partition coefficients. Dynamic partition coefficient tests using Ottawa sand and field NAPL from Hill OU1 were then performed to confirm the partition coefficients measured using the static tests and obtain better estimates of partition coefficients as discussed in Chapter 9. Since the partition coefficients measured using the static and dynamic partition coefficient tests agreed with each other within experimental error, only static partition coefficient tests were used to measure partition coefficients in subsequent experiments. The experimental details regarding static and dynamic partition tests are described in Chapter 7. The error analysis and accuracy of partition coefficients is discussed in Chapter 9. The partition coefficients for several alcohols with Hill OU1 LNAPL and Hill OU2 DNAPL are presented in Table 7.3.

10.2.2 Partitioning Tracer Tests in Clean Field Soil with Field NAPL

The accuracy of NAPL estimation using a partitioning tracer test depends on accurate measurement of the retardation of partitioning tracers. In some instances, field soil may have sufficient organic matter to cause a significant level of

adsorption, retention and thus additional retardation of the alcohols. In this case, the NAPL saturation estimates may be incorrect if the retardation of the tracers due to adsorption by the soil is not factored into the calculations.

In order to measure this retardation of the partitioning tracers by field soil, tracer tests can be conducted in uncontaminated field soil. The retardation can be calculated using the first moments.

Uncontaminated field soil was not obtained from Hill OU1 and hence no tracer experiments were performed to quantify adsorptive retardation. Uncontaminated field soil was obtained from Hill OU2. Tracer tests were conducted in soil columns packed with uncontaminated field soil from Hill OU2 (experiments HILLOU2#7 and HILLOU2#4). Tritium and IPA were used as conservative tracers and several other alcohol tracers were injected into the soil column and the response was measured. Based on the initial partitioning tracer test in uncontaminated field soil, the maximum adsorption of the tracers was less than 5,000 $\mu\text{g/g}$. This corresponds to a retardation of 1.028 and an apparent residual DNAPL saturation of 0.00075 and this number is well below the accuracy of tracer measurements (in other words, these values are considered noise). Based on this it can be concluded that there was negligible adsorption of these tracers by Hill field soil. The details of the experimental procedures and results are presented in Chapters 8 and 9. Negligible values of adsorption of tracers by the Hill field soil can be attributed to extremely low clay and organic content but these values were not measured.

10.2.3 Partitioning Tracer Tests in Contaminated Field Soil

Once procedures for performing tracer tests in clean field soil were well defined, partitioning tracer tests were performed in contaminated field soil. Both contaminated field soil and clean field soil in which field contaminant was injected was used for performing partitioning tracer tests.

Tracer selection was based on retardation factors. For PITT design for the Hill OU1 test, the expected NAPL saturation was between 0.04 and 0.10. Based on this, and using a retardation factor between 1.2 and 2.5, partition coefficients in the range of 4.8 to 13.5 were required. Hence 1-hexanol, (K=4.4) and 2,2-dimethyl-3-pentanol (K=12.9) were suggested as candidates for the field test. Ethanol was chosen as a conservative tracer.

At Hill OU2, the expected DNAPL saturation was between 0.03 and 0.07. Thus, using a retardation factor between 1.2 and 2.5, partition coefficients between 2.7 and 19.9 were required. Hence, 1-pentanol (K=3.8) and 2-ethyl-1-butanol (K=12.5) were suggested as candidates for the field tracer test. The swept pore volume at Hill OU2 is about 14,000 gallons. Assuming a saturation of 0.04, a DNAPL volume on the order of 560 gallons was estimated. The objective of remediation was 97 to 99% DNAPL recovery from this swept volume. This means that the residual DNAPL saturation after surfactant remediation would be on the order of 0.0004 to 0.001. The expected noise in the retardation factor was ± 0.035 . Using a DNAPL saturation between 0.0004 and 0.001 and a retardation factor of 1.05, partition coefficients between 49 and 125 were needed. Hence 1-hexanol (K=30.2), 2,4-dimethyl-3-pentanol (K=49.9) and 1-heptanol (K=140.1) were

recommended as partitioning tracers for the post surfactant PITT for performance assessment.

For the Hill OU1 PITT design, soil packs in experiments OUDNAPL2 and OUDNAPL3 were packed with contaminated field soil. For the Hill OU2 PITT design, partitioning tracer experiments with Hill OU2 field soil were conducted in experiments HILLOU2#3, HILLOU2#4, HILLOU2#5, HILLOU2#7 and HILLOU2#8.

In experiments OUDNAPL2 and OUDNAPL3, a residence time between 5 hours and 10 hours was used for the partitioning tracer tests. In experiment OUDNAPL2, the tracer estimate of the average residual NAPL saturation increased from 0.035 ± 0.009 to 0.060 ± 0.016 when 1.7 cc of NAPL was injected into the soil pack. This corresponded to an increase in saturation of 0.032. Hence the average expected NAPL saturation during the second tracer test was 0.067. Hence it can be observed that the increase in the NAPL estimated using partitioning tracers is consistent the increase in saturation based on the volume of NAPL added. In experiment OUDNAPL3, the average NAPL saturation estimate was around 0.063 ± 0.008 in the first tracer test and 0.061 ± 0.004 in the second tracer test, or about 7% uncertainty in the saturation.

Experiment HILLOU2#1 was carried out to evaluate the performance of partitioning tracers in Ottawa sand Hill DNAPL. The average saturation based on mass balance was 0.245 and the average saturation based on partitioning tracers was 0.234 ± 0.017 . The DNAPL saturation based on mass balance and partitioning tracers agreed to ± 0.011 . The standard deviation of saturation based on partitioning tracer measurements was 7%. Similar results were obtained for column

HILLOU2#4. In columns HILLOU2#1 and HILLOU2#4, a residence time of 9.2 hours was used for the tracer test. In both columns, clean soil was saturated by flooding with DNAPL and following with a waterflood. In experiment HILLOU2#5, contaminated soil was used. This soil pack had a pool of DNAPL as opposed to a uniform DNAPL saturation. A residence time of between 5 to 9 hours for the partitioning tracers was seen to under predict the residual DNAPL saturation. This was remedied in experiment HILLOU2#8 with contaminated field soil when a residence time of 18 to 24 hours was used for the partitioning tracers and excellent results were obtained. In experiment HILLOU2#7, the residual saturation based on mass balance was 0.262 and the residual saturation based on partitioning tracers was 0.255.

In experiments HILLOU2#1, HILLOU2#4, HILLOU2#5, HILLOU2#7 and HILLOU2#8, partitioning tracers were used for performance assessment. The post surfactant DNAPL saturations were between 0.0002 and 0.001. The DNAPL saturation estimates after surfactant flooding agreed with estimates based on mass balance for experiment HILLOU2#7 to within $\pm 1\%$ of the total DNAPL recovered.

10.3 RECOMMENDATIONS FOR FIELD TESTS

10.3.1 HILLOU1

Based on these laboratory results and the concurrent simulation study, ethanol, 1-hexanol and 2,2-dimethyl-3-pentanol were recommended as the tracers to be used in the PITT. Ethanol was the conservative tracer, 1-hexanol ($K=4.4$) and 2,2-dimethyl-3-pentanol ($K=12.9$) were used as the partitioning tracers. A retardation factor of between 1.2 and 2.4 was expected.

10.3.2 Hill OU2

Based on laboratory results, negligible adsorption was measured for partitioning tracers with clean Hill field soil. IPA, 1-pentanol and 2-ethyl-1-butanol were recommended as the tracers. Isopropanol was recommended as the conservative tracer, 1-pentanol ($K=3.87$) and 2-ethyl-1-butanol ($K=12.5$) were recommended as the partitioning tracers. For the post surfactant tracer flood for performance assessment of surfactant remediation, 1-propanol was recommended as the conservative tracer and 1-hexanol ($K=30.2$), 2,4-dimethyl-3-pentanol ($K=49.9$) and 1-heptanol ($K=140.1$) were recommended as the partitioning tracers. For the pre surfactant PITT, retardation factors between 1.1 and 1.8 were expected.

10.4 SURFACTANT SELECTION AND DESIGN

One of the main contributions of this work was the selection of a suitable surfactant solution for use in remediation of the Hill OU2 site at Hill AFB, Utah. Many phase behavior experiments and column experiments were carried out for the design of the surfactant flood at the OU2 DNAPL site at Hill AFB. The field test was divided into two parts, Phase I and Phase II. Phase I consisted of the initial PITT and a small surfactant pre-test in one injector. Phase II consisted of a second PITT, the surfactant flood in a 3X3 line drive well pattern and a final PITT in the same well pattern. The experimental procedures and experimental results for column experiments have been described in Chapters 4, 8 and 9.

10.4.1 Phase Behavior

The surfactants used in this study were anionic surfactants. Several phase behavior experiments were carried out with surfactant, alcohol, polymer and

electrolyte mixtures. Volume fraction diagrams were developed for various surfactant solutions by varying the electrolyte concentrations. The DNAPL solubilization ratios and DNAPL solubilization of various surfactant solutions were also measured. All experiments were carried out at surfactant concentrations greater than the CMC of the surfactant and at a temperature of 23°C but a few were done at the Hill OU2 groundwater temperature of 12.2°C. Hill OU2 groundwater and Hill OU2 source water (Tables 10.2 and 10.3) were used in column experiments and phase behavior experiments with either NaCl or CaCl₂ added to these fresh waters in many of the Phase II experiments.

The surfactants used in this study were sodium diamyl sulfosuccinate, sodium dihexyl sulfosuccinate and sodium dioctyl sulfosuccinate. The alcohols used were IPA and secondary butyl alcohol. The polymer used was xanthan gum and the additional electrolyte used was sodium chloride. Additional studies were carried out using CaCl₂ as an electrolyte to look at the tolerance of the surfactant solutions to the presence of calcium ions (see Table 10.1).

Volume fraction diagrams, contaminant solubility plots and contaminant solubilization ratios were plotted against electrolyte concentration (Chapter 6). Typically, for sodium dihexyl sulfosuccinate solutions, a contaminant solubilization ratio of about 0.3 was observed at lower electrolyte concentrations and a value of approximately 6 at the optimal salinity. These solubilization ratios translated into contaminant solubilities of about 20,000 mg/l at lower electrolyte concentrations and about 600,000 mg/l at optimal salinity.

No NaCl was added the fresh tap water used as the source water for the Phase I test conducted in May of 1996. Contaminant solubilities were measured as

a function of surfactant concentration at 12.2°C. The results are presented in Figure 10.2. It can be seen that even in fresh water, the solubility of the contaminant is enhanced from about 1,100 mg/l to about 78,000 mg/l by using a solution of 8% by weight sodium dihexyl sulfosuccinate. The interfacial tension between the Hill OU2 DNAPL and 8% sodium dihexyl sulfosuccinate was measured as 0.2 dyne/cm. This is much lower than the IFT of 7 dyne/cm measured between the DNAPL and water. These and other data were used in concurrent modeling studies.

During the Phase I field test, the temperature of the effluent appeared to vary between 10°C to 27°C. These data were later found to be erroneous and the best estimates of groundwater temperature at the time is about 12.2°C. However, phase behavior studies using a solution of 8% sodium dihexyl sulfosuccinate, 4% IPA, NaCl in source water at 12.2°C, 15°C, 18°C, 21°C and 23°C were conducted. The volume fraction diagrams and solubility plots are described in detail in Chapter 6. The optimal salinity was plotted against temperature for 8% by weight sodium dihexyl sulfosuccinate and different alcohol concentrations as presented in Figure 10.3. A linear trend in optimal salinity can be observed for the surfactant solutions. This plot was then used to determine the NaCl concentration to be used in the surfactant solution in the Phase II test once accurate subsurface water temperature measurements were obtained.

10.4.2 Column Experiments

In order to design successful tracer and surfactant field tests, it is extremely important to perform a variety of carefully designed laboratory experiments. In

addition to the obvious and commonly performed experiments to measure contaminant recovery from the soil, these laboratory experiments are needed to find out if there are any unexpected adverse interactions between the surfactant and the NAPL or soil, any plugging problems, adsorption and residence time requirements to avoid non-equilibrium effects.

The approach followed for columns experiments was to first perform column experiments using clean Ottawa sand and field DNAPL since Ottawa sand is a very simple standard in our laboratory with very well known characteristics. The interaction between the surfactant and field DNAPL under dynamic conditions can be quantified by measuring the head loss during the surfactant flood and post surfactant waterflood. In the next phase, clean field soil saturated with field DNAPL was used and surfactants were used for remediating contaminated field soil. Partitioning tracers were flushed through clean field soil to find out if the tracers had a detectable adsorption on the soil (none did in this case). Experiments performed at local equilibrium conditions (no kinetic effects) are much easier to interpret and use for modeling and scaleup to the field so these were strongly preferred in this study. This requires slow flow rates and relatively long columns. In the final phase, contaminated field soil was used in soil columns. A summary of all the column experiments performed for design of the Phase I and Phase II tests at Hill AFB is given in Table 10.4. A total of nine experiments were performed. Experiments HILLOU2#1, HILLOU2#2b, HILLOU2#2c and HILLOU2#4 have been described in Shotts (1996). All the other experiments have been described in Chapters 8 and 9.

In order to design the surfactant flood, parameters such as hydraulic gradient across the soil column during surfactant flooding, surfactant adsorption and the final residual DNAPL saturation are needed. The latter data can be used to estimate a capillary desaturation curve for the field soil and DNAPL by calculating capillary and Bond numbers. Each of these parameters and its role in the field design are discussed in the following sections.

10.4.2.1 Hydraulic Gradient Measurement

In many soil column experiments, induced hydraulic gradients were measured during the surfactant flood. These maximum measured hydraulic gradients were compared to the maximum allowable hydraulic gradient for the field. Hydraulic gradients in excess of 1.5 cm/cm in case of solutions without polymer were considered unsuitable for surfactant remediation. Solutions exhibiting such high gradients were considered susceptible to pore plugging due to gels, liquid crystals and emulsions. Hydraulic gradients across the soil packs when no polymer was used were always less than 0.3 cm/cm and in experiments with surfactant/polymer solutions, the induced gradients were between 0.8 to 1.2 cm/cm. These hydraulic gradients were acceptable for the Hill OU2 tests. Lower gradients would be expected in the field as some of the head loss in column experiments occurs at the small entry and exit ports in the columns.

A water containing only 150 mg/l NaCl was used to flush out the surfactant used in experiment HILLOU2#5. A sudden increase in the potential drop (head loss) was observed. Most if not all the calcium ions were likely exchanged by sodium ions on the clays during the surfactant flood and freshwater flood. This

probably caused movement of clays and pore plugging by fines or clays. When the column was flooded with water containing 150 mg/l CaCl_2 , this was reversed and potential drops declined to lower values. Hence, it can be inferred that in order to eliminate/minimize fines production and high hydraulic gradients during the surfactant flood and post-surfactant waterflood, adequate amounts of sodium and calcium ions must be present in the surfactant solution and post-surfactant waterflood.

10.4.2.2 Surfactant Adsorption

Surfactant adsorption was measured using a ^{14}C labeled sodium dihexyl sulfosuccinate prepared at the University of Texas at Austin (Weerasooriya, 1995). Both tritium and the radiolabeled surfactant were injected into three soil columns (HILLOU2#5, HILLOU2#7 and HILLOU2#8) to quantify surfactant adsorption. The details are described in chapters 8 and 9. In all the experiments, HILLOU2#5, HILLOU2#7 and HILLOU2#8, 92.5%, 101% and 96% surfactant was recovered compared to 105%, 103% and 99% tritium recovered from these experiments. Based on these results, it can be inferred that surfactant adsorption is negligible and would not cause any problems during the field test. Based on the retardation of the radiolabeled surfactant, low surfactant adsorption ($<200 \mu\text{g/g}$) was measured in experiment HILLOU2#8. This value of adsorption is so low that it has negligible effect on the field test since 2.5 pore volumes of 8% surfactant were injected and at $200 \mu\text{g/g}$ soil, less than 1% of the injected surfactant would be adsorbed. This was confirmed by the Phase I test.

Also, the surfactant concentrations below the CMC (about 0.2 weight %) were measured in all the experiments at the end of the final waterflood. Below the CMC, the surfactant is not active and can not cause unwanted mobilization of DNAPL so this was the desired state following the field tests.

10.4.2.3 CDC Curves and DNAPL Recovery Mechanism

To understand the capillary desaturation behavior of the DNAPL during surfactant displacements in sandpicks, the interfacial tensions between the Hill DNAPL and the various surfactant solutions were measured. The IFT between the Hill DNAPL and a solution of 4% sodium dihexyl sulfosuccinate in Hill source water was measured as 0.2 dyne/cm. For a solution of 5% sodium diamyl sulfosuccinate in Hill source water, the IFT was measured as 0.4 dyne/cm. These are type I solutions. For sodium dihexyl sulfosuccinate surfactant solutions with Hill DNAPL at optimal salinity, the IFT measured was about 0.01 dyne/cm. Based on these numbers, the trapping number (Jin, 1995; Pennell *et al.*, 1996) was calculated for many column experiments and plotted as shown in Figure 10.4.

From Figure 10.4 it can be seen that at the trapping number (sum of capillary number and bond number for vertical displacements) of about 10^{-4} in some of the Hill OU2 Phase I column experiments, mobilization occurred. The capillary desaturation curve for TCE and Ottawa sand is to the right of the Hill DNAPL data and mobilization would be expected only if the trapping number was greater than 10^{-3} . For the Phase II test conditions, NaCl was added to the solution so the IFT was very low (0.01 dyne/cm) and complete desaturation occurred in these experiments for both Hill DNAPL and TCE (see points at trapping number of

10⁻²). Curves drawn through the data of Delshad (1990) and Pennell *et al.* (1996) are shown on Figure 10.4 for comparison with the data from this study. The differences in all these results are not fully understood but wettability is likely to be one important variable. TCE in Ottawa sand is almost certainly the non-wetting phase and water the wetting phase whereas the Hill DNAPL and soil may have been mixed wet.

After performing several column experiments with a solution of 4% solution of sodium dihexyl sulfosuccinate in Hill source water, (experiments HILLOU2#1, HILLOU2#2b, HILLOU2#4, HILLOU2#5), a solution of sodium diamyl sulfosuccinate which has lower solubilization potential, was used with soil cores contaminated with DNAPL (experiments HILLOU2#2c and HILLOU2#3). Mobilization of DNAPL was observed in experiments HILLOU2#2c and HILLOU2#3.

Sodium dihexyl sulfosuccinate was selected as the preferred surfactant to use at Hill OU2 for both the Phase I and Phase II field tests based upon its overall performance in column tests, its superior solubilization compared to sodium diamyl sulfosuccinate and other factors such as low cost and biodegradability.

10.4.2.4 Performance Assessment

In most of the soil columns, DNAPL saturations were reduced to almost zero after surfactant flooding or greater than 99% of the DNAPL initially present in the soil pack. When possible, these estimates were made based on the weight of the soil columns before contamination of the soil column by the DNAPL and the weight of the soil column after surfactant flooding (mass balance) as well as the use

of partitioning tracers. In instances where contaminated soil was used, partitioning tracers only were used for assessing remediation performance. A comparison of the DNAPL recovery based on mass balance and partitioning tracers is presented in Table 10.5. Since contaminated soil columns were used in experiments HILLOU2#5 and HILLOU2#8, the residual saturation based on mass balance could not be obtained. Apparent residual DNAPL saturations on the order of 0.0004 such as in experiment HILLOU2#1 are so low as to be in the noise and correspond to 99.9% removal of DNAPL. This very small amount of remaining contaminant in such a case is likely to be in some form other than trapped ganglia. In experiment HILLOU2#8, the final contaminant concentration in the effluent was less than 15 mg/l. Lower concentrations could not be achieved due to the presence of Teflon end pieces and nylon tubing in the soil column which caused persistent tails on the order of 10 to 50 mg/l.

10.4.2.5 Selection of a suitable surfactant solution

In all column experiments through experiment HILLOU2#5 surfactant solutions containing 4% surfactant by weight were used for remediation. Subsequently 4% IPA as a cosolvent was used to minimize plugging problems and reduce equilibration times for the surfactant contaminant mixtures. The presence of alcohol lowers the density of the microemulsion. This is extremely important as a microemulsion containing 50,000 mg/l of TCE gas a density of about 1.02 g/cc which is high to promote downward migration.

In an unconfined field test such as Hill OU2, any surfactant solution injected into the ground is greatly diluted by the groundwater. Hence, for good

surfactant performance, a large amount of surfactant must be injected over a long period of time. This can be achieved by either injecting a lower concentration of surfactant for a relatively long period of time or a higher concentration of surfactant for a short period of time. In order to minimize the time for the test, a high surfactant concentration was used. 8% sodium dihexyl sulfosuccinate, 8% IPA, 5,850 mg/l NaCl and 500 ppm xanthan gum polymer was tested in experiment HILLOU2#8.

10.5 RECOMMENDATIONS FOR THE HILLOU2 PHASE I AND THE PHASE II TESTS

Based on all the laboratory experiments and computer simulations (Brown, 1997), a solution of 8% sodium dihexyl sulfosuccinate mixed in Hill source water was recommended as the surfactant solution to be used in the Phase I test. Due to Phase II budget constraints, the polymer was not used as originally recommended. The IPA concentration was lowered to 4% both to minimize problems with the steam stripper used to treat the effluent and the because without polymer the phase behavior was satisfactory with only 4% IPA. The optimum salinity for the final Phase II solution of 8% sodium dihexyl sulfosuccinate (10% by weight Aerosol MA-80I), 4% IPA at 12.2°C was 7,000 mg/l NaCl (added to Hill source water). Approximately 2.5 pore volumes of this solution was injected during Phase I and then flushed with about 8 pore volumes of fresh water. The final residual DNAPL saturation was only 0.0004 based upon the final PITT.

Table 10.1: Summary of phase behavior experiments performed with Hill DNAPL.

% Surfactant		% Alcohol	Electrolyte	Water	XG	T, (K)
C5	C6					
0	4	8 (IPA)	NaCl	DW	500	296
0	4	12 (IPA)	NaCl	DW	500	296
0	8	8 (IPA)	NaCl	DW	500	296
4	4	8 (IPA)	NaCl	DW	500	296
0	4	0 (IPA)	NaCl	Ground	0	296
0	4	8 (IPA)	NaCl	Source	0	296
0	4	8 (IPA)	NaCl	Source	500	296
0	4	4 (IPA)	NaCl	Source	500	296
0	4	4 (Ethanol)	NaCl	Source	500	296
0	8	8 (IPA)	NaCl	Source	500	296
0	8	8 (IPA)	NaCl	Source	500	285.2
0	8	8 (IPA)	CaCl ₂	Source	500	296
0	8	4 (IPA)	NaCl	Source	0	285.2
0	8	4 (IPA)	NaCl	Source	0	288
0	8	4 (IPA)	NaCl	Source	0	291
0	8	4 (IPA)	NaCl	Source	0	294
0	8	4 (IPA)	NaCl	Source	0	296
0	8	2 (IPA)	NaCl	Source	0	285.2
0	8	2 (IPA)	NaCl	Source	0	288
0	8	2 (IPA)	NaCl	Source	0	291
0	8	2 (IPA)	NaCl	Source	0	294
0	8	2 (IPA)	NaCl	Source	0	296

Table 10.2: Cations in Hill groundwater and Hill source water

Cations	Ground Water (mg/l)	Source Water (mg/l)
Aluminum	2.26	< 0.1
Antimony	< 0.1	--
Arsenic	< 0.1	--
Barium	0.1	--
Beryllium	< 0.1	--
Boron	0.276	--
Cadmium	< 0.1	--
Calcium	13.9	73.2
Chromium	< 0.1	--
Cobalt	< 0.1	--
Copper	< 0.1	--
Iron	2.88	0.0277
Lead	< 0.1	--
Magnesium	11.5	17.6
Manganese	0.233	--
Molybdenum	< 0.1	--
Nickel	< 0.1	--
Potassium	11.2	2.18
Selenium	< 0.1	--
Silicon	11.1	--
Silver	< 0.1	--
Sodium	97.4	19.3
Strontium	< 0.1	--
Thallium	< 0.1	--
Vanadium	< 0.1	--
Zinc	< 0.1	--

Table 10.3: Anions in Hill groundwater and Hill source water

Anions	Ground Water (mg/l)	Source Water (mg/l)
Bromide	< 0.1	--
Chloride	37.9	24.5
Fluoride	0.387	--
Sulfate	2.05	19.5

Table 10.4: Summary of column experiments performed for Hill OU2 Phase I and Phase II tests.

Experiment	Soil Type	Description
HILLOU2#1	Ottawa	Partitioning tracers, surfactant
HILLOU2#2b	Ottawa	Surfactant
HILLOU2#2c	Ottawa	Surfactant
HILLOU2#3	Hill OU2	Partitioning tracers, surfactant
HILLOU2#4	Hill OU2	Clean field soil, Partitioning tracers, surfactant, polymer
HILLOU2#5	Hill OU2	Contaminated field soil, Partitioning tracers, radiolabeled surfactant, polymer
HILLOU2#6	Ottawa	Partitioning tracers, radiolabeled surfactant, polymer
HILLOU2#7	Hill OU2	Clean field soil, Partitioning tracers, radiolabeled surfactant, polymer
HILLOU2#8	Hill OU2	Contaminated field soil, Partitioning tracers, radiolabeled surfactant, polymer at 12.2°C

Table 10.5: Performance assessment of surfactant remediation

Experiment	Residual Saturation (mass balance)	Residual Saturation (partitioning tracers)
HILLOU2#1	0.0004	0.0004
HILLOU2#4	-0.0007	0.0070
HILLOU2#5	--	0.0054
HILLOU2#7	-0.0038	0.0002
HILLOU2#8	--	0.0015

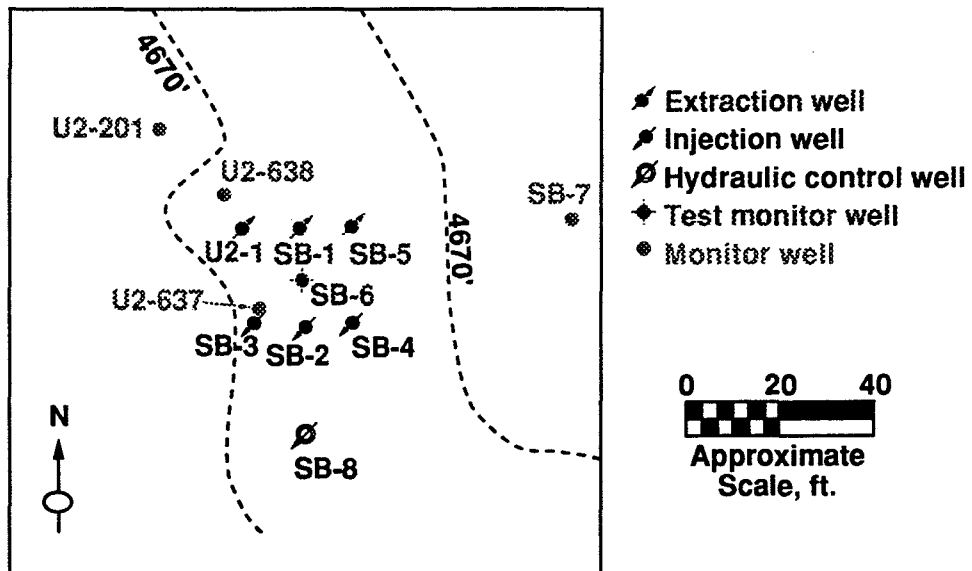


Figure 10.1: Plan view of Hill OU2.

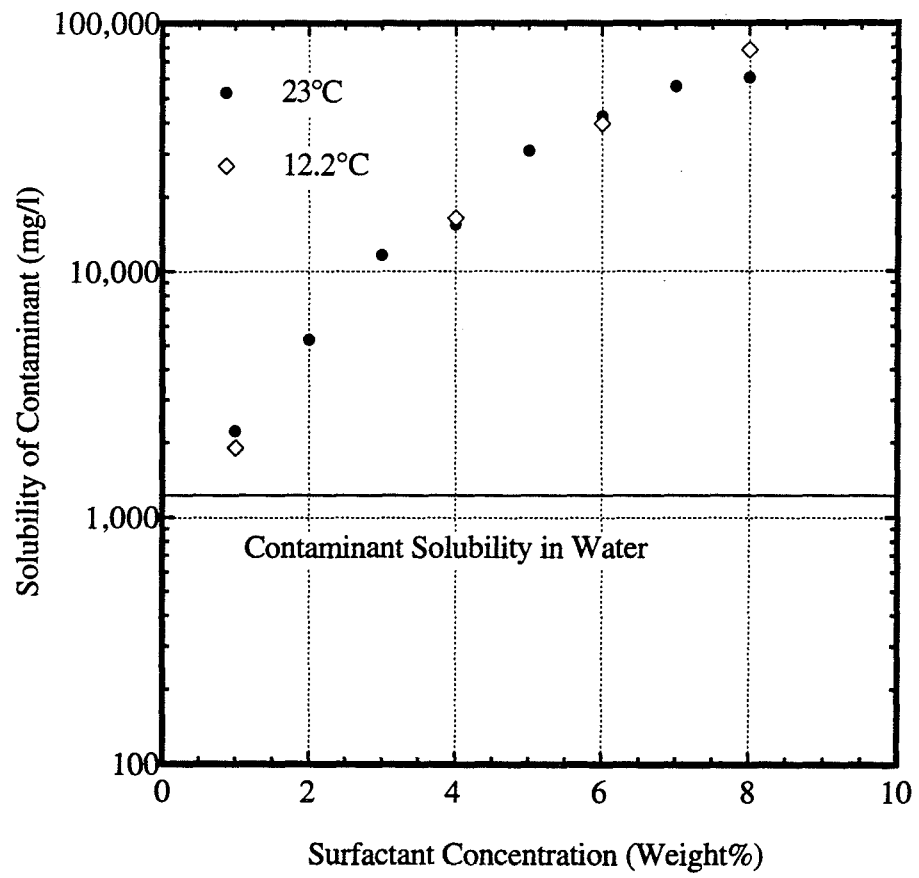


Figure 10.2: Solubility of Hill OU2 contaminants as function of surfactant concentration in Hill source water.

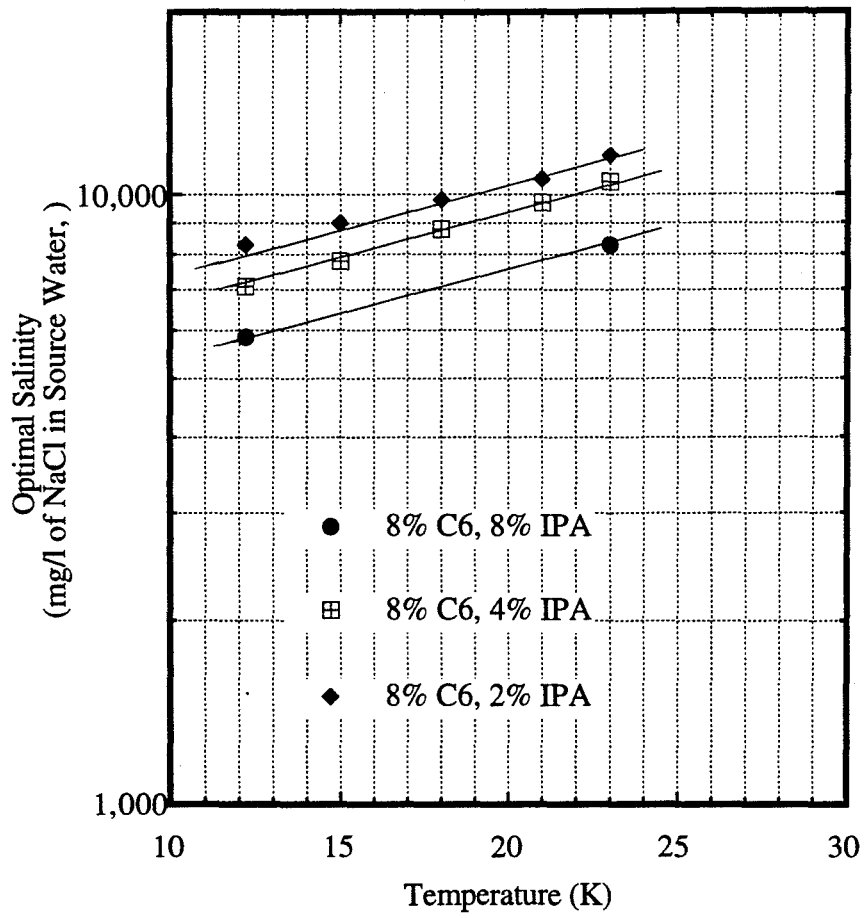


Figure 10.3: Optimal salinity plotted against temperature for a surfactant solution to be used in Hill OU2.

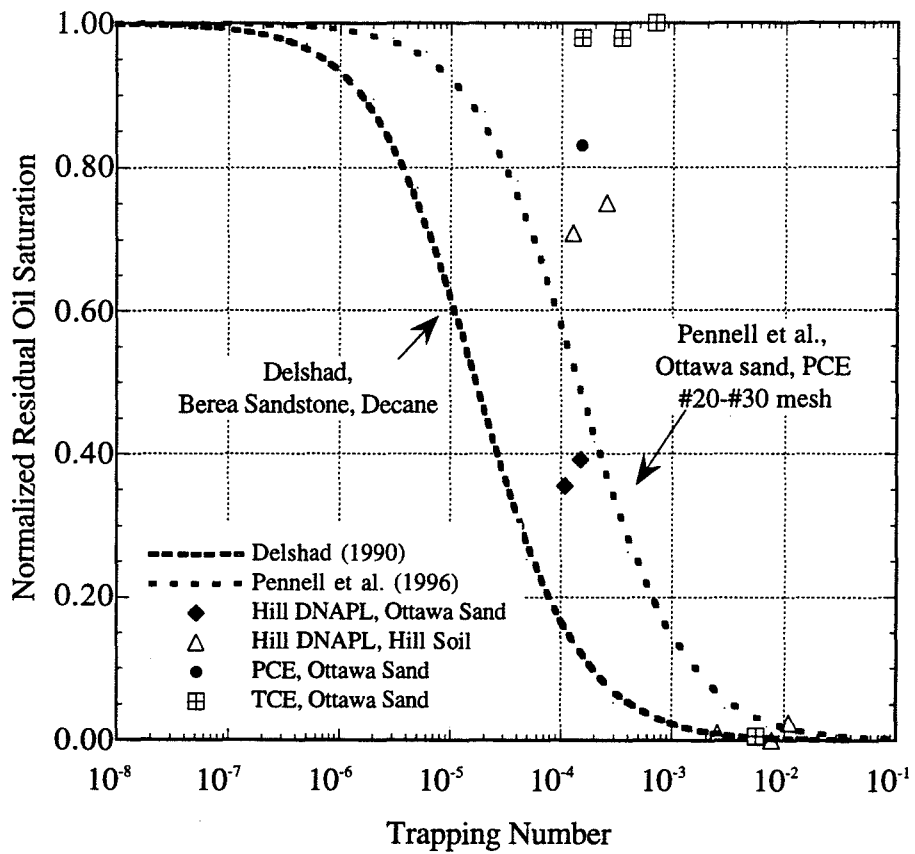


Figure 10.4: Comparison of capillary desaturation data.

Chapter 11: Summary, Conclusions and Future Work

11.1 SUMMARY

The main objectives of this work were development and perfection of experimental procedures for performing partitioning tracer tests for estimation of NAPL and performance of surfactant remediation and identifying suitable surfactant solutions for remediating soils contaminated by nonaqueous phase liquids. In pursuance of these objectives, the following were successfully accomplished:

1. Static partition coefficients were measured for several NAPLs, namely tetrachloroethylene (PCE), trichloroethylene (TCE), jet fuel (JP4), 1,2-dichloroethane, (DCA), 1,1,1-trichloroethane (TCE), trichloromethane (TCM or chloroform), Hill OU1 LNAPL and Hill OU2 DNAPL. A precise relation between the static partition coefficient for alcohol tracers and the solubility of alcohols in water was discovered. A very close match between partition coefficients measured using static experiments and dynamic column experiments was observed. Partition coefficients were also measured for a NAPL mixture consisting of DCA and PCE.
2. Experimental techniques for performing partitioning tracer tests were developed by performing several column experiments to estimate residual NAPL saturation with NAPLs such as PCE, TCE, JP4, Hill OU1 LNAPL and Hill OU2 DNAPL. The residual NAPL saturation based on mass balance and partitioning tracers were observed to agree to within ± 3

saturation percent in all column experiments. Despite low tracer recoveries in some column experiments, residual saturation estimates were still very good.

3. Adsorption of partitioning tracers on Ottawa sand and Hill field soil was measured. The values of adsorption of partitioning tracers by Ottawa sand and three types of field soil were below the error of measurement of tracer tests.
4. Partitioning tracers were used for performance assessment of surfactant remediation and NAPL saturation estimates after surfactant remediation based on mass balance measurements and partitioning tracers agree to within ± 1 saturation percent in all column experiments.
5. Phase behavior experiments were conducted with PCE, TCE, JP4 and Hill OU2 DNAPL with water, alcohol and anionic surfactants. Mostly volume fraction diagrams were developed. Most of the work involved performing salinity scans at a fixed surfactant concentration and fixed temperature. Ternary diagrams were developed for PCE and TCE at 23°C using two different surfactant solutions.
6. The effect of temperature, alcohol concentration, surfactant hydrophobe tail length, xanthan gum polymer and electrolyte type on phase behavior was investigated for TCE and Hill OU2 DNAPL.
7. Surfactant solutions were successfully used to remediate soil columns contaminated by PCE, TCE, jet fuel and Hill OU2 DNAPL. More than 99% of the NAPL was recovered in most of the column experiments.

8. Many surfactant flooding experiments were conducted with aqueous mixtures of surfactant, xanthan gum polymer and alcohols.
9. Both mobilization and solubilization were explored as options for remediation of soil contaminated by NAPLs.
10. Surfactant adsorption by Hill field soil was measured by using radiolabeled surfactant and less than 165 $\mu\text{g/g}$ of surfactant was adsorbed by field soil from Hill AFB.
11. Pressure drops across the contaminated soil columns were measured during surfactant flood and post surfactant flood and was used as a useful tool in surfactant selection.
12. Experimental techniques for laboratory selection of partitioning tracers and surfactants for field applications were perfected. Both surfactant and partitioning tracer tests were carried out successfully at 12.2°C in the lab.
13. Two field partitioning tracer tests (Hill OU1 and Hill OU2) and one field surfactant enhanced aquifer remediation test (Hill OU2) were designed as a direct consequence of all the experiments performed in this work.

11.2 CONCLUSIONS

The conclusions that can be drawn from this work can be divided into two areas, namely partitioning tracer tests and surfactant floods. The most important conclusion is that partitioning tracers can be used to estimate NAPL saturations accurately. They can be used both to estimate residual NAPL saturation and for performance assessment of surfactant remediation by estimating residual NAPL volume after surfactant remediation. This conclusion was reached based on

excellent agreement between NAPL saturation estimated using mass balance and NAPL saturation estimated using partitioning tracers in several column experiments. Based on experimental work presented in this dissertation, the first field LNAPL partitioning tracer test was designed at Hill OU1 and the first unconfined field DNAPL partitioning tracer test was designed.

Laboratory experiments in this work have clearly demonstrated that by designing surfactant floods using a combination of phase behavior and column experiments, up to 99.9% of the contaminant can be recovered and final TCE concentrations in the water can be reduced to less than 1 mg/l after surfactant flooding. In some experiments such low TCE concentrations in the effluent water could not be measured because of the presence of nylon tubing and Teflon end pieces on the columns which caused persistent contaminant tails on the order of 10 to 50 mg/l. Hence, for accurate evaluation of remediation experiments of chlorinate solvents, any column material that will adsorb/desorb the contaminant should be avoided. These results are much more favorable than others reported in the literature for pure contaminants such as TCE or PCE let alone field DNAPLs. The first field surfactant flood to remediate a DNAPL in an unconfined aquifer was designed as a result of the laboratory experiments performed in this work. A final DNAPL saturation of 0.0004 was achieved in the field site as a result of surfactant flooding.

From this work it can be concluded that phase behavior experiments are a very important step to select surfactants with high contaminant solubilization, quick coalescence rates and minimal liquid crystal forming tendencies. Surfactant solutions that form liquid crystals or gels are often non-Newtonian and have high

viscosity and cause problems such as permeability reduction and plugging as evidenced from results in experiments DW#2 and DW#5. Co-solvents such as ethanol or isopropanol can be used to prevent such problems and promote equilibrium microemulsion behavior. Mass transfer kinetics greatly complicate the modeling and scaleup of surfactant remediation, thus it is of great advantage to use solutions that rapidly approach equilibrium behavior during the displacement in the aquifer. These experiments were used to seek out and find the sodium dihexyl sulfosuccinate/isopropanol mixture that performed so well in the Hill OU2 field tests.

The use of xanthan gum polymer as a viscosifier helped in improving the rate of contaminant removal in solubilization experiments as the effluent contaminant concentration was closer to the equilibrium contaminant solubilization as observed in experiment POLYTCE#1. This is due to better contact between the trapped NAPL and the more viscous surfactant/alcohol solution containing polymer. No problems with polymer were observed in column experiments with both pure TCE and Hill DNAPL. No significant difference in the phase behavior was observed with such solutions when sufficient co-solvent was used.

The measurement of hydraulic gradients during a surfactant flood is a very useful tool in quantifying surfactant behavior during transport in a porous medium. Surfactants that are more likely to form macroemulsions, gels and liquid crystals will cause high gradients during the surfactant flood and should be avoided. Acceptable surfactants will show low gradients during the surfactant flood. Low gradients and negligible permeability reduction with Ottawa sand and

Hill field soil were observed when sodium dihexyl sulfosuccinate was used with isopropanol as a cosolvent.

The other more specific conclusions drawn are:

1. Negligible adsorption of alcohol tracers by Ottawa sand and Hill field soil was observed in column experiments.
2. A relationship between the partition coefficient and solubility of alcohol in water was observed for similar types of alcohols on a log-log plot. This was observed for straight chain alcohols, alcohols with one branched methyl group and alcohols with two branched methyl groups.
3. Static and dynamic partition coefficients were observed to agree within experimental error. However dynamic partition coefficients were observed to give better residual saturation estimates when used in soil column experiments.
4. Negligible adsorption of sodium dihexyl sulfosuccinate was observed on Hill OU2 field soil.
5. Surfactant solutions with sodium dihexyl sulfosuccinate were found to be suitable for remediating soil columns contaminated with PCE, TCE and Hill OU2 DNAPL. When co-solvent was used with this surfactant, no decrease in permeability occurred after the surfactant floods and a low hydraulic gradient acceptable in most field tests was observed in all cases.
6. Only about 1 pore volume of surfactant was required to remove almost all the DNAPL from soil columns when optimal salinity was used to give low IFT and mobilization of DNAPL.

7. Surfactant solutions with sodium dioctyl sulfosuccinate without cosolvent were prone to gel/liquid crystal formation with PCE and JP4. Excessive pressure drops were measured in two experiments where sodium dioctyl sulfosuccinate was used.
8. The optimal salinity was observed to decrease as temperature was decreased for sodium dihexyl sulfosuccinate solutions with TCE and Hill OU2 DNAPL.
9. Addition of IPA can be used to decrease the optimal salinity for sodium dihexyl sulfosuccinate solutions with TCE and Hill OU2 DNAPL, but this was accompanied by a decrease in solubilization parameter.
10. The optimal salinity can be decreased and solubilization parameter can be increased by increasing the surfactant hydrophobe length, but a longer hydrophobe would mean a higher probability of gel or liquid crystal formation in surfactant solutions.
11. Persistent tails of low concentration contaminant (≈ 10 mg/l) were found to be caused by adsorption by Teflon end pieces and Nylon tubing and could be eliminated as a laboratory artifact by using all stainless steel columns.
12. Xanthan gum polymer was used to improve the performance of the surfactant solutions by increasing its viscosity without unacceptable increases in hydraulic gradient. The viscosity of the surfactant solution increases about four fold when 500 mg/l xanthan gum is added to the aqueous surfactant solution at shear rates corresponding to interstitial velocities on the order of 10 ft/day.

13. Xanthan gum or other suitable food-grade polymers should be used in future remediation field tests as a very inexpensive and simple method to mitigate the effects of heterogeneity at all scales in the aquifer as well as an aid in hydraulic control of the flood. This will reduce the amount and thus cost of the surfactant needed, shorten the time required to remediate the aquifer and improve the control of the flood.

11.3 FUTURE WORK

The following recommendations are made for future work:

1. The accuracy of the partitioning tracer test can be improved by improving analytical techniques for the analysis of the tracers.
2. The applicability of partitioning tracer experiments in fractured media should be investigated.
3. More research should be carried out to quantify tracer adsorption .
4. The use of perfluorocarbon tracers in saturated zone partitioning tracer tests should be investigated.
6. More experiments should to be done with surfactant-polymer solutions to evaluate the applicability of other types of polymers besides xanthan gum.
7. More research should be done to identify and test surfactant-cosolvent-polymer solutions for use in fractured media.

Nomenclature

A = cross sectional area of porous medium (L^2)

$\frac{1}{a}$ = slope of the tracer response curves plotted on a semi-log scale (T^{-1})

C = Chun Huh constant (which is actually a complex function given by Huh (1979), but varies only a little for many cases of practical interest)

C_b = tracer concentration at time t_b (ML^{-3})

C_D = normalized tracer concentration

$C_{i,NAPL}$ = concentration of tracer species 'i' in the nonaqueous phase at equilibrium (ML^{-3})

$C_{i,I}$ = the concentration of tracer component 'i' in the injected tracer (ML^{-3})

$C_{i,Water}$ = concentrations of tracer species 'i' in the aqueous phase at equilibrium (ML^{-3})

C_o = Initial tracer concentration in porous medium (ML^{-3})

C_S = Concentration of standard (ML^{-3})

C_a^o = alcohol concentration in oil (ML^{-3})

C_a^w = alcohol concentration in water (ML^{-3})

C_a^s = alcohol concentration in surfactant micelles (ML^{-3})

$\Delta\Phi$ = potential drop across porous medium at steady state ($ML^{-1}T^{-2}$)

$\Delta\Phi_j$ = potential drop across porous medium for species 'j' ($ML^{-1}T^{-2}$)

Δp_T = Pressure drop across the transducer ($ML^{-1}T^{-2}$)

f_{N_p} = fraction of NAPL recovered during remediation

γ = Interfacial tension (MT^{-2})

γ_i^∞ = activity coefficient of tracer 'i' at infinite dilution

H = Head loss across the porous medium (L)

H_D = hydraulic gradient across porous medium

k = permeability of porous medium (L^2)

k_{ri} = Relative permeability of phase 'i'

K_d = Distribution coefficient and this is equal to the slope of the linear adsorption isotherm ($M^{-1}L^3$)

K_i = partition coefficient of tracer species 'i'

K_m = ratio of the mole fraction of the compound in the micellar pseudo-phase to the mole fraction of the compound in the aqueous pseudo-phase.

$K_{N,w}^i$ = partition coefficient for tracer species 'i' with NAPL and water

K_a^o = partition coefficient of alcohol between oil and water

K_a^s = partition coefficient of alcohol between surfactant micelles and water

L = length of porous medium (L)

M_i = mass of tracer injected (M)

MSR = molar solubilization ratio

μ = viscosity of flowing fluid ($ML^{-1}T^{-1}$)

N_p = volume of NAPL recovered during surfactant remediation (L^3)

ϕ = porosity of soil

Q = flow rate through porous medium (L^3T^{-1})

Q_i = flow rate of phase 'i' at steady state (L^3T^{-1})

r = radius of soil column (L)

R_f = retardation factor

ρ_a = density of alcohol (ML^{-3})

ρ_b = bulk density of soil (ML^{-3})

ρ_N = density of NAPL (ML^{-3})

ρ_w = density of water (ML^{-3})

ρ_j = Density of fluid flowing through the core (ML^{-3})

ρ_s = density of tracer solution (ML^{-3})

ρ_x = Density of fluid in the lines (ML^{-3})

S_N = residual saturation of NAPL in porous medium

$S_{N,cmc}$ = apparent solubility of a contaminant in moles per liter at the CMC ($Mol.L^{-3}$)

$S_{N,mic}$ = apparent solubility of a contaminant in moles per liter at surfactant concentrations greater than the CMC ($Mol.L^{-3}$)

σ = solubilization parameter

σ_{cme} = contaminant solubilization in microemulsion (ML^{-3})

σ_{C_s} = standard deviation in concentration (ML^{-3})

σ_{w_1} = standard deviation in weight of alcohol added (M)

σ_{W_2} = standard deviation in weight of water added (M)

σ_ρ = standard deviation in density measurements (ML^{-3})

σ_{V_p} = standard deviation in pore volume estimation (L^3)

$\sigma_{W_{sat}}$ = standard deviation in weight of saturated column (M)

$\sigma_{W_{dry}}$ = standard deviation in weight of dry column (M)

σ_{ρ_w} = standard deviation in density measurements (ML^{-3})

σ_{S_N} = standard deviation in NAPL saturation.

$\sigma_{W_{sn}}$ = standard deviation in weight of saturated column (M)

$\sigma_{W_{sat}}$ = standard deviation in weight of dry column (M)

σ_{ρ} = standard deviation in density measurements (ML^{-3})

σ_{K_i} = standard deviation in partition coefficient measurements.

σ_{V_W} = standard deviation in measurement of water volume (L^3).

σ_{V_N} = standard deviation in measurement of NAPL volume (L^3).

σ_o = NAPL solubilization parameter

σ_w = water solubilization parameter

σ_C = standard deviation in measurement of concentrations measured using a GC
(ML^{-3})

t_b = time at which tracer response becomes linear on a semi-log scale (T)

t_D = normalized time or pore volumes injected

\bar{t}_i = first temporal time moment of tracer species 'i' (T^3)

V_A = volume of alcohol (L^3)

V_a^o = volume of alcohol in oil (L^3)

V_a^w = volume of alcohol in water (L^3)

V_a^s = volume of alcohol in surfactant (L^3)

V_{ds} = tracer slug size (L^3)

V_f = the cumulative volume at which the tracer test is terminated (L^3)

V_o = volume of oil (L^3)

V_{me} = Volume of microemulsion (L^3)

V_N = Volume of NAPL solubilized (L^3)

V_p = pore volume of soil pack (L^3)

V_S = Volume of surfactant (L^3)

V_w = Volume of water solubilized (L^3)

V_{wa} = molar volume of water

V_{wp} = volume of water produced during the NAPL flood (L^3)

V_{np} = volume of NAPL produced during the waterflood (L^3)

V_{NAPL} = volume of NAPL at residual NAPL saturation (L^3)

V_W = the volume of the aqueous phase (L^3)

\bar{V} = first temporal volume moment of soil column (L^3)

V_s = tracer slug size (L^3)

\bar{V}^* = movable pore volume of soil medium (L^3)

\bar{V}_i = first temporal volume moment of tracer species 'i' (L^3)

V_f = the cumulative volume at which the tracer test is terminated (L^3)

\bar{V}_p = first temporal volume moment of partitioning tracer (L^3)

\bar{V}_n = first temporal volume moment of conservative tracer (L^3)

V_o' = apparent volume of NAPL solubilized measured using volumetric measurements

W_{dry} = weight of dry column

W_{sat} = weight of saturated column

W_{sn} = weight of soil pack at residual NAPL saturation (M)

W_{sf} = weight of soil pack after surfactant remediation (M)

w_a = weight of alcohol added (M)

W_w = weight of water added (M)

x_i = mole fraction of tracer 'i' in solution

X_a = mole fraction of the contaminant in the aqueous pseudo-phase

X_m = mole fraction of the contaminant in the micellar pseudo-phase

Appendix: A

GC ERRORS IN REPRODUCIBILITY

The standards are mixed by weight using the following formula;

$$C_S = \frac{w_a(\text{mg})}{W_w(\text{g})} \cdot \rho_s \left(\frac{\text{g}}{\text{l}} \right) \quad (\text{A.1})$$

C_S = Concentration of standard

w_a = weight of alcohol added

W_w = weight of water added

ρ_s = density of tracer solution

The uncertainty in measurement can be estimated using the following formula;

$$\frac{\sigma_{C_S}^2}{C_S^2} = \frac{\sigma_{w_1}^2}{w_1^2} + \frac{\sigma_{W_2}^2}{W_2^2} + \frac{\sigma_{\rho}^2}{\rho^2} \quad (\text{A.2})$$

σ_{C_S} = standard deviation in concentration

σ_{w_1} = standard deviation in weight of alcohol added (5 mg)

σ_{W_2} = standard deviation in weight of water added (0.01 g)

σ_{ρ} = standard deviation in density measurements (0.005 g/cc)

Using the above, $\sigma_{C_S} = 0.026$ or 2.6%.

ERRORS IN PORE VOLUME MEASUREMENT BY MASS BALANCE

The formula for determining the pore volume of a soil pack is;

$$V_p = \frac{W_{\text{sat}} - W_{\text{dry}}}{\rho_w} \quad (4.5)$$

V_p = pore volume of soil pack

W_{sat} = weight of saturated core

W_{dry} = weight of dry core

The uncertainty in measurement can be estimated using the following formula;

$$\sigma_{V_p}^2 = \left(\frac{\partial W_{\text{sat}}}{\partial V_p}\right)^2 \sigma_{W_{\text{sat}}}^2 + \left(\frac{\partial W_{\text{dry}}}{\partial V_p}\right)^2 \sigma_{W_{\text{dry}}}^2 + \left(\frac{\partial \rho_w}{\partial V_p}\right)^2 \sigma_{\rho_w}^2 \quad (A.3)$$

σ_{V_p} = standard deviation in pore volume estimation

$\sigma_{W_{\text{sat}}}$ = standard deviation in weight of saturated column (0.01 g)

$\sigma_{W_{\text{dry}}}$ = standard deviation in weight of dry column (0.01 g)

σ_{ρ_w} = standard deviation in density measurements (0.005 g/cc)

Using the above, $\sigma_{V_p} = 0.005$ or 0.5%

ERRORS IN RESIDUAL TCE SATURATION MEASUREMENT BY MASS BALANCE

The formula for determining the pore volume of a soil pack is;

$$S_N = \left(\frac{W_{\text{sn}} - W_{\text{sat}}}{\rho_N - \rho_w}\right) \frac{1}{V_p} \quad (4.19)$$

S_N = residual NAPL saturation

W_{sn} = weight of soil pack at residual NAPL saturation

ρ_N = density of NAPL

ρ_W = density of NAPL

V_p = pore volume of soil pack

W_{sat} = weight of saturated core

W_{dry} = weight of dry core

The uncertainty in measurement can be estimated using the following formula;

$$\begin{aligned} \sigma_{S_N}^2 = & \left(\frac{\partial W_{sn}}{\partial S_N}\right)^2 \sigma_{W_{sn}}^2 + \left(\frac{\partial W_{sat}}{\partial S_N}\right)^2 \sigma_{W_{sat}}^2 + \left(\frac{\partial \rho_w}{\partial S_N}\right)^2 \sigma_{\rho_w}^2 + \\ & \left(\frac{\partial \rho_N}{\partial S_N}\right)^2 \sigma_{\rho_N}^2 + \left(\frac{\partial V_p}{\partial S_N}\right)^2 \sigma_{V_p}^2 \end{aligned} \quad (A.4)$$

σ_{S_N} = standard deviation in NAPL saturation.

$\sigma_{W_{sn}}$ = standard deviation in weight of saturated column (0.01 g)

$\sigma_{W_{sat}}$ = standard deviation in weight of dry column (0.01 g)

σ_{V_p} = standard deviation in pore volume estimation (0.5% of pore volume)

σ_{ρ} = standard deviation in density measurements (0.005 g/cc)

Using the above, $\sigma_{S_N} = 2.5\%$

ERRORS IN STATIC PARTITION COEFFICIENT MEASUREMENT

The formula for determining the static partition coefficient is;

$$K_i = \frac{V_W}{V_N} \left(\frac{C_{i,I}}{C_{i,Water}} - 1 \right) \quad (4.24)$$

K_i = partition coefficient of tracer species 'i'

$C_{i,DNAPL}$ = concentration of tracer species 'i' in the nonaqueous phase at equilibrium.

$C_{i,Water}$ = concentrations of tracer species 'i' in the aqueous phase at equilibrium

V_W = the volume of the aqueous phase

V_N = the volume of the NAPL

$C_{i,I}$ = the concentration of tracer component 'i' in the injected tracer.

The uncertainty in measurement can be estimated using the following formula;

$$\sigma_{K_i}^2 = \left(\frac{\partial V_W}{\partial K} \right)^2 \sigma_{V_W}^2 + \left(\frac{\partial V_N}{\partial K} \right)^2 \sigma_{V_N}^2 + \left(\frac{\partial C_i}{\partial K} \right)^2 \sigma_{C_i}^2 + \left(\frac{\partial C_{i,I}}{\partial K} \right)^2 \sigma_{C_{i,I}}^2 \quad (A.5)$$

σ_{K_i} = standard deviation in partition coefficient measurements.

σ_{V_W} = standard deviation in measurement of water volume (0.05 cc).

σ_{V_N} = standard deviation in measurement of NAPL volume (0.05 cc).

σ_C = standard deviation in measurement of concentrations measured using a GC (6.1% of measured concentration).

Using the above, the error varied between 10-12%.

Bibliography

- Abdul, A.S., T.L. Gibson, and D.N. Rai: "Selection of Surfactants for the Removal of Petroleum Products from Shallow Sandy Aquifers," *Ground Water*, 28(6), p. 920, 1990.
- Abriola, L.M.: "Modeling Multiphase Migration of Organic Chemicals in groundwater Systems: A Review and Assessment," *Environmental Health Perspectives* 88, p.117, 1989.
- Allison, S.B., G.A. Pope, and K. Sepehrnoori: "Analysis of Field Tracers for Reservoir Description," *Journal of Petroleum Science and Engineering*, 5, p. 173, 1991.
- Allred B. and G.O. Brown: "Surfactant-Induced Reductions of Saturated Hydraulic Conductivity and Unsaturated Diffusivity," in *Surfactant - Enhanced Subsurface Remediation Emerging Technologies*, Sabatini, David A., Knox, Robert C., Harwell Jeffrey H. (eds). ACS symposium series 594, American Chemical Society Washington DC, pp. 216-230, 1995.
- Ang, C.C. and A.S. Abdul: "Aqueous Surfactant Flushing of Residual Oil Contamination from Sandy Soil," *Ground Water Monitoring and Review*, 11 (2), p.121, 1991.
- Annable, M.D., P.S.C. Rao, K. Hatfield, W.D. Graham, and A.L. Wood: "Use of Partitioning Tracer for Measuring Residual NAPL Distribution in a Contaminated Aquifer: Preliminary Results from a Field Scale Test," *Proceedings of the second Tracer Workshop, Austin, TX, Nov. 14 & 15, 1994*, edited by T. Bjørnstad and G. Pope, Institute for Energy Technology, N-2007 Kjeller, Norway.
- Annable M.D., P.S.C. Rao, K. Hatfield, W.D. Graham, A.L. Wood and C.G. Enfield: "Use of Partitioning Tracers for Measuring Residual NAPL: Results from a Field-Scale Test," Submitted to *Journal of Environmental Engineering*, 1996.
- Asgharian N., P. Otken, C.K. Sunwoo and W.H. Wade: "Synthesis and Performance of High Efficiency Cosurfactants.1. Model Systems," *Langmuir*, 7 (12), pp.2904-2910, 1991.
- Asgharian N., P. Otken, C.K. Sunwoo and W.H. Wade: "Synthesis and Performance of High Efficiency Cosurfactants.2. Commercial Variants," *Journal Dispersion Science and Technology*, 13 (5), pp.515-525, 1992.

- Baran, J.R. Jr., G.A. Pope, W.H. Wade, and V. Weerasooriya: "Phase Behavior of Water/Perchloroethylene/Anionic Systems," *Langmuir*, 10 (4), p1146, 1994a.
- Baran, J.R. Jr., G.A. Pope, W.H. Wade, V. Weerasooriya, and A. Yapa: "Microemulsion Formation with Chlorinated Hydrocarbon Liquids," *Journal of Colloid Interface Science*, 168 (1), p.67, 1994b.
- Baran, J.R. Jr., G.A. Pope, W.H. Wade, V. Weerasooriya, and A. Yapa: "Microemulsion Formation with Chlorinated Hydrocarbons of Different Polarity Liquids," *Environmental Science and Technology*, 28, pp.1361-1366, 1994c.
- Baran, J.R. Jr., G.A. Pope, W.H. Wade and V. Weerasooriya: "Surfactant Systems for Soil and Aquifer Remediation of JP4 Jet Fuel," *Journal of Dispersion Science and Technology*, 17 (2), pp.131-138, 1996a.
- Baran, J.R. Jr., G.A. Pope, C Schultz, W.H. Wade, V. Weerasooriya, and A. Yapa: "Toxic Spill Remediation of Chlorinated Hydrocarbons Via Microemulsion Formation," in *Surfactants in Solution*, A.K. Chattopadhyay and K.L. Mittal (eds), Marcel Dekker Inc, pp.393-411, 1996b.
- Baran J.R. Jr., G.A. Pope, W.H. Wade and V. Weerasooriya: "Water/Chlorocarbon Winsor I-III-II Microemulsion Phase Behavior with Alkyl Glucamide Surfactants," *Environmental Science and Technology*, 30 (7), pp.2143-2147, 1996c.
- Bourbonais, K.A., G.C. Compeau, L.K. MacClellan, "Evaluating Effectiveness of In Situ Soil Flushing with Surfactants," *Surfactant Enhanced Subsurface Remediation Emerging Technologies*, D.A. Sabatini, R.C. Knox, J.H. Harwell (eds), ACS symposium series 594, American Chemical Society, Washington, DC, pp.161-177, 1995.
- Bourrel, M., R.S. Schechter: *Microemulsions and Related Systems*, Marcel Dekker, New York, 1988.
- Bourrel, M., A.M. Lipow, W.W. Wade, R.S. Schechter, and J.L. Salager, "Properties of Amphiphilic/Oil/Water Systems at an Optimal Formulation of Phase Behavior," SPE 7450, presented at the 53rd Annual Fall Technical Conference and Exhibition of the Society of Petroleum Engineers, Houston, Texas, 1978.
- Brandes D. and K.J. Farley: "Importance of Phase Behavior on the Removal of Residual DNAPLs from Porous Media by Alcohol Flooding," *Water Environment Research*, 65 (7), pp.869-878, 1993.

- Brown C.L.: "Simulation of Surfactant Enhanced Aquifer Remediation of Aquifers Contaminated by Dense Nonaqueous Phase Liquids," M.S. thesis, The University of Texas at Austin, 1993.
- Brown C.L., G.A. Pope, L.M. Abriola and K. Sepehrnoori: "Simulation of Surfactant Enhanced Aquifer Remediation," *Water Resources Research*, 30 (11), p.2959, 1994.
- Brown, C.L.: "Modeling and Design of Surfactant-Enhanced Aquifer Remediation Field Tests," P.h.D. dissertation, The University of Texas at Austin, 1997.
- Brown, C.L., M. Delshad, V. Dwarakanath, D.C. McKinney, G.A. Pope: "Design of a Field-Scale Surfactant Enhanced Remediation of a DNAPL Contaminated Aquifer," Presented at the I&EC Special Symposium American Chemical Society Birmingham, AL, September 9-12, 1996a.
- Brown C.L., M. Delshad, V. Dwarakanath, D.C. McKinney, G. A. Pope, W.H. Wade, R.E. Jackson, J.T. Londergan, H.W. Meinardous: "A Successful Field Demonstration of Surfactant Flushing of an Unconfined Aquifer Contaminated by Chlorinated Solvents," submitted to *Environmental Science and Technology*, 1996b.
- Butler, G.W., R.E. Jackson, J.F. Pickens, and G.A. Pope, "An Interwell Solubilization test for Characterization of Nonaqueous-Phase Liquid Zones," *Surfactant-Enhanced Remediation of Subsurface Contamination*, D.A. Sabatini, R.C. Knox, and J.H. Harwell (eds.), 201-215, May, 1995.
- Camilleri D., A.Fil, G.A. Pope, B.A. Rouse and K. Sepehrnoori: "Improvements in Physical-Property Models Used in Micellar/Polymer Flooding," *SPE Reservoir Engineering*, pp.433-440, Nov 1987.
- Casad B.M. and P.L. Gant: "Reservoir Evaluation Using Partitioning Tracer," U.S. Patent 4,876,449, 1989.
- Causin, E., J. Rochon, and D. Marzorati: "Field Measurements of Remaining Oil Saturation," paper SPE/DOE 20260, *Proceedings of the SPE/DOE 7th Symposium on Enhanced Oil Recovery*, Tulsa, OK, April 22-25, 1990.
- Cayais, J.L., R.S. Schechter and W. H. Wade: "The Measurement of Low Interfacial Tension Via the Spinning Drop Technique," in *Adsorption at Interfaces*, ACS Symposium series, 8, J.R. Gould (ed), American Chemical Society, Washington D.C., 1985.
- Conrad S.H., J.L. Wilson, W.R. Mason and W.J. Peplinski: "Visualization of Residual Organic Liquid Trapped in Aquifers", *Water Resources Research*, 28 (2), pp.467-478, 1992.

- Cooke C.E. Jr.: "Method of Determining Fluid Saturations in Reservoirs," U.S. Patent 3,590,923., 1971.
- Deans, H.A.: "Method of determining fluid saturations in reservoirs," U.S. Patent No. 3,623,842, 1971.
- Delshad, M.: "Trapping of Micellar Fluids in Berea Sandstone," Ph.D. dissertation, The University of Texas at Austin, 1990.
- Delshad, M. G.A. Pope and K. Sepehrnoori: "A Compositional Simulator for Modeling Surfactant Enhanced Aquifer Remediation, 1 Formulation," *Journal of Contaminant Hydrology*, 23, pp.303-327, 1996.
- Demond, A.H. and A.S. Lindner: "Estimation of Interfacial Tension Between Organic Liquids and Water," *Environmental Science Technology*, 27 (12), p. 2318-2331, 1993.
- Descant F.J.: "Simulation of Single Well Tracer Flow," M.S. thesis, The University of Texas at Austin, 1989.
- Diallo M.S., L.M. Abriola and W.J. Weber Jr.: "Solubilization of Nonaqueous Phase Liquid Hydrocarbons in Micellar Solutions of Dodecyl Alcohol Ethoxylates," *Environmental Science and Technology*, 28 (11), pp.1829-1837, 1994.
- Dwarakanath, V., B. Rouse, G.A. Pope, D. Kostarelos, D.R. Shotts, K. Sepehrnoori, and W.H. Wade: "Surfactant Enhanced Remediation of Soil Columns Contaminated by Non Aqueous Phase Liquids," to be submitted to *Journal of Contaminant Hydrology*, 1997.
- Dwarakanath, V., D. R. Shotts, G.A. Pope and W.H. Wade: "Phase Behavior of a Field Dense Nonaqueous Phase Liquid, Alcohol, Electrolyte and Anionic Surfactant Formulations," Paper to be submitted to *Environmental Science and Technology*, 1997.
- Dugstad Ø., T. Bjørnstad and I.A. Hundere: "Measurements of Gas Tracer Retention under Simulated Reservoir Conditions," *Journal of Petroleum Science and Engineering*, 10, pp.17-25, 1993.
- Edgar J.: M.S. thesis, The University of Texas at Austin, in progress
- Edwards D. A., Zhongbao Liu and R.G. Luthy: "Surfactant Enhanced Solubility of Hydrophobic Organic Compounds in Water and Soil-Water Systems," *Organic Substances and Sediments in Water*, R. A. Baker (ed), Lewis Publishers, Chelsea, MI, pp.383-405, 1991a.

- Edwards D. A., R.G. Luthy and Zhongbao Liu: "Solubilization of Polycyclic Hydrocarbons in Micellar Nonionic Surfactant Solutions," *Environmental Science Technology*, 25 (1), pp.127-133, 1991b.
- Ellis, W.D., D.R. Morgan, and S.R. Ranjithan: "Treatment of Contaminated Soils with Aqueous Surfactants," EPA/600/2-85/129, Hazardous Waste Engineering Research Laboratory, November 1986.
- Ferreira, L.E.A.: "Reservoir Characterization Using Single-Well Tracer Tests," Ph.D. dissertation, The University of Texas at Austin, 1992.
- Fetter, C.W.: *Contaminant Hydrogeology*, Macmillan Publishing Company, New York, New York, 1993.
- Fountain, J.C., A. Klimek, M.G. Beikirch, and T.M. Middleton: "The use of surfactants for in situ extraction of organic pollutants from a contaminated aquifer," *Journal of Hazardous Materials*, 28 (3), p. 295, 1991.
- Fountain, J.C.: "Field Tests of Surfactant Flooding Mobility Control of Dense Nonaqueous-phase Liquids," *Transport and Remediation of Subsurface Contaminants Colloidal, Interfacial, and Surfactant Phenomena*, D.A. Sabatini (ed), R.C. Knox, American Chemical Society, Washington, DC, pp.182-191, 1992.
- Fountain, J.C, C. Waddel-Sheets, A. Lagowski, C. Taylor, D. Frazier, and M. Byrne: "Enhanced Removal of Dense Nonaqueous-phase Liquids Using Surfactants Capabilities and Limitations from Field Trials," *Surfactant-Enhanced Subsurface Remediation Emerging Technologies*, D.A. Sabatini, R.C. Knox, J.H. Harwell (eds), ACS 594, American Chemical Society, Washington, DC, pp.177-190, 1995.
- Fountain J.C., R.C. Starr, T. Middleton, M. Beikirch, C. Taylor and D. Hodge:, "A Controlled Field Test of Surfactant-Enhanced Aquifer Remediation," *Ground Water*, 34 (5), pp.910-916, 1996.
- Freeze, G.A., J.C. Fountain, G.A. Pope, and R.E. Jackson: "Modeling the Surfactant-Enhanced Remediation of Perchloroethylene at the Borden Test Site Using the UTCHEM Compositional Simulator," *Surfactant-Enhanced Subsurface Remediation Emerging Technologies*, D.A. Sabatini, R.C. Knox, J.H. Harwell (eds), ACS 594, American Chemical Society, Washington, DC, pp.191-200, 1995.
- Gannon, O.K., P. Bribing, K. Raney, A. Ward, J. Wilson, J.L Underwood, and K.A. Deblak: "Soil Clean Up by In-Situ Surfactant Flushing, III. Laboratory Results," *Journal of Science Technology*, September, pp.1073-1094, 1992.

- Garver F.J.: "The Competition for Chromium in a Berea Core Between Xanthan Biopolymer and the Resident Clays," M.S. thesis, The University of Texas at Austin, 1988.
- Gellar, J.T. and J.R. Hunt: "Mass transfer from nonaqueous phase liquids in water-saturated porous media," *Water Resources Research*, 29 (4), pp.833-845, 1993.
- Glinsmann, G.R.: "Surfactant Flooding with Microemulsions Formed In-Situ-Effect of Oil Characteristics," SPE 8326, proceedings, 54th Annual Technical Conference and Exhibition of the Society of Petroleum Engineers, Las Vegas, Nevada, 1979.
- Graciaa, A.L., N. Fortney, R.S. Schechter, W.H. Wade and S. Yiv: "Criteria for Structuring Surfactant to Maximize Solubilization of Oil and Water I: Commercial Nonionic Surfactants," SPE 9815, proceedings, second joint SPE/DOE Symposium on Enhanced Oil recoverys, Tulsa, OK, 1981.
- Grimberg S.T., C.T. Miller and M.D. Aitken: "Surfactant-Enhanced Dissolution of Phenanthrene into Water for Laminar Flow Conditions," *Environmental Science and Technology*, 30 (10), pp.2967-2974, 1996.
- Harvey, C.F. and S. Gorelick: "Temporal Moment-Generating Equations: Modeling Transport and Mass Transfer in Heterogeneous Aquifers," *Water Resources Research*, 31 (8), pp.1895-1911, 1995.
- Harwell, J.H.: "Factors Affecting Surfactant Performance in Groundwater Remediation Applications," *Transport and Remediation of Subsurface Contaminants Colloidal, Interfacial, and Surfactant Phenomena*, D.A. Sabatini (ed), R.C. Knox, American Chemical Society, Washington, DC, pp.124-132, 1992.
- Healy R.N. and R.L. Reed: "Physicochemical Aspects of Microemulsion Flooding," *SPE Journal*, pp.491-501, Oct 1974.
- Healy R.N., R.L. Reed and C.W. Carpenter Jr.: "A Laboratory Study of Microemulsion Flooding," *SPE Journal*, pp.87-103, Feb 1975.
- Heglund, D.L. and D.C. Tilotta: "Determination of Volatile Organic Compounds in Water by Solid Phase Microextraction and Infrared Spectroscopy," *Environmental Science Technology*, 30 (4), pp.1212-1219, 1996.
- Himmelblau, D.M. and K.B. Bischoff: *Process Analysis and Simulation: Deterministic Systems*, John Wiley & Sons, Inc., New York, 1968.

- Hunt, J.R., N. Sitar and K.S. Udell: "Nonaqueous Phase Liquid Transport and Cleanup 1. Analysis of Mechanisms," *Water Resources Research*, 24 (8), pp.1247-1258, 1988a.
- Hunt, J.R., N. Sitar and K.S. Udell: "Nonaqueous Phase Liquid Transport and Cleanup 2. Experimental Studies," *Water Resources Research*, 24 (8) 1259-1269, 1988b.
- Jackson, R.E. and P.E. Mariner: "Estimating DNAPL Composition and VOC Dilution from Extraction Well Data", *Ground Water*, 33 (3), pp.407-414, 1995.
- Jin, M., M. Delshad, D.C. McKinney, G.A. Pope, K. Sepehrnoori, C. Tilburg, and R.E. Jackson: "Subsurface NAPL Contamination: Partitioning Tracer Test for Detection, Estimation and Remediation Performance Assessment," in *Toxic Substances and Hydrologic Sciences*, edited by A.R. Dutton, American Institute of Hydrology, Minneapolis, MN, p.131, 1994.
- Jin, M.: "Surfactant Enhanced Remediation and Interwell Partitioning Tracer Test for Characterization of NAPL Contaminated Aquifers," Ph.D. dissertation, University of Texas, Austin, 1995.
- Jin, M., M. Delshad, V. Dwarakanath, D.C. McKinney, G.A. Pope, K. Sepehrnoori, C. Tilburg, and R.E. Jackson: "Partitioning Tracer Test for Detection, Estimation and Remediation Performance Assessment of Subsurface Nonaqueous-phase Liquids," *Water Resources Research*, 31 (5), pp.1201, 1995.
- Jin, M. G.W. Butler, R.E. Jackson, P.E. Mariner, G.A. Pope, C.L. Brown and D.C. McKinney: "Partitioning Tracer Testing of DNAPL Zones in Alluvial Aquifers: 1. Introduction," Submitted to *Ground Water*.
- Kan, A.T. and M.B. Tomson: "UNIFAC Prediction of Aqueous and Nonaqueous Solubilities of Chemicals with Environmental Interest," *Environmental Science Technology*, 30 (4), p. 1369-1376, 1996.
- Kertes, A.S. and A.F.M. Barton: "Solubility Data Series: Alcohols with Water," Pergamon Press, New York, 1984.
- Knaepen W.A.I., R. Tijssen and E.A. van den Bergen: "Experimental Aspects of Partitioning Tracer Tests for Residual Oil Saturation Determination With FIA-Based Laboratory Equipment," *SPE Reservoir Engineering*, pp.239-244, 1990.
- Kostarelos, K.: "Surfactants/Polymer Flushing and Partitioning Tracers for Remediation of Dense Nonaqueous Phase Liquid Contaminated Soils," Ph.D. dissertation, The University of Texas at Austin, 1997.

- Kueper, B.H.: "The behavior of dense, non-aqueous phase liquid contaminants in heterogeneous porous media," Ph.D. dissertation, University of Waterloo, Waterloo, Ont., 1989.
- Kueper, B.H., D. Redman, R.C. Starr, S. Reitsma, and Mah: "A Field Experiment to Study the Behaviour of Tetrachloroethylene Below the Water Table: Spatial Distribution of Residual and Pooled DNAPL," *Ground Water*, 31 (5), pp.756-766, 1993.
- Lake, L.W.: *Enhanced Oil Recovery*, Prentice Hall, Englewood Cliffs, NJ, 1989.
- Lalanne-Cassou, C., I. Cormona, L. Fortney, A. Samii, R.S. Schechter, W.H. Wade, U. Weerasooriya and S. Yiv: "Minimizing Cosolvent Requirements for Microemulsions Formed with Binary Surfactant Mixtures," *Journal Dispersion Science and Technology*, 8 (2), pp.137-156, 1987.
- Lenhard, R.J., T.G. Johnson, and J.C. Parker: "Experimental Observations of Nonaqueous-Phase Liquid Subsurface Movement," *Journal of Contaminant Hydrology*, 12, pp.79-101, 1993.
- Lichtenberger G.J.: "Field Applications of Interwell Tracers for Reservoir Characterization of Enhanced Oil Recovery Pilot Areas," SPE 21652, Proceedings of the SPE Symposium on Production Operations, Oklahoma City, 1991.
- Ljosland E., T. Bjørnstad, Ø. Dugstad and I Hundere: "Perfluorocarbon Tracer Studies at the Gullfaks Field in the North Sea," *Journal of Petroleum Science and Engineering*, 10, pp27-38, 1993.
- Lyman, W.J., W. F. Reehl, and D H. Rosenblatt: "Handbook of Chemical Property Estimation Methods," American Chemical Society, Washington, D.C., 1990.
- Mackay, D.M., P.V. Roberts and J.A. Cherry: "Transport of organic contaminants in groundwater," *Environmental Science and Technology*, 19 (5), pp.384-391, 1985.
- Mackay, D.M. and J.A. Cherry: "Groundwater Contamination: Pump and treat Remediation," *Environmental Science and Technology*, 23 (6), pp.630-635, 1989.
- Maroongroge, Vichai.: "Modeling and Application of Tracers for Reservoir Characterization," Ph.D. dissertation, The U. of Texas, Austin (1994).
- Martel R., P.J. Gelinas, J.E. Desnoyers and A. Masson: "Phase Diagrams to Optimize Surfactant Solutions for Oil and DNAPL Recovery in Aquifers," *Ground Water*, 31 (5), pp.789-800, 1993.

- Martel R., P.J. Gelinas: "Surfactant Solutions Developed for NAPL Recovery in Contaminated Aquifers," *Ground Water*, 34 (1), pp.143-154, 1996.
- Mason A. and B.H. Kueper: "Numerical Simulation of Surfactant-Enhanced Solubilization of Pooled DNAPL," *Environmental Science and Technology*, 30 (11), pp.3205-3215, 1996.
- Mayer A.S. and C.T. Miller: "The Influence of Mass Transfer Characteristics and Porous Media Heterogeneity on Nonaqueous Phase Dissolution," *Water Resources Research*, 32 (6), pp.1551-1567, 1996.
- Mercer J.W. and R.M. Cohen: "A Review of Immiscible Fluids in the Subsurface: Properties, Models, Characterization and Remediation," *Journal of Contaminant Hydrology*, 6, pp.107-163, 1990.
- Miller C.T., M.M. Poirer-McNeill and A.S. Mayer: "Dissolution of Trapped Nonaqueous Phase Liquids: Mass Transfer Characteristics," *Water Resources Research*, 26 (11), pp. 2783-2796, 1990.
- Myers D.: "Surfactant Science and Technology," VCH Publishers, Inc. New York, 1988.
- Nash, J.H.: *Field Studies of In-Situ Washing*; EPA/600/2-87/110, U.S. Environmental Protection Agency, Cincinnati, OH, 1987.
- Nelson, R.C. and G.A. Pope: "Phase Relationships and Chemical Flooding," *Society of Petroleum Engineering Journal*, 18(5), p.325, Oct. 1978.
- Nelson N. and M. Brusseau: "Field Study of the Partitioning Tracer Method for Detection of Dense Nonaqueous Phase Liquid in Trichloroethylene-Contaminated Aquifer," *Environmental Science and Technology* 30, (9), pp.2859-2863, 1996.
- Nielsen F., E. Olsen and A. Fredenslund: "Henry's Law Constants and Infinite Dilution Activity Coefficients for Volatile Organic Compounds in Water by a Validated Batch Air Stripping Method," *Environmental Science and Technology*, 28 (12), pp.2133-2138, 1994.
- Oh, K.H., J.R. Baran Jr., W.H. Wade, and V. Weerasooriya: "Temperature Insensitive Microemulsion phase Behavior With Non-Ionic Surfactants," *Journal of Dispersion Science and Technology*, 16 (2), pp.165-168, 1995.
- Okuda I., J.F. McBride, S.N. Gleyzer and C.T. Miller: "Physicochemical Transport Processes Affecting the Removal of Residual DNAPL by Nonionic Surfactant Solutions," *Environmental Science and Technology*, 30 (6), pp.1852-1860, 1996.

- Ooi, K: M.S. thesis, The University of Texas at Austin, in progress
- Oolman, T., S.T. Godard, G.A. Pope, M. Jin, and K. Kirchner: "DNAPL Flow Behavior in a Contaminated Aquifer: Evaluation of Field Data," *GWMR*, 15 (4), pp.125-137, Fall, 1995.
- Palmer, C., D.A. Sabatini, and J.H. Harwell: "Sorption of Hydrophobic Organic Compounds and Nonionic Surfactants with Subsurface Materials," in *Transport and Remediation of Subsurface Contaminants*, ACS Symposium Series, edited by D.A. Sabatini and R.C. Knox, 1992.
- Pankow, J.F. and J.A. Cherry: *Dense Chlorinated Solvents*, Waterloo Press, Portland, OR, 1996.
- Pennell, K.D., L.M. Abriola, W.J. Weber Jr., "Surfactant Enhanced Solubilization of Residual Dodecane in Soil Columns 1. Experimental Investigation," *Environmental Science and Technology*, 27 (12), pp.2332-2340, 1993.
- Pennell, K.D., M. Jin, L.M. Abriola, and G.A. Pope: "Surfactant Enhanced Remediation of Soil Columns Contaminated by Residual Tetrachloroethylene," *Journal of Contaminant Hydrology*, 16 (1), p. 35, May, 1994.
- Pennell, K.D., G.A. Pope and L.M. Abriola: "Influence of Viscous and Buoyancy Forces on the Mobilization of Residual Tetrachloroethylene during Surfactant Flushing," *Environmental Science and Technology*, 30 (4), pp.1328-1335, 1996.
- Peters, R.W., C.D. Montemagno, L. Shem, and B. Lewis: "Surfactant Screening of Diesel Contaminated Soil," *Hazardous Waste and Hazardous Materials*, 9 (2), p. 113, 1992.
- Pitts M.J., K. Wyatt, T.C. Sale and K.R. Piontek: "Utilization of Chemical Enhanced Oil Recovery Technology to Remove Hazardous Oily Waste from Alluvium," SPE 25153, *Proceedings of SPE International Symposium on Oilfield Chemistry*, New Orleans, LA, March 205, 1993.
- Pope, G.A. and M. Bavière: *Basic Concepts in Enhanced Oil Recovery Processes*, *Critical Reports on Applied Chemistry*, 33, M. Bavière (ed.), Elsevier Science Publishing, London, 1991.
- Pope, G.A., K. Sepehrnoori, M. Delshad, B.A. Rouse, V. Dwarakanath, and M. Jin, "NAPL Partitioning Interwell Tracer Test in OU1 Test Cell at Hill Air Force Base, Utah," Final Report, ManTech Environmental Research Services Corp., PO number 94RC0251, GL number 2000-602-4600, 1994a.

- Pope, G.A., M. Jin, V. Dwarakanath, B.A. Rouse, and K. Sepehrnoori, "Partitioning Tracer Tests to Characterize Organic Contaminants," Proceedings of the second Tracer Workshop, Austin, TX, Nov. 14 & 15, 1994b, edited by T. Bjørnstad and G. Pope, Institute for Energy Technology, N-2007 Kjeller, Norway.
- Pope, G.A. and W.H. Wade: "Lessons from Enhanced Oil Recovery Research for Surfactant Enhanced Aquifer remediation," in Surfactant - Enhanced Subsurface Remediation Emerging Technologies, Sabatini, David A., Knox, Robert C., Harwell Jeffrey H. (eds). ACS symposium series 594, American Chemical Society Washington DC, pp. 142-160, 1995.
- Powers S. E., C.O. Loureiro, L.M. Abriola, W.J.Weber Jr.: "Theoretical Study of the Significance of Nonequilibrium Dissolution of Nonaqueous Phase Liquids in Subsurface Systems," Water Resources Research, 27 (4), pp.463-477, 1991.
- Powers S. E., L.M. Abriola, W.J.Weber Jr.: "An Experimental Investigation of NAPL Dissolution in Saturated Subsurface Systems: Steady State Mass Transfer Rates," Water Resources Research, 28 (10), pp.2691-2705, 1992.
- Powers, S.E., L.M. Abriola, J.S. Dunkin, W.J. Weber Jr.: "Phenomenological Models For Transient NAPL-Water Mass-Transfer Processes," Journal of Contaminant Hydrology, 16, pp.1-33, 1994.
- Radian Corporation: "Revised Work Plan for the Surfactant Treatment Study For Operable Unit 2 Hill Air Force Base, Utah," August 1993.
- Reed, R.L. and R.N. Healy: "Some Physiochemical aspects of Microemulsion Flooding: A Review," in Improved Oil Recovery by Surfactant and Polymer Flooding, D.O. Shah and R.S. Schechter (eds), Academic Press, New York, pp.383-437, 1977.
- Renshaw C.E, G.D. Zynda and J.C. Fountain: "Permeability Reductions Induced by Sorption of Surfactant," Water Resources Research, 33 (3), pp.371-378, 1997.
- Richabaugh, J.C., S. Clement, and R.F. Lewis: "Surfactant Scrubbing of Hazardous Chemicals from Soil," Proceedings 41st Purdue Industries Waste Conference, 41, p. 377, 1986.
- Rosen M.J: *Surfactants and Interfacial Phenomena*, John Wiley & Sons, New York, 1988.
- Rouse J. D.and D.A. Sabatini: "Minimizing Surfactant Losses Using Twin-Head Anionic Surfactants in Subsurface Remediation," Environmental Science and Technology, 27 (10), pp.2072-2078, 1993.

- Rouse J. D., D.A. Sabatini, N.E. Deeds and R.E. Brown: "Micellar Solubilization of Unsaturated Hydrocarbon Concentrations As Evaluated by Semiequilibrium Dialysis," *Environmental Science Technology*, 29 (10), pp.2484-2489, 1995.
- Salager J.L., J.C. Morgan, R.S. Schechter and W.H. Wade: "Optimum Formulation of Surfactant/Water/Oil Systems for Minimum Interfacial Tension or Phase Behavior," *SPE Journal*, pp.107-115, April 1979.
- Sale, T C., K.R. Piontek, M. Pitts: "Chemically Enhanced In-Situ Soil Washing," *Proceedings of Petroleum Hydrocarbons and Organic Chemicals in Groundwater*, National Water Well Association, Houston, 1989.
- Sandler, S.I.: "Chemical and Engineering Thermodynamics," John Wiley & Sons, New York, NY, 1989.
- Schwille, F.: *Dense Chlorinated Solvents in Porous and Fractured Media*, translated by J.F. Pankow, Lewis Publishers, Chelsea, MI, 1988.
- Schwarzenbach, R.P., P.M. Gschwend and D.M. Imboden: "Environmental Organic Chemistry," John Wiley and Sons, Inc., New York 1993.
- Sheely, C.Q.: "Description of Field Tests to Determine Residual Oil Saturation by Single-Well Tracer Method," *Journal of Petroleum Technology*, p.194, 1978.
- Sheely, C.Q., Jr. and D.E. Baldwin, Jr.: "Single-Well Tracer Tests for Evaluating Chemically Enhanced Oil Recovery Processes," *Journal of Petroleum Technology*, 34, p.1887, 1982.
- Shiau, B., D.A., Sabatini and J.H. Harwell: "Influence of Rhodamine WT Properties on Sorption and Transport in Subsurface Media," *Ground Water*, 31 (5), pp.913-920, 1993.
- Shiau, B., D.A. Sabatini, and J.H. Harwell: "Properties of Food Grade (Edible) Surfactants Affecting Subsurface Remediation of Chlorinated Solvents," *Environmental Science Technology*, 29 (12), pp.2929-2935, 1995a.
- Shiau, B., J.D. Rouse, D.A. Sabatini, J.H. Harwell, "Surfactant Selection for Optimizing Surfactant Enhanced Subsurface Remediation," *Surfactant Enhanced Subsurface Remediation Emerging Technologies*, D.A. Sabatini, R.C. Knox, J.H. Harwell (eds), ACS symposium series 594, American Chemical Society, Washington, DC, pp.65-81, 1995b.
- Shiau, B.: "Subsurface Remediation of Chlorinated Solvents Using Direct Food Additive Surfactants," Ph.D. dissertation, The University of Oklahoma, Norman, 1995.

- Shiau, B., J.D. Rouse, D.A. Sabatini, J.H. Harwell and D.Q. Vu: "Microemulsion of Mixed Chlorinated Solvents Using Food Grade (Edible) Surfactants," *Environmental Science and Technology*, 30 (1), 1996, pp.97-103.
- Shotts, D.R.: "Surfactant Remediation of Soils Contaminated with Chlorinated Solvents," M.S. thesis, The University of Texas at Austin, 1996.
- Soerens T.S. and D.A. Sabatini: "Cosolvency Effects on Sorption of a Semipolar, Ionogenic Compound (Rhodamine WT) with Subsurface Minerals," *Environmental Science and Technology*, 28 (6), pp.1010-1014, 1994.
- Solley W.B., C.F. Merck and R.R. Pierce: "Estimated Use of Water in the United States in 1985," U.S. Geological Survey Circular 1004, 1988.
- Somasundaram P. and H.S. Hanna: "Physico-Chemical Aspects of Adsorption at Solid/Liquid Interfaces," in *Improved Oil Recovery by Surfactant and Polymer Flooding*, D.O. Shah and R.S. Schechter (eds), Academic Press, New York, pp.205-251, 1977.
- Sorbie, K.S.: *Polymer Improved Oil Recovery*, Blackie and Son Ltd, Bishopbriggs, Glasgow, G64 2NZ, 1991.
- Stegemeier G.L.: "Mechanisms of Entrapment and Mobilization of Oil in Porous Media," in *Improved Oil Recovery by Surfactant and Polymer Flooding*, D.O. Shah and R.S. Schechter (eds), Academic Press, New York, pp.55-91, 1977.
- Studer, J.E., P. Mariner, M. Jin, G.A. Pope, D.C. McKinney, and R. Fate, "Application of a NAPL Partitioning Interwell Tracer Test (PITT) to Support DNAPL Remediation at the Sandia National Laboratories/New Mexico Chemical Waste Landfill," *Proceedings of the Superfund/Hazwaste West Conference*, Las Vegas, NV, May 21-23, 1996.
- Sunwoo C.K. and W.H. Wade: "Optimal Surfactant Structures for Cosurfactant-Free Microemulsion Systems. I. C₁₆ and C₁₄ Guerbet Alcohol Hydrophobes," *Journal Dispersion Science and Technology*, 13 (5), pp. 491-514, 1992.
- Tang, J.S. and B. Harker: "Interwell Tracer Test to Determine Residual Oil Saturation in a Gas-Saturated Reservoir. Part I: Theory and Design," *Journal Canadian Petroleum Technology*, 30 (3), p.76, 1991a.
- Tang, J.S. and B. Harker: "Interwell Tracer Test to Determine Residual Oil Saturation in a Gas-Saturated Reservoir. Part II: field applications," *Journal Canadian Petroleum Technology*, 30 (4), p.34, 1991b.

- Tang, J.S.: "Interwell Tracer Test to Determine Residual Oil Saturation to Waterflood at Judy Creek BHL "A" Pool," *Journal Canadian Petroleum Technology*, 31 (8), p.61, 1992.
- Tham M.J., R.C. Nelson and G.J. Hirasaki : "Study of the Oil Wedge Phenomenon Through the Use of a Chemical Flood Simulator," *SPE Journal*, pp.746-758 Oct. 1983.
- Texas Research Institute Report: "Underground Movement of Gasoline on Groundwater and Enhanced Recovery by Surfactants," Submitted to American Petroleum Institute, Washington D.C., by Texas Research Institute, Inc., Austin, 1979.
- Texas Research Institute Report: "Test Results of Surfactant Enhanced Gasoline Recovery in a Large-Scale Model Aquifer," Submitted to American Petroleum Institute, Washington D.C., by Texas Research Institute, Inc., Austin, 1985.
- Tomich, J.F., R.L. Dalton, Jr., H.A. Deans, and L.K. Shallenberger: "Single-Well Tracer Method to Measure Residual Oil Saturation," *Journal of Petroleum Technology*, 255, p. 211, 1973.
- Trost P.B., G.A. Pouska, M. Day M.: "APS Remediation of a Shallow Aquifer Containing Viscous Oil," *Proceedings of the 6th National RCRA/SUPERFUND Conference New Orleans, L.A. April 1989.*
- Tsaur, K.: "A Study of Polymer/Surfactant Interactions for Micellar/Polymer Flooding Applications," M.S. thesis, The University of Texas at Austin, 1978.
- U.S. EPA, 1991. Dense Nonaqueous Phase Liquids. EPA/540/4-91/002.
- Vigon B.W. and A.J. Rubin: "Practical Considerations in the Surfactant-Aided Mobilization of Contaminants in Aquifers," *Journal Water Pollution Control Federation*, 61 (7), pp.1233-1240, 1989.
- Villaume, J.F.: "Investigations at Sites Contaminated with Dense, Non-aqueous Phase Liquids (NAPLs)," *Groundwater Monitoring Review*, 5 (2), p.60, 1985.
- Wang P., V. Dwarakanath, B.A. Rouse, G.A. Pope and K. Sepehrnoori: "Partition Coefficients for Alcohol Tracers Between Nonaqueous-Phase Liquids and Water from UNIFAC-Solubility Method," In press, *Advances in Water Resources Research*, 1996.
- Weerasooriya, V.,: Personal communication, November, 1995, April, 1996.

- West, C.C.: "Surfactant Enhanced Solubilization of Tetrachloroethylene and Degradation Products in Pump and Treat Remediation," *Transport and Remediation of Subsurface Contaminants Colloidal, Interfacial, and Surfactant Phenomena*, D.A. Sabatini (ed), R.C. Knox, American Chemical Society, Washington, DC, pp.149-158, 1992.
- West, C.C. and J.H. Harwell: "Surfactants and Subsurface Remediation," *Environmental Science and Technology*, 26 (12), 1992, pp.2324-2330.
- Whelan, M.P., E.A. Voudrias, and A.L. Pearce: "DNAPL Pool Dissolution In Saturated Porous Media: Procedure Development and Preliminary Results," *Journal of Contaminant Hydrology*, 15, pp.223-237, 1994.
- Whitley, G.A., G.A. Pope, D.C. McKinney, B.A. Rouse, and P.E. Mariner, "Vadose Zone Nonaqueous-phase Liquid Characterization Using Partitioning Gas Tracers," *Proceedings of the Third International Symposium on In Situ Bioreclamation*, San Diego, CA, 1995.
- Wilson, J. L., S.H. Conrad, W.R. Mason, W. Peplinski and E. Hagan: "Laboratory investigations of residual liquid organics from spills, leaks and disposal of hazardous wastes in groundwater," U.S. EPA Ada. OK, EPA/600/6-90/004, pp.267, 1990.
- Wilson R.D. and D.M. Mackay: "The Use of Sulphur Hexafluoride as a Conservative Tracer in Saturated Sandy Media," *Ground Water*, 31 (5), pp.719-724, 1993.
- Wilson R.D. and D.M. Mackay: "Direct Detection fo Residual Nonaqueous Phase Liquid in the Saturated Zone Using SF₆ as a Partitioning Tracer," *Environmental Science and Technology*, 29 (5), pp.1255-1258, 1995.
- Wilson R.D. and D.M. Mackay: "SF₆ as a Conservative Tracer in Saturated Media with High Intragranular Porosity of High Organic Carbon Content," *Ground Water*, 34 (2), pp.241-249, 1996.
- Winsor, P.A.: *Solvent Properties of Amphiphilic Compounds*, Butterworths, London, 1954.
- Wood, K.N., J.S. Tang and R.J. Lucasavitch: "Interwell Residual Oil Saturation at Leduc Miscible Pilot," paper SPE 20543, *Proceedings of the 65th SPE Annual Technical and Exhibition*, New Orleans, LA, Sept. 23-26, 1990.
- Wreath D.G.: "A Study of Polymerflooding and Residual Oil Saturation," M.S. thesis, The University of Texas at Austin, 1989.
- Yalkowsky S.H. and S. Banerjee: "Aqueous Solubility, Methods of Estimation for Organic Compounds," Marcel Dekker Inc., New York, 1992.

Zemel, B.: *Tracers in the Oil Field, Developments in Petroleum Science*, 43, Elsevier Science, New York, 1995.

Ziegenfuss, P.S.: "The Potential Use of Surfactant and Cosolvent Soil Washing as Adjutant for In-Situ Aquifer Restoration," M.S. thesis, Rice University, Houston, Texas, 1987.

Vita

Varadarajan Dwarakanath was born in Bombay, India on April 30, 1970, the son of Krishnasami Varadarajan and Champa Varadarajan. After graduating from the Delhi Tamil Educational Association High School, Delhi India, in May 1986, he entered The Institute of Technology, Banaras Hindu University. There he earned a Bachelor of Technology degree in Mining Engineering in June 1990. In August 1990 he was admitted to the Graduate School at The University of Texas at Austin. He received his Master of Science in Petroleum Engineering in December 1992. Subsequently he enrolled in the Ph.D. program at The University of Texas at Austin in January 1993.

Permanent address: 27 Alakananda, Shivalik Apts
New Delhi, 110019
India

This dissertation was typed by the author.